Design, Synthesis and Pharmacological Characterization of Oligopeptidic and Non-Peptidic Neuropeptide Y Y_4 Receptor Ligands

DISSERTATION

zur Erlangung des Doktorgrades der Naturwissenschaften (Dr. rer. nat.)
an der Fakultät für Chemie und Pharmazie
der Universität Regensburg

vorgelegt von
Adam Konieczny
aus Krefeld

2020

Die vorliegende Arbeit entstand in der Zeit von Juli 2017 bis November 2020 unter der Leitung von Herrn PD Dr. Max Keller am Institut für Pharmazie der Naturwissenschaftlichen Fakultät IV - Chemie und Pharmazie - der Universität Regensburg.

Das Promotionsgesuch wurde eingereicht im Dezember 2020.

Tag der mündlichen Prüfung: 25.01.2021

Prüfungsausschuss:

Prof. Dr. A. Göpferich	(Vorsitzender)
PD Dr. M. Keller	(Erstgutachter)
Prof. Dr. S. Elz	(Zweitgutachter)
Prof. Dr. J. Wegener	(Drittprüfer)

Für Wioletta, Andreas und David

Acknowledgement and Declaration of Collaborations

An dieser Stelle möchte ich mich herzlich bedanken bei:

Herrn PD Dr. Max Keller für die zahlreichen Tipps, Anmerkungen, Ideen und die hervorragende Betreuung dieser Arbeit. Darüber hinaus vielen Dank für die unermüdliche Geduld und stetige Hilfsbereitschaft bei Fragen aller Art, zu jeder Tages- und Nachtzeit,

Herrn Prof. Dr. Armin Buschauer († 2017) für die Möglichkeit an diesem vielseitigen Projekt arbeiten zu dürfen, auch wenn die Zusammenarbeit leider nur von kurzer Dauer war,

Herrn Prof. Dr. Sigurd Elz für die Übernahme des Zweitgutachtens,

Herrn Prof. Dr. Joachim Wegener für die Teilnahme an der Promotionsprüfung als Drittprüfer,

Herrn Prof. Dr. Achim Göpferich für die Übernahme des Vorsitzes bei der Promotionsprüfung,

Herrn Prof. Dr. Heinrich Sticht, Herrn Marcus Konrad und Herrn Anselm Horn für die Durchführung von MD-Simulationen zur Untersuchung der Y_4R Bindung der zyklischen Peptide (Chapter 5),

Herrn Prof. Dr. Timothy Clark, Herrn Maximilian Schmidt und Herrn Eduard Neu für die Durchführung der Induced-Fit Docking Studien zur Untersuchung der Y_4R Bindung der zyklischen Peptide (Chapter 5),

Herrn Dr. David Wilfing für das Induced-Fit Docking der linearen Peptide an Y_4R Homologiemodellen und die Hilfe bei der Auswertung generierter Daten (Chapter 2 u. 4),

Herrn Dr. Steffen Pockes für die gemeinsame, sportliche Zeit beim SV Moosham,

Herrn Wolfgang Söllner und Herrn Josef Kiermeier für das Messen zahlreicher MS-Spektren und die Hilfe bei der Auswertung der MS-Analysen sowie die fachlichen Diskussionen,

Herrn Fritz Kastner für die stetige Hilfsbereitschaft bei der Vermessung von NMR-Spektren und die Ratschläge bei deren Auswertung,

Frau Dita Fritsch und Frau Elvira Schreiber für die anfängliche Hilfe bei der Kultivierung der CHO-hY_4R-G_{qi5}-mtAEQ Zellen und die Durchführung von Y_4R Radioligand-Bindungsexperimenten,

Frau Brigitte Wenzel für die Kultivierung der SK-N-MC Neuroblastom Zellen, die Durchführung der Y_1R Radioligand-Bindungsexperimente und die Hilfe bei der Vorbereitung des Ca^{2+}-Aequorin Assays,

Frau Susanne Bollwein und Frau Lydia Schneider für die Kultivierung der HEC-1B-hY_5R Zellen und die Durchführung von Y_5R Radioligand-Bindungsexperimenten,

Frau Maria Beer-Krön für die Kultivierung der CHO-hY_2R Zellen und die Durchführung von Sättigungs- und Kompetitionsexperimenten mit [^{3}H]propionyl-pNPY,

Herrn Peter Richthammer für die technische Unterstützung bei der alltäglichen Arbeit im Labor,

Frau Silvia Heinrich für die freundliche Hilfestellung bei bürokratischen Angelegenheiten,

Allen Doktoranden des Lehrstuhls für die kollegiale Zusammenarbeit,

Frau Diana Braun (M.Sc.) für die Unterstützung bei der Synthese und Charakterisierung der linearen Y_4R Liganden (Chapter 2), als Teil ihrer Masterarbeit,

Beiden Forschungspraktikanten Johannes Konrad und Simon Gross für ihre Hilfe bei der Auswertung und Interpretation von computerchemischen Daten (Chapter 4), was über den erforderlichen Rahmen ihres Forschungspraktikums weit hinausgeht,

Allen meinen Freunden, deren namentliche Erwähnung den Rahmen dieser Arbeit sprengen würde. Danke für die tollen gemeinsamen Erlebnisse und die schöne Zeit abseits des Laboralltags,

Meiner wundervollen Frau Julia und meiner Tochter Emma für die Liebe, die sie mir jeden Tag entgegenbringen und dafür, dass sie das Leben lebenswert gestalten,

Zuallerletzt bei meinen liebevollen Eltern Wioletta und Andreas und meinem Bruder David, ohne eure bedingungslose Unterstützung, stetige Hilfe und andauernde Motivation von Beginn an wäre die Arbeit in dieser Form nicht möglich gewesen. Euch ist die vorliegende Dissertation gewidmet.

Publications, Posters, Awards and Professional Training

Publications (published results prior to the submission of this thesis):

Lachmann, D., Konieczny, A., Keller, M., König, B.
Photochromic peptidic NPY Y_4 receptor ligands. *Organic & Biomolecular Chemistry*, **2019**, 17 (9), S. 2467-2478

Spinnler, K., von Krüchten, L., Konieczny, A., Schindler, L., Bernhardt, G., Keller, M.
An alkyne-functionalized arginine for solid-phase synthesis enabling "biorthogonal" peptide conjugation. *ACS Medicinal Chemistry Letters*, **2019**, *11* (3), S. 334-339

Konieczny, A., Braun, D., Wifling, D., Bernhardt, G., Keller, M.
Oligopeptides as neuropeptide Y Y_4 receptor ligands: identification of a high affinity tetrapeptide agonist and a hexapeptide antagonist. *Journal of Medicinal Chemistry*, **2020**, *63* (15), S. 8198-8215

Konieczny, A., Konrad, M., Schmidt, M., Neu, E., Horn, A.H.C., Wifling, D., Gmeiner, P., Clark, T., Sticht, H., Keller, M.
N-terminus to arginine side chain cyclization of linear peptidic neuropeptide Y Y_4 receptor ligands results in picomolar binding constants. *Journal of Medicinal Chemistry*, **2020**, *submitted*

Poster Presentations:

Konieczny A., Buschauer A., Bernhardt G., Keller M.
In search for selective agonists and antagonists for the NPY Y_4 receptor: modifications of the lead compound UR-KK236. *9th International Summer School "Medicinal Chemistry"*, **2018**, Regensburg, Germany.

Konieczny A., Wifling D., Buschauer A., Bernhardt G., Keller M.
New peptidic NPY Y_4 receptor ligands: computational chemistry, synthesis and pharmacological characterization. *8th Austrian Peptide Symposium*, **2018**, Salzburg, Austria.

Konieczny A., Bernhardt G., Keller M.
N-terminus to side chain cyclization of linear peptidic neuropeptide Y Y_4 receptor ligands results in picomolar receptor affinities. *9th Austrian Peptide Symposium*, **2019**, Vienna, Austria.

Poster Awards:

Poster award of the *8th Austrian Peptide Symposium*, **2018**, Salzburg, Austria.

Poster award of the *9th Austrian Peptide Symposium*, **2019**, Vienna, Austria.

Professional Training:

From January 2018 to November 2020 member of the Research Training Group (Graduiertenkolleg 1910) "*Medicinal Chemistry of selective GPCR Ligands*".

Contents

Chapter 1

General Introduction

1.1 The Neuropeptide Y (NPY) Family

Neuropeptide Y (NPY), peptide YY (PYY) and pancreatic polypeptide (PP) constitute a subfamily within the peptide family of neuroendocrine hormones. All three peptides consist of 36 amino acids, share considerable amino acid homology and an amidated C-terminus (Figure 1).[1-3]

NPY YPSKPDNPGEDAPAEDMARYYSALRHYINLITRQRY-NH_2

PYY YPIKPEAPGEDASPEELNRYYASLRHYLNLVTRQRY-NH_2

PP APLEPVYPGDNATPEQMAQYAADLRRYINMLTRPRY-NH_2

Figure 1. Amino acid sequences of human NPY, PYY and PP, members of the neuropeptide Y family. Amino acids are abbreviated using the one-letter code. Amino acids, which are present in all three polypeptides in the same position, are underlined.

NPY, which was firstly isolated by Tatemoto and coworkers from porcine brain in 1982,[4] is extensively expressed in the human body, in particular, in the central and peripheral nervous system.[5,6] Whereas NPY was described to act as a co-transmitter in central noradrenergic synapses, e.g. in the basal ganglia, hypothalamus, hippocampus and amygdala,[7-10] it exerts vasoconstrictor activity in the periphery via the sympathetic nervous system.[11] PYY, discovered in porcine intestine in 1982,[12] appears as a gut hormone, responsible for the regulation of pancreatic and gastric secretion.[4,13] PP, first isolated as a contaminant in chicken insulin in 1968, is also released in the gastrointestinal tract being involved in the regulation of digestion and satiety.[14] Generally, the hormones of the neuropeptide Y family are involved in the regulation of various biological effects and can be implicated in different pathophysiological processes, for example the dysregulation of food intake,[15-17] bone physiology[18-20] and pain,[21-23] as well as mood disorders[24-27] and cancer.[28-32]

X-ray analysis paved the way to a more detailed understanding of the polypeptide tertiary structure. The avian pancreatic polypeptide (aPP) crystal structure was firstly resolved in 1981.[33,34] PP is built up by a N-terminal polyproline-like helix (aa 1-8), followed by a β-turn (aa 9-13) and an antiparallel α-helix (aa 14-31). The C-terminal part (aa 32-36), which is crucial for receptor recognition and binding,[35] proved to be rather flexible. Due to the so called “PP-fold” or hairpin-like conformation, the N- and C-terminus are located in close proximity. Hydrophobic interactions of Pro^2, Pro^5 and Pro^8, all part of the polyproline-like helix, with hydrophobic side-chains of the α-helix, stabilize the tertiary structure of PP. The “PP-fold” was later also proposed for the highly homologous peptide porcine NPY (pNPY) (Figure 2).[36]

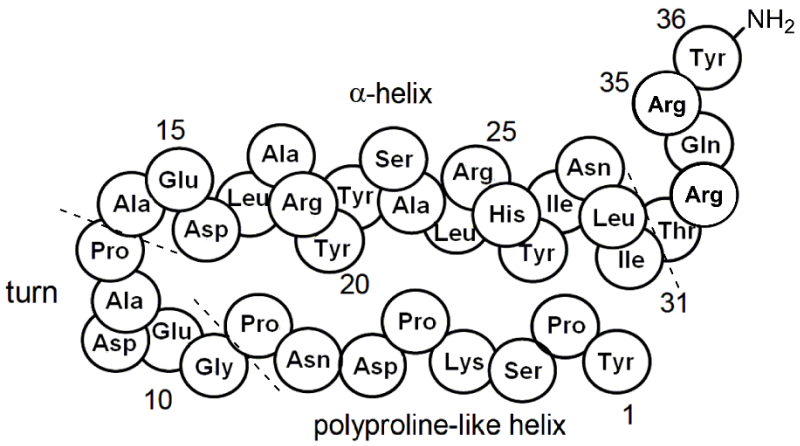

Figure 2. Schematic presentation of the tertiary structure of porcine NPY according to Allen *et al*.[36] Dashed lines indicate four regions: polyproline-like helix (1-8), β-turn (9-13), α-helix (14-31) and flexible C-terminus (32-36).

Subsequently, several groups investigated the three-dimensional structures of NPY and PP in solution using CD spectroscopy, NMR spectroscopy and FRET-based approaches. While some of these studies confirmed the monomeric folded structure of PP,[37,38] others reported contradictory findings, e.g. conformations with a non-helical and flexible N-terminus or dimeric structures, held together by hydrophobic contacts between the N-terminal α-helices.[39-43] It should be mentioned that NMR spectroscopic studies on the conformation of NPY and PP were performed under unphysiological conditions. Therefore, these results should be considered with care regarding the active conformation of NPY under physiological conditions. Interestingly, CD spectroscopy studies revealed various conformations of NPY, depending on temperature, pH-value and the respective peptide concentration. Nevertheless, the monomeric hairpin-like structure seems to be the most favored one,[44] that could be verified for PYY too.[45]

The NPY receptors (YRs) belong to class A (rhodopsin-like) G-protein coupled receptors (GPCRs). Like all GPCRs, they comprise seven transmembrane helices (TM) connected via intracellular (ICL) and extracellular (ECL) loops. Until now, seven different Y receptors (Y_1-Y_8, except Y_3) have been described in vertebrates, and up to five of them (Y_1, Y_2, Y_4, Y_5, Y_6) are present in mammals.[46-55] Noteworthily, the Y_6 receptor acts as a non-functional receptor in most mammalian species and is not expressed in rats.[56] The membrane protein, originally determined as the Y_3 receptor, was later identified as the chemokine receptor 4 (CXCR4) and is thus assigned to the CXC chemokine receptor family.[57] With respect to intracellular signaling, the NPY receptors are $G_{i/0}$ protein coupled mediating the inhibition of cAMP formation[58,59] as well as the activation of phospholipase C, causing an elevation of intracellular (cytosolic) Ca^{2+} levels.[49,50,59-64] Whereas the endogenous YR ligands NPY and PYY prefer the Y_1, Y_2 and Y_5 receptor over the Y_4R, PP is the preferential agonist at the Y_4 receptor,[57] originally classified as the PP_1 receptor.[51] Like NPY, Y_1 and Y_2 receptors are widely distributed throughout the brain.[65-67] The same holds true for the Y_4 and Y_5 receptor but with lower expression levels.[65,68]

Y_4 and Y_5 receptors were mainly found in the ileum, there being responsible for gastric secretion and the mediation of abdominal fullness, a phenomenon that can possibly be exploited for the treatment of obesity. A variety of single nucleotide polymorphisms (SNPs) and gene copy number variations (CNV) are associated with obesity.[69,70] One such CNV region can be found at chromosome 10q11.22 and it encompasses three genes.[71-73] One of these genes is *NPY4R*, encoding the Y_4R. Among the three genes, *NPY4R* is the most likely candidate to play a role in energy metabolism and obesity development. An overview of the most important biological effects, mediated by NPY receptors, is given in Table 1.

Table 1. Overview of the most important biological effects, mediated by NPY receptors.

Receptor	Physiological effect
Y_1	food intake (↑), energy metabolism (↓), anxiolysis, sedation, pain sensitivity (↓), blood pressure (↑) (peripheral effect due to vasoconstriction)
Y_2	food intake (↓), energy metabolism (↑), blood pressure (↓) (additional effect on vascularity), NPY release (↓) (presynaptic autoreceptor), regulation of circadian rhythm
Y_4	gastrointestinal motility (↑), food intake (↓)
Y_5	food intake (↑), anxiety, luteinizing hormone release (↓), regulation of circadian rhythms

Recently, advances in GPCR crystallization paved the way to a more detailed understanding of GPCR ligand binding, activation and dynamics, which was honored with the Nobel Prize in 2012.[74,75] Coming along with optimized GPCR crystallization procedures, more and more GPCR crystal structures have been obtained, covering, in particular, GPCRs, which represent drug targets. In 2018, Zhang et al. reported the crystal structure of the hY_1R in complex with the selective Y_1R antagonists UR-MK299 or BMS-193885.[76] Among other amino acids, $Asp^{6.59}$ of the hY_1R was identified to play a key role in ligand recognition, which had earlier been hypothesized by hY_1R docking studies.[77] Interestingly, the acidic $Asp^{6.59}$ residue is fully conserved among all NPY receptor subtypes. Whereas $Asp^{6.59}$ in the hY_2R and hY_5R interacts with Arg^{33} of NPY, in the hY_1R and hY_4R, the suggested interaction partner of $Asp^{6.59}$ is Arg^{35} of NPY.[77] Xu et al. generated a homology model of the hY_2R in 2013, which was used to suggest binding modes of commercially available peptidic and non-peptidic hY_2R ligands.[78] The C-terminal amino acids Arg^{33} and Arg^{35} of NPY were identified to form salt-bridges with $Asp^{6.59}$ and $Glu^{5.24}$, respectively, of the Y_2R, and the model suggested a hydrogen bond network between $Thr^{2.61}$, $Gln^{3.32}$ and $His^{7.39}$ within the orthosteric binding site of the Y_2R.[78] Additional studies using NMR spectroscopy, molecular modeling and double-cycle mutagenesis investigations underlined the findings of the above mentioned NPY-Y_2R interactions.[79] Based on several available class A GPCR crystal structures, a hY_4R homology model was constructed in complex with the endogenous ligand PP.[80] According to this model, Tyr^{27}, Arg^{33}

and Arg^{35} of PP were involved in interactions with Tyr$^{2.64}$, Asp$^{2.68}$, Asn$^{6.55}$, Asn$^{7.32}$ and Phe$^{7.35}$ of the hY$_4$R, so that the core of the presumed peptide binding pocket was constituted by the upper parts of transmembrane domains 2, 6 and 7 (TM2, TM6, TM7).

1.2 Y_1, Y_2 and Y_5 Receptor Ligands

A first attempt to develop selective Y$_1$R ligands started in the early 1990s by the synthesis of modified and truncated human NPY analogs. Fuhlendorff et al.[81] demonstrated that C-terminal modifications were useful to increase the Y$_1$R selectivity of the peptidic ligands, e.g. [Leu^{31}, Pro^{34}]NPY, exhibiting 80-fold higher Y$_1$R affinity compared to the Y$_2$R. The incorporation of D-amino acids led, e.g. to [D-Arg^{25}, D-His^{26}]NPY, displaying 40-fold higher Y$_1$R over Y$_2$R affinity and a 300-fold higher Y$_1$R affinity compared to Y$_5$R binding.[82] Continuing approaches focused on a size reduction of the peptide structure, e.g. by N-terminal truncation. However, N-terminally truncated NPY analogs, such as NPY(3-36), NPY(13-36) and NPY(18-36), showed low Y$_1$R affinity and were more selective towards the Y$_2$R.[3,83] At the same time, Boehringer-Ingelheim Pharma focused on the development of non-peptide Y$_1$R ligands. An alanine scan of NPY was performed by Beck-Sickinger et al.,[84] which revealed the high importance of the C-terminal sequence of NPY for Y$_1$R binding, especially Arg^{35} and Tyr^{36}. Through structure-activity relationship (SAR) studies, BIBP 3226 (K_i (hY$_1$R): 7 nM), the first non-peptide highly selective Y$_1$R antagonist, mimicking the C-terminal dipeptide of NPY to some extent, was developed (Figure 3).[85] The structure of the argininamide BIBP 3226 was later modified, affording, for example, the (*S*)-configured BIBP 3226 enantiomer, which was 1000 times less potent at the Y$_1$R,[86] or the congener BIBO 3304 (K_i (hY$_1$R): 0.4 nM) (Figure 3), containing an ureidomethly moiety instead of the phenolic hydroxyl group in BIBP 3226.[87] However, BIBP 3226 or BIBO 3304 have not been considered appropriate drug candidates due to disadvantageous pharmacokinetic properties. Derived from BIBP 3226, radiolabeled molecular tools for the hY$_1$R were developed, for example [^{3}H]UR-MK299, a radioligand exhibiting a Y$_1$R dissociation constant in the two-digit picomolar range and a long receptor residence time (Figure 3).[88] Recently, the “cold” form, UR-MK299, proved to be beneficial for the crystallization of the hY$_1$R.[76]

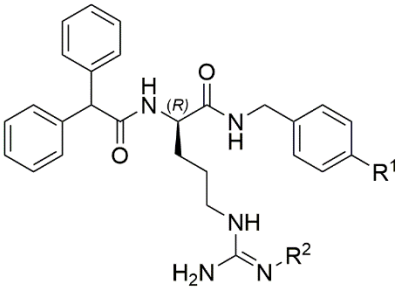

compound	R^1	R^2	K_i or K_D (hY_1R)
BIBP 3226	OH	H	7 nM[a]
BIBO 3304	CH_2-NH-CO-NH_2	H	0.4 nM[b]
[^{3}H]UR-MK299	OH	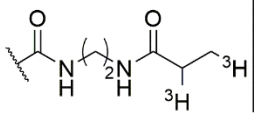	0.044 nM[c]

Figure 3. Structures and Y_1R affinities of the argininamide-type selective Y_1R antagonists BIBP 3226, BIBO 3304 and [^{3}H]UR-MK299. [a]Rudolf *et al*.[85] [b]Wieland *et al*.[87] [c]Keller *et al*.[88]

Compared to NPY, the N-terminally truncated analog NPY(18-36) exhibits an only 6 times lower affinity towards the Y_2R, but 70-fold lower Y_1R binding.[89] For the peptides [Pro^{34}]NPY and [Leu^{31}, Pro^{34}]NPY, low Y_2R affinities were described.[81,90] In 1999, BIIE 0246, the first non-peptide selective Y_2R antagonist, exhibiting Y_2R affinity in the one-digit nanomolar range, was published by Doods et al. (Figure 4).[91] Later, Y_2R antagonists with lower molecular weight were reported, for example JNJ31020028 (Figure 4), developed by Johnson & Johnson with the aid of high throughput screening.[92]

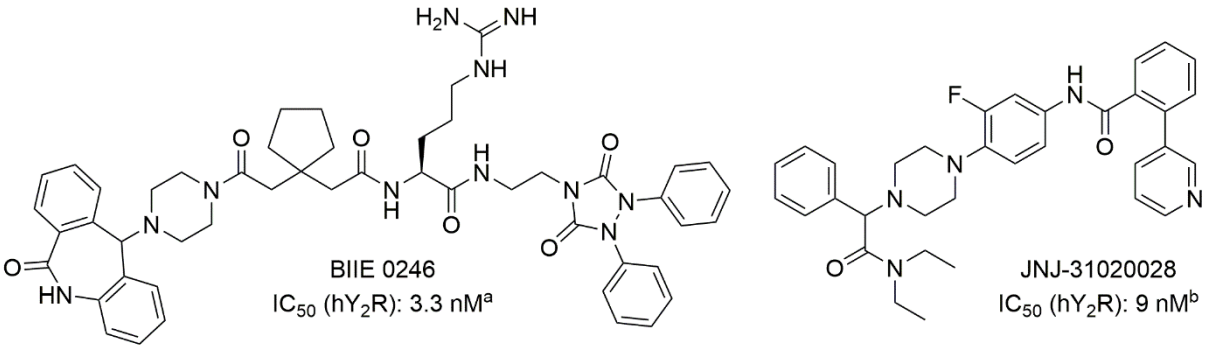

Figure 4. Structures and Y_2R affinities of the non-peptidic selective Y_2R antagonists BIIE 0246 and JNJ-31020028. [a]Doods *et al*.[91] [b]Shoblock *et al*.[92]

The first selective Y_5R ligands were, as in the case of the Y_1R and Y_2R, NPY analogs. For example, Balasubramaniam et al. described [D-Trp^{32}]NPY as a selective Y_5R agonist.[93] Likewise, [Ala^{31},Aib^{32}]NPY, containing the non-proteinogenic amino acid 2-aminoisobutytic acid (Aib), turned out to be a highly potent and selective Y_5R ligand, increasing the feeding behavior of rats.[3,94] The search for new anti-obesity drugs led to highly potent, small-molecule Y_5R antagonists. For example, the Y_5R antagonist CGP 71683A, composed of a naphthylsulfonamide- and a 2,4-diaminoquinazoline moiety, connected via a cyclohexane linker, represents a high-affinity Y_5R antagonist (Figure 5).[62] Due to unfavorable physicochemical properties and off-target effects, this compound did not reach clinical trials. Another example is MK-0557 (Figure 5). This Y_5R antagonist, developed by Merck, showed promising results in the early phases of clinical trials, but studies were later stopped because of the insufficient therapeutic effect.[95]

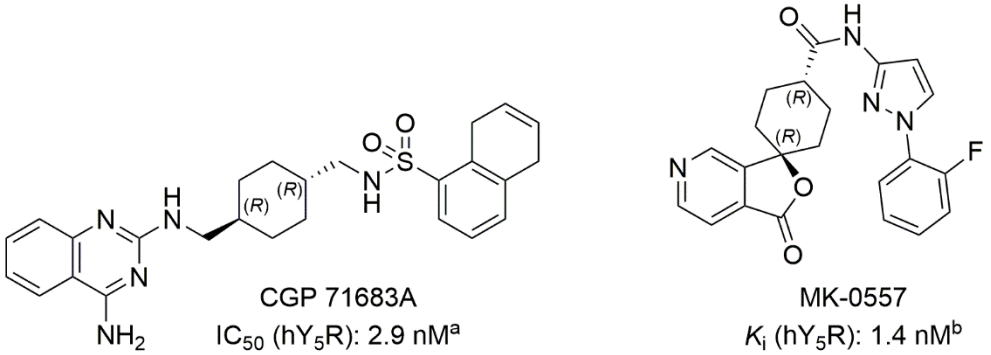

Figure 5. Structures and Y_5R affinities of the selective Y_5R antagonists CGP 71683A and MK-0557. [a]Criscione *et al*.[62] [b]Erondu *et al*.[95]

1.3 Y_4 Receptor Ligands

The Y_4R shares comparably low sequence similarity with the remaining NPY receptor subtypes (42% with the Y_1R, its closest receptor homologue) and plays an exceptional role in the NPY family because of its preferential binding of PP as endogenous ligand.[51] First Y_4R ligands were initially designed as Y_1R antagonists, for example the cyclic peptide GW1229 (Figure 6).[96] Years later, Balasubramaniam et al. published a series of dimeric ligands, constructed by the linkage of two pentapeptides, representing the C-terminal sequence (Tyr-Arg-Leu-Arg-Tyr-NH_2) of GW1229 (Figure 6).[97] The most promising ligand, BVD-74D, exhibited very high Y_4R affinity (K_i (hY_4R): 0.05 nM) and was used for in-vivo studies, investigating the effect of this compound on food intake in mice.[98] In search for radiolabeled hY_4R ligands, homo- and heterodimeric analogs of BVD-74D were synthesized in our work group, affording two high-affinity Y_4R radioligands, i.e. [^{3}H]UR-KK193 and [^{3}H]UR-KK200 (Figure 6).[99] Recently, hexapeptide UR-KK236 (Figure 6), representing the N-terminally argininylated congener of the pentapeptide Tyr-Arg-Leu-Arg-Tyr-NH_2,[100] was reported as a Y_4R partial agonist, exhibiting almost as high hY_4R affinity (K_i: 3.4 nM) as the dimeric ligands UR-KK193 and UR-KK200. Worth mentioning, a dimeric Y_1R ligand approach based on the pharmacophore BIBP 3226, yielded the first non-peptide Y_4R antagonist (UR-MK188, Figure 6) displaying moderate Y_4R affinity (K_i: 130 nM).[101] Interestingly, the optical antipode of UR-MK188, i.e. the *S*,*S*-configured isomer UR-MEK388, showed Y_4R binding comparable to that of UR-MK188, but was inactive at the hY_1R.[101]

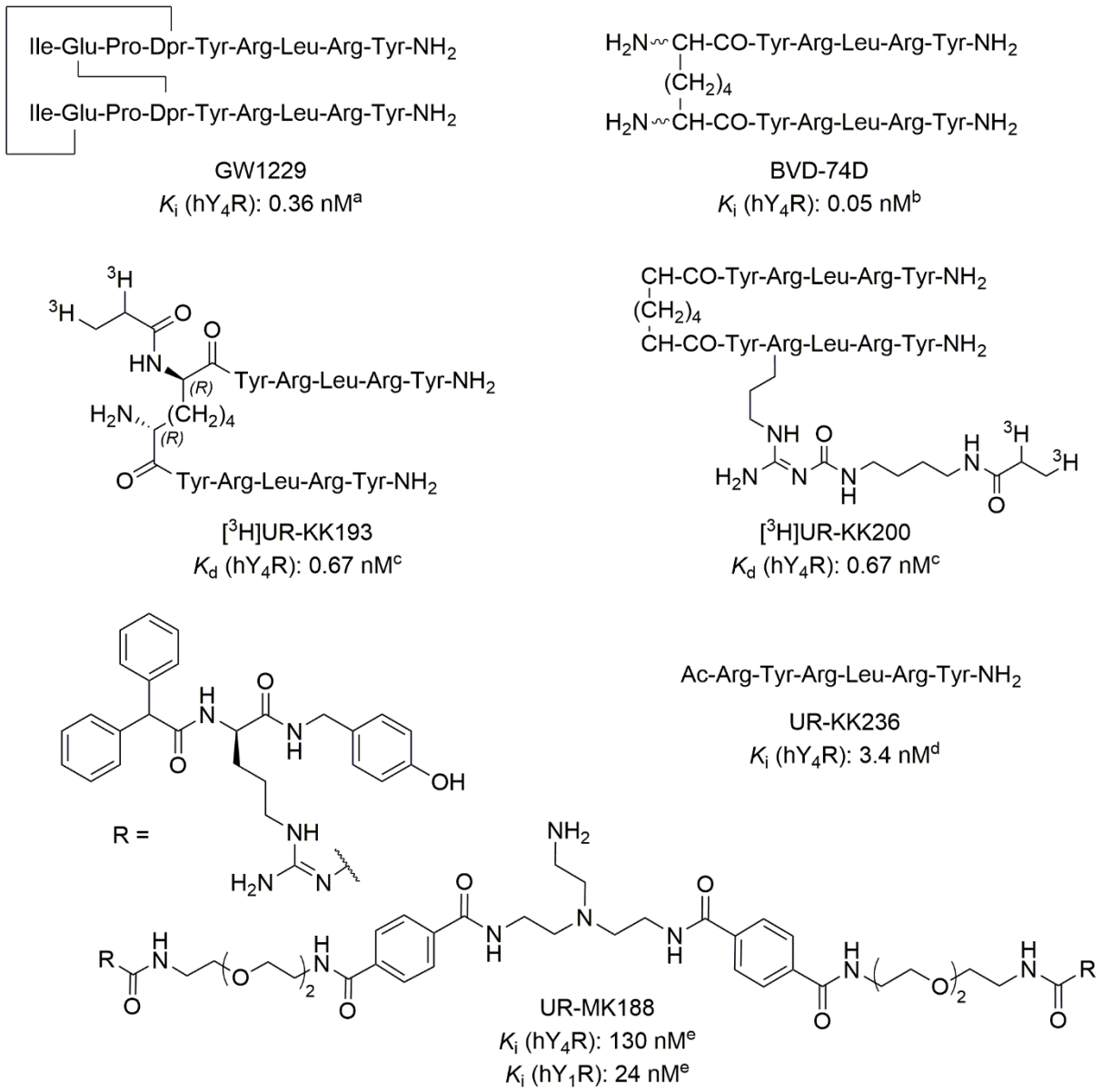

Figure 6. Structures and Y_4R affinities of reported peptide and non-peptide Y_4R ligands. [a]Parker *et al.*[96] [b]Balasubramaniam *et al*.[97] [c]Kuhn *et al*.[99] [d]Kuhn *et al*.[100] [e]Keller *et al*.[101]

Recent approaches also focused on the development of small molecule Y_4R ligands, including positive allosteric modulators (PAMs), which, in general, potentiate binding of the orthosteric receptor ligand by occupying an allosteric binding site of the receptor.[102] Strictly, PAMs exhibit no intrinsic activity, i.e. the modulatory effect can only be observed in conjunction with a ligand simultaneously occupying the orthosteric binding pocket.[103] Surprisingly, the antiparasitic drug niclosamide and the structural variant VU0118748 (Figure 7) were described as weakly active Y_4R PAMs, potentiating the response of PP (elicited at a concentration corresponding to the EC_{20} of PP) by a factor of 3.5 (niclosamide) or 4 (VU0118748) in an inositol phosphate accumulation assay, when used at high concentration (30 µM).[104] Prompted by these results, the structures were later modified to obtain tBPC (*tert*-butylphenoxycyclohexanol), which showed higher Y_4R subtype selectivity and proved to be a Y_4R PAM in a β-arrestin 3

recruitment assay.[105] Compounds **1.1** and **1.2** (Figure 7) belong to a series of patent substances from Bristol-Meyers Squibb that were described as Y_4R PAMs.[106] However, in the used functional assay, measuring the suppression of forskolin-induced cAMP formation, these compounds exhibited intrinsic activity in the absence of the orthosteric agonist. It should be noted that the pharmacological data, characterizing GPCR PAMs, must be interpreted with care because of the high concentrations, in which PAMs are normally used to determine the effect on agonist-mediated receptor activation.[103]

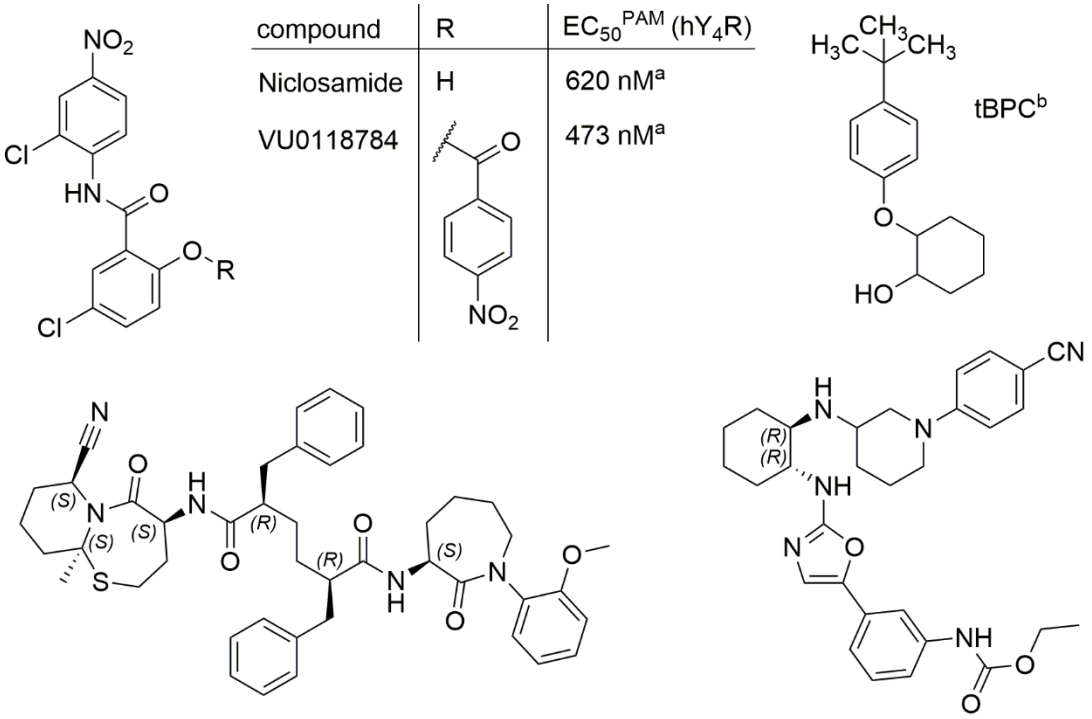

Figure 7. Structures and potencies of reported allosteric Y_4R modulators. [a]Slikowski *et al.*[104] [b]Schubert *et al.*[105] [c]Ewing *et al.*[106]

1.4 Scope of the Thesis

The peptides of the NPY family (NPY, PYY and PP) and their receptors regulate numerous physiological processes, such as gastrointestinal motility and food intake, and were suggested as targets, e.g. for the treatment of obesity.[16,17] Among the human NPY receptor subtypes (Y_1R, Y_2R, Y_4R and Y_5R), the Y_4R seems to play a unique role being primarily involved in the regulation of gastrointestinal functions.[51,107] Concerning therapeutic applications, Y_4R agonists, potentially useful to treat obesity, are more interesting compared to Y_4R antagonists. Whereas a variety of peptide agonists and non-peptide antagonists had been reported for the Y_1R, Y_2R and Y_5R, the available portfolio of Y_4R ligands, especially antagonists, had been limited. Selective Y_4R antagonists are needed as pharmacological tools to investigate the physiological and pathophysiological role of the Y_4R more in detail.

The hexapeptide UR-KK236 (Figure 5),[100] mimicking the amidated C-terminal sequence of PP,[80] had been identified in our work group as a high-affinity Y_4R partial agonist. One objective of this thesis was the synthesis and pharmacological characterization of linear analogs of UR-KK236, including truncated derivatives, to explore the ligand structure with respect to components, essential for Y_4R binding and activation. Modifications had to be achieved, for example, by the incorporation of amino acids such as Trp, GABA, Ala, D-amino acids, as well as other unnatural amino acids. In particular, a bioactivity-retaining reduction of the molecular weight and an inversion of the mode of action (partial agonism) to antagonism were aims of this project.

As cyclic peptides, exhibiting increased rigidity and potentially higher receptor affinity as well as more favorable pharmacokinetic properties compared to their linear analogs, have been used as therapeutics addressing GPCRs and other pharmaceutical target classes,[108,109] cyclic Y_4R ligands derived from UR-KK236 had to be developed. A recently described side chain to C-terminus cyclization of an analog of UR-KK236 resulted in an immense decrease in Y_4R affinity, confirming the necessity of a flexible, linear C-terminus of peptidic Y_4R ligands derived from PP.[100] Therefore, side-chain to N-terminus cyclized analogs of UR-KK236 had to be prepared and the effect on Y_4R affinity had to be studied. For this purpose, amine-functionalized N^{ω}-carbamoylated arginines[110] had to be incorporated to enable a cyclization via (modified) arginine side chains.

Finally, an approach towards the development of small molecule, non-peptidic Y_4R ligands had to be addressed. Former studies had revealed that dimerization of argininamide-type Y_1 receptor antagonists, using long flexible linkers, results in a loss of Y_1 over Y_4 receptor selectivity due to considerably increased Y_4R affinity compared to the monovalent ligands.[101] However, these compounds exhibited high molecular weight, being inappropriate lead

structures. The aim, pursued in this thesis, was the identification of a new, small, non-peptidic lead structure, exhibiting moderate Y_4R affinity and being conveniently synthetically available. This approach had to be supported by computational chemistry, i.e. induced-fit docking studies with virtually designed potential Y_4R ligands using a hY_4R homology model. Based on the reasonability of the binding poses and the obtained score values, a selection of promising compounds had to be synthesized and pharmacologically characterized.

1.5 References

(1) Balasubramaniam, A. A., Neuropeptide Y family of hormones: receptor subtypes and antagonists. *Peptides* **1997**, *18*, 445-457.

(2) Cerda-Reverter, J. M.; Larhammar, D., Neuropeptide Y family of peptides: structure, anatomical expression, function, and molecular evolution. *Biochem. Cell Biol.* **2000**, *78*, 371-392.

(3) Cabrele, C.; Beck-Sickinger, A. G., Molecular characterization of the ligand-receptor interaction of the neuropeptide Y family. *J. Pept. Sci.* **2000**, *6*, 97-122.

(4) Tatemoto, K.; Carlquist, M.; Mutt, V., Neuropeptide Y - a novel brain peptide with structural similarities to peptide YY and pancreatic polypeptide. *Nature* **1982**, *296*, 659-660.

(5) Gray, T. S.; Morley, J. E., Neuropeptide Y: anatomical distribution and possible function in mammalian nervous system. *Life Sci.* **1986**, *38*, 389-401.

(6) Larhammar, D., Evolution of neuropeptide Y, peptide YY and pancreatic polypeptide. *Regul. Pept.* **1996**, *62*, 1-11.

(7) Chronwall, B. M., Anatomy and physiology of the neuroendocrine arcuate nucleus. *Peptides* **1985**, *6*, 1-11.

(8) Fetissov, S. O.; Kopp, J.; Hökfelt, T., Distribution of NPY receptors in the hypothalamus. *Neuropeptides* **2004**, *38*, 175-188.

(9) Enman, N. M.; Sabban, E. L.; McGonigle, P.; Van Bockstaele, E. J., Targeting the neuropeptide Y system in stress-related psychiatric disorders. *Stress--Mol. Behav.* **2015**, *1*, 33-43.

(10) Stanić, D.; Mulder, J.; Watanabe, M.; Hökfelt, T., Characterization of NPY Y_2 receptor protein expression in the mouse brain. II. Coexistence with NPY, the Y_1 receptor, and other neurotransmitter-related molecules. *J. Comp. Neurol.* **2011**, *519*, 1219-1257.

(11) Ekblad, E.; Edvinsson, L.; Wahlestedt, C.; Uddman, R.; Håkanson, R.; Sundler, F., Neuropeptide Y co-exists and co-operates with noradrenaline in perivascular nerve fibers. *Regul. Pept.* **1984**, *8*, 225-235.

(12) Tatemoto, K., Isolation and characterization of peptide YY (PYY), a candidate gut hormone that inhibits pancreatic exocrine secretion. *Proc. Natl. Acad. Sci. U. S. A.* **1982**, *79*, 2514-2518.

(13) Hazelwood, R. L., The pancreatic polypeptide (PP-fold) family: gastrointestinal, vascular, and feeding behavioral implications. *Exp. Biol. Med.* **1993**, *202*, 44-63.

(14) Kimmel, J. R.; Pollock, H. G.; Hazelwood, R. L., Isolation and characterization of chicken insulin. *Endocrinology* **1968**, *83*, 1323-1330.

(15) Kamiji, M. M.; Inui, A., NPY Y_2 and Y_4 receptors selective ligands: promising anti-obesity drugs? *Curr. Trends Med. Chem.* **2007**, *7*, 1734-1742.

(16) Kuo, L. E.; Kitlinska, J. B.; Tilan, J. U.; Li, L.; Baker, S. B.; Johnson, M. D.; Lee, E. W.; Burnett, M. S.; Fricke, S. T.; Kvetnansky, R.; Herzog, H.; Zukowska, Z., Neuropeptide Y acts directly in the periphery on fat tissue and mediates stress-induced obesity and metabolic syndrome. *Nat. Med.* **2007**, *13*, 803-811.

(17) Sato, N.; Ogino, Y.; Mashiko, S.; Ando, M., Modulation of neuropeptide Y receptors for the treatment of obesity. *Expert Opin. Ther. Pat.* **2009**, *19*, 1401-1415.

(18) Meunier, F. A.; Baldock, P. A.; Lee, N. J.; Driessler, F.; Lin, S.; Allison, S.; Stehrer, B.; Lin, E.-J. D.; Zhang, L.; Enriquez, R. F.; Wong, I. P. L.; McDonald, M. M.; During, M.; Pierroz, D. D.; Slack, K.; Shi, Y. C.; Yulyaningsih, E.; Aljanova, A.; Little, D. G.; Ferrari, S. L.; Sainsbury, A.; Eisman, J. A.; Herzog, H., Neuropeptide Y knockout mice reveal a central role of NPY in the coordination of bone mass to body weight. *PLoS ONE* **2009**, *4*, e8415.

(19) Lee, N. J.; Allison, S.; Enriquez, R. F.; Sainsbury, A.; Herzog, H.; Baldock, P. A., Y_2 and Y_4 receptor signalling attenuates the skeletal response of central NPY. *J. Mol. Neurosci.* **2010**, *43*, 123-131.

(20) Ducy, P.; Amling, M.; Takeda, S.; Priemel, M.; Schilling, A. F.; Beil, F. T.; Shen, J.; Vinson, C.; Rueger, J. M.; Karsenty, G., Leptin inhibits bone formation through a hypothalamic relay. *Cell* **2000**, *100*, 197-207.

(21) Seybold, V. S.; McCarson, K. E.; Mermelstein, P. G.; Groth, R. D.; Abrahams, L. G., Calcitonin gene-related peptide regulates expression of neurokinin 1 receptors by rat spinal neurons. *J. Neurosci.* **2003**, *23*, 1816-1824.

(22) Moran, T. D.; Colmers, W. F.; Smith, P. A., Opioid-like actions of neuropeptide Y in rat substantia gelatinosa: Y_1 suppression of inhibition and Y_2 suppression of excitation. *J. Neurophysiol.* **2004**, *92*, 3266-3275.

(23) Brumovsky, P.; Shi, T. S.; Landry, M.; Villar, M. J.; Hökfelt, T., Neuropeptide tyrosine and pain. *Trends Pharmacol. Sci.* **2007**, *28*, 93-102.

(24) Eaton, K.; Sallee, F.; Sah, R., Relevance of neuropeptide Y (NPY) in psychiatry. *Curr. Trends Med. Chem.* **2007**, *7*, 1645-1659.

(25) Wahlestedt, C.; Ekman, R.; Widerlöv, E., Neuropeptide Y (NPY) and the central nervous system: distribution effects and possible relationship to neurological and psychiatric disorders. *Prog. Neuro-Psychopharmacol. Biol. Psychiatry* **1989**, *13*, 31-54.

(26) Thorsell, A.; Slawecki, C. J.; El Khoury, A.; Mathe, A. A.; Ehlers, C. L., The effects of social isolation on neuropeptide Y levels, exploratory and anxiety-related behaviors in rats. *Pharmacol., Biochem. Behav.* **2006**, *83*, 28-34.

(27) Morales-Medina, J. C.; Dumont, Y.; Quirion, R., A possible role of neuropeptide Y in depression and stress. *Brain Res.* **2010**, *1314*, 194-205.

(28) Ruscica, M.; Dozio, E.; Motta, M.; Magni, P., Role of neuropeptide Y and its receptors in the progression of endocrine-related cancer. *Peptides* **2007**, *28*, 426-434.

(29) Hansel, D. E.; Eipper, B. A.; Ronnett, G. V., Neuropeptide Y functions as a neuroproliferative factor. *Nature* **2001**, *410*, 940-944.

(30) Kitlinska, J., Neuropeptide Y (NPY) in neuroblastoma: effect on growth and vascularization. *Peptides* **2007**, *28*, 405-412.

(31) Kitlinska, J., Neuropeptide Y in neural crest-derived tumors: effect on growth and vascularization. *Cancer Lett.* **2007**, *245*, 293-302.

(32) Kitlinska, J.; Abe, K.; Kuo, L.; Pons, J.; Yu, M.; Li, L.; Tilan, J.; Everhart, L.; Lee, E. W.; Zukowska, Z.; Toretsky, J. A., Differential effects of neuropeptide Y on the growth and vascularization of neural crest–derived tumors. *Cancer Res.* **2005**, *65*, 1719-1728.

(33) Reichmann, F.; Holzer, P., Neuropeptide Y: a stressful review. *Neuropeptides* **2016**, *55*, 99-109.

(34) Kloster, E.; Saft, C.; Akkad, D. A.; Epplen, J. T.; Arning, L., Association of age at onset in Huntington disease with functional promoter variations in NPY and NPY_2R. *J. Mol. Med.* **2014**, *92*, 177-184.

(35) Wahlestedt, C.; Yanaihara, N.; Håkanson, R., Evidence for different pre- and post-junctional receptors for neuropeptide Y and related peptides. *Regul. Pept.* **1986**, *13*, 307-318.

(36) Allen, J.; Novotny, J.; Martin, J.; Heinrich, G., Molecular structure of mammalian neuropeptide Y: analysis by molecular cloning and computer-aided comparison with crystal structure of avian homologue. *Proc. Natl. Acad. Sci. U.S.A.* **1987**, *84*, 2532-2536.

(37) Darbon, H.; Bernassau, J. M.; Deleuze, C.; Chenu, J.; Roussel, A.; Cambillau, C., Solution conformation of human neuropeptide Y by ^{1}H nuclear magnetic resonance and restrained molecular dynamics. *Eur. J. Biochem.* **1992**, *209*, 765-771.

(38) Boulanger, Y.; Chen, Y.; Commodari, F.; Senecal, L.; Laberge, A. M.; Fournier, A.; St-Pierre, S., Structural characterizations of neuropeptide tyrosine (NPY) and its agonist analog [Ahx^{5-17}]NPY by NMR and molecular modeling. *Int. J. Pept. Protein. Res.* **1995**, *45*, 86-95.

(39) Bettio, A.; Dinger, M. C.; Beck-Sickinger, A. G., The neuropeptide Y monomer in solution is not folded in the pancreatic-polypeptide fold. *Protein Sci.* **2002**, *11*, 1834-1844.

(40) Cowley, D. J.; Hoflack, J. M.; Pelton, J. T.; Saudek, V., Structure of neuropeptide Y dimer in solution. *Eur. J. Biochem.* **1992**, *205*, 1099-1106.

(41) Monks, S.; Karagianis, G.; Howlett, G.; Norton, R., Solution structure of human neuropeptide Y. *J. Biomol. NMR* **1996**, *8*, 379-390.

(42) Saudek, V.; Pelton, J. T., Sequence-specific proton NMR assignment and secondary structure of neuropeptide Y in aqueous solution. *Biochemistry* **2002**, *29*, 4509-4515.

(43) Lerch, M.; Gafner, V.; Bader, R.; Christen, B.; Folkers, G.; Zerbe, O., Bovine pancreatic polypeptide (bPP) undergoes significant changes in conformation and dynamics upon binding to DPC micelles. *J. Mol. Biol.* **2002**, *322*, 1117-1133.

(44) Nordmann, A.; Blommers, M. J.; Fretz, H.; Arvinte, T.; Drake, A. F., Aspects of the molecular structure and dynamics of neuropeptide Y. *Eur. J. Biochem.* **1999**, *261*, 216-226.

(45) Keire, D. A.; Kobayashi, M.; Solomon, T. E.; Reeve, J. R., Jr., Solution structure of monomeric peptide YY supports the functional significance of the PP-fold. *Biochemistry* **2000**, *39*, 9935-9942.

(46) Sundström, G.; Larsson, T. A.; Xu, B.; Heldin, J.; Larhammar, D., Interactions of zebrafish peptide YYb with the neuropeptide Y-family receptors Y_4, Y_7, Y_{8a}, and Y_{8b}. *Front. Neurosci.* **2013**, *7*, 19-26.

(47) Larhammar, D.; Blomqvist, A. G.; Yee, F.; Jazin, E.; Yoo, H.; Wahlested, C., Cloning and functional expression of a human neuropeptide Y/peptide YY receptor of the Y_1 type. *J. Biol. Chem.* **1992**, *267*, 10935-10938.

(48) Herzog, H.; Hort, Y. J.; Ball, H. J.; Hayes, G.; Shine, J.; Selbie, L. A., Cloned human neuropeptide Y receptor couples to two different second messenger systems. *Proc. Natl. Acad. Sci. U. S. A.* **1992**, *89*, 5794-5798.

(49) Gerald, C.; Walker, M. W.; Vaysse, P. J.; He, C.; Branchek, T. A.; Weinshank, R. L., Expression cloning and pharmacological characterization of a human hippocampal neuropeptide Y/peptide YY Y_2 receptor subtype. *J. Biol. Chem.* **1995**, *270*, 26758-26761.

(50) Bard, J. A.; Walker, M. W.; Branchek, T. A.; Weinshank, R. L., Cloning and functional expression of a human Y_4 subtype receptor for pancreatic polypeptide, neuropeptide Y, and peptide YY. *J. Biol. Chem.* **1995**, *270*, 26762-26765.

(51) Lundell, I.; Blomqvist, A. G.; Berglund, M. M.; Schober, D. A.; Johnson, D.; Statnick, M. A.; Gadski, R. A.; Gehlert, D. R.; Larhammar, D., Cloning of a human receptor of the NPY receptor family with high affinity for pancreatic polypeptide and peptide YY. *J. Biol. Chem.* **1995**, *270*, 29123-29128.

(52) Gerald, C.; Walker, M. W.; Criscione, L.; Gustafson, E. L.; Batzl-Hartmann, C.; Smith, K. E.; Vaysse, P.; Durkin, M. M.; Laz, T. M.; Linemeyer, D. L.; Schaffhauser, A. O.; Whitebread, S.; Hofbauer, K. G.; Taber, R. I.; Branchek, T. A.; Weinshank, R. L., A receptor subtype involved in neuropeptide-Y-induced food intake. *Nature* **1996**, *382*, 168-171.

(53) Weinberg, D. H.; Sirinathsinghji, D. J.; Tan, C. P.; Shiao, L. L.; Morin, N.; Rigby, M. R.; Heavens, R. H.; Rapoport, D. R.; Bayne, M. L.; Cascieri, M. A.; Strader, C. D.; Linemeyer, D. L.; MacNeil, D. J., Cloning and expression of a novel neuropeptide Y receptor. *J. Biol. Chem.* **1996**, *271*, 16435-16438.

(54) Gregor, P.; Feng, Y.; DeCarr, L. B.; Cornfield, L. J.; McCaleb, M. L., Molecular characterization of a second mouse pancreatic polypeptide receptor and its inactivated human homologue. *J. Biol. Chem.* **1996**, *271*, 27776-27781.

(55) Matsumoto, M.; Nomura, T.; Momose, K.; Ikeda, Y.; Kondou, Y.; Akiho, H.; Togami, J.; Kimura, Y.; Okada, M.; Yamaguchi, T., Inactivation of a novel neuropeptide Y/peptide YY receptor gene in primate species. *J. Biol. Chem.* **1996**, *271*, 27217-27220.

(56) Starback, P.; Wraith, A.; Eriksson, H.; Larhammar, D., Neuropeptide Y receptor gene Y_6: multiple deaths or resurrections? *Biochem. Biophys. Res. Commun.* **2000**, *277*, 264-269.

(57) Alexander, S. P. H.; Benson, H. E.; Faccenda, E.; Pawson, A. J.; Sharman, J. L.; Spedding, M.; Peters, J. A.; Harmar, A. J., The concise guide to PHARMACOLOGY 2013/14: G protein-coupled receptors. *Br. J. Pharmacol.* **2013**, *170*, 1459-1581.

(58) Holliday, N. D.; Michel, M. C.; Cox, H. M., NPY receptor subtypes and theier signal transduction. *Neurop. Y Rel. Pept.* **2004**; Vol. 162, 45-73.

(59) Michel, M. C.; Beck-Sickinger, A.; Cox, H.; Doods, H. N.; Herzog, H.; Larhammar, D.; Quirion, R.; Schwartz, T.; Westfall, T., XVI. International union of pharmacology recommendations for the nomenclature of neuropeptide Y, peptide YY, and pancreatic polypeptide receptors. *Pharmacol. Rev.* **1998**, *50*, 143-150.

(60) Grouzmann, E.; Meyer, C.; Burki, E.; Brunner, H., Neuropeptide Y Y_2 receptor signalling mechanisms in the human glioblastoma cell line LN319. *Peptides* **2001**, *22*, 379-386.

(61) Selbie, L. A.; Darby, K.; Schmitz-Peiffer, C.; Browne, C. L.; Herzog, H.; Shine, J.; Biden, T. J., Synergistic interaction of Y_1-neuropeptide Y and alpha 1b-adrenergic receptors in the regulation of phospholipase C, protein kinase C, and arachidonic acid production. *J. Biol. Chem.* **1995**, *270*, 11789-11796.

(62) Criscione, L.; Rigollier, P.; Batzl-Hartmann, C.; Rueger, H.; Stricker-Krongrad, A.; Wyss, P.; Brunner, L.; Whitebread, S.; Yamaguchi, Y.; Gerald, C.; Heurich, R. O.; Walker, M. W.; Chiesi, M.; Schilling, W.; Hofbauer, K. G.; Levens, N., Food intake in free-feeding and energy-deprived lean rats is mediated by the neuropeptide Y_5 receptor. *J. Clin. Invest.* **1998**, *102*, 2136-2145.

(63) Motulsky, H. J.; Michel, M. C., Neuropeptide Y mobilizes Ca^{2+} and inhibits adenylate cyclase in human erythroleukemia cells. *Am. J. Physiol.* **1988**, *255*, 880-885.

(64) Aakerlund, L.; Gether, U.; Fuhlendorff, J.; Schwartz, T. W.; Thastrup, O., Y_1 receptors for neuropeptide Y are coupled to mobilization of intracellular calcium and inhibition of adenylate cyclase. *FEBS Lett.* **1990**, *260*, 73-78.

(65) Kask, A.; Harro, J.; von Hörsten, S.; Redrobe, J. P.; Dumont, Y.; Quirion, R., The neurocircuitry and receptor subtypes mediating anxiolytic-like effects of neuropeptide Y. *Neurosci. Biobehav. Rev.* **2002**, *26*, 259-283.

(66) Kopp, J.; Xu, Z. Q.; Zhang, X.; Pedrazzini, T.; Herzog, H.; Kresse, A.; Wong, H.; Walsh, J. H.; Hökfelt, T., Expression of the neuropeptide Y Y_1 receptor in the CNS of rat and of wild-type and Y_1 receptor knock-out mice. Focus on immunohistochemical localization. *Neuroscience* **2002**, *111*, 443-532.

(67) Eva, C.; Serra, M.; Mele, P.; Panzica, G.; Oberto, A., Physiology and gene regulation of the brain NPY Y_1 receptor. *Front. Neuroendocrinol.* **2006**, *27*, 308-339.

(68) Dumont, Y.; Jacques, D.; Bouchard, P.; Quirion, R., Species differences in the expression and distribution of the neuropeptide Y Y_1, Y_2, Y_4, and Y_5 receptors in rodents, guinea pig, and primates brains. *J. Comp. Neurol.* **1998**, *402*, 372-384.

(69) Loos, R. J. F., Recent progress in the genetics of common obesity. *Br. J. Clin. Pharmacol.* **2009**, *68*, 811-829.

(70) Allison, D. B.; Lindgren, C. M.; Heid, I. M.; Randall, J. C.; Lamina, C.; Steinthorsdottir, V.; Qi, L.; Speliotes, E. K.; Thorleifsson, G.; Willer, C. J., Genome-wide association scan meta-analysis identifies three loci influencing adiposity and fat distribution. *PLoS Genet.* **2009**, *5*, e1000508.

(71) Wang, K.; Li, W. D.; Glessner, J. T.; Grant, S. F. A.; Hakonarson, H.; Price, R. A., Large copy-number variations are enriched in cases with moderate to extreme obesity. *Diabetes* **2010**, *59*, 2690-2694.

(72) Sebat, J., Large-scale copy number polymorphism in the human genome. *Science* **2004**, *305*, 525-528.

(73) Sudmant, P. H.; Kitzman, J. O.; Antonacci, F.; Alkan, C.; Malig, M.; Tsalenko, A.; Sampas, N.; Bruhn, L.; Shendure, J.; Eichler, E. E., Diversity of human copy number variation and multicopy genes. *Science* **2010**, *330*, 641-646.

(74) Kobilka, B., The structural basis of G-protein-coupled receptor signaling (Nobel Lecture). *Angew. Chem., Int. Ed.* **2013**, *52*, 6380-6388.

(75) Lefkowitz, R. J., A brief history of G-protein coupled receptors (Nobel Lecture). *Angew. Chem., Int. Ed.* **2013**, *52*, 6366-6378.

(76) Yang, Z.; Han, S.; Keller, M.; Kaiser, A.; Bender, B. J.; Bosse, M.; Burkert, K.; Kögler, L. M.; Wifling, D.; Bernhardt, G.; Plank, N.; Littmann, T.; Schmidt, P.; Yi, C.; Li, B.; Ye, S.; Zhang, R.; Xu, B.; Larhammar, D.; Stevens, R. C.; Huster, D.; Meiler, J.; Zhao, Q.; Beck-Sickinger, A. G.; Buschauer, A.; Wu, B., Structural basis of ligand binding modes at the neuropeptide Y Y_1 receptor. *Nature* **2018**, *556*, 520–524.

(77) Merten, N.; Lindner, D.; Rabe, N.; Römpler, H.; Mörl, K.; Schöneberg, T.; Beck-Sickinger, A. G., Receptor subtype-specific docking of $Asp^{6.59}$ with C-terminal arginine residues in Y receptor ligands. *J. Biol. Chem.* **2007**, *282*, 7543-7551.

(78) Xu, B.; Fällmar, H.; Boukharta, L.; Pruner, J.; Lundell, I.; Mohell, N.; Gutiérrez-de-Terán, H.; Åqvist, J.; Larhammar, D., Mutagenesis and computational modeling of human G-

protein-coupled receptor Y_2 for neuropeptide Y and peptide YY. *Biochemistry* **2013**, *52*, 7987-7998.

(79) Kaiser, A.; Muller, P.; Zellmann, T.; Scheidt, H. A.; Thomas, L.; Bosse, M.; Meier, R.; Meiler, J.; Huster, D.; Beck-Sickinger, A. G.; Schmidt, P., Unwinding of the C-terminal residues of neuropeptide Y is critical for Y_2 receptor binding and activation. *Angew. Chem. Int. Ed. Engl.* **2015**, *54*, 7446-7449.

(80) Pedragosa-Badia, X.; Sliwoski, G. R.; Dong Nguyen, E.; Lindner, D.; Stichel, J.; Kaufmann, K. W.; Meiler, J.; Beck-Sickinger, A. G., Pancreatic polypeptide is recognized by two hydrophobic domains of the human Y_4 receptor binding pocket. *J. Biol. Chem.* **2014**, *289*, 5846-5859.

(81) Fuhlendorff, J.; Gether, U.; Aakerlund, L.; Langeland-Johansen, N.; Thogersen, H.; Melberg, S. G.; Olsen, U. B.; Thastrup, O.; Schwartz, T. W., [Leu^{31}, Pro^{34}]neuropeptide Y: a specific Y_1 receptor agonist. *Proc. Natl. Acad. Sci. U. S. A.* **1990**, *87*, 182-186.

(82) Mullins, D.; Kirby, D.; Hwa, J.; Guzzi, M.; Rivier, J.; Parker, E., Identification of potent and selective neuropeptide Y Y_1 receptor agonists with orexigenic activity in vivo. *Mol. Pharmacol.* **2001**, *60*, 534-540.

(83) Pedragosa-Badia, X.; Stichel, J.; Beck-Sickinger, A. G., Neuropeptide Y receptors: how to get subtype selectivity. *Front. Endocrinol.* **2013**, *4*, 12-16.

(84) Beck-Sickinger, A. G.; Wieland, H. A.; Wittneben, H.; Willim, K. D.; Rudolf, K.; Jung, G., Complete L-alanine scan of neuropeptide Y reveals ligands binding to Y_1 and Y_2 receptors with distinguished conformations. *Eur. J. Biochem.* **1994**, *225*, 947-58.

(85) Rudolf, K.; Eberlein, W.; Engel, W.; Wieland, H. A.; Willim, K. D.; Entzeroth, M.; Wienen, W.; Beck-Sickinger, A. G.; Doods, H. N., The first highly potent and selective non-peptide neuropeptide Y Y_1 receptor antagonist: BIBP3226. *Eur. J. Pharmacol.* **1994**, *271*, 11-30.

(86) Wieland, H. A.; Willim, K. D.; Entzeroth, M.; Wienen, W.; Rudolf, K.; Eberlein, W.; Engel, W.; Doods, H. N., Subtype selectivity and antagonistic profile of the nonpeptide Y1 receptor antagonist BIBP 3226. *The Journal of pharmacology and experimental therapeutics* **1995**, *275*, 143-149.

(87) Wieland, H. A.; Engel, W.; Eberlein, W.; Rudolf, K.; Doods, H. N., Subtype selectivity of the novel nonpeptide neuropeptide Y Y_1 receptor antagonist BIBO 3304 and its effect on feeding in rodents. *Br. J. Pharmacol.* **1998**, *125*, 549-555.

(88) Keller, M.; Weiss, S.; Hutzler, C.; Kuhn, K. K.; Mollereau, C.; Dukorn, S.; Schindler, L.; Bernhardt, G.; König, B.; Buschauer, A., N^{ω}-Carbamoylation of the argininamide moiety: an avenue to insurmountable NPY Y_1 receptor antagonists and a radiolabeled selective high-affinity molecular tool ([^{3}H]UR-MK299) with extended residence time. *J. Med. Chem.* **2015**, *58*, 8834-8849.

(89) Gehlert, D. R.; Beavers, L. S.; Johnson, D.; Gackenheimer, S. L.; Schober, D. A.; Gadski, R. A., Expression cloning of a human brain neuropeptide Y Y_2 receptor. *Mol. Pharmacol.* **1996**, *49*, 224-228.

(90) Potter, E. K.; Fuhlendorff, J.; Schwartz, T. W., [Pro^{34}]neuropeptide Y selectively identifies postjunctional-mediated actions of neuropeptide Y in vivo in rats and dogs. *Eur. J. Pharmacol.* **1991**, *193*, 15-19.

(91) Doods, H.; Gaida, W.; Wieland, H. A.; Dollinger, H.; Schnorrenberg, G.; Esser, F.; Engel, W.; Eberlein, W.; Rudolf, K., BIIE0246: a selective and high affinity neuropeptide Y Y_2 receptor antagonist. *Eur. J. Pharmacol.* **1999**, *384*, 3-5.

(92) Shoblock, J. R.; Welty, N.; Nepomuceno, D.; Lord, B.; Aluisio, L.; Fraser, I.; Motley, S. T.; Sutton, S. W.; Morton, K.; Galici, R.; Atack, J. R.; Dvorak, L.; Swanson, D. M.; Carruthers, N. I.; Dvorak, C.; Lovenberg, T. W.; Bonaventure, P., In vitro and in vivo characterization of JNJ-31020028 (N-(4-{4-[2-(diethylamino)-2-oxo-1-phenylethyl]piperazin-1-yl}-3-fluorophenyl)-2- pyridin-3-ylbenzamide), a selective brain penetrant small molecule antagonist of the neuropeptide Y Y_2 receptor. *Psychopharmacologia* **2010**, *208*, 265-277.

(93) Balasubramaniam, A.; Sheriff, S.; Johnson, M. E.; Prabhakaran, M.; Huang, Y.; Fischer, J. E.; Chance, W. T., [D-Trp^{32}]neuropeptide Y: a competitive antagonist of NPY in rat hypothalamus. *J. Med. Chem.* **1994**, *37*, 811-815.

(94) Cabrele, C.; Wieland, H. A.; Koglin, N.; Stidsen, C.; Beck-Sickinger, A. G., Ala^{31}-Aib^{32}: identification of the key motif for high affinity and selectivity of neuropeptide Y at the Y_5-receptor. *Biochemistry* **2002**, *41*, 8043-8049.

(95) Erondu, N.; Gantz, I.; Musser, B.; Suryawanshi, S.; Mallick, M.; Addy, C.; Cote, J.; Bray, G.; Fujioka, K.; Bays, H.; Hollander, P.; Sanabria-Bohorquez, S. M.; Eng, W.; Langstrom, B.; Hargreaves, R. J.; Burns, H. D.; Kanatani, A.; Fukami, T.; MacNeil, D. J.; Gottesdiener, K. M.; Amatruda, J. M.; Kaufman, K. D.; Heymsfield, S. B., Neuropeptide Y_5 receptor antagonism does not induce clinically meaningful weight loss in overweight and obese adults. *Cell Metab.* **2006**, *4*, 275-282.

(96) Parker, E. M.; Babij, C. K.; Balasubramaniam, A.; Burrier, R. E.; Guzzi, M.; Hamud, F.; Mukhopadhyay, G.; Rudinski, M. S.; Tao, Z.; Tice, M.; Xia, L.; Mullins, D. E.; Salisbury, B. G., GR231118 (1229U91) and other analogues of the C-terminus of neuropeptide Y are potent neuropeptide Y Y_1 receptor antagonists and neuropeptide Y Y_4 receptor agonists. *Eur. J. Pharmacol.* **1998**, *349*, 97-105.

(97) Balasubramaniam, A.; Mullins, D. E.; Lin, S.; Zhai, W.; Tao, Z.; Dhawan, V. C.; Guzzi, M.; Knittel, J. J.; Slack, K.; Herzog, H.; Parker, E. M., Neuropeptide Y (NPY) Y_4 receptor selective agonists based on NPY(32−36): development of an anorectic Y_4 receptor selective agonist with oicomolar affinity. *J. Med. Chem.* **2006**, *49*, 2661-2665.

(98) Li, J. B.; Asakawa, A.; Terashi, M.; Cheng, K.; Chaolu, H.; Zoshiki, T.; Ushikai, M.; Sheriff, S.; Balasubramaniam, A.; Inui, A., Regulatory effects of Y_4 receptor agonist (BVD-74D) on food intake. *Peptides* **2010**, *31*, 1706-1710.

(99) Kuhn, K. K.; Ertl, T.; Dukorn, S.; Keller, M.; Bernhardt, G.; Reiser, O.; Buschauer, A., High affinity agonists of the neuropeptide Y (NPY) Y_4 receptor derived from the C-terminal pentapeptide of human pancreatic polypeptide (hPP): synthesis, stereochemical discrimination, and radiolabeling. *J. Med. Chem.* **2016**, *59*, 6045-6058.

(100) Kuhn, K. K.; Littmann, T.; Dukorn, S.; Tanaka, M.; Keller, M.; Ozawa, T.; Bernhardt, G.; Buschauer, A., In search of NPY Y_4R antagonists: incorporation of carbamoylated arginine, aza-amino acids, or D-amino acids into oligopeptides derived from the C-termini of the endogenous agonists. *ACS Omega* **2017**, *2*, 3616-3631.

(101) Keller, M.; Kaske, M.; Holzammer, T.; Bernhardt, G.; Buschauer, A., Dimeric argininamide-type neuropeptide Y receptor antagonists: chiral discrimination between Y_1 and Y_4 receptors. *Bioorg. Med. Chem.* **2013**, *21*, 6303-6322.

(102) Thal, D. M.; Glukhova, A.; Sexton, P. M.; Christopoulos, A., Structural insights into G-protein-coupled receptor allostery. *Nature* **2018**, *559*, 45-53.

(103) Liu, X.; Masoudi, A.; Kahsai, A. W.; Huang, L.-Y.; Pani, B.; Staus, D. P.; Shim, P. J.; Hirata, K.; Simhal, R. K.; Schwalb, A. M.; Rambarat, P. K.; Ahn, S.; Lefkowitz, R. J.; Kobilka, B., Mechanism of β_2AR regulation by an intracellular positive allosteric modulator. *Science* **2019**, *364*, 1283-1287.

(104) Sliwoski, G.; Schubert, M.; Stichel, J.; Weaver, D.; Beck-Sickinger, A. G.; Meiler, J., Discovery of small-molecule modulators of the human Y_4 receptor. *PLoS One* **2016**, *11*, e0157146.

(105) Schubert, M.; Stichel, J.; Du, Y.; Tough, I. R.; Sliwoski, G.; Meiler, J.; Cox, H. M.; Weaver, C. D.; Beck-Sickinger, A. G., Identification and characterization of the first selective Y_4 receptor positive allosteric modulator. *J. Med. Chem.* **2017**, *60*, 7605-7612.

(106) Ewing, W. R.; Zhu, Y.; Sun, C.; Huang, Y.; Karatholuvhu, M. S.; Bolton, S. A.; Pasunoori, L.; Mandal, S. K.; Sher, P. M. Diaminocyclohexane compounds as NPY Y_4 receptor modulator and their preparation. 20120716., **2013**.

(107) Thieme, V.; Jolly, N.; Madsen, A. N.; Bellmann-Sickert, K.; Schwartz, T. W.; Holst, B.; Cox, H. M.; Beck-Sickinger, A. G., High molecular weight PEGylation of human pancreatic polypeptide at position 22 improves stability and reduces food intake in mice. *Br. J. Pharmacol.* **2016**, *173*, 3208-3221.

(108) Zorzi, A.; Deyle, K.; Heinis, C., Cyclic peptide therapeutics: past, present and future. *Curr. Opin. Chem. Biol.* **2017**, *38*, 24-29.

(109) Abdalla, M.; McGaw, L., Natural cyclic peptides as an attractive modality for therapeutics: a mini review. *Molecules* **2018**, *23*, 2080-2088.

(110) Keller, M.; Kuhn, K. K.; Einsiedel, J.; Hübner, H.; Biselli, S.; Mollereau, C.; Wifling, D.; Svobodová, J.; Bernhardt, G.; Cabrele, C.; Vanderheyden, P. M. L.; Gmeiner, P.; Buschauer, A., Mimicking of arginine by functionalized N^{ω}-carbamoylated arginine as a new broadly applicable approach to labeled bioactive peptides: high affinity angiotensin, Neuropeptide Y, neuropeptide FF, and neurotensin receptor ligands as examples. *J. Med. Chem.* **2016**, *59*, 1925-1945.

Chapter 2

Oligopeptides as Neuropeptide Y Y_4 Receptor Ligands: Identification of a High-Affinity Tetrapeptide Agonist and a Hexapeptide Antagonist

Note: This chapter was published prior to submission of this thesis.

Konieczny, A.; Braun, D.; Wifling, D.; Bernhardt, G.; Keller, M. Oligopeptides as Neuropeptide Y Y_4 Receptor Ligands: Identification of a High-Affinity Tetrapeptide Agonist and a Hexapeptide Antagonist. *J. Med. Chem*. **2020**, 63, 8198-8215.

The following experiments were performed by co-authors:

D.B.: Synthesis and pharmacological characterization of **2.31**-**2.35**.
D.W.: Induced-fit docking of **2.1**, **2.13** and **2.29** to the hY_4R homology models.

2.1 Introduction

Neuropeptide Y receptors (YRs) are class A (rhodopsin-like) G-protein-coupled receptors (GPCRs), involved in the regulation of numerous central and peripheral biological processes. YRs are stimulated by the highly homologous peptides neuropeptide Y (NPY), peptide YY (PYY) and pancreatic polypeptide (PP), each consisting of 36 amino acids.[1,2] Y_4R is unique in the YR family because of its preferential binding of PP (for a primary structure, see Figure 1) compared to the other subtypes (in human: Y_1R, Y_2R and Y_5R), which are favoring the endogenous agonists NPY and PYY.[3,4] Stimulation of Y_4R mediates a reduction in food intake and increases gastrointestinal motility, therefore, Y_4R agonists are considered as potential antiobesity agents.[5-7] Moreover, studies with Y_4R knockout mice suggested Y_4R as a potential target for the treatment of depression.[8,9] Although several peptidic Y_4R agonists, representing mimics of the C-terminal fragment of hPP (⋯Leu^{31}-Thr^{32}-Arg^{33}-Pro^{34}-Arg^{35}-Tyr^{36}-NH_2), which is crucial for Y_4R binding,[10] are available (e.g. compounds **2.1**-**2.6**, Figure 1),[11-13] only few Y_4R antagonists were reported. For example, compound **2.7** (Figure 1),[14] a dimer of the argininamide-type Y_1R antagonist BIBP3226[15] and analogues of the dimeric peptides **2.3** and **2.4**, containing aza-amino acids (structures not shown),[11] were described as Y_4R antagonists exhibiting high to moderate Y_4R affinity (K_i = 30-134 nM). However, a low-molecular-weight, selective Y_4R antagonist, which could serve as a molecular tool to study the physiological role of Y_4R, is missing to date.

Covalent dimerization of pentapeptide **2.2**, mimicking the C-terminus of hPP,[16] via suberyl linkers, afforded Y_4R partial agonists containing four arginine residues (e.g. compounds **2.3**-**2.5**, see Figure 1). These dimeric peptides showed increased Y_4R affinity compared to **2.2**.[12] Prompted by this finding, the linear hexapeptide **2.1** (UR-KK236), representing the N-terminally arginylated congener of pentapeptide **2.2**, was recently prepared to explore the importance of a third basic amino acid in small peptides, mimicking the C-terminus of hPP.[11] Interestingly, compound **2.1** exhibited considerably higher Y_4R affinity compared to **2.2** (K_i (hY_4R): 3.4 *vs*. 337 nM).[11]

A tritiated analogue of peptide **2.5**, bearing a propionyl residue at the linker moiety, was described as a molecular tool to determine Y_4R affinities.[12] Notably, replacement of the suberyl linker in **2.3** by rigid photochromic scaffolds was well tolerated with respect to Y_4R binding. This approach gave photochromic Y_4R partial agonists with high Y_4R affinity, supporting the hypothesis that the orthosteric binding pocket of Y_4R is occupied by only one of the pentapeptide sequences.[17]

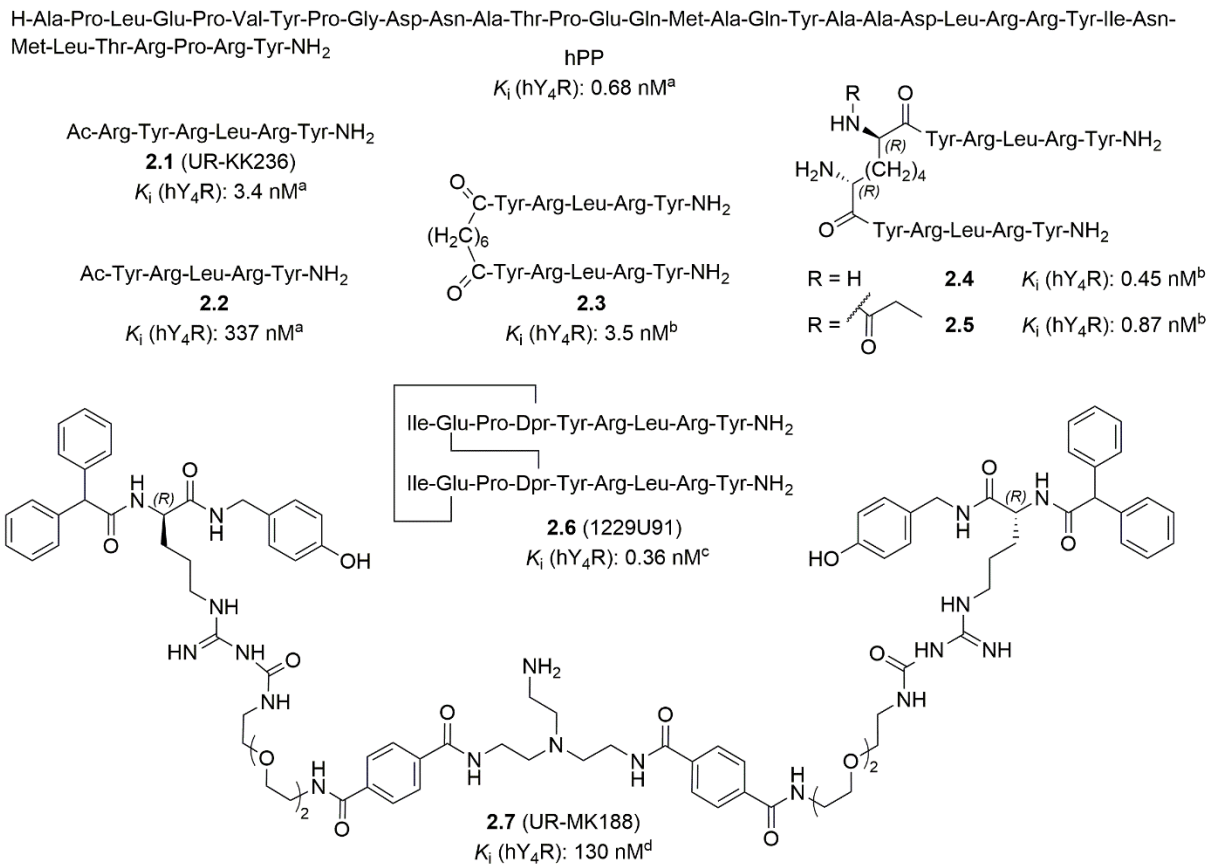

Figure 1. Structures and reported Y_4R affinities of hPP, the Y_4R (partial) agonists **2.1**-**2.6** and the nonpeptide Y_4R antagonist **2.7**. [a]Kuhn *et al*.[11] [b]Kuhn *et al*.[12] [c]Daniels *et al*.[13] [d]Keller *et al*.[14]

Here we describe the synthesis and pharmacological characterization of analogues of hexapeptide **2.1** (cf. Figure 1) reported to be a partial Y_4R agonist with high affinity and pronounced Y_4R selectivity.[11] Compared to the C-terminal sequence of hPP, compound **2.1** contains Leu instead of Pro^{34}, Tyr instead of Thr^{32} and Arg instead of Leu^{31} (see Figure 1). In order to gain more insights into the relevance of individual amino acids and the N-terminus in **2.1** for Y_4R binding and activation, we replaced, for example, Leu by Trp or Pro, inserted various spacers between the N-terminal arginine and the adjacent Tyr, replaced Arg by its nonbasic congener citrulline and prepared analogues with a free (nonacetylated) N-terminus (Figure 2). Moreover, various linear tetrapeptides were prepared, representing N-terminally truncated derivatives of **2.1**. All peptides were characterized with respect to Y_4R affinity by radioligand competition binding, as well as in terms of Y_4R agonism or antagonism in β-arrestin 1 and 2 recruitment assays and in a Ca^{2+}-aequorin assay, measuring G-protein-mediated transient increase in cytosolic Ca^{2+}.

2.2 Results and Discussion

2.2.1 Chemistry

The peptides were prepared on Sieber amide resins by manual solid-phase peptide synthesis (SPPS) according to the Fmoc strategy, applying repeated (double) coupling steps with HBTU/HOBt/*N*,*N*-diisopropylethylamine (DIPEA) as coupling reagents (Scheme 1). N-terminal acetylation (**2.9**, **2.12**, **2.15**, **2.17**-**2.19**, **2.21** and **2.23**-**2.28**) and N-terminal succinylation (**2.20**) were performed by treatment of the Fmoc-deprotected, resin-bound peptide with acetic anhydride and succinic anhydride, respectively. The N-terminally methylated tetrapeptide **2.35** was obtained using Fmoc-NMe-Arg(Pbf)-OH as a building block, which was coupled as an N-terminal amino acid (Scheme 1). Peptides were cleaved from the resin using trifluoroacetic acid (TFA)/CH_2Cl_2 1:3 v/v (two times 20 min at rt), followed by treatment with TFA/H_2O 95:5 v/v to achieve complete side-chain deprotection (Scheme 1).

Scheme 1. Synthesis of the oligopeptides **2.8**-**2.35**.

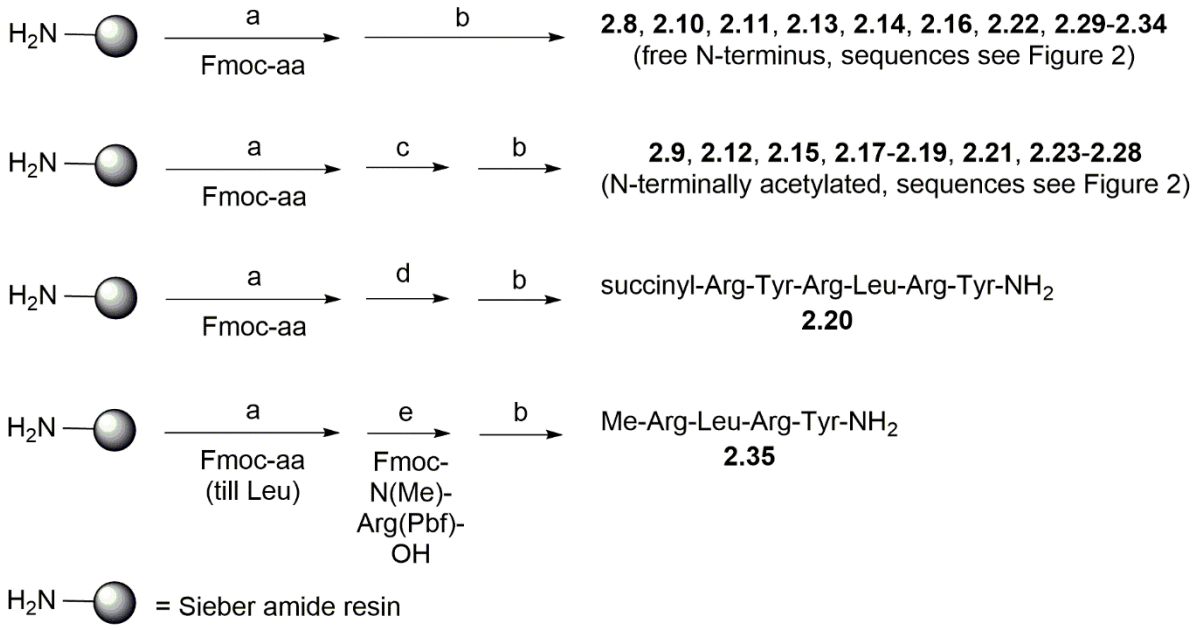

Reagents and conditions: (a) peptide elongation, amino acid coupling: Fmoc-amino acid/HOBt/HBTU/DIPEA (5/5/4.9/10 equiv.), DMF/NMP (8:2), 35 °C, 2 × 45 min ("double" coupling); Fmoc deprotection: 20% piperidine in DMF/NMP (8:2), rt, 2 × 10 min; (b) (1) TFA/CH_2Cl_2 (1:3), rt, 2 × 20 min; (2) TFA/H_2O (95:5), rt, 5 h; (c) acetic anhydride/DIPEA (10/10 equiv.), DMF/NMP (8:2), 35 °C, 45 min; (d) succinic anhydride/DIPEA (10/10 equiv.), DMF/NMP (8:2), 35 °C, 45 min; (e) Fmoc-N(Me)-Arg(Pbf)-OH/HOBt/HBTU/DIPEA (5/5/4.9/10 equiv.), DMF/NMP (8:2), 35 °C, 24 h (single coupling); for overall yields of peptide syntheses, see experimental section.

2.1 (UR-KK236)	Ac-Arg-Tyr-Arg-Leu-Arg-Tyr-NH_2		
2.8	Arg-Tyr-Arg-Leu-Arg-Tyr-NH_2	**2.22**	Trp-Arg-Leu-Arg-Tyr-NH_2
2.9	Ac-Arg-Tyr-Arg-Pro-Arg-Tyr-NH_2	**2.23**	Ac-Arg-Gly-Tyr-Arg-Leu-Arg-Tyr-NH_2
2.10	Arg-Tyr-Arg-Gly-Arg-Tyr-NH_2	**2.24**	Ac-Arg-GABA-Gly-Tyr-Arg-Leu-Arg-Tyr-NH_2
2.11	Arg-Tyr-Arg-Ala-Arg-Tyr-NH_2	**2.25**	Ac-Arg-Gly-Tyr-Arg-Trp-Arg-Tyr-NH_2
2.12	Ac-Arg-Tyr-Arg-Trp-Arg-Tyr-NH_2	**2.26**	Ac-Arg-Gly-Tyr-Arg-Trp-Arg-Trp-NH_2
2.13 (UR-AK1)	Arg-Tyr-Arg-Trp-Arg-Tyr-NH_2	**2.27**	Ac-Arg-Gly-Tyr-Arg-Leu-Arg-Trp-NH_2
2.14	Cit-Tyr-Arg-Leu-Arg-Tyr-NH_2	**2.28**	Ac-Arg-GABA-Tyr-Arg-Trp-Arg-Tyr-NH_2
2.15	Ac-Arg-Tyr-Cit-Leu-Arg-Tyr-NH_2	**2.29** (UR-AK32)	Arg-Leu-Arg-Tyr-NH_2
2.16	Arg-Tyr-Arg-Leu-Cit-Tyr-NH_2	**2.30**	Arg-Trp-Arg-Tyr-NH_2
2.17	Ac-Arg-Trp-Arg-Leu-Arg-Tyr-NH_2	**2.31**	*D*-Arg-Leu-Arg-Tyr-NH_2
2.18	Ac-Arg-Phe-Arg-Leu-Arg-Tyr-NH_2	**2.32**	Arg-*D*-Leu-Arg-Tyr-NH_2
2.19	Ac-Arg-Gly-Arg-Leu-Arg-Tyr-NH_2	**2.33**	Arg-Leu-*D*-Arg-Tyr-NH_2
2.20	Succinyl-Arg-Tyr-Arg-Leu-Arg-Tyr-NH_2	**2.34**	Arg-Leu-Arg-*D*-Tyr-NH_2
2.21	Ac-Arg-Arg-Leu-Arg-Tyr-NH_2	**2.35**	N(Me)Arg-Leu-Arg-Tyr-NH_2

Figure 2. Peptide sequences of the lead compound **2.1** and the synthesized analogues **2.8**-**2.35**. Amino acid replacements or insertions are highlighted in blue (compared to **2.1**) and red (compared to compound **2.29**).

2.2.2 NPY Receptor Binding

Y_4R affinities of the synthesized peptides were determined by radioligand competition binding at live CHO-hY_4R-G_{qi5}-mtAEQ cells[18] using the previously described radioligand [^{3}H]UR-KK200[12] (K_d (hY_4R): 0.68 nM; for structure, see Figure S1, Supporting Information). Radioligand displacement curves are shown in Figure S2 (Supporting Information) and the obtained pK_i values are summarized in Table 1. Removal of the acetyl group in **2.1**, resulting in compound **2.8** (Figure 2), did not affect the Y_4R affinity, suggesting a minor role of the N-terminus of **2.1** for Y_4R binding.

Leu in position 4 of **2.1** was replaced by Pro, which is also present in position 34 in hPP (cf. Figure 1), resulting in compound **2.9**, which displayed considerably lower Y_4R affinity compared to **2.1** (pK_i values of **2.1** and **2.9**: 8.43 and 5.75, respectively). This suggested that the hexapeptidic Y_4R ligands do not tolerate alterations (rigidization and reorientation) of the peptide backbone. Furthermore, Leu^4 in peptide **2.1** or in its equi-active, nonacetylated congener **2.8** was replaced by Gly (**2.10**), Ala (**2.11**), or the bulky aromatic amino acid Trp (**2.12**, **2.13**) to create a series of hexapeptides, bearing nonpolar amino acid residues of various sizes in position 4. Peptides **2.10**-**2.13** exhibited lower Y_4R affinity compared to **2.1** or **2.8** (approximately 1-2 orders of magnitude, see Table 1), showing that Leu^4 in **2.1** or **2.8** is crucial with respect to high Y_4R binding.

In order to explore the importance of the three basic arginine residues in **2.1**, a citrulline scan was performed with respect to these arginines, affording compounds **2.14**, **2.15** and **2.16** (cf. Figure 2).[19] Whereas replacement of Arg^1 by citrulline (**2.14**) did not affect the Y_4R affinity, incorporation of citrulline instead of Arg^3 (**2.15**) and Arg^5 (**2.16**) resulted in a decrease in Y_4R affinity by more than a factor of 10 (see Table 1). This suggested a minor relevance of the basic side chain of Arg^1 for Y_4R binding. However, as previously demonstrated,[11] omitting Arg^1 in **2.1** (compound **2.2**) leads to a considerable decrease in Y_4R affinity (see Figure 1). Concerning Arg^3 and Arg^5, the citrulline scan indicated that these two arginines are involved in key interactions with Y_4R.

Incorporation of Trp, Phe or Gly instead of Tyr^2 in **2.1** afforded congeners (**2.17**-**2.19**) with Y_4R binding constants comparable to that of **2.1** (Table 1), indicating that Tyr^2 in **2.1** plays a minor role for Y_4R binding. N-terminal succinylation instead of acetylation as in **2.1** (peptide **2.20**) and omittance of Tyr^2 in **2.1** (compound **2.21**) did not or only slightly affect Y_4R affinity, being consistent with the aforementioned minor importance of the N-terminus of **2.1** as well as with a minor role of Tyr^2 for Y_4R binding. Strikingly, replacement of the N-terminal Tyr in the previously reported pentapeptide **2.2** (cf. Figure 1) by Trp (peptide **2.22**) led to a considerable increase in Y_4R affinity (reported K_i of **2.2**: 337 nM,[11] pK_i of **2.22**: 8.79). However, an N-terminal extension of **2.22** by one arginine (compound **2.17**) did not lead to a further increase in Y_4R affinity.

As aforementioned, the N-terminal extension of pentapeptide **2.2** (K_i (hY_4R): 337 nM)[11] by one arginine, resulting in hexapeptide **2.1**, led to a considerable increase in Y_4R affinity (K_i: 3.4 nM). Therefore, in order to explore whether an increased distance of the N-terminal Arg in **2.1** to the residual pentapeptide sequence (corresponding to **2.2**) can lead to an even further increased Y_4R affinity, analogues of **2.1** were prepared, containing a glycine or a "GABA-glycine" spacer between Arg^1 and Tyr^2 (**2.23** and **2.24**, cf. Figure 2). Compounds **2.23** and **2.24** showed Y_4R affinities comparable to that of **2.1**. By contrast, insertion of Gly between Arg^1 and Trp^2 in **2.17**, yielding heptapeptide **2.25**, resulted in a more than 10-fold decrease in Y_4R affinity (Table 1). Replacement of the C-terminal tyrosinamide in **2.25** by tryptophanamide, giving heptapeptide **2.26**, resulted in a further decrease in Y_4R binding by approximately 1 order of magnitude. Likewise, replacement of the C-terminal tyrosinamide in **2.23** by tryptophanamide, affording heptapeptide **2.27**, led to a 10-fold decrease in Y_4R affinity. Insertion of GABA between Arg^1 and Tyr^2 in hexapeptide **2.12**, yielding peptide **2.28** (cf. Figure 2), resulted in almost unchanged Y_4R binding (Table 1).

As mentioned above, the N-terminal amino acids in the hexapeptide **2.1** (Arg^1, Tyr^2) seem to be less important for binding of **2.1** to Y_4R. Therefore, tetrapeptide **2.29** was prepared as an N-terminally truncated variant of **2.1**. Compound **2.29** exhibited high Y_4R affinity (pK_i: 8.47)

comparable to that of **2.1** (pK_i: 8.43). This supported the hypothesis that two basic arginine residues, most likely mimicking Arg^{33} and Arg^{35} of hPP (cf. Figure 1), both being crucial for Y_4R binding of hPP,[10] are sufficient in small peptides to achieve high Y_4R affinity. Replacement of Leu in **2.29** by Trp, resulting in **2.30**, caused a considerable decrease in Y_4R binding by two orders of magnitude. A D-amino acid scan applied to tetrapeptide **2.29**, giving peptides **2.31-2.34** (cf. Figure 2), showed that inversion of the stereochemistry of the N-terminal Arg in **2.29** (compound **2.31**) was well tolerated (pK_i (Y_4R) of **2.31**: 8.13). By contrast, in the case of all other amino acids in **2.29**, the inversion of the configuration resulted in a considerably lower Y_4R affinity (tetrapeptides **2.32-2.34**). Finally, N^{α}-methylation of the N-terminal Arg in **2.29** led to a congener (**2.35**), which exhibited the same Y_4R affinity as **2.29** (Table 1).

Table 1. Y_4R binding data of hPP, **2.1** and compounds **2.8**-**2.35**, as well as Y_1, Y_2 and Y_5 receptor binding data of selected compounds.

cmpd.	Y receptor binding				selectivity toward Y_4R (ratio K_i ($Y_{1,2,5}R$) / K_i (Y_4R))		
	pK_i ± SEM / K_i [nM] hY_4R[a]	pK_i / K_i [nM] hY_1R[b]	pK_i / K_i [nM] hY_2R[c]	pK_i / K_i [nM] hY_5R[d]	Y_1R	Y_2R	Y_5R
hPP	9.16 ± 0.03 / 0.69	< 6.5[e] / > 300	< 5.5[e] / > 3000	< 8.0[e] / > 10	> 430	> 4300	> 15
2.1	8.43 ± 0.04 / 3.6	< 5.5[f] / > 3000	< 5.5[f] / > 3000	< 5.5[f] / > 3000	> 830	> 830	> 830
2.8	8.69 ± 0.01 / 2.0	< 5.5 / > 3000	< 5.0 / > 10000	< 5.5 / > 3000	> 1500	> 5000	> 1500
2.9	5.75 ± 0.06 / 1800	n.d.	n.d.	n.d.	-	-	-
2.10	6.73 ± 0.07 / 190	n.d.	n.d.	n.d.	-	-	-
2.11	6.64 ± 0.11 / 240	n.d.	n.d.	n.d.	-	-	-
2.12	7.05 ± 0.13 / 97	n.d.	n.d.	n.d.	-	-	-
2.13	7.57 ± 0.08 / 28	< 5.5 / > 3000	< 5.5 / > 3000	< 5.0 / > 10000	> 110	> 110	> 360
2.14	8.35 ± 0.13 / 4.8	< 5.5 / > 3000	< 5.5 / > 3000	< 5.0 / > 10000	> 630	> 630	> 2100
2.15	6.93 ± 0.04 / 120	n.d.	n.d.	n.d.	-	-	-
2.16	7.25 ± 0.15 / 63	< 5.5 / > 3000	n.d.	n.d.	> 48	-	-
2.17	8.86 ± 0.09 / 1.4	< 6.0 / > 1000	< 6.0 / > 1000	< 6.0 / > 1000	> 710	> 710	> 710
2.18	8.06 ± 0.06 / 8.9	< 6.0 / > 1000	< 5.0 / > 10000	< 6.0 / > 1000	> 110	> 1100	> 110
2.19	8.12 ± 0.08 / 7.9	< 5.5 / > 3000	< 6.0 / > 1000	< 5.5 / > 3000	> 380	> 130	> 380
2.20	8.40 ± 0.04 / 4.0	< 6.5 / > 300	< 5.5 / > 3000	< 5.0 / > 10000	> 75	> 750	> 2500
2.21	7.85 ± 0.07 / 17	< 5.5 / > 3000	< 5.5 / > 3000	< 5.0 / > 10000	> 180	> 180	> 590
2.22	8.79 ± 0.06 / 1.7	< 6.0 / > 1000	< 5.0 / > 10000	< 6.0 / > 1000	> 590	> 5900	> 590
2.23	8.60 ± 0.05 / 2.8	< 6.0 / > 1000	< 5.5 / > 3000	< 5.0 / > 10000	> 360	> 1070	> 3600
2.24	8.40 ± 0.02 / 4.3	< 6.0 / > 1000	< 6.0 / > 1000	< 6.0 / > 1000	> 230	> 230	> 230
2.25	7.55 ± 0.08 / 29	< 5.5 / > 3000	< 5.0 / > 10000	< 5.5 / > 3000	> 100	> 340	> 100
2.26	6.62 ± 0.09 / 250	n.d.	n.d.	n.d.	-	-	-
2.27	7.51 ± 0.11 / 38	< 6.0 / > 1000	< 6.0 / > 1000	< 6.0 / > 1000	> 26	> 26	> 26
2.28	6.81 ± 0.09 / 160	n.d.	n.d.	n.d.	-	-	-
2.29	8.47 ± 0.01 / 3.4	< 5.0 / > 10000	< 5.0 / > 10000	< 5.0 / > 10000	> 2900	> 2900	> 2900
2.30	6.45 ± 0.04 / 350	n.d.	n.d.	n.d.	-	-	-

- **Table 1** continued -

2.31	8.13 ± 0.09 / 7.4	n.d.	n.d.	n.d.	-	-	-
2.32	7.03 ± 0.14 / 93	n.d.	n.d.	n.d.	-	-	-
2.33	5.88 ± 0.11 / 1300	n.d.	n.d.	n.d.	-	-	-
2.34	5.81 ± 0.08 / 1500	n.d.	n.d.	n.d.	-	-	-
2.35	8.41 ± 0.08 / 3.9	< 5.5 / > 3000	< 6.0 / > 1000	< 5.0 / > 10000	> 770	> 260	> 2600

[a]Determined by competition binding at CHO-hY$_4$R-mtAEQ-G$_{qi5}$ cells using [^{3}H]UR-KK200 (K_d = 0.67 nM, c = 1 nM) as radioligand.[12] [b]Determined by competition binding at SK-N-MC neuroblastoma cells using [^{3}H]UR-MK299 (K_d = 0.044 nM, c = 0.15 nM) as radioligand (structure see Figure S1, Supporting Information).[20] [c]Determined by competition binding with [^{3}H]propionyl-pNPY (K_d = 0.14 nM, c = 0.5 nM) at CHO-hY$_2$R cells. [d]Determined by competition binding at HEC-1B-hY$_5$R cells using [^{3}H]propionyl-pNPY (K_d = 4.8 nM, c = 4 nM) as radioligand.[21] [e]pK_i values reported by Berlicki *et al.*[16] [f]pK_i values reported by Kuhn *et al.*[11]
Data represent mean values from three independent experiments performed in triplicate (SEM given for Y$_4$R pK_i values).
n.d.: not determined

For the Y$_4$R agonists **2.8**, **2.14**, **2.17**-**2.24**, **2.27**, **2.29** and **2.35**, exhibiting high Y$_4$R affinity (pK_i > 7.5), as well as for the antagonists **2.13** and **2.25**, complete YR selectivity profiles were determined (Table 1). Compounds **2.8**, **2.13**, **2.14**, **2.17**-**2.19**, **2.21**-**2.25**, **2.29** and **2.35** showed high Y$_4$R selectivity as Y$_1$, Y$_2$ and Y$_5$ receptor affinities were more than 100-fold lower compared to Y$_4$R binding.

2.2.3 Functional Studies at the Human Y$_4$ Receptor

All compounds were investigated with respect to Y$_4$R agonism in the β-arrestin 1 and 2 recruitment assays (HEK293T-ARRB1-Y$_4$R and HEK293T-ARRB2-Y$_4$R cells[11]) and selected peptides (**2.1**, **2.8**-**2.13**, **2.15** and **2.17**-**2.30**) were studied in a Ca^{2+}-aequorin assay (CHO-hY$_4$R-G$_{qi5}$-mtAEQ cells[18]). Except for compounds containing Trp instead of Leu (**2.12**, **2.13**, **2.25**, **2.26** and **2.28**), the synthesized peptides elicited a response in the arrestin recruitment and in the Ca^{2+}-aequorin assay (agonist mode). Complete concentration-effect curves (CEC) (Figure 3 and Figures S3-S5, Supporting Information) were obtained for agonists (**2.1**, **2.8**, **2.14**, **2.16**-**2.24**, **2.27**, **2.29**, **2.31** and **2.35**) exhibiting pK_i values > 7.1 (radioligand competition binding) (Table 2). The respective pEC$_{50}$ values, EC$_{50}$ values and efficacies (relative to hPP) are summarized in Table 2. With efficacies (α) ranging from 0.35 to 0.91, compounds **2.1**, **2.8**, **2.14**, **2.16**-**2.24**, **2.27** and **2.29** proved to be partial agonists irrespective of the type of functional assay (Table 2). Strikingly, the potencies (pEC$_{50}$) of the partial agonists were throughout lower (1.5-2 orders of magnitude) than the respective pK_i values (radioligand competition binding) (Table 2). This discrepancy can be mainly attributed to the absence and presence of sodium ions in the buffers used for binding and functional assays, respectively, as discussed previously.[12,22]

When comparing the potencies (pEC_{50}) and efficacies obtained from the arrestin 1/2 recruitment and the Ca^{2+}-aequorin assay, there were only minor differences (Table 2), showing that the investigated partial agonists were unbiased with respect to the activation of the G-protein pathway and β-arrestin 1/2 recruitment to Y_4R.

Peptides **2.12**, **2.13**, **2.25**, **2.26** and **2.28**, which failed to elicit a response, when studied in the agonist mode (see Figure S6, Supporting Information), were investigated with respect to their antagonistic activities in the arrestin 1/2 recruitment and the Ca^{2+}-aequorin assay. These compounds, which have in common a Trp instead of Leu in the parent compound **2.1**, were capable of completely inhibiting the responses induced by the endogenous agonist hPP (for inhibition curves, see Figure 4A,C,D). The resulting pIC_{50} values were converted to pK_b values, which are presented in Table 2. The differences between the pK_b and pK_i values (antagonists) were much lower compared to the aforementioned differences between the pEC_{50} and pK_i values (partial agonists), being in agreement with the fact that the receptor affinity of antagonists is not increased in the absence of sodium.[23,24] Compound **2.13** was additionally studied with respect to its capability of rightward shifting the CEC of hPP (β-arrestin 1 and Ca^{2+}-aequorin assay). Indeed, in the presence of **2.13** (10 μM), a rightward shift (approximately two log units) and no suppression of the CEC of hPP were observed (Figure 4B,E), supporting the hypothesis of a competitive interaction between hPP and **2.13**.

Table 2. Agonistic (pEC_{50} and EC_{50}) or antagonistic (pK_b) activities of hPP, **2.1** and **2.8**-**2.35**.

cmpd.	β-Arrestin 1[a]		β-Arrestin 2[a]		Ca^{2+}-Aequorin[b]	
	pEC_{50} ± SEM / EC_{50} [nM] or *pK_b ± SEM*	α ± SEM	pEC_{50} ± SEM / EC_{50} [nM] or *pK_b ± SEM*	α ± SEM	pEC_{50} ± SEM / EC_{50} [nM] or *pK_b ± SEM*	α ± SEM
hPP	8.66 ± 0.01 / 2.4	1	8.37 ± 0.02 / 4.1	1	7.96 ± 0.01 / 10.6	1
2.1	6.79 ± 0.07 / 170	0.55 ± 0.02	6.95 ± 0.04 / 120	0.61 ± 0.01	6.74 ± 0.04 / 190	0.75 ± 0.03
2.8	7.29 ± 0.04 / 51	0.71 ± 0.02	7.42 ± 0.05 / 38	0.73 ± 0.05	6.99 ± 0.02 / 100	0.61 ± 0.02
2.9	< 4.50 / > 30000	n.a.	< 4.50 / > 30000	n.a.	< 4.50 / > 30000	n.a.
2.10	< 4.50 / > 30000	n.a.	< 4.50 / > 30000	n.a.	< 4.50 / > 30000	n.a.
2.11	< 4.50 / > 30000	n.a.	< 4.50 / > 30000	n.a.	< 4.50 / > 30000	n.a.
2.12	*7.02 ± 0.02*	-	*6.85 ± 0.05*	-	*7.22* ± 0.02	-
2.13	*7.14 ± 0.02*	-	*6.87 ± 0.04*	-	*7.32* ± 0.05	-
2.14	7.00 ± 0.08 / 100	0.88 ± 0.06	6.83 ± 0.04 / 150	0.64 ± 0.05	n.d.	n.d.
2.15	< 4.50 / > 30000	n.a.	< 4.50 / > 30000	n.a.	< 4.50 / > 30000	n.a.
2.16	5.97 ± 0.13 / 1070	0.61 ± 0.06	6.03 ± 0.08 / 930	0.86 ± 0.09	n.d.	n.d.
2.17	7.17 ± 0.06 / 67	0.79 ± 0.02	7.46 ± 0.03 / 35	0.68 ± 0.03	6.93 ± 0.02 / 120	0.61 ± 0.05
2.18	6.26 ± 0.08 / 550	0.65 ± 0.08	6.50 ± 0.04 / 320	0.63 ± 0.07	6.26 ± 0.01 / 550	0.58 ± 0.06
2.19	6.74 ± 0.09 / 180	0.57 ± 0.02	6.60 ± 0.08 / 250	0.60 ± 0.02	5.92 ± 0.06 / 1200	0.62 ± 0.05
2.20	6.34 ± 0.03 / 460	0.66 ± 0.13	6.37 ± 0.07 / 430	0.86 ± 0.06	6.21 ± 0.05 / 620	0.68 ± 0.04
2.21	6.22 ± 0.04 / 600	0.51 ± 0.07	6.29 ± 0.04 / 510	0.41 ± 0.06	5.60 ± 0.04 / 2500	0.49 ± 0.04
2.22	6.78 ± 0.07 / 160	0.91 ± 0.06	6.83 ± 0.07 / 140	0.70 ± 0.02	6.61 ± 0.08 / 250	0.74 ± 0.02
2.23	6.79 ± 0.08 / 160	0.56 ± 0.02	7.29 ± 0.05 / 51	0.67 ± 0.01	6.97 ± 0.01 / 110	0.64 ± 0.01
2.24	6.77 ± 0.05 / 170	0.64 ± 0.04	6.85 ± 0.04 / 140	0.67 ± 0.03	6.63 ± 0.02 / 230	0.54 ± 0.05
2.25	*6.96 ± 0.05*	-	*7.01 ± 0.03*	-	*7.57* ± 0.07	-
2.26	*6.10 ± 0.06*	-	*5.80 ± 0.08*	-	*6.46* ± 0.03	-
2.27	6.28 ± 0.04 / 520	0.35 ± 0.04	6.45 ± 0.03 / 360	0.47 ± 0.03	6.42 ± 0.06 / 380	0.45 ± 0.16
2.28	*6.22 ± 0.04*	-	*5.87 ± 0.05*	-	*6.91* ± 0.04	-
2.29	6.56 ± 0.01 / 280	0.81 ± 0.05	6.78 ± 0.02 / 170	0.84 ± 0.07	6.36 ± 0.01 / 440	0.54 ± 0.03
2.30	< 4.50 / > 30000	n.a.	< 4.50 / > 30000	n.a.	< 4.50 / > 30000	n.a.
2.31	5.62 ± 0.08 / 2400	0.60 ± 0.03	5.33 ± 0.09 / 4800	1.02 ± 0.06	n.d.	n.d.
2.32	< 4.50 / > 30000	n.a.	< 4.50 / > 30000	n.a.	n.d.	n.d.
2.33	< 4.50 / > 30000	n.a.	< 4.50 / > 30000	n.a.	n.d.	n.d.
2.34	< 4.50 / > 30000	n.a.	< 4.50 / > 30000	n.a.	n.d.	n.d.
2.35	5.61 ± 0.1 / 2500	0.63 ± 0.05	5.93 ± 0.04 / 1200	0.97 ± 0.03	n.d.	n.d.

[a]Agonistic potencies (pEC_{50} and EC_{50}) and intrinsic activities α (relative to the maximum effect elicited by 1 µM hPP, α = 1) determined in a β-arrestin 1 and a β-arrestin 2 recruitment assay at HEK293T-ARRB1-Y_4R cells and HEK293T-ARRB2-Y_4R cells, respectively. When performed in an antagonist mode, the pK_b values (in italics) were obtained by inhibition of the effect elicited by 10 nM hPP. [b]Agonistic potencies (pEC_{50} and EC_{50}) and intrinsic activities α (relative to the maximum effect elicited by 1 µM hPP, α = 1) determined in a Ca^{2+}-aequorin assay using CHO-hY_4R-mtAEQ-G_{qi5} cells. When performed in an antagonist mode, the pK_b values (in italics) were obtained by inhibition of the effect elicited by 100 nM hPP. Data represent mean values from three or four independent experiments (SEM given for pEC_{50}, α and pK_b values).

n.a.: not applicable; n.d.: not determined

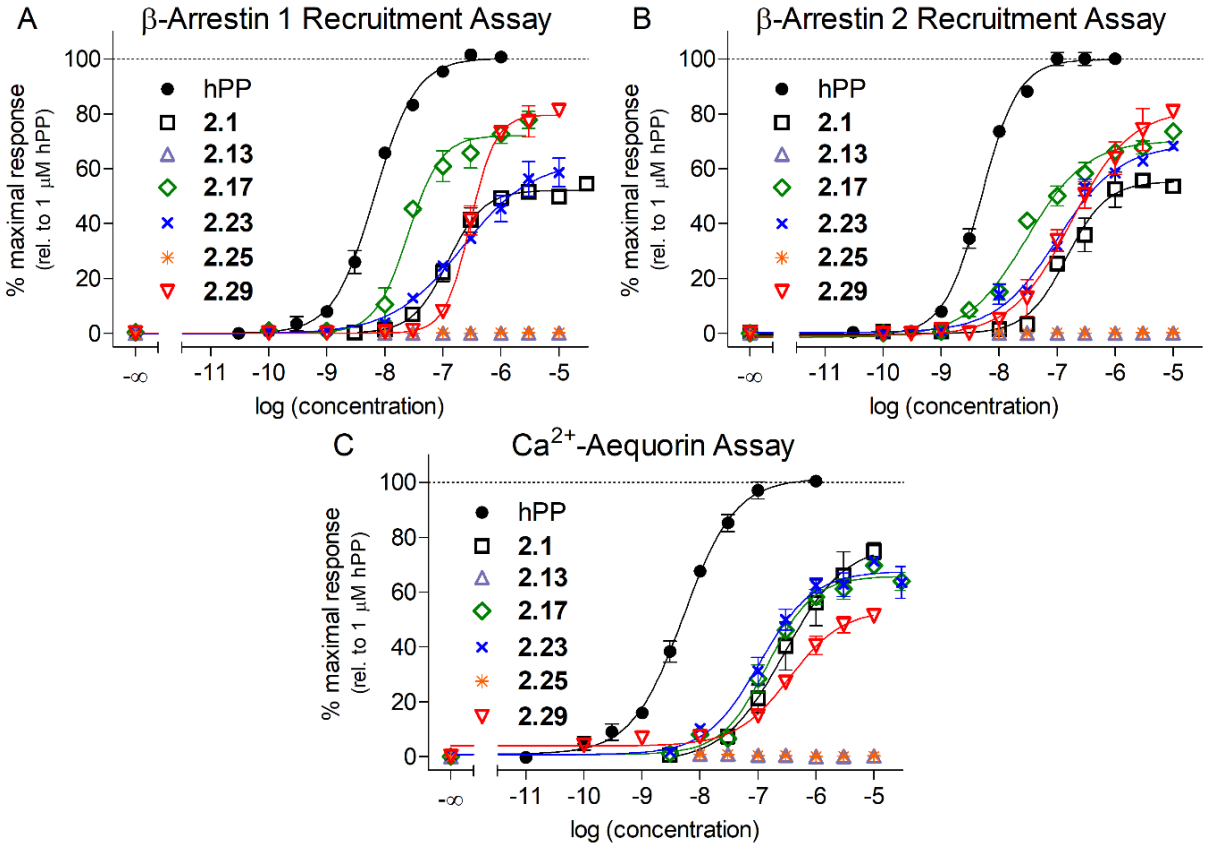

Figure 3. CEC of hPP, **2.1**, **2.13**, **2.17**, **2.23**, **2.25** and **2.29** obtained from a hY_4R β-arrestin 1 recruitment (A), hY_4R β-arrestin 2 recruitment (B) and hY_4R Ca^{2+}-aequorin (C) assay performed with live HEK293T-ARRB1-Y_4R cells, HEK293T-ARRB2-Y_4R cells and CHO-hY_4R-G_{qi5}-mtAEQ cells, respectively. Data represent means ± SEM from at least three independent experiments, each performed in triplicate.

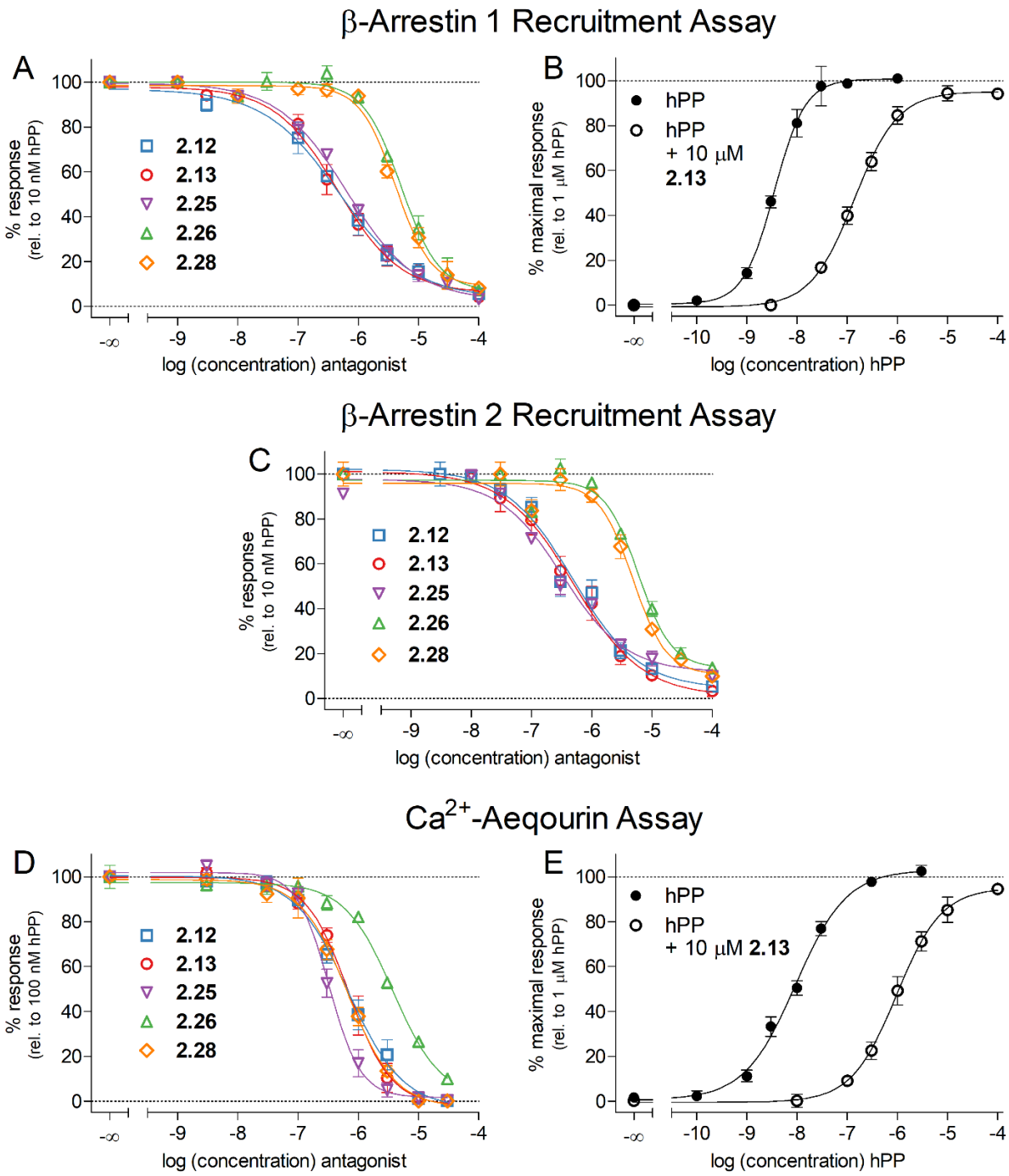

Figure 4. Inhibitory effects of **2.12**, **2.13**, **2.25**, **2.26** and **2.28** on hPP-stimulated hY$_4$R activation determined in hY$_4$R β-arrestin 1 (A, B), hY$_4$R β-arrestin 2 (C) and hY$_4$R Ca^{2+}-aequorin (D, E) assay performed with live HEK293T-ARRB1-Y$_4$R cells, HEK293T-ARRB2-Y$_4$R cells and CHO-hY$_4$R-G$_{qi5}$-mtAEQ cells, respectively. (A) Inhibition of β-arrestin 1 recruitment, elicited by 10 nM hPP, by **2.12**, **2.13**, **2.25**, **2.26** and **2.28**. (B) Effect of **2.13** (10 µM) on the β-arrestin 1 recruitment CEC of hPP. The pK_b value of **2.13**, calculated based on the rightward shift of the CEC according to the Gaddum equation,[25] amounted to 6.63 ± 0.03 (mean ± SEM from three independent experiments). (C) Inhibition of β-arrestin 2 recruitment, elicited by 10 nM hPP, by **2.12**, **2.13**, **2.25**, **2.26** and **2.28**. (D) Inhibition of the intracellular Ca^{2+} mobilization, induced by 100 nM hPP, by **2.12**, **2.13**, **2.25**, **2.26** and **2.28**. (E) Effect of **13** (10 µM) on the intracellular Ca^{2+} mobilization CEC of hPP. The pK_b value of **2.13**, calculated based on the rightward shift of the CEC according to the Gaddum equation,[25] amounted to 7.05 ± 0.05 (mean ± SEM from three independent experiments). Data in A-E represent means ± SEM from at least three independent experiments performed in triplicate. Note: because of to higher apparent potencies of hPP in the arrestin assays (pEC_{50} = 8.66 and 8.37, respectively), compared to the Ca^{2+} aequorin assay (pEC_{50} = 7.96), different hPP concentrations (10 vs. 100 nM) were used for the antagonist mode.

2.2.4 Induced-Fit Docking to the hY_4R

Induced-fit docking to Y_4R was performed with the Y_4R agonists **2.1** and **2.29** and the Y_4R antagonist **2.13** using two different hY_4R homology models: the model, used for agonists **2.1** and **2.29**, was generated based on an active state κ opioid receptor crystal structure (PDB ID: 6B73)[26] (sequence similarity with the hY_4R: 35%) and antagonist **2.13** was docked to a Y_4R model generated from the recently solved inactive state hY_1R crystal structure (PDB ID: 5ZBQ).[27] Docking poses corresponding to the lowest XP GlideScore are presented in Figure 5. The agonists **2.1** and **2.29** exhibited comparable binding poses characterized by a deep location of the C-terminal tyrosinamide within the 7TM bundle, being in contact (H-bond) with $Q222^{5.46}$ of TM V (Figure 5A and 5B). This was in accordance with a previously reported Y_4R binding mode of the agonist hPP, also indicating a deep entering of the C-terminal tyrosinamide into the orthosteric binding pocket.[10] In contrast, the C-terminal tyrosinamide of antagonist **2.13** appeared to be located at the receptor surface (Figure 5C). Moreover, Trp^4 and Arg^5 in **2.13** were located in the region, occupied by the side chain of the C-terminal tyrosine in the agonists **2.1** and **2.29**, reaching the conserved $W278^{6.48}$ (*π*-*π* stacking and *π*-cation interactions, respectively; not indicated in Figure 5) at the bottom of the orthosteric binding pocket (Figure 5C). Irrespective of the binding modes of **2.1**, **2.13** and **2.29**, the basic arginine residues in all ligands showed interactions with the receptor (primarily acidic amino acids such as $E203^{ECL2}$, $E288^{6.58}$, $D289^{6.59}$ and $E293^{ECL3}$), which was consistent with the observed decrease in Y_4R affinity (approximately 1.5 orders of magnitude) upon replacement of arginine by nonbasic citrulline [compounds **2.15** and **2.16** vs peptides **2.1** and **2.8** (*cf*. Figure 2); binding data, see Table 1].

In view of the experimentally proven antagonism of **2.13**, the identified binding pose of this Y_4R ligand is probably incompatible with a contraction of the ligand binding pocket of the receptor required for GPCR activation.[28,29] This might be explained by the positioning of two amino acid residues of peptide **2.13** (Trp^4 and Arg^5, oriented “parallelly”) deeply in the binding pocket, hindering a contraction of the 7TM bundle, instead of only one residue (C-terminal Tyr) as observed for the agonists **2.1** and **2.29**, allowing an inward motion of the TM domains (Figure 5). However, induced-fit docking studies, implicating numerous simplifications, cannot serve for a detailed analysis of the molecular determinants being responsible for the observed antagonism.

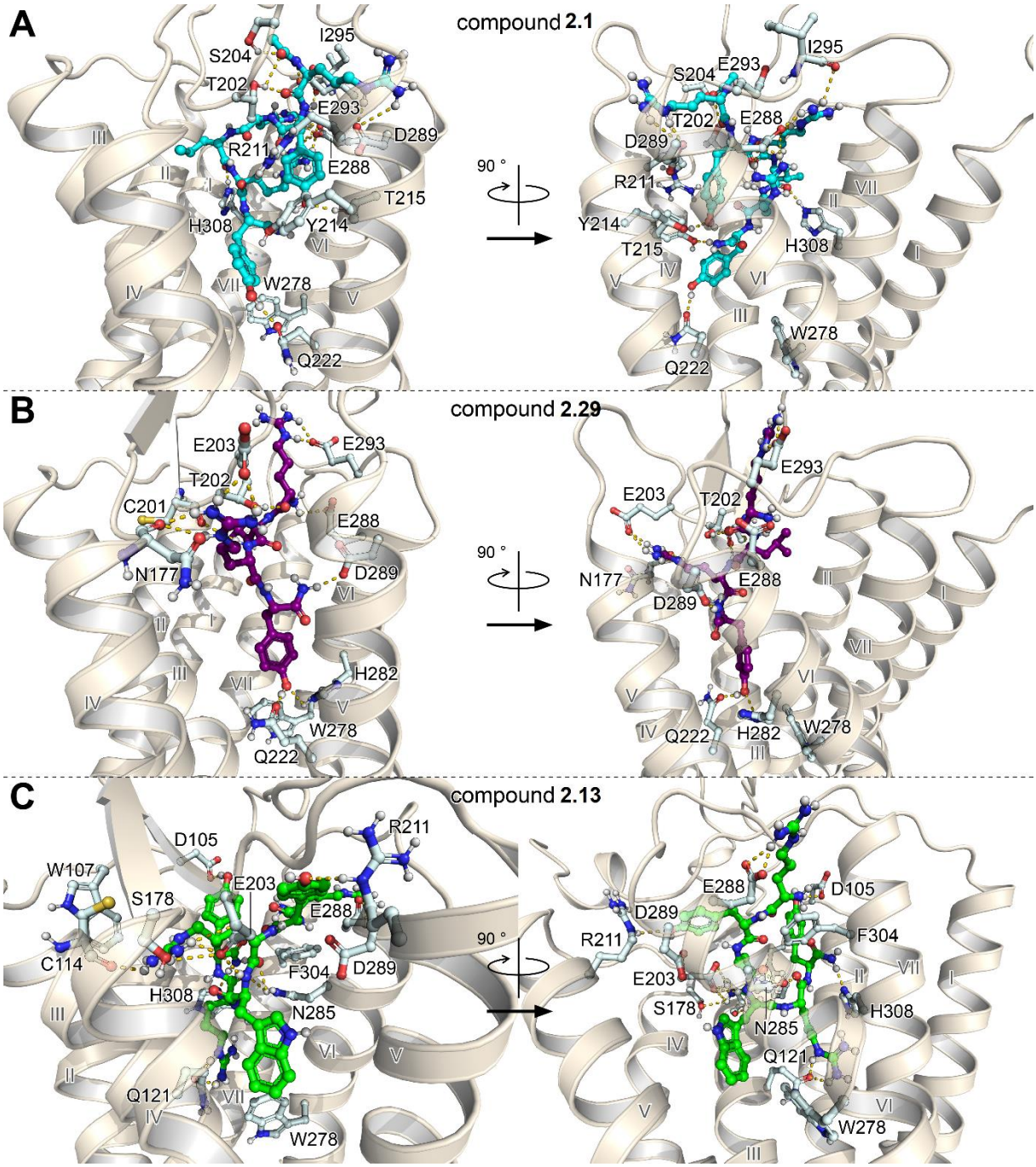

Figure 5. Induced-fit docking poses of the Y_4R agonists **2.1** and **2.29** as well as of the antagonist **2.13** at the homology models of hY_4R. (A) Binding pose of **2.1** (shown in cyan) at a Y_4R homology model generated from the active state κ opioid receptor crystal structure (PDB: 6B73, chain A).[26] (B) Binding pose of **2.29** (shown in purple) at the active state Y_4R homology model used for docking of **2.1** (A). (C) Binding pose of **2.13** (shown in green) at a Y_4R homology model generated from the inactive state hY_1R crystal structure (PDB: 5ZBQ)[27]. Nitrogen and oxygen atoms are shown in blue and red, respectively. Carbon atoms of receptor amino acids are shown in gray. Yellow dashed lines indicate the H-bonds and salt bridges.

2.3 Conclusions

To date, the smallest peptidic Y_4R ligands with high affinity ($pK_i > 8$) have been hexapeptides such as **2.1** (acetyl-Arg-Tyr-Arg-Leu-Arg-Tyr-NH_2). We discovered a tetrapeptide (**2.29**, Arg-Leu-Arg-Tyr-NH_2), representing the smallest Y_4R ligand with high affinity (pK_i: 8.47) known so far. Moreover, replacement of Leu^4 in **2.1** by Trp was identified as a striking structural modification turning Y_4R agonism into antagonism (e.g. compounds **2.12** and **2.13**). These findings may support the development of low-molecular-weight nonpeptidic Y_4R ligands, including antagonists. Such compounds, which are lacking to date, are considered advantageous over peptides in terms of in vivo studies and pharmacokinetics (crossing of the blood-brain barrier). Whereas Y_4R antagonists are needed as pharmacological tools for a better understanding of the physiological role of the Y_4 receptor, Y_4R agonists represent potential therapeutics to treat, for example, obesity.

2.4 Experimental Section

2.4.1 General Experimental Conditions

Protected amino acids Fmoc-Tyr(*t*Bu)-OH, Fmoc-Leu-OH, Fmoc-Arg(Pbf)-OH, Fmoc-Trp-OH, Fmoc-Cit-OH, Fmoc-Phe-OH and Fmoc-Gly-OH were purchased from Carbolution Chemicals (St. Ingbert, Germany). Fmoc-Sieber-PS-resin (0.59 mmol/g), HBTU, N-methyl-2-pyrrolidone (NMP) for peptide synthesis, Fmoc-(*D*)-Tyr(tBu)-OH, Fmoc-(*D*)-Leu-OH and Fmoc-Pro-OH were obtained from Iris Biotech (Marktredwitz, Germany). Fmoc-GABA-OH, Fmoc-Ala-OH, MeOH and TFA were from Merck (Darmstadt, Germany). HOBt hydrate, succinic anhydride and dichloromethane (CH_2Cl_2) were purchased from Acros Organics/Fisher Scientific (Nidderau, Germany). DIPEA was obtained from ABCR (Karlsruhe, Germany) and dimethylformamide (DMF) for peptide synthesis, acetic anhydride, Fmoc-(*D*)-Arg(Pbf)-OH, Fmoc-N(Me)-Arg(Pbf)-OH, gradient grade acetonitrile for high-performance liquid chromatography (HPLC), Triton-X-100 and piperidine were from Sigma-Aldrich (Taufkirchen, Germany). Human PP (hPP) and porcine neuropeptide Y (pNPY) were from SynPeptide (Shanghai, China). Coelenterazine h was purchased from Biotrend (Cologne, Germany). Bacitracin and bovine serum albumin (BSA) were from Serva (Heidelberg, Germany). Pierce D-luciferin (monopotassium salt) was obtained from ThermoFisher Scientific (Nidderau, Germany) and JNJ31020028 was purchased from Cayman Chemicals (Ann Arbor, USA). The syntheses of **2.7**,[14] [^{3}H]UR-MK299,[20] [^{3}H]UR-KK200,[12] BIIE0246[30] and [^{3}H]propionyl-pNPY[20] (used for Y_5R binding studies) were described elsewhere. [^{3}H]Propionyl-pNPY (specific activity: 37.5 Ci/mmol and radiochemical purity: 99%), used for Y_2R binding studies, was prepared according to a previously reported procedure[20] with minor modifications [e.g. anhydrous NMP/DMF (30:70 v/v, 40 μL, supplemented with 0.05 μL of DIPEA) was used instead of 0.1 M sodium borate buffer pH 8.5 (135 μL) and propionyl-pNPY was used instead of pNPY for quantification; radiochemical yield: 26%]. Millipore water was consistently used for the preparation of stock solutions, buffers and eluents for HPLC. Polypropylene reaction vessels (1.5 and 2 mL) from Sarstedt (Nümbrecht, Germany) were used to keep stock solutions and for small-scale reactions (e.g. activation of Fmoc-protected amino acids). NMR spectra were recorded on a Bruker AVANCE 600 instrument with cryogenic probe (^{1}H: 600.3 MHz and ^{13}C: 150.9 MHz) (Bruker, Karlsruhe, Germany). NMR spectra were calibrated based on the solvent residual peaks (^{1}H-NMR, DMSO-d_6: δ = 2.50 ppm; ^{13}C-NMR: DMSO-d_6: δ = 39.50 ppm) and data are reported as follows: ^{1}H-NMR: chemical shift δ in ppm [multiplicity (s = singlet, d = doublet, t = triplet, m = multiplet and br s = broad singlet); integral, coupling constant *J* in Hz] and ^{13}C-NMR: chemical shift δ in ppm. High-resolution mass spectrometry (HRMS) was performed with an Agilent 6540 UHD accurate-mass Q-TOF LC/MS system linked to an Agilent 1290 analytical HPLC system (Agilent Technologies, Santa Clara, CA). Preparative HPLC was

performed with a system from Knauer (Berlin, Germany) consisting of two K-1800 pumps and a K-2001 detector (in the following referred to as “system 1”) or with a Prep 150 LC system from Waters (Eschborn, Germany) comprising a Waters 2545 binary gradient module, a Waters 2489 UV/vis-detector and a Waters fraction collector III (in the following referred to as “system 2”). A Kinetex XB-C18, 5 µm, 250 mm × 21 mm, from Phenomenex (Aschaffenburg, Germany) was used as a reversed-phase (RP) column at a flow rate of 20 mL/min using mixtures of 0.1% aqueous TFA and acetonitrile as the mobile phase. The detection wavelength of 220 nm was used throughout. Collected fractions were lyophilized using a Scanvac CoolSafe 100-9 freeze-dryer (Labogene, Alleroed, Denmark) equipped with a RZ 6 rotary vane vacuum pump (Vacuubrand, Wertheim, Germany). Analytical HPLC analysis was performed with an Agilent 1100 system (Agilent Technologies) composed of a binary pump (G1312A), an autosampler (G1329A), a thermostated column compartment (G1316A) and a diode array detector (G1315B). A Kinetex XB-C18, 5 µm, 250 mm × 4.6 mm (Phenomenex), served as a stationary phase at a flow rate of 0.8 mL/min. Detection was performed at 220 nm and the oven temperature was 25 °C. Mixtures of acetonitrile (A) and 0.1 % aqueous TFA (B) were used as the mobile phase. The following linear gradient was applied: 0-25 min: A/B 10:90 to 30:70; 25-27 min: 30:70 to 95:5 and 27-35 min: 95:5 (isocratic). The injection volume was 50 µL. Retention (capacity) factors k were calculated from the retention times t_R according to $k = (t_R - t_0)/t_0$ (t_0 = dead time).

2.4.2 Compound Characterization

Except for compounds **2.12**, **2.21**, **2.26** and **2.30**, all target compounds were characterized by ^{1}H, ^{13}C and 2D NMR (HSQC, HMBC and ^{1}H COSY) spectroscopy, HRMS and RP-HPLC. Compounds **2.12**, **2.21**, **2.26** and **2.30** were characterized by ^{1}H-NMR, HRMS and RP-HPLC. HPLC purities of all target compounds were ≥ 96%. The analytical data of **2.8**-**2.35** are summarized in Table 3 (chromatograms shown in Appendix).

Table 3. Analytical characterization of peptides **2.8**-**2.35**.

compd.	x-fold hydro-trifluoracetate	MW	overall yield (%)	RP-HPLC purity (%) / t_R [min] / k	HRMS (ESI): *m/z*			NMR[a]
					calcd. for	calcd.	found	
2.8	4	925.11 + 456.09	23	97 / 9.1 / 1.8	$[M+3H]^{3+}$	309.1875	309.1884	^{1}H, ^{13}C, 2D
2.9	3	951.10 + 342.07	25	98 / 19.4 / 5.0	$[M+3H]^{3+}$	317.8472	317.8483	^{1}H, ^{13}C, 2D
2.10	4	869.00 + 456.09	33	99 / 6.3 / 1.0	$[M+3H]^{3+}$	290.4999	290.5008	^{1}H, ^{13}C, 2D
2.11	4	883.03 + 456.09	27	99 / 7.1 / 1.2	$[M+3H]^{3+}$	295.1718	295.1730	^{1}H, ^{13}C, 2D
2.12	3	1040.20 + 342.07	35	97 / 17.0 / 4.3	$[M+3H]^{3+}$	347.5227	347.5240	^{1}H
2.13	4	998.16 + 456.09	32	96 / 16.0 / 4.0	$[M+3H]^{3+}$	333.5192	333.5206	^{1}H, ^{13}C, 2D
2.14	4	926.09 + 456.09	35	98 / 10.8 / 2.4	$[M+3H]^{3+}$	309.5155	309.5166	^{1}H, ^{13}C, 2D

- **Table 3** continued -

2.15	3	968.13 + 342.07	42	97 / 16.0 / 4.0	$[M+3H]^{3+}$	323.5190	323.5202	^{1}H, ^{13}C, 2D
2.16	4	926.09 + 456.09	39	97 / 14.0 / 3.4	$[M+3H]^{3+}$	309.5155	309.5164	^{1}H, ^{13}C, 2D
2.17	3	990.19 + 342.07	33	96 / 15.9 / 3.9	$[M+2H]^{2+}$	495.7909	495.7912	^{1}H, ^{13}C, 2D
2.18	3	951.15 + 342.07	40	98 / 15.5 / 3.8	$[M+2H]^{2+}$	476.2854	476.2856	^{1}H, ^{13}C, 2D
2.19	3	861.02 + 342.07	23	97 / 9.0 / 1.8	$[M+2H]^{2+}$	431.2619	431.2625	^{1}H, ^{13}C, 2D
2.20	3	1053.24 + 342.07	37	97 / 15.0 / 3.7	$[M+3H]^{3+}$	342.5262	342.5273	^{1}H, ^{13}C, 2D
2.21	3	803.97 + 342.07	23	97 / 7.7 / 1.4	$[M+2H]^{2+}$	405.7512	405.7518	^{1}H
2.22	3	791.96 + 342.07	37	99 / 18.1 / 4.6	$[M+2H]^{2+}$	396.7350	396.7362	^{1}H, ^{13}C, 2D
2.23	3	1024.20 + 342.07	70	97 / 16.4 / 4.1	$[M+3H]^{3+}$	342.1982	342.1996	^{1}H, ^{13}C, 2D
2.24	3	1109.31 + 342.07	34	96 / 16.3 / 4.1	$[M+3H]^{3+}$	370.5491	370.5503	^{1}H, ^{13}C, 2D
2.25	3	1097.25 + 342.07	44	96 / 14.1 / 3.4	$[M+3H]^{3+}$	366.5299	366.5320	^{1}H, ^{13}C, 2D
2.26	3	1120.29 + 342.07	41	98 / 17.0 / 4.3	$[M+3H]^{3+}$	374.2019	374.2034	^{1}H
2.27	3	1047.24 + 342.07	40	96 / 17.1 / 4.3	$[M+2H]^{2+}$	524.3016	524.3043	^{1}H, ^{13}C, 2D
2.28	3	1125.31 + 342.07	30	96 / 14.5 / 3.5	$[M+3H]^{3+}$	375.8737	375.8760	^{1}H, ^{13}C, 2D
2.29	3	605.75 + 342.07	34	98 / 5.9 / 0.8	$[M+2H]^{2+}$	303.6954	303.6964	^{1}H, ^{13}C, 2D
2.30	3	678.80 + 342.07	30	97 / 9.4 / 1.9	$[M+2H]^{2+}$	340.1930	340.1940	^{1}H
2.31	3	605.75 + 342.07	21	98 / 8.8 / 1.7	$[M+2H]^{2+}$	303.6954	303.6965	^{1}H, ^{13}C, 2D
2.32	3	605.75 + 342.07	45	98 / 8.5 / 1.6	$[M+2H]^{2+}$	303.6954	303.6962	^{1}H, ^{13}C, 2D
2.33	3	605.75 + 342.07	14	99 / 7.9 / 1.4	$[M+2H]^{2+}$	303.6954	303.6958	^{1}H, ^{13}C, 2D
2.34	3	605.75 + 342.07	22	97 / 8.6 / 1.6	$[M+2H]^{2+}$	303.6954	303.6959	^{1}H, ^{13}C, 2D
2.35	3	619.77 + 228.04	19	98 / 10.9 / 2.4	$[M+2H]^{2+}$	310.7037	310.7038	^{1}H, ^{13}C, 2D

[a]2D-NMR: HSQC, HMBC and COSY.

2.4.3 General Procedure for SPPS: Experimental Protocols and Analytical Data

Peptides were synthesized by manual SPPS according to the Fmoc strategy. Five milliliter Injekt Solo (B. Braun, Melsungen, Germany) or NPRM-JECT (Henke Sass Wolf, Tuttlingen, Germany) syringes, equipped with polyethylene frits (pore size: 35 µm) (Roland Vetter Laborbedarf, Ammerbuch, Germany) were used as reaction vessels. DMF/NMP (8:2 v/v) was used as a solvent for the coupling reactions, Fmoc deprotection and N-terminal acetylation/succinylation. For the initial Fmoc deprotection of the resin and swelling, the resin was treated with 20% piperidine in the solvent at rt for 2 × 20 min. Fmoc-protected L-amino acids were used in 5-fold excess and preactivated with HBTU (4.9 equiv)/HOBt (5 equiv)/DIPEA (10 equiv) in polypropylene reaction vessels for at least 5 min prior to addition to the resin (volume of the solvent: ca. 2.2 mL/mmol Fmoc amino acid). “Double” coupling (2

× 45 min) was performed at 35 °C for all amino acids using a Multi Reax shaker (Heidolph, Schwabach, Germany) covered with a box equipped with a thermostat-controlled heater. After completing the coupling of an Fmoc amino acid, the resin was washed with the solvent (4×) and treated with 20 % piperidine in the solvent at rt for 2 × 10 min, followed by washing of the resin with the solvent (6×). N-Terminally acylated peptides were prepared by treatment of the resin-bound completely elongated peptide with acetic anhydride (10 equiv)/DIPEA (10 equiv) or succinic anhydride (10 equiv)/DIPEA (10 equiv) (**2.20**) in the solvent at rt for 35 min. After coupling and Fmoc deprotection of the final amino acid or after acylation of the N-terminus, the resin was washed with the solvent (6×) and CH_2Cl_2 (treated with K_2CO_3) (4×) followed by cleavage of the resin with CH_2Cl_2/TFA (3:1 v/v) at rt (2 × 20 min). The liquid was separated from the resin by filtration and the resin was washed once with the cleavage reagent. The filtrates were combined in a round-bottom flask and the volatiles were removed by rotary evaporation. The residue was dissolved in TFA/H_2O (95:5 v/v) and the mixture was stirred at rt for 5 h (full side-chain deprotection) and transferred to a 100 mL flask containing water (40 mL), followed by lyophilization and subsequent purification by preparative HPLC.

Arg-Tyr-Arg-Leu-Arg-Tyr-amide tetrakis(hydrotrifluoroacetate) (2.8). Peptide **2.8** was synthesized on a Sieber-amide-PS resin (40 mg, 0.65 mmol/g) according to the general procedure. Purification by preparative HPLC (system 1, gradient: 0-18 min MeCN/0.1% aq TFA 3:97 to 42:58, t_R = 12 min) yielded **2.8** as a white solid (8.3 mg, 23%). ^{1}H-NMR (600 MHz, DMSO-d_6): δ (ppm) 0.80-0.91 (m, 6H), 1.37-1.54 (m, 10H), 1.58-1.76 (m, 5H), 2.63-2.75 (m, 2H), 1.82-2.89 (m, 1H), 2.90-2.96 (m, 1H), 3.02-3.15 (m, 6H), 3.74-3.81 (m, 1H), 4.18-4.24 (m, 1H), 4.25-4.30 (m, 1H), 4.30-4.36 (m, 2H), 4.51-4.57 (m, 1H), 6.60-6.68 (m, 4H), 6.80-7.55 (br s, 12H, interfering with the next three listed signals), 6.96-6.99 (m, 2H), 7.05-7.07 (m, 2H), 7.36-7.40 (m, 2H), 7.63-7.67 (m, 1H), 7.71-7.75 (m, 1H), 7.76-7.84 (m, 2H), 7.93-7.98 (m, 1H), 8.05-8.16 (m, 4H), 8.35-8.40 (m, 1H), 8.47-8.53 (m, 1H), 9.24 (br s, 2H). ^{13}C-NMR (150 MHz, DMSO-d_6): δ (ppm) 21.4, 23.1, 24.0, 24.1, 24.9, 25.1, 28.5, 28.6, 29.0, 36.6, 36.8, 40.2, 40.43, 40.45, 40.8, 50.9, 51.6, 52.2, 52.3, 53.9, 54.3, 114.86 (two carbon atoms), 114.92 (two carbon atoms), 116.0 (TFA), 118.0 (TFA), 127.4, 127.5, 130.0 (two carbon atoms), 130.1 (two carbon atoms), 155.9 (two carbon atoms), 156.77, 156.83, 156.87, 158.7 (q, *J* 32 Hz) (TFA), 168.5, 170.84, 170.85, 171.1, 172.0, 172.7. HRMS (ESI): *m/z* $[M+3H]^{3+}$ calcd. for $[C_{42}H_{71}N_{16}O_8]^{3+}$ 309.1875, found: 309.1884. RP-HPLC (220 nm): 97% (t_R = 9.1 min, *k* = 1.8). $C_{42}H_{68}N_{16}O_8 \cdot C_8H_4F_{12}O_8$ (925.11 + 456.09).

Acetyl-Arg-Tyr-Arg-Pro-Arg-Tyr-amide tris(hydrotrifluoroacetate) (2.9). Peptide **2.9** was synthesized on a Sieber-amide-PS resin (40 mg, 0.65 mmol/g) according to the general procedure. Purification by preparative HPLC (system 1, gradient: 0-18 min MeCN/0.1% aq TFA 3:97 to 42:58, t_R = 11 min) yielded **2.9** as a white solid (7.3 mg, 25%). ^{1}H-NMR (600 MHz,

DMSO-d_6): δ (ppm) 1.36-1.60 (m, 10H), 1.61-1.72 (m, 2H), 1.74-1.90 (m, 6H), 1.98-2.05 (m, 1H), 2.64-2.75 (m, 2H), 2.85-2.92 (m, 2H), 3.00-3.14 (m, 6H), 3.48-3.54 (m, 1H), 3.55-3.60 (m, 1H), 4.10-4.19 (m, 2H), 4.31-4.36 (m, 2H), 4.42-4.50 (m, 2H), 6.59-6.65 (m, 4H), 6.80-7.53 (br s, 12H, interfering with the next three listed signals), 6.94-6.98 (m, 4H), 7.07-7.09 (m, 1H), 7.36-7.38 (m, 1H), 7.62-7.73 (m, 4H), 7.74-7.78 (m, 1H), 8.03-8.08 (m, 1H), 8.12-8.19 (m, 2H), 9,23 (br s, 2H). ^{13}C-NMR (150 MHz, DMSO-d_6): δ (ppm) 22.5, 24.4, 24.6, 25.0 (two carbon atoms), 28.1, 28.7, 28.8, 29.2, 36.5, 36.8, 40.37, 40.38, 40.5, 46.9, 50.0, 52.3, 52.6, 53.6, 53.8, 59.3, 114.8 (two carbon atoms), 114.9 (two carbon atoms), 115.9 (TFA), 117.9 (TFA), 127.4, 127.6, 130.0 (two carbon atoms), 130.1 (two carbon atoms), 155.8 (two carbon atoms), 156.80, 156.82, 156.9, 158.9 (q, *J* 32 Hz) (TFA), 169.6, 169.7, 170.7, 170.9, 171.2, 171.6, 172.8. HRMS (ESI): *m/z* $[M+3H]^{3+}$ calcd. for $[C_{43}H_{69}N_{16}O_9]^{3+}$ 317.8472, found: 317.8483. RP-HPLC (220 nm): 98% (t_R = 19.4 min, k = 5.0). $C_{43}H_{66}N_{16}O_9 \cdot C_6H_3F_9O_6$ (951.10 + 342.07).

Arg-Tyr-Arg-Gly-Arg-Tyr-amide tetrakis(hydrotrifluoroacetate) (2.10). Peptide **2.10** was synthesized on a Sieber-amide-PS resin (40 mg, 0.59 mmol/g) according to the general procedure. Purification by preparative HPLC (system 1, gradient: 0-18 min MeCN/0.1% aq TFA 3:97 to 42:58, t_R = 9 min) yielded **2.10** as a white solid (10.2 mg, 33%). ^{1}H-NMR (600 MHz, DMSO-d_6): δ (ppm) 1.38-1.57 (m, 8H), 1.59-1.66 (m, 1H), 1.66-1.76 (m, 3H), 2.64-2.74 (m, 2H), 2.84-2.91 (m, 1H), 2.94-3.00 (m, 1H), 3.02-3.07 (m, 2H), 3.07-3.14 (m, 4H), 3.68-3.75 (m, 1H), 3.75-3.83 (m, 2H), 4.22-4.29 (m, 2H), 4.30-4.35 (m, 1H), 4.48-4.55 (m, 1H), 6.61-6.68 (m, 4H), 6.80-7.55 (br s, 12H, interfering with the next four listed signals), 6.98-7.01 (m, 2H), 7.03-7.04 (m, 1H), 7.07-7.09 (m, 2H), 7.34-7.35 (m, 1H), 7.61-7.66 (m, 1H), 7.70-7.74 (m, 1H), 7.76-7.81 (m, 1H), 7.91-7.95 (m, 1H), 8.04-8.08 (m, 1H), 8.08-8.14 (m, 4H), 8.32-8.36 (m, 1H), 8.51-8.56 (m, 1H), 9.25 (br s, 2H). ^{13}C-NMR (150 MHz, DMSO-d_6): δ (ppm) 23.9, 24.8, 25.0, 28.5, 29.1, 29.2, 36.4, 36.7, 40.2, 40.39, 40.42, 41.8, 51.6, 52.2, 52.4, 54.2, 54.5, 114.86 (two carbon atoms), 114.94 (two carbon atoms), 116.0 (TFA), 118.0 (TFA), 127.5, 127.7, 130.04 (two carbon atoms), 130.05 (two carbon atoms), 155.8, 155.9, 156.76, 156.82, 156.85, 158.7 (q, *J* 32 Hz) (TFA), 168.5, 168.7, 170.9, 171.0, 171.6, 172.9. HRMS (ESI): *m/z* $[M+3H]^{3+}$ calcd. for $[C_{38}H_{63}N_{16}O_8]^{3+}$ 290.4999, found: 290.5008. RP-HPLC (220 nm): 99% (t_R = 6.3 min, k = 1.0). $C_{38}H_{60}N_{16}O_8 \cdot C_8H_4F_{12}O_8$ (869.00 + 456.09).

Arg-Tyr-Arg-Ala-Arg-Tyr-amide tetrakis(hydrotrifluoroacetate) (2.11). Peptide **2.11** was synthesized on a Sieber-amide-PS resin (40 mg, 0.59 mmol/g) according to the general procedure. Purification by preparative HPLC (system 1, gradient: 0-18 min MeCN/0.1% aq TFA 3:97 to 42:58, t_R = 9 min) yielded **2.11** as a white solid (8.5 mg, 27%). ^{1}H-NMR (600 MHz, DMSO-d_6): δ (ppm) 1.17-1.22 (m, 3H), 1.37-1.46 (m, 2H), 1.46-1.57 (m, 6H), 1.59-1.77 (m, 4H), 2.64-2.74 (m, 2H), 2.83-2.89 (m, 1H), 2.91-2.97 (m, 1H), 3.03-3.14 (m, 6H), 3-78-3-79 (m, 1H), 4.17-4.21 (m, 1H), 4.23-4.30 (m, 2H), 4.31-4.37 (m, 1H), 4.49-4.54 (m, 1H), 6.61-6.67 (m,

4H), 6.80-7.56 (br s, 12H, interfering with the next three listed signals), 6.96-6.98 (m, 2H), 7.06-7.08 (m, 3H), 7.39-7.41 (m, 1H), 7.64-7.68 (m, 1H), 7.72-7.77 (m, 2H), 7.80-7.84 (m, 1H), 7.99-8.03 (m, 1H), 8.07-8.16 (m, 4H), 8.31-8.34 (m, 1H), 8.49-8.53 (m, 1H), 9.23 (br s, 2H). ^{13}C-NMR (150 MHz, DMSO-d_6): δ (ppm) 18.3, 23.9, 24.9, 25.0, 28.5, 28.99, 29.04, 36.5, 36.9, 40.2, 40.4, 40.5, 48.1, 51.6, 52.1, 52.4, 53.8, 54.4, 114.85 (two carbon atoms), 114.93 (two carbon atoms), 115.9 (TFA), 117.9 (TFA), 127.4, 127.5, 130.07 (two carbon atoms), 131.0 (two carbon atoms), 155.8, 156.0, 156.81, 156.85, 156.89, 158.8 (q, *J* 32 Hz) (TFA), 168.5, 170.8, 170.87, 171.89, 172.1, 172.7. HRMS (ESI): *m/z* $[M+3H]^{3+}$ calcd. for $[C_{39}H_{65}N_{16}O_8]^{3+}$ 295.1718, found: 295.1730. RP-HPLC (220 nm): 99% (t_R = 7.1 min, *k* = 1.2). $C_{39}H_{62}N_{16}O_8 \cdot C_8H_4F_{12}O_8$ (883.03 + 456.09).

Acetyl-Arg-Tyr-Arg-Trp-Arg-Tyr-amide tris(hydrotrifluoroacetate) (2.12). Peptide **2.12** was synthesized on a Sieber-amide-PS resin (40 mg, 0.65 mmol/g) according to the general procedure. Purification by preparative HPLC (system 1, gradient: 0-18 min MeCN/0.1% aq TFA 3:97 to 42:58, t_R = 13 min) yielded **2.12** as a white solid (12.5 mg, 35%). ^{1}H-NMR (600 MHz, DMSO-d_6): δ (ppm) 1.33-1.58 (m, 10H), 1.61-1.68 (m, 2H), 1.84 (s, 3H), 2.63-2.69 (m, 1H), 2.69-2.75 (m, 1H), 2.85-2.91 (m, 2H), 2.94-3.09 (m, 7H), 3.11-3.17 (m, 1H), 4.11-4.17 (m, 1H), 4.20-4.27 (m, 2H), 4.33-4.39 (m, 1H), 4.39-4.44 (m, 1H), 4.56-4.61 (m, 1H), 6.59-6.68 (m, 4H), 6.75-7.50 (br s, 12H, interfering with the next seven listed signals), 6.90-6.93 (m, 1H), 6.97-7.01 (m, 4H), 7.02-7.04 (m, 1H), 7.06-7.08 (m, 1H), 7.11-7.12 (m, 1H), 7.29-7.31 (m, 1H), 7.38-7.39 (m, 1H), 7.54-7.63 (m, 4H), 7.76-7.83 (m, 2H), 7.91-7.96 (m, 1H), 8.01-8.08 (m, 2H), 8.13-8.18 (m, 1H), 9.18 (br s, 2H), 10.76 (s, 1H). HRMS (ESI): *m/z* $[M+3H]^{3+}$ calcd. for $[C_{49}H_{72}N_{17}O_9]^{3+}$ 347.5227, found: 347.5240. RP-HPLC (220 nm): 97% (t_R = 17.0 min, *k* = 4.3). $C_{49}H_{69}N_{17}O_9 \cdot C_6H_3F_9O_6$ (1040.20 + 342.07).

Arg-Tyr-Arg-Trp-Arg-Tyr-amide tetrakis(hydrotrifluoroacetate) (2.13). Peptide **2.13** was synthesized on a Sieber-amide-PS resin (40 mg, 0.65 mmol/g) according to the general procedure. Purification by preparative HPLC (system 1, gradient: 0-18 min MeCN/0.1% aq TFA 3:97 to 42:58, t_R = 13 min) yielded **2.13** as a white solid (9.6 mg, 32%). ^{1}H-NMR (600 MHz, DMSO-d_6): δ (ppm) 1.39-1.55 (m, 8H), 1.60-1.75 (m, 4H), 2.59-2.66 (m, 1H), 2.69-2.75 (m, 1H), 2.84-2.91 (m, 2H), 2.93-3.00 (m, 1H), 3.02-3.10 (m, 6H), 3.11-3.17 (m, 1H), 3.74-3.78 (m, 1H), 4.20-4.29 (m, 2H), 4.33-4.40 (m, 1H), 4.47-4.53 (m, 1H), 4.59-4.65 (m, 1H), 6.64 (d, 4H, *J* 8.3 Hz), 6.78-7.53 (br s, 12H, interfering with the next seven signals), 6.90-6.93 (m, 1H), 6.99-7.01 (m, 2H), 7.02-7.04 (m, 1H), 7.05-7.08 (m, 3H), 7.09-7.11 (m, 1H), 7.29-7.31 (m, 1H), 7.40-7.41 (m, 1H), 7.58 (d, 1H, *J* 8.1 Hz), 7.60-7.64 (m, 1H), 7.66-7.72 (m, 1H), 7.76-7.81 (m, 1H), 7.83 (d, 1H, *J* 7.8 Hz), 7.94 (d, 1H, *J* 7.6 Hz), 8.04-8.15 (m, 3H), 8.22 (d, 1H, *J* 7.6 Hz), 8.31 (d, 1H, *J* 7.9 Hz), 8.49 (d, 1H, *J* 7.6 Hz), 9.23 (br s, 2H), 10.76 (s, 1H). ^{13}C-NMR (150 MHz, DMSO-d_6): δ (ppm) 23.9, 24.8, 25.0, 27.9, 28.5, 29.1, 36.4, 38.9, 40.2, 40.5 (two carbon

atoms), 51.6, 52.3, 52.4, 53.0, 54.1, 54.4, 109.7, 111.2, 114.87 (two carbon atoms), 114.92 (two carbon atoms), 116.0 (TFA), 118.0 (TFA), 118.2, 118.5, 120.0, 123.5, 127.3, 127.5, 130.0 (two carbon atoms), 130.1 (two carbon atoms), 136.0, 155.84, 155.89, 156.77, 156.80, 156.84, 158.7 (q, *J* 32 Hz) (TFA), 168.5, 170.9, 171.0, 171.2, 171.3, 172.8. HRMS (ESI): *m/z* $[M+3H]^{3+}$ calcd. for $[C_{47}H_{70}N_{17}O_8]^{3+}$ 333.5192, found: 333.5206. RP-HPLC (220 nm): 96% (t_R = 16.0 min, *k* = 4.0). $C_{47}H_{67}N_{17}O_8 \cdot C_8H_4F_{12}O_8$ (998.16 + 456.09).

Cit-Tyr-Arg-Leu-Arg-Tyr-amide tetrakis(hydrotrifluoroacetate) (2.14). Peptide **2.14** was synthesized on a Sieber-amide-PS resin (40 mg, 0.59 mmol/g) according to the general procedure. Purification by preparative HPLC (system 1, gradient: 0-18 min MeCN/0.1% aq TFA 3:97 to 42:58, t_R = 12 min) yielded **2.14** as a white solid (10.4 mg, 35%). ^{1}H-NMR (600 MHz, DMSO-*d*$_6$): δ (ppm) 0.81-0.89 (m, 6H), 1.36-1.55 (m, 10H), 1.56-1.73 (m, 5H), 2.62-2.75 (m, 2H), 2.80-3.01 (m, 4H), 3.01-3.14 (m, 4H), 3.70-3.79 (m, 1H), 4.18-4.23 (m, 1H), 4.28-4.34 (m, 3H), 4.49-4.54 (m, 1H), 5.53 (br s, 2H), 6.13 (s, 1H), 6.60-6.66 (m, 4H), 6.80-7.20 (br s, 4H, interfering with the next two listed signals), 6.95-6.97 (m, 2H), 7.03-7.06 (m, 3H), 7.20-7.55 (br s, 4H, interfering with the next listed signal), 7.36-7.38 (m, 1H), 7.63-7.70 (m, 2H), 7.76-7.80 (m, 1H), 7.94-8.00 (m, 1H), 8.01-8.12 (m, 4H), 8.27-8.32 (m, 1H), 8.51-8.57 (m, 1H), 9.21 (br s, 2H). ^{13}C-NMR (150 MHz, DMSO-*d*$_6$): δ (ppm) 21.4, 23.1, 24.2, 24.9, 25.0, 25.6, 28.9, 29.0, 29.1, 36.6, 36.8, 38.5, 40.40, 40.43, 40.8, 50.9, 51.8, 52.0, 52.3, 53.9, 54.4, 114.87 (two carbon atoms), 114.94 (two carbon atoms), 115.8 (TFA), 117.8 (TFA), 127.46, 127.47, 130.0 (two carbon signals), 130.1 (two carbon atoms), 155.8, 155.9, 156.79, 156.83, 158.6 (q, *J* 32 Hz) (TFA), 159.1, 168.7, 170.8, 170.9, 171.0, 172.0, 172.7. HRMS (ESI): *m/z* $[M+3H]^{3+}$ calcd. for $[C_{42}H_{70}N_{15}O_9]^{3+}$ 309.5155, found: 309.5166. RP-HPLC (220 nm): 98% (t_R = 10.8 min, *k* = 2.4). $C_{42}H_{67}N_{15}O_9 \cdot C_8H_4F_{12}O_8$ (926.09 + 456.09).

Acetyl-Arg-Tyr-Cit-Leu-Arg-Tyr-amide tris(hydrotrifluoroacetate) (2.15). Peptide **2.15** was synthesized on a Sieber-amide-PS resin (40 mg, 0.65 mmol/g) according to the general procedure. Purification by preparative HPLC (system 1, gradient: 0-18 min MeCN/0.1% aq TFA 3:97 to 42:58, t_R = 13 min) yielded **2.15** as a white solid (14.4 mg, 42%). ^{1}H-NMR (600 MHz, DMSO-*d*$_6$): δ (ppm) 0.81-0.91 (m, 6H), 1.23-1.71 (m, 16H), 1.83 (s, 3H), 2.64-2.74 (m, 2H), 2.82-2.99 (m, 4H), 3.01-3.11 (m, 4H), 4.19-4.36 (m, 5H), 4.41-4.47 (m, 1H), 5.47 (br s, 2H), 6.05 (s, 1H), 6.58-6.65 (m, 4H), 6.73-7.20 (br s, 4H, interfering with the next two listed signals), 6.96-6.99 (m, 4H), 7.03-7.05 (m, 1H), 7.20-7.50 (br s, 4H, interfering with the next listed signal), 7.36-7.38 (m, 1H), 7.53-7.60 (m, 2H), 7.80 (t, 2H, *J* 8.4 Hz), 7.94-7.99 (m, 2H), 8.01-8.07 (m, 2H), 9.17 (br s, 2H). ^{13}C-NMR (150 MHz, DMSO-*d*$_6$): δ (ppm) 21.5, 22.4, 23.1, 24.1, 24.8, 25.0, 26.5, 28.9, 29.1, 29.4, 36.4, 36.8, 38.9, 40.4 (two carbon atoms), 40.6, 51.0, 52.13 (two carbon atoms), 52.17, 53.8, 53.9, 114.8 (two carbon atoms), 114.9 (two carbon atoms), 115.8 (TFA), 117.8 (TFA), 127.5 (two carbon atoms), 130.0 (two carbon atoms), 130.1 (two carbon atoms), 155.78, 155.80, 156.71, 156.72, 158.4 (q, *J* 32 Hz) (TFA), 159.0, 169.5,

170.8, 170.9, 171.3, 171.4, 171.9, 172.7. HRMS (ESI): *m/z* $[M+3H]^{3+}$ calcd. for $[C_{44}H_{72}N_{15}O_{10}]^{3+}$ 323.5190, found: 323.5202. RP-HPLC (220 nm): 97% (t_R = 16.0 min, k = 4.0). $C_{44}H_{69}N_{15}O_{10} \cdot C_6H_3F_9O_6$ (968.13 + 342.07).

Arg-Tyr-Arg-Leu-Cit-Tyr-amide tetrakis(hydrotrifluoroacetate) (2.16). Peptide **2.16** was synthesized on a Sieber-amide-PS resin (40 mg, 0.59 mmol/g) according to the general procedure. Purification by preparative HPLC (system 1, gradient: 0-18 min MeCN/0.1% aq TFA 3:97 to 42:58, t_R = 12 min) yielded **2.16** as a white solid (11.8 mg, 39%). ^{1}H-NMR (600 MHz, DMSO-d_6): δ (ppm) 0.82-0.90 (m, 6H), 1.24-1.38 (m, 2H), 1.39-1.77 (m, 14H), 2.64-2.74 (m, 2H), 2.82-2.99 (m, 4H), 3.07-3.13 (m, 4H), 3.77-3.79 (m, 1H), 4.18-4.22 (m, 1H), 4.25-4.36 (m, 3H), 4.51-4.56 (m, 1H), 5.46 (br s, 2H), 6.04 (s, 1H), 6.60-6.67 (m, 4H), 6.80-7.20 (br s, 4H, interfering with the next three listed signals), 6.96-6.99 (m, 2H), 7.03-7.04 (m, 1H), 7.05-7.07 (m, 2H), 7.20-7.55 (br s, 4H, interfering with the next listed signal), 7.33-7.35 (m, 1H), 7.65-7.69 (m, 1H), 7.72-7.75 (m, 1H), 7.77-7.80 (m, 1H), 7.95-7.99 (m, 1H), 8.02-8.06 (m, 1H), 8.06-8.14 (m, 3H), 8.34-8.38 (m, 1H), 8.49-8.53 (m, 1H), 9.21 (br s, 2H). ^{13}C-NMR (150 MHz, DMSO-d_6): δ (ppm) 21.6, 23.1, 24.0, 24.2, 25.1, 26.4, 28.6, 29.1, 36.6, 36.8, 38.8, 40.2, 40.5, 40.7, 50.9, 51.6, 52.2, 52.4, 53.9, 54.3, 114.87 (two carbon atoms), 114.93 (two carbon atoms), 115.8 (TFA), 117.8 (TFA), 127.4, 127.6, 130.06 (two carbon atoms), 130.11 (two carbon atoms), 155.8, 155.9, 156.8, 156.9, 157.7 (q, J 32 Hz) (TFA), 159.0, 168.5, 170.8, 171.0, 171.0, 171.1, 171.9, 172.7. HRMS (ESI): *m/z* $[M+3H]^{3+}$ calcd. for $[C_{42}H_{70}N_{15}O_9]^{3+}$ 309.5155, found: 309.5164. RP-HPLC (220 nm): 97% (t_R = 14.0 min, k = 3.4). $C_{42}H_{67}N_{15}O_9 \cdot C_8H_4F_{12}O_8$ (926.09 + 456.09).

Acetyl-Arg-Trp-Arg-Leu-Arg-Tyr-amide tris(hydrotrifluoroacetate) (2.17). Peptide **2.17** was synthesized on a Sieber-amide-PS resin (40 mg, 0.65 mmol/g) according to the general procedure. Purification by preparative HPLC (system 1, gradient: 0-18 min MeCN/0.1% aq TFA 3:97 to 42:58, t_R = 14 min) yielded **2.17** as a white solid (10.9 mg, 33%). ^{1}H-NMR (600 MHz, DMSO-d_6): δ (ppm) 0.81-0.91 (m, 6H), 1.32-1.72 (m, 15H), 1.81 (s, 3H), 2.69-2.75 (m, 1H), 2.83-2.89 (m, 1H), 2.97-3.10 (m, 7H), 3.12-3.17 (m, 1H), 4.12-4.16 (m, 1H), 4.18-4.42 (m, 4H), 4.50-4.55 (m, 1H), 6.64 (d, 2H, J 8.4 Hz), 6.72-7.48 (br s, 12H, interfering with the next five listed signals), 6.96-6.99 (m, 2H), 7.05-7.08 (m, 2H), 7.09-7.12 (m, 1H), 7.13-7.14 (m, 1H), 7.31-7.33 (m, 1H), 7.36-7.39 (m, 1H), 7.48-7.62 (m, 4H), 7.68-7.76 (m, 1H), 7.82-7.92 (m, 2H), 8.00-8.12 (m, 3H), 9.19 (br s, 1H), 10.81 (s, 1H). ^{13}C-NMR (150 MHz, DMSO-d_6): δ (ppm) 21.4, 22.4, 23.1, 24.1, 24.9, 25.0, 27.3, 28.6, 28.7, 28.8, 29.0, 36.8, 40.1, 40.4, 40.5, 40.7, 51.1, 52.3, 52.6, 53.3, 53.6, 54.0, 109.7, 111.3, 114.9 (two carbon atoms), 116.0 (TFA), 118.2, 118.3, 120.2, 123.6, 127.3, 127.5, 130.0 (two carbon atoms), 136.0, 155.8, 156.7 (three carbon atoms), 158.4 (q, J 32 Hz) (TFA), 170.0, 170.8, 171.2, 171.6, 171.7, 172.1, 172.7. HRMS (ESI):

m/z $[M+2H]^{2+}$ calcd. for $[C_{46}H_{73}N_{17}O_8]^{2+}$ 495.7909, found: 495.7912. RP-HPLC (220 nm): 96% (t_R = 15.9 min, *k* = 3.9). $C_{46}H_{71}N_{17}O_8 \cdot C_6H_3F_9O_6$ (990.19 + 342.07).

Acetyl-Arg-Phe-Arg-Leu-Arg-Tyr-amide tris(hydrotrifluoroacetate) (2.18). Peptide **2.18** was synthesized on a Sieber-amide-PS resin (40 mg, 0.65 mmol/g) according to the general procedure. Purification by preparative HPLC (system 1, gradient: 0-18 min MeCN/0.1% aq TFA 3:97 to 42:58, t_R = 13 min) yielded **2.18** as a white solid (13.5 mg, 40%). ^{1}H-NMR (600 MHz, DMSO-*d*$_6$): δ (ppm) 0.83-0.91 (m, 6H), 1.28-1.75 (m, 16H), 1.84 (s, 3H), 2.77-2.90 (m, 2H), 2.99-3.13 (m, 7H), 4.10-4.14 (m, 1H), 4.18-4.23 (m, 1H), 4.24-4.42 (m, 3H), 4.49-4.57 (m, 1H), 6.63 (d, 2H, *J* 8.4 Hz), 6.75-7.50 (br s, 12H, interfering with the next five signals), 6.97-6.99 (m, 1H), 7.06-7.07 (m, 1H), 7.09-7.13 (m, 1H), 7.18-7.24 (m, 5H), 7.37-7.40 (m, 1H), 7.55-7.65 (m, 3H), 7.69-7.77 (m, 1H), 7.83-7.89 (m, 1H), 7.89-7.96 (m, 1H), 8.01-8.09 (m, 2H), 8.09-8.15 (m, 1H), 9.24 (br s, 1H). ^{13}C-NMR (150 MHz, DMSO-*d*$_6$): δ (ppm) 21.4, 22.5, 23.1, 24.1, 24.9, 25.0, 28.6, 28.7, 28.9, 36.7, 37.1, 40.3, 40.4, 40.5, 40.7, 51.0, 51.1, 52.6, 53.5, 53.6, 53.9, 114.9 (two carbon atoms), 116.0 (TFA), 118.0 (TFA), 126.3, 127.5, 128.0 (two carbon atoms), 129.2 (two carbon atoms), 129.5, 130.0 (two carbon atoms), 155.8, 156.7 (three carbon atoms), 158.6 (q, *J* 32 Hz) (TFA), 169.9, 170.8, 170.9, 171.1, 171.4, 172.6, 172.7. HRMS (ESI): *m/z* $[M+2H]^{2+}$ calcd. for $[C_{44}H_{72}N_{16}O_8]^{2+}$ 476.2854, found: 476.2856. RP-HPLC (220 nm): 98% (t_R = 15.5 min, *k* = 3.8). $C_{44}H_{70}N_{16}O_8 \cdot C_6H_3F_9O_6$ (951.15 + 342.07).

Acetyl-Arg-Gly-Arg-Leu-Arg-Tyr-amide tris(hydrotrifluoroacetate) (2.19). Peptide **2.19** was synthesized on a Sieber-amide-PS resin (40 mg, 0.65 mmol/g) according to the general procedure. Purification by preparative HPLC (system 1, gradient: 0-18 min MeCN/0.1% aq TFA 3:97 to 42:58, t_R = 11 min) yielded **2.19** as a white solid (7.2 mg, 23%). ^{1}H-NMR (600 MHz, DMSO-*d*$_6$): δ (ppm) 0.79-0.90 (m, 6H), 1.40-1.56 (m, 10H), 1.57-1.75 (m, 4H), 1.85-1.88 (m, 3H), 2.68-2.74 (m, 1H), 2.83-2.90 (m, 1H), 3.01-3.13 (m, 6H), 3.68-3.70 (m, 1H), 3.74-3.79 (m, 1H), 4.13-4.21 (m, 2H), 4.22-4.29 (m, 2H), 4.29-4.34 (m, 1H), 6.63-6.61 (m, 2H), 6.80-7.55 (br s, 12H, interfering with the next four listed signals), 6.96-6.99 (m, 2H), 7.05-7.07 (m, 1H), 7.09-7.13 (m, 1H), 7.34-7.37 (m, 1H), 7.58-7.68 (m, 2H), 7.68-7.76 (m, 2H), 7.87-7.95 (m, 2H), 7.95-8.01 (m, 1H), 8.16-8.21 (m, 1H), 8.29-8.35 (m, 1H), 9.25 (br s, 1H). ^{13}C-NMR (150 MHz, DMSO-*d*$_6$): δ (ppm) 21.4, 22.4, 23.1, 24.1, 24.9, 25.0, 25.1, 28.6, 28.9, 29.0, 36.8, 40.4 (two carbon atoms), 40.4 (two carbon atoms), 42.1, 51.1, 52.3, 52.3, 52.8, 54.0, 114.9 (two carbon atoms), 115.9 (TFA), 117.9 (TFA), 127.5, 130.0 (two carbon atoms), 155.8, 156.7, 156.76, 156.79, 158.8 (q, *J* 32 Hz) (TFA), 169.0, 170.1, 170.9, 171.3, 172.1, 172.2, 172.7. HRMS (ESI): *m/z* $[M+2H]^{2+}$ calcd. for $[C_{37}H_{66}N_{16}O_8]^{2+}$ 431.2619, found: 431.2625. RP-HPLC (220 nm): 97% (t_R = 9.0 min, *k* = 1.8). $C_{37}H_{64}N_{16}O_8 \cdot C_6H_3F_9O_6$ (861.02 + 342.07).

***N*$^{\alpha}$-Succinyl-Arg-Tyr-Arg-Leu-Arg-Tyr-amide tris(hydrotrifluoroacetate) (2.20).** Peptide **2.20** was synthesized on a Sieber-amide-PS resin (40 mg, 0.65 mmol/g) according to the

general procedure. After coupling of the last amino acid and subsequent Fmoc deprotection, the resin was treated with a solutution of succinic anhydride (27.9 mg, 0.236 mmol) and DIPEA (41.1 µL, 0.236 mmol) in DMF/NMP 80:20 v/v (500 µL) at 35 °C for 30 min. The resin was washed with DMF/NMP 80:20 v/v (6×) and CH_2Cl_2 (3×), followed by cleavage off the resin and deprotection according to the general procedure. Purification by preparative HPLC (system 1, gradient: 0-18 min MeCN/0.1% aq TFA 3:97 to 42:58, t_R = 13 min) yielding **2.20** as a white solid (11.0 mg, 37%). ^{1}H-NMR (600 MHz, DMSO-*d*$_6$): δ (ppm) 0.81-0.90 (m, 6H), 1.34-1.57 (m, 11H), 1.57-1.67 (m, 3H), 1.67-1.76 (m, 1H), 2.34-2.47 (m, 4H), 2.67-2.76 (m, 2H), 2.83-2.95 (m, 2H), 2.98-3.13 (m, 6H), 4.11-4.17 (m, 1H), 4.17-4.23 (m, 1H), 4.24-4.35 (m, 3H), 4.38-4.45 (m, 1H), 6.60-6.68 (m, 4H), 6.75-7.55 (br s, 12H, interfering with the next four listed signals, 6.96-7.00 (m, 4H), 7.05-7.07 (m, 1H), 7.09-7.13 (m, 1H), 7.35-7.37 (m, 1H), 7.56-7.66 (m, 3H), 7.69-7.73 (m, 1H), 7.73-7.78 (m, 1H), 7.84-7.89 (m, 1H), 7.99-8.05 (m, 1H), 8.06-8.11 (m, 1H), 8.12-8.17 (m, 1H), 9.31 (br s, 2H). ^{13}C-NMR (150 MHz, DMSO-*d*$_6$): δ (ppm) 21.4, 23.1, 24.1, 24.9, 24.99, 25.02, 28.7, 28.95, 28.96, 29.1, 29.9, 36.3, 36.8, 40.39, 40.41, 40.43, 40.6, 51.0, 52.1, 52.3, 52.6, 54.0, 54.1, 114.86 (two carbon atoms), 114.88 (two carbon atoms), 115.5 (TFA), 117.5 (TFA), 127.49, 127.51, 130.04 (two carbon atoms), 130.07 (two carbon atoms), 155.82, 155.85, 156.8 (three carbon atoms), 158.7 (q, *J* 33 Hz) (TFA), 170.9, 171.11, 171.14, 171.4, 171.8, 172.0, 172.7, 174.0. HRMS (ESI): *m/z* $[M+3H]^{3+}$ calcd. for $[C_{46}H_{75}N_{16}O_{11}]^{3+}$ 342.5262, found: 342.5273. RP-HPLC (220 nm): 97% (t_R = 15.0 min, *k* = 3.7). $C_{46}H_{72}N_{16}O_{11} \cdot C_6H_3F_9O_6$ (1053.24 + 342.07).

Acetyl-Arg-Arg-Leu-Arg-Tyr-amide tris(hydrotrifluoroacetate) (2.21). Peptide **2.21** was synthesized on a Sieber-amide-PS resin (40 mg, 0.65 mmol/g) according to the general procedure. Purification by preparative HPLC (system 1, gradient: 0-18 min MeCN/0.1% aq TFA 3:97 to 42:58, t_R = 11 min) yielded **2.21** as a white solid (6.8 mg, 23%). ^{1}H-NMR (600 MHz, DMSO-*d*$_6$): δ (ppm) 0.80-0.84 (m, 3H), 0.85-0.89 (m, 3H), 1.38-1.56 (m, 11H), 1.56-1.73 (m, 4H), 1.86 (s, 3H), 2.69-2.75 (m, 1H), 2.82-2.90 (m, 1H), 3.03-3.12 (m, 6H), 4.17-4.30 (m, 4H), 4.30-4.35 (m, 1H), 6.60-6.66 (m, 2H), 6.75-7.50 (br s, 12H, interfering with the next four listed signals), 6.96-6.98 (m, 2H), 7.05-7.07 (m, 1H), 7.09-7.14 (m, 1H), 7.36-7.38 (m, 1H), 7.59-7.63 (m, 2H), 7.75-7.79 (m, 1H), 7.85-7.91 (m, 1H), 7.98-8.03 (m, 1H), 8.04-8.14 (m, 2H), 9.19 (br s, 1H). HRMS (ESI): *m/z* $[M+2H]^{2+}$ calcd. for $[C_{35}H_{63}N_{15}O_7]^{2+}$ 405.7512, found: 402.7518. RP-HPLC (220 nm): 97% (t_R = 7.7 min, *k* = 1.4). $C_{35}H_{61}N_{15}O_7 \cdot C_6H_3F_9O_6$ (803.97 + 342.07).

Trp-Arg-Leu-Arg-Tyr-amide tris(hydrotrifluoroacetate) (2.22). Peptide **2.22** was synthesized on a Sieber-amide-PS resin (60 mg, 0.59 mmol/g) according to the general procedure. Purification by preparative HPLC (system 2, gradient: 0-18 min MeCN/0.1% aq TFA 3:97 to 42:58, t_R = 12 min) yielded **2.22** as a white solid (11.8 mg, 37%). ^{1}H-NMR (600

MHz, DMSO-d_6): δ (ppm) 0.82-0.91 (m, 6H), 1.38-1.61 (m, 8H), 1.61-1.68 (m, 2H), 1.68-1.77 (m, 1H), 2.69-2.75 (m, 1H), 2.82-2.88 (m, 1H), 2.97-3.04 (m, 1H), 3.04-3.15 (m, 4H), 3.19-3.25 (m, 1H), 4.03-4.09 (m, 1H), 4.19-4.25 (m, 1H), 4.30-4.37 (m, 2H), 4.38-4.43 (m, 1H), 6.63 (d, 2H, *J* 8.3 Hz), 6.80-7.20 (br s, 4H, interfering with the next four listed signals), 6.96-6.98 (m, 2H), 6.99-7.02 (m, 1H), 7.05-7.07 (m, 1H), 7.09-7.11 (m, 1H), 7.20-7.55 (br s, 4H, interfering with the next two listed signals), 7.20-7.22 (m, 1H), 7.36-7.40 (m, 2H), 7.60-7.64 (m, 1H), 7.68-7.73 (m, 2H), 7.78 (d, 1H, *J* 7.8 Hz), 7.95-8.16 (m, 3H), 8.07 (d, 1H, *J* 7.7 Hz), 8.13 (d, 1H, *J* 7.8 Hz), 8.84 (d, 1H, *J* 7.9 Hz), 9.19 (br s, 1H), 11.01 (s, 1H). ^{13}C-NMR (150 MHz, DMSO-d_6): δ (ppm) 21.4, 23.1 24.2, 24.9, 25.0, 27.5, 29.0, 29.3, 36.8, 40.4 (two carbon atoms), 40.7, 51.0, 52.27 (two carbon atoms), 52.33, 53.9, 106.6, 111.5, 114.9 (two carbon atoms), 116.0 (TFA), 118.0 (TFA), 118.4, 118.5, 121.2, 125.1, 127.0, 127,4, 130.0 (two carbon atoms), 136.4, 155.8, 156.72, 156.79, 158.3 (q, *J* 32 Hz) (TFA), 168.5, 170.7, 170.8, 172.0, 172.6. HRMS (ESI): *m/z* $[M+2H]^{2+}$ calcd. for $[C_{38}H_{59}N_{13}O_6]^{2+}$ 396.7350, found: 396.7362. RP-HPLC (220 nm): 99% (t_R = 18.1 min, *k* = 4.6). $C_{38}H_{57}N_{13}O_6 \cdot C_6H_3F_9O_6$ (791.96 + 342.07).

Acetyl-Arg-Gly-Tyr-Arg-Leu-Arg-Tyr-amide tris(hydrotrifluoroacetate) (2.23). Peptide **2.23** was synthesized on a Sieber-amide-PS resin (40 mg, 0.65 mmol/g) according to the general procedure. Purification by preparative HPLC (system 1, gradient: 0-18 min MeCN/0.1% aq TFA 3:97 to 42:58, t_R = 12 min) yielded **2.23** as a white solid (25.0 mg, 70%). ^{1}H-NMR (600 MHz, DMSO-d_6): δ (ppm) 0.81-0.91 (m, 6H), 1.37-1.58 (m, 11H), 1.58-1.68 (m, 3H), 1.70-1.75 (m, 1H), 1.83-1.88 (m, 3H), 2.60-2.68 (m, 1H), 2.69-2.76 (m, 1H), 2.81-2.92 (m, 2H), 3.01-3.14 (m, 6H), 3.51-3.57 (m, 1H), 3.73-3.79 (m, 1H), 4.18-4.22 (m, 2H), 4.25-4.34 (m, 3H), 4.42-4.47 (m, 1H), 6.59-6.67 (m, 4H), 6.80-7.50 (br s, 12H, interfering with the next four listed signals), 6.96-7.01 (m, 4H), 7.05-7.06 (m, 1H), 7.10-7.13 (m, 1H); 7.35-7.37 (m, 1H), 7.56-7.69 (m, 3H), 7.73-7.79 (m, 1H), 7.86-7.91 (m, 1H), 7.91-7.97 (m, 1H), 8.01-8.04 (m, 1H), 8.10-8.14 (m, 1H), 8.17-8.25 (m, 2H), 9.22 (br s, 1H). ^{13}C-NMR (150 MHz, DMSO-d_6): δ (ppm) 21.40, 21.43, 23.1, 24.1, 24.47, 24.49, 24.9, 25.1, 28.9, 29.0, 36.71, 36.79, 40.36, 40.39, 40.43, 40.7, 41.8, 51.0, 52.2, 52.3, 52.5, 54.0, 54.3, 114.9 (four carbon atoms), 115.7 (TFA), 117.7 (TFA), 127.5, 127.7, 130.0 (four carbon atoms), 155.81, 155.83, 156,75, 156.79 (two carbon atoms), 158.7 (q, *J* 32 Hz) (TFA), 168.6, 168.8, 169.8, 170.9, 171.2, 171.4, 172.0, 172.7. HRMS (ESI): *m/z* $[M+3H]^{3+}$ calcd. for $[C_{46}H_{76}N_{17}O_{10}]^{3+}$ 342.1982, found: 342.1996. RP-HPLC (220 nm): 97% (t_R = 16.4 min, *k* = 4.1). $C_{46}H_{73}N_{17}O_{10} \cdot C_6H_3F_9O_6$ (1024.20 + 342.07).

Acetyl-Arg-GABA-Gly-Tyr-Arg-Leu-Arg-Tyr-amide tris(hydrotrifluoroacetate) (2.24). Peptide **2.24** was synthesized on a Sieber-amide-PS resin (40 mg, 0.65 mmol/g) according to the general procedure. Purification by preparative HPLC (system 1, gradient: 0-18 min MeCN/0.1% aq TFA 3:97 to 42:58, t_R = 13 min) yielded **2.24** as a white solid (12.7 mg, 34%). ^{1}H-NMR (600 MHz, DMSO-d_6): δ (ppm) 0.82-0.90 (m, 6H), 1.35-1.56 (m, 11H), 1.56-1.74 (m,

6H), 1.81-1.88 (m, 3H), 2.07-2.12 (m, 2H), 2.60-2.67 (m, 1H), 2.69-2.75 (m, 1H), 2.83-2.90 (m, 2H), 3.00-3.13 (m, 8H), 3.52-3.58 (m, 1H), 3.69-3.75 (m, 1H), 4.16-4.24 (m, 2H), 4.24-4.35 (m, 3H), 4.43-4.48 (m, 1H), 6.59-6.67 (m, 4H), 6.73-7.54 (br s, 12H, interfering with the next four listed signals), 6.96-7.01 (m, 4H), 7.05-7.06 (m, 1H), 7.09-7.12 (m, 1H), 7.35-7.37 (m, 1H), 7.59-7.64 (m, 2H), 7.65-7.69 (m, 1H), 7.74-7.78 (m, 1H), 7.87-7.91 (m, 1H), 7.96-8.04 (m, 4H), 8.19-8.26 (m, 1H), 9.24 (br s, 2H). ^{13}C-NMR (150 MHz, DMSO-*d*$_6$): δ (ppm) 21.4, 22.5, 23.1, 24.1, 24.9, 25.1, 25.16, 25.22, 28.9, 29.0, 29.3, 32.5, 36.7, 36.8, 38.1, 40.36 (two carbon atoms), 40.42, 40.7, 41.8, 51.0, 52.1, 52.2, 52.3, 54.0, 54.1, 114.9 (four carbon atoms), 115.6 (TFA), 117.6 (TFA), 127.5, 127.6, 130.0 (two carbon atoms), 130.1 (two carbon atoms), 155.8 (two carbon atoms), 156.7, 156.8 (two carbon atoms), 158.7 (q, *J* 33 Hz) (TFA), 168.9, 169.4, 170.8, 171.1, 171.3, 171.4, 172.0, 172.3, 172.7. HRMS (ESI): *m/z* $[M+3H]^{3+}$ calcd. for $[C_{50}H_{83}N_{18}O_{11}]^{3+}$ 370.5491, found: 370.5503. RP-HPLC (220 nm): 96% (t_R = 16.3 min, *k* = 4.1). $C_{50}H_{80}N_{18}O_{11} \cdot C_6H_3F_9O_6$ (1109.31 + 342.07).

Acetyl-Arg-Gly-Tyr-Arg-Leu-Arg-Tyr-amide tris(hydrotrifluoroacetate) (2.25). Peptide **2.25** was synthesized on Sieber-amide-PS resin (40 mg, 0.65 mmol/g) according to the general procedure. Purification by preparative HPLC (system 1, gradient: 0-18 min MeCN/0.1% aq TFA 3:97 to 42:58, t_R = 12 min) yielded **2.25** as a white solid (16.5 mg, 44%). ^{1}H-NMR (600 MHz, DMSO-*d*$_6$): δ (ppm) 1.35-1.56 (m, 9H), 1.58-1.68 (m, 3H), 1.85 (s, 3H), 2.58-2.64 (m, 1H), 2.68-2.74 (m, 1H), 2.80-2.90 (m, 2H), 2.93-2.99 (m, 1H), 3.00-3.10 (m, 6H), 3.10-3.17 (m, 1H), 3.51-3.53 (m, 1H), 3.72-3.77 (m, 1H), 4.16-4.27 (m, 3H), 4.32-4.37 (m, 1H), 4.39-4.45 (m, 1H), 4.54-4.59 (m, 1H), 6.58-6.66 (m, 4H), 6.75-7.50 (br s, 12H, interfering with the next six listed signals), 6.89-6.92 (m, 1H), 6.97-7.03 (m, 6H), 7.05-7.07 (m, 1H), 7.11-7.12 (m, 1H), 7.28-7.30 (m, 1H), 7.36-7.38 (m, 1H), 7.54-7.60 (m, 3H), 7.62-7.67 (m, 1H), 7.78-7.82 (m, 1H), 7.88-7.96 (m, 2H), 8.11-8.19 (m, 3H), 9.18 (br s, 2H), 10.74 (s, 1H). ^{13}C-NMR (150 MHz, DMSO-*d*$_6$): δ (ppm) 22.5, 24.8, 25.0, 25.1, 27.7, 28.8, 29.0, 29.1, 36.6, 36.8, 40.3, 40.39, 40.44, 41.7, 52.2, 52.42, 52.44, 53.2, 54.1, 54.3, 109.8, 111.2, 114.8 (two carbon atoms), 114.9 (two carbon atoms), 116.0 (TFA), 118.0 (TFA), 118.2, 118.5, 120.8, 123.5, 127.3, 127.6, 127.8, 130.0 (two carbon atoms), 130.1 (two carbon atoms), 155.7, 155.8, 156.8 (three carbon atoms), 158.7 (q, *J* 32 Hz) (TFA), 168.6, 169.8, 170.9, 171.2, 171.37, 171.42, 172.0, 172.8. HRMS (ESI): *m/z* $[M+3H]^{3+}$ calcd. for $[C_{51}H_{75}N_{18}O_{10}]^{3+}$ 366.5299, found: 366.5320. RP-HPLC (220 nm): 96% (t_R = 14.1 min, *k* = 3.4). $C_{51}H_{72}N_{18}O_{10} \cdot C_6H_3F_9O_6$ (1097.25 + 342.07).

Acetyl-Arg-Gly-Tyr-Arg-Trp-Arg-Trp-amide tris(hydrotrifluoroacetate) (2.26). Peptide **2.26** was synthesized on a Sieber-amide-PS resin (40 mg, 0.65 mmol/g) according to the general procedure. Purification by preparative HPLC (system 1, gradient: 0-18 min MeCN/0.1% aq TFA 3:97 to 42:58, t_R = 15 min) yielded **2.26** as a white solid (14.1 mg, 41%). ^{1}H-NMR (600 MHz, DMSO-*d*$_6$): δ (ppm) 1.35-1.55 (m, 10H), 1.60-1.69 (m, 3H), 1.85 (s, 3H),

2.80-2.85 (m, 1H), 2.95-3.01 (m, 2H), 3.02-3.09 (m, 6H), 3.11-3.16 (m, 2H), 3.51-3.54 (m, 1H), 3.73-3.79 (m, 1H), 4.17-4.22 (m, 1H), 4.23-4.29 (m, 2H), 4.41-4.46 (m, 1H), 4.47-4.52 (m, 1H), 4.57-4.62 (m, 1H), 6.60-6.64 (m, 2H), 6.70-7.50 (br s, 12H, interfering with the next seven listed signals), 6.89-6.91 (m, 1H), 6.95-6.98 (m, 1H), 6.99-7.07 (m, 5H), 7.11-7.13 (m, 2H), 7.28-7.32 (m, 2H), 7.41-7.44 (m, 1H), 7.45-7.50 (m, 2H), 7.51-7.54 (m, 1H), 7.54-7.61 (m, 2H), 7.87-7.97 (m, 3H), 8.08-8.21 (m, 4H), 9.18 (s, 1H), 10.71-10.75 (m, 1H), 10.76-10.80 (m, 1H). HRMS (ESI): *m/z* $[M+3H]^{3+}$ calcd. for $[C_{53}H_{76}N_{19}O_9]^{3+}$ 374.2019, found: 374.2034. RP-HPLC (220 nm): 98% (t_R = 17.0 min, k = 4.3). $C_{53}H_{73}N_{19}O_9 \cdot C_6H_3F_9O_6$ (1120.29 + 342.07).

Acetyl-Arg-Gly-Tyr-Arg-Leu-Arg-Trp-amide tris(hydrotrifluoroacetate) (2.27). Peptide **2.27** was synthesized on a Sieber-amide-PS resin (40 mg, 0.65 mmol/g) according to the general procedure. Purification by preparative HPLC (system 1, gradient: 0-18 min MeCN/0.1% aq TFA 3:97 to 42:58, t_R = 14 min) yielded **2.27** as a white solid (14.1 mg, 40%). ^{1}H-NMR (600 MHz, DMSO-d_6): δ (ppm) 0.78-0.88 (m, 6H), 1.37-1.56 (m, 11H), 1.59-1.73 (m, 4H), 1.84-1.87 (m, 3H), 2.61-2.67 (m, 1H), 2.83-2.90 (m, 1H), 2.95-3.00 (m, 1H), 3.03-3.13 (m, 7H), 3.51-3.56 (m, 1H), 3.73-3.79 (m, 1H), 4.17-4.33 (m, 4H), 4.40-4.49 (m, 2H), 6.59-6.65 (m, 2H), 6.70-7.50 (br s, 12H, interfering with the next six signals), 6.95-6.97 (m, 1H), 6.99-7.01 (m, 2H), 7.04-7.06 (m, 2H), 7.10-7.11 (m, 1H), 7.30-7.32 (m, 1H), 7.37-7.39 (m, 1H), 7.54-7.63 (m, 4H), 7.82-7.89 (m, 2H), 7.91-7.97 (m, 1H), 8.00-8.04 (m, 1H), 8.09-8.14 (m, 1H), 8.16-8.25 (m, 2H), 9.21 (br s, 1H), 10.78 (s. 1H). ^{13}C-NMR (150 MHz, DMSO-d_6): δ (ppm) 21.4, 22.5, 23.1, 24.1, 24.9, 25.0 (two carbon atoms), 27.8, 28.9 (two carbon atoms), 29.0, 36.7, 40.36, 40.38, 40.44, 40.7, 41.8, 51.0, 52.2, 52.3, 52.4, 53.2, 54.2, 109.8, 111.2, 114.9 (two carbon atoms), 116.0 (TFA), 118.0 (TFA), 118.2, 118.4, 120.8, 123.5, 127.4, 127.7, 130.1 (two carbon atoms), 136.0, 155.8, 156.7 (three carbon atoms), 158.5 (q, J 32 Hz) (TFA), 168.6, 169.8, 171.0, 171.1, 171.4, 172.00, 172.03, 173.07. HRMS (ESI): *m/z* $[M+2H]^{2+}$ calcd. for $[C_{48}H_{76}N_{18}O_9]^{2+}$ 524.3016, found: 524.3043. RP-HPLC (220 nm): 96% (t_R = 17.1 min, k = 4.3). $C_{48}H_{74}N_{18}O_9 \cdot C_6H_3F_9O_6$ (1047.24 + 342.07).

Acetyl-Arg-GABA-Tyr-Arg-Trp-Arg-Tyr-amide tris(hydrotrifluoroacetate) (2.28). Peptide **2.28** was synthesized on a Sieber-amide-PS resin (40 mg, 0.65 mmol/g) according to the general procedure. Purification by preparative HPLC (system 1, gradient: 0-18 min MeCN/0.1% aq TFA 3:97 to 42:58, t_R = 13 min) yielded **2.28** as a white solid (11.3 mg, 30%). ^{1}H-NMR (600 MHz, DMSO-d_6): δ (ppm) 1.34-1.55 (m, 12H), 1.58-1.68 (m, 3H), 1.83-1.86 (s, 3H), 1.99-2.05 (m, 2H), 2.56-2.61 (m, 1H), 2.69-2.74 (m, 1H), 2.80-2.85 (m, 1H), 2.85-2.90 (m, 1H), 2.91-2.99 (m, 3H), 3.03-3.10 (m, 6H), 3.11-3.17 (m, 1H), 4.14-4.20 (m, 1H), 4.20-4.28 (m, 2H), 4.34-4.38 (m, 1H), 4.38-4.44 (m, 1H), 4.56-4.61 (m, 1H), 6.59-6.65 (m, 4H), 6.75-7.48 (br s, 12 H, interfering with the next six listed signals), 6.91-6.93 (m, 1H), 6.99-7.03 (m, 5H), 7.06-7.08 (m, 1H), 7.11-7.12 (m, 1H), 7.29-7.31 (m, 1H), 7.37-7.40 (m, 1H), 7.53-7.59 (m, 3H), 7.62-

7.66 (m, 1H), 7.78-7.83 (m, 1H), 7.91-7.93 (m, 1H), 7.95-7.98 (m, 1H), 8.00-8.04 (m, 1H), 8.11-8.19 (m, 2H), 9.18 (br s, 2H), 10.76 (s, 1H). ^{13}C-NMR (150 MHz, DMSO-d_6): δ (ppm) 22.5, 24.8, 24.9, 25.2, 25.3, 27.7, 29.08, 29.10, 29.2, 32.6, 36.5, 36.8, 38.1, 40.36, 40.40, 40.43, 52.15, 52.18, 52.4, 53.1, 54.1, 54.2, 109.8, 111.2, 114.8 (two carbon atoms), 114.9 (two carbon atoms), 116.1 (TFA), 118.1 (TFA), 118.2, 118.5, 120.8, 123.5, 127.3, 127.6, 128.0, 130.0 (two carbon atoms), 130.1 (two carbon atoms), 136.0, 155.7, 155.8, 156.7 (three carbon atoms), 158.5 (q, *J* 32 Hz) (TFA), 169.4, 170.9, 171.2, 171.4 (two carbon atoms), 171.8, 171.9, 172.8. HRMS (ESI): *m/z* $[M+3H]^{3+}$ calcd. for $[C_{53}H_{79}N_{18}O_{10}]^{3+}$ 375.8737, found: 375.8760. RP-HPLC (220 nm): 96% (t_R = 14.5 min, *k* = 3.5). $C_{53}H_{76}N_{18}O_{10} \cdot C_6H_3F_9O_6$ (1125.31 + 342.07).

Arg-Leu-Arg-Tyr-amide tris(hydrotrifluoroacetate) (2.29). Peptide **2.29** was synthesized on a Sieber-amide-PS resin (40 mg, 0.65 mmol/g) according to the general procedure. Purification by preparative HPLC (system 1, gradient: 0-18 min MeCN/0.1% aq TFA 3:97 to 42:58, t_R = 10 min) yielded **2.29** as a white solid (8.4 mg, 34%). ^{1}H-NMR (600 MHz, DMSO-d_6): δ (ppm) 0.83-0.92 (m, 6H), 1.37-1.57 (m, 7H), 1.61-1.74 (m, 4H), 2.69-2.75 (m, 1H), 2.82-2.87 (m, 1H), 3.03-3.14 (m, 4H), 3.80-3.83 (m, 1H), 4.17-4.22 (m, 1H), 4.31-4.37 (m, 2H), 6.61-6.65 (m, 2H), 6.80-7.20 (br s, 4H, interfering with the next two listed signals), 6.95-6.99 (m, 2H), 7.05-7.08 (m, 1H), 7.20-7.55 (br s, 4H, interfering with the next listed signal), 7.39-7.41 (m, 1H), 7.67-7.72 (m, 1H), 7.72-7.79 (m, 2H), 8.14-8.23 (m, 4H), 8.47-8.54 (m, 1H), 9.22 (br s, 1H). ^{13}C-NMR (150 MHz, DMSO-d_6): δ (ppm) 21.3, 23.1, 24.0 (two carbon atoms), 25.0, 28.4, 28.9, 36.8, 40.2, 40.5, 40.6, 51.2, 51.7, 52.5, 53.8, 114.9 (two carbon atoms), 115.9 (TFA), 117.9 (TFA), 127.4, 130.0 (two carbon atoms), 155.8, 156.8, 156.9, 158.7 (q, *J* 32 Hz) (TFA), 168.3, 170.8, 171.7, 172.7.HRMS (ESI): *m/z* $[M+2H]^{2+}$ calcd. for $[C_{27}H_{49}N_{11}O_5]^{2+}$ 303.6954, found: 303.6964. RP-HPLC (220 nm): 98% (t_R = 5.9 min, *k* = 0.8). $C_{27}H_{47}N_{11}O_5 \cdot C_6H_3F_9O_6$ (605.75 + 342.07).

Arg-Trp-Arg-Tyr-amide tris(hydrotrifluoroacetate) (2.30). Peptide **2.30** was synthesized on a Sieber-amide-PS resin (40 mg, 0.65 mmol/g) according to the general procedure. Purification by preparative HPLC (system 1, gradient: 0-18 min MeCN/0.1% aq TFA 3:97 to 42:58, t_R = 12 min) yielded **2.30** as a white solid (7.9 mg, 30%). ^{1}H-NMR (600 MHz, DMSO-d_6): δ (ppm) 1.40-1.58 (m, 5H), 1.64-1.76 (m, 3H), 2.70-2.77 (m, 1H), 2.86-2.91 (m, 1H), 2.92-2.98 (m, 1H), 3.05-3.13 (m, 4H), 3.16-3.20 (m, 1H), 3.73-3.78 (m, 1H), 4.21-4.25 (m, 1H), 4.36-4.41 (m, 1H), 4.62-4.67 (m, 1H), 6.62-6.66 (m, 2H), 6.80-7.20 (br s, 4H, interfering with the next four listed signals), 6.95-6.97 (m, 1H), 6.99-7.01 (m, 2H), 7.05-7.09 (m, 2H), 7.16-7.18 (m, 1H), 7.20-7.50 (br s, 4H, interfering with the next two listed signals), 7.32-7.34 (m, 1H), 7.42-7.44 (m, 1H), 7.61-7.65 (m, 1H), 7.67-7.72 (m, 2H), 7.77-7.81 (m, 1H), 8.05-8.12 (m, 3H), 8.36-8.41 (m, 1H), 8.54-8.59 (m, 1H), 9.20 (s, 1H), 10.82-10.87 (m, 1H). HRMS (ESI): *m/z* $[M+2H]^{2+}$ calcd. for $[C_{32}H_{48}N_{12}O_5]^{2+}$ 340.1930, found: 340.1940. RP-HPLC (220 nm): 97% (t_R = 9.4 min, *k* = 1.9). $C_{32}H_{46}N_{12}O_5 \cdot C_6H_3F_9O_6$ (678.80 + 342.07).

***D*-Arg-Leu-Arg-Tyr-amide tris(hydrotrifluoroacetate) (2.31).** Peptide **2.31** was synthesized on a Sieber-amide-PS resin (100 mg, 0.59 mmol/g) according to the general procedure. Purification by preparative HPLC (system 1, gradient: 0-30 min MeCN/0.1% aq TFA 8:92 to 45:58, t_R = 9 min) yielded **2.31** as a white solid (12.1 mg, 21%). ^{1}H-NMR (600 MHz, DMSO-d_6): δ (ppm) 0.82-0.89 (m, 6H), 1.37-1.58 (m, 8H), 1.62-1.68 (m, 1H), 1.69-1.74 (m, 2H), 2.70-2.74 (m, 1H), 2.82-2.87 (m, 1H), 3.04-3.10 (m, 2H), 3.10-3.15 (m, 2H), 3.81-3.87 (m, 1H), 4.17-4.23 (m, 1H), 4.32-4.37 (m, 1H), 4.40-4.45 (m, 1H), 6.61-6.65 (m, 2H), 6.90-7.60 (br s, 8H, interfering with the next three listed signals), 6.96-7.00 (m, 2H), 7.07 (s, 1H), 7.40 (s, 1H), 7.69-7.75 (m, 2H), 7.88 (t, 1H, *J* 11.6 Hz), 8.12-8.21 (m, 3H), 8.31 (d, 1H, *J* 7.7 Hz), 8.65 (d, 1H, *J* 8.4 Hz), 9.20 br s, 1H). ^{13}C-NMR (150 MHz, DMSO-d_6): δ (ppm) 21.2, 23.1, 24.1, 24.2, 25.1, 28.5, 28.9, 36.9, 40.0, 40.5, 41.1, 50.9, 51.8, 52.5, 53.8, 114.8 (two carbon atoms), 127.5, 130.1 (two carbon atoms), 155.8, 156.8, 156.9, 168.1, 170.7, 171.6, 172.7. HRMS (ESI): *m/z* $[M+2H]^{2+}$ calcd. for $[C_{27}H_{49}N_{11}O_5]^{2+}$ 303.6954, found: 303.6965. RP-HPLC (220 nm): 98% (t_R = 8.8 min, *k* = 1.7). $C_{27}H_{47}N_{11}O_5 \cdot C_6H_3F_9O_6$ (605.75 + 342.07).

Arg-*D*-Leu-Arg-Tyr-amide tris(hydrotrifluoroacetate) (2.32). Peptide **2.32** was synthesized on a Sieber-amide-PS resin (100 mg, 0.59 mmol/g) according to the general procedure. Purification by preparative HPLC (system 1, gradient: 0-30 min MeCN/0.1% aq TFA 8:92 to 45:58, t_R = 9 min) yielded **2.32** as a white solid (26.1 mg, 45%). ^{1}H-NMR (600 MHz, DMSO-d_6): δ (ppm) 0.84 (d, 3H, *J* 6.4 Hz), 0.88 (d, 3H, *J* 6.3 Hz), 1.36-1.51 (m, 8H), 1.60-1.74 (m, 3H), 2.66-2.71 (m, 1H), 2.82-2.88 (m, 1H), 3.02-3.08 (m, 2H), 3.09-3.15 (m, 2H), 3.81-3.86 (m, 1H), 4.20-4.25 (m, 1H), 4.31-4.37 (m, 1H), 4.45-4.51 (m, 1H), 6.63-6.67 (m, 2H), 6.90-7.60 (br s, 8H, interfering with the next three listed signals), 7.02-7.04 (m, 2H), 7.08 (s, 1H), 7.54 (s, 1H), 7.70 (t, 1H, *J* 10.8 Hz),7.84-7.87 (m, 1H), 7.88-7.92 (t, 1H, *J* 11.8 Hz), 8.14-8.19 (m, 3H), 8.46 (d, 1H, *J* 8.5 Hz), 8.71 (d, 1H, *J* 8.6 Hz), 9.26 (br s, 1H). ^{13}C-NMR (150 MHz, DMSO-d_6): δ (ppm) 21.2, 23.1, 24.1, 24.2, 25.1, 28.5, 28.9, 36.9, 40.0, 40.5, 41.1, 50.9, 51.8, 52.5, 53.8, 114.8 (two carbon atoms), 127.5, 130.1 (two carbon atoms), 155.8, 156.8, 156.9, 168.1, 170.7, 171.6, 172.7. HRMS (ESI): *m/z* $[M+2H]^{2+}$ calcd. for $[C_{27}H_{49}N_{11}O_5]^{2+}$ 303.6954, found: 303.6962. RP-HPLC (220 nm): 98% (t_R = 8.5 min, *k* = 1.6). $C_{27}H_{47}N_{11}O_5 \cdot C_6H_3F_9O_6$ (605.75 + 342.07).

Arg-Leu-*D*-Arg-Tyr-amide tris(hydrotrifluoroacetate) (2.33). Peptide **2.33** was synthesized on a Sieber-amide-PS resin (100 mg, 0.59 mmol/g) according to the general procedure. Purification by preparative HPLC (system 1, gradient: 0-30 min MeCN/0.1% aq TFA 8:92 to 45:58, t_R = 9 min) yielded **2.33** as a white solid (8.4 mg, 14%). ^{1}H-NMR (600 MHz, DMSO-d_6): δ (ppm) 0.85-0.89 (m, 6H), 1.14-1.21 (m, 1H), 1.21-1.29 (m, 1H), 1.29-1.37 (m, 1H), 1.38-1.54 (m, 5H), 1.55-1.63 (m, 1H), 1.63-1.71 (m, 2H), 2.61-2.67 (m, 1H), 2.91-2.95 (m, 1H), 2.96-3.03 (m, 2H), 3.05-3.12 (m, 2H), 3.77-3.84 (m, 1H), 4.22-4.27 (m, 1H), 4.32-4.37 (m, 1H), 4.41-4.46 (m, 1H), 6.62-6.66 (m, 2H), 6.80-7.60 (br s, 8H, interfering with the next three listed signals),

6.99-7.02 (m, 2H), 7.09-7.13 (m, 1H), 7.45-7.48 (m, 1H), 7.62 (t, 1H, *J* 11.4 Hz), 7.69 (t, 1H, *J* 11.5 Hz), 8.13-8.20 (m, 4H), 8.36 (d, 1H, *J* 7.8 Hz), 8.51 (d, 1H, *J* 7.9 Hz), 9.20 (s, 1H). ^{13}C-NMR (150 MHz, DMSO-d_6): δ (ppm) 22.1, 23.4, 24.5, 24.6, 25.2, 28.8, 29.6, 37.4, 40.4. 40.5, 41.6, 51.6, 52.2, 52.5, 54.6, 115.3 (two carbon atoms), 128.4, 130.6 (two carbon atoms), 156.3, 157.2, 157.3, 168.6, 171.3, 172.0, 173.8. HRMS (ESI): *m/z* $[M+2H]^{2+}$ calcd. for $[C_{27}H_{49}N_{11}O_5]^{2+}$ 303.6954, found: 303.6958. RP-HPLC (220 nm): 99% (t_R = 7.9 min, *k* = 1.4). $C_{27}H_{47}N_{11}O_5 \cdot C_6H_3F_9O_6$ (605.75 + 342.07).

Arg-Leu-Arg-*D*-Tyr-amide tris(hydrotrifluoroacetate) (2.34). Peptide **2.34** was synthesized on a Sieber-amide-PS resin (100 mg, 0.59 mmol/g) according to the general procedure. Purification by preparative HPLC (system 1, gradient: 0-30 min MeCN/0.1% aq TFA 8:92 to 45:58, t_R = 9 min) yielded **2.34** as a white solid (13.7 mg, 22%). ^{1}H-NMR (600 MHz, DMSO-d_6): δ (ppm) 0.87 (d, 6H, *J* 6.6 Hz), 1.34-1.41 (m, 1H), 1.41-1.46 (m, 2H), 1.49-1.57 (m, 3H), 1.61-1.67 (m, 1H), 1.66-1.72 (m, 2H), 2.58-2.65 (m, 1H), 2.91-2.96 (m, 1H), 3.00 (q, 2H, *J* 6.8 Hz), 3.06-3.14 (m, 2H), 3.77-3.85 (m, 1H), 4.15 (q, 1H, *J* 7.2 Hz), 4.29-4.37 (m, 2H), 6.60-6.66 (m, 2H), 6.80-7.50 (br s, 8H, interfering with the next three listed signals), 6.96-7.01 (m, 2H), 7.09-7.12 (m, 1H), 7.36-7.40 (m, 2H), 7.64 (t, 1H, *J* 5.7 Hz), 7.78 (t, 1H, *J* 5.9 Hz), 8.05 (d, 1H, *J* 8.5 Hz), 8.14-8.21 (m, 4H), 8.52 (d, 1H, *J* 7.5 Hz), 9.22 (s, 1H). ^{13}C-NMR (150 MHz, DMSO-d_6): δ (ppm) 21.4, 23.1, 24.0, 24.1, 24.7, 28.4, 28.7, 36.9, 40.3, 40.7, 43.7, 51.3, 51.7, 52.5, 54.1, 114.9 (two carbon atoms), 127.9, 130.1 (two carbon atoms), 155.8, 156.8, 156.9, 168.3, 170.9, 171.8, 173.1. HRMS (ESI): *m/z* $[M+2H]^{2+}$ calcd. for $[C_{27}H_{49}N_{11}O_5]^{2+}$ 303.6954, found: 303.6959. RP-HPLC (220 nm): 97% (t_R = 8.6 min, *k* = 1.6). $C_{27}H_{47}N_{11}O_5 \cdot C_6H_3F_9O_6$ (605.75 + 342.07).

N$^{\alpha}$-methyl-Arg-Leu-Arg-Tyr-amide tris(hydrotrifluoroacetate) (2.35). Peptide **2.35** was synthesized on a Sieber-amide-PS resin (100 mg, 0.59 mmol/g) according to the general procedure. Purification by preparative HPLC (system 1, gradient: 0-30 min MeCN/0.1% aq TFA 8:92 to 45:58, t_R = 9 min) yielded **2.35** as a white solid (11.4 mg, 19%). ^{1}H-NMR (600 MHz, DMSO-d_6): δ (ppm) 0.85-0.91 (m, 6H), 1.36-1.55 (m, 7H), 1.57-1.73 (m, 4H), 1.73-1.78 (m, 1H), 2.47 (s, 3H), 2.69- 2.75 (m, 1H), 2.82-2.88 (m, 1H), 3.04-3.14 (m, 4H), 3.76 (s, 1H), 4.20 (q, 1H, *J* 7.7 Hz), 4.34 (q, 1H, *J* 7.8 Hz), 4.38-4.44 (m, 1H), 6.61-6.65 (m, 2H), 6.80-7.50 (br s, 8H, interfering with the next three listed signals), 6.95-6.98 (m, 2H), 7.05-7.08 (m, 1H), 7.40-7.42 (m, 1H), 7.64 (t, 1H, *J* 5.7 Hz), 7.71-7.77 (m, 2H), 8.22 (d, 1H, *J* 7.6 Hz), 8.68-8.77 (m, 1H), 9.19 (s, 1H). ^{13}C-NMR (150 MHz, DMSO-d_6): δ (ppm) 21.1, 23.1, 23.8, 24.2, 25.0, 26.9, 28.9, 31.1, 36.9, 40.0, 40.4, 40.5, 51.2, 52.5, 53.8, 60.0, 114.9 (two carbon atoms), 127.4, 130.0 (two carbon atoms), 155.8, 156.8, 156.9, 167.0, 170.8, 171.5, 172.7. HRMS (ESI): *m/z* $[M+2H]^{2+}$ calcd. for $[C_{28}H_{51}N_{11}O_5]^{2+}$ 310.7037, found: 310.7038. RP-HPLC (220 nm): 98% (t_R = 10.9 min, *k* = 2.4). $C_{28}H_{49}N_{11}O_5 \cdot C_4H_2F_6O_4$ (619.77 + 228.04).

2.4.4 Pharmacological Assays

Cell Culture. Cells were cultured in 75 cm^2 flasks (Sarstedt, Nümbrecht, Germany) in a humidified atmosphere (95% air, 5% CO_2) at 37 °C. SK-N-MC neuroblastoma cells,[20] CHO-hY_4R-G_{qi5}-mtAEQ cells,[18] HEC-1B-hY_5R cells,[21] HEK293T-ARRB1-hY_4R cells and HEK293T-ARRB2-hY_4R cells[11] were cultured as described previously. CHO-hY_2R cells (Perkin Elmer, Rodgau, Germany) were cultured in Ham's F-12 supplemented with 5% fetal calf serum (FCS) and 400 µg/mL of G418 (Fisher Scientific).

Buffers and media used for binding and functional assays. *Buffer I*: a hypotonic sodium-free HEPES buffer (25 mM HEPES, 2.5 mM $CaCl_2$ and 1 mM $MgCl_2$, pH 7.4) supplemented with 1% BSA (Serva, Heidelberg, Germany) and 0.1 mg/mL of bacitracin (Serva) used for binding experiments at Y_2R and Y_4R. *Buffer II*: an isotonic sodium-containing HEPES buffer (150 mM NaCl, 10 mM HEPES, 25 mM $NaHCO_3$, 2.5 mM $CaCl_2$ and 5 mM KCl) supplemented with 1% BSA used for binding experiments at Y_1R and Y_5R. *Buffer III*: an isotonic sodium-containing HEPES buffer supplemented with 120 mM NaCl, 25 mM HEPES, 1.5 mM $CaCl_2$, 1 mM $MgCl_2$, 5 mM KCl and 10 mM D-glucose used for the functional Ca^{2+}-aequorin Y_4R assay. *L15 medium*: phenol red-free Leibovitz's L-15 medium (140 mM NaCl, 1.3 mM $CaCl_2$, 1 mM $MgCl_2$, various amino acids and vitamins, pH 7.4) (Thermo Fischer Scientific, Nidderau, Germany) supplemented with 10 mM HEPES and 5% FCS used for the seeding of cells 1 day prior to the β-arrestin 1 and β-arrestin 2 recruitment assays.

Radioligand binding assays. Y_1R binding. Radioligand competition binding experiments at Y_1R-expressing SK-N-MC neuroblastoma cells were performed in *buffer II* as described previously using [^{3}H]UR-MK299 (K_d = 0.044 nM and c = 0.15 nM) as a radioligand.[20] For each compound, three independent experiments were performed in triplicate.

Y_2R binding. Competition binding studies at hY_2R were performed on CHO-hY_2R cells (purchased from PerkinElmer, product no. ES-352-C, lot no. 460-167-A) at 23 ± 1 °C using [^{3}H]propionyl-pNPY (specific activity 37.5 Ci/mmol) as a radioligand. One day prior to the experiment, cells were seeded in tissue culture (TC)-treated white 96-well plates with a clear bottom (Corning, catalog no. 3610) at a density that gave 80-90% confluency on the day of experiment. The culture medium was removed by suction and the cells were washed with *buffer I* (without BSA and bacitracin) (200 µL) and covered with 160 µL (competition and unspecific binding) and 180 µL (total binding) of *buffer I*. To determine total binding, a 5 nM solution of [^{3}H]propionyl-pNPY (20 µL) in *buffer I* [prepared in "siliconized" (Sigmacote, Sigma) polypropylene tubes] was added. To determine the displacing effect of a compound of interest and to determine unspecific binding, *buffer I* (20 µL), containing the compound of interest (10-fold concentrated), or a mixture of BIIE0246 and JNJ31020028 (each 50 µM, final

concentration 5 μM) (unspecific binding) was added, followed by addition of a 5 nM solution of [^{3}H]propionyl-pNPY (20 μL) in *buffer I*. During the incubation period of 2 h, the plates were gently shaken. After incubation, the binding buffer was removed by suction and the cells were washed twice with ice-cold phosphate-buffered saline. To each well, 25 μL of lysis solution (8 M urea, 3 M acetic acid and 1% Triton-X-100 in water) was added, the plates were shaken for 30 min and liquid scintillator (Ultima Gold, PerkinElmer) (200 μL) was added to each well. Plates were sealed with a transparent sealing tape (permanent seal for microplates, PerkinElmer, product no. 1450-461) and turned upside down several times to achieve complete mixing. The plates were kept in the dark for 1 h, followed by measurement of radioactivity (ccpm) with a MicroBeta2 plate counter (PerkinElmer). For each compound, three independent experiments were performed in triplicate.

Prior to the competition binding experiments, the K_d value of [^{3}H]propionyl-pNPY was determined by saturation binding applying the same conditions (buffer, temperature, incubation time, unspecific binding, etc.) (for saturation isotherms, see Figure S7A, Supporting Information). The obtained K_d value amounted to 0.14 ± 0.03 nM [mean value ± standard error of the mean (SEM) from three independent determinations performed in triplicate]. For assay validation, the Y_2R affinity of the standard Y_2R ligand BIIE0246 was determined by competition binding with [^{3}H]propionyl-pNPY (for radioligand displacement curve, see Figure S7B, Supporting Information). The obtained pK_i value amounted to 8.0 ± 0.05 (mean ± SEM from two independent experiments performed in triplicate), being in good agreement with the reported Y_2R affinities of BIIE0246 (K_i: 2.6 nM[31] and pK_i: 8.0[32]).

Y_4R binding. Radioligand competition binding experiments at Y_4R were performed in *buffer I* as reported previously using CHO-hY_4R-G_{qi5}-mtAEQ cells and [^{3}H]UR-KK200 (K_d = 0.67 nM and c = 1 nM) as a radioligand.[12] Three (**2.8**-**2.12**, **2.14**-**2.16**, **2.18**-**2.24**, **2.26**-**2.29** and **2.31**-**2.35**) or four (**2.13**, **2.17**, **2.25** and **2.30**) independent experiments were performed in triplicate.

Y_5R binding. Radioligand competition binding experiments at Y_5R were performed as described previously in *buffer II* at 23 ± 1 °C using HEC-1B-hY_5R cells and [^{3}H]propionyl-pNPY (specific activity: 27.4 Ci/mmol) (K_d = 4.8 nM and c = 4 nM) as a radioligand.[12] For each compound, three independent experiments were performed in triplicate. Specific binding data (Y_4R) were analyzed by a four-parameter logistic fit [log(inhibitor) vs response – variable slope; GraphPad Prism 5.0, GraphPad Software, San Diego, CA] to obtain pIC_{50} values. The latter were converted to pK_i values according to the Cheng-Prusoff equation[33] (logarithmic form).

β-Arrestin recruitment assay. One day before the experiment, HEK293T-ARRB1-Y_4R and HEK293T-ARRB2-Y_4R cells[11] were trypsinized, centrifugated and resuspended in *L15 medium* at a density of 1.0 Mio cells/mL (agonist mode) or 1.25 Mio cells/mL (antagonist mode). For

seeding of the cells in white, TC-treated, flat-bottom 96-well microtiter plates [VWR (catalog no. 736-0119), Ismaning, Germany], 80 µL (agonist mode) or 70 µL (antagonist mode) of the respective cell suspension were added to each well and the plates were kept in a humidified atmosphere (95% air and 5% CO_2) at 37 °C overnight. The microtiter plates were removed from the incubator and kept for 5 min at rt. For agonist mode, D-luciferin (potassium salt) (10 µL of a 10 mM stock solution) was added to each well, followed by immediate baseline acquisition for 20 min (10 plate reads) using a preheated (37 °C) EnSpire multimode plate reader (Perkin Elmer, Rodgau, Germany) (settings: 1 s per well measurement time, by rows bidirectional). Subsequently, the compound of interest (10 µL of a 10-fold concentrated solution in *L15 medium*) was added [controls: addition of 10 µL of neat *L15 medium* (0% effect) and 10 µL of a 10 µM hPP solution (100% effect)] and bioluminescence was recorded for 40 min (20 plate reads). For the antagonist mode, D-luciferin (potassium salt) (10 µL of a 10 mM stock solution) and the compound of interest (10 µL of a 10-fold concentrated solution in *L15 medium*) were added followed by baseline acquisition for 20 min. hPP (10 µL of a 100 nM solution in *L15 medium*) was added [controls: addition of 10 µL of neat *L15 medium* instead of the antagonist and 10 µL of a 100 nM hPP solution (100% effect) or another 10 µL of neat *L15 medium* (0% effect)] immediately, followed by data acquisition (20 entire plate reads). For each compound, three independent experiments were performed in triplicate. Relative luminescences [100% = 1 µM hPP (agonist mode) or 10 nM hPP (antagonist mode), 0% = neat buffer] were plotted against log(concentration of agonist or antagonist) and analyzed by four-parameter logistic fits (GraphPad Prism 5.0) to obtain pEC_{50} (agonists) or pIC_{50} values. The latter were converted to pK_b values according to the Cheng-Prusoff equation[33] (logarithmic form) using the pEC_{50} values of hPP determined in the absence of antagonist [pEC_{50} (β-arrestin 1) = 8.66 and pEC_{50} (β-arrestin 2) = 8.37]. Efficacies α (maximum effect relative to 1 µM hPP) of (partial) agonists were calculated from the upper plateaus of the CEC. In the case of rightward shifted concentration-effect curves in the presence of **2.13** (fixed concentration: 10 µM), the pEC_{50} shift of hPP was used to estimate the antagonist pK_b according to the Gaddum equation[25] (β-arrestin 1 assay).

Ca^{2+}-aequorin assay. CHO-hY_4-G_{qi5}-mtAEQ cells[18] were grown to 80-90% confluency, trypsinized and centrifuged at 1200 rpm for 5 min. The supernatant was removed, cells were resuspended in phenol red-free Dulbecco's modified Eagle's medium supplemented with 1% FCS and adjusted to a density of 10 Mio cells/mL. Coelenterazine h (1 mM stock solution in MeOH) was added (final concentration: 2 µM) and the cell suspension was incubated at rt for 2 h in the dark, followed by dilution with *buffer III*, to reach a density of 0.5 Mio cells/mL and incubated under gentle stirring at rt for 3 h in the dark. White 96-well plates (Lumitrac 200, Greiner Bio-One, Frickenhausen, Germany) were prefilled with 18 µL of a solution of the compound of interest (10-fold concentrated compared to the final concentration) in *buffer III*

supplemented with 1% BSA and 100 µg/mL of bacitracin [controls: 18 µL of a solution of hPP (10 µM, resulting in a final concentration of 1 µM) in *buffer III* supplemented with 1% BSA and 100 µg/mL of bacitracin (maximum effect) and 18 µL of 'neat' *buffer III* supplemented with 1% BSA and 100 µg/mL of bacitracin (0% control)]. Measurements were performed with a GENios Pro plate reader (Tecan, Salzburg, Austria). The cell suspension (162 µL) was injected into each well of the plate and the emitted luminescence was recorded for 43 s in kinetic mode (peak 1), followed by injection of 1% Triton-X-100 in *buffer III* (20 µL) (cell lysis to release the remaining aequorin) and recording of the signal for 22 s (peak 2). For the antagonist mode, the compound of interest (2 µL of a 100-fold concentrated solution in *buffer III* supplemented with 1% BSA and 100 µg/mL of bacitracin) was added to the empty wells of a white 96-well plate, followed by the addition of 178 µL of the cell suspension [controls: 2 µL of 'neat' *buffer III* supplemented with 1% BSA and 100 µg/mL of bacitracin instead of antagonist (reference effect in the absence of antagonist) and 22 µL of 'neat' *buffer III* supplemented with 1% BSA and 100 µg/mL of bacitracin (no addition of hPP, 0% control)]. After a preincubation period of 15 min, the measurement was started by injecting 20 µL of a 1 µM solution of hPP (final concentration: 100 nM) in *buffer III* supplemented with 1% BSA and 100 µg/mL of bacitracin, and signals were recorded as in the agonist mode (Triton X-100 added after 43 s). For each compound, three independent experiments were performed in triplicate. Areas under the curve were calculated using GraphPad Prism 5.0 (GraphPad software). Fractional luminescences [calculated by dividing the area of peak 1 by the total area (peaks 1 and 2)] were normalized (100% = fractional luminescence obtained from 1 µM hPP, 0% = basal effect in the absence of agonist and antagonist; GraphPad Prism 5.0) and relative responses were plotted against log(concentration of agonist) or log(concentration of antagonist), followed by fitting according to a four-parameter logistic equation [log(agonist) vs response – variable slope or log(inhibitor) vs. response – variable slope; GraphPad Prism 5.0] to obtain pEC_{50} and pIC_{50} values, respectively. The latter were converted to pK_b values according to the Cheng-Prusoff equation[33] (logarithmic form) using the pEC_{50} value of hPP determined in the absence of antagonist (pEC_{50} = 7.96). Efficacies α (maximum effect relative to 1 µM hPP) of (partial) agonists were calculated from the upper plateaus of the CEC. In the case of rightward-shifted CEC in the presence of **2.13** (fixed concentration: 10 µM), the pEC_{50} shift of hPP was used to estimate the antagonist pK_b according to the Gaddum equation.[25]

2.4.5 Induced-Fit Docking at Y_4R

Two homology models of hY_4R were prepared based on the inactive state hY_1R (PDB ID: 5ZBQ)[27] and the active state κ opioid receptor (PDB: 6B73, chain A)[26] crystal structures using Modeller[34] within the UCSF Chimera package version 1.13 (Resource for Biocomputing,

Visualization and Informatics at the University of California, San Francisco, CA).[35] The receptor models contained disulfide bridges between Cys114$^{3.25}$ and Cys201^{ECL2} and between the N-terminal Cys^{34} and Cys298$^{7.29}$ in TM7. Coordinates other than ligand and receptor molecules were removed. The Y_4R models were further refined using the protein preparation wizard (Schrödinger LLC, Portland, OR, USA). The N- and C-termini were capped by the introduction of acetyl and methylamide groups, respectively, and amino acid side chains containing hydrogen bond donors and acceptors were optimized for hydrogen bonding. Histidine residues were simulated in the uncharged form as the N^{ε}-H tautomer. Residues other than histidine were simulated in their dominant protonation state at pH 7. Ligand (**2.1**, **2.13** and **2.29**) geometries were energetically optimized using the LigPrep module (Schrödinger LLC). Guanidine groups and primary amine groups in **2.1**, **2.13** and **2.29** were protonated, resulting in net charges of +3, +4 and +3, respectively.

Induced-fit docking of **2.1** and **2.29** to the active state Y_4R model and of **2.13** to the inactive state Y_4R model was performed using the induced-fit docking module (Schrödinger LLC). Initially, ligands were docked within a box of 46 × 46 × 46 Å^3 around the crystallographic binding poses of the co-crystallized ligands using the standard protocol. Redocking was performed in the extended precision mode. From the obtained induced-fit docking results of each Y_4R model/ligand combination, the pose (ligand-receptor complex) corresponding to the lowest XP GlideScore (reflecting the lowest free energy of binding) was selected for analysis. Figures showing molecular structures of Y_4R in complex with **2.1**, **2.13**, or **2.29** were generated with PyMOL molecular graphics system, version 2.3.0 (Schrödinger LLC). Apparent molecular interactions (H-bonds, salt bridges, π-π and π-cation) between the ligands and Y_4R were determined with the Maestro interface (Schrödinger LLC).

2.5 Supporting Information

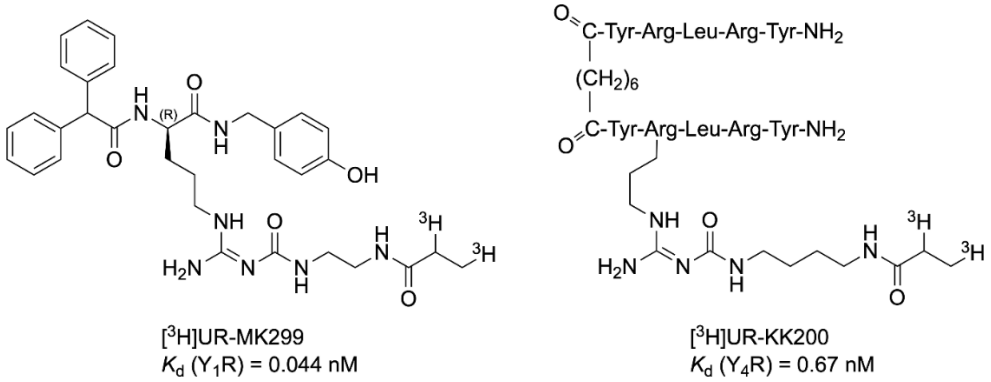

Figure S1. Structures of the tritiated Y_1R antagonist [^{3}H]UR-MK299 and of the tritiated Y_4R agonist [^{3}H]UR-KK200.

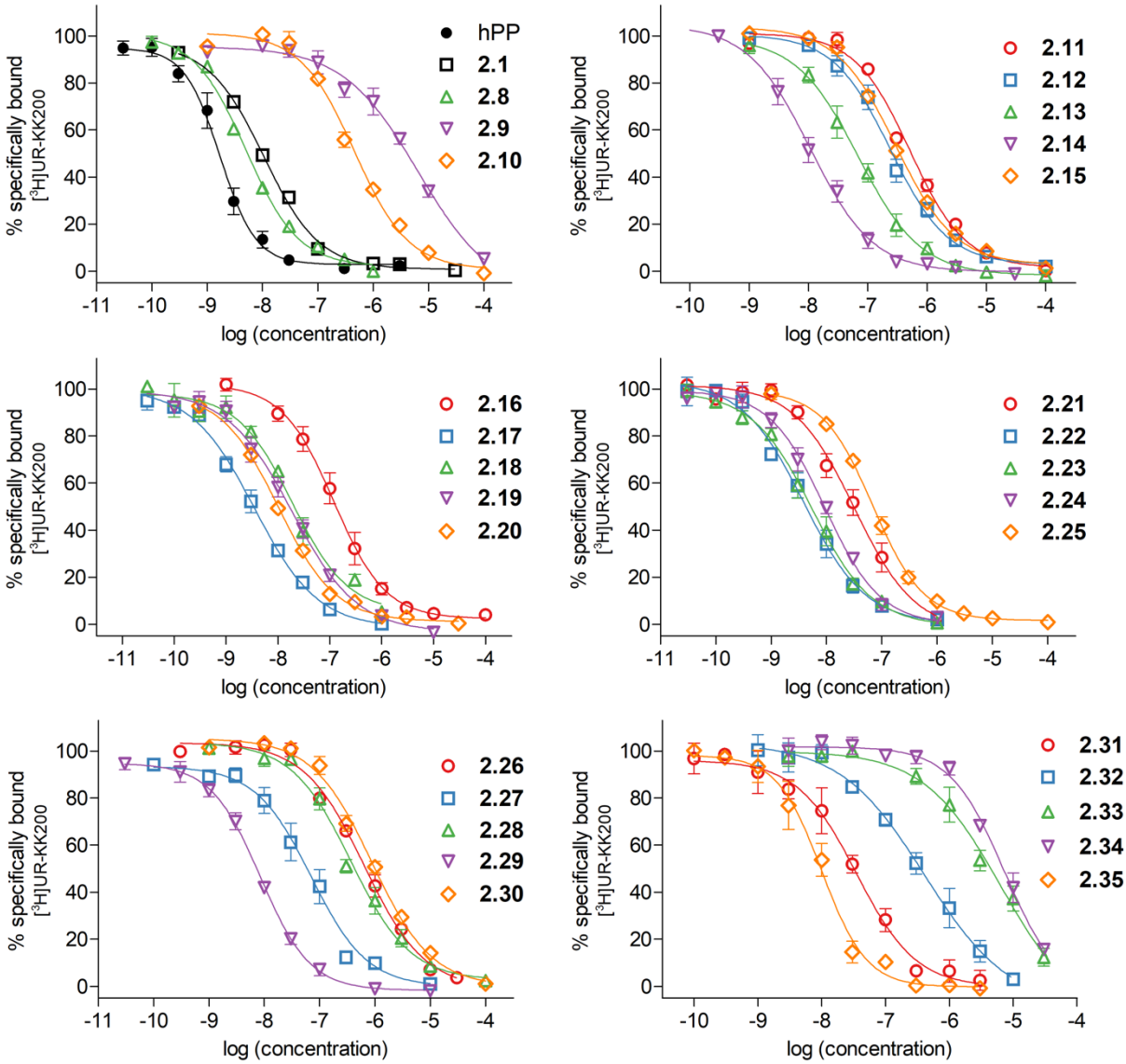

Figure S2. Radioligand displacement curves of hPP, **2.1** (UR-KK236) and compounds **2.8**-**2.35** obtained from competition binding experiments with [^{3}H]UR-KK200 (K_d = 0.67 nM, c = 1 nM) performed with CHO-hY_4R-mtAEQ-G_{qi5} cells. Data represent means ± SEM from at least three independent experiments, each performed in triplicate. Data were analyzed by four parametric logistic fits (GraphPad Prism 5).

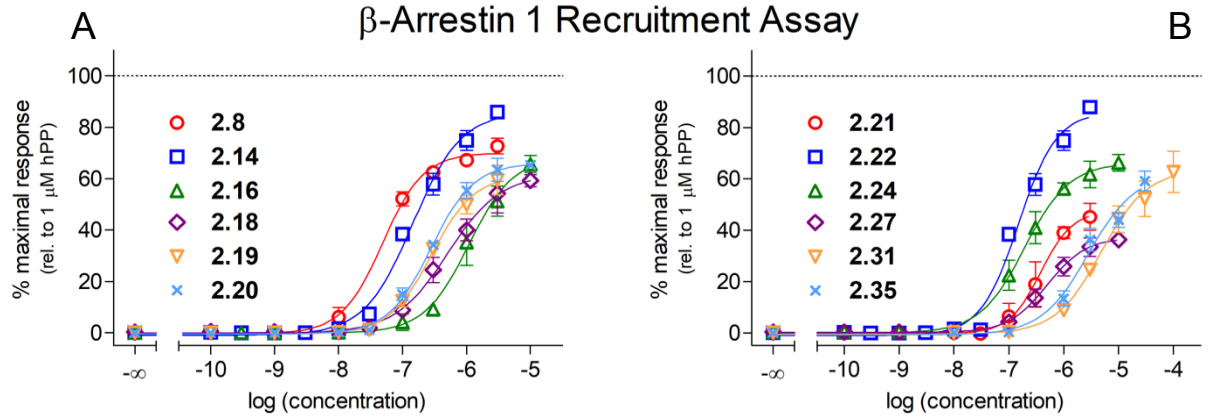

Figure S3. Concentration-response curves of compounds (A) **2.8**, **2.14**, **2.16**, **2.18**, **2.19** and **2.20**, (B) **2.21**, **2.22**, **2.24**, **2.27**, **2.31** and **2.35**, obtained from a hY$_4$R β-arrestin 1 recruitment assay performed with live HEK293T-ARRB1-Y$_4$R cells. Data represent means ± SEM from at least three independent experiments, each performed in triplicate.

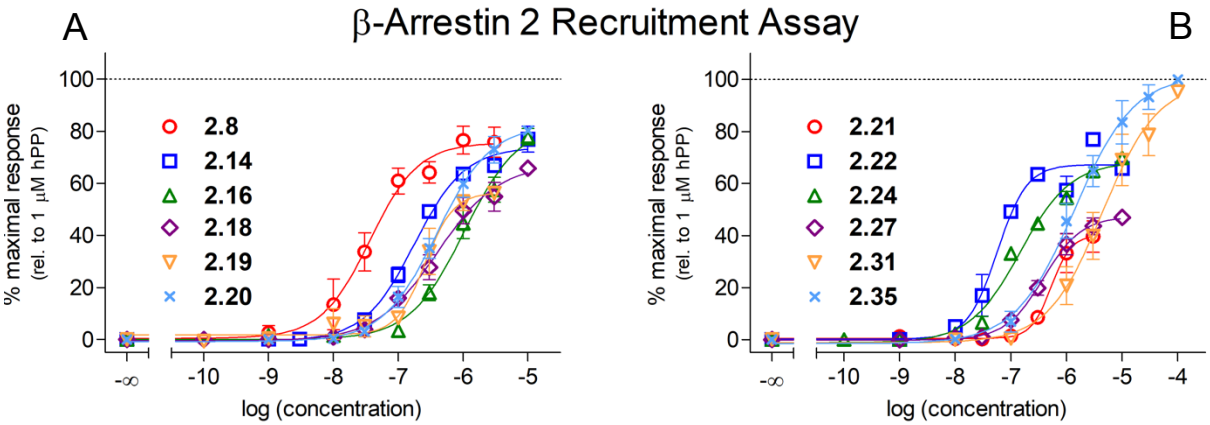

Figure S4. Concentration-response curves of compounds (A) **2.8**, **2.14**, **2.16**, **2.18**, **2.19** and **2.20**, (B) **2.21**, **2.22**, **2.24**, **2.27**, **2.31** and **2.35**, obtained from a hY$_4$R β-arrestin 2 recruitment assay performed with live HEK293T-ARRB2-Y$_4$R cells. Data represent means ± SEM from at least three independent experiments, each performed in triplicate.

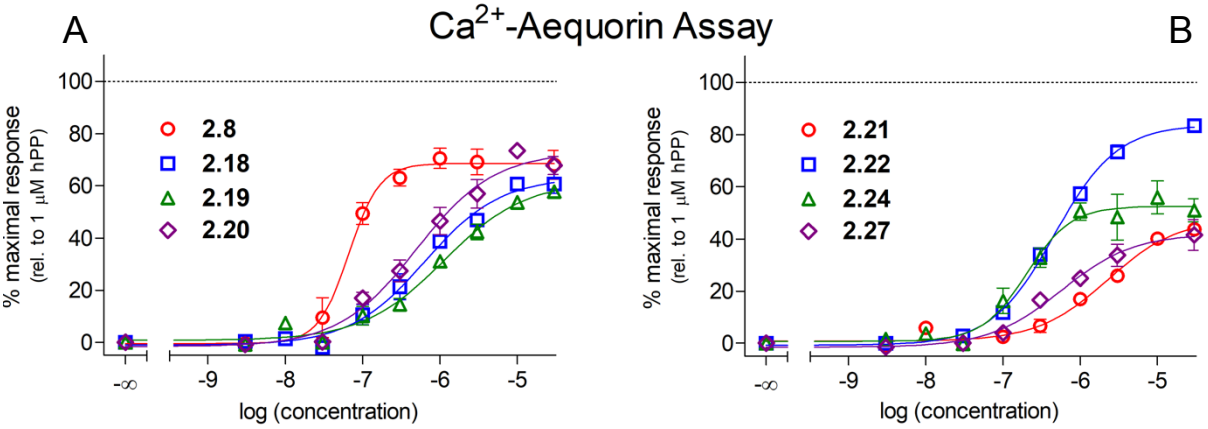

Figure S5. Concentration-response curves of compounds (A) **2.8**, **2.18**, **2.19** and **2.20**, (B) **2.21**, **2.22**, **2.24** and **2.27**, obtained from a hY$_4$R Ca^{2+}-aequorin assay performed with live CHO-hY$_4$-G$_{qi5}$-mtAEQ cells. Data represent means ± SEM from at least three independent experiments, each performed in triplicate.

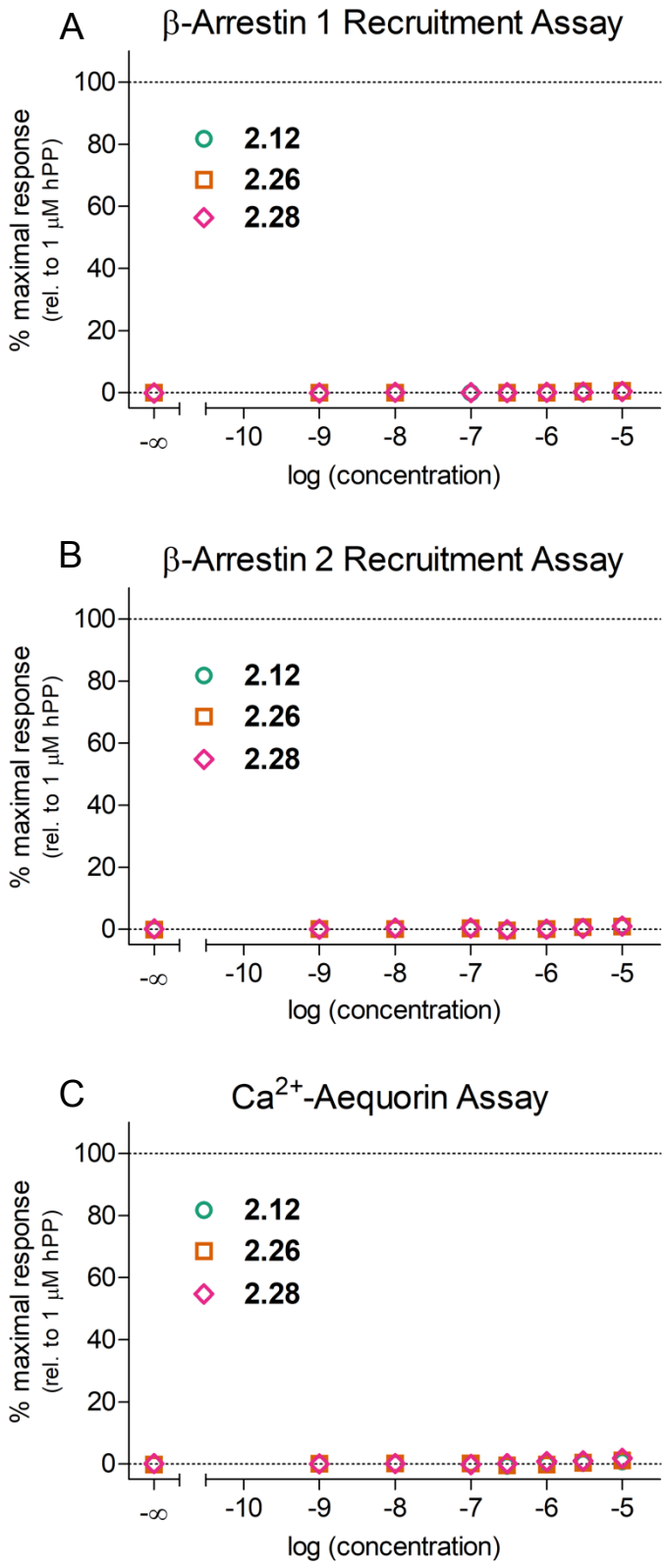

Figure S6. Y_4R functional activities of compounds **2.12**, **2.26**, and **2.28**, when the assay was performed in the agonist mode. (A) Induced β-arrestin recruitment in HEK239T-ARRB1-Y_4R cells. (B) Induced β-arrestin recruitment in HEK239T-ARRB2-Y_4R cells. (C) Induced intracellular Ca^{2+} mobilization in CHO-hY_4R-mtAEQ-G_{qi5} cells. Data represent means ± SEM from at least three independent experiments, each performed in triplicate.

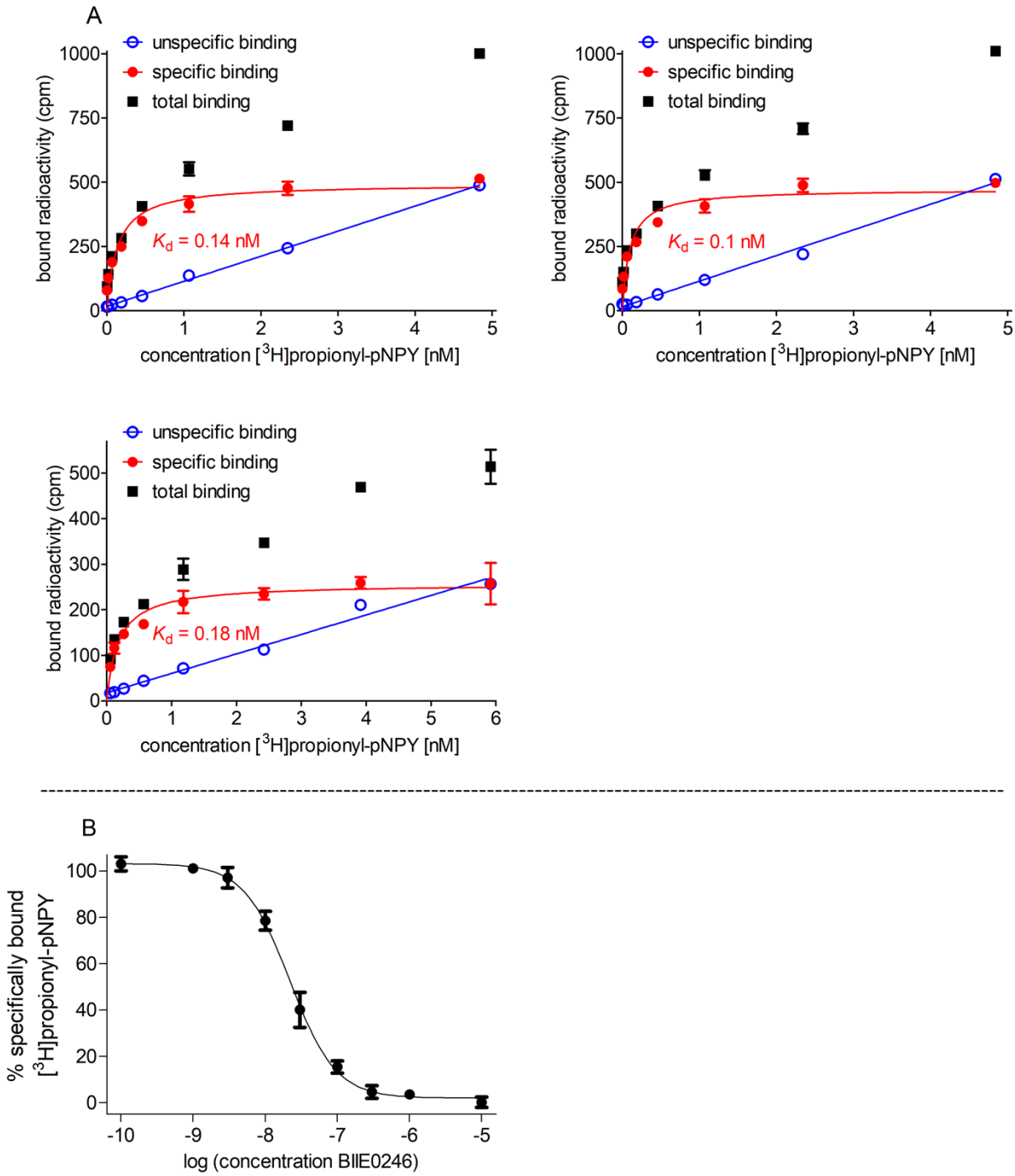

Figure S7. Characterization of [^{3}H]-propionyl-pNPY binding at intact CHO-hY_2R cells. (A) Saturation isotherms (red) from three saturation binding experiments. Data represent mean values ± SEM (total and unspecific binding) or calculated values ± (maximum) propagated error (specific binding) from three individual experiments performed in triplicate. (B) Displacement curve of [^{3}H]-propionyl-pNPY from competition binding experiments with the Y_2R standard antagonist BIIE0246. Data represent mean values ± SEM from two independent experiments, each performed in triplicate. Determined K_i value of BIIE0246: 9.7 nM ± 0.07.

2.6 References

(1) Balasubramaniam, A. A., Neuropeptide Y family of hormones: receptor subtypes and antagonists. *Peptides* **1997**, *18*, 445-457.

(2) Cabrele, C.; Beck-Sickinger, A. G., Molecular characterization of the ligand-receptor interaction of the neuropeptide Y family. *J. Pept. Sci.* **2000**, *6*, 97-122.

(3) Cerda-Reverter, J. M.; Larhammar, D., Neuropeptide Y family of peptides: structure, anatomical expression, function, and molecular evolution. *Biochem. Cell Biol.* **2000**, *78*, 371-392.

(4) Zhang, L.; Bijker, M. S.; Herzog, H., The neuropeptide Y system: pathophysiological and therapeutic implications in obesity and cancer. *Pharmacol. Ther.* **2011**, *131*, 91-113.

(5) Lundell, I.; Blomqvist, A. G.; Berglund, M. M.; Schober, D. A.; Johnson, D.; Statnick, M. A.; Gadski, R. A.; Gehlert, D. R.; Larhammar, D., Cloning of a human receptor of the NPY receptor family with high affinity for pancreatic polypeptide and peptide YY. *J. Biol. Chem.* **1995**, *270*, 29123-29128.

(6) Thieme, V.; Jolly, N.; Madsen, A. N.; Bellmann-Sickert, K.; Schwartz, T. W.; Holst, B.; Cox, H. M.; Beck-Sickinger, A. G., High molecular weight PEGylation of human pancreatic polypeptide at position 22 improves stability and reduces food intake in mice. *Br. J. Pharmacol.* **2016**, *173*, 3208-3221.

(7) Li, J. B.; Asakawa, A.; Terashi, M.; Cheng, K.; Chaolu, H.; Zoshiki, T.; Ushikai, M.; Sheriff, S.; Balasubramaniam, A.; Inui, A., Regulatory effects of Y_4 receptor agonist (BVD-74D) on food intake. *Peptides* **2010**, *31*, 1706-1710.

(8) Painsipp, E.; Wultsch, T.; Edelsbrunner, M. E.; Tasan, R. O.; Singewald, N.; Herzog, H.; Holzer, P., Reduced anxiety-like and depression-related behavior in neuropeptide Y Y_4 receptor knockout mice. *Genes, Brain Behav.* **2008**, *7*, 532-542.

(9) Tasan, R. O.; Lin, S.; Hetzenauer, A.; Singewald, N.; Herzog, H.; Sperk, G., Increased novelty-induced motor activity and reduced depression-like behavior in neuropeptide Y (NPY)–Y_4 receptor knockout mice. *Neuroscience* **2009**, *158*, 1717-1730.

(10) Pedragosa-Badia, X.; Sliwoski, G. R.; Dong Nguyen, E.; Lindner, D.; Stichel, J.; Kaufmann, K. W.; Meiler, J.; Beck-Sickinger, A. G., Pancreatic polypeptide is recognized by two hydrophobic domains of the human Y_4 receptor binding pocket. *J. Biol. Chem.* **2014**, *289*, 5846-5859.

(11) Kuhn, K. K.; Littmann, T.; Dukorn, S.; Tanaka, M.; Keller, M.; Ozawa, T.; Bernhardt, G.; Buschauer, A., In search of NPY Y_4R antagonists: incorporation of carbamoylated arginine, aza-amino acids, or D-amino acids into oligopeptides derived from the C-termini of the endogenous agonists. *ACS Omega* **2017**, *2*, 3616-3631.

(12) Kuhn, K. K.; Ertl, T.; Dukorn, S.; Keller, M.; Bernhardt, G.; Reiser, O.; Buschauer, A., High affinity agonists of the neuropeptide Y (NPY) Y_4 receptor derived from the C-

terminal pentapeptide of human pancreatic polypeptide (hPP): synthesis, stereochemical discrimination, and radiolabeling. *J. Med. Chem.* **2016**, *59*, 6045-6058.

(13) Daniels, A. J.; Matthews, J. E.; Slepetis, R. J.; Jansen, M.; Viveros, O. H.; Tadepalli, A.; Harrington, W.; Heyer, D.; Landavazo, A.; Leban, J. J.; Spaltenstein, A., High-affinity neuropeptide Y receptor antagonists. *Proc. Natl. Acad. Sci. USA* **1995**, *92*, 9067-9071.

(14) Keller, M.; Kaske, M.; Holzammer, T.; Bernhardt, G.; Buschauer, A., Dimeric argininamide-type neuropeptide Y receptor antagonists: chiral discrimination between Y_1 and Y_4 receptors. *Bioorg. Med. Chem.* **2013**, *21*, 6303-6322.

(15) Rudolf, K.; Eberlein, W.; Engel, W.; Wieland, H. A.; Willim, K. D.; Entzeroth, M.; Wienen, W.; Beck-Sickinger, A. G.; Doods, H. N., The first highly potent and selective non-peptide neuropeptide Y Y_1 receptor antagonist: BIBP3226. *Eur. J. Pharmacol.* **1994**, *271*, R11-30.

(16) Berlicki, Ł.; Kaske, M.; Gutiérrez-Abad, R.; Bernhardt, G.; Illa, O.; Ortuño, R. M.; Cabrele, C.; Buschauer, A.; Reiser, O., Replacement of $Thr^{32}$and Gln^{34} in the C-terminal neuropeptide Y fragment 25–36 by cis-cyclobutane and cis-cyclopentane β-amino acids shifts selectivity toward the Y_4receptor. *J. Med. Chem.* **2013**, *56*, 8422-8431.

(17) Lachmann, D.; Konieczny, A.; Keller, M.; König, B., Photochromic peptidic NPY Y_4 receptor ligands. *Org. Biomol. Chem.* **2019**, *17*, 2467-2478.

(18) Ziemek, R.; Schneider, E.; Kraus, A.; Cabrele, C.; Beck-Sickinger, A. G.; Bernhardt, G.; Buschauer, A., Determination of affinity and activity of ligands at the human neuropeptide Y Y_4 receptor by flow cytometry and aequorin luminescence. *J. Recept. Signal Transduct. Res.* **2007**, *27*, 217-233.

(19) Bartleson, C.; Luo, S.; Graves, D. J.; Martin, B. L., Arginine to citrulline replacement in substrates of phosphorylase kinase. *Biochim. Biophys. Acta, Protein Struct. Mol. Enzymol.* **2000**, *1480*, 23-28.

(20) Keller, M.; Weiss, S.; Hutzler, C.; Kuhn, K. K.; Mollereau, C.; Dukorn, S.; Schindler, L.; Bernhardt, G.; König, B.; Buschauer, A., N^{ω}-Carbamoylation of the argininamide moiety: an avenue to insurmountable NPY Y_1 receptor antagonists and a radiolabeled selective high-affinity molecular tool ([^{3}H]UR-MK299) with extended residence time. *J. Med. Chem.* **2015**, *58*, 8834-8849.

(21) Moser, C.; Bernhardt, G.; Michel, J.; Schwarz, H.; Buschauer, A., Cloning and functional expression of the hNPY Y_5 receptor in human endometrial cancer (HEC-1B) cells. *Can. J. Physiol. Pharmacol.* **2000**, *78*, 134-142.

(22) Dukorn, S.; Littmann, T.; Keller, M.; Kuhn, K.; Cabrele, C.; Baumeister, P.; Bernhardt, G.; Buschauer, A., Fluorescence- and radiolabeling of [Lys^4,$Nle^{17,30}$]hPP yields molecular tools for the NPY Y_4 receptor. *Bioconjugate Chem.* **2017**, *28*, 1291-1304.

(23) Katritch, V.; Fenalti, G.; Abola, E. E.; Roth, B. L.; Cherezov, V.; Stevens, R. C., Allosteric sodium in class A GPCR signaling. *Trends Biochem. Sci.* **2014**, *39*, 233-244.

(24) White, K. L.; Eddy, M. T.; Gao, Z.-G.; Han, G. W.; Lian, T.; Deary, A.; Patel, N.; Jacobson, K. A.; Katritch, V.; Stevens, R. C., Structural connection between activation microswitch and allosteric sodium site in GPCR signaling. *Structure* **2018**, *26*, 259-269.

(25) Gaddum, J. H., Quantitative effects of antagonistic drugs. *J. Physiol.* **1937**, *89*, 7-9.

(26) Che, T.; Majumdar, S.; Zaidi, S. A.; Kormos, C.; McCorvy, J. D.; Wang, S.; Mosier, P. D.; Uprety, R.; Vardy, E.; Krumm, B. E.; Han, G. W.; Lee, M. Y.; Pardon, E.; Steyaert, J.; Huang, X. P.; Strachan, R. T.; Tribo, A. R.; Pasternak, G. W.; Carroll, I. F.; Stevens, R. C.; Cherezov, V.; Katritch, V.; Wacker, D.; Roth, B. L., Crystal Structure of a nanobody-stabilized active state of the kappa-opioid receptor. *Cell* **2018**, *172,* 55-67.

(27) Yang, Z.; Han, S.; Keller, M.; Kaiser, A.; Bender, B. J.; Bosse, M.; Burkert, K.; Kögler, L. M.; Wifling, D.; Bernhardt, G.; Plank, N.; Littmann, T.; Schmidt, P.; Yi, C.; Li, B.; Ye, S.; Zhang, R.; Xu, B.; Larhammar, D.; Stevens, R. C.; Huster, D.; Meiler, J.; Zhao, Q.; Beck-Sickinger, A. G.; Buschauer, A.; Wu, B., Structural basis of ligand binding modes at the neuropeptide Y Y_1 receptor. *Nature* **2018**, *556*, 520–524.

(28) Manglik, A.; Kruse, A. C., Structural basis for G protein-coupled receptor activation. *Biochemistry* **2017**, *56*, 5628-5634.

(29) Weis, W. I.; Kobilka, B. K., The molecular basis of G protein–coupled receptor activation. *Annu. Rev. Biochem.* **2018**, *87*, 897-919.

(30) Pluym, N.; Brennauer, A.; Keller, M.; Ziemek, R.; Pop, N.; Bernhardt, G.; Buschauer, A., Application of the guanidine-acylguanidine bioisosteric approach to argininamide-type NPY Y(2) receptor antagonists. *ChemMedChem* **2011**, *6*, 1727-38.

(31) Ziemek, R.; Brennauer, A.; Schneider, E.; Cabrele, C.; Beck-Sickinger, A. G.; Bernhardt, G.; Buschauer, A., Fluorescence- and luminescence-based methods for the determination of affinity and activity of neuropeptide Y_2 receptor ligands. *Eur. J. Pharmacol.* **2006**, *551*, 10-18.

(32) Goumain, M.; Voisin, T.; Lorinet, A.-M.; Ducroc, R.; Tsocas, A.; Rozé, C.; Rouet-Benzineb, P.; Herzog, H.; Balasubramaniam, A.; Laburthe, M., The peptide YY-preferring receptor mediating inhibition of small intestinal secretion is a peripheral Y_2 receptor: pharmacological evidence and molecular cloning. *Mol. Pharmacol.* **2001**, *60*, 124-134.

(33) Cheng, Y.; Prusoff, W. H., Relationship between the inhibition constant (K_I) and the concentration of inhibitor which causes 50 per cent inhibition (IC_{50}) of an enzymatic reaction. *Biochem. Pharmacol.* **1973**, *22*, 3099-3108.

(34) Šali, A.; Blundell, T. L., Comparative protein modelling by satisfaction of spatial restraints. *J. Mol. Biol.* **1993**, *234*, 779-815.

(35) Pettersen, E. F.; Goddard, T. D.; Huang, C. C.; Couch, G. S.; Greenblatt, D. M.; Meng, E. C.; Ferrin, T. E., UCSF Chimera - a visualization system for exploratory research and analysis. *J. Comput. Chem.* **2004**, *25*, 1605-161.

Chapter 3

Incorporation of Unnatural Amino Acids into the Oligopeptidic Y_4R Partial Agonist UR-AK32

3.1 Introduction

Until now, the large majority of known hY_4R ligands are peptides, which are structurally related to the C-terminal sequence of the physiological neurotransmitter human pancreatic polypeptide (hPP), a linear, C-terminally amidated 36 amino acid peptide. For example, the N-terminal acetylated hexapeptide **3.1** represents a high-affinity Y_4R partial agonist (K_i (hY_4R): 3.4 nM) (Figure 1).[1] Structure-activity relationship studies based on **3.1** (amino acid replacement, sequence truncation, etc.) afforded tetrapeptide **3.2** (UR-AK32), a Y_4R partial agonist with hY_4R affinity (K_i (hY_4R): 3.4 nM) comparable to that of **3.1**.[2] Peptide **3.2**, obtained by N-terminal truncation of **3.1**, represents, among ligands with meaningful Y_4R affinity (K_i < 1 µM), the Y_4R ligand with the lowest molecular weight known so far (Figure 1). **3.2** acted as a partial agonist in a Ca^{2+} aequorin assay (measuring G-protein mediated increase in cytosolic Ca^{2+}) (EC_{50} = 288 nM, α = 0.54), as well as in β-arrestin 1 and 2 recruitment assays (EC_{50} (β-arrestin 1) = 275 nM, α = 0.81; EC_{50} (β-arrestin 2) = 166 nM, α = 0.84).

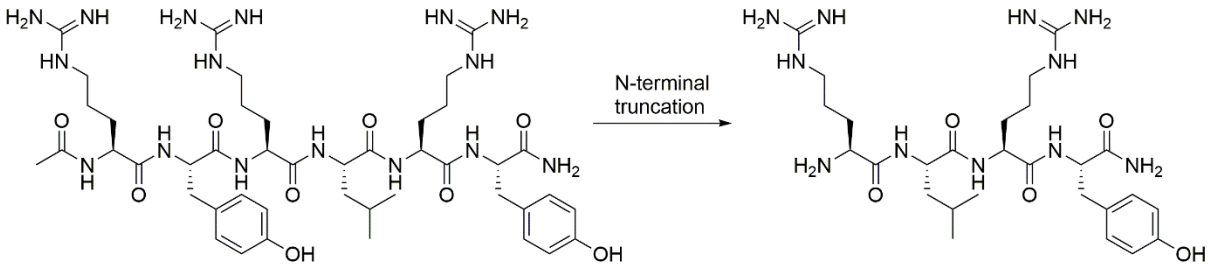

3.1 (UR-KK236)
K_i (hY_4R): 3.4 nM[a]

3.2 (UR-AK32)
K_i (hY_4R): 3.4 nM[b]

Figure 1. Structures and Y_4R affinities (K_i values) of **3.1** and the N-terminally truncated analog **3.2**, both acting as partial agonists at the hY_4R. [a]Kuhn *et al.*[1] [b]Konieczny *et al.*[2]

The objective of this project was the replacement of individual amino acids in **3.2** by various commercially available unnatural amino acids in order to explore how these structural modifications effect Y_4R affinity and, possibly, also the mode of action (agonism *vs.* antagonism). Peptide synthesis procedures were improved over the last 20 years and many modified amino acids, prepared for SPPS, are commercially available as Fmoc- and side-chain protected building blocks, giving synthetic access to a large group of divers peptidic derivatives.[3-5] Therefore, we incorporated a series of unnatural amino acids into lead compound **3.2**. Many unnatural amino acids represent congeners, homologues and/or optical antipodes of native amino acids, missing functional groups or bearing additional functionalities. The incorporation of unnatural amino acids by SPPS enables a convenient structural modification of bioactive peptides.[6,7] The unnatural amino acids, which were used to replace natural amino acids in **3.2** are shown in Figure 2.

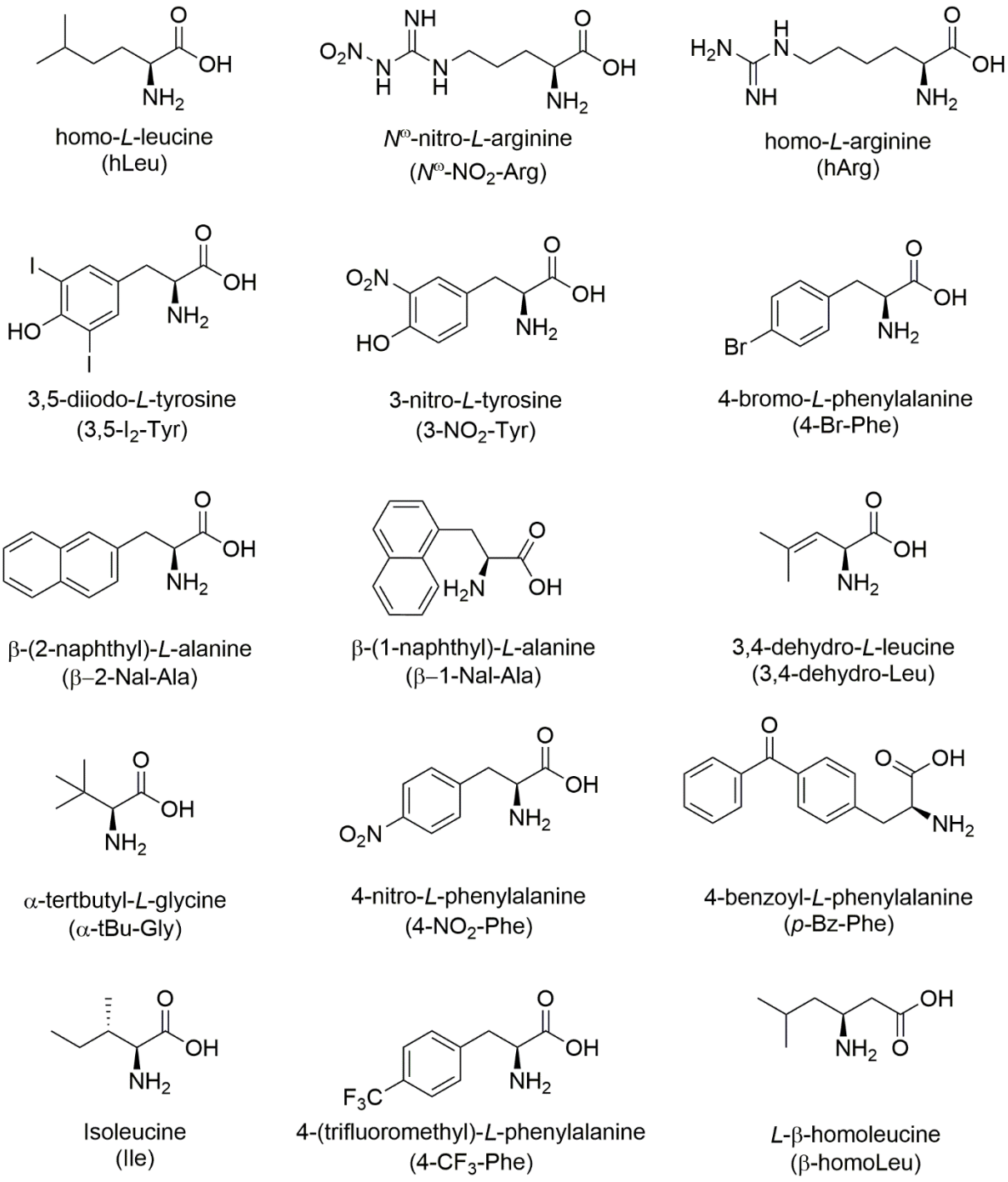

Figure 2. Structures and designations of unnatural amino acids, which were incorporated into lead compound **3.2** (UR-AK32).

3.2 Results and Discussion

3.2.1 Chemistry

Peptide synthesis was performed on a Sieber-amide resin following the standard Fmoc protocol (coupling reagents: HOBt/HBTU/DIPEA) and applying a double coupling procedure. Protecting groups were removed by treatment with TFA/water 95:5. All prepared oligopeptides (**3.3**-**3.24**, sequences listed in Figure 3) were purified by preparative HPLC.

hPP H-Ala-Pro-Leu-Glu-Pro-Val-Tyr-Pro-Gly-Asp-Asn-Ala-Thr-Pro-Glu-Gln-Met-Ala-Gln-Tyr-Ala-Ala-Asp-Leu-Arg-Arg-Tyr-Ile-Asn-Met-Leu-Thr-Arg-Pro-Arg-Tyr-NH_2

3.2	Arg-Leu-Arg-Tyr-NH_2	**3.14**	Arg-Leu-hArg-Tyr-NH_2
3.3	N^{ω}-NO_2-Arg-Leu-Arg-Tyr-NH_2	**3.15**	Arg-Leu-N^{ω}-NO_2-Arg-Tyr-NH_2
3.4	hArg-Leu-Arg-Tyr-NH_2	**3.16**	Arg-Trp-Arg-4-NO_2-Phe-NH_2
3.5	Arg-α-tBu-Gly-Arg-Tyr-NH_2	**3.17**	Arg-Leu-Arg-*p*-Bz-Phe-NH_2
3.6	Arg-hLeu-Arg-Tyr-NH_2	**3.18**	Arg-Leu-Arg-4-CF_3-Phe-NH_2
3.7	Arg-Ile-Arg-Tyr-NH_2	**3.19**	Arg-Leu-Arg-3,5-I_2-Tyr-NH_2
3.8	Arg-Ala-Arg-Tyr-NH_2	**3.20**	Arg-Leu-Arg-3-NO_2-Tyr-NH_2
3.9	Arg-β-1-Nal-Ala-Arg-Tyr-NH_2	**3.21**	Arg-Leu-Arg-4-Br-Phe-NH_2
3.10	Arg-β-2-Nal-Ala-Arg-Tyr-NH_2	**3.22**	Arg-Trp-Arg-β-2-Nal-Ala-NH_2
3.11	Arg-*p*-Bz-Phe-Arg-Tyr-NH_2	**3.23**	Arg-Leu-Arg-β-1-Nal-Ala-NH_2
3.12	2,3-dehydro-Leu-Arg-Tyr-NH_2	**3.24**	Tyr-Arg-Leu-Arg-NH_2
3.13	Arg-β-homoLeu-Arg-NH_2		

Figure 3. Peptide sequences of hPP, the lead compound **3.2** and the synthesized analogs **3.3**-**3.24**. Modifications are highlighted in blue (compared to **3.2**). For structures and abbreviations of unnatural amino acids see Figure 2.

3.2.2 Competition Binding Experiments at the Human Y_4 Receptor

For radioligand competition binding studies at the hY_4R, the Y_4R radioligand [^{3}H]UR-KK200[8] (structure see Figure 1, Appendix) was used, a dimeric pentapeptide, containing a suberic acid linker and a tritiated propionyl moiety at an N^{ω}-carbamoylated arginine side chain.[9] Binding experiments were performed at live CHO-hY_4R-G_{qi5}-mtAEQ cells[10] stably expressing human Y_4 receptors. The obtained pK_i values are summarized in Table 1, the effects of the respective structural modifications on Y_4R binding (nearly no effect, moderate decrease or

strong decrease) are schematically indicated in Figure 4, and exemplary radioligand displacement curves are depicted in Figure 5.

Lead compound **3.2** was the result of studies concerning the C-terminal fragment of hPP and its crucial significance for Y_4R binding.[2,11] The exchange of Arg^1 in **3.2** by $hArg^1$ (compound **3.4**) resulted in retained Y_4R affinity (pK_i: 8.32), compared to **3.2**. Tetrapeptide **3.14**, containing hArg in position 3, showed slightly decreased hY_4R affinity (pK_i: 7.87) (Figure 4, Table 1). Replacement of Arg^1 by a non-basic[12] N^{ω}-NO_2-Arg^1 (**3.3**) was unfavorable with respect to Y_4R binding (70-fold decrease in affinity). Likewise, incorporation of N^{ω}-NO_2-Arg instead of Arg^3 (**3.15**) resulted in a drastic decrease (145-fold) in Y_4R affinity (Table 1), showing that a basic group is of importance in these positions. This underlined the necessity of at least one (**3.12**), better two guanidines or related basic groups in the peptide sequence.

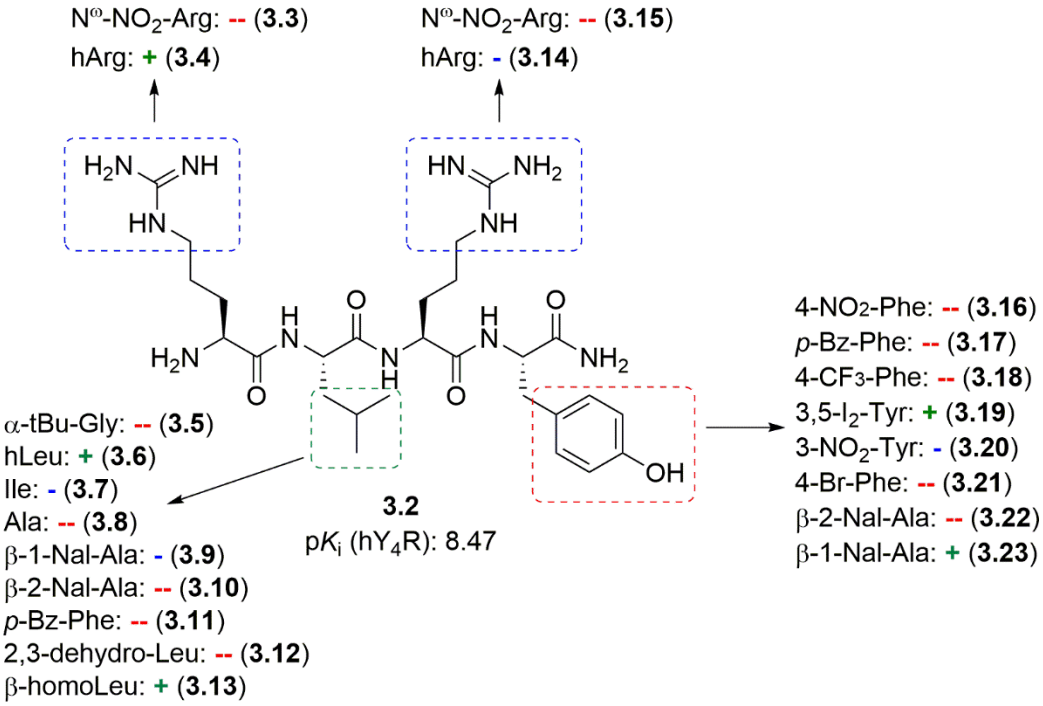

Figure 4. Structural modifications of lead compound **3.2** achieved by the incorporation of unnatural amino acids instead of Arg^1 or Arg^3 (guanidine groups highlighted by blue dashed boxes), Leu^2 (side chain highlighted by green dashed box) or Tyr^4 (side chain highlighted by red dashed box). For abbreviations of unnatural amino acids see Figure 2. The symbols (+), (-) and (--) indicate whether the modification did not affect Y_4R affinity (pK_i: > 8) compared to the parent compound **3.2**, led to a moderate decrease in Y_4R affinity (pK_i: 7-8), or resulted in a marked decrease in Y_4R affinity (pK_i: < 7).

Leu^2 in **3.2**, containing a hydrophobic *iso*-butyl side-chain, proved to be an unfavorable position for amino acid replacement with respect to Y_4R binding. The replacement of Leu^2 by amino acids with bulky aromatic side chains such as naphthalene (**3.9**, **3.10**) or benzophenone (**3.11**) was not tolerated. Interestingly, in the case of **3.9**, containing β-1-Nal-Ala^2, the decrease in Y_4R affinity was less pronounced compared to **3.10**, containing the isomer β-2-Nal-Ala^2 (pK_i: 7.08 *vs.* 5.92). Elongation of the Leu^2 side chain in **3.2** by one methylene group ($hLeu^2$, **3.6**)

had almost no impact on Y_4R affinity (pK_i of **3.6**: 8.18) (Table 1). In contrast, replacement of Leu^2 by Ile^2 (**3.7**) resulted in a significant decrease in Y_4R binding (pK_i of **3.7**: 7.25). Truncation of the Leu^2 side chain in **3.2** (α-*t*Bu-Gly^2, **3.5**; Ala^2, **3.8**), went along with a massive decrease in Y_4R affinity (Table 1, Figure 4).

Compound **3.19** (pK_i: 8.68), containing 3,5-I_2-Tyr^4, exhibited Y_4R affinity comparable to that lead compound **3.2** (pK_i: 8.47). Possibly, the electron-withdrawing inductive effect (-*I* effect) of the two iodine substituents, resulting in a pronounced positive partial charge (δ+) of the phenolic hydroxyl group,[13] could be beneficial with respect to Y_4R affinity.[14] Whereas replacement of Tyr^4 in **3.2** by β-2-Nal-Ala^4 (**3.22**) resulted in decreased Y_4R affinity, exchange of Tyr^4 by β-1-Nal-Ala^4 (**3.23**) showed retained Y_4R affinity (pK_i: 6.49 *vs*. 8.39), indicating a strong dependence from the orientation of the naphthalene moiety in the binding pocket. Compounds **3.16, 3.17**, **3.18** and **3.21**, containing various unnatural amino acids instead of Tyr^4 in **3.2** (*cf*. Figures 2 and 3, exhibited low Y_4R affinity (Table 1). Finally, an inversion of the peptide sequence of **3.2** led to a loss of Y_4R affinity (**3.24**).

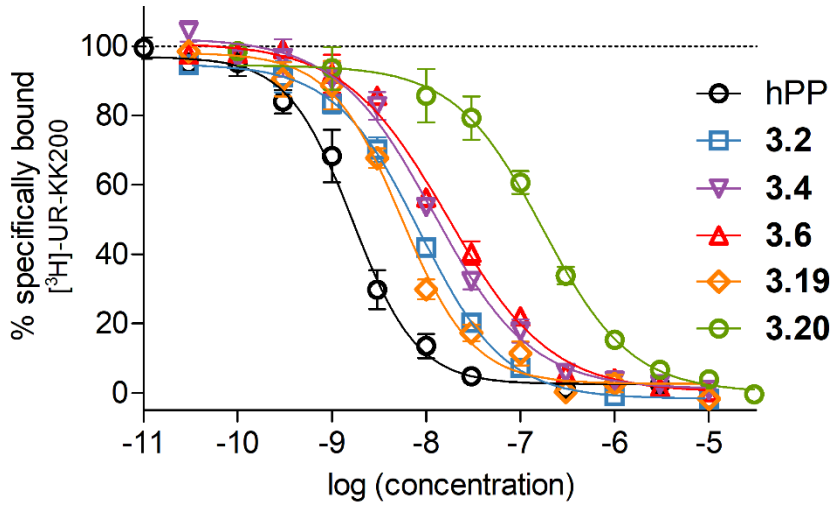

Figure 5. Radioligand displacement curves from competition binding experiments with [^{3}H]UR-KK200 (K_d (hY_4R): 0.67 nM, c = 1 nM) and hPP, **3.2**, **3.4**, **3.6**, **3.19** or **3.20** performed at CHO-hY_4R-mtAEQ-G_{qi5} cells. Data represent means ± SEM from at least three independent experiments performed in triplicate.

Table 1. Y_4R binding data (pK_i ± SEM, K_i) of hPP and compounds **3.2**-**3.24** as well as Y_1, Y_2, and Y_5 receptor binding data (pK_i), agonistic activities (pEC_{50}) and efficacies (α) of selected compounds.

compd.	Y receptor binding (pK_i ± SEM, K_i)				β-Arrestin 1[e]		β-Arrestin 2[e]		Ca^{2+}-Aequorin[f]	
	hY_4R[a]	hY_1R[b]	hY_2R[c]	hY_5R[d]	pEC_{50} ± SEM	α ± SEM	pEC_{50} ± SEM	α ± SEM	pEC_{50} ± SEM	α ± SEM
hPP	9.16 ± 0.03 / 0.69	< 6.5[g]	< 5.5[g]	< 8.0[g]	8.66 ± 0.01	1	8.37 ± 0.02	1	7.96 ± 0.01	1
3.2	8.47 ± 0.01 / 3.4	< 5.0[h]	< 5.0[h]	< 5.0[h]	6.56 ± 0.07	0.51 ± 0.00	6.78 ± 0.02	0.84 ± 0.07	6.36 ± 0.01	0.54 ± 0.03
3.3	6.73 ± 0.11 / 215	n.d.	n.d.	n.d.	n.d.	n.d.	n.d.	n.d.	n.d.	n.d.
3.4	8.32 ± 0.05 / 4.8	< 6.0	< 5.0	< 5.0	6.53 ± 0.02	0.54 ± 0.06	6.54 ± 0.04	0.68 ± 0.04	6.15 ± 0.08	0.53 ± 0.05
3.5	5.90 ± 0.04 / 1280	n.d.	n.d.	n.d.	n.d.	n.d.	n.d.	n.d.	n.d.	n.d.
3.6	8.18 ± 0.04 / 6.7	< 5.5	< 5.0	< 5.5	6.29 ± 0.04	0.59 ± 0.09	6.41 ± 0.07	0.67 ± 0.08	6.11 ± 0.05	0.59 ± 0.07
3.7	7.25 ± 0.13 / 63	n.d.	n.d.	n.d.	< 4.5	n.a.	< 4.5	n.a.	n.d.	n.d.
3.8	< 5.0 / -	n.d.	n.d.	n.d.	n.d.	n.d.	n.d.	n.d.	n.d.	n.d.
3.9	7.08 ± 0.05 / 84	< 5.5	< 5.0	< 5.5	n.d.	n.d.	n.d.	n.d.	n.d.	n.d.
3.10	5.92 ± 0.05 / 1200	n.d.	n.d.	n.d.	n.d.	n.d.	n.d.	n.d.	n.d.	n.d.
3.11	5.89 ± 0.05 / 1300	n.d.	n.d.	n.d.	n.d.	n.d.	n.d.	n.d.	n.d.	n.d.
3.12	6.11 ± 0.07 / 794	< 5.5	n.d.	n.d.	n.d.	n.d.	n.d.	n.d.	n.d.	n.d.
3.13	8.24 ± 0.07 / 6.2	< 5.5	< 5.0	< 5.0	5.60 ± 0.10	0.63 ± 0.05	6.10 ± 0.04	0.91 ± 0.02	5.89 ± 0.07	0.79 ± 0.02
3.14	7.87 ± 0.15 / 15	< 5.0	< 6.0	< 5.5	5.99 ± 0.06	0.54 ± 0.04	6.08 ± 0.02	0.57 ± 0.05	6.17 ± 0.04	0.59 ± 0.05
3.15	6.31 ± 0.05 / 495	n.d.	n.d.	n.d.	n.d.	n.d.	n.d.	n.d.	n.d.	n.d.
3.16	5.94 ± 0.07 / 1190	n.d.	n.d.	n.d.	n.d.	n.d.	n.d.	n.d.	n.d.	n.d.
3.17	5.84 ± 0.06 / 1490	n.d.	n.d.	n.d.	n.d.	n.d.	n.d.	n.d.	n.d.	n.d.
3.18	6.03 ± 0.12 / 1090	n.d.	n.d.	n.d.	n.d.	n.d.	n.d.	n.d.	n.d.	n.d.
3.19	8.68 ± 0.04 / 2.1	< 5.0	< 6.0	< 5.0	7.45 ± 0.05	0.72 ± 0.06	7.53 ± 0.03	0.72 ± 0.02	6.67 ± 0.06	0.37 ± 0.07
3.20	7.20 ± 0.04 / 64	< 5.0	< 5.0	< 5.5	n.a.	n.a.	n.a.	n.a.	n.a.	n.a.
3.21	6.65 ± 0.05 / 226	< 5.5	n.d.	n.d.	n.d.	n.d.	n.d.	n.d.	n.d.	n.d.
3.22	6.49 ± 0.05 / 334	< 5.0	n.d.	n.d.	n.d.	n.d.	n.d.	n.d.	n.d.	n.d.
3.23	8.39 ± 0.12 / 5.2	< 6.0	< 5.0	< 5.0	6.56 ± 0.03	0.66 ± 0.04	6.49 ± 0.07	0.68 ± 0.03	6.35 ± 0.04	0.59 ± 0.03
3.24	< 5.0 / -	n.d.	n.d.	n.d.	n.d.	n.d.	n.d.	n.d.	n.d.	n.d.

[a]Determined by competition binding at CHO-hY_4R-mtAEQ-G_{qi5} cells using [^{3}H]UR-KK200 (K_d = 0.67 nM, c = 1 nM)[8] as radioligand. [b]Determined by competition binding at SK-N-MC neuroblastoma cells using [^{3}H]UR-MK299 (K_d = 0.044 nM, c = 0.15 nM)[15] as radioligand. [c]Determined by competition binding with [^{3}H]propionyl-pNPY (K_d = 0.14, nM, c = 0.5 nM) at CHO-hY_2R cells.[2] [d]Determined by competition binding at HEC-1B-hY_5 cells using [^{3}H]propionyl-pNPY (K_d = 4.8 nM, c = 4 nM)[16] as radioligand. [e]Agonistic potencies (pEC_{50}) and intrinsic activities α (relative to 1 µM hPP, α = 1) determined in a β-arrestin 1 and a β-arrestin 2 recruitment assay at HEK293T-ARRB1-Y_4R cells and HEK293T-ARRB2-Y_4R cells, respectively. [f]Agonistic potencies (pEC_{50}) and intrinsic activities α (relative to 1 µM hPP, α = 1) determined in a Ca^{2+}-aequorin assay using CHO-hY_4R-mtAEQ-G_{qi5} cells. [g]pK_i values reported by Berlicki *et al.*[17] [h]pK_i values reported by Konieczny *et al.*[2] Data represent mean values ± SEM (pK_i, pEC_{50}, α) or mean values (K_i) from three independent experiments performed in triplicate.

n.a.: not applicable

n.d.: not determined

3.2.3 NPY Receptor Subtype Selectivity

Lead compound **3.2** was characterized as a high affinity Y_4R ligand showing high Y_4R selectivity over the remaining human YR subtypes, i.e. Y_1R, Y_2R and Y_5R.[2] For selected peptides (**3.4**, **3.6**, **3.9**, **3.13**, **3.14**, **3.19**, **3.20**, **3.23**) complete NPY receptor selectivity profiles were determined (Table 1). In the case of the studied compounds, incorporation of unnatural amino acids did not affect Y_4R selectivity, i.e. Y_1, Y_2 and Y_5 receptor affinities were in the same range as Y_1, Y_2 and Y_5 receptor binding data of **3.2**.

3.2.4 Functional Studies at the Human Y_4 Receptor

Functional characterization was performed by studying a selection of the synthesized peptides (compounds with a pK_i (hY_4R) > 7.0) in a β-arrestin 1 and 2 recruitment assay (live HEK293T-ARRB1-Y_4R cells and HEK293T-ARRB2-Y_4R cells, respectively[1]), measuring recruitment of β-arrestin to the Y_4R upon receptor activation. In order to investigate the activation of the G-protein mediated signaling pathway, an aequorin-Ca^{2+} assay (live CHO-hY_4R-G_{qi5}-mtAEQ cells[10]) was performed, measuring the increase in intracellular (cytosolic) calcium. In all three assays, the studied compounds (**3.4**, **3.6**, **3.7**, **3.13**, **3.14**, **3.19**, **3.20** and **3.23**) elicited a response when investigated in agonist mode, i.e. these peptides acted as partial Y_4R agonists (Figure 6 A-C). The obtained pEC_{50} values and intrinsic activities α are summarized in Table 1. The discrepancies between the potencies (pEC_{50}) and the respective pK_i values can be mainly attributed to the presence or absence of sodium ions in the used buffers for the functional assays and the radioligand binding assay, respectively, as observed and discussed previously for other peptidic Y_4R agonists.[1,2,18]

It should be mentioned that the observed differences between functional data (pEC_{50}, α) obtained from the Ca^{2+}-aequorin assay and the β-arrestin recruitment assays were low, i.e. the studied Y_4R partial agonists were unbiased with respect to the activation of the G-protein and the arrestin signaling pathways.[19,20] Tetrapeptide **3.19**, containing 3,5-I_2-Tyr^4, displayed slightly higher pEC_{50} values (pEC_{50} = 7.45 (β-arrestin 1); pEC_{50} = 7.53 (β-arrestin 2); pEC_{50} = 6.72 (Ca^{2+}-aequorin)) compared to parent compound **3.2**, but the efficacies α were lower than those of **3.2**. Incorporation of 3-NO_2-Tyr^4 (**3.20**) instead of Tyr^4 in **3.2** resulted in a decrease in Y_4R activity in all three types of assay, however, compound **3.20** was characterized as a weak partial agonist. Future modifications in the 3-NO_2 substituted phenolic ring of Tyr^4 in **3.2** could be an approach to change the mode of action from agonism to antagonism.

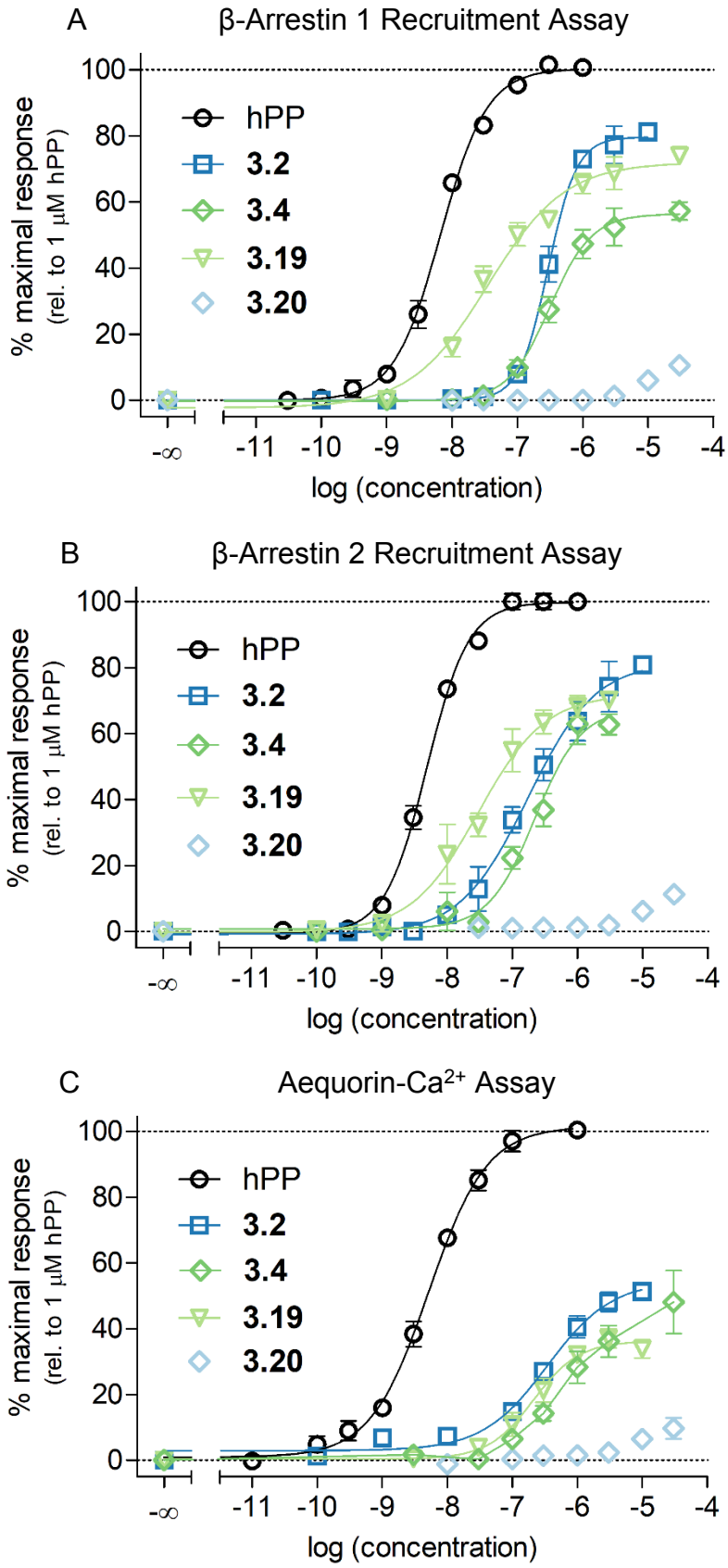

Figure 6. Concentration-response curves of hPP, **3.2**, **3.4**, **3.19** and **3.20** obtained from a hY$_4$R β-arrestin 1 recruitment (A), a hY$_4$R β-arrestin 2 recruitment (B) and a hY$_4$R Ca^{2+}-aequorin (C) assay performed with live HEK293T-ARRB1-Y$_4$R cells, HEK293T-ARRB2-Y$_4$R cells and CHO-hY$_4$-G$_{qi5}$-mtAEQ cells, respectively. Data represent means ± SEM from at least three independent experiments performed in triplicate.

3.3 Conclusion

Through incorporation of unnatural amino acids in oligopeptide **3.2**, a new series of tetrapeptides, acting as Y_4R ligands, was prepared. However, no compound showed a significant increase in Y_4R affinity compared to **3.2** and all analogs proved to be partial Y_4R agonists, i.e. no Y_4R receptor antagonist was obtained by the pursued approach. In future studies, computational chemistry approaches, based on Y_4R homology models, might support the development of non-peptidic Y_4R ligands, including antagonists, derived from tetrapeptide **3.2**.

3.4 Experimental section

3.4.1 General Experimental Conditions

Protected amino acids Fmoc-Tyr(*t*Bu)-OH, Fmoc-Leu-OH, Fmoc-Arg(Pbf)-OH, Fmoc-Bpa-OH, Fmoc-Phe(4-NO_2)-OH and Fmoc-Phe(4-CF_3)-OH were purchased from Carbolution Chemicals (St. Ingbert, Germany). Fmoc-Sieber-PS-resin (0.59 mmol/g), HBTU, N-methyl-2-pyrrolidone (NMP) for peptide synthesis, Fmoc-Tyr(3-NO_2)-OH, Fmoc-Arg(N^{ω}-NO_2)-OH, Fmoc-Tyr(3,5-I_2)-OH and Fmoc-2,3-dehydro-Leu were obtained from Iris Biotech (Marktredwitz, Germany). Fmoc-Ala-OH, MeOH, trifluoroacetic acid, Fmoc-hArg(Pbf)-OH, Fmoc-hLeu-OH, Fmoc-Phe(4-Br)-OH and Fmoc-β-homoleu-OH were from Merck (Darmstadt, Germany). HOBt hydrate and dichloromethane (CH_2Cl_2) were purchased from Acros Organics/Fisher Scientific (Nidderau, Germany). *N,N*-diisopropylethylamine (DIPEA) was obtained from ABCR (Karlsruhe, Germany) and DMF for peptide synthesis, acetic anhydride, gradient grade acetonitrile for HPLC, Triton X-100 and piperidine were from Sigma-Aldrich (Taufkirchen, Germany). Human pancreatic polypeptide (hPP) and porcine neuropeptide Y (pNPY) were from SynPeptide (Shanghai, China). Coelenterazine h was purchased from Biotrend (Cologne, Germany), bacitracin and bovine serum albumin (BSA) were from Serva (Heidelberg, Germany). Pierce™ D-Luciferin (monopotassium salt) was obtained from ThermoFisher Scientific (Nidderau, Germany). The syntheses of radioligands [^{3}H]UR-MK299,[15] [^{3}H]UR-KK200[8] and [^{3}H]propionyl-pNPY[15] were described elsewhere. Millipore water was consistently used for the preparation of stock solutions, buffers and eluents for HPLC. Polypropylene reaction vessels (1.5 and 2 mL) from Sarstedt (Nümbrecht, Germany) were used to keep stock solutions and for small-scale reactions (e.g. activation of Fmoc protected amino acids). NMR spectra were recorded on a Bruker Avance 600 instrument with cryogenic probe (^{1}H: 600.3 MHz, ^{13}C: 150.9 MHz) (Bruker, Karlsruhe, Germany). NMR spectra were calibrated based on the solvent residual peaks (^{1}H-NMR, DMSO-d_6: δ = 2.50 ppm; ^{13}C-NMR: DMSO-d_6: δ = 39.50 ppm) and data are reported as follows: ^{1}H-NMR: chemical shift δ in ppm (multiplicity (s = singlet, d = doublet, t = triplet, m = multiplet, br s = broad singlet), integral, coupling constant *J* in Hz), ^{13}C-NMR: chemical shift δ in ppm. High resolution mass spectrometry (HRMS) was performed with an Agilent 6540 UHD Accurate-Mass Q-TOF LC/MS system linked to an Agilent 1290 analytical HPLC system (Agilent Technologies, Santa Clara, CA). Preparative HPLC was performed with a system from Knauer (Berlin, Germany) consisting of two K-1800 pumps and a K-2001 detector (in the following referred to as “system 1”), or with a Prep 150 LC system from Waters (Eschborn, Germany), comprising a Waters 2545 binary gradient module, a Waters 2489 UV/vis-detector and a Waters fraction collector III (in the following referred to as “system 2”). A Kinetex XB-C18, 5 µm, 250 mm × 21 mm from Phenomenex (Aschaffenburg, Germany) was used as RP-column at a flow rate of 20 mL/min

using mixtures of 0.1% aqueous TFA and acetonitrile as mobile phase. A detection wavelength of 220 nm was used throughout. Collected fractions were lyophilized using a Scanvac CoolSafe 100-9 freeze-dryer (Labogene, Alleroed, Denmark) equipped with a RZ 6 rotary vane vacuum pump (Vacuubrand, Wertheim, Germany). Analytical HPLC analysis was performed with an Agilent 1100 system (Agilent Technologies) composed of a binary pump (G1312A), an autosampler (G1329A), a thermostated column compartment (G1316A) and a diode array detector (G1315B). A Kinetex XB-C18, 5 µm, 250 mm × 4.6 mm (Phenomenex) served as stationary phase at a flow rate of 0.8 mL/min. Detection was performed at 220 nm, the oven temperature was 25 °C. Mixtures of acetonitrile (A) and 0.1 % aqueous TFA (B) were used as mobile phase. The following linear gradient was applied: 0-25 min: A/B 10:90-30:70, 25-27 min: 30:70-95:5, 27-35 min: 95:5 (isocratic). The injection volume was 50 µL. Retention (capacity) factors k were calculated from the retention times t_R according to $k = (t_R - t_0)/t_0$ (t_0 = dead time).

3.4.2 Compound Characterization

Except of compound **3.11**, all target compounds were characterized by ^{1}H-, ^{13}C- and 2D-NMR spectroscopy (2D: HSQC, HMBC, ^{1}H-COSY), HRMS and RP-HPLC. Compound **3.11** was characterized by ^{1}H-NMR, HRMS and RP-HPLC. HPLC purities of all target compounds were ≥ 95% (chromatograms shown in Appendix).

3.4.3 General Procedure for Solid-Phase Peptide Synthesis

Peptides were synthesized by manual SPPS according to the Fmoc strategy. 5-mL Injekt Solo (B. Braun, Melsungen, Germany) or NPRM-JECT (Henke Sass Wolf, Tuttlingen, Germany) syringes, equipped with polyethylene frits (pore size: 35 µm) (Roland Vetter Laborbedarf, Ammerbuch, Germany) were used as reaction vessels. DMF/NMP (8:2 v/v) was used as solvent (referred to as “solvent” in the following) for the coupling reactions and Fmoc deprotection. For initial Fmoc deprotection of the resin and swelling, the resin was treated with 20% piperidine in solvent at rt for 2 × 20 min. Fmoc protected L-amino acids and unnatural amino acids were used in 5-fold excess and preactivated with HBTU (4.9 equiv.)/HOBt (5 equiv.)/DIPEA (10 equiv.) in polypropylene reaction vessels for at least 5 min prior to addition to the resin (volume of solvent: ca. 2.2 mL/mmol Fmoc-amino acid). “Double” coupling (2 × 45 min) was performed at 35 °C for all amino acids using a Multi Reax shaker (Heidolph, Schwabach, Germany) covered with a box equipped with a thermostat-controlled heater. After completed coupling of an Fmoc-aa, the resin was washed with solvent (4 ×) and treated with 20 % piperidine in solvent at rt for 2 × 10 min followed by washing of the resin with solvent (6

×). N-terminally acylated peptides were prepared by treatment of the resin-bound, completely elongated peptide with acetic anhydride (10 equiv.)/DIPEA (10 equiv.) in solvent at rt for 35 min. After coupling and Fmoc deprotection of the final amino acid or after acylation of the N-terminus, the resin was washed with solvent (6 ×) and CH_2Cl_2 (treated with K_2CO_3) (4 ×) followed by cleavage off the resin with CH_2Cl_2/TFA (3:1 v/v) at rt (2 × 20 min). The liquid was separated from the resin by filtration and the resin was washed once with the cleavage reagent. The filtrates were combined in a round-bottom flask and the volatiles were removed by rotary evaporation. The residue was dissolved in TFA/H_2O (95:5 v/v), the mixture was stirred at rt for 5 h (full side-chain deprotection) and transferred to a 100-mL flask containing water (40 mL) followed by lyophilization and subsequent purification by preparative HPLC.

3.4.4 Experimental Protocols and Analytical Data

***N*$^{\omega}$-Nitro-Arg-Leu-Arg-Tyr-amide tris(hydrotrifluoroacetate) (3.3).** Peptide **3.3** was synthesized on a Sieber-Amide-PS resin (40 mg, 0.59 mmol/g) according to the general procedure. Purification by preparative HPLC (system 1, gradient: 0-18 min MeCN/0.1% aq TFA 3:97-42:58, t_R = 10 min) yielded **3.3** as a yellow solid (6.6 mg, 28%). ^{1}H-NMR (600 MHz, DMSO-d_6): δ (ppm) 0.86 (d, 3H, *J* 6.6 Hz), 0.89 (d, 3H, *J* 6.6 Hz), 1.37-1.76 (m, 12H), 2.67-2.75(m, 1H), 2.82-2.87 (m, 1H), 3.07 (q, 2 H, *J* 6.2 Hz), 3.17 (s, 2H), 3.78-3.83 (m, 1H), 4.20-4.26 (m, 1H), 4.33-4.39 (m, 2H), 6.62 (d, 2H, *J* 8.5 Hz), 6.80-7.54 (br s, 4H, interfering with the next three listed signals), 6.96-6.98 (m, 2H), 7.04-7.06 (m, 1H), 7.37-7.40 (m, 1H), 7.61 (t, 1H, *J* 5.6 Hz), 7.72-8.25 (m, 7H), 8.43-8.61 (m, 2H), 9.19 (br s, 1H). ^{13}C-NMR (150 MHz, DMSO-d_6): δ (ppm) 21.4, 23.1, 24.0 (two carbon atoms), 24.9, 28.5, 29.0, 36.8, 40.0, 40.4, 40.7, 51.1, 51.7, 52.3, 53.8, 114.9 (two carbon atoms), 115.9 (TFA), 117.9 (TFA), 127.5, 130.0 (two carbon atoms), 155.9, 156.8 (two carbon atoms), 158.4 (q, *J* 32 Hz) (TFA), 168.3, 170.8, 171.6, 172.7. HRMS (ESI): *m/z* $[M+2H]^{2+}$ calcd. for $[C_{27}H_{48}N_{12}O_7]^{2+}$ 326.1879, found: 326.1885. RP-HPLC (220 nm): 98% (t_R = 12.1 min, *k* = 2.8). $C_{27}H_{46}N_{12}O_7 \cdot C_6H_3F_9O_6$ (650.74 + 342.07).

***N*$^{\varepsilon}$-Amidinyl-Lys-Leu-Arg-Tyr-amide tris(hydrotrifluoroacetate) (3.4).** Peptide **3.4** was synthesized on a Sieber-Amide-PS resin (40 mg, 0.59 mmol/g) according to the general procedure. Purification by preparative HPLC (system 1, gradient: 0-18 min MeCN/0.1% aq TFA 3:97-42:58, t_R = 10 min) yielded **3.4** as a white solid (6.3 mg, 28%). ^{1}H-NMR (600 MHz, DMSO-d_6): δ (ppm) 0.86 (d, 3H, *J* 6.6 Hz), 0.89 (d, 3H, *J* 6.6 Hz), 1.30-1.37 (m, 2H), 1.39-1.55 (m, 7H), 1.60-1.75 (m, 4H), 2.69-2.75 (m, 1H), 2.82-2.87 (m, 1H), 3.06 (q, 4H, *J* 6.6 Hz), 3.76-3.82 (m, 1 H), 4.17-4.23 (m, 1H), 4.30-4.38 (m, 2H), 6.62 (d, 2H, *J* 8.5 Hz), 6.80-7.20 (br s, 4H, interfering with the next two listed signals), 6.96-6.98 (m, 2H), 7.05-7.07 (m, 1H), 7.20-7.55 (br s, 4H, interfering with the next listed signal), 7.38-7.39 (m, 1H), 7.68 (t, 1H, *J* 5.4 Hz),

7.71-7.77 (m, 2H), 8.08-8.17 (m, 3H), 8.20 (d, 1H, *J* 7.9 Hz), 8.51 (d, 1H, *J* 7.9 Hz), 9.21 (br s, 1H). ^{13}C-NMR (150 MHz, DMSO-*d*$_6$): δ (ppm) 21.3, 21.4, 23.1, 24.0, 24.9, 27.8, 28.9, 30.6, 36.8, 40.4, 40.5, 40.6, 51.1, 51.8, 52.4, 53.8, 114.9 (two carbon atoms), 115.9 (TFA), 117.9 (TFA), 127.4, 130.0 (two carbon atoms), 155.82, 156.8 (two carbon atoms), 158.6 (q, *J* 32 Hz) (TFA), 168.5, 170.8, 171.7, 172.6. HRMS (ESI): *m/z* $[M+2H]^{2+}$ calcd. for $[C_{28}H_{51}N_{11}O_5]^{2+}$ 310.7032, found: 310.7035. RP-HPLC (220 nm): 99% (t_R = 10.9 min, *k* = 2.4). $C_{28}H_{49}N_{11}O_5 \cdot C_6H_3F_9O_6$ (619.77 + 342.07).

Arg-(*S*)-2-*tert*-butyl-Gly-Arg-Tyr-amide tris(hydrotrifluoroacetate) (3.5). Peptide **3.5** was synthesized on a Sieber-Amide-PS resin (40 mg, 0.59 mmol/g) according to the general procedure. Purification by preparative HPLC (system 1, gradient: 0-18 min MeCN/0.1% aq TFA 3:97-42:58, t_R = 9 min) yielded **3.5** as a white solid (6.6 mg, 30%). ^{1}H-NMR (600 MHz, DMSO-*d*$_6$): δ (ppm) 0.91 (s, 9H), 1.39-1.56 (m, 5H), 1.59-1.69 (m, 3H), 2.71-2.77 (m, 1H), 2.80-2.86 (m, 1H), 3.04-3.13 (m, 4H), 3.96-4.00 (m, 1H), 4.21-4.28 (m, 2H), 4.32-4.37 (m, 1H), 6.60-6.63 (m, 2H), 6.80-7.20 (br s, 4H, interfering with the next two listed signals), 6.96-6.99 (m, 2H), 7.01-7.02 (m, 1H), 7.20-7.55 (br s, 4H, interfering with the next listed signal), 7.38-7.39 (m, 1H), 7.68-7.73 (m, 1H), 7.82-7.87 (m, 2H), 8.10-8.14 (m, 1H), 8.15-8.23 (m, 3H), 8-30-8-34 (m, 1H), 9.20 (br s, 1H). ^{13}C-NMR (150 MHz, DMSO-*d*$_6$): δ (ppm) 24.2, 24.8, 26.6 (three carbon atoms), 28.6, 29.0, 34.2, 36.7, 40.1, 40.5, 51.6, 52.3, 54.0, 60.2, 114.9 (two carbon atoms), 115.9 (TFA), 117.9 (TFA), 127.5, 129.9 (two carbon atoms), 155.5, 156.8, 156.9, 158.7 (q, *J* 32 Hz) (TFA), 168.3, 168.4, 170.7, 172.8. HRMS (ESI): *m/z* $[M+2H]^{2+}$ calcd. for $[C_{27}H_{49}N_{11}O_5]^{2+}$ 303.6954, found: 303.6956. RP-HPLC (220 nm): 98% (t_R = 9.0 min, *k* = 1.8). $C_{27}H_{47}N_{11}O_5 \cdot C_6H_3F_9O_6$ (605.75 + 342.07).

Arg-(*S*)-(3-methylbut-1-yl)-Gly-Arg-Tyr-amide tris(hydrotrifluoroacetate) (3.6). Peptide **3.6** was synthesized on a Sieber-Amide-PS resin (40 mg, 0.59 mmol/g) according to the general procedure. Purification by preparative HPLC (system 1, gradient: 0-18 min MeCN/0.1% aq TFA 3:97-42:58, t_R = 11 min) yielded **3.6** as a white solid (7.9 mg, 35%). ^{1}H-NMR (600 MHz, DMSO-*d*$_6$): δ (ppm) 0.83 (d, 3H, *J* 1.5 Hz), 0.84 (d, 3H, *J* 1.5 Hz), 1.09-1.18 (m, 1H), 1.18-1.26 (m, 1H), 1.39-1.57 (m, 7H), 1.61-1.73 (m, 4H), 2.68-2.74 (m, 1H), 2.81-2.86 (m, 1H), 3.07 (q, 2H, *J* 6.4 Hz), 3.10 (q, 2H, *J* 6.6 Hz), 3.80-3.86 (m, 1H), 4.18-4.24 (m, 1H), 4.24-4.30 (m, 1H), 4.32-4.37 (m, 1H), 6.62 (d, 2H, *J* 8.5 Hz), 6.80-7.20 (br s, 4H, interfering with the next two listed signals), 6.96-6.98 (m, 2H), 7.05-7.06 (m, 1H), 7.20-7.55 (br s, 4H, interfering with the next listed signal), 7.40-7.42 (m, 1H), 7.64-7.69 (m, 1H), 7.71-7.78 (m, 2H), 8.11-8.23 (m, 4H), 8.51 (d, 1H, *J* 7.7 Hz), 9.12 (br s, 1H). ^{13}C-NMR (150 MHz, DMSO-*d*$_6$): δ (ppm) 22.3, 22.5, 24.0, 25.0, 27.4, 28.5, 29.0, 34.3, 37.0, 40.1, 40.5, 51.7, 52.4, 53.0, 53.8, 114.9 (two carbon atoms), 116.0 (TFA), 118.0 (TFA), 127.4, 130.1 (two carbon atoms), 155.8, 156.8, 156.9, 158.7 (q, *J* 32 Hz) (TFA), 168.3, 170.9, 171.2, 172.7. HRMS (ESI): *m/z* $[M+2H]^{2+}$

calcd. for $[C_{28}H_{51}N_{11}O_5]^{2+}$ 310.7032, found: 310.7038. RP-HPLC (220 nm): 96% (t_R = 14.1 min, k = 3.4). $C_{28}H_{49}N_{11}O_5 \cdot C_6H_3F_9O_6$ (619.77 + 342.07).

Arg-Ile-Arg-Tyr-amide tris(hydrotrifluoroacetate) (3.7). Peptide **3.7** was synthesized on a Sieber-Amide-PS resin (100 mg, 0.59 mmol/g) according to the general procedure. Purification by preparative HPLC (system 1, gradient: 0-18 min MeCN/0.1% aq TFA 8:92-45:55, t_R = 9 min) yielded **3.7** as a white solid (34.2 mg, 59%). ^{1}H-NMR (600 MHz, DMSO-d_6): δ (ppm) 0.79-0.83 (m, 6H), 1.03-1.11 (m, 1H), 1.37-1.57 (m, 6H), 1.61-1.76 (m, 4H), 2.70-2.75 (m, 1H), 2.80-2.86 (m, 1H), 3.04-3.13 (m, 4H), 3.85-3.91 (m, 1H), 4.22-4.27 (m, 2H), 4.35 (q, 1H, *J* 5.8 Hz), 6.60-6.65 (m, 2H), 6.8-7.5 (br s, 8H, interfering with the next three listed signals), 6.96-6.99 (m, 2H), 7.02-7.04 (m, 1H), 7.39-7.41 (m, 1H), 7.67 (t, 1H, *J* 5.7 Hz), 7.76 (t, 1H, *J* 5.9 Hz), 7.83 (d, 1H, *J* 7.9 Hz), 8.12-8.20 (m, 4H), 8.41 (d, 1H, *J* 8.3 Hz), 9.20 (s, 1H). ^{13}C-NMR (150 MHz, DMSO-d_6): δ (ppm) 11.6, 15.7, 24.6, 24.6, 25.4, 29.0, 29.6, 37.3, 40.5, 40.6, 40.9, 52.1, 52.8, 54.4, 57.6, 115.3 (two carbon atoms), 127.9, 130.4 (two carbon atoms), 156.3, 157.3, 157.3, 168.8, 170.9, 171.3, 173.2. HRMS (ESI): *m/z* $[M+2H]^{2+}$ calcd. for $[C_{27}H_{49}N_{11}O_5]^{2+}$ 303.6954, found: 303.6967. RP-HPLC (220 nm): 97% (t_R = 9.2 min, k = 1.8). $C_{27}H_{47}N_{11}O_5 \cdot C_6H_3F_9O_2$ (605.75 + 342.07).

Arg-Leu-Ala-Tyr-amide bis(hydrotrifluoroacetate) (3.8). Peptide **3.8** was synthesized on a Sieber-Amide-PS resin (40 mg, 0.59 mmol/g) according to the general procedure. Purification by preparative HPLC (system 1, gradient: 0-18 min MeCN/0.1% aq TFA 3:97-42:58, t_R = 14 min) yielded **3.8** as a white solid (9.7 mg, 42%). ^{1}H-NMR (600 MHz, DMSO-d_6): δ (ppm) 0.85-0.91 (m, 6H), 1.17 (d, 3H, *J* 7.1 Hz), 1.43-1.48 (m, 2H), 1.48-1.55 (m, 2H), 1.60-1.73 (m, 3H), 2.69-2.75 (m, 1H), 2.83-2.88 (m, 1H), 3.10 (q, 2H, *J* 6.7 Hz), 3.78-3.84 (m, 1H), 4.18-4.23 (m, 1H), 4.29-4.33 (m, 1H), 4.34-4.38 (m, 1H), 6.61-6.65 (m, 2H), 6.90-7.55 (br s, 4H, interfering with the next three listed signals), 6.96-6.99 (m, 2H), 7.05-7.07 (m, 1H), 7.35-7.37 (m, 1H), 7.66-7.70 (m, 1H), 7.72-7.77 (m, 1H), 8.13-8.25 (m, 4H), 8.48-8.54 (m, 1H), 9.20 (br s, 1H). ^{13}C-NMR (150 MHz, DMSO-d_6): δ (ppm) 17.9, 21.4, 23.1, 23.98, 23.99, 28.4, 36.8, 40.2, 40.6, 48.4, 51.0, 51.7, 53.8, 114.8 (two carbon atoms), 115.9 (TFA), 117.9 (TFA), 127.5, 130.1 (two carbon atoms), 155.8, 156.8, 168.2, 171.4, 171.6, 172.7. HRMS (ESI): *m/z* $[M+H]^+$ calcd. for $[C_{24}H_{41}N_8O_5]^+$ 521.3194, found: 521.3200. RP-HPLC (220 nm): 98% (t_R = 8.0 min, k = 1.5). $C_{24}H_{40}N_8O_5 \cdot C_4H_2F_6O_4$ (520.64 + 228.01).

(*S*)-2-Amino-*N*-((*S*)-1-(((*S*)-1-(((*S*)-1-amino-3-(4-hydroxyphenyl)-1-oxopropan-2-yl)amino)-5-guanidino-1-oxopentan-2-yl)amino)-3-(naphthalen-1-yl)-1-oxopropan-2-yl)-5-guanidinopentanamide tris(hydrotrifluoroacetate) (3.9). Peptide **3.9** was synthesized on a Sieber-Amide-PS resin (40 mg, 0.59 mmol/g) according to the general procedure. Purification by preparative HPLC (system 2, gradient: 0-18 min MeCN/0.1% aq TFA 3:97-42:58, t_R = 14 min) yielded **3.9** as a white solid (10.9 mg, 45%). ^{1}H-NMR (600 MHz, DMSO-

d$_6$): δ (ppm) 1.41-1.56 (m, 5H), 1.63-1.75 (m, 3H), 2.72-2.77 (m, 1H), 2.86-2.92 (m, 1H), 3.05-3.12 (m, 4H), 3.28-3.32 (m, 1H), 3.50-3.51 (m, 1H), 3.73-3.75 (m, 1H), 4.24-4.28 (m, 1H), 4.35-4.40 (m, 1H), 4.76-4.82 (m, 1H), 6.64-6.67 (m, 2H), 6.80-7.20 (br s, 4H, interfering with the next two listed signals), 7.02-7.04 (m, 2H), 7.07-7.08 (m, 1H), 7.20-7.50 (br s, 4H, interfering with the next two listed signals), 7.33-7.35 (m, 2H), 7.45-7.46 (m, 1H), 7.51-7.57 (m, 2H), 7.60-7.63 (m, 1H), 7.67-7.71 (m, 1H), 7.78-7.81 (m, 1H), 7.85-7.88 (m, 1H), 7.89-7.94 (m, 1H), 8.06-8.16 (m, 3H), 8.21-8.25 (m, 1H), 8.33-8.36 (m, 1H), 8.72-8.76 (m, 1H), 9.12 (br s, 1H). ^{13}C-NMR (150 MHz, DMSO-*d*$_6$): δ (ppm) 24.0, 24.9, 28.4, 29.0, 34.5, 36.9, 40.2, 40.5, 51.7, 52.6, 53.1, 54.0, 114.9 (two carbon atoms), 115.9 (TFA), 117.9 (TFA), 123.8, 125.4, 125.6, 126.1, 126.9, 127.1, 127.6, 128.5, 130.1 (two carbon atoms), 131.6, 133.0, 133.3, 155.9, 156.7, 156.8, .158.4 (q, *J* 32 Hz) (TFA), 168.6, 170.68, 170.72, 172.8. HRMS (ESI): *m/z* $[M+2H]^{2+}$ calcd. for $[C_{34}H_{49}N_{11}O_5]^{2+}$ 345.6954, found: 345.6963. RP-HPLC (220 nm): 97% (t_R = 16.4 min, *k* = 4.1). $C_{34}H_{47}N_{11}O_5 \cdot C_6H_3F_9O_6$ (689.82 + 342.07).

(*S*)-2-Amino-*N*-((*S*)-1-(((*S*)-1-(((*S*)-1-amino-3-(4-hydroxyphenyl)-1-oxopropan-2-yl)amino)-5-guanidino-1-oxopentan-2-yl)amino)-3-(naphthalen-2-yl)-1-oxopropan-2-yl)-5-guanidinopentanamide tris(hydrotrifluoroacetate) (3.10). Peptide **3.10** was synthesized on a Sieber-Amide-PS resin (40 mg, 0.59 mmol/g) according to the general procedure. Purification by preparative HPLC (system 2, gradient: 0-18 min MeCN/0.1% aq TFA 3:97-42:58, t_R = 14 min) yielded **3.10** as a white solid (13.7 mg, 57%). ^{1}H-NMR (600 MHz, DMSO-*d*$_6$): δ (ppm) 1.44-1.57 (m, 5H), 1.64-1.74 (m, 3H), 2.71-2.77 (m, 1H), 2.86-2.91 (m, 1H), 2.92-2.99 (m, 1H), 3.04-3.13 (m, 4H), 3.21-3.27 (m, 1H), 3.74-3.76 (m, 1H), 4.24-4.27 (m, 1H), 4.39-4.43 (m, 1H), 4.70-4.76 (m, 1H), 6.62-6.67 (m, 2H), 7.74-7.20 (br s, 4H, interfering with the next two listed signals), 6.99-7.02 (m, 2H), 7.08-7.09 (m, 1H), 7.20-7.56 (br s, 4H, interfering with the next listed signal), 7.44-7.51 (m, 4H), 7.59-7.66 (m, 2H), 7.77-7.89 (m, 5H), 7.99-8.09 (m, 3H), 8.45-8.49 (m, 1H), 8.58-8.62 (m, 1H), 9.19 (br s, 1H). ^{13}C-NMR (150 MHz, DMSO-*d*$_6$): δ (ppm) 23.9, 25.0, 28.5, 29.1, 36.9, 37.5, 40.2, 40.5, 51.6, 52.6, 53.8, 54.0, 114.8 (two carbon atoms), 115.8 (TFA), 117.8 (TFA), 125.5, 126.0, 127.3, 127.39, 127.45, 127.47, 127.51, 127.7, 130.1 (two carbon atoms), 131.9, 132.9, 135.1, 155.8, 156.70, 156.72, 158.3 (q, *J* 32 Hz) (TFA), 168.6, 170.7, 170.8, 172.7. HRMS (ESI): *m/z* $[M+2H]^{2+}$ calcd. for $[C_{34}H_{49}N_{11}O_5]^{2+}$ 345.6954, found: 345.6963. RP-HPLC (220 nm): 98% (t_R = 17.1 min, *k* = 4.3). $C_{34}H_{47}N_{11}O_5 \cdot C_6H_3F_9O_6$ (689.82 + 342.07).

(*S*)-2-Amino-*N*-((*S*)-1-(((*S*)-1-(((*S*)-1-amino-3-(4-hydroxyphenyl)-1-oxopropan-2-yl)amino)-5-guanidino-1-oxopentan-2-yl)amino)-3-(4-benzoylphenyl)-1-oxopropan-2-yl)-5-guanidinopentanamide tris(hydrotrifluoroacetate) (3.11). Peptide **3.11** was synthesized on a Sieber-Amide-PS resin (40 mg, 0.59 mmol/g) according to the general procedure. Purification by preparative HPLC (system 1, gradient: 0-18 min MeCN/0.1% aq TFA 3:97-

42:58, t_R = 13 min) yielded **3.11** as a white solid (11.9 mg, 46%). ^{1}H-NMR (600 MHz, DMSO-d_6): 1.43-1.56 (m, 5H), 1.64-1.73 (m, 3H), 2.69-2.76 (m, 1H), 2.84-2.92 (m, 2H), 3.06-3.12 (m, 4H), 3.13-3.17 (m, 1H), 3.77-3.78 (m, 1H), 4.23-4.26 (m, 1H), 4.37-4.42 (m, 1H), 4.66-4.71 (m, 1H), 6.60-6.63 (m, 2H), 6.75-7.20 (br s, 4H, interfering with the next two listed signals), 6.96-6.98 (m, 2H), 7.07-7.09 (m, 1H), 7.20-7.50 (br s, 4H, interfering with the next listed signal), 7.43-7.48 (m, 3H), 7.55-7.59 (m, 3H), 7.60-7.64 (m, 1H), 7.66-7.73 (m, 5H), 7.82-7.86 (m, 1H), 8.03-8.12 (m, 3H), 8.43-8.47 (m, 1H), 8.61-8.65 (m, 1H), 9.15 (br s, 1H). HRMS (ESI): *m/z* $[M+2H]^{2+}$ calcd. for $[C_{37}H_{51}N_{11}O_6]^{2+}$ 372.7006, found: 372.7011. RP-HPLC (220 nm): 98% (t_R = 18.8 min, k = 4.8). $C_{37}H_{49}N_{11}O_6 \cdot C_6H_3F_9O_6$ (743.87 + 342.07).

(*E*)-2-Amino-*N*-((*S*)-1-(((*S*)-1-amino-3-(4-hydroxyphenyl)-1-oxopropan-2-yl)amino)-5-guanidino-1-oxopentan-2-yl)-4-methylpent-2-enamide di(hydrotrifluoroacetate) (3.12). Peptide **3.12** was synthesized on a Sieber-Amide-PS resin (40 mg, 0.59 mmol/g) according to the general procedure. Purification by preparative HPLC (system 1, gradient: 0-18 min MeCN/0.1% aq TFA 3:97-42:58, t_R = 15 min) yielded **3.12** as a white solid (8.4 mg, 53%). ^{1}H-NMR (600 MHz, DMSO-d_6): δ (ppm) 0.88-0.91 (m, 6H), 1.31-1.44 (m, 2H), 1.55-1.63 (m, 1H), 1.65-1.73 (m, 1H), 2.00-2.07 (m, 1H), 2.64-2.74 (m, 3H), 2.84-2.89 (m, 1H), 3.01-3.07 (m, 2H), 4.22-4.27 (m, 1H), 4.33-4.38 (m, 1H), 6.60-6.63 (m, 2H), 6.75-7.50 (br s, 4H, interfering with the next three listed signals), 6.97-6.99 (m, 2H), 7.03-7.05 (m, 1H), 7.39-7.43 (m, 1H), 7.51-7.55 (m, 1H), 8.00 (d, 1H, *J* 8.2 Hz), 8.37 (d, 1H, *J* 8.3 Hz), 8.99-9.34 (br s, 1H). ^{13}C-NMR (150 MHz, DMSO-d_6): δ (ppm) 22.28, 22.30, 23.7, 24.9, 28.8, 36.8, 40.3, 45.2, 52.3, 54.0, 114.8 (two carbon atoms), 127.6, 130.1 (two carbon atoms), 155.8, 156.7, 158.3 (q, *J* 32 Hz) (TFA), 161.0, 170.1, 172.7, 198.3. HRMS (ESI): *m/z* $[M+H]^+$ calcd. for $[C_{21}H_{34}N_7O_4]^+$ 449.2488, found: 449.2510. RP-HPLC (220 nm): 98% (t_R = 21.9 min, k = 5.8). $C_{21}H_{33}N_7O_4 \cdot C_4H_2F_6O_4$ (447.54 + 228.01).

(*N*-Arginyl-3-amino-3-[2-methylpropyl]-propionyl)Arg-Tyr-amide tris(hydrotrifluoroacetate) (3.13). Peptide **3.13** was synthesized on a Sieber-Amide-PS resin (100 mg, 0.59 mmol/g) according to the general procedure. Purification by preparative HPLC (system 1, gradient: 0-18 min MeCN/0.1% aq TFA 8:92-45:55, t_R = 9 min) yielded **3.13** as a white solid (11.2 mg, 19%). ^{1}H-NMR (600 MHz, DMSO-d_6): δ (ppm) 0.81-0.85 (m, 6H), 1.11-1.18 (m, 1H), 1.31-1.37 (m, 1H), 1.40-1.52 (m, 5H), 1.55-1.63 (m, 2H), 1.64-1.73 (m, 2H), 2.23-2.33 (m, 2H), 2.67-2.74 (m, 1H), 2.87 (dd, 1H, *J* 5.4 Hz), 3.03-3.08 (m, 2H), 3.08-3.13 (m, 2H), 3.67-3.74 (m, 1H), 4.12-4.18 (m, 1H), 4.19-4.24 (m, 1H), 4.30-4.35 (m, 1H), 6.62-6.65 (m, 2H), 6.8-7.5 (br s, 8H, interfering with the next three listed signals), 6.97-7.00 (m, 2H), 7.05-7.06 (m, 1H), 7.38-7.41 (m, 1H), 7.67 (t, 1H, *J* 5.7 Hz), 7.76 (t, 1H, *J* 5.9 Hz), 7.85 (d, 1H, *J* 8.1 Hz), 8.11-8.14 (m, 1H), 8.14-8.17 (m, 3H), 8.27 (d, 1H, *J* 8.6 Hz), 9.21 (s, 1H). ^{13}C-NMR (150 MHz, DMSO-d_6): δ (ppm) 21.5, 23.4, 24.0, 24.0, 25.0, 28.3, 29.1, 36.8, 40.2, 40.4, 41.4, 42.8, 44.8,

51.9, 52.3, 54.0, 114.9 (two carbon atoms), 127.7, 130.1 (two carbon atoms), 155.8, 156.8, 156.8, 167.4, 169.9, 171.1, 172.9. HRMS (ESI): *m/z* $[M+2H]^{2+}$ calcd. for $[C_{28}H_{52}N_{11}O_5]^{2+}$ 310.7037, found: 310.7047. RP-HPLC (220 nm): 95% (t_R = 10.2 min, *k* = 2.1). $C_{28}H_{49}N_{11}O_5 \cdot C_6H_3F_9O_2$ (619.77 + 342.07).

(*S*)-*N*-((*S*)-1-Amino-3-(4-hydroxyphenyl)-1-oxopropan-2-yl)-2-((*S*)-2-((*S*)-2-amino-5-guanidinopentanamido)-4-methylpentanamido)-6-guanidinohexanamide tris(hydrotrifluoroacetate) (3.14). Peptide **3.14** was synthesized on a Sieber-Amide-PS resin (40 mg, 0.59 mmol/g) according to the general procedure. Purification by preparative HPLC (system 2, gradient: 0-18 min MeCN/0.1% aq TFA 3:97-42:58, t_R = 10 min) yielded **3.14** as a white solid (8.9 mg, 39%). ^{1}H-NMR (600 MHz, DMSO-*d*$_6$): δ (ppm) 0.83-0.90 (m, 6H), 1.16-1.30 (m, 2H), 1.40-1.56 (m, 7H), 1.58-1.73 (m, 4H), 2.69-2.74 (m, 1H), 2.81-2.87 (m, 1H), 3.01-3.06 (m, 2H), 3.06-3.13 (m, 2H), 3.79-3.83 (m, 1H), 4.13-4.17 (m, 1H), 4.31-4.37 (m, 2H), 6.60-6.64 (m, 2H), 6.80-7.20 (br s, 4H, interfering with the next two listed signals), 6.95-6.98 (m, 2H), 7.07-7.08 (m, 1H), 7.20-7.55 (br s, 4H, interfering with the next listed signal), 7.38-7.40 (m, 1H), 7.67-7.70 (m, 1H), 7.73-7.80 (m, 2H), 8.13-8.22 (m, 4H), 8.47-8.52 (m, 1H), 9.21 (br s, 1H). ^{13}C-NMR (150 MHz, DMSO-*d*$_6$): δ (ppm) 21.3, 22.3, 23.1, 23.99, 24.01, 28.1, 28.4, 31.4, 36.8, 40.2, 40.6, 40.7, 51.2 ,51.7, 52.7, 53.8, 114.8 (two carbon atoms), 115.8 (TFA), 117.8 (TFA), 127.5, 130.0 (two carbon atoms), 155.8, 156.8, 156.9, 158.8 (q, *J* 32 Hz) (TFA), 168.2, 171.0, 171.6, 172.9. HRMS (ESI): *m/z* $[M+2H]^{2+}$ calcd. for $[C_{28}H_{51}N_{11}O_5]^{2+}$ 310.7032, found: 310.7039. RP-HPLC (220 nm): 98% (t_R = 10.8 min, *k* = 2.4). $C_{28}H_{49}N_{11}O_5 \cdot C_6H_3F_9O_6$ (619.77 + 342.07).

(*S*)-2-Amino-*N*-((*S*)-1-(((*S*)-1-(((*S*)-1-amino-3-(4-hydroxyphenyl)-1-oxopropan-2-yl)amino)-5-(3-nitroguanidino)-1-oxopentan-2-yl)amino)-4-methyl-1-oxopentan-2-yl)-5-guanidinopentanamide tris(hydrotrifluoroacetate) (3.15). Peptide **3.15** was synthesized on a Sieber-Amide-PS resin (40 mg, 0.59 mmol/g) according to the general procedure. Purification by preparative HPLC (system 2, gradient: 0-18 min MeCN/0.1% aq TFA 3:97-42:58, t_R = 11 min) yielded **3.15** as a yellow solid (7.4 mg, 32%). ^{1}H-NMR (600 MHz, DMSO-*d*$_6$): δ (ppm) 0.83-0.91 (m, 6H), 1.40-1.56 (m, 7H), 1.60-1.72 (m, 4H), 2.68-2.73 (m, 1H), 2.81-2.87 (m, 1H), 3.07-3.16 (m, 4H), 3.80-3.82 (m, 1H), 4.16-4.22 (m, 1H), 4.31-4.36 (m, 2H), 6.60-6.64 (m, 2H), 6.80-7.50 (br s, 4H, interfering with the next three listed signals), 6.95-6.98 (m, 2H), 7.04-7.07 (m, 1H), 7.37-7.39 (m, 1H), 7.60-8.37 (br s, 2H, interfering with the next two listed signals), 7.66-7.76 (m, 2H), 8.13-8.21 (m, 5H), 8.38-8.58 (m, 2H), 9.18 (br s, 1H). ^{13}C-NMR (150 MHz, DMSO-*d*$_6$): δ (ppm) 21.4, 23.1, 23.99, 24.01 (two carbon atoms), 28.4, 29.1, 36.9, 40.2, 40.3, 40.6, 51.3, 51.7, 52.4, 53.8, 114.9 (two carbon atoms), 116.0 (TFA), 118.0 (TFA), 127.5, 130.0 (two carbon atoms), 155.8, 156.8 (two carbon atoms), 158.5 (q, *J* 32 Hz) (TFA), 168.3, 170.9, 171.7, 172.7. HRMS (ESI): *m/z* $[M+2H]^{2+}$ calcd. for $[C_{27}H_{48}N_{12}O_7]^{2+}$

326.1879, found: 326.1889. RP-HPLC (220 nm): 98% (t_R = 12.5 min, k = 3.2). $C_{27}H_{46}N_{12}O_7 \cdot C_6H_3F_9O_6$ (650.74 + 342.07).

(*S*)-2-Amino-*N*-((*S*)-1-(((*S*)-1-(((*S*)-1-amino-3-(4-nitrophenyl)-1-oxopropan-2-yl)amino)-5-guanidino-1-oxopentan-2-yl)amino)-4-methyl-1-oxopentan-2-yl)-5-guanidinopentanamide tris(hydrotrifluoroacetate) (3.16). Peptide **3.16** was synthesized on a Sieber-Amide-PS resin (40 mg, 0.59 mmol/g) according to the general procedure. Purification by preparative HPLC (system 1, gradient: 0-18 min MeCN/0.1% aq TFA 3:97-42:58, t_R = 12 min) yielded **3.16** as a yellow solid (9.7 mg, 42%). ^{1}H-NMR (600 MHz, DMSO-d_6): δ (ppm) 0.81-0.86 (m, 6H), 1.34-1.56 (m, 7H); 1.59-1.65 (m, 2H), 1.67-1.73 (m, 2H), 2.92-2.99 (m, 1H), 3.02-3.17 (m, 5H), 3.79-3.84 (m, 1H), 4.15-4.21 (m, 1H), 4.30-4.36 (m, 1H), 4.49-4.55 (m, 1H), 6.80-7.20 (br s, 4H, interfering with the next listed signal), 7.18-7.20 (m, 1H), 7.20-7.60 (br s, 4H, interfering with the next two listed signals), 7.47-7.50 (m, 2H), 7.54-7.56 (m, 1H), 7.70-7.74 (m, 1H), 7.78-7.82 (m, 1H), 7.95-7.99 (m, 1H), 8.10-8.14 (m, 2H), 8.16-8.23 (m, 4H), 8.47-8.51 (m, 1H). ^{13}C-NMR (150 MHz, DMSO-d_6): δ (ppm) 21.3, 23.0, 23.9, 24.0, 25.0, 28.4, 28.9, 37.5, 40.1, 40.4, 40.6, 51.1, 51.7, 52.5, 52.9, 115.8 (TFA), 117.8 (TFA), 123.0 (two carbon atoms), 130.5 (two carbon atoms), 146.1, 146.2, 156.8, 156.9, 158.7 (q, J 32 Hz) (TFA), 168.3, 171.0, 171.6, 172.0. HRMS (ESI): *m/z* $[M+2H]^{2+}$ calcd. for $[C_{27}H_{48}N_{12}O_6]^{2+}$ 318.1904, found: 318.1912. RP-HPLC (220 nm): 98% (t_R = 17.2 min, k = 4.4). $C_{27}H_{46}N_{12}O_6 \cdot C_6H_3F_9O_6$ (634.74 + 342.07).

(*S*)-2-Amino-*N*-((*S*)-1-(((*S*)-1-(((*S*)-1-amino-3-(4-benzoylphenyl)-1-oxopropan-2-yl)amino)-5-guanidino-1-oxopentan-2-yl)amino)-4-methyl-1-oxopentan-2-yl)-5-guanidinopentanamide tris(hydrotrifluoroacetate) (3.17). Peptide **3.17** was synthesized on a Sieber-Amide-PS resin (40 mg, 0.59 mmol/g) according to the general procedure. Purification by preparative HPLC (system 1, gradient: 0-18 min MeCN/0.1% aq TFA 3:97-42:58, t_R = 15 min) yielded **3.17** as a white solid (10.8 mg, 42%). ^{1}H-NMR (600 MHz, DMSO-d_6): δ (ppm) 0.80-0.84 (m, 6H), 1.39-1.56 (m, 7H), 1.60-1.72 (m, 4H), 2.92-2.98 (m, 1H), 3.05-3.13 (m, 5H), 3.79-3.83 (m, 1H), 4.19-4.24 (m, 1H), 4.32-4.37 (m, 1H), 4.49-4.54 (m, 1H), 6.80-7.20 (br s, 4H, interfering with the next listed signal), 7.16-7.18 (m, 1H), 7.20-7.58 (br s, 4H, interfering with the next three listed signals), 7.38-7.40 (m, 2H), 7.52-7.54 (m, 1H), 7.55-7.57 (m, 2H), 7.64-7.74 (m, 6H), 7.79-7.82 (m, 1H), 7.93-7.96 (m, 1H), 8.14-8.25 (m, 4H), 8.48-8.52 (m, 1H). ^{13}C-NMR (150 MHz, DMSO-d_6): δ (ppm) 21.3, 23.1, 23.9, 24.0, 25.0, 28.4, 28.9, 37.6, 40.1, 40.4, 40.7, 51.2, 51.7, 52.4, 53.2, 115.9 (TFA), 117.9 (TFA), 128.5 (two carbon atoms), 129.4 (two carbon atoms), 129.5 (two carbon atoms), 129.6 (two carbon atoms), 132.5, 135.0, 137.2, 143.0, 156.8, 156.7, 158.8 (q, J 32 Hz) (TFA), 168.3, 171.0, 171.7, 172.2, 195.5. HRMS (ESI): *m/z* $[M+2H]^{2+}$ calcd. for $[C_{34}H_{53}N_{11}O_5]^{2+}$ 347.7110, found: 347.7119. RP-HPLC (220 nm): 98% (t_R = 23.8 min, k = 6.4). $C_{34}H_{51}N_{11}O_5 \cdot C_6H_3F_9O_6$ (693.85 + 342.07).

(*S*)-2-Amino-*N*-((*S*)-1-(((*S*)-1-(((*S*)-1-amino-1-oxo-3-(4-(trifluoromethyl)phenyl)propan-2-yl)amino)-5-guanidino-1-oxopentan-2-yl)amino)-4-methyl-1-oxopentan-2-yl)-5-guanidinopentanamide tris(hydrotrifluoroacetate) (3.18). Peptide **3.18** was synthesized on a Sieber-Amide-PS resin (40 mg, 0.59 mmol/g) according to the general procedure. Purification by preparative HPLC (system 1, gradient: 0-18 min MeCN/0.1% aq TFA 3:97-42:58, t_R = 16 min) yielded **3.18** as a white solid (11.4 mg, 48%). ^{1}H-NMR (600 MHz, DMSO-d_6): δ (ppm) 0.82-0.87 (m, 6H), 1.37-1.56 (m, 7H), 1.60-1.72 (m, 4H), 2.89-2.95 (m, 1H), 3.03-3.12 (m, 5H), 3.79-3.84 (m, 1H), 4.16-4.21 (m, 1H), 4.31-4.36 (m, 1H), 4.45-4.50 (m, 1H), 6.90-7.20 (br s, 4H, interfering with the next listed signal), 7.15-7.16 (m, 1H), 7.20-7.55 (br s, 4H, interfering with the next two listed signals), 7.40-7.42 (m, 2H), 7.50-7.52 (m, 1H), 7.57-7.61 (m, 2H), 7.73-7.77 (m, 1H), 7.81-7.85 (m, 1H), 7.90-7.93 (m, 1H), 8.16-8.25 (m, 4H), 8.49-8.52 (m, 1H). ^{13}C-NMR (150 MHz, DMSO-d_6): δ (ppm) 21.3, 23.0, 23.95, 24.00, 25.0, 28.4, 28.9, 37.4, 40.1, 40.4, 40.6, 51.2, 51.7, 52.5, 53.1, 115.9 (TFA), 117.9 (TFA), 123.5, 124.76, 124.78, 125.3, 130.0 (two carbon atoms), 142.5, 156.87, 156.92, 158.9 (q, *J* 32 Hz) (TFA), 168.3, 171.0, 171.7, 172.2. HRMS (ESI): *m/z* $[M+2H]^{2+}$ calcd. for $[C_{28}H_{48}F_3N_{11}O_4]^{2+}$ 329.6916, found: 329.6922. RP-HPLC (220 nm): 97% (t_R = 23.3 min, *k* = 6.2). $C_{28}H_{46}F_3N_{11}O_4 \cdot C_6H_3F_9O_6$ (657.74 + 342.07).

(*S*)-2-Amino-*N*-((*S*)-1-(((*S*)-1-(((*S*)-1-amino-3-(4-hydroxy-3,5-diiodophenyl)-1-oxopropan-2-yl)amino)-5-guanidino-1-oxopentan-2-yl)amino)-4-methyl-1-oxopentan-2-yl)-5-guanidinopentanamide tris(hydrotrifluoroacetate) (3.19). Peptide **3.19** was synthesized on a Sieber-Amide-PS resin (40 mg, 0.59 mmol/g) according to the general procedure. Purification by preparative HPLC (system 2, gradient: 0-18 min MeCN/0.1% aq TFA 3:97-42:58, t_R = 14 min) yielded **3.19** as a white solid (8.4 mg, 30%). ^{1}H-NMR (600 MHz, DMSO-d_6): δ (ppm) 0.85-0.92 (m, 6H), 1.42-1.59 (m, 7H), 1.62-1.73 (m, 4H), 2.63-2.69 (m, 1H), 2.82-2.88 (m, 1H), 3.05-3.14 (m, 4H), 3.78-3.83 (m, 1H), 4.13-4.18 (m, 1H), 4.30-4.38 (m, 2H), 6.78-7.20 (br s, 4H, interfering with the next listed signal), 7.15-7.18 (m, 1H), 7.20-7.55 (br s, 4H, interfering with the next listed signal), 7.48-7.52 (m, 1H), 7.57 (s, 2H), 7.61-7.65 (m, 1H), 7.67-7.71 (m, 1H), 7.75-7.78 (m, 1H), 8.11-8.19 (m, 3H), 8.22-8.26 (m, 1H), 8.46-8.50 (m, 1H), 9.37 (s, 1H). ^{13}C-NMR (150 MHz, DMSO-d_6): δ (ppm) 21.3, 23.2, 24.0 (two carbon atoms), 25.0, 28.4, 29.1, 35.6, 40.2 (two carbon atoms), 40.5, 51.2, 51.7, 52.7, 53.5, 86.7 (two carbon atoms), 116.1 (TFA), 118.1 (TFA), 133.6, 139.6 (two carbon atoms), 153.8, 156.7, 156.8, 158.4 (q, *J* 32 Hz) (TFA), 168.2, 171.0, 171.7, 172.2. HRMS (ESI): *m/z* $[M+2H]^{2+}$ calcd. for $[C_{27}H_{47}I_2N_{11}O_5]^{2+}$ 429.5920, found: 429.5921. RP-HPLC (220 nm): 99% (t_R = 21.5 min, *k* = 5.7). $C_{27}H_{45}I_2N_{11}O_5 \cdot C_6H_3F_9O_6$ (857.54 + 342.07).

(*S*)-2-Amino-*N*-((*S*)-1-(((*S*)-1-(((*S*)-1-amino-3-(4-hydroxy-3-nitrophenyl)-1-oxopropan-2-yl)amino)-5-guanidino-1-oxopentan-2-yl)amino)-4-methyl-1-oxopentan-2-yl)-5-

guanidinopentanamide tris(hydrotrifluoroacetate) (3.20). Peptide **3.20** was synthesized on a Sieber-Amide-PS resin (40 mg, 0.59 mmol/g) according to the general procedure. Purification by preparative HPLC (system 1, gradient: 0-18 min MeCN/0.1% aq TFA 3:97-42:58, t_R = 12 min) yielded **3.20** as a yellow solid (5.1 mg, 22%). ^{1}H-NMR (600 MHz, DMSO-d_6): δ (ppm) 0.83-0.90 (m, 6H), 1.38-1.58 (m, 7H), 1.59-1.74 (m, 4H), 2.78-2.82 (m, 1H), 2.93-2.98 (m, 1H), 3.04-3.13 (m, 4H), 3.79-3.84 (m, 1H), 4.14-4.19 (m, 1H), 4.31-4.36 (m, 1H), 4.39-4.44 (m, 1H), .6.80-7.20 (br s, 4H, interfering with the next two listed signals), 7.02-7.04 (m, 1H), 7.14-7.16 (m, 1H), 7.20-7.55 (br s, 4H, interfering with the next two listed signals), 7.37-7.39 (m, 1H), 7.49-7.50 (m, 1H), 7.69-7.72 (m, 1H), 7.73-7.75 (m, 1H), 7.77-7.80 (m, 1H), 7.84-7.89 (m, 1H), 8.14-8.24 (m, 4H), 8.45-8.50 (m, 1H), 10.91 (br s, 1H). ^{13}C-NMR (150 MHz, DMSO-d_6): δ (ppm) 21.3, 23.1, 23.97, 23.99, 25.0, 28.4, 28.9, 36.4, 40.1, 40.4, 40.6, 51.2, 51.7, 52.5, 53.4, 115.9 (TFA), 117.9 (TFA), 118.9, 125.3, 128.7, 136.0, 136.4, 151.0, 156.8, 156.9, 158.7 (q, *J* 32 Hz) (TFA), 168.3, 171.0, 171.7, 172.3. HRMS (ESI): *m/z* $[M+2H]^{2+}$ calcd. for $[C_{27}H_{48}N_{12}O_7]^{2+}$ 326.1879, found: 326.1883. RP-HPLC (220 nm): 98% (t_R = 16.3 min, *k* = 4.1). $C_{27}H_{46}N_{12}O_7 \cdot C_6H_3F_9O_6$ (650.74 + 342.07).

(*S*)-2-Amino-*N*-((*S*)-1-(((*S*)-1-(((*S*)-1-amino-3-(4-bromophenyl)-1-oxopropan-2-yl)amino)-5-guanidino-1-oxopentan-2-yl)amino)-4-methyl-1-oxopentan-2-yl)-5-guanidinopentanamide tris(hydrotrifluoroacetate) (3.21). Peptide **3.21** was synthesized on a Sieber-Amide-PS resin (40 mg, 0.59 mmol/g) according to the general procedure. Purification by preparative HPLC (system 1, gradient: 0-18 min MeCN/0.1% aq TFA 3:97-42:58, t_R = 14 min) yielded **3.21** as a light brown solid (6.3 mg, 26%). ^{1}H-NMR (600 MHz, DMSO-d_6): δ (ppm) 0.85 (d, 3H, *J* 6.6 Hz), 0.87 (d, 3H, *J* 6.6 Hz), 1.34-1.55 (m, 7H), 1.58-1.74 (m, 4H), 2.75-2.82 (m, 1H), 2.91-2.97 (m, 1H), 3.02-3.12 (m, 4H), 3.77-3.84 (m, 1H), 4.15-4.20 (m, 1H), 4.31-4.36 (m, 1H), 4.38-4.43 (m, 1H), 6.80-7.20 (br s, 4H, interfering with the next listed signal), 7.12-7.15 (m, 3H), 7.20-7.55 (br s, 4H, interfering with the next two listed signals), 7.40-7.43 (m, 2H), 7.47-7.48 (m, 1H), 7.68 (t, 1H, *J* 5.4 Hz), 7.75 (t, 1H, *J* 5.6 Hz), 7.84 (d, 1H, *J* 8.0 Hz), 8.13-8.19 (m, 3H), 8.21 (d, 1H, *J* 7.6 Hz), 8.49 (d, 1H, *J* 7.7 Hz). ^{13}C-NMR (150 MHz, DMSO-d_6): δ (ppm) 21.3, 23,1, 23.98, 23.99, 25.0, 28.4, 28.9, 37.0, 40.2, 40.4, 40.7, 51.1, 51.7, 52.5, 53.2, 116.0 (TFA), 117.9 (TFA), 119.5, 130.8 (two carbon atoms), 131.4 (two carbon atoms), 137.0, 156.8, 156.8, 158.6 (q, *J* 32 Hz) (TFA), 168.2, 170.9, 171.6, 172.2. HRMS (ESI): *m/z* $[M+2H]^{2+}$ calcd. for $[C_{27}H_{48}BrN_{12}O_7]^{2+}$ 335.6532, found: 335.6528. RP-HPLC (220 nm): 98% (t_R = 21.8 min, *k* = 5.8). $C_{27}H_{46}BrN_{12}O_7 \cdot C_6H_3F_9O_6$ (668.64 + 342.07).

(*S*)-2-Amino-*N*-((*S*)-1-(((*S*)-1-(((*S*)-1-amino-3-(naphthalen-2-yl)-1-oxopropan-2-yl)amino)-5-guanidino-1-oxopentan-2-yl)amino)-4-methyl-1-oxopentan-2-yl)-5-guanidinopentanamide tris(hydrotrifluoroacetate) (3.22). Peptide **3.22** was synthesized on a Sieber-Amide-PS resin (40 mg, 0.59 mmol/g) according to the general procedure.

Purification by preparative HPLC (system 1, gradient: 0-18 min MeCN/0.1% aq TFA 3:97-42:58, t_R = 15 min) yielded **3.22** as a white solid (7.8 mg, 34%). ^{1}H-NMR (600 MHz, DMSO-d_6): δ (ppm) 0.80-0.87 (m, 6H), 1.34-1.56 (m, 7H), 1.59-1.72 (m, 4H), 2.98-3.05 (m, 3H), 3.06-3.11 (m, 2H), 3.14-3.19 (m, 1H), 3.79-3.82 (m, 1H), 4.15-4.21 (m, 1H), 4.30-4.36 (m, 1H), 4.52-4.47 (m, 1H), 6.80-7.20 (br s, 4H, interfering with the next listed signal), 7.14-7.15 (m, 1H), 7.20-7.55 (br s, 4H, interfering with the next two listed signals), 7.38-7.40 (m, 1H), 7.44-7.50 (m, 3H), 7.64-7.67 (m, 1H), 7.68 (s, 1H), 7.73-7.76 (m, 1H), 7.78-7.82 (m, 2H), 7.83-7.86 (m, 1H), 7.87-7.90 (m, 1H), 8.12-8.20 (m, 3H), 8.21-8.24 (m, 1H), 8.47-8.50 (m, 1H). ^{13}C-NMR (150 MHz, DMSO-d_6): δ (ppm) 21.3, 23.1, 23.95, 23.98, 24.9, 28.4, 28.9, 37.8, 40.1, 40.4, 40.6, 51.2, 51.7, 52.6, 53.5, 116.0 (TFA), 118.0 (TFA), 125.4, 125.9, 127.36, 127.39, 127.40, 127.44, 127.8, 131.8, 132.9, 135.2, 156.76, 156.82, 158.6 (q, *J* 32 Hz) (TFA), 168.2, 170.9, 171.7, 172.5. HRMS (ESI): *m/z* $[M+2H]^{2+}$ calcd. for $[C_{31}H_{51}N_{11}O_4]^{2+}$ 320.7057, found: 320.7060. RP-HPLC (220 nm): 98% (t_R = 23.2 min, *k* = 6.2). $C_{31}H_{49}N_{11}O_4 \cdot C_6H_3F_9O_6$ (639.81 + 342.07).

(*S*)-2-Amino-*N*-((*S*)-1-(((*S*)-1-(((*S*)-1-amino-3-(naphthalen-1-yl)-1-oxopropan-2-yl)amino)-5-guanidino-1-oxopentan-2-yl)amino)-4-methyl-1-oxopentan-2-yl)-5-guanidinopentanamide tris(hydrotrifluoroacetate) (3.23). Peptide **3.23** was synthesized on a Sieber-Amide-PS resin (40 mg, 0.59 mmol/g) according to the general procedure. Purification by preparative HPLC (system 1, gradient: 0-18 min MeCN/0.1% aq TFA 3:97-42:58, t_R = 15 min) yielded **3.23** as a white solid (7.0 mg, 30%). ^{1}H-NMR (600 MHz, DMSO-d_6): δ (ppm) 0.84-0.91 (m, 6H), 1.32-1.38 (m, 1H), 1.39-1.56 (m, 6H), 1.57-1.72 (m, 4H), 3.02-3.11 (m, 4H), 3.24-3.29 (m, 1H), 3.44-3.46 (m, 1H), 3.78-3.84 (m, 1H), 4.15-4.20 (m, 1H), 4.32-4.37 (m, 1H), 4.55-4.60 (m, 1H), 6.90-7.20 (br s, 4H, interfering with the next listed signal), 7.13-7.14 (m, 1H), 7.20-7.50 (br s, 4H, interfering with the next two listed signals), 7.32-7.34 (m, 1H), 7.37-7.40 (m, 2H), 7.50-7.57 (m, 2H), 7.62-7.67 (m, 1H), 7.70-7.74 (m, 1H), 7.76-7.80 (m, 1H), 7.90-7.92 (m, 1H), 7.99-8.02 (m, 1H), 8.12-8.19 (m, 3H), 8.21-8.26 (m, 2H), 8.47-8.52 (m, 1H). ^{13}C-NMR (150 MHz, DMSO-d_6): δ (ppm) 21.4, 23.1, 23.98, 24.01, 25.0, 28.4, 28.8, 34.9, 40.1, 40.4, 40.6, 51.2, 51.7, 52.6, 53.1, 116.0 (TFA), 118.0 (TFA), 123.8, 125.3, 125.5, 126.0, 127.0, 127.2, 128.5, 131.7, 133.3, 133.5, 156.7, 156.8, 158.5 (q, *J* 32 Hz) (TFA), 168.2, 171.0, 171.7, 172.6. HRMS (ESI): *m/z* $[M+2H]^{2+}$ calcd. for $[C_{31}H_{51}N_{11}O_4]^{2+}$ 320.7057, found: 320.7061. RP-HPLC (220 nm): 98% (t_R = 22.5 min, *k* = 6.0). $C_{31}H_{49}N_{11}O_4 \cdot C_6H_3F_9O_6$ (639.81 + 342.07).

Tyr-Arg-Leu-Arg-amide tris(hydrotrifluoroacetate) (3.24). Peptide **3.24** was synthesized on a Sieber-Amide-PS resin (40 mg, 0.59 mmol/g) according to the general procedure. Purification by preparative HPLC (system 1, gradient: 0-18 min MeCN/0.1% aq TFA 3:97-42:58, t_R = 12 min) yielded **3.24** as a white solid (11.8 mg, 39%). ^{1}H-NMR (600 MHz, DMSO-d_6): δ (ppm) 0.84-0.92 (m, 6H), 1.41-1.59 (m, 8H), 1.60-1.74 (m, 3H), 2.76-2.82 (m, 1H), 2.94-

3.01 (m, 1H), 3.06-3.16 (m, 4H), 3.97-4.01 (m, 1H), 4.17-4.22 (m, 1H), 4.29-4.34 (m, 1H), 4.35-4.41 (m, 1H), 6.65-6.71 (m, 2H), 6.85-7.20 (br s, 4H, interfering with the next two listed signals), 7.00-7.03 (m, 2H), 7.11-7.12 (m, 1H), 7.20-7.60 (br s, 4H, interfering with the next listed signal), 7.41-7.43 (m, 1H), 7.76-7.81 (m, 2H), 7.84-7.88 (m, 1H), 8.00-8.10 (m, 3H), 8.20-8.15 (m, 1H), 8.70-8.75 (m, 1H), 9.39 (br s, 1H). ^{13}C-NMR (150 MHz, DMSO-d_6): δ (ppm) 21.3, 23.1, 24.2, 25.0, 25.1, 29.3, 29.4, 36.1, 40.3, 40.4, 40.7, 51.3, 51.8, 52.2, 53.4, 115.3 (two carbon atoms), 115.9 (TFA), 117.9 (TFA), 124.5, 130.5 (two carbon atoms), 156.6, 156.8, 156.9, 158.7 (q, *J* 32 Hz) (TFA), 168.0, 170.7, 171.7, 173.3. HRMS (ESI): *m/z* $[M+2H]^{2+}$ calcd. for $[C_{42}H_{69}N_{15}O_9]^{2+}$ 303.6954, found: 303.6959. RP-HPLC (220 nm): 99% (t_R = 5.8 min, *k* = 0.8). $C_{27}H_{47}N_{11}O_5 \cdot C_6H_3F_9O_6$ (605.75 + 342.07).

3.4.5 Pharmacology

Cell Culture, Buffers and Media Used for Binding and Functional Assays. Described in chapter 2.

Radioligand Binding Assays at the hY_1R, hY_2R, hY_4R and hY_5R. Described in chapter 2.

β-Arrestin 1 and 2 Recruitment Assay. Described in chapter 2.

Ca^{2+}-Aequorin Assay. Described in chapter 2.

3.5 References

(1) Kuhn, K. K.; Littmann, T.; Dukorn, S.; Tanaka, M.; Keller, M.; Ozawa, T.; Bernhardt, G.; Buschauer, A., In search of NPY Y_4R antagonists: incorporation of carbamoylated arginine, aza-amino acids, or D-amino acids into oligopeptides derived from the C-termini of the endogenous agonists. *ACS Omega* **2017**, *2*, 3616-3631.

(2) Konieczny, A.; Braun, D.; Wifling, D.; Bernhardt, G.; Keller, M., Oligopeptides as neuropeptide Y Y_4 receptor ligands: identification of a high-affinity tetrapeptide agonist and a hexapeptide antagonist. *J. Med. Chem.* **2020**, *63*, 8198-8215.

(3) Góngora-Benítez, M.; Tulla-Puche, J.; Albericio, F., Handles for Fmoc solid-phase synthesis of protected peptides. *ACS Comb. Sci.* **2013**, *15*, 217-228.

(4) Behrendt, R.; White, P.; Offer, J., Advances in Fmoc solid-phase peptide synthesis. *J. Pept. Sci.* **2016**, *22*, 4-27.

(5) Hansen, P. R.; Oddo, A., Fmoc solid-phase peptide synthesis. *Methods Mol. Biol.* **2015**, *1348*, 33-50.

(6) O'Donnell, M. J.; Zhou, C.; Scott, W. L., Solid-phase unnatural peptide synthesis (UPS). *J. Am. Chem. Soc.* **1996**, *118*, 6070-6071.

(7) Hodgson, D. R. W.; Sanderson, J. M., The synthesis of peptides and proteins containing non-natural amino acids. *Chem. Soc. Rev.* **2004**, *33*, 422-437.

(8) Kuhn, K. K.; Ertl, T.; Dukorn, S.; Keller, M.; Bernhardt, G.; Reiser, O.; Buschauer, A., High affinity agonists of the neuropeptide Y (NPY) Y_4 receptor derived from the C-terminal pentapeptide of human pancreatic polypeptide (hPP): synthesis, stereochemical discrimination, and radiolabeling. *J. Med. Chem.* **2016**, *59*, 6045-6058.

(9) Keller, M.; Kuhn, K. K.; Einsiedel, J.; Hübner, H.; Biselli, S.; Mollereau, C.; Wifling, D.; Svobodová, J.; Bernhardt, G.; Cabrele, C.; Vanderheyden, P. M. L.; Gmeiner, P.; Buschauer, A., Mimicking of arginine by functionalized N^{ω}-carbamoylated arginine as a new broadly applicable approach to labeled bioactive peptides: high affinity angiotensin, Neuropeptide Y, neuropeptide FF, and neurotensin receptor ligands as examples. *J. Med. Chem.* **2016**, *59*, 1925-1945.

(10) Ziemek, R.; Schneider, E.; Kraus, A.; Cabrele, C.; Beck-Sickinger, A. G.; Bernhardt, G.; Buschauer, A., Determination of affinity and activity of ligands at the human neuropeptide Y Y_4 receptor by flow cytometry and aequorin luminescence. *J. Recept. Signal Transduct. Res.* **2007**, *27*, 217-233.

(11) Pedragosa-Badia, X.; Sliwoski, G. R.; Dong Nguyen, E.; Lindner, D.; Stichel, J.; Kaufmann, K. W.; Meiler, J.; Beck-Sickinger, A. G., Pancreatic polypeptide is recognized by two hydrophobic domains of the human Y_4 receptor binding pocket. *J. Biol. Chem.* **2014**, *289*, 5846-5859.

(12) Nepali, K.; Lee, H.-Y.; Liou, J.-P., Nitro-group-containing drugs. *J. Med. Chem.* **2018**, *62*, 2851-2893.

(13) Wilcken, R.; Zimmermann, M. O.; Lange, A.; Joerger, A. C.; Boeckler, F. M., Principles and applications of halogen bonding in medicinal chemistry and chemical biology. *J. Med. Chem.* **2013**, *56*, 1363-1388.

(14) Lu, Y.; Liu, Y.; Xu, Z.; Li, H.; Liu, H.; Zhu, W., Halogen bonding for rational drug design and new drug discovery. *Expert Opin. Drug Discovery* **2012**, *7*, 375-383.

(15) Keller, M.; Weiss, S.; Hutzler, C.; Kuhn, K. K.; Mollereau, C.; Dukorn, S.; Schindler, L.; Bernhardt, G.; König, B.; Buschauer, A., N^{ω}-Carbamoylation of the argininamide moiety: an avenue to insurmountable NPY Y_1 receptor antagonists and a radiolabeled selective high-affinity molecular tool ([^{3}H]UR-MK299) with extended residence time. *J. Med. Chem.* **2015**, *58*, 8834-8849.

(16) Moser, C.; Bernhardt, G.; Michel, J.; Schwarz, H.; Buschauer, A., Cloning and functional expression of the hNPY Y_5 receptor in human endometrial cancer (HEC-1B) cells. *Can. J. Physiol. Pharmacol.* **2000**, *78*, 134-142.

(17) Berlicki, L.; Kaske, M.; Gutierrez-Abad, R.; Bernhardt, G.; Illa, O.; Ortuno, R. M.; Cabrele, C.; Buschauer, A.; Reiser, O., Replacement of Thr^{32} and Gln^{34} in the C-terminal neuropeptide Y fragment 25-36 by cis-cyclobutane and cis-cyclopentane beta-amino acids shifts selectivity toward the Y_4 receptor. *J. Med. Chem.* **2013**, *56*, 8422-8431.

(18) Dukorn, S.; Littmann, T.; Keller, M.; Kuhn, K.; Cabrele, C.; Baumeister, P.; Bernhardt, G.; Buschauer, A., Fluorescence- and radiolabeling of [Lys^4,$Nle^{17,30}$]hPP yields molecular tools for the NPY Y_4 receptor. *Bioconjugate Chem.* **2017**, *28*, 1291-1304.

(19) Wisler, J. W.; Xen, K.; Thomsen, A. R.; Lefkowitz, R. J., Recent developments in biased agonism. *Curr. Opin. Cell Biol.* **2014**, *61*, 342-356.

(20) Luttrell, L. M., Minireview: more than just a hammer: ligand “bias” and pharmaceutical discovery. *Mol. Endocrinol.* **2014**, *28*, 281-294.

Chapter 4

Computer-Aided Design, Synthesis and Pharmacological Characterization of Small Molecule NPY Y_4 Receptor Ligands Using Peptides as Lead Structures

4.1 Introduction

The neuropeptide Y (NPY) receptor family is part of 118 peptide-binding, class A G-protein coupled receptors (GPCRs) and comprise four functional subtypes (Y_1R, Y_2R, Y_4R, Y_5R).[1,2] Noteworthy, the Y_4R plays a special role in the NPY family because of its preferential binding of pancreatic polypeptide (PP) over NPY and peptide YY (PYY), which show higher affinity to the other subtypes.[3] Through structure-activity relationship studies of PP analogs, it was possible to identify the most crucial part responsible for Y_4R binding, that is, the amidated C-terminal sequence of the 36 amino acid peptide. This resulted, amongst others, in the linear tetrapeptide **4.3** (UR-AK32), a high affinity Y_4R selective partial agonist.[4] The non-peptide Y_4R ligand (*R*,*R*)-**4.1** (UR-MK188, Figure 1) resulted from a bivalent ligand approach, based on the argininamide-type Y_1R antagonist (BIBP3226[5]).[6] Whereas (*R*,*R*)-**4.1** binds as antagonist to the Y_1 and Y_4 receptor, its optical antipode, i.e. the (*S*,*S*)-enantiomer, exhibits no Y_1R affinity (Figure 1). Nevertheless, more small molecule, non-peptide Y_4R ligands are required, not only for the use as molecular tools (e.g. fluorescent- and radioligands), but also as pharmacological tools for further investigations of the physiological meaning of the hY_4R and its role as a potential target for the treatment of obesity.[7,8]

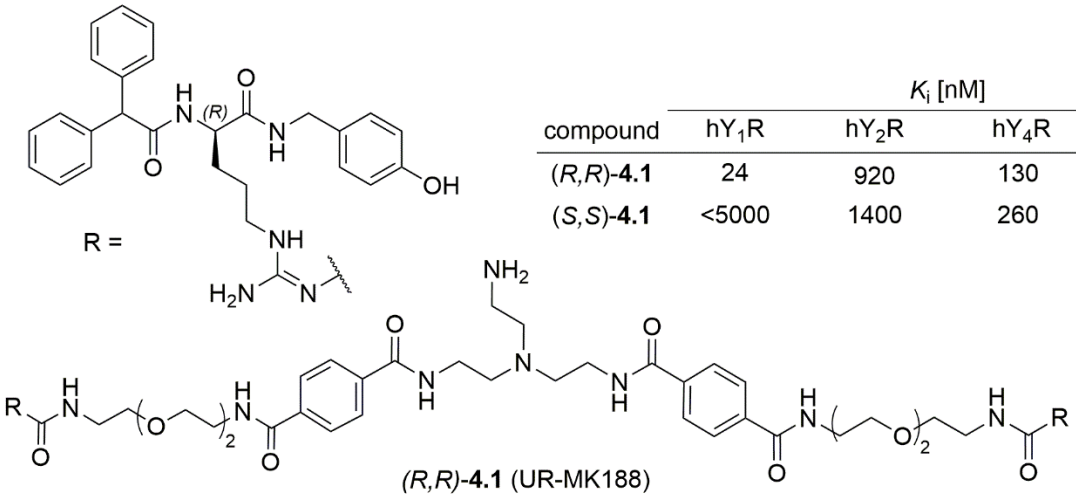

compound	K_i [nM] hY_1R	hY_2R	hY_4R	hY_5R
(*R*,*R*)-**4.1**	24	920	130	<5000
(*S*,*S*)-**4.1**	<5000	1400	260	<5000

Figure 1. Structure and YR selectivity profile of the bivalent Y_1/Y_4-receptor antagonist (*R*,*R*)-**4.1** and the respective (*S*,*S*)-enantiomer. Data taken from Keller *et al.*[6]

With the increasing knowledge, gained in the field of GPCR crystallization during the last few years, numerous crystal structures were reported, not only bound to agonists, antagonists and partial agonists, but also in complex with allosteric modulators.[9-11] Data of these crystal structures are available online on the Brookhaven Protein Data Bank (PDB).[12] In general, structures from already crystallized receptors, which share high sequence similarity to the respective investigated receptor, are used as templates, to generate homology models for non-crystallized GPCRs.[13] These homology models are an opportunity to obtain preliminary insights into key ligand-receptor interactions and residues, responsible for receptor binding

and activation.[14] Besides MD simulations, docking studies are a popular method to suggest the ligand binding mode at or in a receptor.

The objective was to transfer the peptide structure of already known Y_4R ligands into new small molecules and, ideally, to establish a pharmacophore model for future modifications. As template, we selected three peptides with known Y_4R affinities and studied the binding poses in complex with a hY_4R homology model, generated from the recent solved crystal structure of the hY_1R.[15] Important amino acids, which form the orthosteric binding pocket of the hY_4R, were identified through induced-fit docking studies of selected peptidic Y_4R ligands. Based on this information, we tried to design new core structures of small-molecule Y_4R ligands. All virtually created compounds were docked to the Y_4R model (induced-fit docking) and the results were evaluated using a scoring system (XPGlide-, MMGBSA-score) and by manually inspecting the respective binding pose. Some of the most promising compounds were subsequently synthesized and characterized by radioligand competition binding experiments and in a functional β-arrestin 2 recruitment assay.

4.2 Results and Discussion

4.2.1 Induced-Fit Docking Studies

It is important to mention that no active state Y receptor crystal structure is available to date, so that an active state homology model was not involved in our studies. Therefore, the results from docking studies of partial agonists **4.2** and **4.3** in complex with the hY_4R homology model, based on the inactive conformation of the hY_1R,[15] must be interpreted very carefully. Moreover, all virtually created compounds were docked to this Y_4R model. In general, only small ligands are appropriate for induced-fit docking studies. Large molecules, for example the endogenous Y_4R ligand PP, are too flexible (high number of degrees of freedom) or are too bulky to fit into the orthosteric binding pocket, a challenge, which cannot be adequately addressed by contemporary computational chemistry.

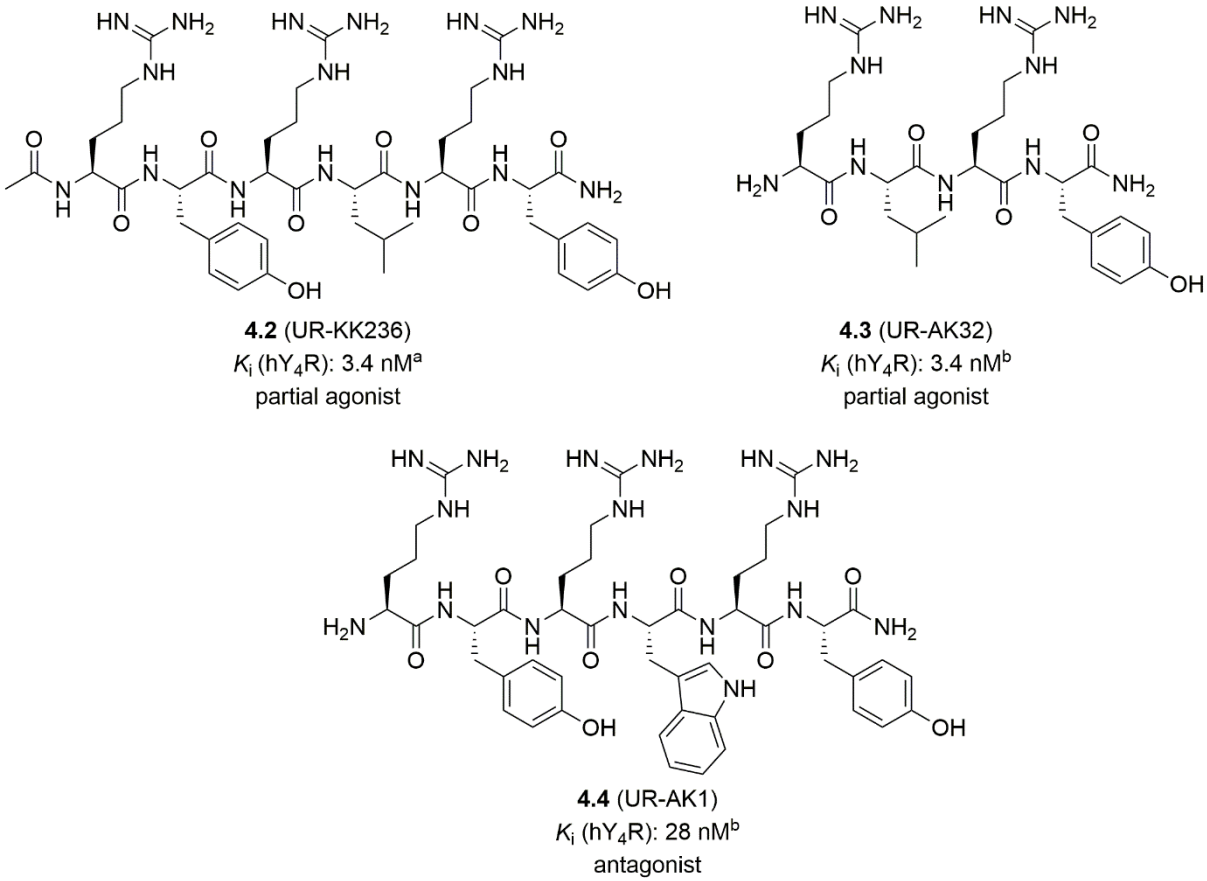

Figure 2. Structures, affinities and functional activities (agonism vs. antagonism) of selected peptidic Y_4R ligands (**4.2**-**4.4**), which were docked to a hY_4R homology model using induced-fit docking. [a]Kuhn *et al*.[16] [b]Konieczny *et al*.[4]

As mentioned above, three linear peptides (**4.2**-**4.4**, Figure 2) were chosen for induced-fit docking studies, all characterized with respect to hY_4R binding as well as in functional studies. **4.2**-**4.4** were docked to the Y_4R homology model using the LipPrep and induced-fit docking modules, which are implemented in the Schrödinger Suite (Figure 3 A-C).[17] The Y_4R homology model was generated from the recently published crystal structure of the hY_1R (PDB ID: 5ZBQ, inactive state),[15] sharing the highest sequence similarity to the hY_4R among all NPY receptor subtypes.[3] The two partial agonists **4.2** and **4.3** exhibited comparatively similar binding poses (Figure 3A and 3B). In both cases, the amidated C-terminal Tyr deeply reached into the orthosteric binding pocket. The phenolic Tyr side-chain pointed into the receptor interior and showed a *π*-*π* interaction with W278$^{6.48}$. In the case of tetrapeptide **4.3**, a salt bridge was additionally evident between the hydroxyl group of the C-terminal Tyr and Q222$^{5.46}$. Near the receptor surface, a hydrophilic cluster (D105$^{2.68}$, E203^{ECL2}, E288$^{6.58}$ and D289$^{6.59}$) of the hY_4R was involved in receptor-ligand interactions. The basic guanidine groups of the arginine side-chains in **4.2**-**4.4** were the main interaction partners by forming salt-bridges and H-bonds with D105$^{2.68}$, E203^{ECL2}, N285$^{6.55}$, E288$^{6.58}$ and D289$^{6.59}$. This underlined the hypothesis that at least two basic groups are indispensable to achieve high Y_4R affinity.

Compound **4.4** was pharmacologically characterized as an antagonist. Accordingly, this compound showed a different Y_4R binding mode compared to the partial agonists **4.2** and **4.3** (Figure 3C). Instead of the C-terminal Tyr, as in the case of the partial agonists, the aromatic indole ring of Trp^4 in **4.4** was interacting with $W278^{6.48}$ in the receptor interior. The amidated C-terminal Tyr in **4.4** was oriented towards the receptor surface (Figure 3C). The role of the basic guanidine groups of Arg^1 and Arg^5 in **4.4** was comparable to Arg^1 and Arg^3 in **4.3**. They were part of key interactions with hydrophilic amino acids $D105^{2.68}$, $E203^{ECL2}$ and $D289^{6.59}$.

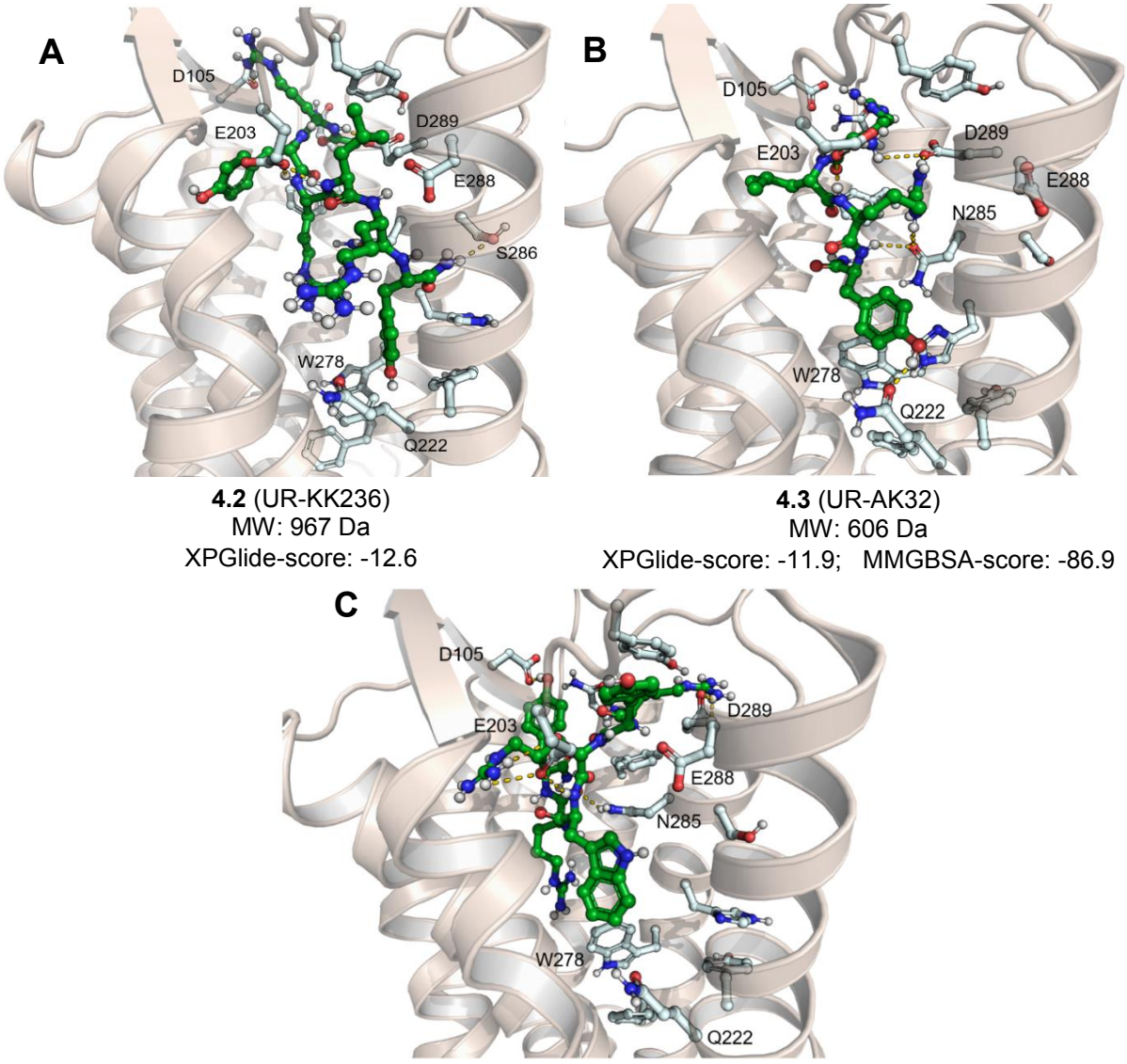

4.2 (UR-KK236)
MW: 967 Da
XPGlide-score: -12.6

4.3 (UR-AK32)
MW: 606 Da
XPGlide-score: -11.9; MMGBSA-score: -86.9

4.4 (UR-AK1)
MW: 998 Da
XPGlide-score.: -13.8

Figure 3. Y_4R binding poses of **4.2** (A), **4.3** (B) and **4.4** (C) obtained by induced-fit docking to a homology model of the hY_4R (derived from the crystal structure of the hY_1R in the inactive state (PDB ID: 5ZBQ))[15]. Nitrogen and oxygen atoms are shown in blue and red, respectively, and carbon atoms are shown in green (ligands) or grey (amino acids of the receptor). Yellow dashed lines indicate H-bonds and salt bridges.

Whereas the MMGBSA-score is a standard method in docking experiments,[18] calculated by multiple parameters, for example, free energies of the respective ligand, receptor and ligand-receptor complex, the XPGlide-score is a useful tool, for the identification of favorable energetic states of the investigated compounds.[19,20] Ideally, promising compounds exhibited scores, as low as possible, in both scoring systems. In the case of ligands **4.2** and **4.4**, no MMGBSA-scores were obtained by induced-fit docking, what is a general problem for investigations of peptides in Schrödinger Suite. The program has problems to differ between peptidic ligand and the respective receptor. Tetrapeptide **4.3** elicited a MMGBSA-score of -86.9. The achieved XPGlide-scores were all in the same range (**4.2** = -12.6; **4.3** = -11.9; **4.4** = -13.8) (Figure 3). Interestingly, tetrapeptide **4.3** was able to compete with **4.2** and **4.4**, with respect to the XPGlide-score, although **4.3** has a markedly smaller molecular weight (MW) and less residues for receptor-ligand interactions.

The binding poses and the XPGlide-/MMGBSA-scores suggested important receptor amino acids, responsible for receptor-ligand interactions in the orthosteric binding pocket of the hY_4R. Seven residues were identified to play an important role for hY_4R recognition and binding of the studied ligands: $D105^{2.68}$, $E203^{ECL2}$, $Q222^{5.46}$, $W278^{6.48}$, $N285^{6.55}$, $E288^{6.58}$ and $D289^{6.59}$ (Figure 4A). This is in agreement with reported mutagenesis studies that proved the importance of TM2 and TM6, in particular $D105^{2.68}$, $N285^{6.55}$, $E288^{6.58}$ and $D289^{6.59}$ for Y_4R binding of PP.[21]

Our model indicated two different clusters in the hY_4R, a hydrophobic cluster ($Q222^{5.46}$, $W278^{6.48}$, $N285^{6.55}$), present in the receptor interior, and a hydrophilic cluster ($D105^{2.68}$, $E203^{ECL2}$, $E288^{6.58}$, $D289^{6.59}$) at the receptor surface (Figure 4B). The hydrophobic cluster seemed to be part of the presumed Y_4R orthosteric binding pocket, typically located in the receptor interior. Moreover, the relevant amino acids of the hydrophilic cluster are partially identical, observed for allosteric vestibule at the receptor surface of the M_2 receptor.[22-24] Therefore, both clusters can potential guide the design of new, non-peptide Y_4R ligands. Accordingly, a hypothetical Y_4R ligand should contain an aromatic ring system and, at least, one or two basic residues connected by a flexible linker. Based on the docking results, it was possible to obtain more information about the distance between the basic groups, the bulkiness of the aromatic ring system as well as the length of the linker.

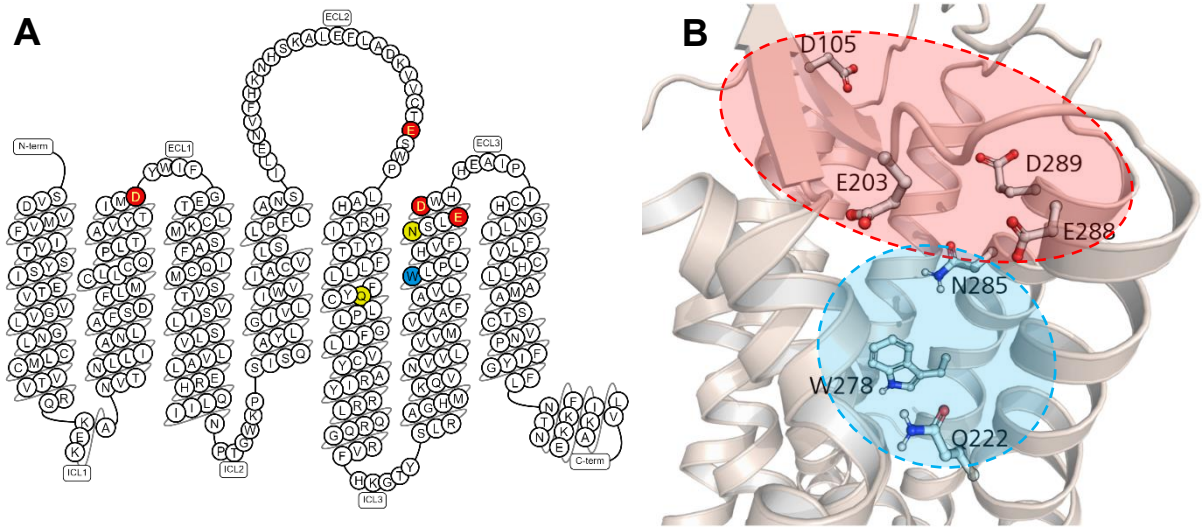

Figure 4. Representations of the hY_4R and important amino acids responsible for receptor-ligand interactions. A: Snake plot (generated by GPCR data base)[25] of the hY_4R. Amino acids with charged side-chains are highlighted in red ($D105^{2.68}$, $E203^{ECL2}$, $E288^{6.58}$, $D289^{6.59}$), amino acids with polar-uncharged side-chains are highlighted in yellow ($Q222^{5.46}$, $N285^{6.55}$) and one amino acid with a hydrophobic side-chain is highlighted in blue ($W278^{6.48}$). B: hY_4R homology model (based on the crystal structure of the hY_1R (PDB ID: 5ZBQ)),[15] highlighting the hydrophobic cluster ($Q222^{5.46}$, $W278^{6.48}$, $N285^{6.55}$) in the receptor interior (in blue) and the hydrophilic cluster ($D105^{2.68}$, $E203^{ECL2}$, $E288^{6.58}$, $D289^{6.59}$) at the receptor surface (in red). Important amino acids were additionally assigned by Ballosteros-Weinstein numbering.[26]

After the identification of essential hY_4R residues, we focused on the translation of the peptide structure into an entire new non-peptide structure. For this purpose, four cyclic core scaffolds were chosen (Figure 5), to which the aforementioned aromatic ring system and two basic residues had to be attached.

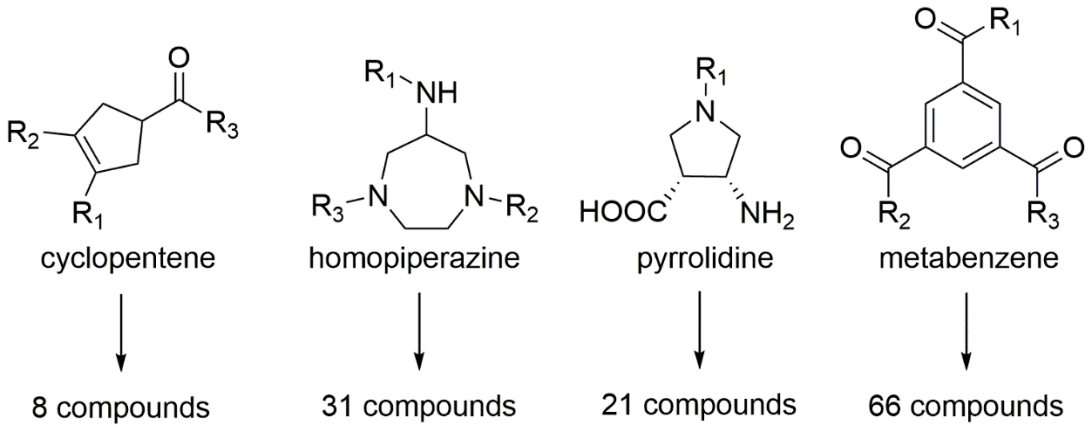

Figure 5. Core structures and number of derived virtual non-peptide Y_4R ligands, which docked to the Y_4R homology model using induced-fit docking. The exact structures of all compounds are provided as SMILES-strings in the appendix.

The first set of screened Y_4R ligands (**4.5**-**4.8**) is shown in Figure 6. In these compounds, the amidated L-tyrosine residue was directly attached to the core structure, only in compound **4.6**, a malonic acid linker was inserted. Two basic guanidine groups were also attached to the core structures, in the case of **4.5** and **4.7**, separated by a C_3-linker, in the case of **4.6** and **4.8**,

separated by a C_4-linker, the latter being superior to the C_3 linker with respect to the score values obtained by induced-fit docking.

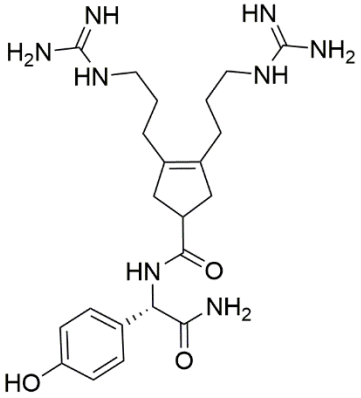

4.5
(cyclopentene core)
MW: 473 Da
XPGlide-score: -12.6
MMGBSA-score: -87.7

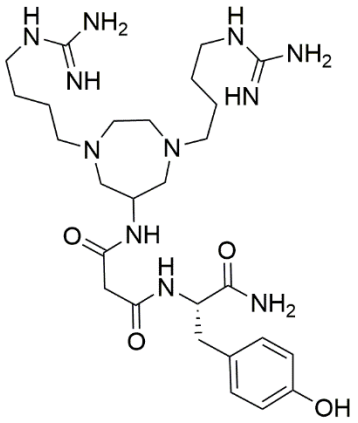

4.6
(homopiperazine core)
MW: 593 Da
XPGlide-score: -18.0
MMGBSA-score: -122.7

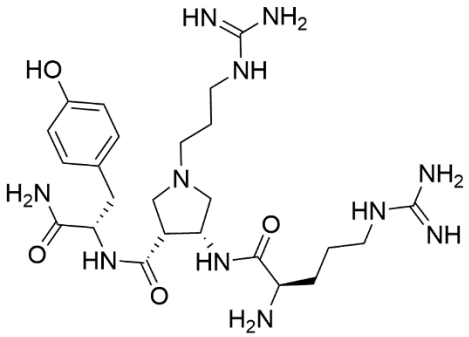

4.7
(pyrrolidine core)
MW: 552 Da
XPGlide-score: -19.7
MMGBSA-score: -106.3

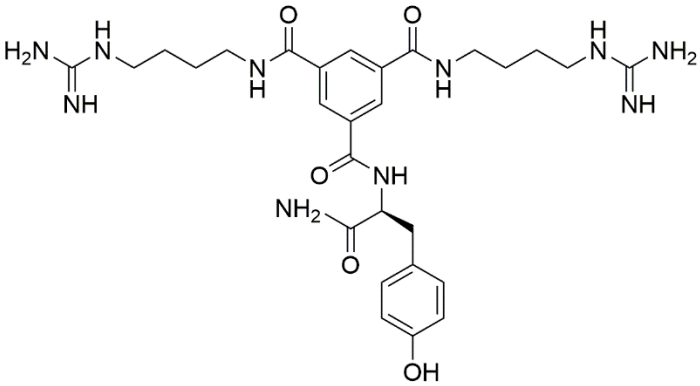

4.8
(metabenzene core)
MW: 598 Da
XPGlide-score: -16.4
MMGBSA-score: -111.5

Figure 6. Structures, molecular weight (MW) as well as XPGlide- and MMGBSA-scores (induced-fit docking) of the virtually designed potential Y_4R ligands **4.5**-**4.8**.

The structures **4.5**-**4.8** were the starting point for the screening of over 140 compounds (SMILES-strings of all virtually screened compounds are listed in the Appendix), all containing one of the core scaffolds shown in Figure 5. For example, replacement of the tyrosine moiety by other heterocycles, variation of the linker structure and length as well as a bioisoteric exchange of the guanidine residues were considered. The design of the structures was an iterative process, i.e. after induced-fit docking of a subset of compounds, new structural modifications were guided by the XPGlide and MMGBSA scores.

It is important to mention that the docking scores correlated inversely with the molecular weight of the virtual ligands. This means that heavy-weight structures exhibited per se lower XPGlide-

and MMGBSA-scores, compared to small molecules, because of the higher number of degrees of freedom and additional potential contacts to the receptor (Figure 7A).

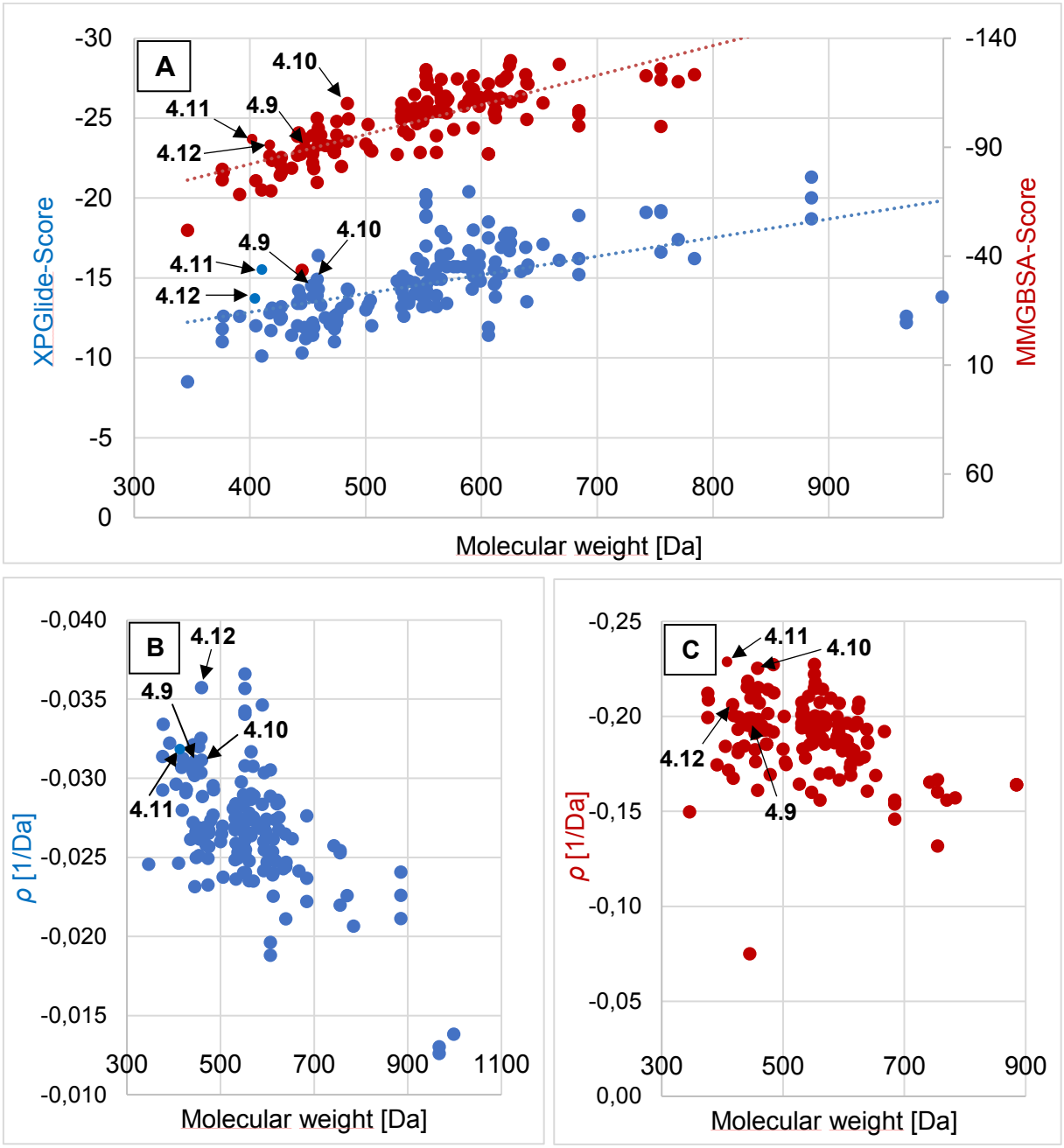

Figure 7. Demonstration of the dependence of the XPGlide-/MMGBSA-scores from the molecular weight of the docked potential Y_4R ligands. A: Correlation between the molecular weight (x-axis) and the XPGlide-/MMGBSA-score (y-axis). B: Scatter diagram of the molecular weight (x-axis) plotted against parameter ρ (y-axis, explained below) resulted from the XPGlide-score. C: Scatter diagram of the molecular weight (x-axis) plotted against parameter ρ (y-axis, explained below) resulted from the MMGBSA-score. Structures of **4.9**-**4.12** are shown in Figure 8.

Therefore, we did not only focus on the score values, i.e. also the plausibility of the binding pose was considered and a kind of normalized score (parameter *ρ*) was calculated by dividing the XPGlide or the MMGBSA sore by the MW of the potential ligand:

$$\rho = \frac{\text{XPGlide score or MMGBSA score}}{\text{Molecular weight}} \qquad [\frac{1}{Da}]$$

Plotting parameter *ρ* against the MW of the docked structures provided a more accurate judgment in terms of the hypothetical "qualification" as a lead structure for the development of non-peptide Y_4R ligands (Figure 7B, 7C). In other words, the combination of a small value of *ρ* with a low MW indicated a promising compound.

The induced-fit docking studies suggested a variety of potential Y_4R ligands, from which **4.9**-**4.12** were the most promising ones (Figure 8A). The entire screening process effected three major modifications. The first one was related to the moiety mimicking the phenolic side-chain of tyrosine. A bulkier and more hydrophobic heterocycle appeared to be more favorable for the occupation of the hydrophobic hY_4R sub pocket. Therefore, we first incorporated a quinoline ring, which was later replaced by a 1*H*-pyrrolo[3,4-*b*]quinoline-1,3(2*H*)-dione heterocycle (see structures of **4.9**-**4.12** in Figure 8A), showing interactions with $Q222^{5.46}$ and $W278^{6.48}$ (induced-fit docking, Figure 8B).

Moreover, a linker was introduced between the 1*H*-pyrrolo[3,4-*b*]quinoline-1,3(2*H*)-dione moiety and the cyclic core scaffold. The docking process indicated the importance of a flexible linker with an optimal length of approximately two (**4.9** and **4.11**) or three (**4.12**) atom bonds.

Modifications in terms of the hydrophilic and basic structure elements were very broad. Therefore, compounds **4.9**-**4.12** exhibited quite diverse basic moieties (an "arginine side-chain" in **4.9**, a tetrahydropyrimidine moiety in **4.10**, a guanidine moiety attached to a phenyl ring in **4.11**, or two aminomethyl groups attached to a phenyl ring in **4.12**; Figure 8A).

A

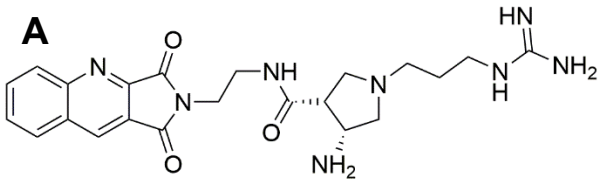

4.9
MW: 453 Da
XPGlide-/MMGBSA-score: -14.5 / -88.2
ρ(XPGlide/MW): -0.0320; ρ(MMGBSA/MW): -0.1946

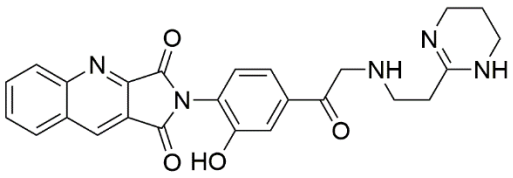

4.10
MW: 458 Da
XPGlide-/MMGBSA-score: -14.9 / -103.2
ρ(XPGlide/MW): -0.0325; ρ(MMGBSA/MW): -0.2253

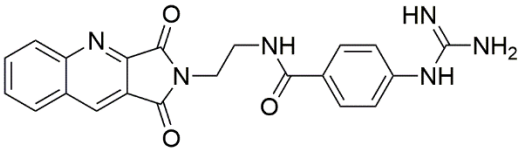

4.11
MW: 402 Da
XPGlide-/MMGBSA-score: -13.5 / -92.3
ρ(XPGlide/MW): -0.0336; ρ(MMGBSA/MW): -0.2296

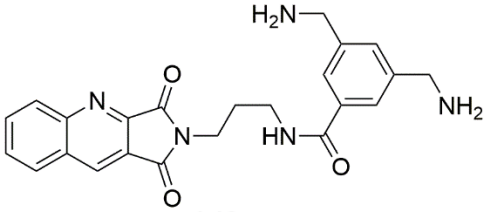

4.12
MW: 417 Da
XPGlide-/MMGBSA-score: -15.5 / -84.1
ρ(XPGlide/MW): -0.0372; ρ(MMGBSA/MW): -0.2017

B

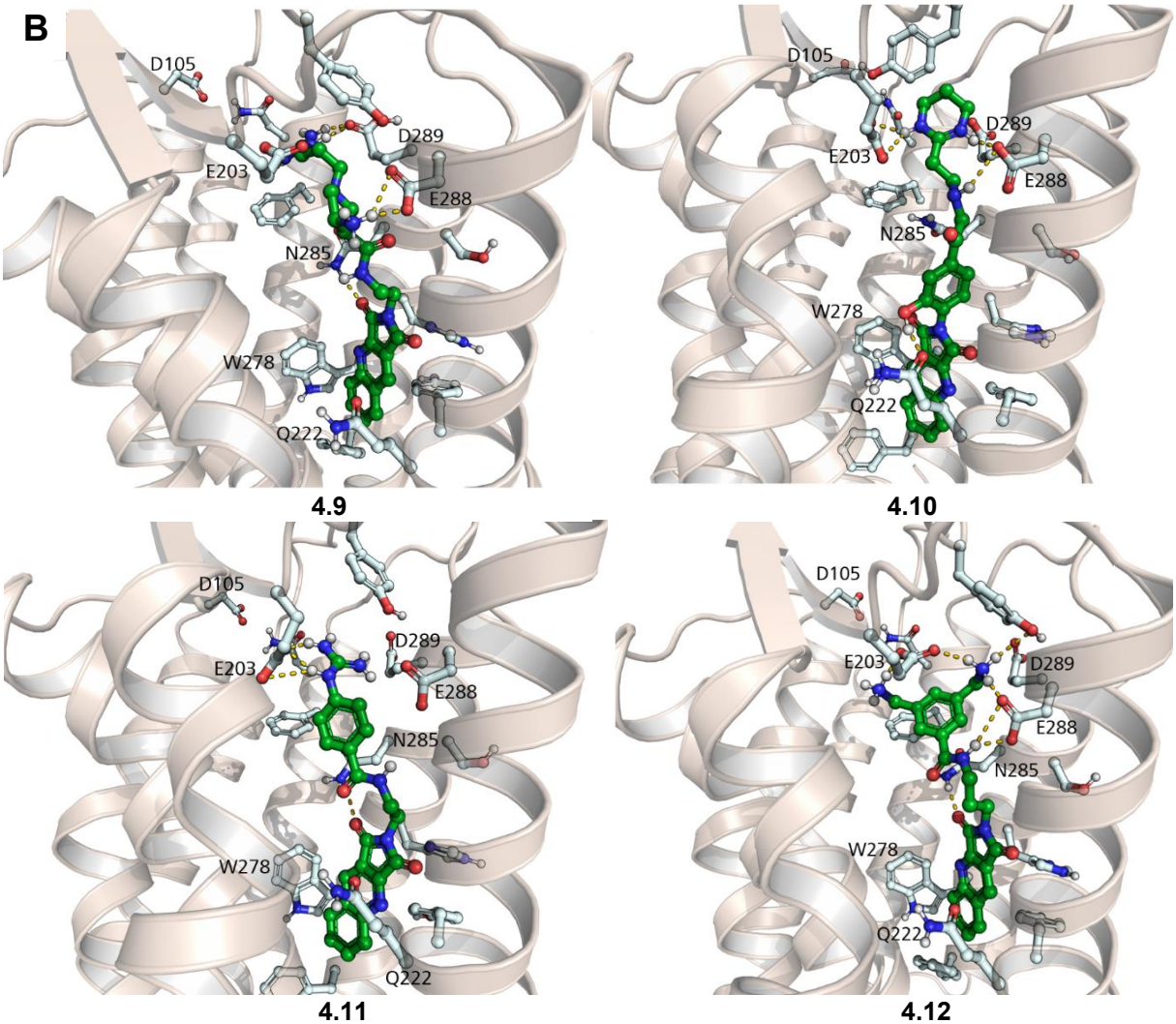

Figure 8. A: Structure, MW, XPGlide and MMGBSA scores, and parameter *ρ* selected, potential non-peptide Y_4R ligands **4.9**-**4.12**. B: Y_4R binding poses of **4.9**-**4.12** obtained by induced-fit docking to a Y_4R homology model (derived from the crystal structure of the hY_1R (PDB ID: 5ZBQ))[15]. Nitrogen, oxygen and carbon atoms are shown in blue, red and green, respectively. Yellow dashed lines indicate H-bonds and salt bridges.

Regarding the induced-fit docking binding poses of compounds **4.9**-**4.12** (Figure 8B), similarities could be found with respect to the identified interactions of the peptidic Y_4R ligands **4.2**-**4.4** (cf. Figure 3). As expected, the 1*H*-pyrrolo[3,4-*b*]quinoline-1,3(2*H*)-dione heterocycle, mimicking the C-terminal tyrosine residue of the peptides, was embedded in the hydrophobic cluster in the interior of the hY_4R showing contacts to $Q222^{5.46}$, $W278^{6.48}$, $N285^{6.55}$, and the basic residues in **4.9**-**4.12** showed contacts to acidic amino acids residues at the receptor surface, as also observed for peptides **4.2**-**4.4** (Figure 3).

Based on these results, obtained by computational chemistry, we decided to synthesize and characterize compounds **4.11** and **4.12**. They exhibited the lowest molecular weight of all studied structures and yielded comparatively low XPGlide-/MMGBSA-scores. In addition, the 1*H*-pyrrolo[3,4-*b*]quinoline-1,3(2*H*)-dione heterocycle in **4.11** and **4.12** was replaced by a 1*H*-benzo[*f*]isoindole-1,3(2*H*)-dione moiety.

4.2.2 Synthesis of Potential Non-Peptidic Y_4R Ligands

4-Guanidinobenzoic acid (**4.13**) and 3,5-bis(aminomethyl)benzoic acid (**4.14**) (both commercially available) were double Boc-protected by using di-*tert*-butyl dicarbonate to give **4.15** and **4.16**, respectively (Scheme 1).

Scheme 1. Synthesis of the Boc-protected compounds **4.15** and **4.16**.

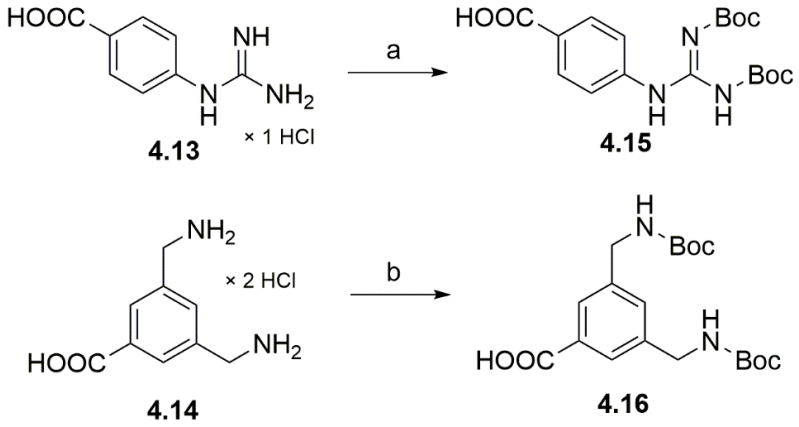

Reagents and conditions: (a) Boc_2O (2 equiv.), 0.5 M NaOH/MeCN (2:1 v/v), dioxane, 0 °C to rt, overnight, 40%; (b) Boc_2O (2 equiv.), 0.5 M NaOH, dioxane/THF (2:1 v/v), 0 °C to rt, overnight, 41%.

The acid anhydride naphtho[2,3-*c*]furan-1,3-dione (**4.18**) was used as starting material for the synthesis of imides **4.23** and **4.24** (Scheme 2). For the synthesis of the imides **4.21** and **4.22**, quinoline-2,3-dicarboxylic acid (**4.17**) was used. The intermediate anhydride of **4.17** was formed by using the strong dehydrating reagent phosphorus pentoxide, followed by the addition of mono-Boc protected amines **4.19** and **4.20** (one-pot reaction) and subsequent Boc-

deprotection. Unfortunately, these conditions gave the products **4.21** and **4.22** only in very low yields because of the preferential formation of an amide bond with one of the carboxylic acid groups. Compounds **4.21**-**4.24** were used for amide bond formation with **4.15** or **4.16**, followed by Boc-deprotection to afford compounds **4.11**, **4.12** and **4.25**-**4.30** (Scheme 2). For an exchange of the two primary amines in **4.12** by two guanidine groups, *tert*-butyl (Z)-(((*tert*-butoxycarbonyl)amino)(1*H*-pyrazol-1-yl)methylene)carbamate (**4.31**) was used as guanidinylating reagent to synthesize compound **4.32** from **4.12**.

Scheme 2. Synthesis of compounds **4.11**, **4.12**, **4.25**-**4.30** and **4.32**.

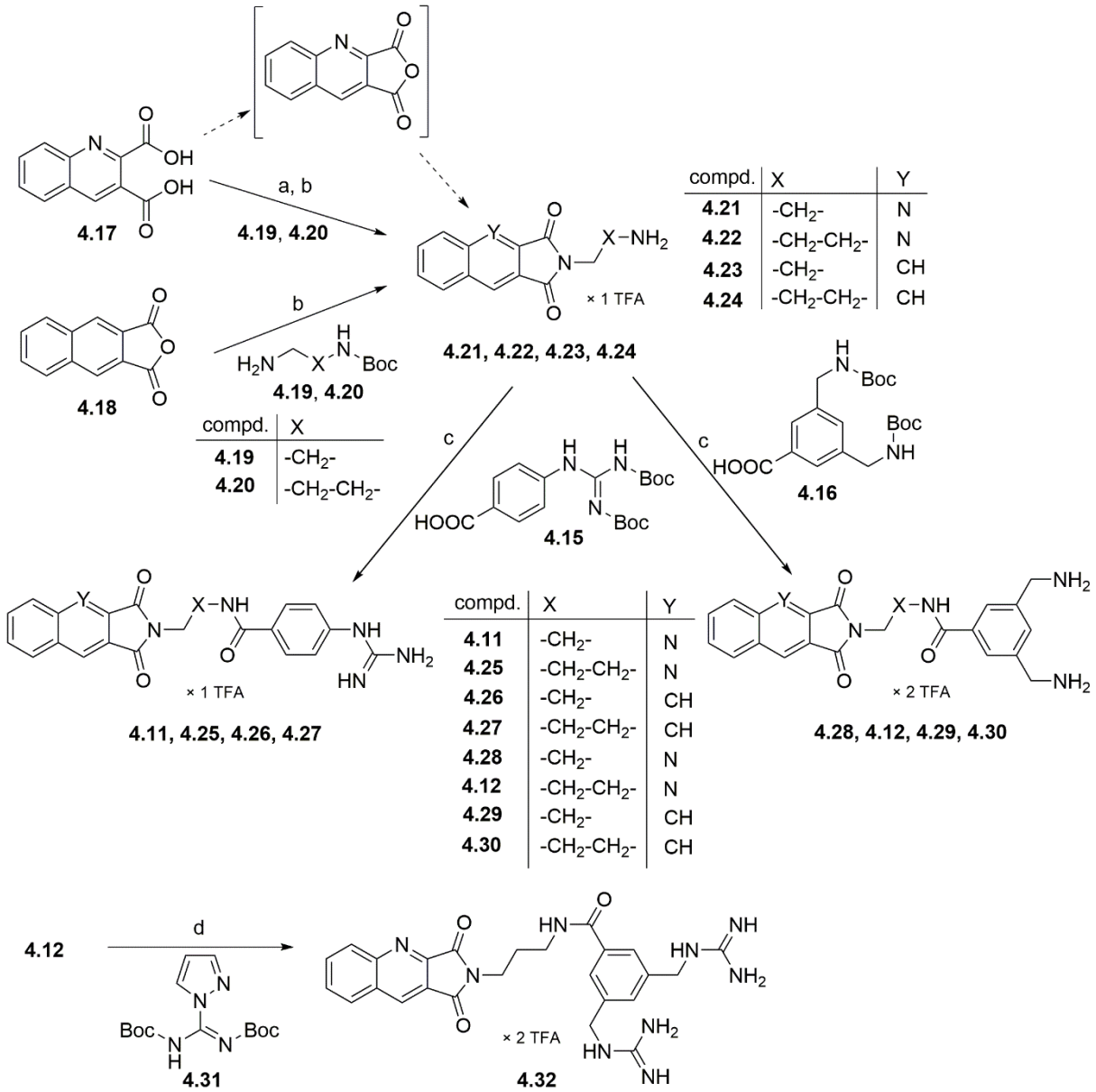

Reagents and conditions: (a) P_4O_{10}, THF, reflux, 1 h; (b) (1) THF, reflux, 1,5 h, (2) CH_2Cl_2/TFA (2:1 v/v), rt, 5 h, 9-24%; (c) (1) HOBt/HBTU/DIPEA (5/5/4.9/10 equiv.), DMF/NMP (8:2 v/v), 35 °C, 3 h, (2) CH_2Cl_2/TFA (2:1 v/v), rt, 24 h, 44-83%; (d) (1) Et_3N (3.5 equiv.), CH_2Cl_2 (anhydrous), rt, 2h, (2) CH_2Cl_2/TFA (2:1 v/v), rt, 24 h, 70%.

4.2.3 Competition Binding and Functional Studies at the Human Y_4 Receptor

All target compounds were characterized by radioligand competition binding at live CHO-hY_4R-G_{qi5}-mtAEQ cells[27] using the previously described radioligand [^{3}H]UR-KK200[28] (K_d (hY_4R): 0.68 nM). Unfortunately, compounds **4.11** and **4.25**-**4.30** displayed no Y_4R affinity (see Figure 9 and Table 1). By contrast, a complete radioligand displacement curve could be obtained in the case of compound **4.12** (pK_i (hY_4R): 5.72) (Figure 9). The transformation of both primary amine groups into guanidine moieties (**4.32**) resulted in slightly increased Y_4R affinity (pK_i: 6.03, Table 1). Compound **4.32** proved to be the ligand with the highest Y_4R affinity in this series.

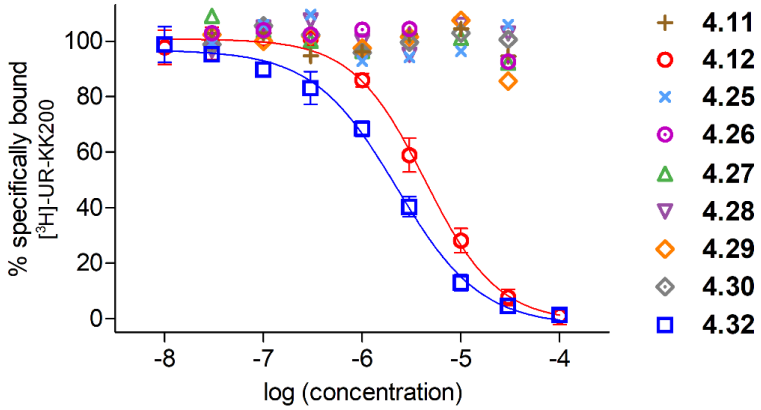

Figure 9. Radioligand displacement curves obtained from competition binding experiments with [^{3}H]UR-KK200 (K_d(hY_4R): 0.65 nM) and **4.12** or **4.32**, performed at CHO-hY_4R-mtAEQ-G_{qi5} cells. Data represent means ± SEM from at least three independent experiments performed in triplicate. In the case of **4.12** and **4.32**, data was analyzed by four parametric logistic fits (GraphPad Prism 5).

Table 1. Y_4R binding data of hPP and compounds **4.11**, **4.12**, **4.25**-**4.30** and **4.32**.

compd.	pK_i ± SEM / K_i [nM] (hY_4R)[a]
hPP	9.16 ± 0.03 / 0.69
4.11	< 4.0 / -
4.12	5.72 ± 0.1 / 2000
4.25	< 4.0 / -
4.26	< 4.0 / -
4.27	< 4.0 / -
4.28	< 4.0 / -
4.29	< 4.0 / -
4.30	< 4.0 / -
4.32	6.03 ± 0.07 / 960

[a]Determined by competition binding at CHO-hY_4R-mtAEQ-G_{qi5} cells using [^{3}H]UR-KK200 (K_d = 0.67 nM, c = 1 nM)[28] as radioligand. Data represent mean values ± SEM (pK_i) or mean values (K_i) from three independent experiments performed in triplicate.

Additionally, all compounds were investigated in a β-arrestin 2 recruitment assay (HEK293T-ARRB2-Y_4R cells[16]) to determine the respective mode of action. In agonist mode, compounds **4.11** and **4.25**-**4.30** elicited no arrestin recruitment to the Y_4R (data not shown). However, compounds **4.12** and **4.32** induced β-arrestin 2 recruitment at high concentrations (> 10 µM) (Figure 10). Therefore, it can be assumed that **4.12** and **4.32** act as partial or full agonists at the hY_4R. Investigations in antagonist mode were not carried out due to lacking Y_4R binding of **4.11** and **4.25**-**4.30**. Worth mentioning, small molecule, non-peptidic GPCR agonists are very rare (for example morphine at the µ-opioid receptor).[29] The discrepancy between binding data (pK_i) and the potency of **4.12** and **4.32** estimated in the β-arrestin recruitment assay (pEC_{50} < 4, cf. Figure 10) can be mainly attributed to the absence or presence of sodium ions in the used buffers for the radioligand binding and the functional assay, respectively, and was discussed previously for compounds **4.3** and **4.4** as well.[4,28,30]

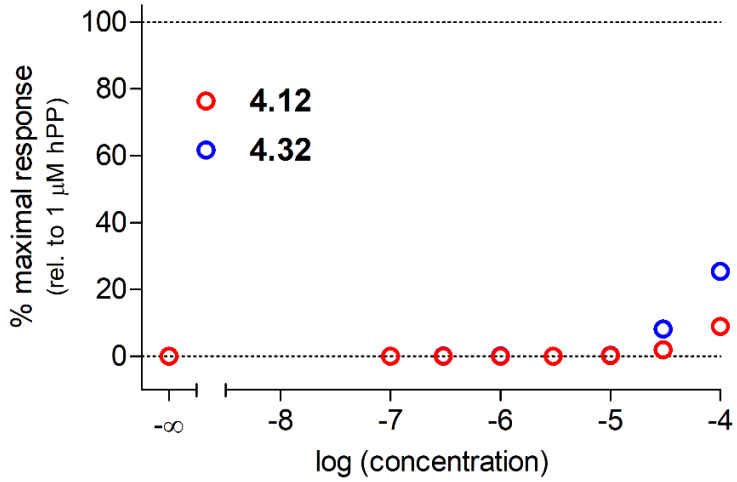

Figure 10. Effects of **4.12** and **4.32** on Y_4R mediated β-arrestin 2 recruitment determined at live HEK293T-ARRB2-Y_4R cells. Data represent means ± SEM from at least three independent experiments performed in triplicate.

4.3 Conclusion

Based on docking studies using a Y_4R homology model and using peptidic Y_4R ligands as lead structures, compound **4.12** (pK_i (hY_4R) = 6.02) (UR-AK113) could be identified as a new non-peptide lead structure, which can potentially support the development of low molecular weight, non-peptidic Y_4R ligands. Substructures in **4.12**, which are suggested to be modified in future studies, are highlighted in Figure 11.

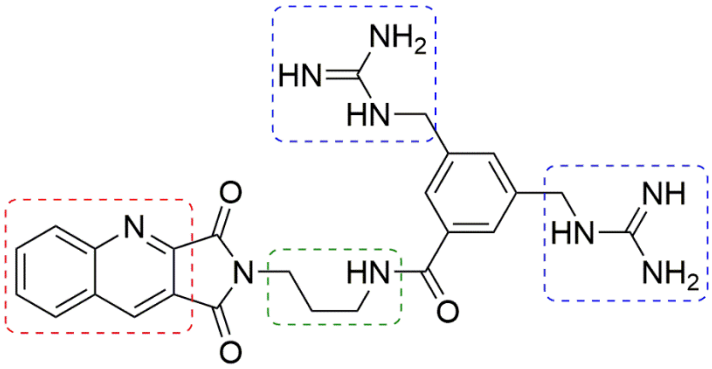

4.32

Figure 11. Structure of the non-peptide Y_4R ligand **4.32**. Colored dashed boxes indicate positions for possible future modifications.

4.4 Experimental Section

4.4.1 General Experimental Conditions

HBTU and N-methyl-2-pyrrolidone (NMP) for peptide synthesis were obtained from Iris Biotech (Marktredwitz, Germany). Trifluoroacetic acid was from Merck (Darmstadt, Germany). HOBt hydrate, tetrahydrofurane (THF), dichloromethane (CH_2Cl_2) and anhydrous $MgSO_4$ were purchased from Acros Organics/Fisher Scientific (Nidderau, Germany). *N*,*N*-diisopropylethylamine (DIPEA), 3,5-bisaminomethylbenzoic acid dihydrochloride (**4.14**), quinoline-2,3-dicarboxylic acid (**4.17**), *tert*-butyl-3-aminopropylcarbamate (**4.20**), *tert*-butyl-2-aminoethylcarbamate (**4.19**) and 4-guanidinobenzoic acid hydrochlorate (**4.13**) were obtained from ABCR (Karlsruhe, Germany) and DMF for peptide synthesis as well as gradient grade acetonitrile for HPLC were from Sigma-Aldrich (Taufkirchen, Germany). 2,3-Naphthalenedicarboxylic anhydride (**4.18**), di-*tert*-butyl dicarbonate and P_4O_{10} were from TCI (Eschborn, Germany). Human pancreatic polypeptide (hPP) was from SynPeptide (Shanghai, China). Bacitracin and bovine serum albumin (BSA) were from Serva (Heidelberg, Germany). Pierce™ D-Luciferin (monopotassium salt) was obtained from ThermoFisher Scientific (Nidderau, Germany). The synthesis of [^{3}H]UR-KK200 was described elsewhere.[28] Polypropylene reaction vessels (1.5 and 2 mL) from Sarstedt (Nümbrecht, Germany) were used to store stock solutions. Millipore water was consistently used for the preparation of stock solutions, buffers and eluents for HPLC. NMR spectra were recorded on a Bruker Avance 400 (^{1}H: 400 MHz, ^{13}C: 100 MHz) and a Bruker Avance 600 instrument with cryogenic probe (^{1}H: 600.3 MHz, ^{13}C: 150.9 MHz) (Bruker, Karlsruhe, Germany). NMR spectra were calibrated based on the solvent residual peaks (^{1}H-NMR, DMSO-d_6: δ = 2.50 ppm; ^{13}C-NMR: DMSO-d_6: δ = 39.50 ppm) and data are reported as follows: 1H-NMR: chemical shift δ in ppm (multiplicity (s = singlet, d = doublet, t = triplet, m = multiplet, br s = broad singlet); integral, coupling constant *J* in Hz), ^{13}C-NMR: chemical shift δ in ppm. High resolution mass spectrometry (HRMS) was performed with an Agilent 6540 UHD Accurate-Mass Q-TOF LC/MS system coupled to an Agilent 1290 analytical HPLC system (Agilent Technologies, Santa Clara, CA). Preparative HPLC was performed with a system from Knauer (Berlin, Germany) consisting of two K-1800 pumps and a K-2001 detector (in the following referred to as “system 1”), or with a Prep 150 LC system from Waters (Eschborn, Germany), comprising a Waters 2545 binary gradient module, a Waters 2489 UV/vis-detector and a Waters fraction collector III (in the following referred to as “system 2”). A Kinetex XB-C18, 5 µm, 250 mm × 21 mm from Phenomenex (Aschaffenburg, Germany) was used as RP-column at a flow rate of 20 mL/min using mixtures of 0.1% aqueous TFA and acetonitrile as mobile phase. The detection wavelength of 220 nm was used throughout. Collected fractions were lyophilized using a Scanvac CoolSafe 100-9 freeze-dryer (Labogene, Alleroed, Denmark) equipped with a RZ 6

rotary vane vacuum pump (Vacuubrand, Wertheim, Germany). Analytical HPLC analysis was performed with an Agilent 1100 system (Agilent Technologies) composed of a binary pump (G1312A), an autosampler (G1329A), a thermostated column compartment (G1316A) and a diode array detector (G1315B). A Kinetex XB-C18, 5 µm, 250 mm × 4.6 mm (Phenomenex) served as stationary phase at a flow rate of 0.8 mL/min. Detection was performed at 220 nm, the oven temperature was 25 °C. Mixtures of acetonitrile (A) and 0.1 % aqueous TFA (B) were used as mobile phase. The following linear gradient was applied: 0-25 min: A/B 10:90-40:60, 25-27 min: 30:70-95:5, 27-35 min: 95:5 (isocratic). The injection volume was 50 µL. Retention (capacity) factors *k* were calculated from the retention times t_R according to $k = (t_R - t_0)/t_0$ (t_0 = dead time).

4.4.2 Compound Characterization

Intermediate compounds **4.21**-**4.24** were characterized by ^{1}H- and ^{13}C-NMR spectroscopy (^{1}H: 400 MHz, ^{13}C: 100 MHz) and HRMS. Compound **4.25** was characterized by ^{1}H-NMR spectroscopy (600 MHz), HRMS and RP-HPLC. Compounds **4.11**, **4.12**, **4.26**-**4.30** and **4.32** were characterized by ^{1}H- and ^{13}C-NMR spectroscopy (^{1}H: 600 MHz, ^{13}C: 150 MHz) as well as by 2D-NMR spectroscopy (^{1}H COSY, HSQC, HMBC), HRMS and RP-HPLC. HPLC purities of all target compounds were ≥95% (chromatograms shown in Appendix).

Annotation concerning the ^{1}H-NMR spectra of **4.28**, **4.30** and **4.32**: proton signals that interfered with the broad water peak at ~ 3.5 ppm were identified by 2D NMR and by additionally recording ^{1}H-NMR spectra in DMSO-d_6/D_2O (4:1 v/v) leading to a shift of the water signal to higher ppm values.

4.4.3 Chemistry: Experimental Protocols and Analytical Data

***N*-(2-(1,3-Dioxo-1,3-dihydro-2*H*-pyrrolo[3,4-*b*]quinolin-2-yl)ethyl)-4-guanidinobenzamide hydrotrifluoroacetate (4.11).** HOBt (21.8 mg, 0.143 mmol), HBTU (53.0 mg, 0.14 mmol) and DIPEA (49.6 µL, 0.285 mmol) were added to a solution of **4.15** (10.8 mg, 0.029 mmol) in DMF/NMP 80:20 v/v (10 mL) and the mixture was stirred at rt for 15 min. Amine **4.21** (10.1 mg, 0.029 mmol) was added and stirring was continued at 35 °C for 3 h. The volatiles were removed under reduced pressure, the residue was dissolved in a mixture of CH_2Cl_2/TFA 2:1 v/v and the solution was stirred at rt for 24 h. After evaporation of the volatiles, purification by preparative HPLC (system 2, gradient: 0-18 min MeCN/0.1% aq TFA 3:97-40:60, t_R = 12.4 min) yielded **4.11** as a white solid (12.3 mg, 84%). ^{1}H-NMR (600 MHz, DMSO-d_6): δ (ppm) 3.58-3.63 (m, 2H), 3.85-3.91 (m, 2H), 7.25-7.29 (m, 2H), 7,68 (s, 4H),

7.76-7.79 (m, 2H), 7.85-7.88 (m, 1H), 8.01-8.05 (m, 1H), 8.29-8.33 (m, 2H), 8.62-8.66 (m, 1H), 9.00 (s, 1H), 10.07 (s, 1H). ^{13}C-NMR (150 MHz, DMSO-*d*$_6$): δ (ppm) 37.4, 38.1, 123.1 (two carbon atoms), 123.3, 128.4, 128.5 (two carbon atoms), 129.3, 130.37, 130.42, 131.5, 132.4, 132.8, 138.4, 149.6, 151.0, 155.6, 165.7, 166.0, 166.1. HRMS (ESI): *m/z* $[M+H]^+$ calcd. for $[C_{21}H_{19}N_6O_3]^+$ 403.1513, found: 403.1513. RP-HPLC (220 nm): 99% (t_R = 16.3 min, *k* = 4.1). $C_{21}H_{18}N_6O_3 \cdot C_2H_1F_3O_2$ (402.41 + 114.02).

3,5-Bis(aminomethyl)-*N*-(3-(1,3-dioxo-1,3-dihydro-2*H*-pyrrolo[3,4-*b*]quinolin-2-yl)propyl)benzamide bis(hydrotrifluoroacetate) (4.12). HOBt (20.8 mg, 0.136 mmol), HBTU (50.5 mg, 0.136 mmol) and DIPEA (47.3 µL, 0.272 mmol) were added to a solution of **4.16** (10.3 mg, 0.027 mmol) in DMF/NMP 80:20v/v (10 mL) and the mixture was stirred at rt for 15 min. Amine **4.22** (10.0 mg, 0.027 mmol) was added and stirring was continued at 35 °C for 3 h. The volatiles were removed under reduced pressure, the residue was dissolved in a mixture of CH_2Cl_2/TFA 2:1 v/v and the solution was stirred at rt for 24 h. After evaporation of the volatiles, purification by preparative HPLC (system 2, gradient: 0-18 min MeCN/0.1% aq TFA 3:97-40:60, t_R = 10.3 min) yielded **4.12** as a white solid (14.0 mg, 80%). ^{1}H-NMR (600 MHz, DMSO-*d*$_6$): δ (ppm) 1.92-1.98 (m, 2H), 3.38-3.41 (m, 2H), 3.76 (t, 2H, *J* 7.3 Hz), 4.07 (s, 4H), 7.61-7.64 (m, 1H), 7.85-7.89 (m, 1H), 7.96-7.99 (m, 2H), 8.01-8.05 (m, 1H), 8.23-8.37 (m, 8H), 8.59 (t, 1H, *J* 5.7 Hz), 8.97-9.00 (m, 1H). ^{13}C-NMR (150 MHz, DMSO-*d*$_6$): δ (ppm) 28.0, 36.0, 37.2, 42.0 (two carbon atoms), 123.2, 127.8 (two carbon atoms), 128.5, 129.3, 130.39, 130.44, 131.9, 132.5, 132.8, 134.5 (two carbon atoms), 135.3, 149.6, 150.9, 165.6, 166.0, 166.1. HRMS (ESI): *m/z* $[M+2H]^{2+}$ calcd. for $[C_{23}H_{25}N_5O_3]^{2+}$ 209.5973, found: 209.5980. RP-HPLC (220 nm): 97% (t_R = 12.3 min, *k* = 2.8). $C_{23}H_{23}N_5O_3 \cdot C_4H_2F_6O_4$ (417.47 + 228.04).

(*Z*)-4-(2,3-Bis(*tert*-butoxycarbonyl)guanidino)benzoic acid (4.15). 4-Guanidinobenzoic acid (**4.14**) (209 mg, 0.968 mmol) was dissolved in 0.5 M NaOH/MeCN 2:1 v/v (10 mL) and the solution was cooled to 0 °C under vigorously stirring. Boc_2O (482 mg, 1.936 mmol), dissolved in dioxane (10 mL), was added dropwise to the mixture by using a dropping funnel over a period of 30 min. The reaction mixture was allowed to warm up to rt and stirring was continued overnight. After addition of H_2O (30 mL), organic solvents were evaporated under reduced pressure. The aqueous phase was treated with CH_2Cl_2 (3 × 100 mL) and the collected organic phases were combined and dried over $MgSO_4$. Removal of CH_2Cl_2 under reduced pressure yielded **4.15** as a white-grey solid (148 mg, 40%). ^{1}H-NMR (400 MHz, DMSO-*d*$_6$): δ (ppm) 1.39-1.43 (m, 18H), 7.02-7.09 (m, 2H), 7.23 (s, 1H), 7.78-7.85 (m, 2H), 10.83 (s, 1H), 12.63 (br s, 1H). ^{13}C-NMR (100 MHz, DMSO-*d*$_6$): δ (ppm) 28.9 (six carbon atoms), 77.2, 81.3, 116.9 (two carbon atoms), 121.0, 128.3 (two carbon atoms), 142.3, 152.9, 156.9, 157.2, 169.0. HRMS (ESI): *m/z* $[M+H]^+$ calcd. for $[C_{18}H_{26}N_3O_6]^+$ 380.1816, found: 380.1821. $C_{18}H_{25}N_3O_6$ (379.41).

3,5-Bis(((*tert*-butoxycarbonyl)amino)methyl)benzoic acid (4.16). 3,5-bis(aminomethyl)benzoic acid (**4.13**) (324 mg, 1.50 mmol) was dissolved in 0.5 M NaOH (10 mL) and the solution was cooled to 0 °C under vigorously stirring. Boc_2O (890 mg, 4.112 mmol), dissolved in dioxane (10 mL), was added dropwise to the mixture by using a dropping funnel over a period of 30 min. The reaction mixture was allowed to warm up to rt and stirring was continued overnight. After addition of H_2O (30 mL), organic solvents were evaporated under reduced pressure. The aqueous phase was treated with CH_2Cl_2 (3 × 100 mL) and the collected organic phases were combined and dried over $MgSO_4$. Removal of CH_2Cl_2 under reduced pressure yielded **4.16** as an orange solid (233 mg, 41%). ^{1}H-NMR (400 MHz, DMSO-d_6): δ (ppm) 1.38-1.41 (m, 18H), 4.13-4.18 (m, 4H), 7.33 (s, 1H), 7.42-7.48 (m, 2H), 7.68-7.72 (m, 2H), 12.9 (br s, 1H). ^{13}C-NMR (100 MHz, DMSO-d_6): δ (ppm) 29.7 (six carbon atoms), 43.6 (two carbon atoms), 78.4 (two carbon atoms), 126.7 (two carbon atoms), 130.3, 131.4, 141.1 (two carbon atoms), 156.3 (two carbon atoms), 167.8. HRMS (ESI): *m/z* $[M+H]^+$ calcd. for $[C_{18}H_{29}N_2O_6]^+$ 381.2020, found: 381.2019. $C_{19}H_{28}N_2O_6$ (380.44).

2-(2-Aminoethyl)-1*H*-pyrrolo[3,4-*b*]quinoline-1,3(2*H*)-dione hydrotrifluoroacetate (4.21). Compound **4.17** (200 mg, 0.92 mmol) was dissolved in anhydrous THF (100 mL). After portionwise P_4O_{10} addition (1.3 g, 4.6 mmol), the mixture was vigorously stirred under reflux for 1 h. Mono-Boc-diamine **4.19** (147 mg, 0.92 mmol) was added to the round-bottom flask and the suspension was stirred for additional 1.5 h, reflux conditions were maintained. After cooling down to rt, solid material was removed by filtration, the filtrate collected and the volatiles removed under reduced pressure. Purification by preparative HPLC (system 1, gradient: 0-18 min MeCN/0.1% aq TFA 5:95-42:58, t_R = 9.3 min) yielded Boc-protected product as a white solid. The residue was dissolved in a mixture of CH_2Cl_2/TFA 2:1 v/v and the solution was stirred at rt for 5 h. The volatiles were evaporated, the residue was resolved in H_2O/MeCN 9:1 v/v (100 mL) and lyophilized. Product **4.21** was obtained as a white solid (28.1 mg, 9%). ^{1}H-NMR (400 MHz, DMSO-d_6): δ (ppm) 3.24-3.28 (m, 2H), 3.75-3.81 (m, 2H), 7.49-7.55 (m, 1H), 7.61-7.65 (m, 1H), 8.00-8.04 (m, 1H), 8.46-8.51 (m, 4H), 9.51 (s, 1H). ^{13}C-NMR (100 MHz, DMSO-d_6): δ (ppm) 38.1, 42.8, 126.8, 127.1, 129.2, 129.4, 130.1, 133.1, 135.6, 150.1, 156.5, 165.9, 167.3. HRMS (ESI): *m/z* $[M+H]^+$ calcd. for $[C_{13}H_{12}N_3O_2]^+$ 242.0924, found: 242.0922. $C_{13}H_{11}N_3O_2$ (241.25 + 114.02).

2-(3-Aminopropyl)-1*H*-pyrrolo[3,4-*b*]quinoline-1,3(2*H*)-dione hydrotrifluoroacetate (4.22). Compound **4.17** (200 mg, 0.92 mmol) was dissolved in anhydrous THF (100 mL). After portionwise P_4O_{10} addition (1.3 g, 4.6 mmol), the mixture was vigorously stirred under reflux for 1 h. Mono-Boc-diamine **4.20** (160 mg, 0.92 mmol) was added to the round-bottom flask and the suspension was stirred for additional 1.5 h, reflux conditions were maintained. After cooling down to rt, solid material was removed by filtration, the filtrate collected and the

volatiles removed under reduced pressure. Purification by preparative HPLC (system 1, gradient: 0-18 min MeCN/0.1% aq TFA 5:95-42:58, t_R = 9.6 min) yielded Boc-protected product as a white solid. The residue was dissolved in a mixture of CH_2Cl_2/TFA 2:1 v/v and the solution was stirred at rt for 5 h. The volatiles were evaporated, the residue was resolved in H_2O/MeCN 9:1 v/v (100 mL) and lyophilized. Product **4.22** was obtained as a white solid (34.5 mg, 10%). ^{1}H-NMR (400 MHz, DMSO-*d*$_6$): δ (ppm) 2.20-2.25 (m, 2H), 3.33-3.39 (m, 2H), 3.99-4.05 (m, 2H), 7.71-7.75 (m, 1H), 8.00-8.06 (m, 1H), 8.27-8.31 (m, 1H), 8.64-8.69 (m, 4H), 9.44 (s, 1H). ^{13}C-NMR (100 MHz, DMSO-*d*$_6$): δ (ppm) 27.1, 38.7, 43.1, 125.9, 127.1, 127.2, 129.7, 129.9, 134.1, 138.6, 150.1, 156.9, 165.6, 167.3. HRMS (ESI): *m/z* $[M+H]^+$ calcd. for $[C_{14}H_{14}N_3O_2]^+$ 256.1080, found: 256.1081. $C_{14}H_{13}N_3O_2 \cdot C_2H_1F_3O_2$ (255.28 + 114.02).

2-(2-Aminoethyl)-1*H*-benzo[*f*]isoindole-1,3(2*H*)-dione hydrotrifluoroacetate (4.23). Anhydride **4.18** (300 mg, 1.51 mmol) was added to a round-bottom flask and dissolved in EtOH (150 mL). After addition of **4.19** (242 mg, 1.51 mmol), the mixture was vigorously stirred under reflux for 2 h. The volatiles were evaporated under reduced pressure and the residue was dissolved in THF (10 mL). The crude product was purified by column chromatography (THF) to obtain Boc-protected product as white solid. The residue was dissolved in a mixture of CH_2Cl_2/TFA 2:1 v/v and the solution was stirred at rt for 5 h. The volatiles were evaporated, the residue was resolved in H_2O/MeCN 9:1 v/v (400 mL) and lyophilized. Product **4.23** was obtained as a white solid (103.5 mg, 19%). ^{1}H-NMR (400 MHz, DMSO-*d*$_6$): δ (ppm) 3.31-3.35 (m, 2H), 4.01-4.06 (m, 2H), 6.98-7.08 (m, 2H), 8.03-8.10 (m, 2H), 8.52 (s, 3H), 8.91 (s, 2H). ^{13}C-NMR (100 MHz, DMSO-*d*$_6$): δ (ppm) 38.2, 43.4, 127.9 (two carbon atoms), 128.3 (two carbon atoms), 128.9 (two carbon atoms), 133.7 (two carbon atoms), 134.5 (two carbon atoms), 169.2 (two carbon atoms). HRMS (ESI): *m/z* $[M+H]^+$ calcd. for $[C_{14}H_{13}N_2O_2]^+$ 241.0972, found: 241.0982. $C_{14}H_{12}N_2O_2 \cdot C_2H_1F_3O_2$ (240.26 + 114.02).

2-(3-Aminopropyl)-1*H*-benzo[*f*]isoindole-1,3(2*H*)-dione hydrotrifluoroacetate (4.24). Anhydride **4.18** (300 mg, 1.51 mmol) was added to a round-bottom flask and dissolved in EtOH (150 mL). After addition of **4.20** (242 mg, 1.51 mmol), the mixture was vigorously stirred under reflux for 2 h. The volatiles were evaporated under reduced pressure and the residue was dissolved in THF (10 mL). The crude product was purified by column chromatography (THF) to obtain Boc-protected product as white solid. The residue was dissolved in a mixture of CH_2Cl_2/TFA 2:1 v/v and the solution was stirred at rt for 5 h. The volatiles were evaporated, the residue was resolved in H_2O/MeCN 9:1 v/v (400 mL) and lyophilized. Product **4.24** was obtained as a white solid (133.7 mg, 24%). ^{1}H-NMR (400 MHz, DMSO-*d*$_6$): δ (ppm) 2.45-2.50 (m, 2H), 3.51-3.56 (m, 2H), 4.09-4.12 (m, 2H), 7.20-7.27 (m, 2H), 8.21-8.25 (m, 2H), 8.55 (s, 3H), 8.91 (s, 2H). ^{13}C-NMR (100 MHz, DMSO-*d*$_6$): δ (ppm) 27.9, 38.7, 42.9, 128.1 (two carbon atoms), 129.0 (two carbon atoms); 129.7 (two carbon atoms), 132.7 (two carbon atoms), 135.2

(two carbon atoms), 168.9 (two carbon atoms). HRMS (ESI): *m/z* $[M+H]^+$ calcd. for $[C_{15}H_{15}N_2O_2]^+$ 255.1128, found: 255.1125. $C_{15}H_{14}N_2O_2 \cdot C_2H_1F_3O_2$ (255.30 + 114.02).

***N*-(3-(1,3-Dioxo-1,3-dihydro-2*H*-pyrrolo[3,4-*b*]quinolin-2-yl)propyl)-4-guanidinobenzamide hydrotrifluoroacetate (4.25).** HOBt (20.8 mg, 0.136 mmol), HBTU (50.5 mg, 0.133 mmol) and DIPEA (47.3 µL, 0.272 mmol) were added to a solution of 4.15 (10.3 mg, 0.027 mmol) in DMF/NMP 80:20 v/v (10 mL) and the mixture was stirred at rt for 15 min. Amine **4.22** (10.0 mg, 0.027 mmol) was added and stirring was continued at 35 °C for 3 h. The volatiles were removed under reduced pressure, the residue was dissolved in a mixture of CH_2Cl_2/TFA 2:1 v/v and the solution was stirred at rt for 24 h. After evaporation of the volatiles, purification by preparative HPLC (system 2, gradient: 0-18 min MeCN/0.1% aq TFA 3:97-40:60, t_R = 13.3 min) yielded **4.25** as a white solid (9.3 mg, 65%). ^{1}H-NMR (600 MHz, DMSO-d_6): δ (ppm)1.91-1.97 (m, 2H), 3.35-3.39 (m, 2H), 3.72-3.77 (m, 2H), 7.28-7.32 (m, 2H), 7.53 (s, 4H), 7.84-7.88 (m, 1H), 7.89-7.93 (m, 2H), 8.00-8.06 (m, 1H), 8.29-8.33 (m, 2H), 8.53-8.59 (m, 1H), 8.98 (s, 1H), 9.81 (s, 1H). HRMS (ESI): *m/z* $[M+H]^+$ calcd. for $[C_{22}H_{21}N_6O_3]^+$ 417.1670, found: 417.1671. RP-HPLC (220 nm): 99% (t_R = 17.3 min, k = 4.4). $C_{22}H_{20}N_6O_3 \cdot C_2H_1F_3O_2$ (416.44 + 114.02).

***N*-(2-(1,3-Dioxo-1,3-dihydro-2*H*-benzo[*f*]isoindol-2-yl)ethyl)-4-guanidinobenzamide hydrotrifluoroacetate (4.26).** HOBt (21.8 mg, 0.143 mmol), HBTU (53.0 mg, 0.14 mmol) and DIPEA (49.6 µL, 0.285 mmol) were added to a solution of 4.15 (10.8 mg, 0.029 mmol) in DMF/NMP 80:20 v/v (10 mL) and the mixture was stirred at rt for 15 min. Amine **4.23** (10.1 mg, 0.029 mmol) was added and stirring was continued at 35 °C for 3 h. The volatiles were removed under reduced pressure, the residue was dissolved in a mixture of CH_2Cl_2/TFA 2:1 v/v and the solution was stirred at rt for 24 h. After evaporation of the volatiles, purification by preparative HPLC (system 1, gradient: 0-18 min MeCN/0.1% aq TFA 3:97-60:40, t_R = 12.8 min) yielded **4.26** as a white solid (10.7 mg, 73%). ^{1}H-NMR (600 MHz, DMSO-d_6): δ (ppm) 3.56-3.60 (m, 2H), 3.81-3.85 (m, 2H), 7.27 (d, 2H, *J* 8.7 Hz), 7.60 (s, 4H), 7.74-7.83 (m, 4H), 8.23-8.29 (m, 2H), 8.51 (s, 2H), 8.66 (t, 1H, *J* 5.9 Hz), 9.93 (s, 1H). ^{13}C-NMR (150 MHz, DMSO-d_6): δ (ppm) 37.6, 37.9, 123.2 (two carbon atoms), 124.1 (two carbon atoms), 127.7 (two carbon atoms), 128.5 (two carbon atoms), 129.2 (two carbon atoms), 130.2 (two carbon atoms), 131.7, 134.9 (two carbon atoms), 138.2, 155.5, 165.6, 167.6 (two carbon atoms). HRMS (ESI): *m/z* $[M+H]^+$ calcd. for $[C_{22}H_{20}N_5O_3]^+$ 402.1561, found: 402.1564. RP-HPLC (220 nm): 97% (t_R = 21.0 min, k = 5.5). $C_{22}H_{19}N_5O_3 \cdot C_2H_1F_3O_2$ (401.43 + 114.02).

***N*-(3-(1,3-Dioxo-1,3-dihydro-2*H*-benzo[*f*]isoindol-2-yl)propyl)-4-guanidinobenzamide hydrotrifluoroacetate (4.27).** HOBt (20.8 mg, 0.136 mmol), HBTU (50.5 mg, 0.133 mmol) and DIPEA (47.3 µL, 0.272 mmol) were added to a solution of 4.15 (10.2 mg, 0.027 mmol) in DMF/NMP 80:20 v/v (10 mL) and the mixture was stirred at rt for 15 min. Amine **4.24** (10.0

mg, 0.027 mmol) was added and stirring was continued at 35 °C for 3 h. The volatiles were removed under reduced pressure, the residue was dissolved in a mixture of CH_2Cl_2/TFA 2:1 v/v and the solution was stirred at rt for 24 h. After evaporation of the volatiles, purification by preparative HPLC (system 1, gradient: 0-18 min MeCN/0.1% aq TFA 3:97-60:40, t_R = 13.8 min) yielded **4.27** as a white solid (9.1 mg, 64%). ^{1}H-NMR (600 MHz, DMSO-d_6): δ (ppm) 1.88-1.95 (m, 2H), 3.34 (q, 2H, *J* 6.4 Hz), 3.70 (t, 2H, *J* 7.4 Hz), 7.28-7.32 (m, 2H), 7.63 (s, 4H), 7.76-7.81 (m, 2H), 7.88-7.92 (m, 2H), 8.24-8.29 (m, 2H), 8.50 (s, 2H), 8.53-8.57 (m, 1H), 10.0 (s, 1H). ^{13}C-NMR (150 MHz, DMSO-d_6): δ (ppm) 28.1, 35.8, 37.0, 123.3 (two carbon atoms), 124.3 (two carbon atoms), 127.5 (two carbon atoms), 128.6 (two carbon atoms), 129.2 (two carbon atoms), 130.3 (two carbon atoms), 131.7, 135.0 (two carbon atoms), 138.2, 155.6, 165.2, 167.5 (two carbon atoms). HRMS (ESI): *m/z* $[M+H]^+$ calcd. for $[C_{23}H_{22}N_5O_3]^+$ 416.1717, found: 416.1724. RP-HPLC (220 nm): 99% (t_R = 22.6 min, *k* = 6.0). $C_{23}H_{21}N_5O_3 \cdot C_2H_1F_3O_2$ (415.45 + 114.02).

3,5-Bis(aminomethyl)-*N*-(2-(1,3-dioxo-1,3-dihydro-2*H*-pyrrolo[3,4-*b*]quinolin-2-yl)ethyl)benzamide bis(hydrotrifluoroacetate) (4.28). HOBt (21.8 mg, 0.143 mmol), HBTU (53.0 mg, 0.140 mmol) and DIPEA (49.6 µL, 0.285 mmol) were added to a solution of 4.16 (10.8 mg, 0.029 mmol) in DMF/NMP 80:20 v/v (10 mL) and the mixture was stirred at rt for 15 min. Amine **4.21** (10.1 mg, 0.029 mmol) was added and stirring was continued at 35 °C for 3 h. The volatiles were removed under reduced pressure, the residue was dissolved in a mixture of CH_2Cl_2/TFA 2:1 v/v and the solution was stirred at rt for 24 h. After evaporation of the volatiles, purification by preparative HPLC (system 2, gradient: 0-18 min MeCN/0.1% aq TFA 3:97-40:60, t_R = 9.5 min) yielded **4.28** as a white solid (11.8 mg, 64%). ^{1}H-NMR (600 MHz, DMSO-d_6): δ (ppm) 3.61-3.64 (m, 2H), 3.89-3.92 (m, 2H), 4.03-4.07 (m, 4H), 7.65 (s, 1H), 7.84-7.88 (m, 1H), 7.89-7.92 (m, 2H), 8.00-8.04 (m, 1H), 8.27-8.42 (m, 8H), 8.78-8.82 (m, 1H), 8.98 (s, 1H). ^{13}C-NMR (150 MHz, DMSO-d_6): δ (ppm) 37.6, 37.9, 42.0 (two carbon atoms), 116.0 (TFA), 118.0 (TFA), 123.2, 127.7 (two carbon atoms), 128.5, 129.4, 130.37, 130.42, 132.0, 132.5, 132.8, 134.5 (two carbon atoms), 135.2, 149.6, 151.0, 158.3 (q, *J* 32 Hz) (TFA), 165.96, 166.00, 166.04. HRMS (ESI): *m/z* $[M+2H]^{2+}$ calcd. for $[C_{22}H_{23}N_5O_3]^{2+}$ 202.5895, found: 202.5899. RP-HPLC (220 nm): 97% (t_R = 11.2 min, *k* = 2.5). $C_{22}H_{21}N_5O_3 \cdot C_4H_2F_6O_4$ (403.44 + 228.04)

3,5-Bis(aminomethyl)-*N*-(2-(1,3-dioxo-1,3-dihydro-2*H*-benzo[*f*]isoindol-2-yl)ethyl)benzamide bis(hydrotrifluoroacetate) (4.29). HOBt (21.8 mg, 0.143 mmol), HBTU (53.0 mg, 0.140 mmol) and DIPEA (49.6 µL, 0.285 mmol) were added to a solution of 4.16 (10.8 mg, 0.029 mmol) in DMF/NMP 80:20 v/v (10 mL) and the mixture was stirred at rt for 15 min. Amine **4.23** (10.0 mg, 0.029 mmol) was added and stirring was continued at 35 °C for 3 h. The volatiles were removed under reduced pressure, the residue was dissolved in a mixture

of CH_2Cl_2/TFA 2:1 v/v and the solution was stirred at rt for 24 h. After evaporation of the volatiles, purification by preparative HPLC (system 1, gradient: 0-18 min MeCN/0.1% aq TFA 3:97-60:40, t_R = 10.5 min) yielded **4.29** as a white solid (8.0 mg, 44%). ^{1}H-NMR (600 MHz, DMSO-*d*$_6$): δ (ppm) 3.59-3.62 (m, 2H), 3.83-3.87 (m, 2H), 4.02-4.08 (m, 4H), 7.64 (s, 1H), 7.76-7.81 (m, 2H), 7.87-7.92 (m, 2H), 8.23-8.41 (m, 8H), 8.49 (s, 2H), 8.77 (t, 1H, *J* 6.0 Hz). ^{13}C-NMR (150 MHz, DMSO-*d*$_6$): δ (ppm) 37.7, 37.8, 42.0 (two carbon atoms), 124.2 (two carbon atoms), 127.6 (two carbon atoms), 127.7 (two carbons atoms), 129.2 (two carbon atoms, 130.2 (two carbon atoms), 131.9, 134.5 (two carbon atoms), 135.0 (two carbon atoms), 135.1, 165.8, 167.6 (two carbon atoms). HRMS (ESI): *m/z* $[M+2H]^{2+}$ calcd. for $[C_{23}H_{24}N_4O_3]^{2+}$ 202.0919, found: 202.0925. RP-HPLC (220 nm): 98% (t_R = 15.1 min, *k* = 3.7). $C_{23}H_{22}N_4O_3 \cdot C_4H_2F_6O_4$ (402.45 + 228.04).

3,5-Bis(aminomethyl)-*N*-(3-(1,3-dioxo-1,3-dihydro-2*H*-benzo[*f*]isoindol-2-yl)propyl)benzamide bis(hydrotrifluoroacetate) (4.30). HOBt (20.8 mg, 0.136 mmol), HBTU (50.5 mg, 0.133 mmol) and DIPEA (47.3 µL, 0.272 mmol) were added to a solution of 4.16 (10.3 mg, 0.027 mmol) in DMF/NMP 80:20 v/v (10 mL) and the mixture was stirred at rt for 15 min. Amine **4.24** (10.3 mg, 0.027 mmol) was added and stirring was continued at 35 °C for 3 h. The volatiles were removed under reduced pressure, the residue was dissolved in a mixture of CH_2Cl_2/TFA 2:1 v/v and the solution was stirred at rt for 24 h. After evaporation of the volatiles, purification by preparative HPLC (system 1, gradient: 0-18 min MeCN/0.1% aq TFA 3:97-60:40, t_R = 11.5 min) yielded **4.30** as a white solid (13.7 mg, 79%). ^{1}H-NMR (600 MHz, DMSO-*d*$_6$): δ (ppm) 1.90-1.96 (m, 2H), 3.37-3.38 (m, 2H), 3.70-3.73 (m, 2H), 4.05-4.10 (m, 4H), 7.61-7.63 (m, 1H), 7.77-7.81 (m, 2H), 7.96-7.98 (m, 2H), 8.24-8.34 (m, 8H), 8.51 (s, 2H), 8.56-8.60 (m, 1H). ^{13}C-NMR (150 MHz, DMSO-*d*$_6$): δ (ppm) 28.2, 35.8, 37.2, 42.0 (two carbon atoms), 124.3 (two carbon atoms), 127.5 (two carbon atoms), 127.8 (two carbon atoms), 129.3 (two carbon atoms), 130.3 (two carbon atoms), 131.9, 134.5 (two carbon atoms), 135.0 (two carbon atoms), 135.3, 165.5, 167.5 (two carbon atoms). HRMS (ESI): *m/z* $[M+2H]^{2+}$ calcd. for $[C_{24}H_{26}N_4O_3]^{2+}$ 209.0997, found: 209.0995. RP-HPLC (220 nm): 97% (t_R = 16.5 min, *k* = 4.1). $C_{24}H_{24}N_4O_3 \cdot C_4H_2F_6O_4$ (416.48 + 228.04).

***N*-(3-(1,3-Dioxo-1,3-dihydro-2*H*-pyrrolo[3,4-*b*]quinolin-2-yl)propyl)-3,5-bis(guanidinomethyl)benzamide bis(hydrotrifluoroacetate) (4.32).** Compound **4.30** (20.0 mg, 0.031 mmol) was dissolved in anhydrous CH_2Cl_2 (10 mL). *Tert*-butyl (Z)-(((*tert*-butoxycarbonyl)amino)(1*H*-pyrazol-1-yl)methylene)carbamate (**4.31**) (20.2 mg, 0.065 mmol) and Et_3N (15.0 µL, 0.109 mmol) were added and the mixture was stirred for 2 h at room temperature. The volatiles were removed under reduced pressure, the residue was dissolved in a mixture of CH_2Cl_2/TFA 2:1 v/v and the solution was stirred at rt for 24 h. After evaporation of the volatiles, purification by preparative HPLC (system 1, gradient: 0-18 min MeCN/0.1%

aq TFA 3:97-60:40, t_R = 10.1 min) yielded **4.32** as a white solid (16.0 mg, 70%). ^{1}H-NMR (600 MHz, DMSO-d_6): δ (ppm) 1.91-1.98 (m, 2H), 3.35-3.38 (m, 2H), 3.72-3.78 (m, 2H), 4.40-4.44 (m, 4H), 6.95-7.70 (br s, 8H, interfering with the next listed signals), 7.36-7.37 (m, 1H), 7.73-7.76 (m, 2H), 7.84-7.89 (m, 1H), 8.01-8.05 (m, 1H), 8.09-8.15 (m, 2H), 8.29-8.34 (m, 2H), 8.58-8.64 (m, 1H), 8.98 (s, 1H). ^{13}C-NMR (150 MHz, DMSO-d_6): δ (ppm) 28.0, 36.0, 37.1, 43.9 (two carbon atoms), 116.1 (TFA), 118.1 (TFA), 123.2, 125.3 (two carbon atoms), 128.5, 128.6, 129.3, 130.39, 130.44, 132.5, 132.8, 135.2, 137.8 (two carbon atoms), 149.6, 150.9, 156.9 (two carbon atoms), 158.5 (q, *J* 32 Hz) (TFA), 165.8, 165.97, 166.00. HRMS (ESI): *m/z* $[M+2H]^{2+}$ calcd. for $[C_{25}H_{29}N_9O_3]^{2+}$ 251.6191, found: 251.6200. RP-HPLC (220 nm): 99% (t_R = 16.3 min, *k* = 4.1). $C_{25}H_{27}N_9O_3 \cdot C_4H_2F_6O_4$ (501.55 + 228.04).

4.4.4 Computational Chemistry & Pharmacology

Induced-Fit Docking. Described in chapter 2.

Cell Culture, Buffers and Media Used for Cellular Assays. Described in chapter 2.

Radioligand Binding Assay at the hY$_4$R. Described in chapter 2.

β-Arrestin 2 Recruitment Assay. Described in chapter 2.

4.5 References

(1) Balasubramaniam, A. A., Neuropeptide Y family of hormones: receptor subtypes and antagonists. *Peptides* **1997**, *18*, 445-457.

(2) Cerda-Reverter, J. M.; Larhammar, D., Neuropeptide Y family of peptides: structure, anatomical expression, function, and molecular evolution. *Biochem. Cell Biol.* **2000**, *78*, 371-392.

(3) Lundell, I.; Blomqvist, A. G.; Berglund, M. M.; Schober, D. A.; Johnson, D.; Statnick, M. A.; Gadski, R. A.; Gehlert, D. R.; Larhammar, D., Cloning of a human receptor of the NPY receptor family with high affinity for pancreatic polypeptide and peptide YY. *J. Biol. Chem.* **1995**, *270*, 29123-29128.

(4) Konieczny, A.; Braun, D.; Wifling, D.; Bernhardt, G.; Keller, M., Oligopeptides as neuropeptide Y Y_4 receptor ligands: identification of a high-affinity tetrapeptide agonist and a hexapeptide antagonist. *J. Med. Chem.* **2020**, *63*, 8198-8215.

(5) Rudolf, K.; Eberlein, W.; Engel, W.; Wieland, H. A.; Willim, K. D.; Entzeroth, M.; Wienen, W.; Beck-Sickinger, A. G.; Doods, H. N., The first highly potent and selective non-peptide neuropeptide Y Y_1 receptor antagonist: BIBP3226. *Eur. J. Pharmacol.* **1994**, *271*, 11-30.

(6) Keller, M.; Kaske, M.; Holzammer, T.; Bernhardt, G.; Buschauer, A., Dimeric argininamide-type neuropeptide Y receptor antagonists: chiral discrimination between Y_1 and Y_4 receptors. *Bioorg. Med. Chem.* **2013**, *21*, 6303-6322.

(7) Li, J. B.; Asakawa, A.; Terashi, M.; Cheng, K.; Chaolu, H.; Zoshiki, T.; Ushikai, M.; Sheriff, S.; Balasubramaniam, A.; Inui, A., Regulatory effects of Y_4 receptor agonist (BVD-74D) on food intake. *Peptides* **2010**, *31*, 1706-1710.

(8) Olza, J.; Gil-Campos, M.; Leis, R.; Ruperez, A. I.; Tojo, R.; Canete, R.; Gil, A.; Aguilera, C. M., Influence of variants in the NPY gene on obesity and metabolic syndrome features in Spanish children. *Peptides* **2013**, *45*, 22-27.

(9) Rosenbaum, D. M.; Zhang, C.; Lyons, J. A.; Holl, R.; Aragao, D.; Arlow, D. H.; Rasmussen, S. G. F.; Choi, H.-J.; DeVree, B. T.; Sunahara, R. K.; Chae, P. S.; Gellman, S. H.; Dror, R. O.; Shaw, D. E.; Weis, W. I.; Caffrey, M.; Gmeiner, P.; Kobilka, B. K., Structure and function of an irreversible agonist-β_2 adrenoceptor complex. *Nature* **2011**, *469*, 236-240.

(10) Wu, B.; Chien, E. Y. T.; Mol, C. D.; Fenalti, G.; Liu, W.; Katritch, V.; Abagyan, R.; Brooun, A.; Wells, P.; Bi, F. C.; Hamel, D. J.; Kuhn, P.; Handel, T. M.; Cherezov, V.; Stevens, R. C., Structures of the CXCR4 chemokine GPCR with small-molecule and cyclic peptide antagonists. *Science* **2010**, *330*, 1066-1071.

(11) Liu, X.; Masoudi, A.; Kahsai, A. W.; Huang, L.-Y.; Pani, B.; Staus, D. P.; Shim, P. J.; Hirata, K.; Simhal, R. K.; Schwalb, A. M.; Rambarat, P. K.; Ahn, S.; Lefkowitz, R. J.;

Kobilka, B., Mechanism of β_2AR regulation by an intracellular positive allosteric modulator. *Science* **2019**, *364*, 1283-1287.

(12) Berman, H. M., The protein data bank. *Nucleic Acids Res.* **2000**, *28*, 235-242.

(13) Loo, J. S. E.; Emtage, A. L.; Ng, K. W.; Yong, A. S. J.; Doughty, S. W., Assessing GPCR homology models constructed from templates of various transmembrane sequence identities: Binding mode prediction and docking enrichment. *J. Mol. Graphics Modell.* **2018**, *80*, 38-47.

(14) Hui, W.-Q.; Cheng, Q.; Liu, T.-Y.; Ouyang, Q., Homology modeling, docking, and molecular dynamics simulation of the receptor GALR2 and its interactions with galanin and a positive allosteric modulator. *J. Mol. Model.* **2016**, *22*, 90-105.

(15) Yang, Z.; Han, S.; Keller, M.; Kaiser, A.; Bender, B.J.; Bosse, M.; Burkert, K.; Kögler, L.M.; Wifling, D.; Bernhardt, G.; Plank, N.; Littmann, T.; Schmidt, P.; Yi, C.; Li, B.; Ye, S.; Zhang, R.; Xu, B.; Larhammar, D.; Stevens, R.C.; Huster, D.; Meiler, J.; Zhao, Q.; Beck-Sickinger, A. G.; Buschauer A. & Wu B., Structural basis of ligand binding modes at the neuropeptide Y Y_1 receptor. *Nature* **2018**, *556*, 520–524.

(16) Kuhn, K. K.; Littmann, T.; Dukorn, S.; Tanaka, M.; Keller, M.; Ozawa, T.; Bernhardt, G.; Buschauer, A., In search of NPY Y_4R antagonists: incorporation of carbamoylated arginine, aza-amino acids, or D-amino acids into oligopeptides derived from the C-termini of the endogenous agonists. *ACS Omega* **2017**, *2*, 3616-3631.

(17) Sherman, W.; Day, T.; Jacobson, M. P.; Friesner, R. A.; Farid, R., Novel procedure for modeling ligand/receptor induced fit effects. *J. Med. Chem.* **2006**, *49*, 534-553.

(18) Genheden, S.; Ryde, U., The MM/PBSA and MM/GBSA methods to estimate ligand-binding affinities. *Expert Opin. Drug Discovery* **2015**, *10*, 449-461.

(19) Friesner, R. A.; Banks, J. L.; Murphy, R. B.; Halgren, T. A.; Klicic, J. J.; Mainz, D. T.; Repasky, M. P.; Knoll, E. H.; Shelley, M.; Perry, J. K.; Shaw, D. E.; Francis, P.; Shenkin, P. S., Glide: a new approach for rapid, accurate docking and scoring. 1. method and assessment of docking accuracy. *J. Med. Chem.* **2004**, *47*, 1739-1749.

(20) Halgren, T. A.; Murphy, R. B.; Friesner, R. A.; Beard, H. S.; Frye, L. L.; Pollard, W. T.; Banks, J. L., Glide: a new approach for rapid, accurate docking and scoring. 2. enrichment factors in database screening. *J. Med. Chem.* **2004**, *47*, 1750-1759.

(21) Pedragosa-Badia, X.; Sliwoski, G. R.; Dong Nguyen, E.; Lindner, D.; Stichel, J.; Kaufmann, K. W.; Meiler, J.; Beck-Sickinger, A. G., Pancreatic polypeptide is recognized by two hydrophobic domains of the human Y_4 receptor binding pocket. *J. Biol. Chem.* **2014**, *289*, 5846-5859.

(22) Christopoulos, A., G protein-coupled receptor allosterism and complexing. *Pharmacol. Rev.* **2002**, *54*, 323-374.

(23) Dror, R. O.; Pan, A. C.; Arlow, D. H.; Borhani, D. W.; Maragakis, P.; Shan, Y.; Xu, H.; Shaw, D. E., Pathway and mechanism of drug binding to G-protein-coupled receptors. *Proc. Natl. Acad. Sci. U. S. A.* **2011**, *108*, 13118-13123.

(24) Bock, A.; Merten, N.; Schrage, R.; Dallanoce, C.; Bätz, J.; Klöckner, J.; Schmitz, J.; Matera, C.; Simon, K.; Kebig, A.; Peters, L.; Müller, A.; Schrobang-Ley, J.; Tränkle, C.; Hoffmann, C.; De Amici, M.; Holzgrabe, U.; Kostenis, E.; Mohr, K., The allosteric vestibule of a seven transmembrane helical receptor controls G-protein coupling. *Nat. Commun.* **2012**, *3*, 345-361.

(25) Pándy-Szekeres, G.; Munk, C.; Tsonkov, T. M.; Mordalski, S.; Harpsøe, K.; Hauser, A. S.; Bojarski, A. J.; Gloriam, D. E., GPCRdb in 2018: adding GPCR structure models and ligands. *Nucleic Acids Res.* **2018**, *46*, 440-446.

(26) Ballesteros, J. A.; Weinstein, H., Integrated methods for the construction of three-dimensional models and computational probing of structure-function relations in G protein-coupled receptors. *Methods Neurosci.* **1995**, *25*, 366-428.

(27) Ziemek, R.; Schneider, E.; Kraus, A.; Cabrele, C.; Beck-Sickinger, A. G.; Bernhardt, G.; Buschauer, A., Determination of affinity and activity of ligands at the human neuropeptide Y Y_4 receptor by flow cytometry and aequorin luminescence. *J. Recept. Signal Transduction* **2008**, *27*, 217-233.

(28) Kuhn, K. K.; Ertl, T.; Dukorn, S.; Keller, M.; Bernhardt, G.; Reiser, O.; Buschauer, A., High affinity agonists of the neuropeptide Y (NPY) Y_4 receptor derived from the C-terminal pentapeptide of human pancreatic polypeptide (hPP): synthesis, stereochemical discrimination, and radiolabeling. *J. Med. Chem.* **2016**, *59*, 6045-6058.

(29) Huang, W.; Manglik, A.; Venkatakrishnan, A. J.; Laeremans, T.; Feinberg, E. N.; Sanborn, A. L.; Kato, H. E.; Livingston, K. E.; Thorsen, T. S.; Kling, R. C.; Granier, S.; Gmeiner, P.; Husbands, S. M.; Traynor, J. R.; Weis, W. I.; Steyaert, J.; Dror, R. O.; Kobilka, B. K., Structural insights into μ-opioid receptor activation. *Nature* **2015**, *524*, 315-321.

(30) Dukorn, S.; Littmann, T.; Keller, M.; Kuhn, K.; Cabrele, C.; Baumeister, P.; Bernhardt, G.; Buschauer, A., Fluorescence- and radiolabeling of [Lys^4,$Nle^{17,30}$]hPP yields molecular tools for the NPY Y_4 receptor. *Bioconjugate Chem.* **2017**, *28*, 1291-1304.

Chapter 5

N-Terminus to Arginine Side Chain Cyclization of Linear Peptidic Neuropeptide Y Y_4 Receptor Ligands Results in Picomolar Binding Constants

Note: This chapter was submitted for publication in corporation with partners prior to submission of this thesis.

Konieczny, A., Konrad, M., Schmidt, M., Neu, E., Horn, A.H.C., Wifling, D., Gmeiner, P., Clark, T., Sticht, H., Keller, M. N-Terminus to Arginine Side Chain Cyclization of Linear Peptidic Neuropeptide Y Y_4 Receptor Ligands Results in Picomolar Binding Constants. *J. Med. Chem.*, **2020**, *submitted*.

The following experiments were performed by co-authors:

M.K., A.H.: MD simulations of **2.18** and **2.24**.
M.S., E.N.: Induced-fit docking of **2.18** and **2.24** to the hY_4R homology model.

5.1 Introduction

In humans, the neuropeptide Y (NPY) receptor family comprises four physiologically relevant class A-type G-protein coupled receptors (GPCRs), designated Y_1R, Y_2R, Y_4R and Y_5R, which couple preferentially to pertussis toxin sensitive $G_{i/o}$-type G-proteins.[1] The endogenous ligands of NPY receptors are the homologous linear peptides neuropeptide Y (NPY), peptide YY (PYY) and pancreatic polypeptide (PP), all consisting of 36 amino acids.[1] The amidated C-terminus of these peptides (-Arg-Tyr-NH_2) is crucial for receptor recognition.[2] Within the NPY family, PP is peculiar as it prefers the Y_4R over the other three subtypes.[3,4] Physiologically, the Y_4R is involved in the regulation of gastrointestinal motility, pancreatic secretion and food intake as well as central effects such as anxiolysis and depression,[5-9] thus, it represents a potential drug target. To date, numerous potent peptidic Y_4R ligands, representing mimics of the C-terminal sequences of NPY or PP, have been described.[10-13]

For example, the dimeric and cyclic peptide **5.1** (Figure 1), exhibiting antagonistic activity at the Y_1R,[11] was reported to act as a potent agonist at the Y_4R.[14] A selection of described small oligopeptidic (4-6 amino acids) Y_4R ligands (**5.2-5.7**) is also shown in Figure 1. Interestingly, pentapeptide **5.2**, representing a monomeric analogue of the high-affinity dimeric Y_4R partial agonist BVD-74D (structure not shown),[15] exhibits considerably lower Y_4R affinity and potency compared to the dimeric ligand.[10,15] However, the N-terminally argininylated congener of **5.2** (hexapeptide **5.3**, Figure 1), displaying approximately 100fold higher Y_4R affinity compared to **5.2** (Figure 1), demonstrates that high Y_4R affinity can be also achieved with monomeric oligopeptides.[10,12] Notably, also N-terminal truncation of pentapeptide **5.2** by one amino acid, yielding tetrapeptide **5.4**, resulted in an approximately 100fold increase in Y_4R binding compared to **5.2** (Figure 1).[13] Replacement of Arg^3 in hexapeptide **5.3** by an amino-functionalized N^{ω}-carbamoylated arginine[16] did not affect Y_4R binding (compound **5.5**, Figure 1).[10] However, C-terminus to side chain cyclization of **5.5** via the modified arginine residue resulted in marked decrease in Y_4R binding (cyclic peptide **5.6**),[10] confirming the importance of a flexible linear amidated C-terminus for peptidic Y_4R ligands mimicking the C-terminus of the endogenous NPY receptor ligands. Noteworthily, the incorporation of Trp^4 instead of Leu^4 in **5.3**, giving hexapeptide **5.7**, turned Y_4R agonism into antagonism.[13]

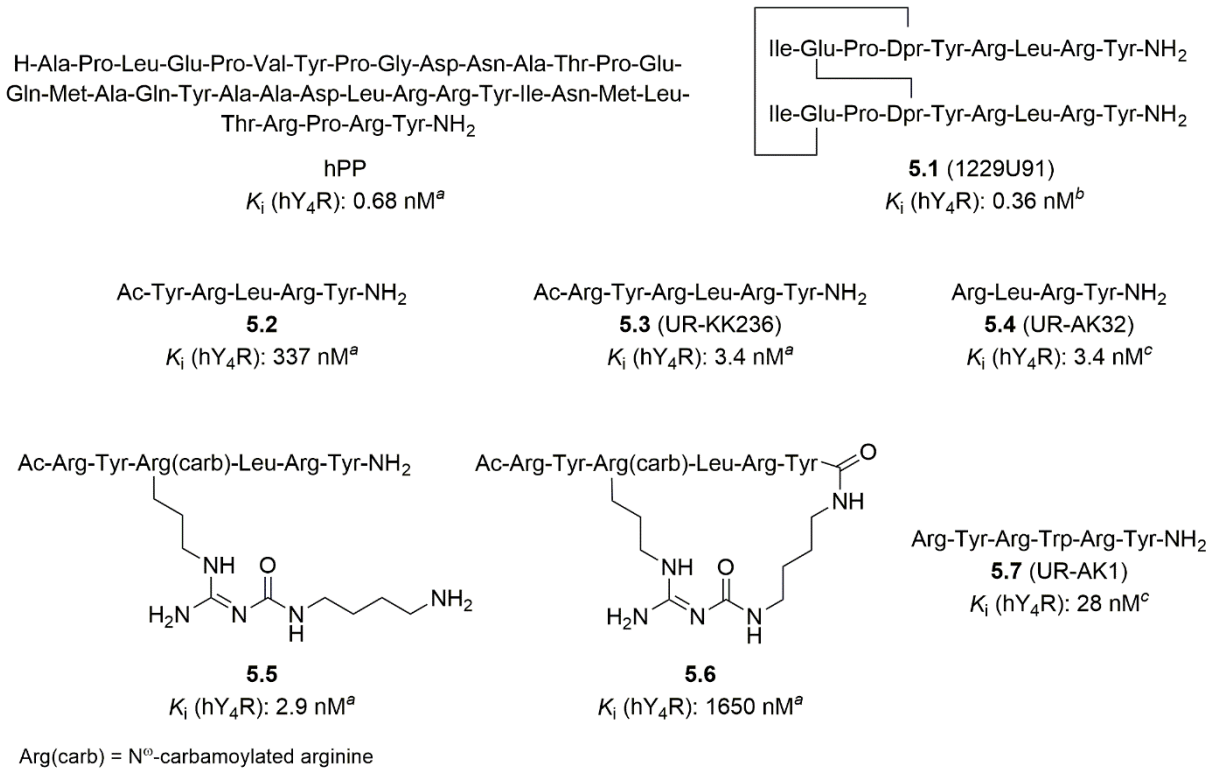

Figure 1. Structures and reported hY_4R affinities of hPP and peptides **5.1**-**5.7**. Whereas hPP and **5.1**-**5.6** represent Y_4R (partial) agonists, peptide **5.7** acts as a Y_4R antagonist. [a]Kuhn *et al.*[10] [b]Daniels *et al.*[11] [c]Konieczny *et al.*[13]

As cyclic peptides harbor the potential of exhibiting higher bioactivity and stability as well as more drug-like properties compared to their linear analogues,[17-19] we were aiming at cyclic peptidic Y_4R ligands derived from hexapeptide **5.3**. Unlike the approach pursued for the synthesis of cyclic peptide **5.6** (C-terminus to side chain cyclization), the series of cyclic peptides, presented in this work, was prepared by N-terminus to side chain cyclization. For this purpose, linear analogues of hexapeptide **5.3** were prepared, containing an amino-functionalized N^{ω}-carbamoylated arginine instead of Arg^3 or Arg^5 and a succinylated N-terminus. Subsequently, by cyclization via the succinyl residue and the amino-functionalized arginine side chain, cyclic derivatives were obtained featuring increased rigidity, but still exhibiting a flexible linear C-terminus (Figure 2). Additional modifications were performed by replacing, for example, Tyr^2 or Leu^4 in the sequence of **5.3**, by Trp, in order to test whether this modification will lead to Y_4R antagonists. According to our hypothesis, the weakly basic carbamoylated arginine ($pK_a \approx 8$),[20] embedded in the macrocycle, is crucial for high Y_4R affinity. Therefore, we also prepared cyclic analogues containing a non-basic N^{δ}-acylated ornithine instead of the N^{ω}-carbamoylated arginine. All linear and cyclic peptides were characterized in terms of Y_4R binding (radioligand competition binding assay) and in three different functional assays, namely a β-arrestin 1 and 2 recruitment assay as well as a Ca^{2+}-aequorin assay. Moreover, selected peptides were investigated with respect to stability in

buffer and human plasma, and the putative interactions of two cyclic peptides with the Y_4R were studied by molecular dynamics simulations.

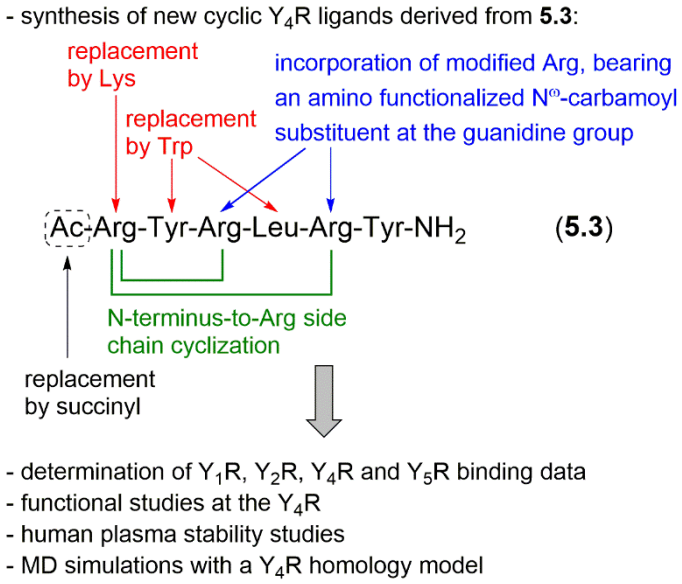

Figure 2. Rational of the present study.

5.2 Results and Discussion

5.2.1 Chemistry

The N^{ω}-carbamoylated arginine building blocks **5.8**[16] and **5.9**, containing a tetramethylene or a trimethylene spacer in the N^{ω}-carbamoyl substituent (Figure 3), were used for the replacement of Arg^3 or Arg^5 in hexapeptide **3**. The compatibility of **5.8** with solid-phase peptide synthesis (SPPS) was shown previously.[16,21] Compound **5.9** was synthesized based on the procedure reported for the preparation of **5.8**[16] (for detailed conditions see Scheme S1, Supporting Information).

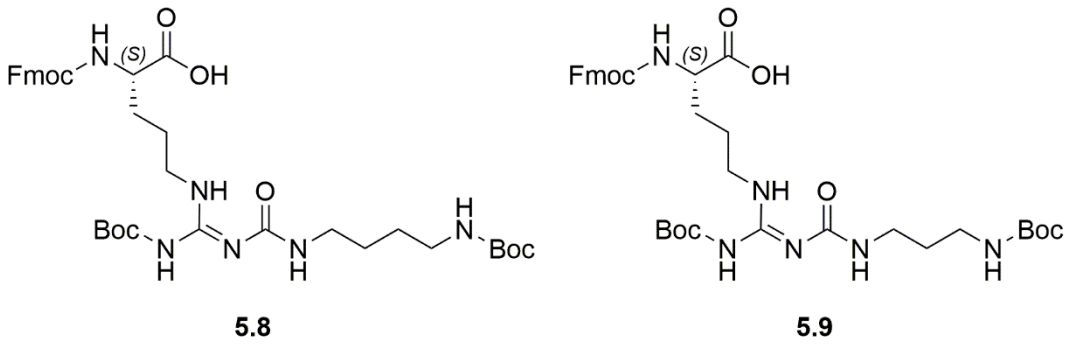

Figure 3. Structures of the N^{ω}-carbamoylated arginine building blocks **5.8**[16] and **5.9**.

The preparation of the "guanidine-free" ornithine derivative **5.13**, representing a congener of **5.8**, is outlined in Scheme 1. Compound **5.10**[22] was acylated at the delta amino group with Boc-Gly-OH using HOBt/HBTU/DIPEA as coupling reagents, followed by Boc-deprotection in the presence of TFA, to yield intermediate **5.11**. Amine **5.11** was acylated with *N*-Boc aminopentanoic acid under the conditions used for acylation of **5.10**, to obtain **5.12**. Cleavage of the benzyl ester moiety in **5.12** under hydogenolytic conditions afforded the Fmoc- and Boc-protected ornithine derivative **5.13**, which was used for SPPS.

Scheme 1. Synthesis of ornithine derivative **5.13**, containing, compared to arginine derivative **5.8**, two amide moieties and a methylene group instead of the carbamoylguanidine group in **5.8**.

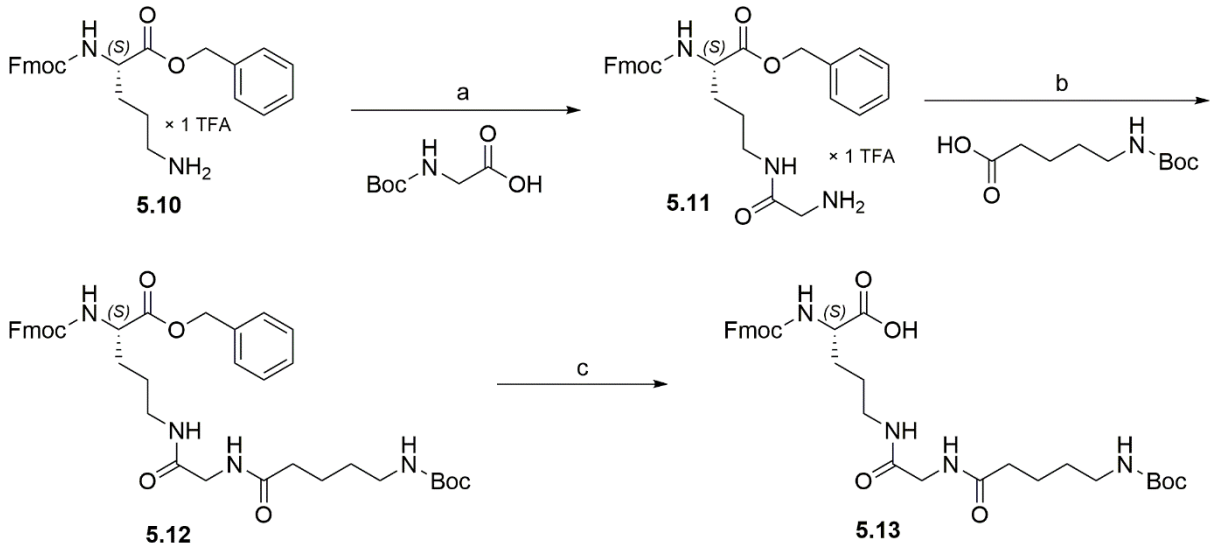

Reagents and conditions: (a) (1) HOBt, HBTU, DIPEA, DMF (anhydrous), rt, 24 h; (2) TFA/CH_2Cl_2 (1:4), rt, 2 h, 89%; (b) HOBt, HBTU, DIPEA, DMF (anhydrous), rt, 24 h, 73%; (c) 10% Pd/C, H_2, EtOH, rt, 20 min, 52%.

All linear peptides (precursor peptides of the cyclic peptides **5.14**-**5.16** and **5.35** as well as peptides **5.17**, **5.19**, **5.21**, **5.23**, **5.25**, **5.27**, **5.29**, **5.31** and **5.33**) were synthesized on a Sieber amide resin by Fmoc strategy SPPS. HBTU/HOBt/DIPEA were used as coupling reagents throughout. Whereas in the case of standard (natural) Fmoc amino acids the coupling procedure was repeated ("double" coupling), coupling of **5.8**, **5.9** and **5.13** was performed in one step (Scheme 2). The cyclic heptapeptides **5.14** and **5.15**, and the cyclic octapeptide **5.16**, included as reference compounds being devoid of an N^{ω}-carbamoylated arginine, were prepared in solution from the respective fully deprotected precursor peptides using PyBOP/HOBt/DIPEA as coupling reagents (Scheme 2). Peptides **5.14** and **5.15** were obtained by amide bond formation between the N-terminal Gly^1 and the Glu^4 (**5.14**) or Asp^4 (**5.15**) residue. Cyclic octapeptide **5.16** resulted from amide bond formation between the N-terminal Arg^1 and the Glu^4 residue.

The linear peptides **5.17**, **5.19**, **5.21**, **5.23**, **5.25**, **5.27**, **5.29**, **5.31** and **5.33**, representing precursors for the synthesis of the cyclic peptides **5.18**, **5.20**, **5.22**, **5.24**, **5.26**, **5.28**, **5.30**, **5.32** and **5.34**, were prepared as N-terminally succinylated peptides (Scheme 2, Figure 4) because cyclization to the amino-functionalized arginine side chains required a carboxy-functionalized N-terminus. N-terminal succinylation of the resin-bound, Fmoc-deprotected peptides was performed using a mixture of succinic anhydride/DIPEA 10:10 v/v, followed by cleavage from the resin with TFA/CH_2Cl_2 1:3 v/v, side chain deprotection by treatment with TFA/H_2O 95:5 v/v, and purification by preparative HPLC to give **5.17**, **5.19**, **5.21**, **5.23**, **5.25**, **5.27**, **5.29**, **5.31** and **5.33** (Scheme 2, Figure 4).

Scheme 2. Synthesis of cyclic peptides **5.14**-**5.16** and linear peptides **5.17**, **5.19**, **5.21**, **5.23**, **5.25**, **5.27**, **5.29**, **5.31** and **5.33**.

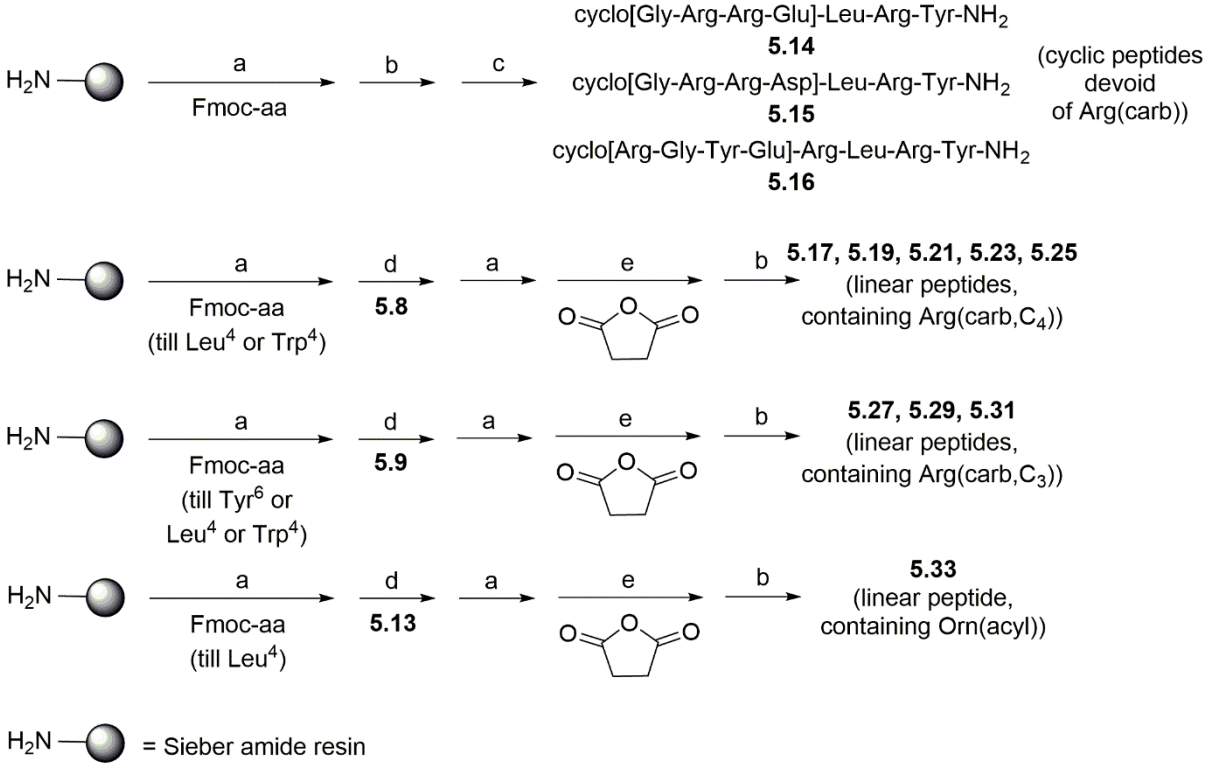

Reagents and conditions: (a) peptide elongation, amino acid coupling: Fmoc-amino acid/HOBt/HBTU/DIPEA (5/5/4.9/10 equiv.), DMF/NMP (8:2), 35 °C, 2 × 45 min ("double" coupling); Fmoc deprotection: 20% piperidine in DMF/NMP (8:2), rt, 2 × 10 min; (b) (1) TFA/CH_2Cl_2 (1:3), rt, 2 × 20 min; (2) TFA/H_2O (95:5), rt, 5 h; (c) HOBt/PyBOP/DIPEA (5/5/10 equiv.), DMF/NMP (8:2), rt, 24 h; (d) building blocks **5.8**, **5.9** or **5.13**/HOBt/HBTU/DIPEA (3/3/2.95/6 equiv.), DMF/NMP (8:2), 35 °C, 24 h ("single" coupling); (e) succinic anhydride/DIPEA (10/10 equiv.), DMF/NMP (8:2), 35 °C, 30 min; overall yields of SPPS: 18-33%.

5.3	Ac-Arg-Tyr-Arg-Leu-Arg-Tyr-NH_2
5.14	cyclo[Gly-Arg-Arg-Glu]-Leu-Arg-Tyr-NH_2
5.15	cyclo[Gly-Arg-Arg-Asp]-Leu-Arg-Tyr-NH_2
5.16	cyclo[Arg-Gly-Tyr-Glu]-Arg-Leu-Arg-Tyr-NH_2
5.17	succinyl-Arg-Tyr-Arg(carb,C_4)-Leu-Arg-Tyr-NH_2
5.18	cyclo[succinyl-Arg-Tyr-Arg(carb,C_4)]-Leu-Arg-Tyr-NH_2
5.19	succinyl-Arg-Arg(carb,C_4)-Leu-Arg-Tyr-NH_2
5.20	cyclo[succinyl-Arg-Arg(carb,C_4)]-Leu-Arg-Tyr-NH_2
5.21	succinyl-Lys-Tyr-Arg(carb,C_4)-Leu-Arg-Tyr-NH_2
5.22	cyclo[succinyl-Lys-Tyr-Arg(carb,C_4)]-Leu-Arg-Tyr-NH_2
5.23	succinyl-Arg-Trp-Arg(carb,C_4)-Leu-Arg-Tyr-NH_2
5.24	cyclo[succinyl-Arg-Trp-Arg(carb,C_4)]-Leu-Arg-Tyr-NH_2
5.25	succinyl-Arg-Tyr-Arg(carb,C_4)-Trp-Arg-Tyr-NH_2
5.26	cyclo[succinyl-Arg-Tyr-Arg(carb,C_4)]-Trp-Arg-Tyr-NH_2
5.27	succinyl-Arg-Tyr-Arg(carb,C_3)-Leu-Arg-Tyr-NH_2
5.28	cyclo[succinyl-Arg-Tyr-Arg(carb,C_3)]-Leu-Arg-Tyr-NH_2
5.29	succinyl-Arg-Tyr-Arg(carb,C_3)-Trp-Arg-Tyr-NH_2
5.30	cyclo[succinyl-Arg-Tyr-Arg(carb,C_3)]-Trp-Arg-Tyr-NH_2
5.31	succinyl-Arg-Tyr-Arg-Leu-Arg(carb,C_3)-Tyr-NH_2
5.32	cyclo[succinyl-Arg-Tyr-Arg-Leu-Arg(carb,C_3)]-Tyr-NH_2
5.33	succinyl-Arg-Tyr-Orn(acyl)-Leu-Arg-Tyr-NH_2
5.34	cyclo[succinyl-Arg-Tyr-Orn(acyl)]-Leu-Arg-Tyr-NH_2
5.35	cyclo[succinyl-Arg-Tyr-Arg(carb,C_4)]-Leu-NH_2

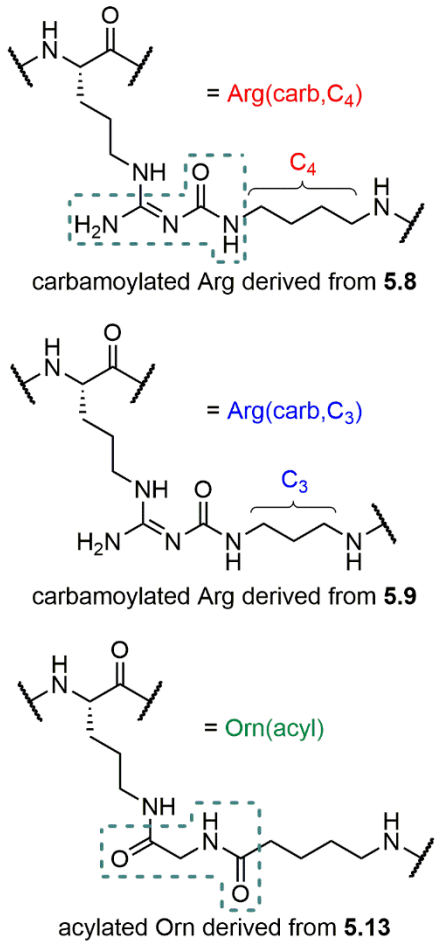

Figure 4. Peptide sequences of parent hexapeptide **5.3** and the synthesized linear or cyclic analogs **5.14**-**5.35**. Replacement of amino acids in **5.3** by natural amino acids and insertions of amino acids into the sequence of **5.3** are marked in grey. Replacement of Arg^3 or Arg^5 in **5.3** by an N^{ω}-carbamoylated arginine (derived from **5.8** or **5.9**) or by the modified ornithine derived from **5.13** are highlighted in green, red and blue, respectively.

The cyclic peptides **5.18**, **5.20**, **5.22**, **5.24**, **5.26**, **5.28**, **5.30** and **5.32** were obtained from the respective linear precursor peptides by amide bond formation between the N-terminal succinyl group and the primary amine group of the N^{ω}-carbamoylated arginine residues derived from **5.8** or **5.9** using HOBt/PyBOP/DIPEA as coupling reagents (Scheme 3). The concentrations of the linear precursor peptides in the reaction mixtures, which were shaken at rt for 24 h, were in the range of 4-12 µM. Purification of the target peptides was performed with preparative HPLC. Using the same procedure, cyclic peptide **5.34** was prepared from **5.33** by cyclization via the N-terminal succinyl group and the primary amine group of the N^{δ}-acylated ornithine residue derived from **5.13**. The cyclic tetrapeptide **5.35**, representing a C-terminally

truncated analogue of **5.18**, was prepared using the procedure for the synthesis of **5.18**, but the C-terminal amino acids Arg[5] and Tyr[6] were omitted (Scheme 3).

Scheme 3. Synthesis of the cyclic peptides **5.18**, **5.20**, **5.22**, **5.24**, **5.26**, **5.28**, **5.30**, **5.32**, **5.34** and **5.35**.

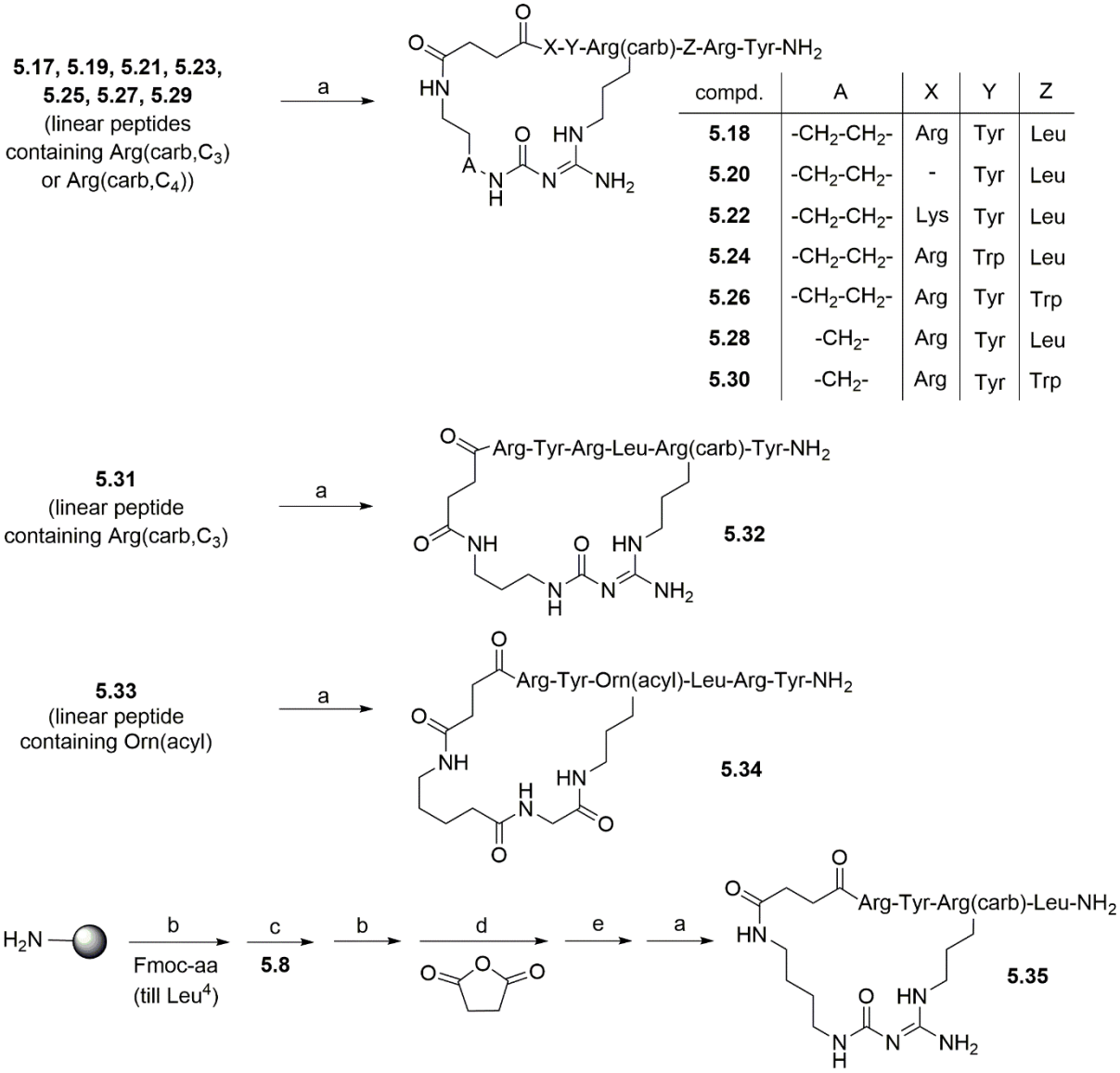

compd.	A	X	Y	Z
5.18	-CH_2-CH_2-	Arg	Tyr	Leu
5.20	-CH_2-CH_2-	-	Tyr	Leu
5.22	-CH_2-CH_2-	Lys	Tyr	Leu
5.24	-CH_2-CH_2-	Arg	Trp	Leu
5.26	-CH_2-CH_2-	Arg	Tyr	Trp
5.28	-CH_2-	Arg	Tyr	Leu
5.30	-CH_2-	Arg	Tyr	Trp

Reagents and conditions: (a) HOBt/PyBOP/DIPEA (5/5/10 equiv.), DMF/NMP (8:2), rt, 24 h; (b) peptide elongation, amino acid coupling: Fmoc-amino acid/HOBt/HBTU/DIPEA (5/5/4.9/10 equiv.), DMF/NMP (8:2), 35 °C, 2 × 45 min ("double" coupling); Fmoc deprotection: 20% piperidine in DMF/NMP (8:2), rt, 2 × 10 min; (c) building block **5.8**/HOBt/HBTU/DIPEA (3/3/2.95/6 equiv.), DMF/NMP (8:2), 35 °C, 24 h ("single" coupling); (d) succinic anhydride/DIPEA (10/10 equiv.), DMF/NMP (8:2), 35 °C, 30 min; (e) (1) TFA/CH_2Cl_2 (1:3), rt, 2 × 20 min; (2) TFA/H_2O (95:5), rt, 5 h; overall yields of cyclic peptides: 60% (**5.18**), 50% (**5.20**), 71% (**5.22**), 53% (**5.24**), 45% (**5.26**), 52% (**5.28**), 60% (**5.30**), 55% (**5.32**), 75% (**5.34**), 54% (**5.35**).

5.2.2 NPY Y_4 Receptor Binding

Y_4 receptor affinities (summarized in Table 1) were determined in competition binding experiments at live CHO-hY_4R-G_{qi5}-mtAEQ cells[23] using the previously described radioligand [^{3}H]**5.36**[21] (K_d (hY_4R): 0.68 nM) (for structure see Figure S1, Supporting Information). Radioligand displacement curves are shown in Figure 5 and Figure S2 (Supporting Information). The cyclic heptapeptides **5.14** and **5.15**, containing, compared to the linear hexapeptide **5.3**, Arg instead Tyr^2, Glu (**5.14**) or Asp (**5.15**) instead of Arg^3 and being N-terminally extended by one glycine (*cf.* Figure 4), showed approximately 40-50fold lower Y_4R binding compared to **5.3**. This indicated that replacement of Tyr^2 (previously shown to play a minor role for Y_4R binding[13]) in **5.3** by Arg, as well as replacement of Arg^3 by an acidic amino acid and cyclization via the latter to the N-terminus is unfavorable for Y_4R binding (Table 1). By contrast, the cyclic octapeptide **5.16**, containing, compared to **5.3**, an inserted Glu in between Tyr^2 and Arg^3 as well as an inserted Gly in between Arg^1 and Tyr^2, and being cyclized via the N-terminus and the Glu side chain (see Figure 4), exhibited Y_4R affinity comparable to that of parent peptide **5.3** (Table 1).

When looking at the Y_4R affinities of the linear peptides **5.17**, **5.19**, **5.21**, **5.23**, **5.25**, **5.27**, **5.29**, **5.31** and **5.33**, peptides **5.17**, **5.19**, **5.21** and **5.23** showed almost unchanged Y_4R binding compared to **5.3** (< 3fold decrease or increase), i.e. the structural modifications compared to **5.3**, present in **5.17**, **5.19**, **5.21** and **5.23** (*cf.* Figure 4), did not affect Y_4R binding. The linear precursor peptide **5.27**, containing Arg(carb,C_3) instead of Arg^3 in **5.3** and an N-terminal succinyl residue, displayed slightly increased, i.e. approximately 5fold higher Y_4R affinity than **5.3**. In contrast to **5.27**, the linear hexapeptides **5.25**, **5.29**, **5.31** and **5.33** showed circa 10fold lower Y_4R affinity compared to **5.3**. When comparing the structures of these compounds with the sequences of the other linear peptides, the reasons for the decrease in Y_4R binding are obvious: in peptides **5.25** and **5.29** it can be attributed to the presence of Trp^4 instead of Leu^4, in peptide **5.31** it is caused by the presence of an N^{ω}-carbamoylated arginine (Arg(carb,C_3)) in position 5, and in the case of **5.33** it is mediated by the N^{δ}-acylated ornithine (derived from **5.13**) incorporated instead of Arg^3.

Table 1. Y_4R binding data of hPP, **5.3** and peptides **5.14**-**5.35**, as well as Y_1, Y_2 and Y_5 receptor binding data of selected compounds.

cmpd.	Y receptor binding				selectivity toward Y_4R (ratio K_i ($Y_{1,2,5}$R) / K_i (Y_4R))		
	pK_i ± SEM / K_i [nM] hY_4R[a]	pK_i / K_i [nM] hY_1R[b]	pK_i / K_i [nM] hY_2R[c]	pK_i / K_i [nM] hY_5R[d]	Y_1R	Y_2R	Y_5R
hPP	9.16 ± 0.03 / 0.69	6.35[e] / 440	< 5.5[e] / > 3000	7.75[e] / 17	> 630	> 4300	> 20
5.3	8.47 ± 0.04 [f] / 3.4	< 5.5[f] / > 3000	< 5.5[f] / > 3000	< 5.5[f] / > 3000	> 830	> 830	> 830
5.14	6.93 ± 0.09 / 150	n.d.	n.d.	n.d.	-	-	-
5.15	6.86 ± 0.09 / 170	n.d.	n.d.	n.d.	-	-	-

- **Table 1** continued -

5.16	8.28 ± 0.03 / 5.3	n.d.	n.d.	n.d.	-	-	-
5.17	8.90 ± 0.09 / 1.3	< 5.0 / > 10000	< 5.0 / > 10000	< 5.0 / > 10000	> 7600	> 7600	> 7600
5.18	10.36 ± 0.11 / 0.048	< 5.5 / > 3000	< 5.0 / > 10000	< 6.0 / > 3000	> 60000	> 200000	> 60000
5.19	7.99 ± 0.06 / 10	< 5.0 / > 10000	n.d.	n.d.	> 1000	-	-
5.20	8.60 ± 0.09 / 2.6	< 5.0 / > 10000	n.d.	n.d.	> 3800	-	-
5.21	8.16 ± 0.07 / 7.1	n.d.	n.d.	n.d.	-	-	-
5.22	9.63 ± 0.02 / 0.24	< 5.5 / > 3000	< 5.0 / > 10000	< 5.5 / > 3000	> 12000	> 40000	> 12000
5.23	8.71 ± 0.13 / 2.1	< 5.0 / > 10000	< 5.5 / > 3000	< 5.0 / > 10000	> 4700	> 1400	> 4700
5.24	10.48 ± 0.04 / 0.033	< 5.0 / > 10000	< 5.0 / > 10000	< 6.0 / > 3000	> 300000	> 300000	> 90000
5.25	7.36 ± 0.15 / 50	< 5.5 / > 3000	< 5.5 / > 3000	< 5.0 / > 10000	> 60	> 60	> 200
5.26	8.80 ± 0.06 / 1.6	< 5.5 / > 3000	< 5.0 / > 10000	< 5.0 / > 10000	> 1800	> 6200	> 6200
5.27	9.19 ± 0.07 / 0.66	< 5.0 / > 10000	< 5.0 / > 10000	< 5.0 / > 10000	> 15000	> 15000	> 15000
5.28	9.93 ± 0.14 / 0.13	< 5.0 / > 10000	< 5.5 / > 3000	< 6.0 / > 3000	> 76000	> 23000	> 23000
5.29	7.25 ± 0.08 / 63	< 5.0 / > 10000	< 5.5 / > 3000	< 5.5 / > 3000	> 150	> 47	> 47
5.30	7.54 ± 0.03 / 28	< 5.0 / > 10000	< 5.0 / > 10000	< 5.0 / > 10000	> 350	> 350	> 350
5.31	7.30 ± 0.09 / 53	n.d.	n.d.	n.d.	-	-	-
5.32	6.87 ± 0.09 / 140	n.d.	n.d.	n.d.	-	-	-
5.33	7.02 ± 0.04 / 97	n.d.	n.d.	n.d.	-	-	-
5.34	8.18 ± 0.07 / 6.7	n.d.	n.d.	n.d.	-	-	-
5.35	5.72 ± 0.11 / 2040	n.d.	n.d.	n.d.	-	-	-

[a]Determined by competition binding at CHO-hY_4R-mtAEQ-G_{qi5} cells using [^{3}H]**5.36** (K_d = 0.67 nM, c = 1 nM) as radioligand.[21] [b]Determined by competition binding at SK-N-MC neuroblastoma cells using [^{3}H]**5.37** (K_d = 0.044 nM, c = 0.15 nM) as radioligand.[24] [c]Determined by competition binding with [^{3}H]propionyl-pNPY (K_d = 0.14 nM, c = 0.5 nM) at CHO-hY_2R cells.[13] [d]Determined by competition binding at HEC-1B-hY_5R cells using [^{3}H]propionyl-pNPY (K_d = 4.8 nM, c = 4 nM) as radioligand[25] (for structures of all used radioligands see Figure S1, Supporting Information). [e]Berlicki *et al*;[12] reported K_i values were converted to pK_i values [f]pK_i values reported by Kuhn *et al*.[10]
Data represent mean values from three independent experiments performed in triplicate (SEM given for Y_4R pK_i values).
n.d.: not determined

Except for **5.30** and **5.32**, all cyclic peptides (**5.18**, **5.20**, **5.22**, **5.24**, **5.26**, **5.28** and **5.34**) showed higher Y_4R affinity compared to the respective linear precursor peptides. The increase in Y_4R binding, presumably caused by an entropically more favorable binding process, was most pronounced (ca. 60fold) for the cyclization of **5.23**, resulting in **5.24**. With pK_i values of 10.36 and 10.48, respectively, the cyclic hexapeptides **5.18** and **5.24** exhibited the highest Y_4R affinities among the studied compounds (Table 1). The cyclic peptide **5.30**, containing Trp in position 4, displayed Y_4R affinity comparable to that of its linear precursor **5.29** (pK_i values: 7.54 and 7.25, respectively). In the case of the compound pair **5.31**/**5.32**, cyclization of **5.31**, affording **5.32**, resulted in a slight decrease in Y_4R affinity (pK_i: 7.30 vs. 6.87), showing that cyclization via an N^{ω}-carbamoylated arginine in position 5, going along with a reduction of the flexibility of the C-terminal tripeptide sequence, is unfavorable for Y_4R binding.

For an evaluation of the importance of the weakly basic carbamoylguanidine group in the macrocycle of high-affinity cyclic peptides such **5.18** for Y_4R binding, peptide **5.34** was synthesized as a congener of **5.18**. While peptide **5.34** contains two non-basic amide moieties and a methylene group instead of the carbamoylguanidine moiety in **5.18**, keeping the size of the macrocycle unvaried (*cf*. Scheme 3 and Figure 4), no other modifications are present in **5.34** compared to **5.18**. Compound **5.34** exhibited >100fold lower Y_4R affinity than **5.18** (pK_i: 8.18 vs. 10.36), demonstrating the need of a basic group, supposed to interact with an acidic residue of the Y_4R, in the macrocycle of **5.18**. Y_4R binding of the cyclic tetrapeptide **5.35**, representing a C-terminally truncated congener of cyclic hexapeptide **5.18**, was lower, compared to **5.18**, by four orders of magnitude (pK_i: 5.72 vs. 10.36), confirming the utmost importance of the linear C-terminus of the presented class of peptidic Y_4R ligands.

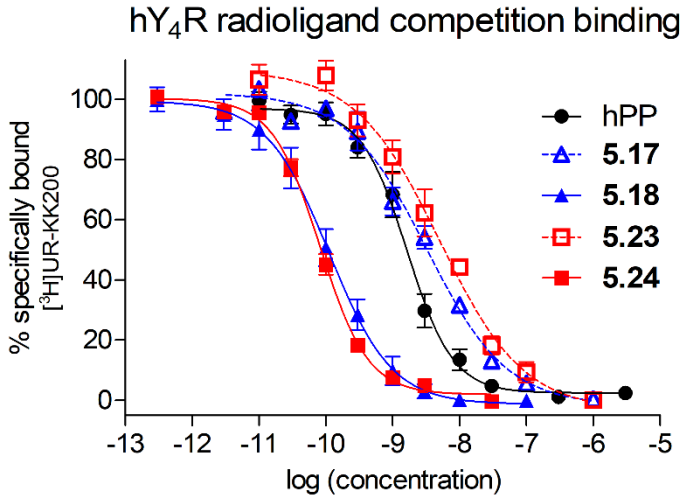

Figure 5. Radioligand displacement curves of hPP and peptides **5.17**, **5.18**, **5.23** and **5.24**, obtained from competition binding experiments with [^{3}H]**5.36** (K_d = 0.67 nM, c = 1 nM) performed with CHO-hY_4R-mtAEQ-G_{qi5} cells. Dashed lines (blue, red) indicate linear peptides (**5.17**, **5.23**), solid lines (blue, red) represent cyclic peptides (**5.18**, **5.24**). Data represent means ± SEM from at least three independent experiments, each performed in triplicate.

5.2.3 NPY Receptor Subtype Selectivity

For peptides **5.17**, **5.18** and **5.22-5.30**, Y_4R selectivity was assessed by determination of Y_1, Y_2 and Y_5 receptor binding data in previously used radioligand competition binding assays[13,16,21] (Table 1). Due to very low affinities of the investigated compounds at the Y_1, Y_2 and Y_5 receptor, pK_i values could not be determined. Peptides **5.17**, **5.18**, **5.22-5.24**, **5.26-5.28** and **5.30** exhibited at least more than 300fold higher Y_4R affinity compared to the NPY receptor subtypes Y_1, Y_2 and Y_5. In the case of the linear peptides **5.25** and **5.29**, Y_4R selectivity was less pronounced. Notably, as peptide cyclization caused no marked increase in Y_1, Y_2 and Y_5 receptor affinity, the cyclic peptides **5.18** and **5.24**, exhibiting very high Y_4R

affinity (pK_i > 10), showed excellent Y_4R selectivities (> 50,000fold over the Y_1, Y_2 and Y_5 receptor).

5.2.4 Functional Studies at the Human Y_4 Receptor

Except of peptide **5.35**, all peptides (**5.14**-**5.34**) were investigated in previously described β-arrestin 1 and 2 recruitment assays[10] with respect to Y_4R agonism. Except for the linear hexapeptides **5.25** and **5.29**, both containing a Trp in position 4, these compounds were capable of stimulating β-arrestin 1 and 2 recruitment to the Y_4 receptor (Figure 6A and 6B, Figure S3A and S3B, Supporting Information). In the case of compounds **5.14**, **5.15** and **5.31**-**5.33**, complete concentration-response curves could not be obtained (data not shown) due to low potencies (pEC_{50} < 4.5). In the β-arrestin 1 assay, only the cyclic peptide **5.24**, containing a Trp in position 2, proved to be a full agonist (Figure 6A, Table 2). Peptides **5.16**-**5.23**, **5.26**-**5.28**, **5.30** and **5.34** acted as partial agonists with intrinsic activities α of 0.35-0.90. In the β-arrestin 2 assay, none of the studied compounds showed full agonism (Figure 6B). The intrinsic activities of **5.16**-**5.24**, **5.26**-**5.28**, **5.30** and **5.34** were in the range of 0.47-0.83 (Table 2). Compounds **5.25** and **5.29**, which elicited no response in the agonist mode, were studied in antagonist mode using a fixed concentration (10 nM) of the agonist hPP approximately corresponding to the pEC_{80} of hPP. Like the recently reported peptidic Y_4R antagonist **5.7** (Figure 1), **5.25** and **5.29** were capable of completely inhibiting hPP mediated arrestin recruitment (Figure 7A and 7B). The corresponding pK_b values of **5.25** and **5.29** were in excellent agreement with their pK_i values obtained from radioligand competition binding studies (cf. Tables 1 and 2). Interestingly, the cyclic peptides derived from the linear precursor peptides **5.25** and **5.29**, i.e. **5.26** and **5.30**, proved to be partial Y_4R agonists in the β-arrestin 1 and 2 recruitment assays (Figure 7A and 7B), showing that N-terminus to side chain cyclization of peptidic Y_4R antagonists, such as **5.25** and **5.29**, leads to an inversion of the mode of action.

Table 2. Agonistic (pEC_{50}, EC_{50}) or antagonistic (pK_b) Y_4R activities of hPP, **5.3** and **5.14**-**5.35**.

cmpd.	β-Arrestin 1[a]		β-Arrestin 2[a]		Ca^{2+}-Aequorin[b]	
	pEC_{50} ± SEM / EC_{50} [nM] or *pK_b ± SEM*	α ± SEM	pEC_{50} ± SEM / EC_{50} [nM] or *pK_b ± SEM*	α ± SEM	pEC_{50} ± SEM / EC_{50} [nM] or *pK_b ± SEM*	α ± SEM
hPP	8.66[c] / 2.4	1	8.37[c] / 4.1	1	7.96[c] / 10.6	1
5.3	6.79[c] / 170	0.55	6.95[c] / 120	0.61	6.74[c] / 190	0.75
5.14	< 4.5	n.a.	< 4.5	n.a.	< 4.5	n.a.
5.15	< 4.5	n.a.	< 4.5	n.a.	< 4.5	n.a.
5.16	6.54 ± 0.07 / 290	0.64 ± 0.07	6.75 ± 0.05 / 180	0.74 ± 0.05	6.17 ± 0.07 / 670	0.48 ± 0.02
5.17	6.80 ± 0.05 / 160	0.75 ± 0.08	6.85 ± 0.09 / 140	0.83 ± 0.07	6.69 ± 0.02 / 210	0.70 ± 0.03

- **Table 2** continued -

5.18	8.44 ± 0.03 / 3.6	0.68 ± 0.05	8.80 ± 0.04 / 1.7	0.73 ± 0.03	8.57 ± 0.03 / 2.7	0.82 ± 0.02
5.19	6.00 ± 0.02 / 990	0.71 ± 0.08	6.12 ± 0.02 / 760	0.60 ± 0.07	n.d.	n.d.
5.20	6.74 ± 0.04 / 180	0.87 ± 0.03	7.03 ± 0.07 / 94	0.83 ± 0.05	6.44 ± 0.04 / 350	0.61 ± 0.05
5.21	6.57 ± 0.04 / 270	0.57 ± 0.03	6.53 ± 0.03 / 300	0.61 ± 0.03	n.d.	n.d.
5.22	7.85 ± 0.06 / 14	0.61 ± 0.06	7.89 ± 0.04 / 13	0.67 ± 0.04	7.59 ± 0.05 / 25	0.75 ± 0.03
5.23	6.94 ± 0.08 / 120	0.67 ± 0.03	6.79 ± 0.09 / 160	0.76 ± 0.03	6.98 ± 0.05 / 110	0.67 ± 0.02
5.24	9.00 ± 0.03 / 1.0	0.98 ± 0.05	8.78 ± 0.03 / 2.1	0.80 ± 0.07	9.00 ± 0.07 / 0.99	0.84 ± 0.02
5.25	*7.07 ± 0.07*	-	*6.84 ± 0.01*	-	*7.12 ± 0.03*	-
5.26	6.90 ± 0.09 / 130	0.84 ± 0.08	7.02 ± 0.03 / 96	0.83 ± 0.06	6.72 ± 0.09 / 200	0.61 ± 0.04
5.27	7.31 ± 0.05 / 50	0.61 ± 0.01	6.89 ± 0.04 / 130	0.71 ± 0.06	6.75 ± 0.09 / 180	0.65 ± 0.01
5.28	8.45 ± 0.06 / 3.5	0.90 ± 0.09	8.27 ± 0.05 / 5.4	0.87 ± 0.03	7.82 ± 0.05 / 15	0.83 ± 0.02
5.29	*6.91 ± 0.04*	-	*7.05 ± 0.02*	-	*7.04 ± 0.08*	-
5.30	6.28 ± 0.04 / 520	0.35 ± 0.04	6.45 ± 0.03 / 360	0.47 ± 0.03	6.42 ± 0.06 / 380	0.45 ± 0.16
5.31	< 4.5	n.a.	< 4.5	n.a.	< 4.5	n.a.
5.32	< 4.5	n.a.	< 4.5	n.a.	< 4.5	n.a.
5.33	< 4.5	n.a.	< 4.5	n.a.	< 4.5	n.a
5.34	6.29 ± 0.08 / 510	0.56 ± 0.07	6.41 ± 0.04 / 390	0.57 ± 0.01	6.11 ± 0.02 / 780	0.59 ± 0.07

[a]Agonistic potencies (pEC_{50}/EC_{50}) and intrinsic activities α (relative to the maximum effect elicited by 1 μM hPP, α = 1) determined in a β-arrestin 1 and a β-arrestin 2 recruitment assay at HEK293T-ARRB1-Y_4R cells and HEK293T-ARRB2-Y_4R cells, respectively. When performed in antagonist mode, pK_b values (in italics) were obtained by inhibition of the effect elicited by 10 nM hPP. [b]Agonistic potencies (pEC_{50}, EC_{50}) and intrinsic activities α (relative to the maximum effect elicited by 1 μM hPP, α = 1) determined in a Ca^{2+}-aequorin assay using CHO-hY_4R-mtAEQ-G_{qi5} cells. When performed in antagonist mode, pK_b values (in italics) were obtained by inhibition of the effect elicited by 100 nM hPP. [c]pEC_{50}, EC_{50} and α values reported by Konieczny *et al.*[13]
Data represent mean values from three or four independent experiments (SEM given for pEC_{50}, α and pK_b values).
n.a.: not applicable
n.d.: not determined

In addition to the functional characterization in the arrestin recruitment assays, peptides **5.14**-**5.18**, **5.20** and **5.22**-**5.34** were investigated in a previously reported Ca^{2+}-aequorin assay[23] (CHO-hY_4-G_{qi5}-mtAEQ cells) measuring the increase in intracellular Ca^{2+} via Y_4R mediated activation of a chimeric G protein. The results were comparable with those obtained from the arrestin assays: compounds **5.25** and **5.29** elicited no response, peptides **5.14**, **5.15** and **5.31**-**5.33** induced an increase in intracellular Ca^{2+}, but their potencies were too low (pEC_{50} < 4.5) to generate full concentration-response curves, and compounds **5.16**-**5.24**, **5.26**-**5.28**, **5.30** and **5.34** acted as partial agonist exhibiting intrinsic activities α between 0.45 and 0.84 (Table 2, Figure 6C, Figures S3C and S4C, Supporting Information). Notably, the cyclic oligopeptides **5.18** and **5.24** showed higher Y_4R potencies compared to the endogenous Y_4R agonist hPP (Table 2).

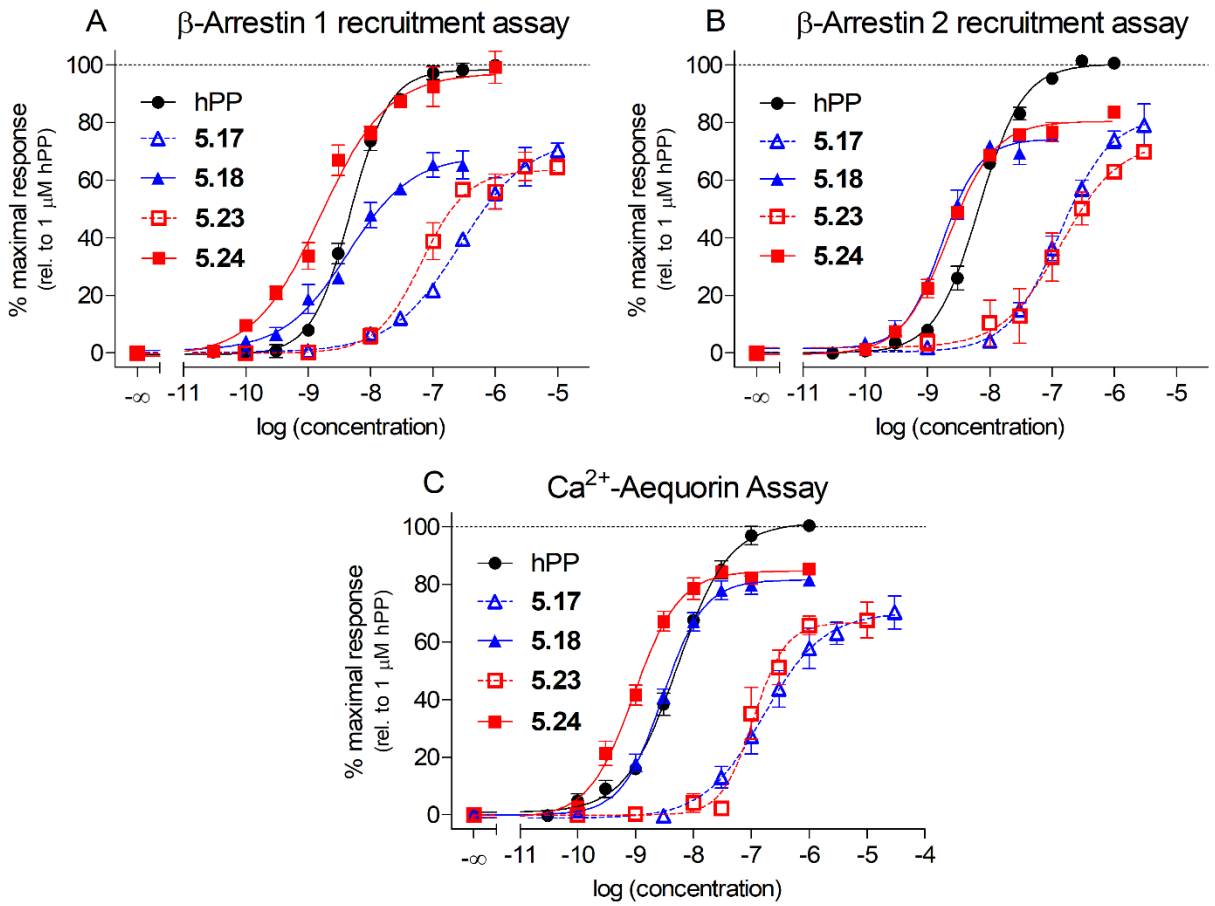

Figure 6. Concentration-response curves of hPP and peptides **5.17**, **5.18**, **5.23** and **5.24**, obtained from a hY_4R β-arrestin 1 recruitment (A), a hY_4R β-arrestin 2 recruitment (B) and a hY_4R Ca^{2+}-aequorin (C) assay performed with live HEK293T-ARRB1-Y_4R cells, HEK293T-ARRB2-Y_4R cells and CHO-hY_4-G_{qi5}-mtAEQ cells, respectively, in agonist mode. Dashed lines (blue, red) indicate linear peptides (**5.17**, **5.23**) and solid lines (blue, red) represent cyclic peptides (**5.18**, **5.24**). Data represent means ± SEM from at least three independent experiments, each performed in triplicate.

As in the case of the arrestin assays, the investigation of the antagonists **5.25** and **5.29** in antagonist mode revealed a complete inhibition of the signal elicited by hPP (Figure 7C) and the pK_b values of **5.25** and **5.29** were in good accordance with the respective pK_i values (Tables 1 and 2). Moreover, similarly to the arrestin assays, the cyclic counterparts of **5.25** and **5.29**, i.e. **5.26** and **5.30**, proved to be partial agonists in the Ca^{2+} aequorin assay (Figure 7C).

Unlike the pK_b and pK_i values of the antagonists **5.25** and **5.29**, being in good agreement, the potencies (pEC_{50}) of the agonists were consistently lower compared to the respective pK_i values (Tables 1 and 2). As discussed previously, this can be mainly attributed to the presence (functional studies) and absence (binding studies) of sodium ions in the used buffers.[13,21,26] As sodium acts as an allosteric modulator in many GPCRs, stabilizing the inactive state of the receptor,[27,28] the affinity of agonists, preferring the active receptor conformation, is potentially higher when determined in sodium-free buffers. By contrast, the receptor affinity of silent antagonists is not or only slightly affected by the absence of sodium ions, as demonstrated for

the Y_4R antagonists **5.25** and **5.29**. It should be noted that binding studies at NPY receptors, typically involving radiolabeled peptidic agonists, are usually performed in sodium-free buffers because by the omittance of sodium the consumption of radioligand and the extent of unspecific binding can be considerably reduced due to higher receptor affinities of the used radiolabeled peptides.

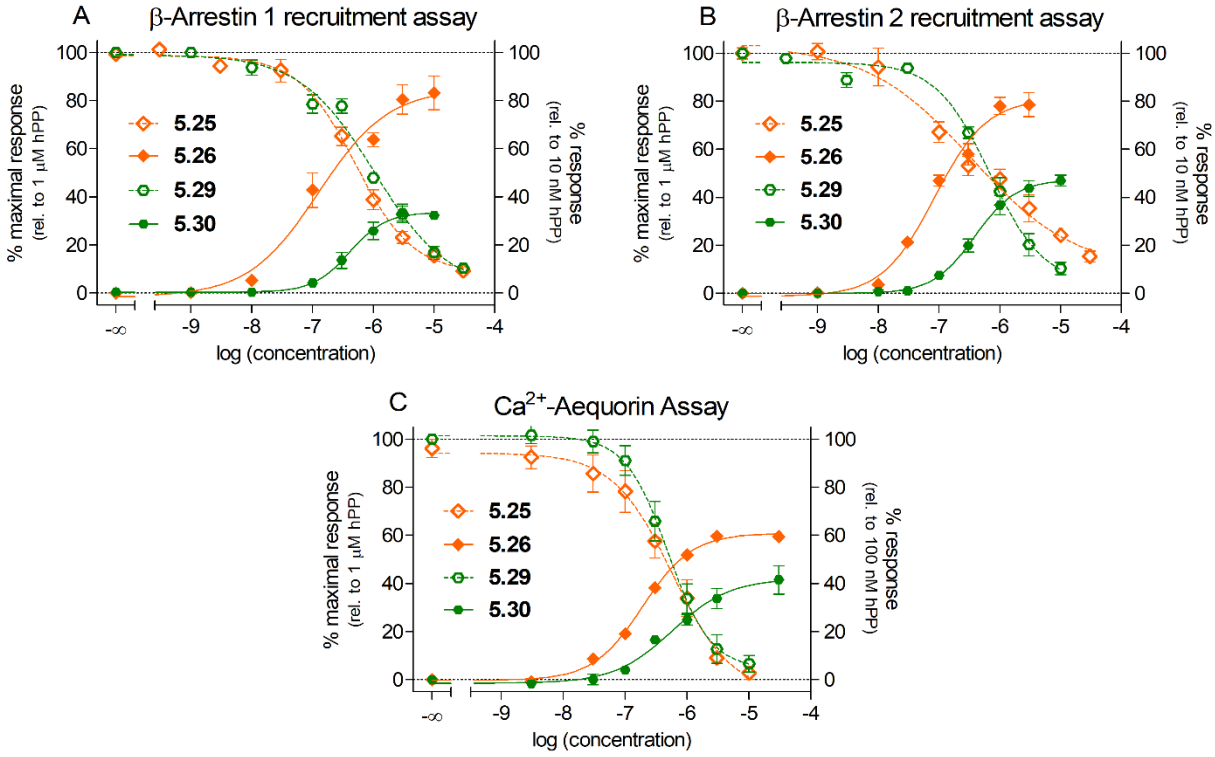

Figure 7. Y_4R functional activities of **5.25**, **5.26**, **5.29** and **5.30** determined in a β-arrestin 1 and 2 recruitment and a Ca^{2+}-aequorin assay. (A) Induced β-arrestin 1 recruitment (**5.26** and **5.30**, plotted on the left Y-axis) or inhibition of hPP (c = 10 nM) induced β-arrestin 1 recruitment (**5.25** and **5.29**, plotted on the right Y-axis) in live HEK293T-ARRB1-Y_4R cells. (B) Induced β-arrestin 2 recruitment (**5.26** and **5.30**, plotted on the left Y-axis) or inhibition of hPP (c = 10 nM) induced β-arrestin 1 recruitment (**5.25** and **5.29**, plotted on the right Y-axis) in live HEK293T-ARRB2-Y_4R cells. (C) Induced intracellular Ca^{2+} mobilization (**5.26** and **5.30**, plotted on left Y-axis) or inhibition of hPP (c = 100 nM) induced Ca^{2+} mobilization (**5.25** and **5.29**) in CHO-hY_4-G_{qi5}-mtAEQ cells. Dashed lines indicate linear peptides (**5.25**, **5.29**) and solid lines cyclic peptides (**5.26**, **5.30**). Data represent means ± SEM from at least three independent experiments, each performed in triplicate.

5.2.5 Stability in PBS and Human Plasma

The chemical stability of the high affinity Y_4R ligands **5.18** and **5.24** was investigated in PBS (pH 7.4) at rt over a period of 48 h. Under these conditions, these peptides proved to be stable (Figure S5, Supporting Information). In order to explore the stability of the presented type of peptides against enzymatic cleavage, the cyclic peptides **5.18** and **5.24** as well as the previously reported linear hexapeptide **5**, also containing a carbamoylated arginine (*cf*. Figure 1), were incubated in human plasma at 37 °C for up to 6 h, followed by precipitation of plasma

proteins and HPLC analysis (for recoveries see Table S1, Supporting Information). These studies revealed moderate stabilities for **5.5**, **5.18** and **5.24** in human plasma, exhibiting half-lives in the range of 2-3 h (Table 3). The cyclic peptides **5.18** and **5.24** showed almost no higher stability compared to the linear peptide **5**. This was in accordance with the location of the identified major cleavage site, i.e. the Leu^4-Arg^5 bond in the C-terminal, non-cyclized part of **5.18** and **5.24** (Figure 8).

Table 3. In vitro plasma stabilities of **5.5**, **5.18** and **5.24** determined at 37 °C.

compd.	% intact peptide in plasma after the given incubation time[a]				estimated $t_{1/2}$ [h][b]
	30 min	1 h	2 h	6 h	
5.5	>99	77 ± 2.8	38 ± 1.6	9 ± 0.1	1.8
5.18	>99	>99	58 ± 1.3	22 ± 0.4	3.2
5.24	94 ± 2.7	87 ± 4.2	57 ± 2.1	19 ± 0.6	2.5

[a]The initial concentration of the peptide in human plasma/PBS (1:2 v/v) was 100 µM. Data represent means (± SEM) from three independent experiments (SEM not given when no decompensation was observed). [b]Determined by non-linear regression (two-parameter monoexponential decline) including t = 0 (100%).

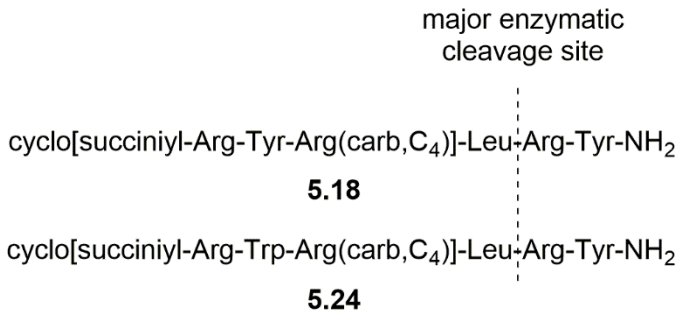

Figure 8. Major enzymatic cleavage site of **5.18** and **5.24**, identified by LC-HRMS analysis after incubation in human plasma. Fragments other than the indicated cleavage products were not found.

5.2.6 MD Simulations

For induced-fit docking of the high affinity Y_4R agonists **5.18** and **5.24** to the Y_4R and subsequent refinement by MD simulations, a recently reported homology model of the Y_4R derived from the active state κ opioid receptor crystal structure (PDB ID: 6B73, chain A[29]) was used.[13]

Four MD simulation runs of 1 µs length were performed for each ligand: two runs with Cα-restraints on the helices of the receptor and two runs without restraints. Since the topology of Y_4R proved to be stable in the absence of Cα-restraints (Figure S6, Supporting Information), all subsequent analyses were performed based on the unrestrained simulations.

The receptor-ligand complexes are shown in Figure 9 for the representative cluster structures. As previously found for linear peptidic Y_4R agonists such as **5.3** and **5.4**,[13] both cyclic ligands were oriented with their exocyclic flexible C-terminus towards the inside of the receptor (Tyr^6 of **5.18** and **5.24** located in close vicinity to $W278^{6.48}$). During the simulations, Tyr^6 showed tight hydrophobic interactions (Figure S7, Supporting Information), and no marked polar interactions for the tyrosine side chain or the C-terminal amide group were detected. The experimental observation that a C-terminal amide is strongly preferred compared to a terminal carboxyl group (investigated for structurally related linear oligopeptidic Y_4R ligands[10]) may most likely be explained by the highly unfavorable desolvation energy resulting from the placement of a charged carboxyl group in a rather hydrophobic environment. Similar to Tyr^6, the aromatic side chain in position 2 (Tyr^2 in **5.18**, Trp^2 in **5.24**) also showed tight hydrophobic interactions and no stable polar interactions. The van der Waals interaction energies of Trp^2 in **5.24** were slightly stronger compared to Tyr^2 in **5.18** (Figure S7, Supporting Information), being in line with the slightly higher Y_4R affinity of **5.24** compared to **5.18**.

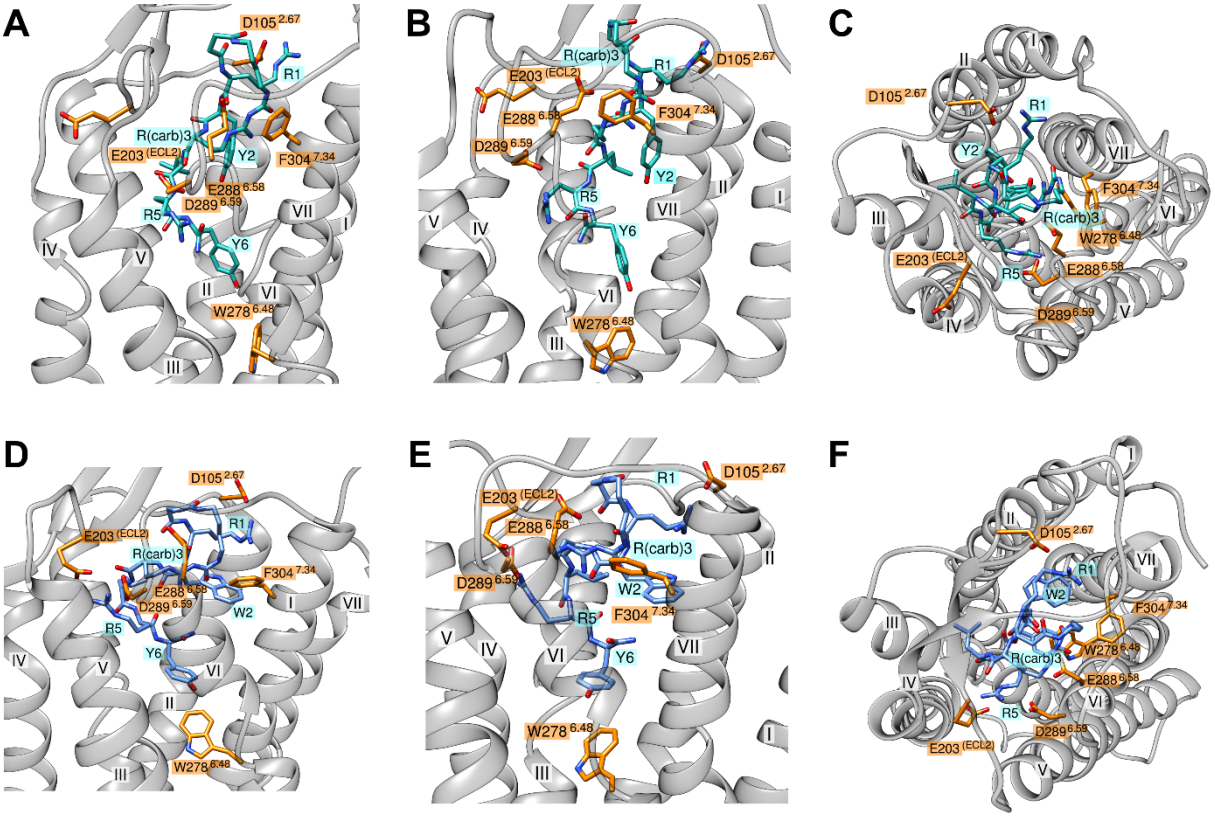

Figure 9. Binding poses of **5.18** and **5.24** at a homology model of the hY_4R obtained from molecular dynamics simulations. Images in A-C and in D-F show the representative structure from the most populated cluster of the Y_4R-**5.18** and Y_4R-**5.24** simulations, respectively. The views shown in B and C as well as in E and F were obtained by a rotation of ca. 90° around the vertical (B, E) or horizontal (C, F) axis, compared to A and D, respectively. Nitrogen and oxygen atoms are shown in blue and red, respectively. Carbon atoms of receptor amino acids are shown in orange and carbon atoms of **5.18** and **5.24** are shown in cyan and blue, respectively.

A very important aspect of the ligand-Y_4R complexes are distinct electrostatic interactions formed between the positively charged arginine residues of the ligand and acidic amino acid residues of the Y_4R (Figure 9). The three most frequent ionic interactions were the following: Arg^1-$D105^{2.67}$, $Arg(carb)^3$-$E288^{6.58}$ and Arg^5-$D289^{6.59}$. After a local conformational rearrangement of the ECL2, an additional electrostatic interaction was formed between Arg^5 and $E203^{ECL2}$ for both ligands in one of the simulations. The patterns of ionic interactions were in good agreement with those observed in a previous study of structurally similar linear peptidic ligands.[13] Details of the observed ionic interactions between **5.18** and Y_4R as well as **5.24** and Y_4R are shown in Figures S8 and S9 (Supporting Information).

A comprehensive overview of all interactions observed in the four simulations is given in Figures S10A-D (Supporting Information). Notably, a tight interaction between $Arg(carb)^3$ and $E288^{6.58}$ was consistently detected in all four simulation runs suggesting a high relevance of the positively charged basic carbamoyl guanidine moiety being located in the macrocycle. In addition to the salt bridge formed by $Arg(carb)^3$ and $E288^{6.58}$, a cation-π interaction was present between the positively charged carbamoylguanidine groups of $Arg(carb)^3$ and the phenyl ring of $F304^{7.34}$ in some of the simulations. These findings were in agreement with the experimental observation that replacement of the basic carbamoylguanidine moiety in **5.18** by two non-basic amide groups (reference compound **5.34**) resulted in a more than 100fold decrease in Y_4R binding (cf. Table 1).

5.3 Conclusion

Replacement of the N-terminal acetyl group by a succinyl moiety and incorporation of an amino-functionalized N^{ω}-carbamoylated arginine instead of Arg^3 or Arg^5 in the hexapeptide acetyl-Arg-Tyr-Arg-Leu-Arg-Tyr-NH_2 (**5.3**) gave linear precursor peptides, which were conveniently cyclized in solution via the succinyl group and the modified arginine side chain. Cyclization via Arg^3 resulted in an up to 60fold increase in Y_4R affinity compared to the linear precursor peptides. Using this novel approach, we discovered two cyclic peptidic Y_4R agonists (**5.18**, **5.24**), exhibiting higher Y_4R potency, affinity and selectivity than the endogenous agonist hPP. This had not been achieved before with small peptides such as hexapeptides. The study demonstrates that the guanidine/carbamoylguanidine bioisosteric approach, reported to be useful for peptide labeling via arginine residues,[16,21,30,31] can be successfully exploited for the preparation of cyclic peptidic receptor ligands with high affinity. Whereas the macrocycle in **5.18** (UR-AK86c) and **5.24** (UR-AK95c) proved to be stable against proteolytic cleavage when incubated in human plasma, the exocyclic C-terminal tripeptide sequence, shown to be crucial for Y_4R binding, harbors a proteolytic cleavage site (amide bond between Leu^4 and Arg^5). Applying known strategies for peptide backbone stabilization, such as N^{α}-methylation, this can be addressed in future studies. The identified cyclic Y_4R agonists represent promising lead structures for the design and synthesis of labeled high-affinity Y_4R ligands, which are needed for binding assays involving “physiological” buffers, i.e. sodium-containing buffers. As cyclic peptides are potentially superior to linear peptides with respect to in vivo studies and pharmacokinetics, the presented compound class might support the development of Y_4R ligands, which are orally available and capable of penetrating across the blood brain barrier. Moreover, due to their reduced flexibility, Y_4R agonists such as **5.18** and **5.24** are considered useful tools for the crystallization of the Y_4R in the active state.

5.4 Experimental Section

5.4.1 General Experimental Conditions

The protected amino acids Fmoc-Tyr(*t*Bu)-OH, Fmoc-Leu-OH, Fmoc-Arg(Pbf)-OH, Fmoc-Trp-OH, Boc-Gly-OH and Fmoc-Gly-OH were purchased from Carbolution Chemicals (St. Ingbert, Germany). Fmoc-Sieber-PS-resin (0.59 mmol/g), HBTU, *N*-methyl-2-pyrrolidinone (NMP) for peptide synthesis, Fmoc-Glu-OH, Fmoc-Asp-OH and PyBOP were obtained from Iris Biotech (Marktredwitz, Germany). Fmoc-Lys-OH, gradient grade MeOH for HPLC and trifluoroacetic acid were from Merck (Darmstadt, Germany). HOBt hydrate, succinic anhydride and dichloromethane (CH_2Cl_2) were purchased from Acros Organics/Fisher Scientific (Nidderau, Germany). *N,N*-diisopropylethylamine (DIPEA), *tert*-butyl (3-aminopropyl)carbamate and 5-((*tert*-butoxycarbonyl)amino)pentanoic acid were obtained from ABCR (Karlsruhe, Germany). DMF for peptide synthesis, palladium on activated charcoal (10% Pd basis), EtOH, gradient grade acetonitrile for HPLC, Triton X-100 and piperidine were from Sigma-Aldrich (Taufkirchen, Germany). Human pancreatic polypeptide (hPP) and porcine neuropeptide Y (pNPY) were from SynPeptide (Shanghai, China). Coelenterazine h was purchased from Biotrend (Cologne, Germany). Bacitracin and bovine serum albumin (BSA) were from Serva (Heidelberg, Germany). Pierce™ D-Luciferin (monopotassium salt) was obtained from ThermoFisher Scientific (Nidderau, Germany). Deuterated solvents were from Deutero (Kastellaun, Germany). The syntheses of **5.5**,[10] **5.8**,[16] [^{3}H]**5.36**,[21] [^{3}H]**5.37**[24] and [^{3}H]propionyl-pNPY (specific activity: 27.4 Ci/mmol)[13] were described elsewhere. Compound **5.10** was prepared according to a described procedure.[16] Millipore water was consistently used for the preparation of stock solutions, buffers and eluents for HPLC. Polypropylene reaction vessels (1.5 and 2 mL) from Sarstedt (Nümbrecht, Germany) were used to keep stock solutions and for small-scale reactions (e.g. activation of Fmoc protected amino acids). NMR spectra were recorded on a Bruker Avance 400 (^{1}H: 400 MHz, ^{13}C: 100 MHz) or a Bruker Avance 600 instrument with cryogenic probe (^{1}H: 600.3 MHz, ^{13}C: 150.9 MHz) (Bruker, Karlsruhe, Germany). NMR spectra were calibrated based on the solvent residual peaks (^{1}H-NMR, DMSO-d_6: δ = 2.50 ppm; ^{13}C-NMR, DMSO-d_6: δ = 39.50 ppm) and data are reported as follows: ^{1}H-NMR: chemical shift δ in ppm (multiplicity (s = singlet, d = doublet, t = triplet, m = multiplet, br s = broad singlet); integral, coupling constant *J* in Hz), ^{13}C-NMR: chemical shift δ in ppm. High resolution mass spectrometry (HRMS) was performed with an Agilent 6540 UHD Accurate-Mass Q-TOF LC/MS system coupled to an Agilent 1290 analytical HPLC system (Agilent Technologies. Santa Clara, CA). Preparative HPLC was performed with a system from Knauer (Berlin, Germany) consisting of two K-1800 pumps and a K-2001 detector (in the following referred to as “system 1”), or with a Prep 150 LC system from Waters (Eschborn, Germany), comprising a Waters 2545 binary gradient module, a Waters 2489 UV/Vis-detector

and a Waters fraction collector III (in the following referred to as “system 2”). A Kinetex XB-C18, 5 µm, 250 mm × 21 mm from Phenomenex (Aschaffenburg, Germany) was used as RP-column at a flow rate of 20 mL/min using mixtures of acetonitrile and 0.1% aqueous TFA as mobile phase. The detection wavelength was set to 220 nm. Collected fractions were lyophilized using a Scanvac CoolSafe 100-9 freeze-dryer (Labogene, Alleroed, Denmark) equipped with a RZ 6 rotary vane vacuum pump (Vacuubrand, Wertheim, Germany). Analytical HPLC analysis was performed with a system from Agilent Technologies composed of a 1290 Infinity binary pump equipped with a degasser, a 1290 Infinity autosampler, a 1290 Infinity thermostated column compartment, a 1260 Infinity diode array detector, and a 1260 Infinity fluorescence detector. A Kinetex-XB C18, 2.6 µm, 100 × 3 mm (Phenomenex) served as stationary phase at a flow rate of 0.5 mL/min. Detection was performed at 220 nm and the oven temperature was 25 °C. Mixtures of acetonitrile (A) and 0.04% aqueous TFA (B) were used as mobile phase. The following linear gradients were applied: compounds **5.15**-**5.20** and **5.22**-**5.35**: 0-14 min: A/B 10:90-30:70, 14-16 min: 30:70-95:5, 16-20 min: 95:5 (isocratic); compounds **5.14** and **5.21**: 0-14 min: A/B 5:95-25:75, 14-16 min: 25:75-95:5, 16-20 min: 95:5 (isocratic). The injection volume was 20 µL. Retention (capacity) factors k were calculated from the retention times t_R according to $k = (t_R - t_0)/t_0$ (t_0 = dead time).

5.4.2 Compound Characterization

Compounds **5.9** and **5.13** were characterized by ^{1}H-NMR and ^{13}C-NMR spectroscopy and HRMS. Except for compounds **5.20**, **5.24**, **5.26**, **5.28**, **5.30**, **5.32** and **5.35**, all target compounds were characterized by ^{1}H-NMR, ^{13}C-NMR and 2D-NMR (^{1}H-COSY, HSQC, HMBC) spectroscopy, HRMS and RP-HPLC. Compounds **5.20**, **5.24**, **5.26**, **5.28**, **5.30**, **5.32** and **5.35** were characterized by ^{1}H-NMR, HRMS and RP-HPLC. HPLC purities of all peptides were ≥ 96%. An overview about the analytical data of **5.14**-**5.35** is given in Table 4 (chromatograms shown in Appendix).

Annotation concerning the ^{1}H-NMR spectra (solvent: DMSO-d_6) of **5.18**, **5.22** and **5.34**. In order to allow an integration of the signals interfering with the broad water signal at ca. 3.5 ppm, ^{1}H-NMR spectra were additionally recorded in DMSO-d_6/D_2O (4:1 v/v).

Table 4. Analytical characterization of target peptides **5.14**-**5.35**.

compd.	x-fold hydro-trifluoroacetate	MW	overall yield (%)	RP-HPLC purity (%) / t_R [min] / k	HRMS (ESI): m/z			NMR[a]
					calcd. for	calcd.	found	
5.14	3	930.09 + 342.07	54	99 / 4.9 / 4.3	$[M+3H]^{3+}$	310.8509	310.8520	^{1}H, ^{13}C, 2D
5.15	3	916.06 + 342.07	54	98 / 3.3 / 2.6	$[M+3H]^{3+}$	306.1790	306.1800	^{1}H, ^{13}C, 2D
5.16	3	1093.26 + 342.07	58	96 / 3.6 / 2.9	$[M+3H]^{3+}$	365.2053	365.2063	^{1}H, ^{13}C, 2D

- **Table 4** continued -

5.17	4	1139.33 + 456.09	26	98 / 3.1 / 2.4	$[M+3H]^{3+}$	380.5526	380.5538	^{1}H, ^{13}C, 2D
5.18	3	1121.32 + 342.07	60	99 / 5.6 / 5.1	$[M+3H]^{3+}$	374.5491	374.5499	^{1}H, ^{13}C, 2D
5.19	4	976.16 + 456.09	33	96 / 3.3 / 2.6	$[M+4H]^{4+}$	244.9004	244.9018	^{1}H, ^{13}C, 2D
5.20	3	958.14 + 342.07	50	99 / 3.9 / 3.2	$[M+3H]^{3+}$	320.1946	320.1956	^{1}H
5.21	4	1111.32 + 456.09	22	99 / 4.5 / 3.9	$[M+3H]^{3+}$	371.2172	371.2182	^{1}H, ^{13}C, 2D
5.22	3	1093.30 + 342.07	71	97 / 3.8 / 3.1	$[M+2H]^{2+}$	547.3169	547.3179	^{1}H, ^{13}C, 2D
5.23	4	1162.37 + 456.09	28	99 / 6.3 / 5.8	$[M+4H]^{4+}$	291.4203	291.4209	^{1}H, ^{13}C, 2D
5.24	3	1144.35 + 342.07	53	98 / 9.3 / 9.1	$[M+3H]^{3+}$	382.2211	382.2223	^{1}H
5.25	4	1212.39 + 456.09	33	98 / 4.4 / 3.8	$[M+3H]^{3+}$	404.8843	404.8850	^{1}H, ^{13}C, 2D
5.26	3	1194.37 + 342.07	45	99 / 3.4 / 2.7	$[M+3H]^{3+}$	398.8808	398.8816	^{1}H
5.27	4	1125.90 + 456.09	22	97 / 3.2 / 2.5	$[M+3H]^{3+}$	375.8807	375.8811	^{1}H, ^{13}C, 2D
5.28	3	1107.29 + 342.07	52	99 / 4.9 / 4.3	$[M+3H]^{3+}$	369.8772	369.8783	^{1}H
5.29	4	1198.36 + 456.09	18	99 / 6.6 / 6.2	$[M+3H]^{3+}$	400.2125	400.2129	^{1}H, ^{13}C, 2D
5.30	3	1180.34 + 342.07	60	97 / 7.8 / 7.5	$[M+3H]^{3+}$	394.2089	394.2100	^{1}H
5.31	4	1125.30 + 456.09	24	99 / 4.5 / 3.9	$[M+3H]^{3+}$	375.8807	375.8813	^{1}H, ^{13}C, 2D
5.32	3	1107.29 + 342.07	55	98 / 3.1 / 2.4	$[M+3H]^{3+}$	369.8772	369.8797	^{1}H
5.33	3	1153.35 + 342.07	31	98 / 7.8 / 7.5	$[M+3H]^{3+}$	385.2207	385.2210	^{1}H, ^{13}C, 2D
5.34	2	1135.34 + 228.04	75	98 / 8.9 / 8.7	$[M+3H]^{3+}$	379.2172	379.3277	^{1}H, ^{13}C, 2D
5.35	2	801.95 + 228.04	54	98 / 3.9 / 3.2	$[M+2H]^{2+}$	401.7378	401.7381	^{1}H

[a]2D-NMR: ^{1}H-COSY, HSQC and HMBC

5.4.3 General Procedure for Solid-Phase Peptide Synthesis

Peptides were synthesized by manual SPPS according to the Fmoc strategy. 5-mL Injekt Solo (B. Braun, Melsungen, Germany) or NPRM-JECT (Henke Sass Wolf, Tuttlingen, Germany) syringes, equipped with polyethylene frits (pore size: 35 µm) (Roland Vetter Laborbedarf, Ammerbuch, Germany) were used as reaction vessels. DMF/NMP (8:2 v/v) was used as solvent for the coupling reactions and the cleavage of Fmoc groups. For initial Fmoc deprotection of the resin and swelling, the resin was treated with 20% piperidine in solvent at rt for 2 × 20 min. Protected natural L-amino acids were used in 5fold excess and preactivated with HBTU (4.9 equiv.)/HOBt (5 equiv.)/DIPEA (10 equiv.) in polypropylene reaction vessels for at least 5 min prior to addition to the resin (volume of the solvent: ca. 2.2 mL/mmol Fmoc-amino acid). In the case of standard (natural) Fmoc-amino acids, “double” coupling (2 × 45 min) was performed at 35 °C. Building blocks **5.8**, **5.9** or **5.13** were used in 3fold excess, preactivated with HBTU (2.95 equiv.)/HOBt (3 equiv.)/DIPEA (6 equiv.) (volume of solvent: ca. 1.6 mL/mmol building block **5.8**, **5.9** or **5.13**), and the reaction was performed at 35 °C for 24

h ("single" coupling). During coupling reactions, syringes were shaken using a Multi Reax shaker (Heidolph, Schwabach, Germany) covered with a box, which was equipped with a thermostat-controlled heater. After completed coupling of an Fmoc-aa, the resin was washed with solvent (4 ×) and treated with 20 % piperidine in solvent at rt for 2 × 10 min followed by washing of the resin with solvent (6 ×). After coupling and Fmoc deprotection of the final amino acid, and, in the case of **5.17**, **5.19**, **5.21**, **5.23**, **5.25**, **5.27**, **5.29**, **5.31** and **5.33** subsequent treatment with succinic anhydrate (see experimental procedures of the respective linear peptides), the resin was washed with solvent (6 ×) and CH_2Cl_2 (treated with K_2CO_3) (4 ×) followed by cleavage off the resin with CH_2Cl_2/TFA (3:1 v/v) at rt (2 × 20 min, performed in the syringe). After completed cleavage, the resin was washed once with CH_2Cl_2/TFA (3:1 v/v). The collected liquid phases were combined in a round-bottom flask and the volatiles were removed by rotary evaporation. The residue was dissolved in TFA/H_2O (95:5 v/v), the mixture was stirred at rt for 5 h (full side chain deprotection) and transferred to a 100-mL round-bottom flask containing water (40 mL) followed by lyophilization and subsequent purification by preparative HPLC.

5.4.4 Experimental Protocols and Analytical Data

Benzyl-(*S*)-2-((((9*H*-fluoren-9-yl)methoxy)carbonyl)amino)-5-(2-aminoacetamido) pentanoate hydrotrifluoroacetate (5.11). HOBt (1.10 g, 7.166 mmol), HBTU (2.72 g, 7.166 mmol) and DIPEA (2.50 mL, 14.3 mmol) were added to a solution of Boc-Gly-OH (1.2 g, 3.583 mmol) in anhydrous DMF (50 mL) and the mixture was stirred at rt for 15 min. Amine **5.10** (3.0 g, 3.583 mmol) was added and stirring was continued at 35 °C for 24 h. The mixture was transferred to a separating funnel, CH_2Cl_2 (300 mL) was added and the solution was treated with H_2O (4 × 300 mL). The organic phase was dried over $MgSO_4$ and the solvent was removed under reduced pressure. Purification by column chromatography (eluent: THF) afforded the Boc-protected intermediate as a yellowish solid. A mixture of CH_2Cl_2/TFA 4:1 v/v (5 mL) was added and the solution was stirred at rt for 3 h followed by evaporation of the volatiles to yield **5.11** as a yellow oil (1.95 g, 89%). ^{1}H-NMR (400 MHz, DMSO-d_6): δ (ppm) 1.38-1.54 (m, 3H), 1.61-1.72 (m, 1H), 2.30-2.34 (m, 1H), 2.58-2.66 (m, 2H), 3.92-3.99 (m, 1H), 4.01-4.07 (m, 1H), 4.09-4.16 (m, 1H), 4.17-4.23 (m, 1H), 4.95 (s, 2H), 7.09-7.20 (m, 8H), 7.21-7.25 (m, 2H), 7.49-7.62 (m, 5H), 7.67-7.72 (m, 3H), 7.76 (s, 1H). ^{13}C-NMR (100 MHz, DMSO-d_6): δ (ppm) 24.3, 27.9, 31.1, 36.1, 47.1, 54.0, 66.2, 66.5, 120.5 (two carbon atoms), 125.57, 125.61, 127.5 (two carbon atoms), 128.1 (two carbon atoms), 128.2 (two carbon atoms), 128.5, 128.8 (two carbon atoms), 136.3, 141.2 (two carbon atoms), 144.20, 144.24, 156.7, 158.9 (q, *J* 32 Hz) (TFA), 172.4 (two carbon atoms). HRMS (ESI): *m/z* $[M+H]^+$ calcd. for $[C_{29}H_{32}N_3O_5]^+$ 502.2336, found: 502.2337. $C_{29}H_{31}N_3O_5 \cdot C_2H_1F_3O_2$ (501.58 + 114.02).

Benzyl-(*S*)-18-((((9*H*-fluoren-9-yl)methoxy)carbonyl)amino)-2,2-dimethyl-4,10,13-trioxo-3-oxa-5,11,14-triazanonadecan-19-oate (5.12). HOBt (659 mg, 4.552 mmol), HBTU (1.70 g, 4.552 mmol) and DIPEA (1.57 mL, 9.104 mmol) were added to a solution of 5-((*tert*-butoxycarbonyl)amino)pentanoic acid (500 mg, 2.301 mmol) in anhydrous DMF (40 mL) and the mixture was stirred at rt for 15 min. Amine **5.11** (1.40 g, 2.301 mmol) was added and stirring was continued at 35 °C for 24 h. The mixture was transferred to a separating funnel, CH_2Cl_2 (200 mL) was added and the solution was treated with H_2O (3 × 170 mL). The organic phase was dried over $MgSO_4$ and the solvent was removed under reduced pressure. Purification by column chromatography (eluent: THF) afforded **5.12** as a white solid (1.18 g, 73%). ^{1}H-NMR (400 MHz, DMSO-d_6): δ (ppm) 1.13-1.27 (m, 2H), 1.34-1.39 (m, 9H), 1.40-1.78 (m, 6H), 2.00-2.07 (m, 2H), 2.84-2.93 (m, 2H), 2.98-3.06 (m, 2H), 3.35 (s, 2H), 3.98-4.14 (m, 2H), 4.16-4.37 (m, 3H), 5.11 (s, 2H), 6.71-6.79 (m, 1H), 7.27-2.38 (m, 7H), 7.38-7.45 (m, 2H), 7.68-7.77 (m, 3H), 7.80-7.92 (m, 3H). ^{13}C-NMR (100 MHz, DMSO-d_6): δ (ppm) 21.2, 23.1, 26.3, 28.5, 28.7 (three carbon atoms), 29.6, 35.5, 38.3, 47.1, 54.3, 60.0, 66.2, 66.3, 77.8, 120.6 (two carbon atoms), 125.68, 125.71, 127.53, 127.54, 128.1 (two carbon atoms), 128.2 (two carbon atoms), 128.5, 128.9 (two carbon atoms), 136.4, 141.2 (two carbon atoms), 144.2, 144.3, 156.0, 156.6, 165.1, 172.3, 172.7. HRMS (ESI): *m/z* $[M+H]^+$ calcd. for $[C_{39}H_{49}N_4O_8]^+$ 701.3545, found: 701.3550. $C_{39}H_{48}N_4O_8$ (700.83).

(*S*)-18-((((9*H*-Fluoren-9-yl)methoxy)carbonyl)amino)-2,2-dimethyl-4,10,13-trioxo-3-oxa-5,11,14-triazanonadecan-19-oic acid (5.13). In a two-necked round-bottom flask, **5.12** (1.0 g, 1.428 mmol) was dissolved in EtOH (45 mL) under an atmosphere of argon followed by the addition of a 10% Pd/C catalyst (200 mg). The suspension was vigorously stirred under an atmosphere of hydrogen at rt for 20 min and the catalyst was removed by filtration through a pad of celite. The volatiles were removed by evaporation and the product was purified by column chromatography (eluent: THF/MeOH 10:1 to 1:1). The solvent of the collected fraction was removed under reduced pressure and water (300 mL) was added to the residue. Lyophilization yielded **5.13** as a white powder (453 mg, 52%). ^{1}H-NMR (400 MHz, DMSO-d_6): δ (ppm) 1.24-1.31 (m, 5H), 1.48-1.62 (m, 8H), 1.90-1.96 (m, 2H), 2.66-2.76 (m, 4H), 2.82-2.90 (m, 2H), 2.99 (s, 3H), 3.66-3.75 (m, 1H), 4.00-4.12 (m, 3H), 6.42-6.50 (m, 2H), 6.57-6.62 (m, 1H), 7.10-7.18 (m, 2H), 7.20-7.25 (m, 2H), 7.51-7.59 (m, 2H), 7.63-7.73 (m, 3H), 7.78-7.83 (m, 1H), 12.56 (br s, 1H). ^{13}C-NMR (100 MHz, DMSO-d_6): δ (ppm) 21.8, 22.5, 25.9, 28.2 (three carbon atoms), 29.0, 29.1, 33.4, 34.8, 41.9, 46.7, 54.0, 65.6, 77.3, 120.1, 123.0, 124.9 (two carbon atoms), 125.3, 127.1, 127.6, 128.0, 140.7 (two carbon atoms), 143.8, 143.9, 155.6, 156.0, 164.6, 168.8, 172.3. HRMS (ESI): *m/z* $[M+H]^+$ calcd. for $[C_{32}H_{43}N_4O_8]^+$ 611.3075, found: 611.3077. $C_{32}H_{42}N_4O_8$ (610.71).

(5*S*,8*S*,11*S*)-*N*-((*S*)-1-(((*S*)-1-(((*S*)-1-Amino-3-(4-hydroxyphenyl)-1-oxopropan-2-yl)amino)-5-guanidino-1-oxopentan-2-yl)amino)-4-methyl-1-oxopentan-2-yl)-5,8-bis(3-

guanidinopropyl)-3,6,9,14-tetraoxo-1,4,7,10-tetraazacyclotetradecane-11-carboxamide tris(hydrotrifluoroacetate) (5.14). A solution of PyBOP (31.7 mg, 0.061 mmol) in DMF/NMP 80:20 v/v (500 µL) was added to a stirred solution of the linear precursor peptide (17.1 mg, 12.183 µmol) (prepared by SPPS), HOBt (9.3 mg, 0.061 mmol) and DIPEA (21 µL, 0.122 mmol) in DMF/NMP 80:20 v/v (500 µL) and stirring was continued at rt overnight. 0.1% aq TFA (30 mL) was added followed by freeze-drying and purification by preparative HPLC (system 1, gradient: 0–18 min MeCN/0.1% aq TFA 3:97–42:58, t_R = 11 min) affording **5.14** as a white solid (8.3 mg, 54%). ^{1}H-NMR (600 MHz, DMSO-d_6): δ (ppm) 0.79-0.88 (m, 6H), 1.38-1.76 (m, 16H), 1.84-1.92 (m, 1H), 2.18-2.30 (m, 2H), 2.68-2.74 (m, 1H), 2.83-2.87 (m, 1H), 3.02-3.13 (m, 6H), 4.18-4.31 (m, 4H), 4.31-4.36 (m, 1H), 4.37-4.43 (m, 1H), 6.61-6.65 (m, 2H), 6.75-7.55 (br s, 12H, interfering with the next three listed signals), 6.95-6.99 (m, 2H), 7.04-7.05 (m, 1H), 7.35-7.37 (m, 1H), 7.60-7.64 (m, 1H), 7.72-7.79 (m, 3H), 7.96-8.00 (m, 1H), 8.01-8.13 (m, 5H), 8.23-8.28 (m, 1H), 8.54-8.59 (m, 1H), 9.19 (br s, 1H). ^{13}C-NMR (150 MHz, DMSO-d_6): δ (ppm) 21.4, 23.1, 24.1, 24.9, 24.95, 24.98, 27.5, 28.9, 29.0, 29.6, 30.1, 36.8, 40.1, 40.40, 40.41, 40.5, 40.6, 50.9, 51.8, 52.1, 52.2, 52.3, 53.9, 114.9 (two carbon atoms), 116.0 (TFA), 118.0 (TFA), 127.5, 130.0 (two carbon atoms), 155.8, 156.8, 156.9 (two carbon atoms), 158.8 (q, *J* 32 Hz) (TFA), 165.8, 170.85, 170.93 (two carbon atoms), 171.1, 172.0, 172.7, 174.1. HRMS (ESI): *m/z* $[M+3H]^{3+}$ calcd. for $[C_{40}H_{70}N_{17}O_9]^{3+}$ 310.8509, found: 310.8520. RP-HPLC (220 nm): 99% (t_R = 4.9 min, *k* = 4.3). $C_{40}H_{67}N_{17}O_9 \cdot C_6H_3F_9O_6$ (930.09 + 342.07).

(5*S*,8*S*,11*S*)-*N*-((*S*)-1-(((*S*)-1-(((*S*)-1-Amino-3-(4-hydroxyphenyl)-1-oxopropan-2-yl)amino)-5-guanidino-1-oxopentan-2-yl)amino)-4-methyl-1-oxopentan-2-yl)-5,8-bis(3-guanidinopropyl)-3,6,9,13-tetraoxo-1,4,7,10-tetraazacyclotridecane-11-carboxamide tris(hydrotrifluoroacetate) (5.15). A solution of PyBOP (36.0 mg, 0.069 mmol) in DMF/NMP 80:20 v/v (500 µL) was added to a stirred solution of the linear precursor peptide (19.2 mg, 13.817 µmol) (prepared by SPPS), HOBt (10.6 mg, 0.069 mmol) and DIPEA (24.1 µL, 0.138 mmol) in DMF/NMP 80:20 v/v (500 µL) and stirring was continued at rt overnight. 0.1% aq TFA (30 mL) was added followed by freeze-drying and purification by preparative HPLC (system 1, gradient: 0–18 min MeCN/0.1% aq TFA 3:97–42:58, t_R = 11 min) yielding **5.15** as a white solid (9.4 mg, 54%). ^{1}H-NMR (600 MHz, DMSO-d_6): δ (ppm) 0.80-0.90 (m, 6H), 1.19-1.69 (m, 15H), 1.69-1.78 (m, 1H), 2.56-2.61 (m, 1H), 2.68-2.75 (m, 2H), 2.83-2.88 (m, 1H), 3.01-3.14 (m, 6H), 3.84-3.90 (m, 1H), 4.09-4.16 (m, 2H), 4.16-4.21 (m, 1H), 4.25-4.35 (m, 2H), 4.58-4.64 (m, 1H), 6.61-6.65 (m, 2H), 6.70-7.48 (br s, 12H, interfering with the next three listed signals), 6.96-6.99 (m, 2H), 7.04-7.06 (m, 1H), 7.31-7.36 (m, 2H), 7.48-7.52 (m, 1H), 7.58-7.62 (m, 1H), 7.63-7.67 (m, 1H), 7.68-7.72 (m, 1H), 7.74-7.79 (m, 1H), 7.81-7.87 (m, 1H), 7.91-7.95 (m, 1H), 7.97-8.02 (m, 1H), 8.04-8.08 (m, 1H), 8.44-8.49 (m, 1H), 9.17 (s, 1H). ^{13}C-NMR (150 MHz, DMSO-d_6): δ (ppm) 21.5, 23.1, 24.0, 24.9, 25.1, 25.3, 27.1, 28.00, 28.03, 28.09, 36.8, 40.2, 40.4, 40.48, 40.53, 43.8, 49.8, 50.3, 51.2, 51.6, 52.1, 52.3, 114.8 (two carbon atoms), 127.5, 130.0 (two

carbon atoms), 155.8, 156.64, 156.68, 156.70, 158.3 (q, *J* 32 Hz) (TFA), 169.6, 170.0, 170.2, 170.5, 170.8, 171.4, 172.0, 170.6. HRMS (ESI): *m/z* $[M+3H]^{3+}$ calcd. for $[C_{39}H_{68}N_{17}O_9]^{3+}$ 306.1790, found: 306.1800. RP-HPLC (220 nm): 98% (t_R = 3.3 min, *k* = 2.6). $C_{40}H_{65}N_{17}O_9 \cdot C_6H_3F_9O_6$ (916.06 + 342.07).

(2*S*,8*S*)-*N*-((6*S*,9*S*,12*S*)-1,17-Diamino-6-(((*S*)-1-amino-3-(4-hydroxyphenyl)-1-oxopropan-2-yl)carbamoyl)-1,17-diimino-9-isobutyl-8,11-dioxo-2,7,10,16-tetraazaheptadecan-12-yl)-2-(3-guanidinopropyl)-8-(4-hydroxybenzyl)-3,6,9,14-tetraoxo-1,4,7,10-tetraazacyclotetradecane-11-carboxamide tris(hydrotrifluoroacetate) (5.16). A solution of PyBOP (24.9 mg, 0.048 mmol) in DMF/NMP 80:20 v/v (500 µL) was added to a stirred solution of the linear precursor peptide (15.0 mg, 9.574 µmol) (prepared by SPPS), HOBt (7.3 mg, 0.048 mmol) and DIPEA (16.7 µL, 0.096 mmol) in DMF/NMP 80:20 v/v (500 µL) and stirring was continued at rt overnight. 0.1% aq TFA (30 mL) was added followed by freeze-drying and purification by preparative HPLC (system 1, gradient: 0-18 min MeCN/0.1% aq TFA 3:97–42:58, t_R = 13 min) yielding **5.16** as a white solid (7.9 mg, 58%). ^{1}H-NMR (600 MHz, DMSO-*d*$_6$): δ (ppm) 0.78-0.91 (m, 6H), 1.36-1.88 (m, 17H), 1.98-2.06 (m, 1H), 2.14-2.22 (m, 1H), 2.63-2.67 (m, 1H), 2.69-2.75 (m, 1H), 2.84-2.89 (m, 1H), 2.96-3.02 (m, 1H), 3.04-3.14 (m, 6H), 3.25-3.35 (m, 2H), 3.85-3.90 (m, 1H), 3.93-3.98 (m, 1H), 3.98-4.04 (m, 1H), 4.18-4.24 (m, 2H), 4.24-4.29 (m, 1H), 4.29-4.34 (m, 1H), 4.45-4.51 (m, 1H), 6.60-6.65 (m, 4H), 6.70-7.46 (br s, 12H, interfering with the next three listed signals), 6.94-6.99 (m, 4H), 7.05-7.07 (m, 1H), 7.32-7.34 (m, 1H), 7.47-7.49 (m, 1H), 7.50-7.58 (m, 2H), 7.59-7.64 (m, 1H), 7.69-7.77 (m, 2H), 7.91-7.96 (m, 1H), 8.09-8.14 (m, 1H), 8.47-8.53 (m, 1H), 8.53-8.57 (m, 1H), 9.17 (br s, 2H). ^{13}C-NMR (150 MHz, DMSO-*d*$_6$): δ (ppm) 21.4, 23.1, 24.1, 24.47, 24.52, 24.8, 25.0, 25.3, 26.4, 28.6, 28.86, 28.90, 35.3, 36.7, 40.3, 40.4 (two carbon atoms), 40.5, 51.1, 52.2, 52.3, 53.2, 54.0, 54.2, 55.6, 114.81 (two carbon atoms), 114.84 (two carbon atoms, 127.5, 127.8, 130.0 (two carbon atoms), 130.4 (two carbon atoms), 155.6, 155.8, 156.66, 156.67, 156.68, 158.2 (q, *J* 32 Hz) (TFA), 169.4, 170.8, 171.2, 171.9., 172.0, 172.67, 172.70, 173.2, 174.0. HRMS (ESI): *m/z* $[M+3H]^{3+}$ calcd. for $[C_{49}H_{79}N_{18}O_{11}]^{3+}$ 365.2053, found: 365.2063. RP-HPLC (220 nm): 96% (t_R = 3.6 min, *k* = 2.9). $C_{49}H_{76}N_{18}O_{11} \cdot C_6H_3F_9O_6$ (1093.26 + 342.07).

***N*$^{\alpha}$-Succinyl-Arg-Tyr-*N*$^{\omega}$-[(4-aminobutyl)aminocarbonyl]Arg-Leu-Arg-Tyr-amide tetrakis(hydrotrifluoroacetate) (5.17).** Peptide **5.17** was synthesized on a Fmoc-Sieber-PS resin (75 mg, 0.59 mmol/g) according to the general procedure. After coupling of the last amino acid and subsequent Fmoc deprotection, the resin was treated with a solution of succinic anhydride (52.3 mg, 0.443 mmol) and DIPEA (77.1 µL, 0.443 mmol) in DMF/NMP 80:20 v/v (500 µL) at 35 °C for 30 min. The resin was washed with DMF/NMP 80:20 v/v (6 ×) and CH_2Cl_2 (3 ×), followed by cleavage off the resin and deprotection according to the general procedure. Purification by preparative HPLC (system 2, gradient: 0–18 min MeCN/0.1% aq TFA 3:97–42:58, t_R = 14 min) yielded **5.17** as a white solid (18.4 mg, 26%). ^{1}H-NMR (600 MHz, DMSO-

d_6): δ (ppm) 0.81-0.89 (m, 6H), 1.37-1.66 (m, 18H), 1.70-1.76 (m, 1H), 2.34-2.46 (m, 4H), 2.68-2.75 (m, 2H), 2.76-2.82 (m, 2H), 2.83-2.88 (m, 1H), 2.89-2.94 (m, 1H), 3.02-3.13 (m, 6H), 3.21-3.27 (m, 2H), 4.11-4.16 (m, 1H), 4.18-4.22 (m, 1H), 4.24-4.35 (m, 3H), 4.38-4.43 (m, 1H), 6.60-6.65 (m, 4H), 6.80-7.20 (br s, 4H, interfering with the next two listed signals), 6.96-7.00 (m, 4H), 7.05-7.06 (m, 1H), 7.20-7.50 (br s, 4H, interfering with the next listed signal), 7.34-7.36 (m, 1H), 7.58-7.67 (m, 3H), 7.69-7.86 (m, 6H), 8.01-8.05 (m, 1H), 8.07-8.11 (m, 1H), 8.12-8.16 (m, 1H), 8.46 (br s, 2H), 9.03 (s, 1H), 9.22 (br s, 2H), 10.58 (s, 1H), 12.18 (s, 1H). ^{13}C-NMR (150 MHz, DMSO-*d_6*): δ (ppm) 21.4, 23.1, 24.1, 24.4, 24.5, 24.9, 25.0, 25.9, 28.7, 28.8, 28.9, 29.1, 29.9, 36.2, 36.8, 38.5, 38.6, 40.37, 40.41, 40.5, 40.6, 51.0, 52.1, 52.3, 52.6, 53.9, 54.1, 114.9 (four carbon atoms), 116.0 (TFA), 118.0 (TFA), 127.47, 127.50, 130.0 (four carbon atoms), 153.8, 153.9, 155.81, 155.84, 156.78 (two carbon atoms), 158.8 (q, *J* 32 Hz) (TFA), 170.8, 171.1, 171.2, 171.5, 171.8, 172.0, 172.7, 174.0. HRMS (ESI): *m/z* $[M+3H]^{3+}$ calcd. for $[C_{51}H_{85}N_{18}O_{12}]^{3+}$ 380.5526, found: 380.5538. RP-HPLC (220 nm): 98% (t_R = 3.1 min, *k* = 2.4). $C_{51}H_{82}N_{18}O_{12} \cdot C_8H_4F_{12}O_8$ (1139.33 + 456.09).

(9*S*,12*S*,15*S*)-*N*-((*S*)-1-(((*S*)-1-(((*S*)-1-Amino-3-(4-hydroxyphenyl)-1-oxopropan-2-yl)amino)-5-guanidino-1-oxopentan-2-yl)amino)-4-methyl-1-oxopentan-2-yl)-15-(3-guanidinopropyl)-12-(4-hydroxybenzyl)-4-imino-2,11,14,17,20-pentaoxo-1,3,5,10,13,16,21-heptaazacyclopentacosane-9-carboxamide tris(hydrotrifluoroacetate) (5.18). Peptide **5.17** (7.9 mg, 4.954 µmol), HOBt (3.8 mg, 0.025 mmol) and DIPEA (8.6 µL, 0.050 mmol) were dissolved in DMF/NMP 80:20 v/v (500 µL) in a round-bottom flask. Under stirring, a solution of PyBOP (12.9 mg, 0.025 mmol) in DMF/NMP 80:20 v/v (500 µL) was added and the mixture was stirred at rt overnight. 0.1% aq TFA (30 mL) was added followed by freeze-drying and purification by preparative HPLC (system 1, gradient: 0–18 min MeCN/0.1% aq TFA 3:97–42:58, t_R = 15 min) to yield **5.18** as a white solid (4.4 mg, 60%). ^{1}H-NMR (600 MHz, DMSO-*d_6*): δ (ppm) 0.80-0.90 (m, 6H), 1.34-1.58 (m, 15H), 1.59-1.68 (m, 3H), 1.72-1.78 (m, 1H), 2.28-2.41 (m, 4H), 2.68-2.73 (m, 1H), 2.75-2.81 (m, 1H), 2.81-2.90 (m, 2H), 2.91-2.96 (m, 1H), 3.01-3.15 (m, 6H), 3.18-3.35 (m, 4H), 4.03-4.11 (m, 1H), 4.17-4.22 (m, 1H), 4.24-4.38 (m, 4H), 6.61-6.68 (m, 4H), 6.80-7.20 (br s, 4H, interfering with the next two listed signals), 6.97-7.02 (m, 4H), 7.05-7.06 (m, 1H), 7.20-7.50 (br s, 4H, interfering with the next listed signal), 7.33-7.35 (m, 1H), 7.54-7.61 (m, 1H), 7.63-7.71 (m, 2H), 7.73-7.77 (m, 1H), 7.80-7.85 (m, 1H), 7.88-7.99 (m, 3H), 8.03-8.10 (m, 1H), 8.15 (s, 1H), 8.36 (s, 2H), 9.16-9.32 (m, 2H), 10.51 (s, 1H). ^{13}C-NMR (150 MHz, DMSO-*d_6*): δ (ppm) 21.4, 23.1, 24.1, 24.3, 24.9, 25.1, 25.9, 26.5, 28.6 (two carbon atoms), 28.9, 31.1, 31.3, 35.6, 36.8, 38.1, 38.8, 40.2, 40.37, 40.41, 40.5, 51.2, 51.8, 52.4, 53.1, 54.0, 54.9, 114.88 (two carbon atoms), 114.94 (two carbon atoms), 116.0 (TFA), 118.0 (TFA), 127.6, 127.7, 129.9 (two carbon atoms), 130.1 (two carbon atoms), 153.8, 154.0, 155.8, 155.9, 156.81, 156.84, 158.9 (q, *J* 32 Hz) (TFA), 170.9, 171.1, 171.3, 171.5, 172.0, 172.1, 172.7, 172.8. HRMS (ESI): *m/z* $[M+3H]^{3+}$ calcd. for $[C_{51}H_{83}N_{18}O_{11}]^{3+}$

374.5491, found: 374.5499. RP-HPLC (220 nm): 99% (t_R = 5.6 min, k = 5.1). $C_{51}H_{80}N_{18}O_{11} \cdot C_6H_3F_9O_6$ (1121.32 + 342.07).

***N*$^{\alpha}$-Succinyl-Arg-*N*$^{\omega}$-[(4-aminobutyl)aminocarbonyl]Arg-Leu-Arg-Tyr-amide tetrakis(hydrotrifluoroacetate) (5.19).** Peptide **5.19** was synthesized on a Fmoc-Sieber-PS resin (75 mg, 0.59 mmol/g) according to the general procedure. After coupling of the last amino acid and subsequent Fmoc deprotection, the resin was treated with a solution of succinic anhydride (52.3 mg, 0.443 mmol) and DIPEA (77.1 µL, 0.443 mmol) in DMF/NMP 80:20 v/v (500 µL) at 35 °C for 30 min. The resin was washed with DMF/NMP 80:20 v/v (6 ×) and CH_2Cl_2 (3 ×), followed by cleavage off the resin and deprotection according to the general procedure. Purification by preparative HPLC (system 2, gradient: 0–18 min MeCN/0.1% aq TFA 3:97–42:58, t_R = 11 min) yielded **5.19** as a white solid (21.1 mg, 33%). ^{1}H-NMR (600 MHz, DMSO-d_6): δ (ppm) 0.81 (d, 3H, *J* 6.6 Hz), 0.86 (d, 3H, *J* 6.6 Hz), 1.35-1.75 (m, 19H), 2.32-2.45 (m, 4H), 2.68-2.74 (m, 1H), 2.75-2.81 (m, 2H), 2.82-2.88 (m, 1H), 3.02-3.13 (m, 6H), 3.17-3.29 (m, 3H), 4.15-4.29 (m, 4H), 4.30-4.35 (m, 1H), 6.63 (d, 2H, *J* 8.4 Hz), 6.80-7.20 (br s, 4H, interfering with the next two listed signals), 6.96-6.99 (m, 2H), 7.05-7.07 (m, 1H), 7.20-7.50 (br s, 4H, interfering with the next listed signal), 7.34-7.36 (m, 1H), 7.58 (s, 1H), 7.60-7.66 (m, 2H), 7.70-7.81 (m, 4H), 7.84 (d, 1H, *J* 7.6 Hz), 7.99 (d, 1H, *J* 7.5 Hz), 8.04 (d, 1H, *J* 7.7 Hz), 8.16 (d, 1H, *J* 7.5 Hz), 8.45 (br s, 2H,), 9.02 (s, 1H), 9.20 (br s, 1H), 10.52 (s, 1H). ^{13}C-NMR (150 MHz, DMSO-d_6): δ (ppm) 21.3, 23.1, 24.1, 24.4, 24.6, 24.9, 25.0, 26.0, 28.7, 28.9, 29.0, 29.1, 29.9, 36.8, 38.5, 38.6, 40.4, 40.5 (two carbon atoms), 40.6, 51.0, 52.2, 52.3, 52.4, 53.9, 114.9 (two carbon atoms), 115.9 (TFA), 117.8 (TFA), 127.5, 130.0 (two carbon atoms), 153.7, 153.9, 155.8, 156.75, 156.77, 158.7 (q, *J* 32 Hz) (TFA), 170.8, 171.2, 171.6, 171.8, 172.0, 172.7, 173.9. HRMS (ESI): *m/z* $[M+4H]^{4+}$ calcd. for $[C_{42}H_{77}N_{17}O_{10}]^{4+}$, 244.9004, found: 244.9018. RP-HPLC (220 nm): 96% (t_R = 3.3 min, k = 2.6). $C_{42}H_{73}N_{17}O_{10} \cdot C_8H_4F_{12}O_8$ (976.16 + 456.09).

(9*S*,12*S*)-*N*-((S)-1-(((*S*)-1-(((*S*)-1-Amino-3-(4-hydroxyphenyl)-1-oxopropan-2-yl)amino)-5-guanidino-1-oxopentan-2-yl)amino)-4-methyl-1-oxopentan-2-yl)-12-(3-guanidinopropyl)-4-imino-2,11,14,17-tetraoxo-1,3,5,10,13,18-hexaazacyclodocosane-9-carboxamide tris(hydrotrifluoroacetate) (5.20). Peptide **5.19** (8.7 mg, 6.074 µmol), HOBt (4.7 mg, 0.030 mmol) and DIPEA (10.6 µL, 0.061 mmol) were dissolved in DMF/NMP 80:20 v/v (500 µL) in a round-bottom flask. Under stirring, a solution of PyBOP (15.8 mg, 0.030 mmol) in DMF/NMP 80:20 v/v (500 µL) was added and stirring was continued at rt overnight. 0.1% aq TFA (30 mL) was added followed by freeze-drying and purification by preparative HPLC (system 2, gradient: 0–18 min MeCN/0.1% aq TFA 3:97–42:58, t_R = 10 min) to yield **5.20** as a white solid (4.1 mg, 50%). ^{1}H-NMR (600 MHz, DMSO-d_6): δ (ppm) 0.79-0.91 (m, 6H), 1.22-1.29 (m, 1H), 1.34-1.70 (m, 16H), 1.73-1.79 (m, 1H), 2.28-2.36 (m, 2H), 2.78-2.84 (m, 1H), 2.88-2.98 (m, 3H), 3.00-3.08 (m, 4H), 3.09-3.15 (m, 2H), 3.95-4.02 (m, 1H), 4.13-4.19 (m, 1H), 4.21-4.28 (m, 2H), 4.29-4.34 (m, 1H), 4.41-4.48 (m, 1H), 6.61-6.66 (m, 2H), 6.80-7.20 (br s,

4H, interfering with the next two listed signals), 6.98-7.01 (m, 2H), 7.16-7.18 (m, 1H), 7.20-7.53 (br s, 4H, interfering with the next two listed signals), 7.41-7.46 (m, 2H), 7.48-7.51 (m, 1H), 7.55-7.63 (m, 2H), 7.63-7.67 (m, 1H), 7.68-7.74 (m, 1H), 7.81-7.86 (m, 1H), 7.87-8.04 (m, 5H), 8.17-8.38 (m, 3H), 9.17-9.32 (m, 2H), 10.31 (s, 1H). HRMS (ESI): *m/z* $[M+3H]^{3+}$ calcd. for $[C_{42}H_{74}N_{17}O_9]^{3+}$ 320.1946, found: 320.1956. RP-HPLC (220 nm): 99% (t_R = 3.9 min, k = 3.2). $C_{42}H_{71}N_{17}O_9 \cdot C_6H_3F_9O_6$ (958.14 + 342.07).

***N*$^{\alpha}$-Succinyl-Lys-Tyr-*N*$^{\omega}$-[(4-aminobutyl)aminocarbonyl]Arg-Leu-Arg-Tyr-amide tetrakis(hydrotrifluoroacetate) (5.21).** Peptide **5.21** was synthesized on a Fmoc-Sieber-PS resin (75 mg, 0.59 mmol/g) according to the general procedure. After coupling of the last amino acid and subsequent Fmoc deprotection, the resin was treated with a solution of succinic anhydride (52.3 mg, 0.443 mmol) and DIPEA (77.1 µL, 0.443 mmol) in DMF/NMP 80:20 v/v (500 µL) at 35 °C for 30 min. The resin was washed with DMF/NMP 80:20 v/v (6 ×) and CH_2Cl_2 (3 ×), followed by cleavage off the resin and deprotection according to the general procedure. Purification by preparative HPLC (system 1, gradient: 0–18 min MeCN/0.1% aq TFA 3:97–42:58, t_R = 12 min) yielded **5.21** as a white solid (16.2 mg, 22%). ^{1}H-NMR (600 MHz, DMSO-d_6): δ (ppm). ^{13}C-NMR (150 MHz, DMSO-d_6): δ (ppm) 0.81-0.90 (m, 6H), 1.14-1.27 (m, 2H), 1.39-1.66 (m, 18H), 1.70-1.76 (m, 1H), 2.33-2.47 (m, 4H), 2.68-2.75 (m, 4H), 2.76-2.82 (m, 2H), 2,83-2,88 (m, 1H), 2.90-2.95 (m, 1H), 3.03-3.14 (m, 4H), 3.21-3.28 (m, 2H), 4.06-4.11 (m, 1H), 4.17-4.22 (m, 1H), 4.24-4.35 (m, 3H), 4.37-4.42 (m, 1H), 6.60-6.66 (m, 4H), 6.80-7.50 (br s, 4H, interfering with the next three listed signals), 6.96-7.00 (m, 4H), 7.04-7.07 (m, 1H), 7.32-7.37 (m, 1H), 7.58-7.63 (m, 1H), 7.64-7.70 (m, 2H), 7.72-7.87 (m, 8H), 7.99-8.03 (m, 1H), 8.04-8.08 (m, 1H), 8.10-8.14 (m, 1H), 8.46 (br s, 2H), 9.03 (s, 1H), 9.11 (br s, 2H), 10.54 (s, 1H), 12.2 (br s, 1H). ^{13}C-NMR (150 MHz, DMSO-d_6): δ (ppm) 21.4, 22.2, 23.1, 24.1, 24.4, 24.6, 24.9, 25.9, 26.6, 28.8, 28.9, 29.1, 29.9, 30.9, 36.2, 36.8, 38.5, 38.6, 38.7, 40.4, 40.5 40.6, 51.1, 52.2, 52.3, 52.9, 53.9, 54.2, 114.8 (two carbon atoms), 114.9 (two carbon atoms), 116.0 (TFA), 118.0 (TFA), 127.5 (two carbon atoms), 130.0 (four carbon atoms), 153.8, 153.9, 155.81, 155.83, 156.8, 158.7 (q, J 32 Hz) (TFA), 170.8, 171.1, 171.3, 171.7, 171.8, 172.0, 172.7, 174.0. HRMS (ESI): *m/z* $[M+3H]^{3+}$ calcd. for $[C_{51}H_{85}N_{16}O_{12}]^{3+}$ 371.2172, found: 371.2182. RP-HPLC (220 nm): 99% (t_R = 4.5 min, k = 3.9). $C_{51}H_{82}N_{16}O_{12} \cdot C_8H_4F_{12}O_8$ (1111.32 + 456.09).

(9*S*,12*S*,15*S*)-*N*-((*S*)-1-(((*S*)-1-(((*S*)-1-Amino-3-(4-hydroxyphenyl)-1-oxopropan-2-yl)amino)-5-guanidino-1-oxopentan-2-yl)amino)-4-methyl-1-oxopentan-2-yl)-15-(4-aminobutyl)-12-(4-hydroxybenzyl)-4-imino-2,11,14,17,20-pentaoxo-1,3,5,10,13,16,21-heptaazacyclopentacosane-9-carboxamide tris(hydrotrifluoroacetate) (5.22). Peptide **5.21** (15.9 mg, 10.140 µmol), HOBt (7.8 mg, 0.051 mmol) and DIPEA (17.7 µL, 0.101 mmol) were dissolved in DMF/NMP 80:20 v/v (500 µL) in a round-bottom flask. Under stirring, a solution of PyBOP (26.4 mg, 0.051 mmol) in DMF/NMP 80:20 v/v (500 µL) was added and stirring was continued at rt overnight. 0.1% aq TFA (30 mL) was added followed by freeze-

drying and purification by preparative HPLC (system 2, gradient: 0–18 min MeCN/0.1% aq TFA 3:97–42:58, t_R = 11 min) to yield **5.22** as a white solid (10.4 mg, 71%). ^{1}H-NMR (600 MHz, DMSO-d_6): δ (ppm) 0.81-0.90 (m, 6H), 1.16-1.27 (m, 2H), 1.33-1.68 (m, 18H), 1.71-1.79 (m, 2H), 2.26-2.37 (m, 3H), 2.68-2.80 (m, 4H), 2.80-2.90 (m, 2H), 2.91-2.96 (m, 1H), 3.01-3.09 (m, 3H), 3.10-3.17 (m, 1H), 3.17-3.23 (m, 1H), 3.25-3.33 (m, 2H), 3.99-4.05 (m, 1H), 4.18-4.23 (m, 1H), 4.25-4.38 (m, 4H), 6.60-6.66 (m, 4H), 6.70-7.43 (br s, 4H, interfering with the next three listed signals), 6.96-7.02 (m, 4H,), 7.05-7.07 (m, 1H), 7.34-7.37 (m, 1H), 7.46-7.55 (m, 2H), 7.62-7.71 (m, 3H), 7.72-7.75 (m, 1H), 7.79-7.82 (m, 1H), 7.84-7.87 (m, 1H), 7.88-7.94 (m, 1H), 7.94-7.99 (m, 1H), 8.03-8.14 (m, 2H), 8.31 (s, 2H), 9.04-9.32 (m, 3H), 9.99 (s, 1H). ^{13}C-NMR (150 MHz, DMSO-d_6): δ (ppm) 21.3, 22.3, 23.1, 24.1, 24.8, 26.0, 26.5, 26.6 (two carbon atoms), 28.7, 28.9, 30.9, 31.2, 35.7, 36.8, 38.1, 38.7 (two carbon atoms), 38.8, 40.3, 40.4, 40.5, 50.6, 51.1, 51.7, 52.3, 53.9, 54.6, 114.9 (four carbon atoms), 116.0 (TFA), 118.0 (TFA), 127.5, 127.7, 129.9 (two carbon atoms), 130.0 (two carbon atoms), 153.7, 154.4, 155.78, 155.82, 156.6, 158.4 (q, *J* 32 Hz) (TFA), 170.8, 171.0, 171.2, 171.5, 171.9, 172.1, 172.6, 172.7. HRMS (ESI): *m/z* $[M+2H]^{2+}$ calcd. for $[C_{51}H_{82}N_{16}O_{11}]^{2+}$ 547.3169, found: 547.3179. RP-HPLC (220 nm): 97% (t_R = 3.8 min, *k* = 3.1). $C_{51}H_{80}N_{16}O_{11} \cdot C_6H_3F_9O_6$ (1093.30 + 342.07).

***N*$^{\alpha}$-Succinyl-Arg-Trp-*N*$^{\omega}$-[(4-aminobutyl)aminocarbonyl]Arg-Leu-Arg-Tyr-amide tetrakis(hydrotrifluoroacetate) (5.23).** Peptide **5.23** was synthesized on a Fmoc-Sieber-PS resin (75 mg, 0.59 mmol/g) according to the general procedure. After coupling of the last amino acid and subsequent Fmoc deprotection, the resin was treated with a solution of succinic anhydride (52.3 mg, 0.443 mmol) and DIPEA (77.1 µL, 0.443 mmol) in DMF/NMP 80:20 v/v (500 µL) at 35 °C for 30 min. The resin was washed with DMF/NMP 80:20 v/v (6 ×) and CH_2Cl_2 (3 ×), followed by cleavage off the resin and deprotection according to the general procedure. Purification by preparative HPLC (system 2, gradient: 0–18 min MeCN/0.1% aq TFA 3:97–42:58, t_R = 12 min) yielded **5.23** as a white solid (19.8 mg, 28%). ^{1}H-NMR (600 MHz, DMSO-d_6): δ (ppm) 0.83 (d, 3H, *J* 6.3 Hz), 0.86 (d, 3H, *J* 6.3 Hz), 1.34-1.69 (m, 18H), 1.70-1.78 (m, 1H), 2.30-2.45 (m, 4H), 2.69-2.74 (m, 1H), 2.75-2.85 (m, 2H), 2.83-2.88 (m, 1H), 2.98-3.17 (m, 8H), 3.20-3.26 (m, 2H), 4.10-4.17 (m, 1H), 4.17-4.23 (m, 1H), 4.23-4.37 (m, 3H), 4.45-4.56 (m, 1H), 6.63 (d, 2H, *J* 8.1 Hz), 6.74-7.20 (br s, 4H, interfering with the next three listed signals), 6.95-6.99 (m, 3H), 7.04-7.07 (m, 2H), 7.14-7.16 (m, 1H), 7.20-7.50 (br s, 4H, interfering with the next listed signal), 7.31-7.35 (m, 2H), 7.53-7.64 (m, 4H), 7.67-7.87 (m, 6H), 8.01 (d, 1H, *J* 7.6 Hz), 8.08 (d, 1H, *J* 7.5 Hz), 8.12 (d, 1H, *J* 7.3 Hz), 8.44 (br s, 2H), 9.00 (s, 1H), 9.18 (s, 1H), 10.44 (s, 1H), 10.80 (s, 1H), 12.51 (br s, 1H). ^{13}C-NMR (150 MHz, DMSO-d_6): δ (ppm) 21.4, 23.1, 24.1, 24.3, 24.5, 24.8, 24.9, 25.9, 27.2, 28.6, 28.8, 28.9, 29.0, 29.8, 36.8, 38.4 (two carbon atoms), 40.0, 40.38, 40.40, 40.6, 51.1, 52.3, 52.3, 52.7, 53.6, 53.9, 109.7, 111.3, 114.8 (two carbon atoms), 117.8, 118.2, 120.9, 123.6, 127.2, 127.5, 130.0 (two carbon atoms), 136.0, 153.7, 153.8, 155.7, 156.7 (two carbon atoms), 158.4 (q, *J* 32 Hz) (TFA), 170.8, 171.1, 171.6,

171.7, 171.9, 172.0, 172.7, 174.0. HRMS (ESI): *m/z* $[M+4H]^{4+}$ calcd. for $[C_{53}H_{87}N_{19}O_{11}]^{4+}$ 291.4203, found: 291.4209. RP-HPLC (220 nm): 99% (t_R = 6.3 min, k = 5.8). $C_{53}H_{83}N_{19}O_{11} \cdot C_8H_4F_{12}O_8$ (1162.37 + 456.09).

(9*S*,12*S*,15*S*)-12-((1*H*-Indol-3-yl)methyl)-*N*-((*S*)-1-(((*S*)-1-(((*S*)-1-amino-3-(4-hydroxyphenyl)-1-oxopropan-2-yl)amino)-5-guanidino-1-oxopentan-2-yl)amino)-4-methyl-1-oxopentan-2-yl)-15-(3-guanidinopropyl)-4-imino-2,11,14,17,20-pentaoxo-1,3,5,10,13,16,21-heptaazacyclopentacosane-9-carboxamide tris(hydrotrifluoroacetate) (5.24). Peptide **5.23** (11.4 mg, 7.044 µmol), HOBt (5.4 mg, 0.035 mmol) and DIPEA (12.3 µL, 0.070 mmol) were dissolved in DMF/NMP 80:20 v/v (500 µL) in a round-bottom flask. Under stirring, a solution of PyBOP (18.3 mg, 0.035 mmol) in DMF/NMP 80:20 v/v (500 µL) was added and the mixture was stirred at rt overnight. 0.1% aq TFA (30 mL) was added followed by lyophilization and purification by preparative HPLC (system 2, gradient: 0–18 min MeCN/0.1% aq TFA 3:97–42:58, t_R = 13 min) to afford **5.24** as a white solid (4.5 mg, 53%). ^{1}H-NMR (600 MHz, DMSO-d_6): δ (ppm) 0.81-0.91 (m, 6H), 1.21-1.29 (m, 1H), 1.31-1.57 (m, 15H), 1.58-1.68 (m, 3H), 1.71-1.79 (m, 1H), 2.27-2.38 (m, 4H), 2.66-2.75 (m, 2H), 2.79-2.91 (m, 2H), 2.96-3.25 (m, 8H), 4.04-4.09 (m, 1H), 4.18-4.23 (m, 1H), 4.25-4.34 (m, 3H), 4.43-4.49 (m, 1H), 6.46-6.56 (m, 1H), 6.61-6.65 (m, 2H), 6.66-7.20 (br s, 4H, interfering with the next three listed signals), 6.96-7.00 (m, 3H), 7.05-7.08 (m, 2H), 7.15-7.17 (m, 1H), 7.20-7.56 (br s, 4H, interfering with the next three listed signals), 7.32-7.36 (m, 2H), 7.39-7.44 (m, 2H), 7.49-7.57 (m, 2H), 7.68-7.78 (m, 2H), 7.85-7.93 (m, 1H), 7.93-7.80 (m, 2H), 8.05-8.17 (m, 2H), 8.22-8.34 (m, 2H), 9.08-9.19 (m, 2H), 9,77 (s, 1H), 10.80 (s, 1H). HRMS (ESI): *m/z* $[M+3H]^{3+}$ calcd. for $[C_{53}H_{84}N_{19}O_{10}]^{3+}$ 382.2211, found: 382.2223. RP-HPLC (220 nm): 98% (t_R = 9.3 min, k = 9.1). $C_{53}H_{81}N_{19}O_{10} \cdot C_6H_3F_9O_6$ (1144.35 + 342.07).

***N*$^{\alpha}$-Succinyl-Arg-Tyr-*N*$^{\omega}$-[(4-aminobutyl)aminocarbonyl]Arg-Trp-Arg-Tyr-amide tetrakis(hydrotrifluoroacetate) (5.25).** Peptide **5.25** was synthesized on a Fmoc-Sieber-PS resin (75 mg, 0.59 mmol/g) according to the general procedure. After coupling of the last amino acid and subsequent Fmoc deprotection, the resin was treated with a solution of succinic anhydride (52.3 mg, 0.443 mmol) and DIPEA (77.1 µL, 0.443 mmol) in DMF/NMP 80:20 v/v (500 µL) at 35 °C for 30 min. The resin was washed with DMF/NMP 80:20 v/v (6 ×) and CH_2Cl_2 (3 ×), followed by cleavage off the resin and deprotection according to the general procedure. Purification by preparative HPLC (system 2, gradient: 0–18 min MeCN/0.1% aq TFA 3:97–42:58, t_R = 11 min) yielded **5.25** as a white solid (24.2 mg, 33%). ^{1}H-NMR (600 MHz, DMSO-d_6): δ (ppm) 1.34-1.59 (m, 14H), 1.61-1.70 (m, 2H), 2.31-2.46 (m, 5H), 2.63-2.74 (m, 2H), 2.75-2.72 (m, 2H), 2.85-2.92 (m, 2H), 2.94-3.22 (m, 10H), 4.14 (m, 1H), 4.20-4.27 (m, 2H), 4.33-4.42 (m, 2H), 4.58 (m, 1H), 6.59-6.66 (m, 4H), 6.75-7.20 (br s, 4H, interfering with the next five signals), 6.90-6.93 (m, 1H), 6.98-7.01 (m, 4H), 7.02-7.04 (m, 1H), 7.06-7.07 (m, 1H), 7.11-7.12 (m, 1H), 7.20-7.50 (br s, 4H, interfering with the next two listed signals), 7.29-7.31 (m, 1H),

7.36-7.38 (m, 1H), 7.54-7.65 (m, 4H), 7.67-7.84 (m, 5H), 7.88 (d, 1H, *J* 7.6 Hz), 8.04 (d, 1H, *J* 7.5 Hz), 8.11 (d, 1 H, *J* 7.5 Hz), 8.16 (d, 1H, *J* 7.5 Hz), 8.41 (br s, 2H), 8.99 (s, 1H), 9.20 (br s, 2H). 10.51 (br s, 1H), 10.75 (s, 1H). ^{13}C-NMR (150 MHz, DMSO-d_6): δ (ppm) 24.3, 24.4, 24.8, 24.9, 25.9, 27.7, 28.7, 28.9, 29.0, 29.1, 29.9, 36.6, 36.8, 38.5, 38.6, 40.3, 40.4, 40.5, 50.2, 52.45, 52.51, 53.2, 54.06, 54.12, 109.8, 111.2, 114.84 (two carbon atoms), 114.86 (two carbon atoms), 115.9 (TFA), 117.9 (TFA), 118.2, 118.5, 120.8, 123.5, 127.3, 127.6 (two carbon atoms), 130.0 (two carbon atoms), 130.1 (two carbon atoms), 136.0, 153.7, 153.9, 155.79, 155.82, 156.7 (two carbon atoms), 158.7 (q, *J* 32 Hz) (TFA), 170.9, 171.2, 171.26, 171.33, 171.5, 171.8, 172.8, 174.0. HRMS (ESI): *m/z* $[M+3H]^{3+}$ calcd. for $[C_{56}H_{84}N_{19}O_{12}]^{3+}$ 404.8843, found: 404.8850. RP-HPLC (220 nm): 98% (t_R = 4.4 min, *k* = 3.8). $C_{56}H_{81}N_{19}O_{12} \cdot C_8H_4F_{12}O_8$ (1212.39 + 456.09).

(9*R*,12*R*,15*R*)-N-((*R*)-1-(((*R*)-1-(((*R*)-1-Amino-3-(4-hydroxyphenyl)-1-oxopropan-2-yl)amino)-5-guanidino-1-oxopentan-2-yl)amino)-3-(1*H*-indol-3-yl)-1-oxopropan-2-yl)-15-(3-guanidinopropyl)-12-(4-hydroxybenzyl)-4-imino-2,11,14,17,20-pentaoxo-1,3,5,10,13,16,21-heptaazacyclopentacosane-9-carboxamide tris(hydrotrifluoroacetate) (5.26). Peptide **5.25** (10.5 mg, 6.293 µmol), HOBt (4.8 mg, 0.031 mmol) and DIPEA (11.0 µL, 0.063 mmol) were dissolved in DMF/NMP 80:20 v/v (500 µL) in a round-bottom flask. Under stirring, a solution of PyBOP (16.4 mg, 0.031 mmol) in DMF/NMP 80:20 v/v (500 µL) was added and stirring was continued at rt overnight. 0.1% aq TFA (30 mL) was added followed by freeze-drying and purification by preparative HPLC (system 2, gradient: 0–18 min MeCN/0.1% aq TFA 3:97–42:58, t_R = 12 min) to yield **5.26** as a white solid (3.9 mg, 45%). ^{1}H-NMR (600 MHz, DMSO-d_6: δ (ppm) 1.22-1.27 (m, 1H), 1.34-1.47 (m, 12H), 1.48-1.54 (m, 2H), 1.56-1.60 (m, 1H), 1.62-1.68 (m, 2H), 2.28-2.37 (m, 4H), 2.68-2.77 (m, 2H), 2.81-2.91 (m, 3H), 2.93-3.08 (m, 7H), 3.12-3.16 (m, 2H), 4.04-4.11 (m, 1H), 4.20-4.29 (m, 2H), 4.32-4.38 (m, 2H), 4.56-4.61 (m, 1H), 6.48-6.58 (m, 1H), 6.62-6.66 (m, 4H), 6.70-7.20 (br s, 4H, interfering with the next five listed signals), 6.92-6.94 (m, 1H), 6.98-7.03 (m, 5H), 7.03-7.05 (m, 1H), 7.06-7.08 (m, 1H), 7.11-7.13 (m, 1H), 7.20-7.60 (br s, 4H, interfering with the next five listed signals), 7.29-7.31 (m, 1H), 7.36-7.39 (m, 1H), 7.43-7.47 (m, 2H), 7.49-7.54 (m, 1H), 7.56-7.60 (m, 1H), 7.76-7.80 (m, 1H), 7.87-7.91 (m, 1H), 7.92-7.96 (m, 1H), 7.96-8.00 (m, 1H), 8.06-8.16 (m, 2H), 8.25-8.31 (m, 1H), 9.08-9.24 (m, 3H), 9.95 (br s, 1H), 10.73-10.78 (m, 1H). HRMS (ESI): *m/z* $[M+3H]^{3+}$ calcd. for $[C_{56}H_{82}N_{19}O_{11}]^{3+}$ 398.8808, found: 398.8816. RP-HPLC (220 nm): 99% (t_R = 3.4 min, *k* = 2.7). $C_{56}H_{79}N_{19}O_{11} \cdot C_6H_3F_9O_6$ (1194.37 + 342.07).

***N*$^{\alpha}$-Succinyl-Arg-Tyr-*N*$^{\omega}$-[(3-aminopropyl)aminocarbonyl]Arg-Leu-Arg-Tyr-amide tetrakis(hydrotrifluoroacetate) (5.27).** Peptide **5.27** was synthesized on a Fmoc-Sieber-PS resin (75 mg, 0.59 mmol/g) according to the general procedure. After coupling of the last amino acid and subsequent Fmoc deprotection, the resin was treated with a solution of succinic anhydride (52.3 mg, 0.443 mmol) and DIPEA (77.1 µL, 0.443 mmol) in DMF/NMP 80:20 v/v

(500 µL) at 35 °C for 30 min. The resin was washed with DMF/NMP 80:20 v/v (6 ×) and CH_2Cl_2 (3 ×), followed by cleavage off the resin and deprotection according to the general procedure. Purification by preparative HPLC (system 2, gradient: 0–18 min MeCN/0.1% aq TFA 3:97–42:58, t_R = 10 min) yielded **5.27** as a white solid (13.3 mg, 22%). ^{1}H-NMR (600 MHz, DMSO-d_6): δ (ppm) 0.81-0.90 (m, 6H), 1.37-1.67 (m, 14H), 1.69-1.77 (m, 3H), 2.36-2.47 (m, 3H), 2.68-2.75 (m, 2H), 2.78-2.88 (m, 4H), 2.89-2.99 (m, 2H), 3.01-3.10 (m, 4H), 3.13-3.20 (m, 2H), 3.21-3.28 (m, 2H), 4.10-4.16 (m, 1H), 4.17-4.23 (m, 1H), 4.24-4.35 (m, 3H), 4.38-4.43 (m, 1H), 6.59-6.68 (m, 4H), 6.80-7.20 (br s, 4H, interfering with the next three listed signals), 6.96-7.01 (m, 4H), 7.04-7.08 (m, 2H), 7.10-7.13 (m, 1H), 7.20-7.55 (br s, 4H, interfering with the next listed signal), 7.34-7.37 (m, 1H), 7.61-7.67 (m, 2H), 7.68-7.75 (m, 2H), 7.78-7.86 (m, 3H), 8.00-8.12 (m, 2H), 8.12-8.17 (m, 1H), 8.36-8.56 (m, 2H), 9.01 (s, 1H), 9.22 (br s, 1H), 10.42-10.72 (m, 1H), 12.15 (br s, 1H). ^{13}C-NMR (150 MHz, DMSO-d_6): δ (ppm) 21.4, 21.8, 22.6, 23.1, 24.1, 24.9, 25.0, 27.2, 28.7, 28.8, 29.1, 29.9, 36.4, 36.6 (two carbon atoms), 36.8, 40.3, 40.4, 40.5, 40.6, 51.0, 52.2, 52.3, 52.6, 53.9, 54.1, 114.9 (four carbon atoms), 115.8 (TFA), 117.8 (TFA), 127.47, 127.50, 130.0 (four carbon atoms), 153.7, 154.0, 155.81, 155.84, 156.8 (two carbon atoms), 158.7 (q, *J* 32 Hz), 170.8, 171.1, 171.2, 171.5, 171.8, 172.0, 172.7, 174.0. HRMS (ESI): *m/z* $[M+3H]^{3+}$ calcd. for $[C_{50}H_{83}N_{18}O_{12}]^{3+}$ 375.8807, found: 375.8811. RP-HPLC (220 nm): 97% (t_R = 3.2 min, *k* = 2.5). $C_{50}H_{80}N_{18}O_{12} \cdot C_8H_4F_{12}O_8$ (1125.30 + 456.09).

(15*S*,18*S*,21*S*)-*N*-((*S*)-1-(((*S*)-1-(((*S*)-1-Amino-3-(4-hydroxyphenyl)-1-oxopropan-2-yl)amino)-5-guanidino-1-oxopentan-2-yl)amino)-4-methyl-1-oxopentan-2-yl)-15-(3-guanidinopropyl)-18-(4-hydroxybenzyl)-2-imino-4,10,13,16,19-pentaoxo-1,3,5,9,14,17,20-heptaazacyclotetracosane-21-carboxamide tris(hydrotrifluoroacetate) (5.28). Peptide **5.27** (7.8 mg, 4.930 µmol), HOBt (3.8 mg, 0.025 mmol) and DIPEA (8.6 µL, 0.049 mmol) were dissolved in DMF/NMP 80:20 v/v (500 µL) in a round-bottom flask. Under stirring, a solution of PyBOP (12.8 mg, 0.025 mmol) in DMF/NMP 80:20 v/v (500 µL) was added and the mixture was stirred at rt overnight. 0.1% aq TFA (30 mL) was added followed by lyophilization and purification by preparative HPLC (system 2, gradient: 0–18 min MeCN/0.1% aq TFA 3:97–42:58, t_R = 11 min) to yield **5.28** as a white solid (3.7 mg, 52%). ^{1}H-NMR (600 MHz, DMSO-d_6): δ (ppm) 0.84-0.89 (m, 6H), 1.35-1.70 (m, 19H), 1.72-1.77 (m, 1H), 2.28-2.35 (m, 3H), 2.70-2.73 (m, 1H), 2.75-2.81 (m, 1H), 2.84-2.89 (m, 1H), 2.90-2.98 (m, 2H), 2.99-3.09 (m, 5H), 3.15-3.21 (m, 2H), 3.91-4.06 (m, 1H), 4.17-4.23 (m, 1H), 4.24-4.41 (m, 4H), 6.61-6.95 (br s, 4H, interfering with the next listed signal), 6.61-6.66 (m, 4H), 6.95-7.44 (br s, 4H, interfering with the next three listed signals), 6.97-6.99 (m, 3H), 7.04-7.13 (m, 3H), 7.35-7.44 (m, 4H), 7.70-7.74 (m 1H), 7.75-7.81 (m, 1H), 7.87 (s, 2H), 7.96-8.04 (m, 2H), 8.12-8.33 (m, 3H), 9.15-9.19 (m, 2H), 9.61-9.81 (m, 1H). HRMS (ESI): *m/z* $[M+3H]^{3+}$ calcd. for $[C_{50}H_{81}N_{18}O_{11}]^{3+}$ 369.8772, found: 369.8783. RP-HPLC (220 nm): 99% (t_R = 4.9 min, *k* = 4.3). $C_{50}H_{78}N_{18}O_{11} \cdot C_6H_3F_9O_6$ (1107.29 + 342.07).

N^{α}-Succinyl-Arg-Tyr-N^{ω}-[(3-aminopropyl)aminocarbonyl]Arg-Trp-Arg-Tyr-amide tetrakis(hydrotrifluoroacetate) (5.29). Peptide **5.29** was synthesized on a Fmoc-Sieber-PS resin (75 mg, 0.59 mmol/g) according to the general rocedure. After coupling of the last amino acid and subsequent Fmoc deprotection, the resin was treated with a solution of succinic anhydride (52.3 mg, 0.443 mmol) and DIPEA (77.1 µL, 0.443 mmol) in DMF/NMP 80:20 v/v (500 µL) at 35 °C for 30 min. The resin was washed with DMF/NMP 80:20 v/v (6 ×) and CH_2Cl_2 (3 ×), followed by cleavage off the resin and deprotection according to the general procedure. Purification by preparative HPLC (system 2, gradient: 0–18 min MeCN/0.1% aq TFA 3:97–42:58, t_R = 11 min) yielded **5.29** as a white solid (11.6 mg, 18%). ^{1}H-NMR (600 MHz, DMSO-d_6): δ (ppm) 1.31-1.78 (m, 15H), 2.34-2.46 (m, 4H), 2.65-2.74 (m, 2H), 2.77-2.83 (m, 2H), 2.85-2.91 (m, 2H), 2.96-3.07 (m, 5H), 3.15-3.22 (m, 4H), 4.12-4.16 (m, 1H), 4.20-4.26 (m, 2H), 4.33-4.42 (m, 2H), 4.55-4.61 (m, 1H), 6.60-6.66 (m, 4H), 6.80-7.20 (br s, 4H, interfering with the next five listed signals), 6.90-6.93 (m, 1H), 6.98-7.01 (m, 4H), 7.02-7.04 (m, 1H), 7.06-7.08 (m, 1H), 7.11-7.12 (m, 1H), 7.20-7.43 (br s, 4H, interfering with the next two listed signals), 7.29-7.31 (m, 1H), 7.36-7.38 (m, 1H), 7.55-7.62 (m, 3H), 7.65-7.69 (m, 1H), 7.70-7.74 (m, 1H), 7.75-7.84 (m, 4H), 7.86-7.90 (m, 1H), 8.01-8.06 (m, 1H), 8.09-8.13 (m, 1H), 8.14-8.18 (m, 1H), 8.43 (br s, 2H), 8.97 (s, 1H), 9.19 (br s, 2H), 10.57 (br s, 1H), 10.75 (s, 1H), 12.18 (br s, 1H). ^{13}C-NMR (150 MHz, DMSO-d_6): δ (ppm) 24.4, 24.8, 24.9, 27.2, 27.7, 28.7, 28.9, 29.0, 29.1, 29.9, 36.2, 36.5, 36.6, 36.8, 40.37, 40.42, 40.5, 52.3, 52.4, 52.5, 53.2, 54.05, 54.10, 109.8, 111.2, 114.8 (two carbon atoms), 114.9 (two carbon atoms), 116.0 (TFA), 118.0 (TFA), 118.2, 118.5, 120.8, 123.5, 127.3, 127.56, 127.62, 130.0 (two carbon atoms), 130.1 (two carbon atoms), 136.0, 153.7, 155.78, 155.82, 156.7 (three carbon atoms), 158.6 (q, *J* 32 Hz) (TFA), 170.9, 171.1, 171.26, 171.32, 171.5, 171.8, 172.8, 174.0. HRMS (ESI): *m/z* $[M+3H]^{3+}$ calcd. for $[C_{55}H_{82}N_{18}O_{12}]^{3+}$ 400.2125, found: 400.2129. RP-HPLC (220 nm): 99% (t_R = 6.6 min, *k* = 6.2). $C_{55}H_{79}N_{19}O_{12} \cdot C_8H_4F_{12}O_8$ (1198.36 + 456.09).

(15*S*,18*S*,21*S*)-*N*-((*S*)-1-(((*S*)-1-(((*S*)-1-Amino-3-(4-hydroxyphenyl)-1-oxopropan-2-yl)amino)-5-guanidino-1-oxopentan-2-yl)amino)-3-(1*H*-indol-3-yl)-1-oxopropan-2-yl)-15-(3-guanidinopropyl)-18-(4-hydroxybenzyl)-2-imino-4,10,13,16,19-pentaoxo-1,3,5,9,14,17,20-heptaazacyclotetracosane-21-carboxamide tris(hydrotrifluoroacetate) (5.30). Peptide **5.29** (6.9 mg, 4.171 µmol), HOBt (3.2 mg, 0.021 mmol) and DIPEA (7.3 µL, 0.042 mmol) were dissolved in DMF/NMP 80:20 v/v (500 µL) in a round-bottom flask. Under stirring, a solution of PyBOP (10.9 mg, 0.030 mmol) in DMF/NMP 80:20 v/v (500 µL) was added and stirring was continued at rt overnight. 0.1% aq TFA (30 mL) was added followed by freeze-drying and purification by preparative HPLC (system 2, gradient: 0–18 min MeCN/0.1% aq TFA 3:97–42:58, t_R = 12 min) to afford **5.30** as a white solid (3.3 mg, 60%). ^{1}H-NMR (600 MHz, DMSO-d_6): δ (ppm) 1.20-1.29 (m, 2H), 1.32-1.58 (m, 12H), 1.61-1.71 (m, 3H), 2.30-2.34 (m, 2H), 2.69-2.78 (m, 2H), 2.85-3.07 (m, 9H), 3.10-3.17 (m, 3H), 4.00-4.07 (m, 1H), 4.19-4.29

(m, 2H), 4.32-4.38 (m, 2H), 4.54-4.59 (m, 1H), 6.52 (s, 1H), 6.62-6.66 (m, 4H), 6.70-7.20 (br s, 4H, interfering with the next five listed signals), 6.92-6.94 (m, 1H), 6.99-7.02 (m, 4H), 7.03-7.05 (m, 1H), 7.06-7.11 (m, 2H), 7.13-7.15 (m, 1H), 7.20-7.48 (br s, 4H, interfering with the next three listed signals), 7.29-7.31 (m, 1H), 7.36-7.38 (m, 1H), 7.40-7.48 (m, 3H), 7.56-7.59 (m, 1H), 7.74-7.79 (m, 1H), 7.84-7.92 (m, 3H), 7.95-8.00 (m, 1H), 8.04-8.15 (m, 2H), 8.18-8.28 (m, 2H), 9.17-9.19 (m, 2H), 10.02 (br s, 1H), 10.75 (br s, 1H). HRMS (ESI): *m/z* $[M+3H]^{3+}$ calcd. for $[C_{50}H_{80}N_{19}O_{11}]^{3+}$ 394.2089, found: 394.2100. RP-HPLC (220 nm): 97% (t_R = 7.8 min, k = 7.5). $C_{50}H_{77}N_{19}O_{11} \cdot C_6H_3F_9O_6$ (1180.34 + 342.07).

N^{α}-Succinyl-Arg-Tyr-Arg-Leu-N^{ω}-[(3-aminopropyl)aminocarbonyl]Arg-Tyr-amide tetrakis(hydrotrifluoroacetate) (5.31). Peptide **5.31** was synthesized on a Fmoc-Sieber-PS resin (75 mg, 0.59 mmol/g) according to the general procedure. After coupling of the last amino acid and subsequent Fmoc deprotection, the resin was treated with a solution of succinic anhydride (52.3 mg, 0.443 mmol) and DIPEA (77.1 µL, 0.443 mmol) in DMF/NMP 80:20 v/v (500 µL) at 35 °C for 30 min. The resin was washed with DMF/NMP 80:20 v/v (6 ×) and CH_2Cl_2 (3 ×), followed by cleavage off the resin and deprotection according to the general procedure. Purification by preparative HPLC (system 2, gradient: 0–18 min MeCN/0.1% aq TFA 3:97–42:58, t_R = 10 min) yielded **5.31** as a white solid (14.4 mg, 24%). ^{1}H-NMR (600 MHz, DMSO-d_6): δ (ppm) 0.84 (d, 3H, *J* 6.3 Hz), 0.88 (d, 3H, *J* 6.5 Hz), 1.35-1.68 (m, 15H), 1.69-1.76 (m, 3H), 2.33-2.47 (m, 4H), 2.66-2.75 (m, 2H), 2.79-2.83 (m, 2H), 2.84-2.88 (m, 1H), 2.89-2.94 (m, 1H), 3.01-3.06 (m, 2H), 3.07-3.12 (m, 2H), 3.15-3.24 (m, 4H), 4.11-4.16 (m, 1H), 4.19-4.23 (m, 1H), 4.24-4.34 (m, 3H), 4.39-4.45 (m, 1H), 6.58-6.69 (m, 4H), 6.80-7.20 (br s, 4H, interfering with the next three listed signals), 6.96-7.00 (m, 4H), 7.06-7.07 (m, 1H), 7.08-7.12 (m, 1H), 7.20-7.50 (br s, 4H, interfering with the next listed signal), 7.35-7.38 (m, 1H), 7.60-7.63 (m, 1H), 7.64-7.71 (m, 2H), 7.75-7.84 (m, 4H), 7.85-7.89 (m, 1H), 8.01-8.04 (m, 1H), 8.06-8-10 (m, 1H), 8.14 (d, 1H, *J* 7.4 Hz), 8.47 (br s, 2H), 9.00 (s, 1H), 9.25 (br s, 2H), 10.40-10.70 (m, 1H). ^{13}C-NMR (150 MHz, DMSO-d_6): δ (ppm) 21.4, 23.1, 24.1, 24.3, 25.0, 27.2, 28.7, 28.8, 28.9, 29.0, 29.1, 29.9, 36.3, 36.5, 36.7 (two carbon atoms), 40.4 (two carbon atoms), 40.5, 40.6, 51.0, 52.1, 52.3, 52.6, 54.0, 54.1, 114.84 (two carbon atoms), 114.87 (two carbon atoms), 115.9 (TFA), 117.9 (TFA), 127.46, 127.49, 130.03 (two carbon atoms), 130.06 (two carbon atoms), 153.7, 153.9, 155.8 (two carbon atoms), 156.8 (two carbon atoms), 158.7 (q, *J* 32 Hz) (TFA), 170.8, 171.0, 171.1, 171.4, 171.8, 172.0, 172.7, 174.0. HRMS (ESI): *m/z* $[M+3H]^{3+}$ calcd. for $[C_{50}H_{83}N_{18}O_{12}]^{3+}$ 375.8807, found: 375.8813. RP-HPLC (220 nm): 99% (t_R = 4.5 min, k = 3.9). $C_{50}H_{80}N_{18}O_{12} \cdot C_8H_4F_{12}O_8$ (1125.30 + 456.09).

(15*S*,18*S*,21*S*,24*S*,27*S*)-*N*-((*S*)-1-Amino-3-(4-hydroxyphenyl)-1-oxopropan-2-yl)-15,21-bis(3-guanidinopropyl)-18-(4-hydroxybenzyl)-2-imino-24-isobutyl-4,10,13,16,19,22,25-heptaoxo-1,3,5,9,14,17,20,23,26-nonaazacyclotriacontane-27-carboxamide tris(hydrotrifluoroacetate) (5.32). Peptide **5.31** (9.5 mg, 6.007 µmol), HOBt (4.6 mg, 0.030

mmol) and DIPEA (10.5 µL, 0.060 mmol) were dissolved in DMF/NMP 80:20 v/v (500 µL) in a round-bottom flask. Under stirring, a solution of PyBOP (17.1 mg, 0.030 mmol) in DMF/NMP 80:20 v/v (500 µL) was added and the mixture was stirred at rt overnight. 0.1% aq TFA (30 mL) was added followed by freeze-drying and purification by preparative HPLC (system 2, gradient: 0–18 min MeCN/0.1% aq TFA 3:97–42:58, t_R = 10 min) to yield **5.32** as a white solid (4.8 mg, 55%). ^{1}H-NMR (600 MHz, DMSO-d_6): δ (ppm) 0.79-0.92 (m, 6H), 1.23-1.28 (m, 5H), 1.35-1.68 (m, 16H), 1.70-1.80 (m, 3H), 2.23-2.29 (m, 1H), 2.67-2.73 (m, 1H), 2.87-3.03 (m, 8H), 3.60-3.65 (m, 1H), 3.85-3.92 (m, 1H), 4.09-4.14 (m, 1H), 4.16-4.29 (m, 3H), 4.30-4.34 (m, 1H), 6.60-7.20 (br s, 4H, interfering with the next three listed signals), 6.61-6.69 (m, 4H), 6.99-7.05 (m, 4H), 7.06-7.09 (m, 1H), 7.20-7.60 (br s, 4H, interfering with the next two listed signals), 7.29-7.32 (m, 1H), 7.41-7.51 (m, 4H), 7.62-7.69 (m, 1H), 7.71-7.83 (m, 3H), 7.95-8.04 (m, 1H), 8.19 (br s, 2H), 8.56 (s, 1H), 9.04 (s, 1H), 9.15 (s, 1H), 9.20 (s, 1H), 9.73 (s, 1H). HRMS (ESI): *m/z* $[M+3H]^{3+}$ calcd. for $[C_{50}H_{81}N_{18}O_{11}]^{3+}$ 369.8772, found: 369.8797. RP-HPLC (220 nm): 98% (t_R = 3.1 min, k = 2.4). $C_{50}H_{78}N_{18}O_{11} \cdot C_6H_3F_9O_6$ (1107.29 + 342.07).

(6*S*,9*S*,12*S*,15*S*,18*S*)-1-Amino-6-(((*S*)-1-amino-3-(4-hydroxyphenyl)-1-oxopropan-2-yl)carbamoyl)-12-(3-(2-(5-aminopentanamido)acetamido)propyl)-18-(4-guanidinobutyl)-15-(4-hydroxybenzyl)-1-imino-9-isobutyl-8,11,14,17,20-pentaoxo-2,7,10,13,16,19-hexaazatricosan-23-oic-acid tris(hydrotrifluoroacetate) (5.33). Peptide **5.33** was synthesized on a Fmoc-Sieber-PS resin (75 mg, 0.59 mmol/g) according to the general procedure. After coupling of the last amino acid and subsequent Fmoc deprotection, the resin was treated with a solution of succinic anhydride (52.3 mg, 0.443 mmol) and DIPEA (77.1 µL, 0.443 mmol) in DMF/NMP 80:20 v/v (500 µL) at 35 °C for 30 min. The resin was washed with DMF/NMP 80:20 v/v (6 ×) and CH_2Cl_2 (3 ×), followed by cleavage off the resin and deprotection according to the general procedure. Purification by preparative HPLC (system 1, gradient: 0–18 min MeCN/0.1% aq TFA 3:97–42:58, t_R = 12 min) yielded **5.33** as a white solid (27.6 mg, 31%). ^{1}H-NMR (600 MHz, DMSO-d_6): δ (ppm) 0.81-0.90 (m, 6H), 1.21-1.37 (m, 4H), 1.38-1.57 (m, 14H), 1.58-1.71 (m, 5H), 2.34-2.47 (m, 4H), 2.66-2.80 (m, 6H), 2.83-2.94 (m, 2H), 3.00-3.11 (m, 4H), 4.14-4.34 (m, 6H), 4.40-4.46 (m, 1H), 6.60-6.66 (m, 4H), 6.90-7.20 (br s, 4H, interfering with the next two listed signals), 6.96-6.99 (m, 4H), 7.04-7.07 (m, 1H), 7.20-7.63 (br s, 4H, interfering with the next listed signal), 7.34-7.36 (m, 1H), 7.74-7.81 (m, 4H), 7.84-7.90 (m, 5H), 7.93-8.02 (m, 3H), 8.06-8.15 (m, 2H), 9.26 (s, 2H), 12.18 (br s, 1H). ^{13}C-NMR (150 MHz, DMSO-d_6): δ (ppm) 21.5, 22.38, 22.42, 23.1, 24.3, 25.0, 25.1, 26.70 (two carbon atoms), 26.72, 28.9, 29.0, 29.3, 30.0, 31.1, 31.3, 36.6, 36.8, 38.8 (two carbon atoms), 40.1, 40.45, 40.49, 40.6, 51.3, 52.4, 52.5, 52.8, 54.1, 54.2, 114.96 (two carbon atoms), 115.00 (two carbon atoms), 116.1 (TFA), 118.1 (TFA), 127.5, 127.6, 130.1 (two carbon atoms), 130.2 (two carbon atoms), 155.93, 155.94. 157.0 (two carbon atoms), 159.2 (q, J 32 Hz) (TFA), 171.0, 171.1, 171.4, 171.6, 171.8, 172.1, 172.3, 172.9, 174.1. HRMS (ESI): *m/z* $[M+3H]^{3+}$ calcd. for

$[C_{53}H_{87}N_{16}O_{13}]^{3+}$ 385.2207, found: 385.2210. RP-HPLC (220 nm): 98% (t_R = 7.8 min, k = 7.5). $C_{53}H_{84}N_{16}O_{13} \cdot C_6H_3F_9O_6$ (1153.35 + 342.07).

(2*S*,5*S*,8*S*)-*N*-((*S*)-1-(((*S*)-1-(((*S*)-1-Amino-3-(4-hydroxyphenyl)-1-oxopropan-2-yl)amino)-5-guanidino-1-oxopentan-2-yl)amino)-4-methyl-1-oxopentan-2-yl)-2-(4-guanidinobutyl)-5-(4-hydroxybenzyl)-3,6,13,16,22,25-hexaoxo-1,4,7,12,15,21-hexaazacyclopentacosane-8-carboxamide bis(hydrotrifluoroacetate) (5.34). Peptide **5.33** (15.7 mg, 10.48 µmol), HOBt (8.0 mg, 0.052 mmol) and DIPEA (18.3 µL, 0.105 mmol) were dissolved in DMF/NMP 80:20 v/v (500 µL) in a round-bottom flask. Under stirring, a solution of PyBOP (27.3 mg, 0.052 mmol) in DMF/NMP 80:20 v/v (500 µL) was added and stirring was continued at rt overnight. 0.1% aq TFA (30 mL) was added followed by lyophilization and purification by preparative HPLC (system 1, gradient: 0–18 min MeCN/0.1% aq TFA 3:97–42:58, t_R = 12 min) to yield **5.34** as a white solid (10.7 mg, 75%). ^{1}H-NMR (600 MHz, DMSO-d_6): δ (ppm) 0.80-0.90 (m, 6H), 1.09-1.17 (m, 1H), 1.28-1.58 (m, 17H), 1.59-1.71 (m, 5H), 2.33-2.48 (m, 3H), 2.68-2.79 (m, 4H), 2.80-2.98 (m, 4H), 2.99-3.08 (m, 4H), 3.80-3.83 (m, 1H), 3.99-4.02 (m, 1H), 4.13-4.23 (m, 3H), 4.24-4.33 (m, 2H), 6.59-6.69 (m, 4H), 6.80-7.20 (br s, 4H, interfering with the next two listed signals), 6.96-7.02 (m, 4H), 7.05-7.07 (m, 1H), 7.20-7.54 (br s, 4H, interfering with the next listed signal), 7.25-7.27 (m, 1H), 7.56-7.60 (m, 1H), 7.62-7.83 (m, 10H), 8.02-8.07 (m, 1H), 8.41-8.46 (m, 1H), 9.23 (br s, 2H). ^{13}C-NMR (150 MHz, DMSO-d_6): δ (ppm) 21.5, 22.4, 22.5, 23.1, 24.1, 24.8, 25.2, 26.6, 26.7 (two carbon atoms), 28.1, 28.2, 28.7, 30.0, 30.6, 30.7, 35.9, 36.7, 38.6 (two carbon atoms), 40.3, 40.4, 40.5, 51.4, 52.5, 53.1, 54.2, 55.2, 55.4, 114.9 (two carbon atoms), 115.0 (two carbon atoms), 115.9 (TFA), 117.9 (TFA), 127.7, 127.9, 129.8 (two carbon atoms), 130.1 (two carbon atoms), 155.8, 155.9, 156.78, 156.84, 158.8 (q, J 32 Hz) (TFA), 170.0, 170.9, 171.4, 171.8, 171.9, 172.1, 172.2, 172.7, 172.8, 174.1. HRMS (ESI): *m/z* $[M+3H]^{3+}$ calcd. for $[C_{53}H_{85}N_{16}O_{12}]^{3+}$ 379.2172, found: 379.2177. RP-HPLC (220 nm): 98% (t_R = 8.9 min, k = 8.7). $C_{53}H_{82}N_{16}O_{12} \cdot C_4H_2F_6O_4$ (1135.34 + 228.04).

(9*S*,12*S*,15*S*)-*N*-((*S*)-1-amino-4-methyl-1-oxopentan-2-yl)-15-(3-guanidinopropyl)-12-(4-hydroxybenzyl)-4-imino-2,11,14,17,20-pentaoxo-1,3,5,10,13,16,21-heptaazacyclopentacosane-9-carboxamide bis(hydrotrifluoroacetate) (5.35). A solution of PyBOP (10.9 mg, 0.021 mmol) in DMF/NMP 80:20 v/v (500 µL) was added to a stirred solution of the linear precursor peptide (6.9 mg, 4.171 µmol) (prepared by SPPS), HOBt ((3.2 mg, 0.021 mmol) and DIPEA (7.3 µL, 0.042 mmol) in DMF/NMP 80:20 v/v (500 µL) and stirring was continued at rt overnight. 0.1% aq TFA (30 mL) was added followed by freeze-drying and purification by preparative HPLC (system 2, gradient: 0–18 min MeCN/0.1% aq TFA 3:97–42:58, t_R = 9 min) yielding **5.35** as a white solid (9.4 mg, 54%). ^{1}H-NMR (600 MHz, DMSO-d_6): δ (ppm) 0.76-0.93 (m, 6H), 7.36-7.68 (m, 15H), 2.77-2.84 (m, 1H), 2.88-2.97 (m, 3H), 2.99-3.08 (m, 4H), 3.09-3.15 (m, 2H), 4.13-4.19 (m, 1H), 4.21-4.28 (m, 2H), 4.29-4.34 (m, 1H), 4.41-4.48 (m, 1H), 6.60-6.67 (m, 2H), 6.80-7.20 (br s, 4H, interfering with the next two listed

signals), 6.97-7.01 (m, 2H), 7.16-7.19 (m, 1H), 7.20-7.52(br s, 4H, interfering with the next two listed signals), 7.42-7.44 (m, 1H), 7.48-7.51 (m, 1H), 7.69-7.75 (m, 1H), 7.81-7.86 (m, 1H), 7.89-7.99 (m, 4H), 8.19-8.33 (m, 2H), 9.22-9.27 (m, 1H), 10.30 (s, 1H). HRMS (ESI): *m/z* $[M+2H]^{2+}$ calcd. for $[C_{36}H_{61}N_{13}O_8]^{2+}$ 401.7378, found: 401.7381. RP-HPLC (220 nm): 98% (t_R = 3.9 min, k = 3.2). $C_{36}H_{59}N_{13}O_8 \cdot C_4H_2F_6O_4$ (801.95 + 228.04).

5.4.5 Pharmacological Assays

Cell Culture. Cells were cultured in 75 cm^2 flasks (Sarstedt, Nümbrecht, Germany) in a humidified atmosphere (95% air, 5% CO_2) at 37 °C. The culture media used to maintain SK-N-MC neuroblastoma cells,[24] CHO-hY_2R cells,[13] CHO-hY_4-G_{qi5}-mtAEQ cells,[23] HEC-1B-hY_5 cells,[25] HEK293T-ARRB1-hY_4R and HEK293T-ARRB2-hY_4R cells[10] were described elsewhere.

Buffers and Media used for Binding and Functional Assays. Buffer I (used for binding experiments at the Y_2R and Y_4R): a hypotonic sodium-free HEPES buffer (25 mM HEPES, 2.5 mM $CaCl_2$, 1 mM $MgCl_2$, pH 7.4) supplemented with BSA (Serva, Heidelberg, Germany) (1%) and 0.1 mg/mL bacitracin (Serva). Buffer II (used for binding experiments at the Y_1R and Y_5R): an isotonic sodium-containing HEPES buffer (150 mM NaCl, 10 mM HEPES, 25 mM $NaHCO_3$, 2.5 mM $CaCl_2$, 5 mM KCl) supplemented with 1% BSA. Buffer III (used for the functional Ca^{2+}-aequorin Y_4R assay): an isotonic sodium-containing HEPES buffer, containing 120 mM NaCl, 25 mM HEPES, 1.5 mM $CaCl_2$, 1 mM $MgCl_2$, 5 mM KCl and 10 mM D-glucose. L15 medium (used for the β-arrestin recruitment assays): phenol red-free Leibovitz's L-15 medium (140 mM NaCl, 1.3 mM $CaCl_2$, 1 mM $MgCl_2$, various amino acids and vitamins, pH 7.4) (Thermo Fischer Scientific, Nidderau, Germany) supplemented with 10 mM HEPES and 5% FCS.

Radioligand Binding Assays. Y_1R Binding. Competition binding experiments at Y_1R-expressing SK-N-MC neuroblastoma cells were performed in *buffer II* as described previously using the radioligand [^{3}H]**5.37** (K_d = 0.044 nM, used concentration: 0.15 nM).[24]

Y_2R Binding. Competition binding experiments at CHO-hY_2R cells were performed in *buffer I* as previously reported using the radioligand [^{3}H]propionyl-pNPY (K_d = 0.14 nM, used concentration: 0.5 nM).[13]

Y_4R Binding. Competition binding experiments at CHO-hY_4-G_{qi5}-mtAEQ cells were performed using the previously described radioligand [^{3}H]**5.36** (K_d = 0.67 nM, used concentration: 1 nM).[21] Cells were grown to 80-100% confluency. The culture medium was replaced by *buffer I* (without BSA and bacitracin) and the cells were scraped off the culture flask followed by centrifugation for 5 min at 300g. The supernatant was discarded and the cells were resuspended in *buffer I*

at a density of 500,000 cells/mL. 20 µL of a 10fold concentrated solution of the compound of interest in *buffer I*, neat *buffer I* (total binding) or 20 µL of a 10fold concentrated solution of hPP in *buffer I* (10 µM, final concentration: 1 µM), and 20 µL of a 10fold concentrated solution of [^{3}H]**5.36** in *buffer I* (10 nM, final concentration: 1 nM) were added per well in Primaria 96-well plates (Corning Life Sciences, Oneonta, NY). 160 µL of the cell suspension were added to each well followed by incubation at 23 °C under gentle shaking for 90 min. Cells were collected on GF/C filters (Whatman, Maidstone, UK) (pretreated with 0.3% polyethylenimine for 30 min) using a Brandel Harvester (Brandel, Gaithersburg, MD, USA) and were washed twice with cold (4 °C) PBS. Filter pieces for each well were punched out and transferred into 1450-401 96-well plates (PerkinElmer). Scintillation cocktail (200 µL, Rotiscint Eco Plus, Carl Roth GmbH, Karlsruhe, Germany) was added and the plates were sealed with a 1450−461 transparent sealing tape (PerkinElmer). After incubation in the dark for at least 60 min, radioactivity (ccpm) was measured with a MicroBeta2 plate counter (PerkinElmer).

Y_5R Binding. Competition binding experiments at HEC-1B-hY_5 cells were performed in *buffer II* as described previously using the radioligand [^{3}H]propionyl-pNPY (K_d = 4.8 nM, used concentration: 4 nM).[21]

All radioligand competition binding assays were performed at 23 ± 1 °C. In the case of Y_1R, Y_2R and Y_5R binding studies, no curve fitting was performed due to low radioligand displacement. Specific binding data obtained from Y_4R binding studies were analyzed by a four parameter logistic fit (log(inhibitor) vs. response – variable slope; GraphPad Prism 5.0, GraphPad Software, San Diego, CA) to obtain pIC_{50} values. The latter were converted to pK_i values according to the Cheng-Prusoff equation[32] (logarithmic form).

***β*-Arrestin Recruitment Assay.** The assay was performed with live HEK293T-ARRB1-Y_4R and HEK293T-ARRB2-Y_4R cells[10] in L15 medium as described previously.[13] Measurements were performed with EnSpire multimode plate reader (Perkin Elmer, Rodgau, Germany). Relative luminescences (100% = 1 µM hPP (agonist mode) or 10 nM hPP (antagonist mode), 0% = neat buffer) were plotted against log(concentration of agonist or antagonist) and analyzed by four-parameter logistic fits (GraphPad Prism 5.0) to obtain pEC_{50} (agonists) or pIC_{50} (antagonists) values. Efficacies α (maximum effect relative to 1 µM hPP) of (partial) agonists were calculated based on the upper plateaus of the concentration-response curves. pEC_{50} values of hPP amounted to 8.66 (β-arrestin 1) and 8.37 (β-arrestin 2) (see also Table 2).

Ca^{2+}-Aequorin Assay. The assay was perfomed with live CHO-hY_4R-G_{qi5}-mtAEQ cells and buffer III as described previously.[23,13] Measurements were performed with a GENius Pro plate reader (Tecan, Salzburg, Austria). Areas under the curve were calculated using GraphPad Prism 5.0 (GraphPad software). Fractional luminescences (calculated by dividing the area of peak 1 by the total area (peaks 1 and 2)) were normalized (100% = fractional luminescence

obtained from 1 µM hPP (agonist mode) or 100 nM hPP (antagonist mode), 0% = basal effect in the absence of agonist; GraphPad Prism 5.0) and relative responses were plotted against log(concentration of agonist) or log(concentration of antagonist) followed by fitting according to a four-parameter logistic equation (log(agonist) vs. response – variable slope, or log(inhibitor) vs. response – variable slope; GraphPad Prism 5.0) to obtain pEC_{50} and pIC_{50} values, respectively. Efficacies α (maximum effect relative to 1 µM hPP) of (partial) agonists were calculated based on the upper plateaus of the concentration-response curves. Note: due to a lower pEC_{50} value of hPP determined in the Ca^{2+}-aequorin assay (pEC_{50} = 7.96) compared to the arrestin assays (pEC_{50} = 8.66 and 8.37, respectively), different concentrations of hPP were used in antagonist mode (Ca^{2+}-aequorin assay: 100 nM, arrestin assay: 10 nM).

5.4.6 Stabilities in Human Plasma and PBS

Stability in Human Plasma. The investigation of the stabilities of **5.5**, **5.18** and **5.24** in human plasma was performed using a reported protocol.[33] 1-Methyl-D-tryptophane (**5.41**) was used as internal standard. Samples were analyzed by analytical RP-HPLC using the system and conditions as described under general experimental conditions (purity controls), but applying a different linear gradient: 0-14 min: MeCN/0.04% aq. TFA 12:88-25:75, 14-15 min: 25:75-95:5, 15-19 min: 95:5 (isocratic). Based on four-point calibrations, peak areas were transformed into concentrations (µM) and percent recoveries of the peptides (determined for two concentrations in plasma: 4 µM and 80 µM) and the internal standard **5.41** were calculated based on the average values of the 100% reference samples (see Table S1, Supporting Information). Recovery ratios were obtained by dividing the recovery of the peptide by the recovery of **5.41** for each individual sample followed by the calculation of mean recovery ratios (n = 5, cf. Table S1, Supporting Information). In the case of the determination of plasma stabilities, recoveries of **5.5**, **5.18** and **5.24** were calculated by multiplying the recovery of **5.41**, obtained for each individual sample, with the mean recovery ratio obtained for the concentration of 80 µM (incubation times 0.5, 1 and 2 h in the case of **5**, all incubation times in the case of **5.18** and **5.24**) or obtained for the concentration of 4 µM (incubation time of 6 h, **5**). The plasma concentrations of **5.5**, **5.18** and **5.24** were obtained by dividing the determined concentrations of **5.5**, **5.18** and **5.24** (RP-HPLC) by the respective recovery. The major degradation products of peptides **5.5**, **5.18** and **5.24** were identified by LC-HRMS analysis (LC-MS instrument see general experimental conditions).

Chemical Stability in Buffer. The chemical stabilities of peptides **5.18** and **5.24** were investigated in PBS (pH 7.4). The incubation of compounds **5.18** and **5.24** was started by addition of 3 µL of a 5 mM peptide stock solution into 147 µL PBS (pH 7.4, autoclaved) to give a final concentration of 100 µM. After 0 h, 6 h, 24 h and 48 h, an aliquot (25 µL) was taken and

diluted with MeCN/0.04% TFA (1:9 v/v) (25 µL) to obtain a solution with a final peptide concentration of 50 µM. 20 µL of this solution were analyzed by RP-HPLC using the system and conditions as described under general experimental conditions (purity controls), but applying a different linear gradient: 0-14 min: MeCN/0.04% aq. TFA 10:90-30:70, 14-15 min: 30:70-95:5, 15-19 min: 95:5 (isocratic).

5.4.7 Induced-Fit Docking and MD Simulations

Geometries of the ligands **5.18** and **5.24** were prepared and energetically optimized using the LigPrep module (Schrödinger LLC). Both arginine residues and the carbamoylguanidine group within the macrocycle were protonated, resulting in a formal charge of +3 for each ligand. A recently described hY_4R homology model, generated from the active state κ opioid receptor crystal structure (PDB-ID: 6B73, chain A^{29}),[13] served as Y_4 receptor and was prepared by means of the Protein Preparation Wizard module (Schrödinger LLC). Amino acid side chains containing hydrogen bond donors and acceptors were optimized for hydrogen bonding and were modeled in their dominant protonation state at pH 7. As a van-der-Waals scaling of 0.5 for both the receptor and the ligands lead to unreasonable initial GLIDE docking poses (tunneling effects), a van-der-Waals scaling of 0.6 was used for the receptor and the ligands (note: at van-der-Waals scaling ≥ 0.7, the ligands did not enter the orthosteric binding pocket). This approach resulted in docking poses (lowest scores) where the C-terminal tyrosine of **5.18** and **5.24** was deeply located in the orthosteric binding pocket. These ligand-receptor complexes were used as initial coordinates for refinement by MD simulations. The lowest-energy GPCR-ligand complexes from the docking served as starting structures. Tleap was used to assign ff99SB parameters[34,35] to the protein structure obtained from docking. The parametrization of the ligands **5.18** and **5.24** for MD simulations is described in the Supporting Information. Prior to embedding the receptor into the membrane, a first minimization run was conducted to reduce steric tensions in the docking model. Using sander from Amber18, 500 steps of the steepest descent algorithm followed by 4,500 steps of the conjugate gradient algorithm were carried out. The MD simulations including membrane embedding, equilibration and production phase followed the overall strategy described previously for GPCR-ligand complexes.[36,37] In the first step, the protein as well as the ligand coordinates were translated into the Gromacs[38] file formats by amb2gmx.pl. A pre-equilibrated dioleoylphosphatidylcholine (DOPC) bilayer,[39] solvated in SPC water,[40] was used as membrane in which the protein ligand complex was embedded. Prior to the final minimization, the gmx genion functionality was used for electrical neutralization. Due to the system size, the minimization was conducted step wise; after minimizing only water molecules and ions with restraints on all other atoms, the restraints were solely placed on the Cα carbons and lastly no restrains were placed at all. Regarding the

restraints, harmonic potentials with a force constant of 10 kcal·mol^{-1}·Å^{-2} in each cartesian direction were used. Each step was subdivided in a similar fashion as in the aforementioned minimization procedure, but with 2,500 steepest descent steps followed by 2,500 conjugate gradient steps. The equilibration was run as a series of 300 MD simulations, each with a length of 100ps. Position restraints were applied to the receptor and ligand atoms during these runs to keep the system stable while adjusting to the membrane. A Berendsen thermostat[41] was used to keep the temperature constant at 310 K. The resulting system was then used for the production runs. A time step of 2 fs was chosen for all systems including the production runs. Surface-tension coupling was used applying a reference pressure of 1 bar and a reference surface tension of 1.1 nm·bar. In all simulations, periodic boundary conditions were applied and the SHAKE algorithm[42] was used for covalent bonds with hydrogen atoms. An overview of the performed simulations is given in Table 5.

Table 5. Overview of the performed MD simulations.

Simulation name	Compound	Cα-restraints	Simulation time	#Atoms	#Water molecules	#DOPC molecules
run 1	**5.18**		1 µs	99,883	20,765	236
run 2	**5.18**		1 µs			
run 3	**5.18**	×	1 µs			
run 4	**5.18**	×	1 µs			
run 1	**5.24**		1 µs	99,601	20,762	234
run 2	**5.24**		1 µs			
run 3	**5.24**	×	1 µs			
run 4	**5.24**	×	1 µs			

Post-processing and subsequent analysis were mainly performed using cpptraj from AmberTools 18. For the assessment of contacts, the nativecontacts command was used with a specified distance criterion of 5 Å. Distances were evaluated using the distance command, while the vdw-energies were calculated with the lie routine. Clustering was performed over both unrestrained runs for **5.18** and **5.24**, respectively. For both ligands, the most populated cluster is predominantly found in run2. Plots were created with gnuplot using a Bezier smoothing function. The structure visualization was done with UCSF Chimera.[43]

5.5 Supporting Information

Scheme S1. Synthesis of the arginine derivative **5.9**.

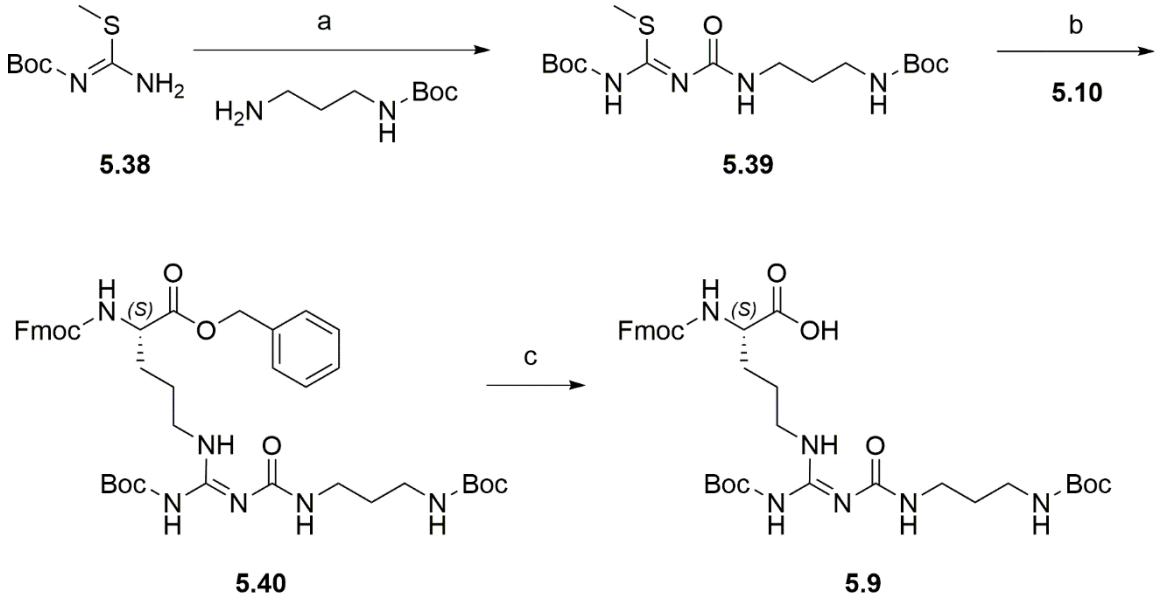

Reagents and conditions: (a) triphosgene, DIPEA, CH_2Cl_2 (anhydrous), rt, 0.5 + 3 h, 80%; (b) $HgCl_2$, DIPEA, CH_2Cl_2 (anhydrous), rt, 3 h, 62%; (c) 10% Pd/C, H_2, acetic acid, isopropyl alcohol, rt, 6 h, 39%.

***N*-*tert*-Butoxycarbonyl-*N'*-[3-(*tert*-butoxycarbonylamino)propyl]aminocarbonyl-*S*-methylisothiourea (5.39).** The reaction was carried out in a 250 mL round bottom flask that was evacuated, heated and then argon purged prior to the reaction. A solution of *tert*-butyl (3-aminopropyl)carbamate (3.8 g, 21.0 mmol) and DIPEA (11.0 mL, 63.0 mmol) in anhydrous CH_2Cl_2 (60 mL) was added dropwise to a solution of triphosgene (2.81 g, 9.45 mmol) in anhydrous CH_2Cl_2 (20 mL) over a period of 30 min, *N*-Boc-*S*-methylisothiourea (**5.38**) (4.0 g, 21.0 mmol) was added and stirring was continued at rt for 3 h. The mixture was treated with H_2O (3 × 200 mL), the organic phases were combined and dried over anhydrous $MgSO_4$ and the solvent was evaporated under reduced pressure. Purification by column chromatography (eluent: light petroleum/CH_2Cl_2/EtOAc 4:2:1 to CH_2Cl_2/EtOAc 1:1) afforded **5.39** as a pale yellow solid (6.55 g, 80%). ^{1}H-NMR (400 MHz, DMSO-d_6): 1.35-1.43 (m, 18H), 2.15-2.18 (m, 2H), 2.67 (s, 3H), 3.65-3.71 (m, 4H), 6.91 (s, 1H), 7.65 (s, 1H), 13.22 (s, 1H). ^{13}C-NMR (100 MHz, DMSO-d_6): δ (ppm) 17.2, 27.9, 28.3 (six carbon atoms), 35.6, 41.7, 78.9, 83.7, 154.3, 155.3, 157.1, 167.7. HRMS (ESI): *m/z* $[M+H]^+$ calcd. for $[C_{16}H_{31}N_4O_5S]^+$ 391.2010, found: 391.2025. $C_{16}H_{30}N_4O_5S$ (390.50).

(*S*)-Benzyl-17-((((9*H*-fluoren-9-yl)methoxy)carbonyl)amino)-12-((*tert*-butoxycarbonyl)amino)-2,2-dimethyl-4,10-dioxo-3-oxa-5,9,11,13-tetraazaoctadec-11-en-18-oate (5.40). Compounds **5.10** (8.58 g, 15.36 mmol) and **5.39** (6.0 g, 15.36 mmol) were dissolved in anhydrous CH_2Cl_2 (200 mL), followed by the addition of $HgCl_2$ (6.26 g, 23.04 mmol) and DIPEA (8.02 mL, 46.08 mmol). The mixture was stirred at rt for 3 h, solid material

was removed by centrifugation and decantation and the volatiles of the combined supernatants were removed under reduced pressure (solid material was washed twice). The residue was dried *in vacuo* overnight and purification by column chromatography (eluent: CH_2Cl_2/EtOAc 20:1 to CH_2Cl_2/EtOAc 2:1) yielded **5.40** as a colorless, crystalline solid (7.49 g, 62%). ^{1}H-NMR (400 MHz, DMSO-d_6): 1.35-1.55 (m, 24H), 2.91-3.02 (m, 4H), 3.40-3.43 (m, 2H), 3.32-3.39 (m, 2H), 3.45-3.55 (m, 4H), 3.90-3.97 (m, 2H), 4.12-4.16 (m, 2H), 5.35 (s, 2H), 7.32-7.46 (m, 4H), 7.55-7.62 (m, 3H), 7.67-7.72 (m, 2H), 7.81-7.86 (m, 2H), 8.11-8.13 (m, 1H). ^{13}C-NMR (100 MHz, DMSO-d_6): δ (ppm) 23.2, 24.6, 28.2 (six carbon atoms), 29.1, 35.6, 37.8, 42.3, 47.1, 56.9, 65.4, 65.6, 79.2, 84.2, 121.3 (two carbons atoms), 124.3 (two carbon atoms), 124.8 (two carbon atoms), 126.1 (two carbon atoms), 126.4 (two carbon atoms), 127.5, 128.8 (two carbon atoms), 134.9, 141.3 (two carbon atoms), 143.9, 144.1, 151.3, 153.4, 155.8, 155.9, 168.3, 171.8. HRMS (ESI): *m/z* $[M+H]^+$ calcd. for $[C_{42}H_{55}N_6O_9]^+$ 787.4025, found: 787.4040. $C_{42}H_{54}N_6O_9$ (786.93).

(*S*)-17-((((9*H*-Fluoren-9-yl)methoxy)carbonyl)amino)-12-((*tert*-butoxycarbonyl)amino)-2,2-dimethyl-4,10-dioxo-3-oxa-5,9,11,13-tetraazaoctadec-11-en-18-oic acid (5.9). Under an atmosphere of argon, precursor **5.40** (7.0 g, 8.901 mmol) and acetic acid (20 µL) were dissolved in 2-propanol (65 mL) in a two-necked round-bottom flask. A 10% Pd/C catalyst (700 mg) was added and the suspension was vigorously stirred under an atmosphere of hydrogen at rt for 6 h (additional catalyst was added after 2.5 h (400 mg) and 3.5 h (280 mg)). The catalyst was removed by filtration through a pad of celite, followed by evaporation of the volatiles. The product was purified by column chromatography (eluent: MeCN/EtOH 40:1 to 10:1). The major part of the solvent of the product fraction was removed under reduced pressure. Water (500 mL) was added to the residue and lyophilization yielded **5.9** as a white powder (2.42 g, 39%). ^{1}H-NMR (400 MHz, DMSO-d_6): δ (ppm) 1.25-1.67 (m, 25H), 1.69-1.83 (m, 1H), 2.86-3.08 (m, 4H), 3.16-3.31 (m, 2H), 3.81-3.93 (m, 1H), 4.17-4.36 (m, 3H), 6.69-6.83 (m, 1H), 6.91-6.04 (m, 1H), 7.24-7.44 (m, 4H), 7.56-7.76 (m, 2H), 7.82-7.90 (m, 2H), 8.20 (s, 0.5H), 9.14 (s, 0.5H), 11.09 (s, 0.5H), 12.44-12.70 (m, 0.5H). ^{13}C-NMR (100 MHz, DMSO-d_6): δ (ppm) 25.4, 27.7, 28.1, 28.2 (six carbon atoms), 36.9, 37.7, 46.8, 55.0, 65.4, 77.4, 81.9, 118.0, 120.1 (two carbon atoms), 125.2, 127.1 (two carbon atoms), 127.6 (two carbon atoms), 140.8 (two carbon atoms), 143.8, 144.1, 152.5, 153.1, 154.7, 156.4, 162.7, 164.4, 175.3. HRMS (ESI): *m/z* $[M+H]^+$ calcd. for $[C_{35}H_{49}N_6O_9]^+$ 697.3556, found: 697.3559. $C_{35}H_{48}N_6O_9$ (696.80).

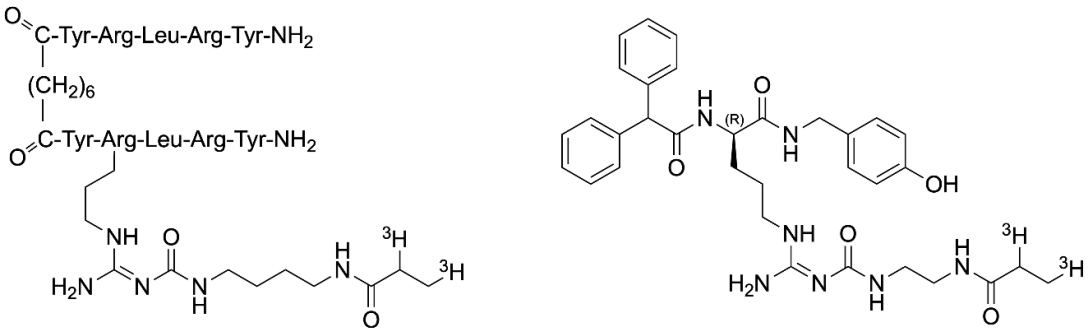

H-Tyr-Pro-Ser-Lys-Pro-Asp-Asn-Pro-Gly-Glu-Asp-Ala-Pro-Ala-Glu-Asp-Leu-Ala-Arg-Tyr-Tyr-Ser-Ala-Leu-Arg-His-Tyr-Ile-Asn-Leu-Ile-Thr-Arg-Gln-Arg-Tyr-NH_2

[^{3}H]propionyl-pNPY
K_d (hY_2R): 0.14 nM
K_d (hY_5R): 4.8 nM

Figure S1. Structures of the tritiated Y_4R partial agonist [^{3}H]**5.36**, the tritiated Y_1R antagonist [^{3}H]**5.37** and the tritiated Y_1R, Y_2R and Y_5R agonist [^{3}H]propionyl-pNPY.

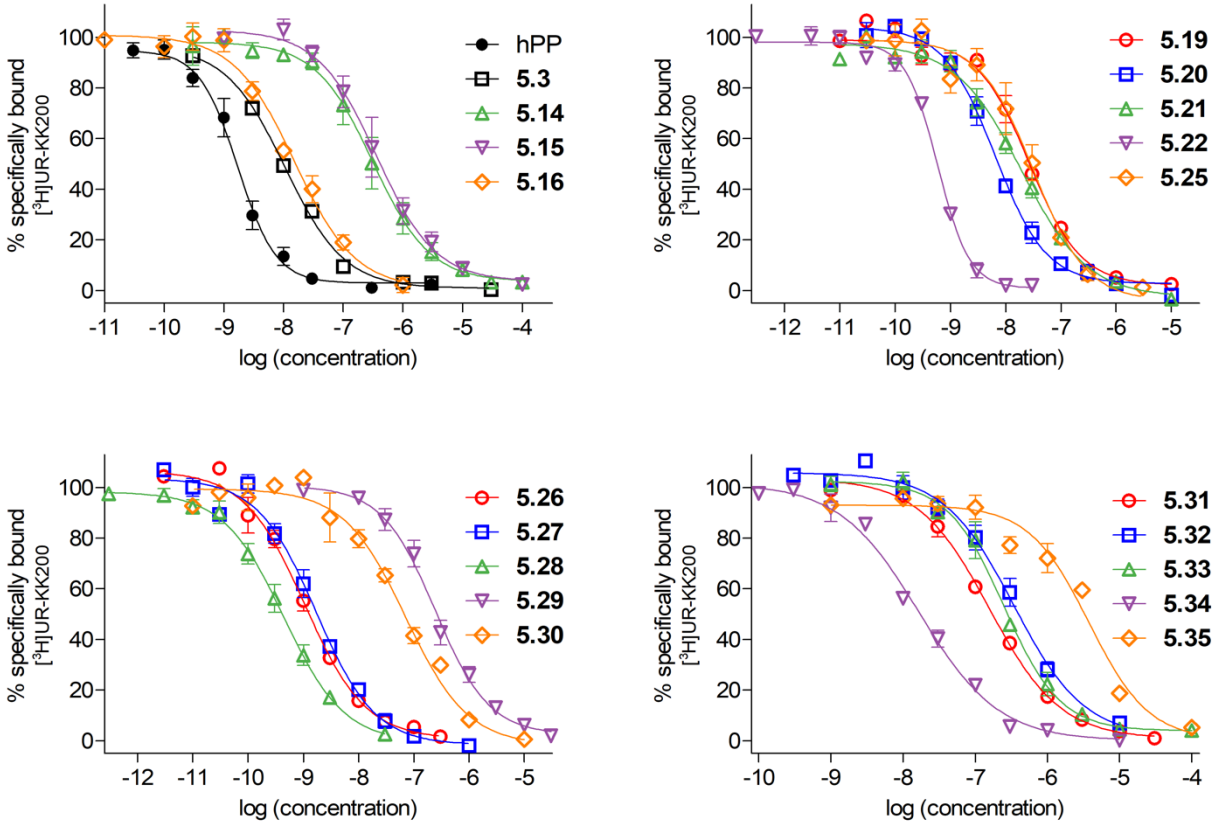

Figure S2. Radioligand displacement curves obtained from competition binding experiments with [^{3}H]**5.36** (K_d = 0.67 nM, c = 1 nM) and hPP, **5.3**, **5.14**-**5.16**, **5.19**-**5.22** or **5.25**-**5.35**, performed with CHO-hY_4R-mtAEQ-G_{qi5} cells. Data represent means ± SEM from at least three independent experiments, each performed in triplicate. Data were analyzed by four parametric logistic fits (GraphPad Prism 5).

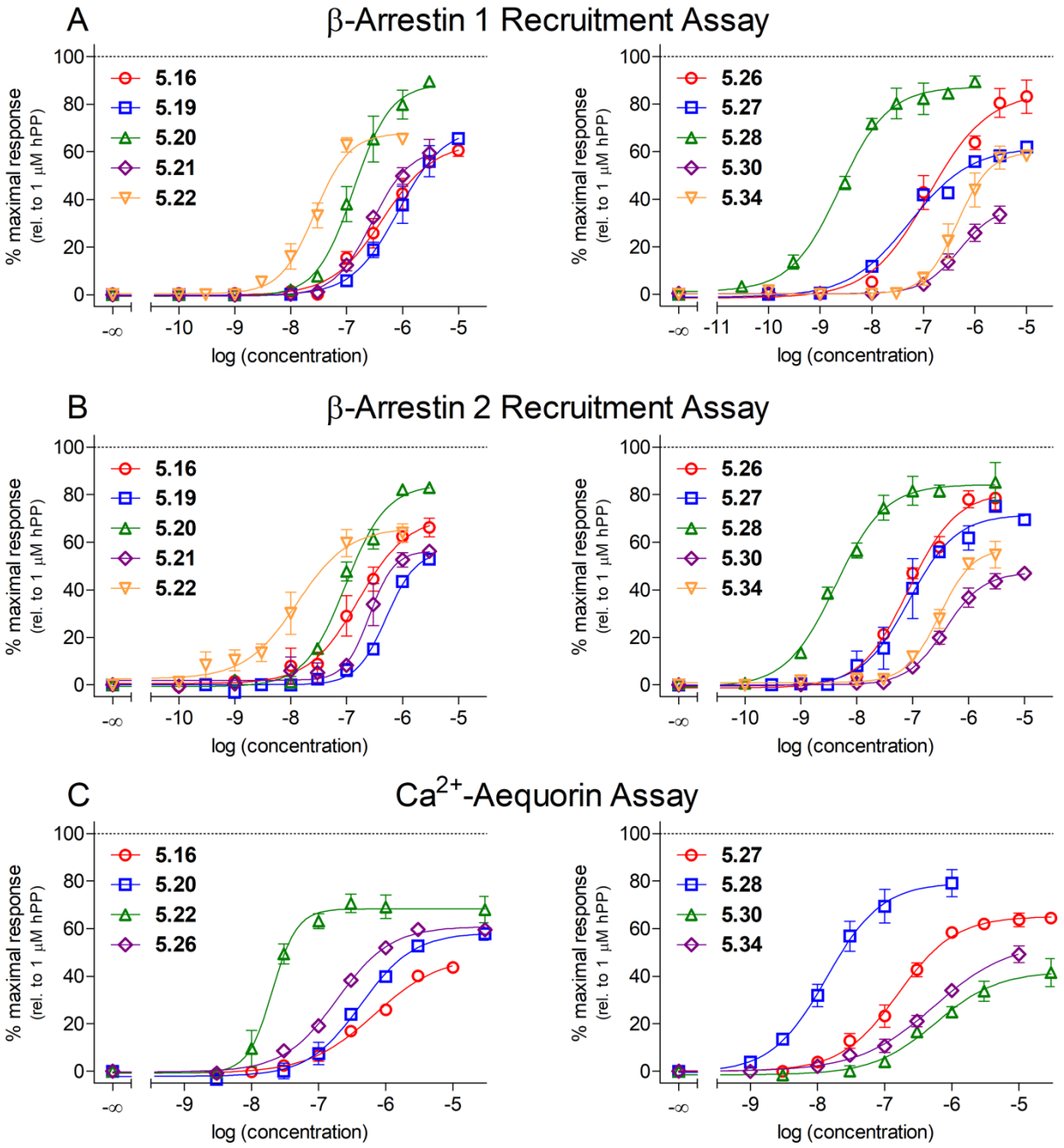

Figure S3. Y_4R agonism of selected compounds determined in a β-arrestin 1 recruitment assay, a β-arrestin 2 recruitment assay and a Ca^{2+}-aequorin assay. Panel A: concentration-response curves of compounds **5.16**, **5.19**-**5.22**, **5.26**-**5.28**, **5.30** and **5.34** obtained from a hY_4R β-arrestin 1 recruitment assay performed with live HEK293T-ARRB1-Y_4R cells. Panel B: concentration-response curves of compounds **5.16**, **5.19**-**5.22**, **5.26**-**5.28**, **5.30** and **5.34** obtained from a hY_4R β-arrestin 2 recruitment assay performed with live HEK293T-ARRB2-Y_4R cells. Panel C: concentration-response curves of compounds **5.16**, **5.20**, **5.22**, **5.26**-**5.28**, **5.30** and **5.34** obtained from a hY_4R Ca^{2+}-aequorin assay performed with live CHO-hY_4-G_{qi5}-mtAEQ cells. Data in A-C represent means ± SEM from at least three independent experiments, each performed in triplicate. Data were analyzed by four parametric logistic fits (GraphPad Prism 5).

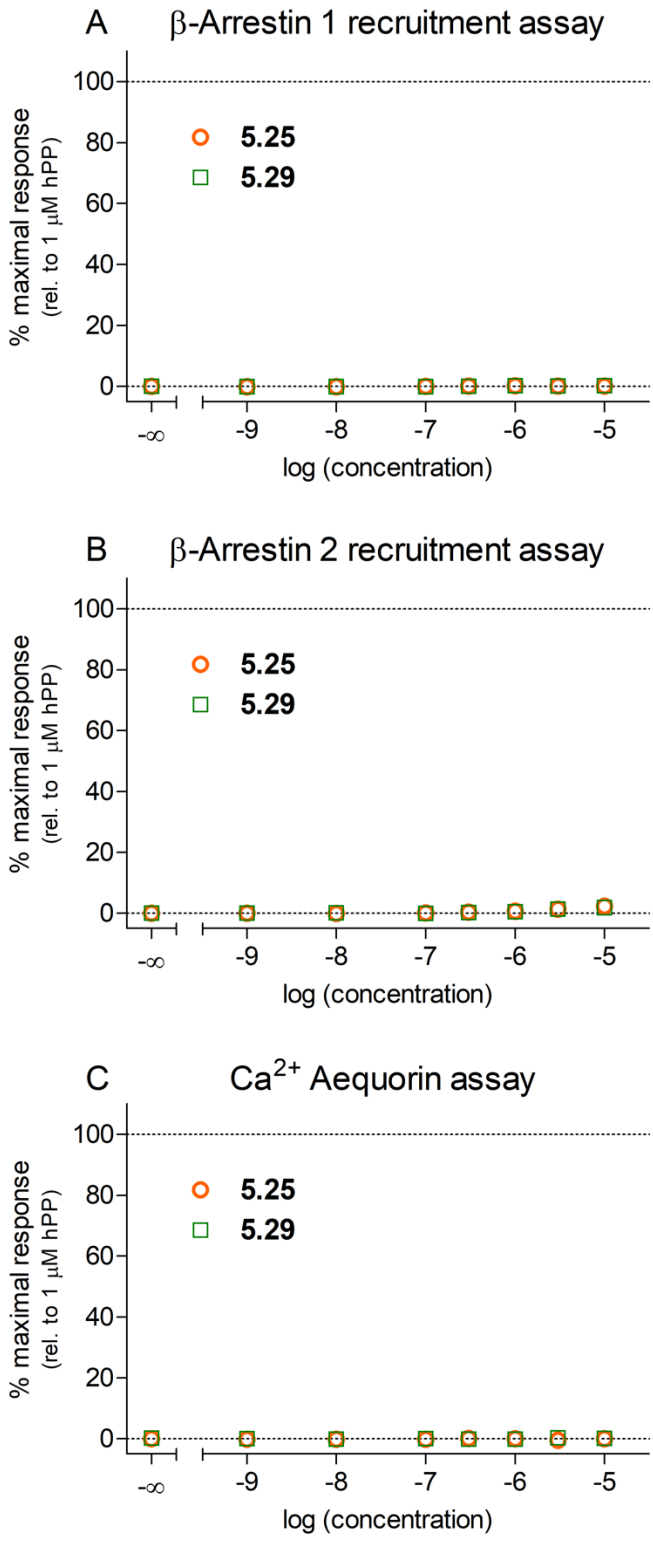

Figure S4. Investigation of compounds **5.25** and **5.29** in various functional Y_4R assays performed in agonist mode. (A) β-arrestin 1 recruitment studied in HEK239T-ARRB1-Y_4R cells. (B) β-arrestin 2 recruitment studied in HEK239T-ARRB2-Y_4R cells. (C) Intracellular Ca^{2+} mobilization measured in CHO-hY_4R-mtAEQ-G_{qi5} cells. In all assays, **5.25** and **5.29** elicited no response up to concentrations of 10 µM. Data represent means ± SEM from at least three independent experiments, each performed in triplicate.

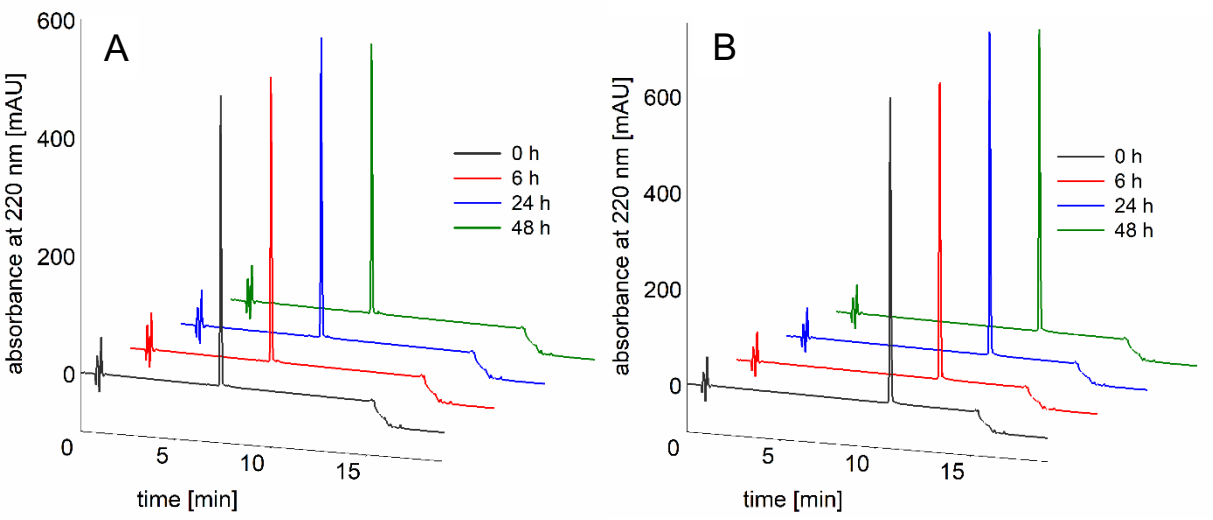

Figure S5. Reversed-phase HPLC analysis of peptides **5.18** (A) and **5.24** (B) after incubation in phosphate buffered saline (PBS) at pH 7.4 for up to 48 h. Both peptides showed no decompensation.

Table S1. Recoveries of peptides **5.5**, **5.18** and **5.24** from human plasma/PBS (1:2 v/v) for two different concentrations (80 µM and 4 µM) and ratios of peptide recovery over recovery of internal standard 1-Methyl-D-tryptophan (**5.41**).

compd.	peptide concentration 80 µM			peptide concentration 4 µM		
	recovery peptide (%)[a]	recovery **5.41** (%)[a]	ratio[b]	recovery peptide (%)[a]	recovery **5.41** (%)[a]	ratio[b]
5.5	33	100	0.34	37	99	0.37
	30	100	0.31	35	101	0.35
	31	99	0.31	40	97	0.41
	29	100	0.29	39	98	0.39
	31	101	0.30	39	100	0.39
			0.31 ± 0.01			0.38 ± 0.01
5.18	41	100	0.41	61	101	0.61
	42	101	0.42	62	100	0.62
	44	98	0.45	67	99	0.68
	43	101	0.42	61	101	0.60
	44	99	0.44	62	97	0.64
			0.43 ± 0.01			0.63 ± 0.01
5.24	36	96	0.36	61	100	0.61
	39	98	0.39	60	99	0.60
	38	100	0.38	61	102	0.61
	38	100	0.38	63	95	0.63
	39	96	0.39	66	99	0.66
			0.38 ± 0.01			0.62 ± 0.01

[a]Recoveries of peptides **5.5**, **5.18** and **5.24** as well as internal standard **5.41** from human plasma/PBS (1:2 v/v) using peptide concentrations of 80 µM or 4 µM and an internal standard concentration of 10 µM (five independent experiments). [b]Ratios of peptide recovery over recovery of **5.41** calculated for individual experiments, as well as mean recovery ratios ± SEM.

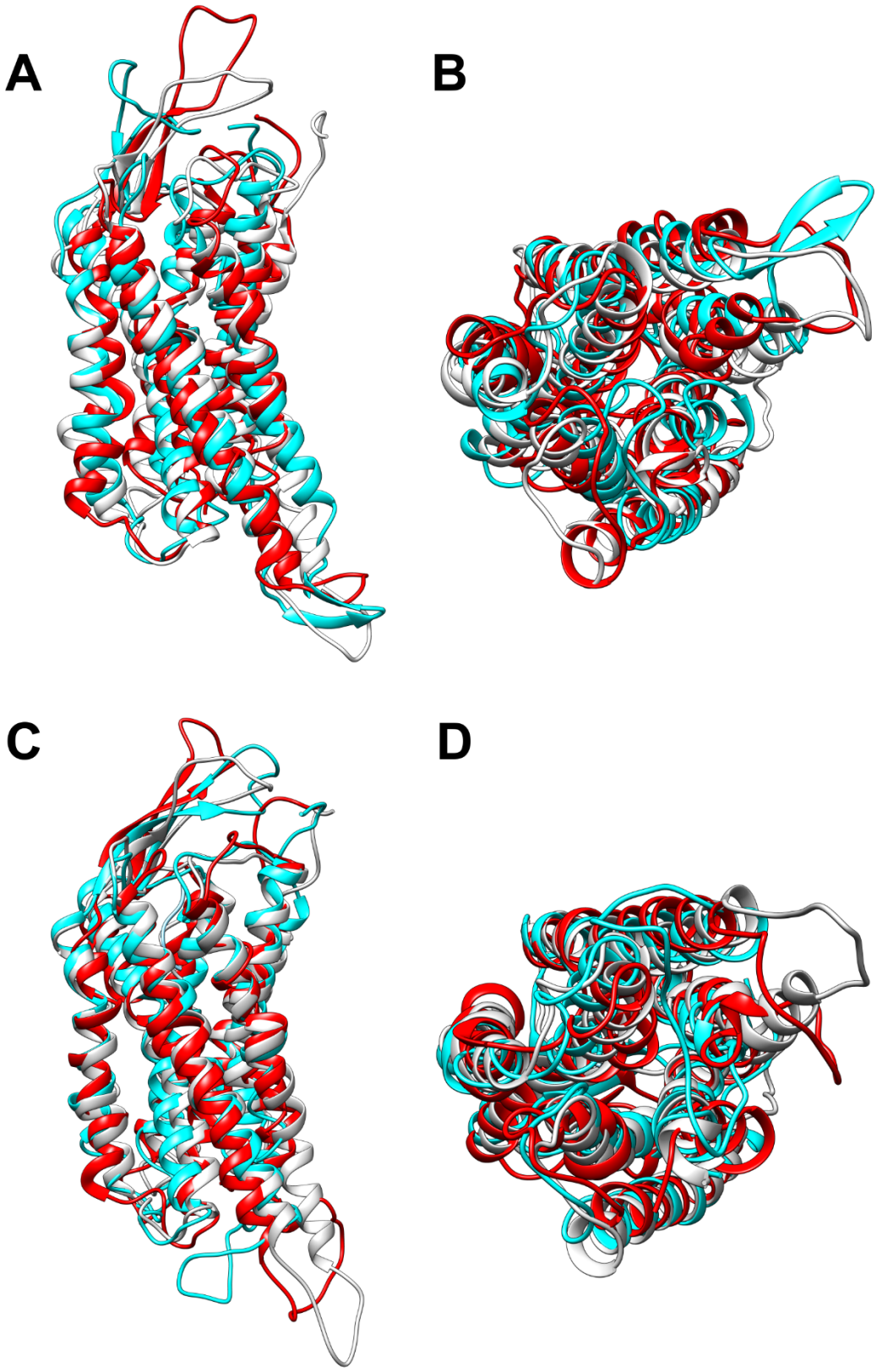

Figure S6. Conformational stability of the hY_4R homology models during the unrestrained MD simulations. (A, B) Overlay of the final structures resulting from run 1 (red) and run 2 (cyan) of the Y_4R-**5.18** complex with the initial structure of the homology model (white). (C, D) Overlay of the final structures resulting from run 1 (red) and run 2 (cyan) of the Y_4R-**5.24** complex with the initial structure of the homology model (white). The views of the two images within a panel differ by a rotation of ca. 90° around the horizontal axis.

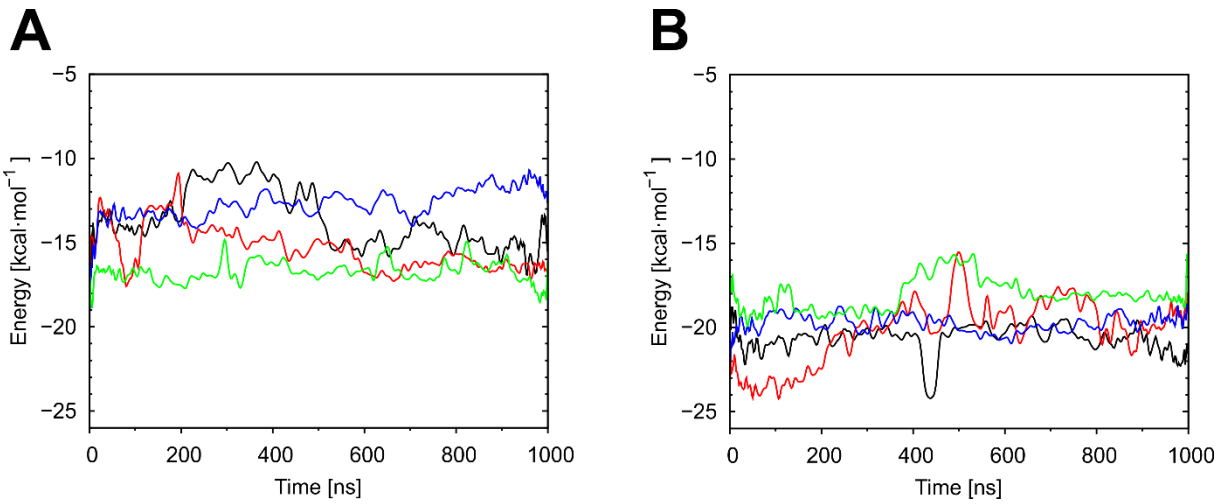

Figure S7. Van der Waals interaction energies of the aromatic amino acid residues in **5.18** and **5.24**. (A) vdW interaction energy of Tyr^{2} (**5.18**) and Trp^{2} (**5.24**) over the simulation time of each individual run. (B) vdW interaction energy of Tyr^{6} over the simulation time of each individual run. Curves for **5.18** (run 1), **5.18** (run 2), **5.24** (run 1), and **5.24** (run 2) are colored in black, blue, red and green, respectively.

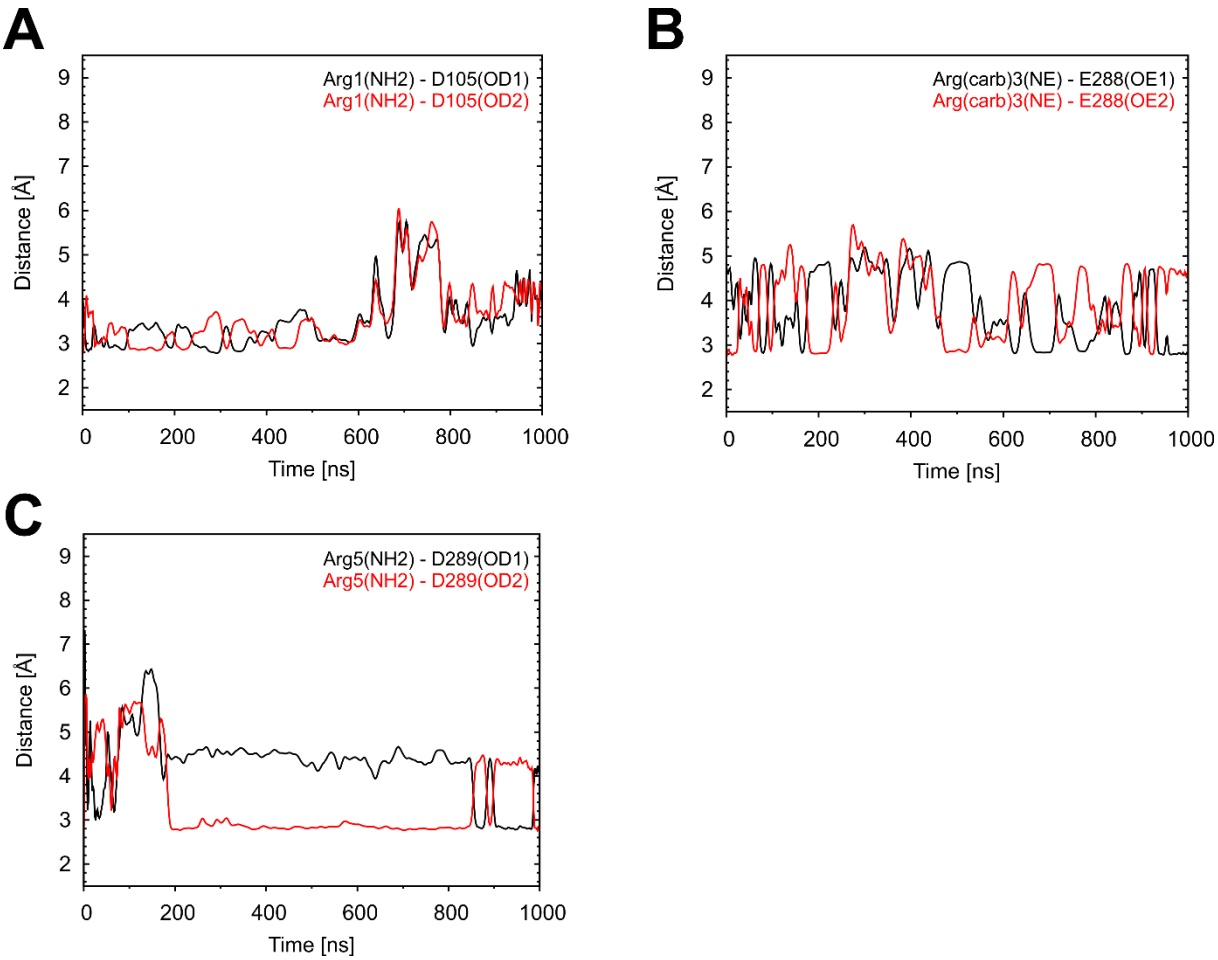

Figure S8. Key electrostatic interactions observed in run 2 of the simulation of the Y$_4$R-**5.18** complex. The following ionic ligand-receptor interactions are shown: (A) Arg^{1}-D105, (B) Arg(carb)^{3}-E288, (C) Arg^{5}-D289.

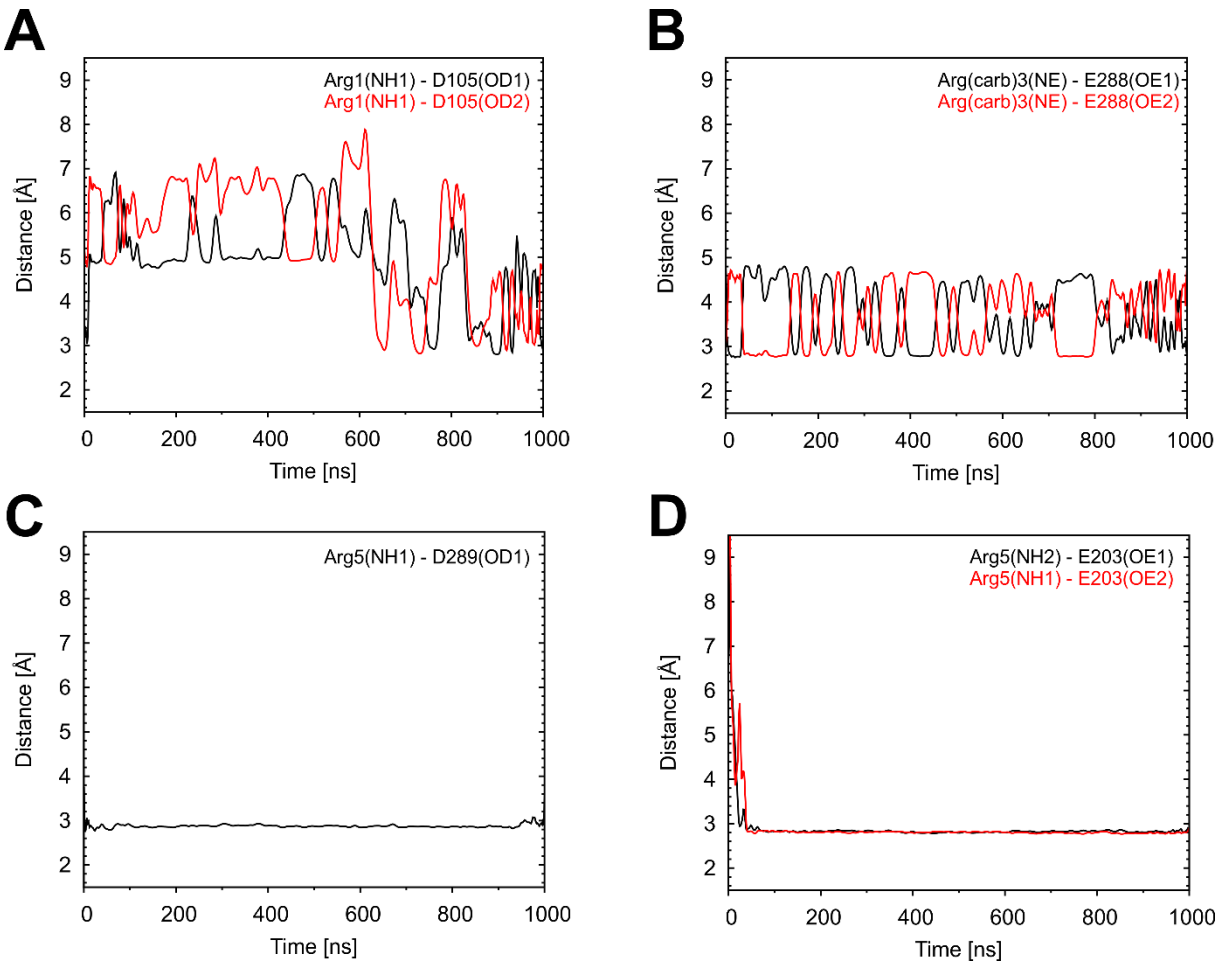

Figure S9. Key electrostatic interactions observed in run 2 of the simulation of the Y_4R-**5.24** complex. The following ionic ligand-receptor interactions are shown: (A) Arg^1-D105, (B) $Arg(carb)^3$-E288, (C) Arg^5-D289 and (D) Arg^5-E203.

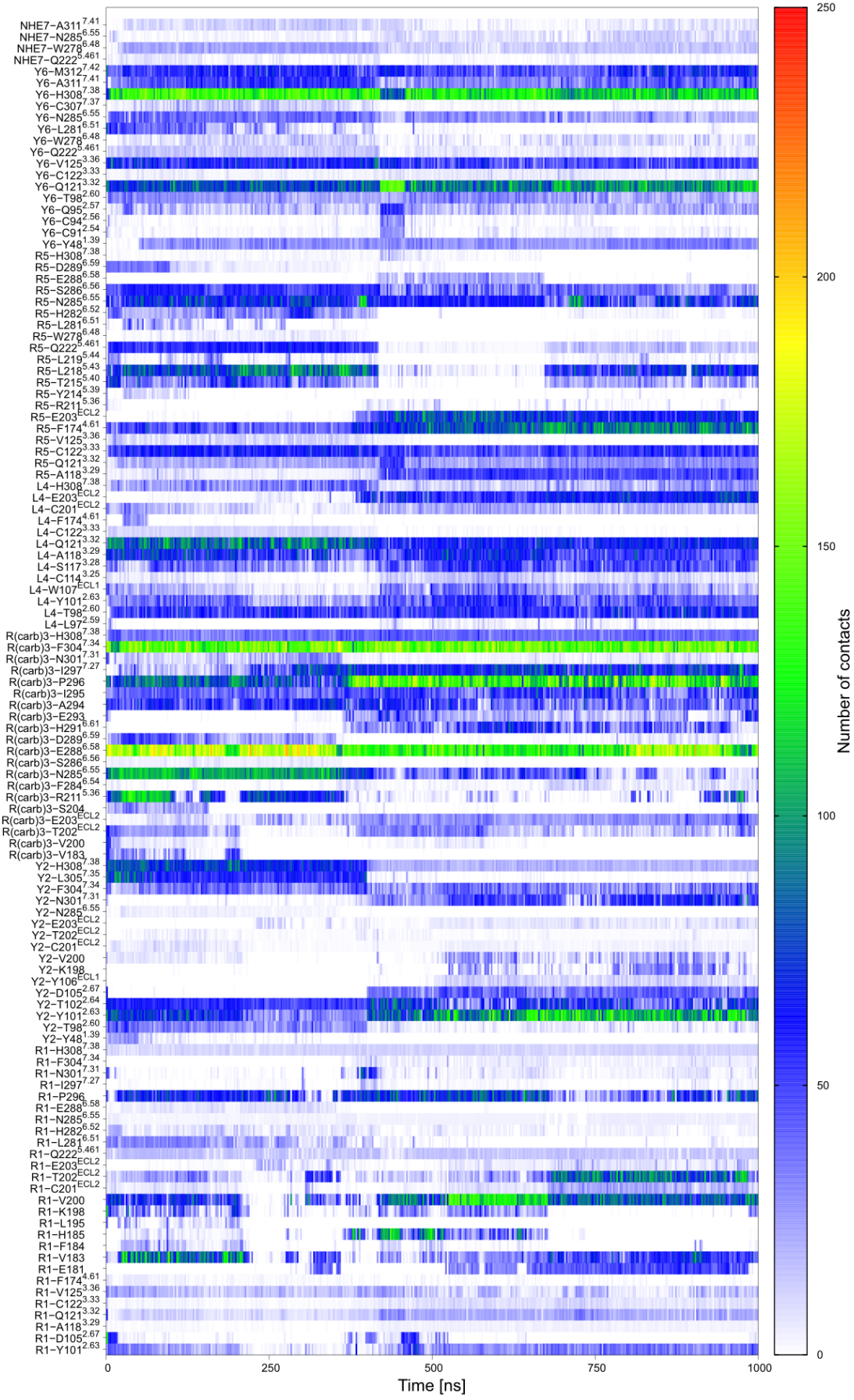

Figure S10A. Number of contacts between **5.18** (run 1) and the indicated Y_4R residues over the simulation time. The number of contacts is color-encoded (vertical scale bar).

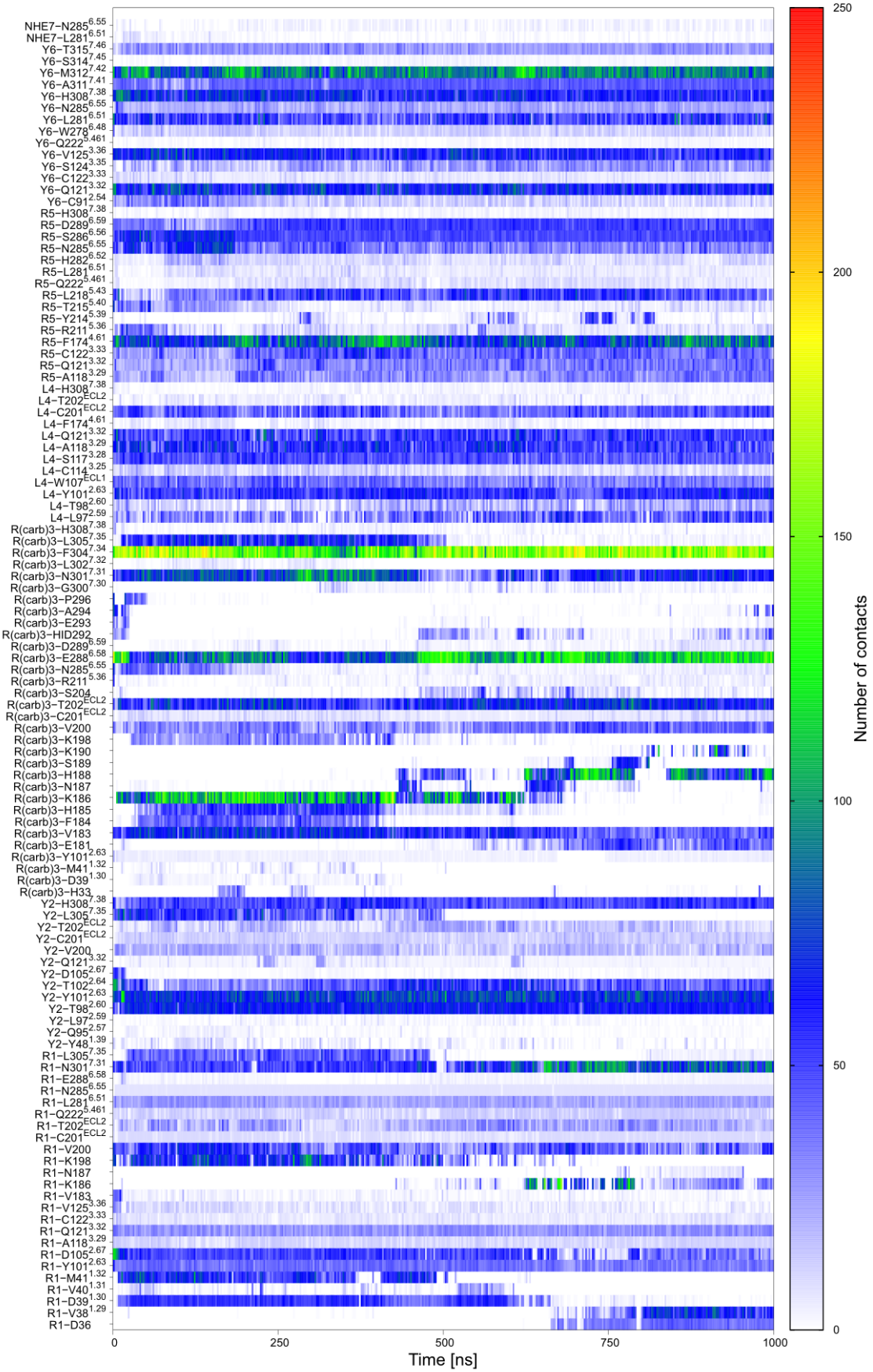

Figure S10B. Number of contacts between **5.18** (run 2) and the indicated Y_4R residues over the simulation time. The number of contacts is color-encoded (vertical scale bar).

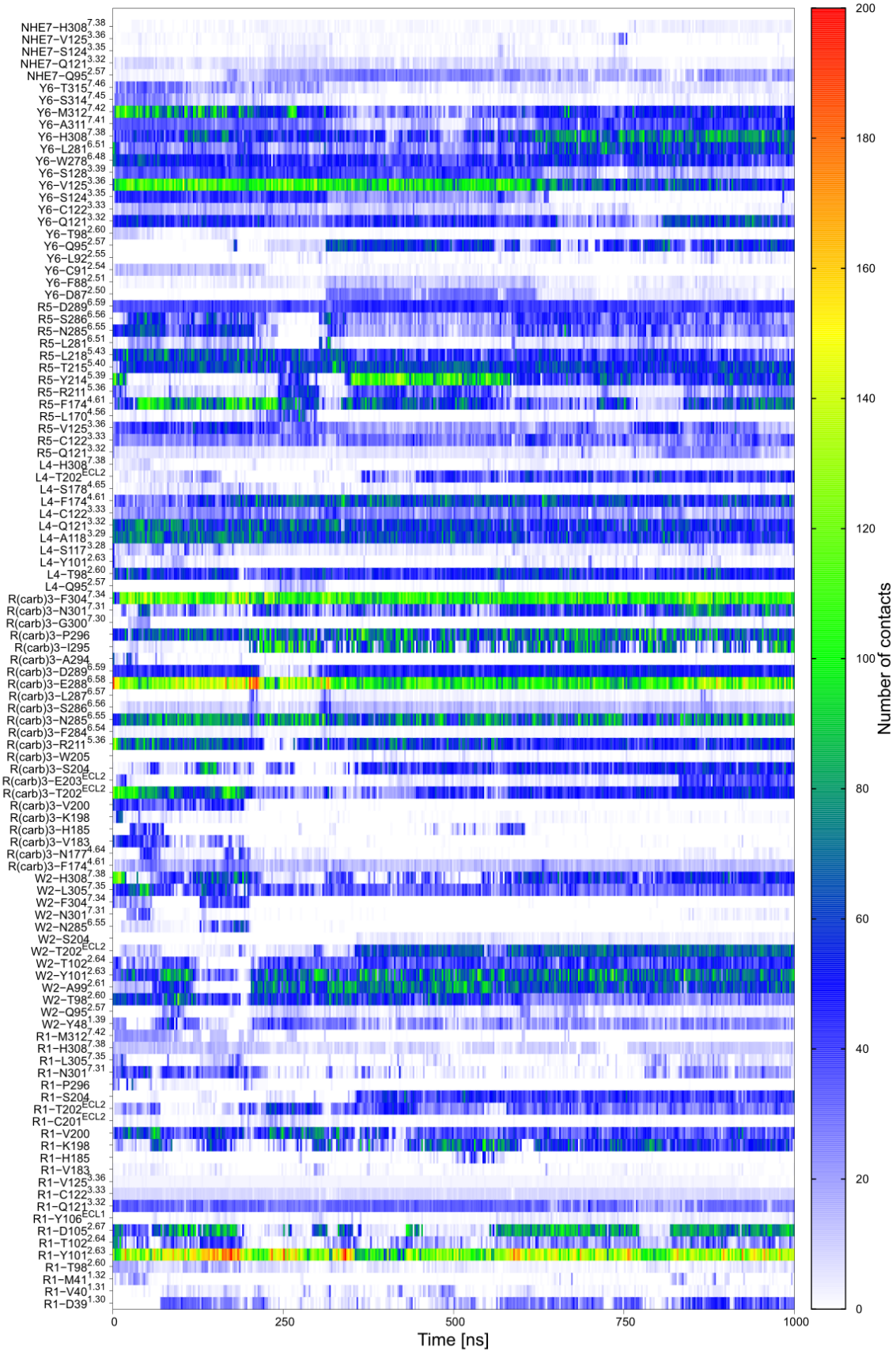

Figure S10C. Number of contacts between **5.24** (run 1) and the indicated Y_4R residues over the simulation time. The number of contacts is color-encoded (vertical scale bar).

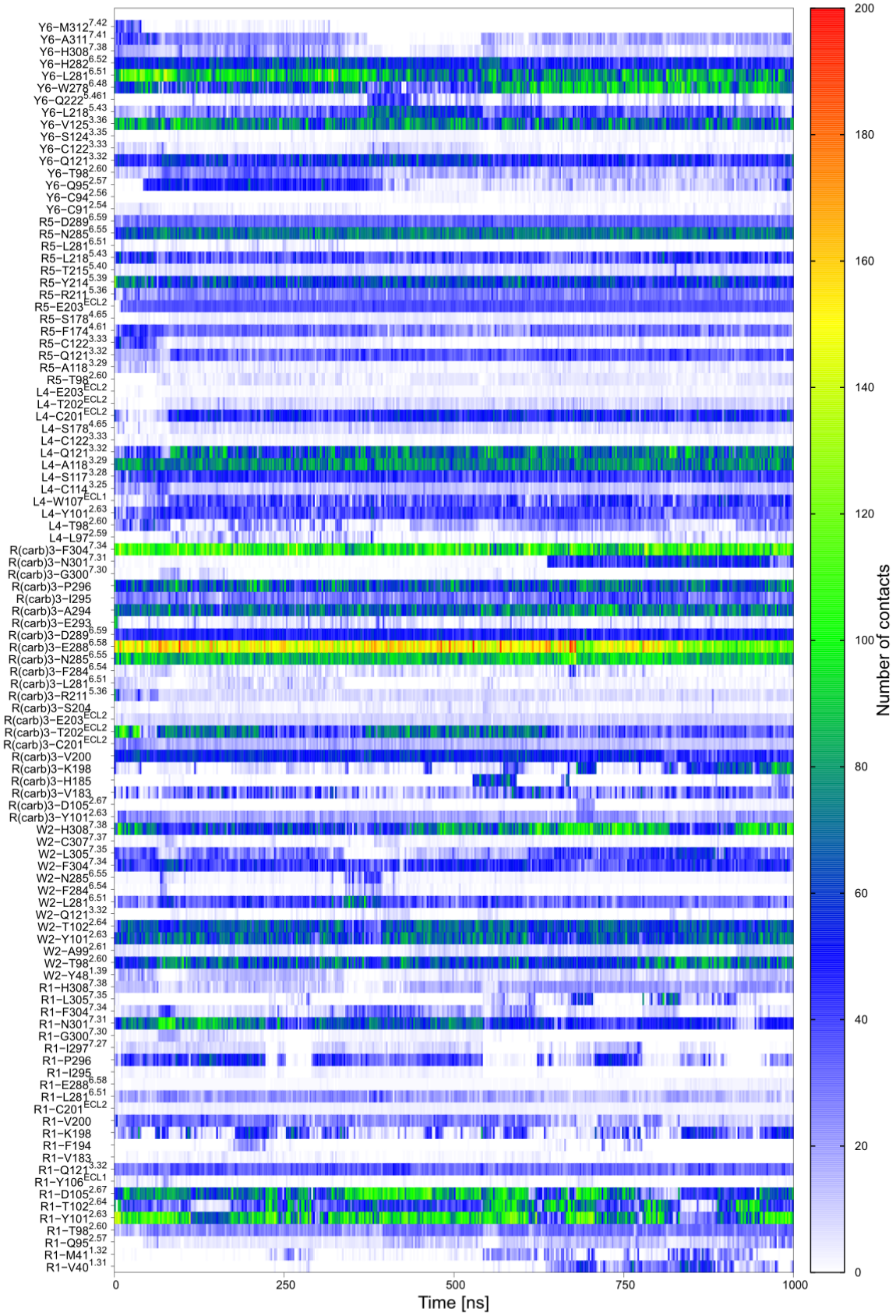

Figure S10D. Number of contacts between **5.24** (run 2) and the indicated Y_4R residues over the simulation time. The number of contacts is color-encoded (vertical scale bar).

Parametrization of the Y_4R ligands **5.18** and **5.24** for MD simulations.

The macrocycles of the cyclic peptides **5.18** and **5.24** contain the side chain of a non-canonical amino acid (carbamoylated arginine (Arg(carb)); cf. Figure 4 and Scheme 3, main article) that lacks force field parameters in existing force field libraries. This carbamoylated arginine residue forms a bridge to the succinyl group attached to the N-terminal amino group of Arg[1]. For parametrization, this succinyl group was treated as part of the R(carb) residue, resulting in an extended moiety that was henceforth termed RLX (Figure S11).

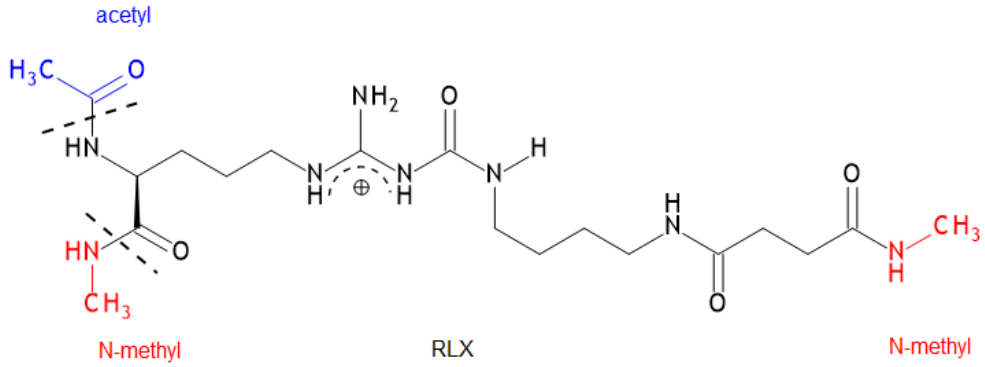

Figure S11. Lewis structure of the modified arginine used for parameterization in **5.18** and **5.24**. Capping groups are shown in blue (acetyl) or red (N-methyl). Peptide bonds within the peptide backbone are marked with dashed lines. (The scheme was created with BioviaDraw20.1 [Daussault Systèmes 2020])

In a first approach, we assigned standard GAFF parameters to the entire ligand. However, the resulting ligand exhibited an unfavorable conformational geometry (e.g. nonplanar guanidino and amide groups) in preliminary MD simulations. Therefore, we pursued a different approach, i.e. ff99SB parameters were used for the canonical ligand amino acids and ff99-compatible parameters were created for RLX allowing to treat the latter as a modified amino acid.

For atomic charge generation, the general protocol[44] recommended for ff99 force fields was followed: a model system for the RLX residue (Figure S11) in an extended conformation was generated (with Avogadro[45]), thereby capping the N-terminus with an acetyl group and the C-terminus and the side chain with an N-methyl group. The carbamoylguanidine group was protonated yielding a total residue charge of +1. This isolated RLX structure was geometry optimized at the HF/6-31G* level of theory using Gaussian, followed by a frequency calculation at the same level to ensure that the identified stationary point was a true minimum. Afterwards, RESP charges were generated via PyRED/REDServer[46] applying charge constraints to peptide bond atoms similar to ff99SB. Finally, general ff99 atom types were assigned and remaining force field parameters were adopted from ff99SB. Amber parameter files for RLX are available as separate supplementary files. Topology files for the simulation were created with leap from the Amber package, and ligand cyclization was implemented via the bond command.

5.6 References

1. Michel, M. C.; Beck-Sickinger, A.; Cox, H.; Doods, H. N.; Herzog, H.; Larhammar, D.; Quirion, R.; Schwartz, T.; Westfall, T., XVI. International union of pharmacology recommendations for the nomenclature of neuropeptide Y, peptide YY, and pancreatic polypeptide receptors. *Pharmacol. Rev.* **1998**, *50*, 143-150.
2. Pedragosa-Badia, X.; Sliwoski, G. R.; Dong Nguyen, E.; Lindner, D.; Stichel, J.; Kaufmann, K. W.; Meiler, J.; Beck-Sickinger, A. G., Pancreatic polypeptide is recognized by two hydrophobic domains of the human Y_4 receptor binding pocket. *J. Biol. Chem.* **2014**, *289*, 5846-5859.
3. Cerda-Reverter, J. M.; Larhammar, D., Neuropeptide Y family of peptides: structure, anatomical expression, function, and molecular evolution. *Biochem. Cell Biol.* **2000**, *78*, 371-392.
4. Silva, A. P.; Cavadas, C.; Grouzmann, E., Neuropeptide Y and its receptors as potential therapeutic drug targets. *Clin. Chim. Acta* **2002**, *326*, 3-25.
5. Sainsbury, A.; Shi, Y.-C.; Zhang, L.; Aljanova, A.; Lin, Z.; Nguyen, A. D.; Herzog, H.; Lin, S., Y_4 receptors and pancreatic polypeptide regulate food intake via hypothalamic orexin and brain-derived neurotropic factor dependent pathways. *Neuropeptides* **2010**, *44*, 261-268.
6. Li, J. B.; Asakawa, A.; Terashi, M.; Cheng, K.; Chaolu, H.; Zoshiki, T.; Ushikai, M.; Sheriff, S.; Balasubramaniam, A.; Inui, A., Regulatory effects of Y_4 receptor agonist (BVD-74D) on food intake. *Peptides* **2010**, *31*, 1706-1710.
7. Khandekar, N.; Berning, B. A.; Sainsbury, A.; Lin, S., The role of pancreatic polypeptide in the regulation of energy homeostasis. *Mol. Cell. Endocrinol.* **2015**, *418*, 33-41.
8. Painsipp, E.; Wultsch, T.; Edelsbrunner, M. E.; Tasan, R. O.; Singewald, N.; Herzog, H.; Holzer, P., Reduced anxiety-like and depression-related behavior in neuropeptide Y Y_4 receptor knockout mice. *Genes, Brain Behav.* **2008**, *7*, 532-542.
9. Verma, D.; Hörmer, B.; Bellmann-Sickert, K.; Thieme, V.; Beck-Sickinger, A. G.; Herzog, H.; Sperk, G.; Tasan, R. O., Pancreatic polypeptide and its central Y_4 receptors are essential for cued fear extinction and permanent suppression of fear. *Br. J. Pharmacol.* **2016**, *173*, 1925-1938.
10. Kuhn, K. K.; Littmann, T.; Dukorn, S.; Tanaka, M.; Keller, M.; Ozawa, T.; Bernhardt, G.; Buschauer, A., In search of NPY Y_4R antagonists: incorporation of carbamoylated arginine, aza-amino acids, or D-amino acids into oligopeptides derived from the C-termini of the endogenous agonists. *ACS Omega* **2017**, *2*, 3616-3631.
11. Daniels, A. J.; Matthews, J. E.; Slepetis, R. J.; Jansen, M.; Viveros, O. H.; Tadepalli, A.; Harrington, W.; Heyer, D.; Landavazo, A.; Leban, J. J.; Spaltenstein, A., High-affinity neuropeptide Y receptor antagonists. *Proc. Natl. Acad. Sci. USA* **1995**, *92*, 9067-9071.

12. Berlicki, Ł.; Kaske, M.; Gutiérrez-Abad, R.; Bernhardt, G.; Illa, O.; Ortuño, R. M.; Cabrele, C.; Buschauer, A.; Reiser, O., Replacement of $Thr^{32}$and Gln^{34} in the C-terminal neuropeptide Y fragment 25–36 by cis-cyclobutane and cis-cyclopentane β-amino acids shifts selectivity toward the Y_4receptor. *J. Med. Chem.* **2013**, *56*, 8422-8431.
13. Konieczny, A.; Braun, D.; Wifling, D.; Bernhardt, G.; Keller, M., Oligopeptides as neuropeptide Y Y_4 receptor ligands: identification of a high-affinity tetrapeptide agonist and a hexapeptide antagonist. *J. Med. Chem.* **2020**, *63*, 8198-8215.
14. Schober, D. A.; Van Abbema, A. M.; Smiley, D. L.; Bruns, R. F.; Gehlert, D. R., The neuropeptide Y Y_1 antagonist, 1229U91, a potent agonist for the human pancreatic polypeptide-preferring (NPY Y_4) receptor. *Peptides* **1998**, *19*, 537-542.
15. Balasubramaniam, A.; Mullins, D. E.; Lin, S.; Zhai, W.; Tao, Z.; Dhawan, V. C.; Guzzi, M.; Knittel, J. J.; Slack, K.; Herzog, H.; Parker, E. M., Neuropeptide Y (NPY) Y_4 receptor selective agonists based on NPY(32−36): development of an anorectic Y_4 receptor selective agonist with oicomolar affinity. *J. Med. Chem.* **2006**, *49*, 2661-2665.
16. Keller, M.; Kuhn, K. K.; Einsiedel, J.; Hübner, H.; Biselli, S.; Mollereau, C.; Wifling, D.; Svobodová, J.; Bernhardt, G.; Cabrele, C.; Vanderheyden, P. M. L.; Gmeiner, P.; Buschauer, A., Mimicking of arginine by functionalized $N^{(\omega)}$-carbamoylated arginine as a new broadly applicable approach to labeled bioactive peptides: high affinity angiotensin, Neuropeptide Y, neuropeptide FF, and neurotensin receptor ligands as examples. *J. Med. Chem.* **2016**, *59*, 1925-1945.
17. Zorzi, A.; Deyle, K.; Heinis, C., Cyclic peptide therapeutics: past, present and future. *Curr. Opin. Chem. Biol.* **2017**, *38*, 24-29.
18. Abdalla, M.; McGaw, L., Natural cyclic peptides as an attractive modality for therapeutics: a mini review. *Molecules* **2018**, *23*, 2080-2088.
19. Peterson, E. M. a. M. L., Macrocycles are great cycles: applications, opportunities and challenges of synthetic macrocycles in drug discovery. *J. Med. Chem.* **2011**, *54*, 1961-2004.
20. Hutzler, C., Synthesis and pharmacological activity of new neuropeptide Y receptor ligands: from *N*,*N*-disubstituted alkanamides to highly potent argininamide-type Y_1 antagonists. Doctoral thesis. University of Regensburg, Regensburg, Germany. **2001**.
21. Kuhn, K. K.; Ertl, T.; Dukorn, S.; Keller, M.; Bernhardt, G.; Reiser, O.; Buschauer, A., High affinity agonists of the neuropeptide Y (NPY) Y_4 receptor derived from the C-terminal pentapeptide of human pancreatic polypeptide (hPP): synthesis, stereochemical discrimination, and radiolabeling. *J. Med. Chem.* **2016**, *59*, 6045-6058.
22. Cherkupally, P.; Ramesh, S.; Govender, T.; Kruger, H. G.; de la Torre, B. G.; Albericio, F., An efficient solid-phase strategy for total synthesis of naturally occurring amphiphilic

marine siderophores: amphibactin-T and moanachelin ala-B. *Org. Biomol. Chem.* **2015**, *13*, 4760-4768.

23. Ziemek, R.; Schneider, E.; Kraus, A.; Cabrele, C.; Beck-Sickinger, A. G.; Bernhardt, G.; Buschauer, A., Determination of affinity and activity of ligands at the human neuropeptide Y Y_4 receptor by flow cytometry and aequorin luminescence. *J. Recept. Signal Transduct. Res.* **2007**, *27*, 217-233.
24. Keller, M.; Weiss, S.; Hutzler, C.; Kuhn, K. K.; Mollereau, C.; Dukorn, S.; Schindler, L.; Bernhardt, G.; König, B.; Buschauer, A., N^{ω}-Carbamoylation of the argininamide moiety: an avenue to insurmountable NPY Y_1 receptor antagonists and a radiolabeled selective high-affinity molecular tool ([^{3}H]UR-MK299) with extended residence time. *J. Med. Chem.* **2015**, *58*, 8834-8849.
25. Moser, C.; Bernhardt, G.; Michel, J.; Schwarz, H.; Buschauer, A., Cloning and functional expression of the hNPY Y_5 receptor in human endometrial cancer (HEC-1B) cells. *Can. J. Physiol. Pharmacol.* **2000**, *78*, 134-142.
26. Dukorn, S.; Littmann, T.; Keller, M.; Kuhn, K.; Cabrele, C.; Baumeister, P.; Bernhardt, G.; Buschauer, A., Fluorescence- and radiolabeling of [Lys^4,Nle^{17,30}]hPP yields molecular tools for the NPY Y_4 receptor. *Bioconjugate Chem.* **2017**, *28*, 1291-1304.
27. Katritch, V.; Fenalti, G.; Abola, E. E.; Roth, B. L.; Cherezov, V.; Stevens, R. C., Allosteric sodium in class A GPCR signaling. *Trends Biochem. Sci.* **2014**, *39*, 233-244.
28. White, K. L.; Eddy, M. T.; Gao, Z.-G.; Han, G. W.; Lian, T.; Deary, A.; Patel, N.; Jacobson, K. A.; Katritch, V.; Stevens, R. C., Structural connection between activation microswitch and allosteric sodium site in GPCR signaling. *Structure* **2018**, *26*, 259-269.
29. Che, T.; Majumdar, S.; Zaidi, S. A.; Kormos, C.; McCorvy, J. D.; Wang, S.; Mosier, P. D.; Uprety, R.; Vardy, E.; Krumm, B. E.; Han, G. W.; Lee, M. Y.; Pardon, E.; Steyaert, J.; Huang, X. P.; Strachan, R. T.; Tribo, A. R.; Pasternak, G. W.; Carroll, I. F.; Stevens, R. C.; Cherezov, V.; Katritch, V.; Wacker, D.; Roth, B. L., Crystal structure of a nanobody-stabilized active state of the kappa-opioid receptor. *Cell* **2018**, *172*, 55-67.
30. Keller, M.; Mahuroof, S. A.; Hong Yee, V.; Carpenter, J.; Schindler, L.; Littmann, T.; Pegoli, A.; Hübner, H.; Bernhardt, G.; Gmeiner, P.; Holliday, N. D., Fluorescence labeling of neurotensin(8–13) via arginine residues gives molecular tools with high receptor affinity. *ACS Med. Chem. Lett.* **2019**, *11*, 16-22.
31. Spinnler, K.; von Krüchten, L.; Konieczny, A.; Schindler, L.; Bernhardt, G.; Keller, M., An alkyne-functionalized arginine for solid-phase synthesis enabling “bioorthogonal” peptide conjugation. *ACS Med. Chem. Lett.* **2019**, *11*, 334,339.
32. Cheng, Y.; Prusoff, W. H., Relationship between the inhibition constant (K_I) and the concentration of inhibitor which causes 50 per cent inhibition (IC_{50}) of an enzymatic reaction. *Biochem. Pharmacol.* **1973**, *22*, 3099-3108.

33. Pegoli, A.; Wifling, D.; Gruber, C. G.; She, X.; Hübner, H.; Bernhardt, G.; Gmeiner, P.; Keller, M., Conjugation of short peptides to dibenzodiazepinone-type muscarinic acetylcholine receptor ligands determines M_2R selectivity. *J. Med. Chem.* **2019**, *62*, 5358-5369.
34. Hornak, V.; Abel, R.; Okur, A.; Strockbine, B.; Roitberg, A.; Simmerling, C., Comparison of multiple Amber force fields and development of improved protein backbone parameters. *Proteins: Struct., Funct., Genet.* **2006**, *65*, 712-725.
35. Wang, J.; Cieplak, P.; Kollman, P. A., How well does a restrained electrostatic potential (RESP) model perform in calculating conformational energies of organic and biological molecules? *J. Comput. Chem.* **2000**, *21*, 1049-1074.
36. Söldner, C. A.; Horn, A. H. C.; Sticht, H., Binding of histamine to the H1 receptor—a molecular dynamics study. *J. Mol. Model.* **2018**, *24*, 346-362.
37. Söldner, C. A.; Horn, A. H. C.; Sticht, H., A metadynamics-based protocol for the determination of GPCR-ligand binding modes. *Int. J. Mol. Sci.* **2019**, *20*, 1970-1982.
38. Berendsen, H. J. C.; van der Spoel, D.; van Drunen, R., GROMACS: a message-passing parallel molecular dynamics implementation. *Comput. Phys. Commun.* **1995**, *91*, 43-56.
39. Siu, S. W. I.; Vácha, R.; Jungwirth, P.; Böckmann, R. A., Biomolecular simulations of membranes: physical properties from different force fields. *J. Chem. Phys.* **2008**, *128*, 125103.
40. Toukan, K.; Rahman, A., Molecular-dynamics study of atomic motions in water. *Phys. Rev. B: Condens. Matter Mater. Phys.* **1985**, *31*, 2643-2648.
41. Berendsen, H. J. C.; Postma, J. P. M.; van Gunsteren, W. F.; DiNola, A.; Haak, J. R., Molecular dynamics with coupling to an external bath. *J. Chem. Phys.* **1984**, *81*, 3684-3690.
42. Ryckaert, J.-P.; Ciccotti, G.; Berendsen, H. J. C., Numerical integration of the cartesian equations of motion of a system with constraints: molecular dynamics of n-alkanes. *J. Comput. Phys.* **1977**, *23*, 327-341.
43. Pettersen, E. F.; Goddard, T. D.; Huang, C. C.; Couch, G. S.; Greenblatt, D. M.; Meng, E. C.; Ferrin, T. E., UCSF Chimera - a visualization system for exploratory research and analysis. *J. Comput. Chem.* **2004**, *25*, 1605-1612.
44. Cieplak, P.; Cornell, W. D.; Bayly, C.; Kollman, P. A.; Application of the multimolecule and multiconformational RESP methodology to biopolymers: charge derivation for DNA, RNA, and proteins. *J. Comput. Chem.* **1995**, *16*, 1357-1377.
45. Hanwell, M. D.; Curtis, D. E.; Lonie, D. C.; Vandermeersch, T.; Zurek, E.; Hutchison, G. R., Avogadro: an advanced semantic chemical editor, visualization, and analysis platform. *J. Cheminf.* **2012**, *4*, 35-45.

46. Vanquelef, E.; Simon, S.; Marquant, G.; Garcia, E.; Klimerak, G.; Delepine, J. C.; Cieplak, P.; Dupradeau, F.-Y., R.E.D. Server: a web service for deriving RESP and ESP charges and building force field libraries for new molecules and molecular fragments. *Nucleic Acids Res. 2011*, *39*, W511-W517.

Chapter 6

Summary

6. Summary

The 36-amino acid peptides neuropeptide Y (NPY), peptide YY (PYY) and pancreatic polypeptide (PP) exert their biological effects via activation of four G protein-coupled receptors (Y_1R, Y_2R, Y_4R and Y_5R), contributing to the regulation of numerous (patho)physiological processes, such as feeding behavior, pain sensitivity, seizures and anxiety. Among the NPY receptors, the Y_4R is unique, as it preferably binds PP over NPY and PYY. For a better understanding of the physiological role of the Y_4R and to explore its relevance as a potential drug target, selective Y_4R ligands are needed. Therefore, the aim of this work was the discovery of selective Y_4R agonists and antagonists, including peptidic and non-peptidic ligands.

The hexapeptide UR-KK236 (Ac-Arg-Tyr-Arg-Leu-Arg-Tyr-NH_2, **2.1**), a high affinity Y_4R partial agonist (K_i = 3.4 nM), was used as lead structure for the development of new Y_4R agonists and antagonists. N-terminal truncation of **2.1** by two amino acids resulted in a tetrapeptide (Arg-Leu-Arg-Tyr-NH_2) (UR-AK32, **2.29**) acting as Y_4R partial agonist and showing as high Y_4R affinity (K_i = 3.4 nM) as **2.1**. Replacement of individual amino acids in **2.29** by unnatural amino acids such as naphthylalanine, β-homoleucine, 4-nitrophenylalanine and D-configured amino acids did not result in increased Y_4R affinity. However, compound **2.29**, representing the smallest high-affinity Y_4R ligand to date, might serve as a lead structure for the development of non-peptidic Y_4R ligands in future projects. Interestingly, replacement of Leu^4 in **2.1** by Trp was identified as a key modification to turn Y_4R agonism into antagonism (e.g. UR-AK1 (**2.13**), Arg-Tyr-Arg-Trp-Arg-Tyr-NH_2). Compound **2.13**, exhibiting a pK_i of 7.57 (radioligand competition binding), behaved as an antagonist in Y_4R β-arrestin-1 and β-arrestin-2 recruitment assays, as well as in a Y_4R Ca^{2+} aequorin assay measuring G-protein activation (K_b values: 7.14, 6.87 and 7.32, respectively). The results from induced-fit docking studies, using homology models of the Y_4R, suggested a different binding pose for the antagonist **2.13** compared to the agonists **2.1** and **2.29**, being consistent with the experimental data.

Moreover, based on the structures of **2.1**, **2.13** and **2.29** and their key interactions with the Y_4R, suggested by induced-fit docking studies, potential non-peptidic Y_4R ligands with low molecular weight (< 503 g/mole) were designed. The virtual Y_4R ligands were investigated by induced-fit docking using a Y_4R homology model, and one series of compounds, containing a 3,5-bis(aminomethyl)benzoyl and a tricyclic 1*H*-pyrrolo[3,4-*b*]quinoline-1,3(2*H*)-dione moiety, was synthesized. Most of these compounds did not bind to the Y_4R, but two compounds (UR-AK113, UR-AK118) displayed Y_4R binding. The more potent ligand, UR-AK113 (**4.32**), containing two basic guanidine groups, exhibited a pK_i value of 6.03 and showed agonistic behavior in a β-arrestin 2 recruitment assay. In future approaches, **4.32** can potentially serve as a template for the synthesis of non-peptidic Y_4R ligands showing higher Y_4R affinity.

Besides the discovery of the aforementioned peptidic Y_4R antagonists, a major achievement of this work was the introduction of N-terminus-to-arginine side chain cyclized hexapeptides as a new class of Y_4R (partial) agonists exhibiting high Y_4R potency, affinity and selectivity. Among these compounds, UR-AK86c (cyclo[succinyl-Arg-Tyr-Arg(carb)]-Leu-Arg-Tyr-NH_2, **5.18**) and UR-AK95c (cyclo[succinyl-Arg-Trp-Arg(carb)]-Leu-Arg-Tyr-NH_2, **5.24**) (note: Arg(carb) stands for an amino-functionalized N^{ω}-carbamoylated arginine) showed the highest Y_4R affinities with pK_i values > 10. Worth mentioning, the non-cyclized, linear precursor peptides of **5.18** and **5.24** exhibited considerably lower Y_4R affinity (27-fold and 64-fold, respectively). Stability studies with **5.18** and **5.24** in human plasma at 37 °C revealed rather low plasma stabilities (half-lives of ca. 2 h) due to proteolytic cleavage within the linear C-terminal tripeptide sequence (amide bond between Leu^4 and Arg^5), which is crucial for Y_4R binding. Therefore, structural optimizations of the cyclic peptides are required with respect to metabolic stability and in vivo applications. Notably, cyclic peptides such as **5.24**, exhibiting even higher Y_4R affinity than the endogenous ligand hPP, represent attractive lead structures for the synthesis of new Y_4R radio- and fluorescent-ligands, and can possibly be used as tools to support the crystallization of the hY_4R in its active state.

In summary, the approaches pursued in this thesis afforded new useful Y_4R ligands, which can serve as pharmacological tools to study the physiological role of the NPY Y_4 receptor, or as lead structures for future ligand development including labeled molecular tools for the Y_4R.

Chapter 7

Appendix

7.1 Appendix Chapter 2

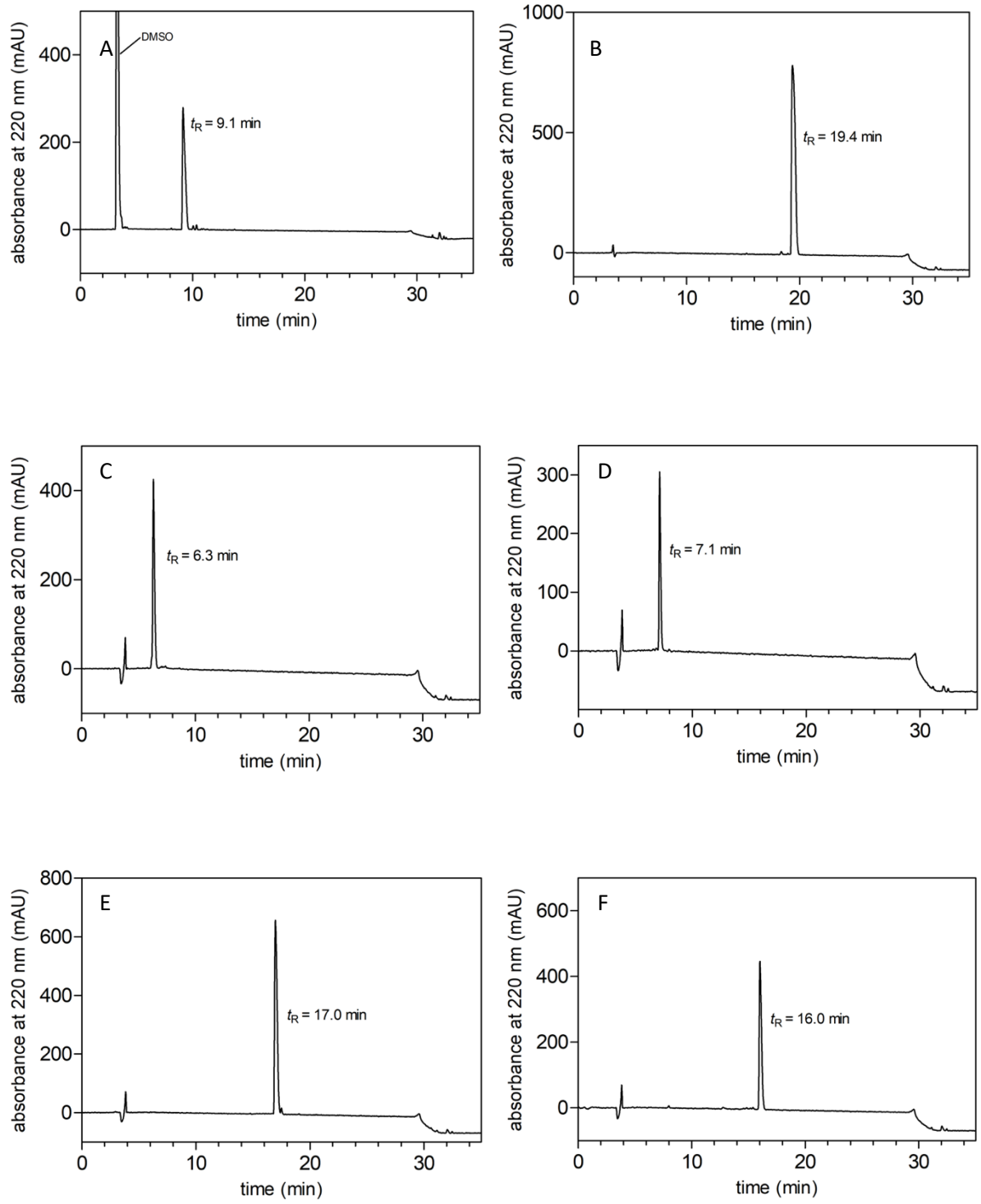

RP-HPLC analysis of compound **2.8** (A), **2.9** (B), **2.10** (C), **2.11** (D), **2.12** (E) and **2.13** (F).

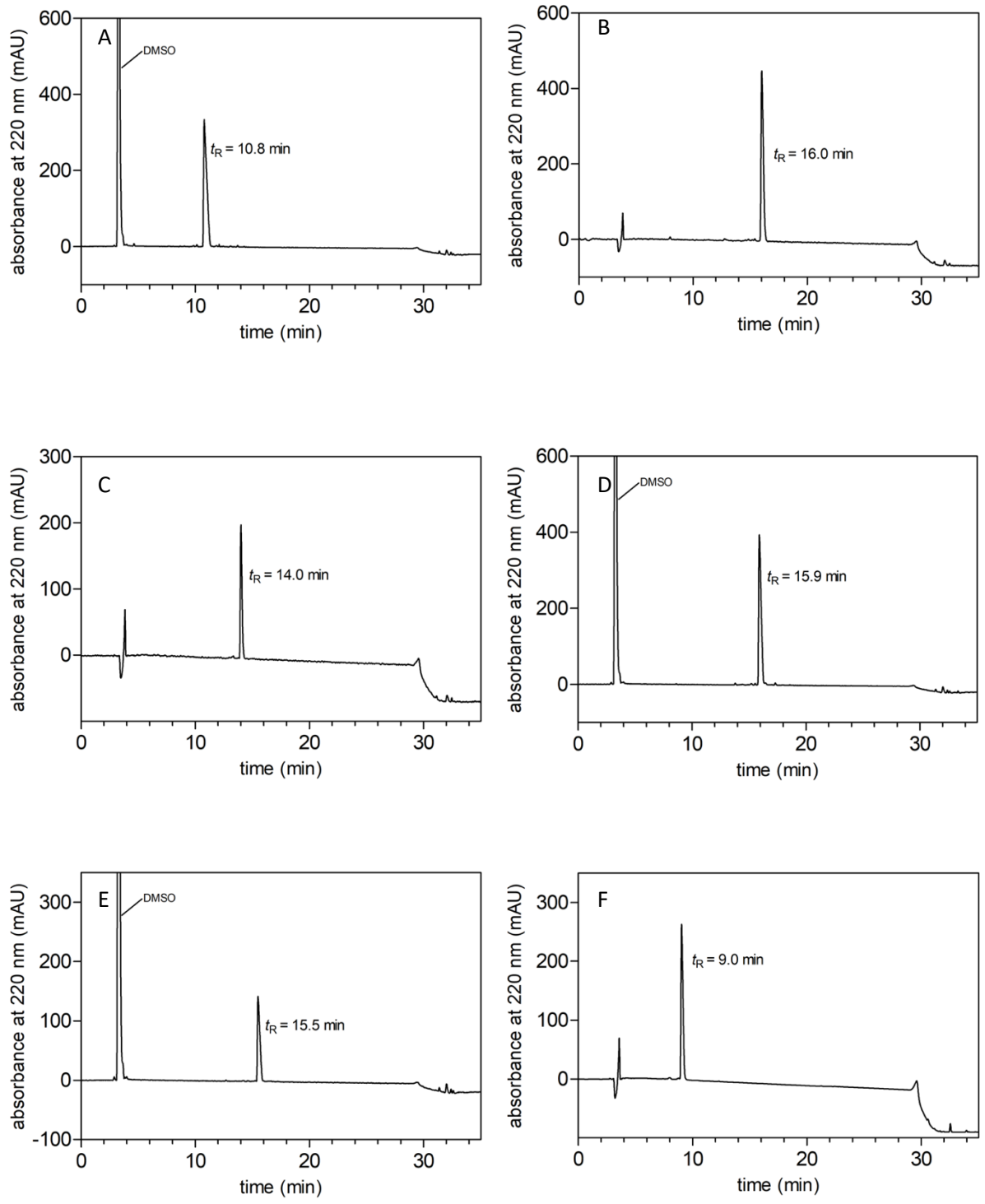

RP-HPLC analysis of compound **2.14** (A), **2.15** (B), **2.16** (C), **2.17** (D), **2.18** (E) and **2.19** (F).

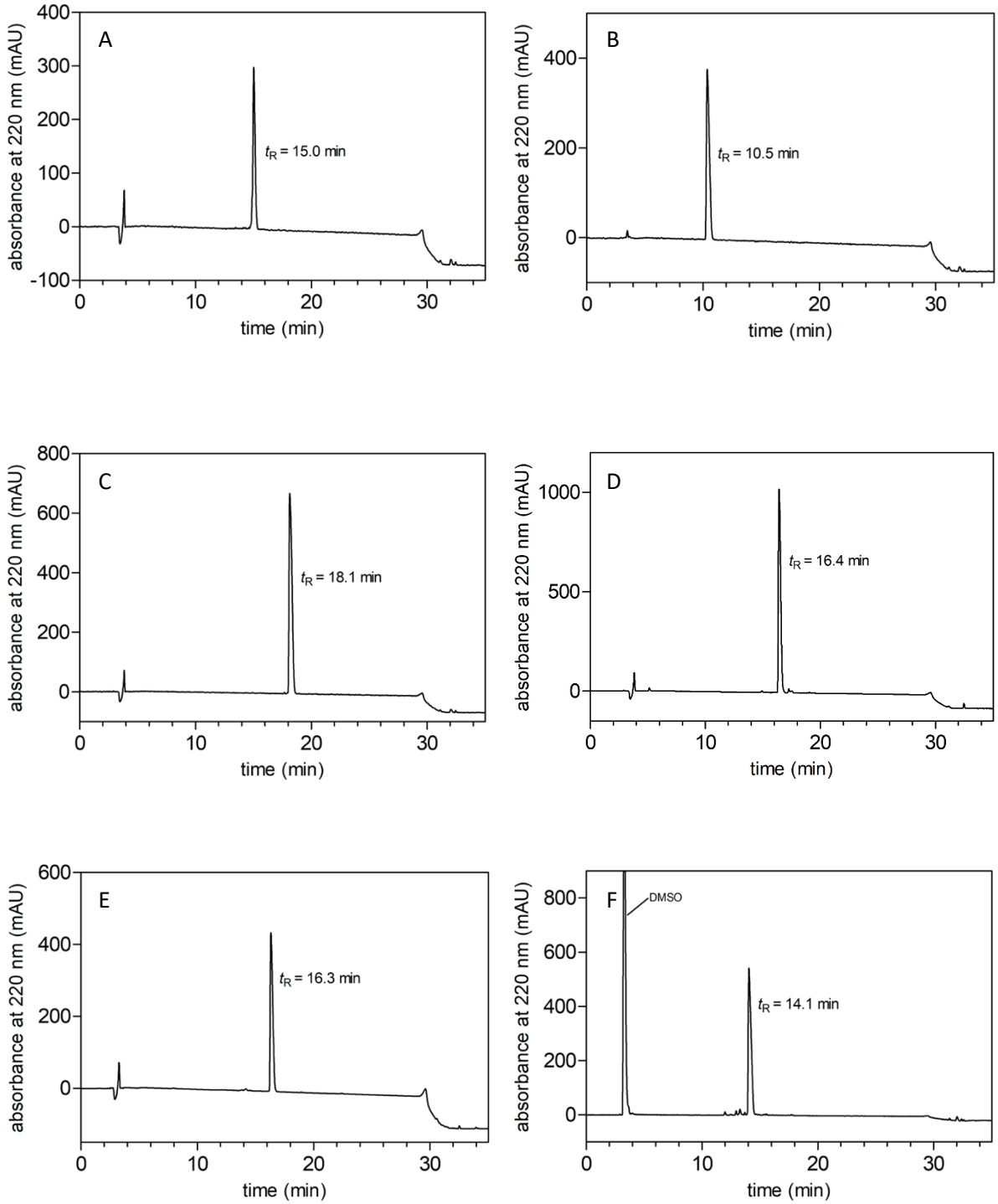

RP-HPLC analysis of compound **2.20** (A), **2.21** (B), **2.22** (C), **2.23** (D), **2.24** (E) and **2.25** (F).

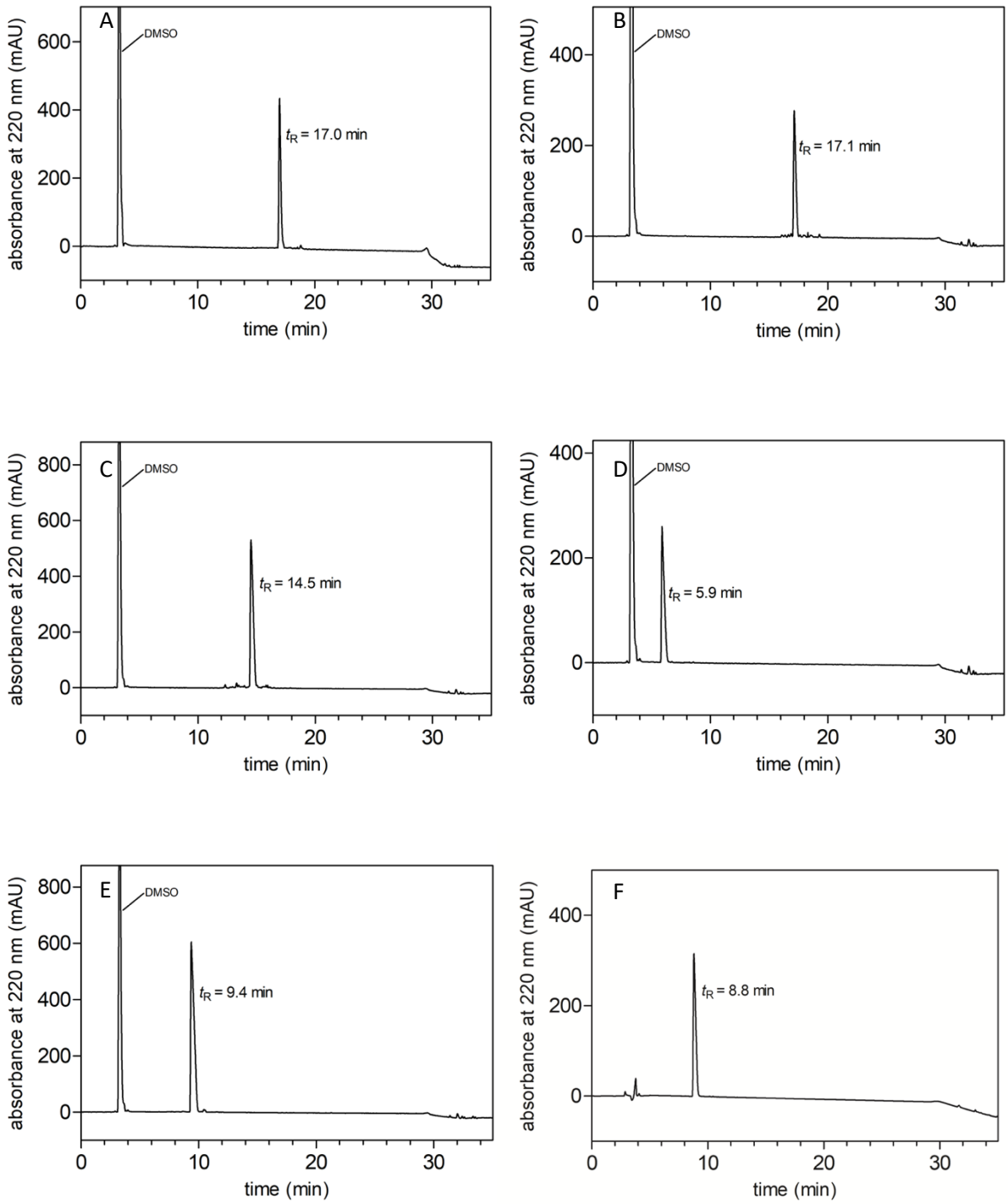

RP-HPLC analysis of compound **2.26** (A), **2.27** (B), **2.28** (C), **2.29** (D), **2.30** (E) and **2.31** (F).

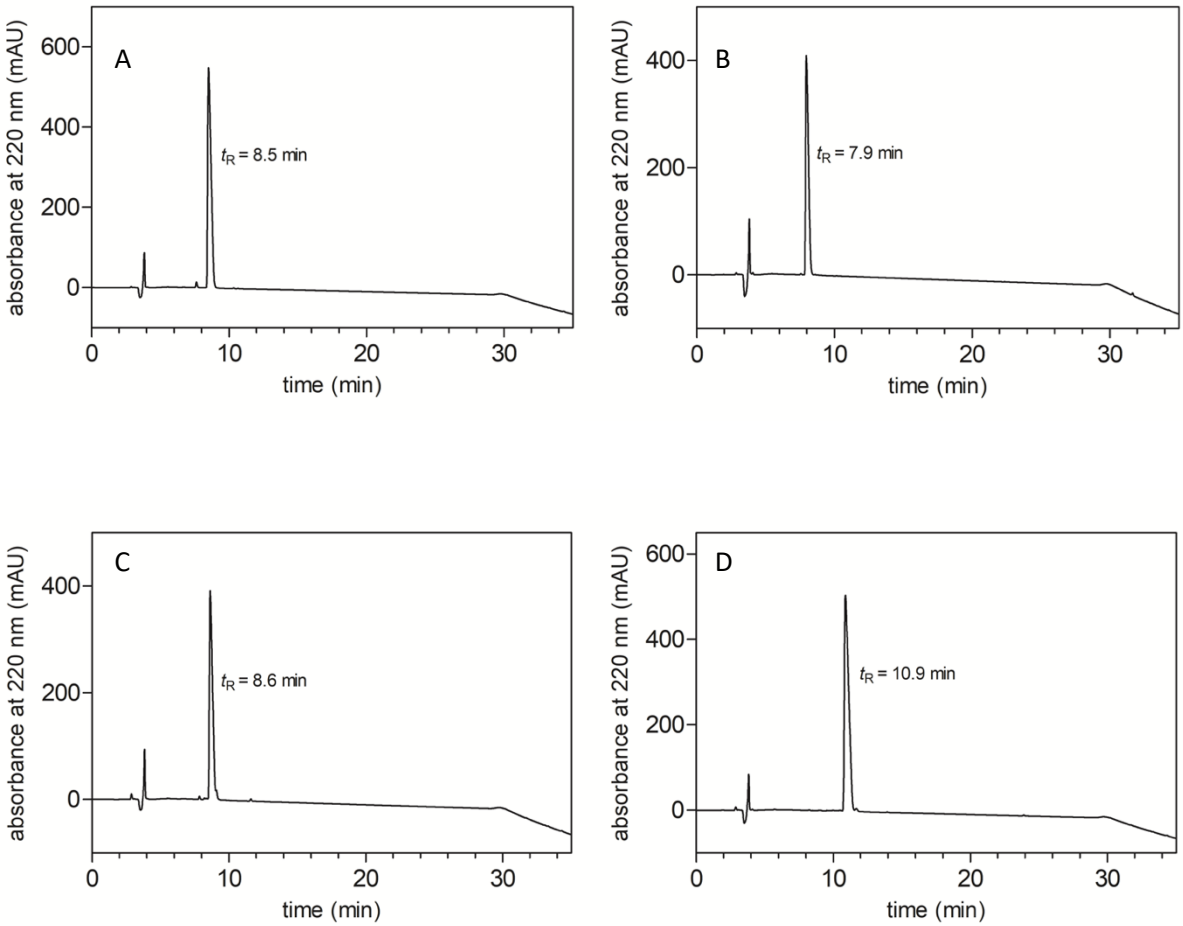

RP-HPLC analysis of compound **2.32** (A), **2.33** (B), **2.34** (C) and **2.35** (D).

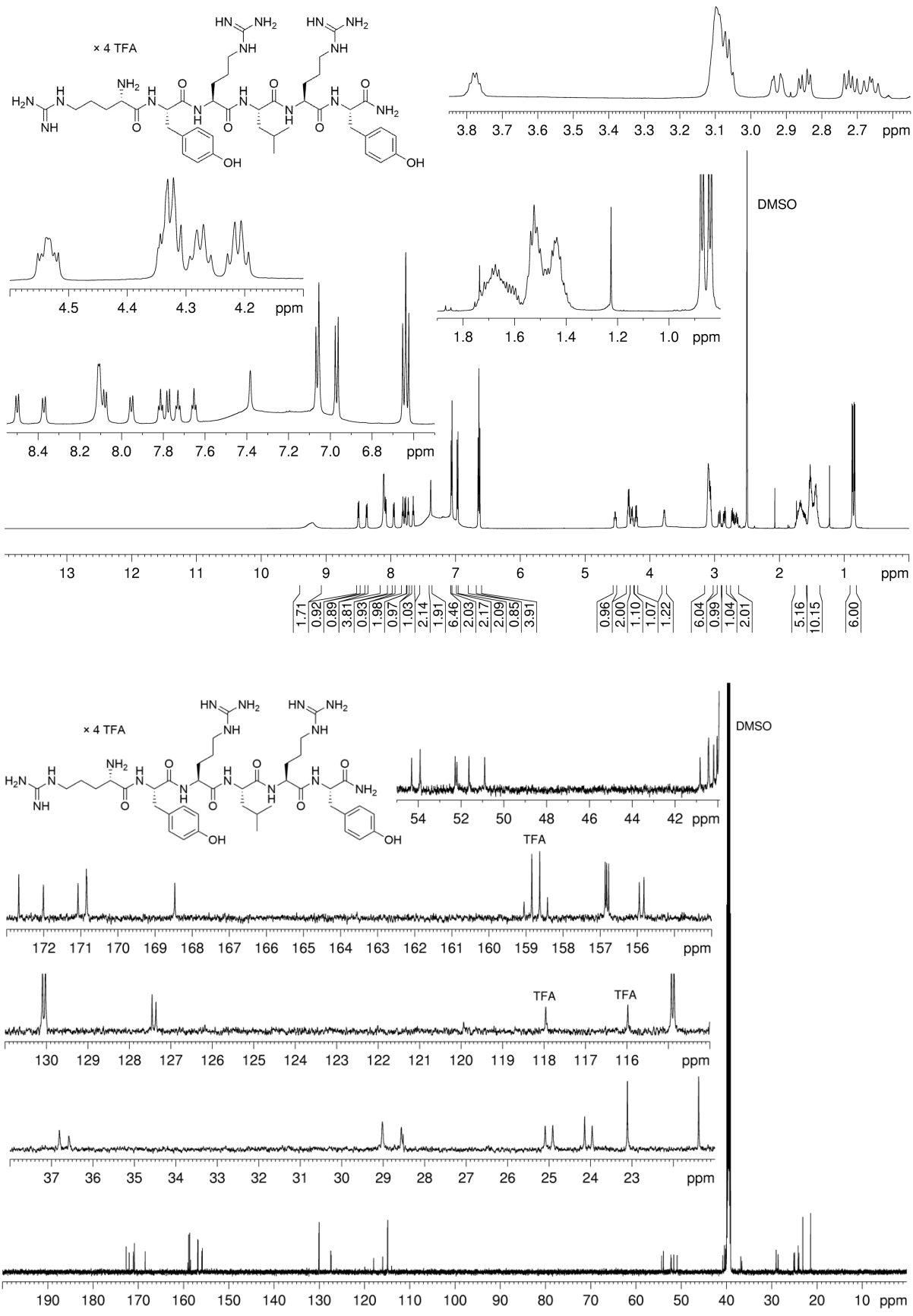

^{1}H-NMR (600 MHz, DMSO-d_6) and ^{13}C-NMR (150 MHz, DMSO-d_6) spectrum of compound **2.8**

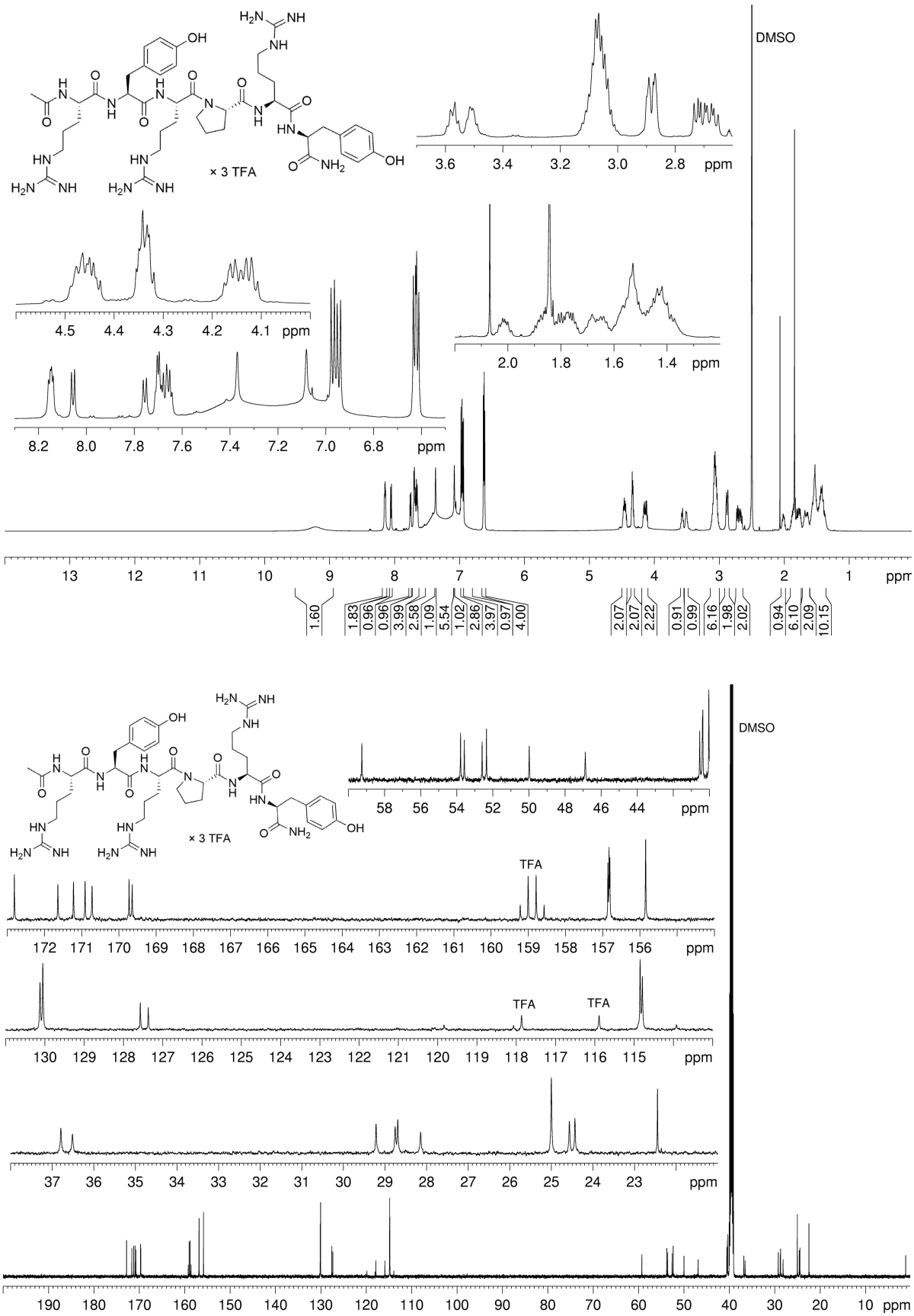

^{1}H-NMR (600 MHz, DMSO-d_6) and ^{13}C-NMR (150 MHz, DMSO-d_6) spectrum of compound **2.9**

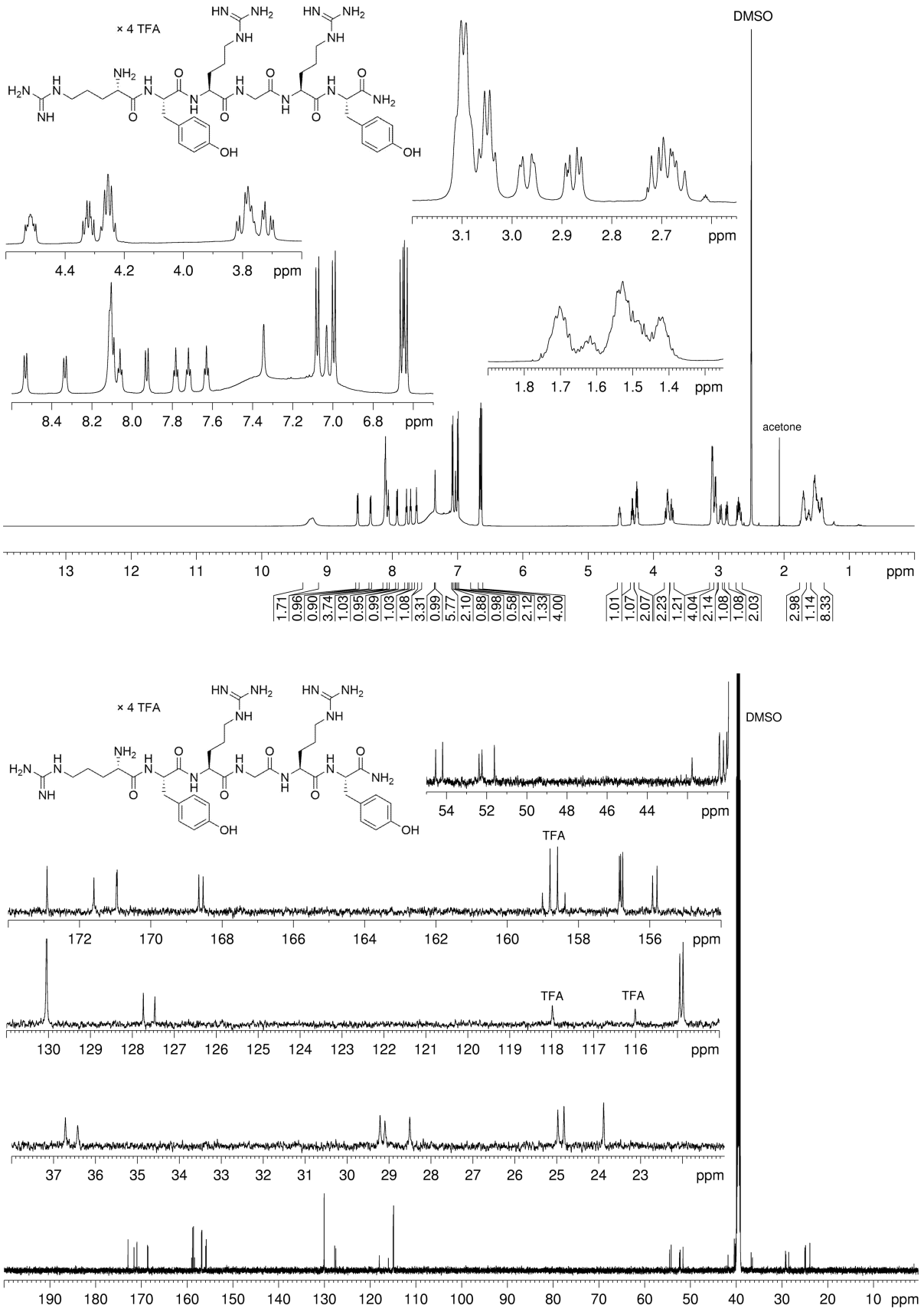

^{1}H-NMR (600 MHz, DMSO-d_6) and ^{13}C-NMR (150 MHz, DMSO-d_6) spectrum of compound **2.10**

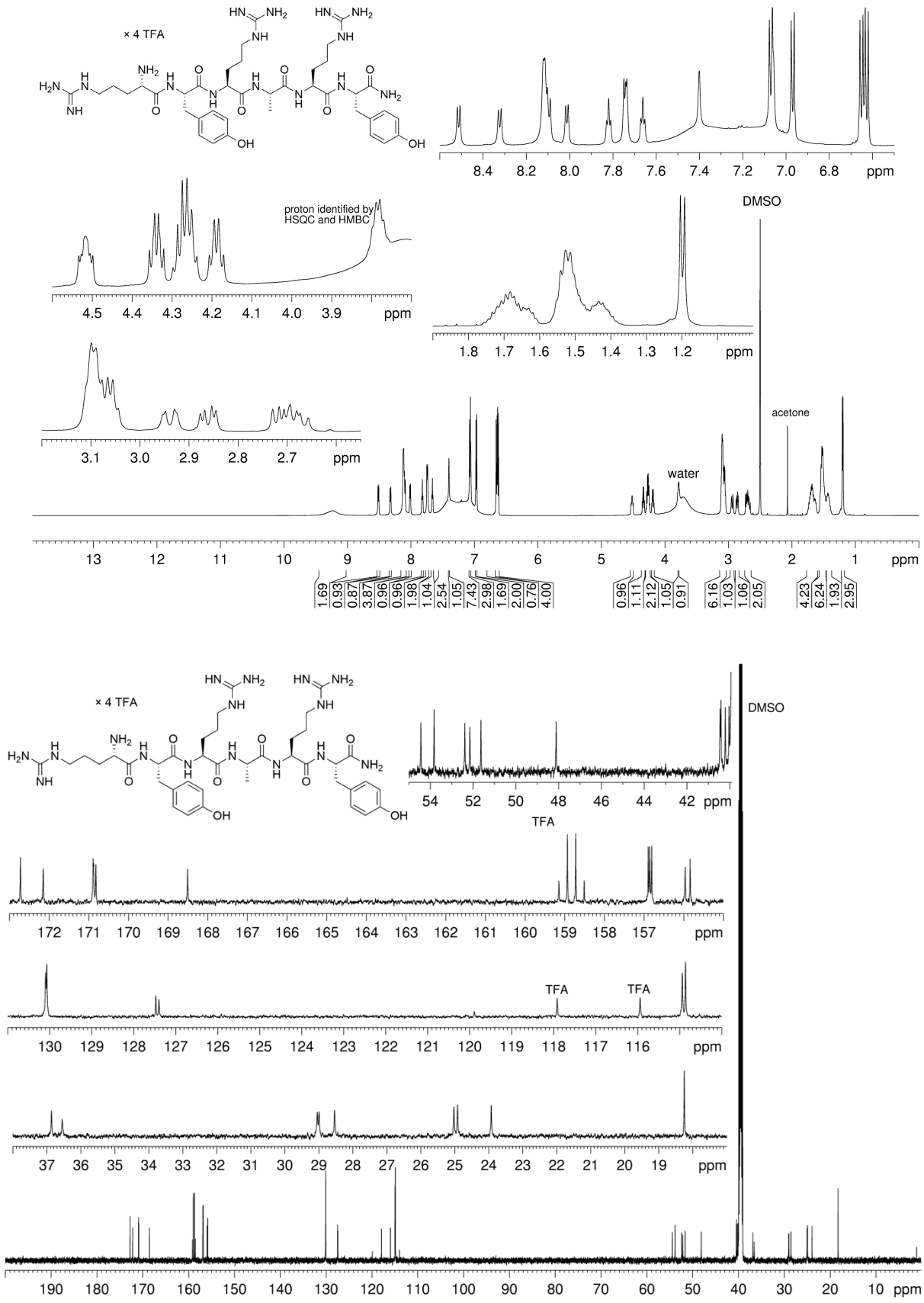

^{1}H-NMR (600 MHz, DMSO-d_6) and ^{13}C-NMR (150 MHz, DMSO-d_6) spectrum of compound **2.11**

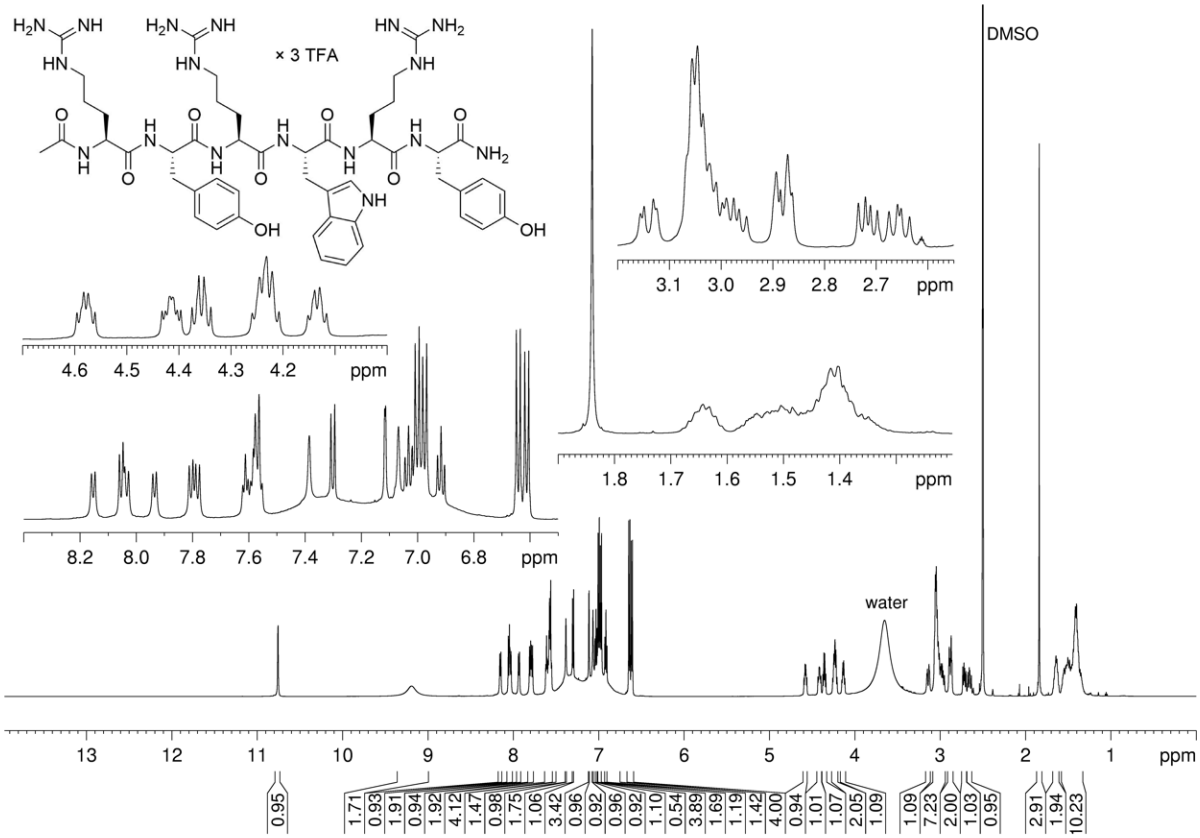

^{1}H-NMR (600 MHz, DMSO-d_6) spectrum of compound **2.12**

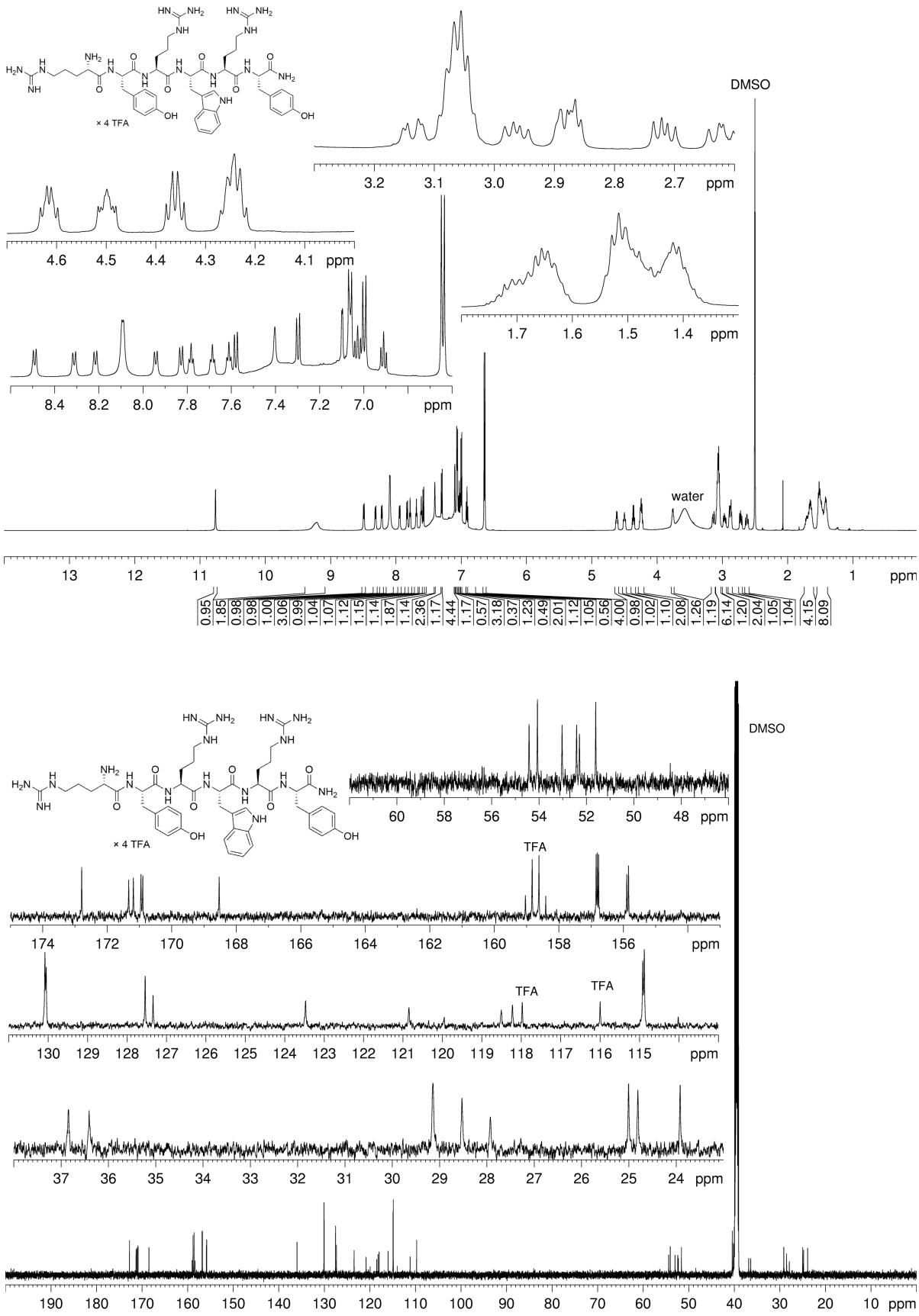

^{1}H-NMR (600 MHz, DMSO-d_6) and ^{13}C-NMR (150 MHz, DMSO-d_6) spectrum of compound **2.13**

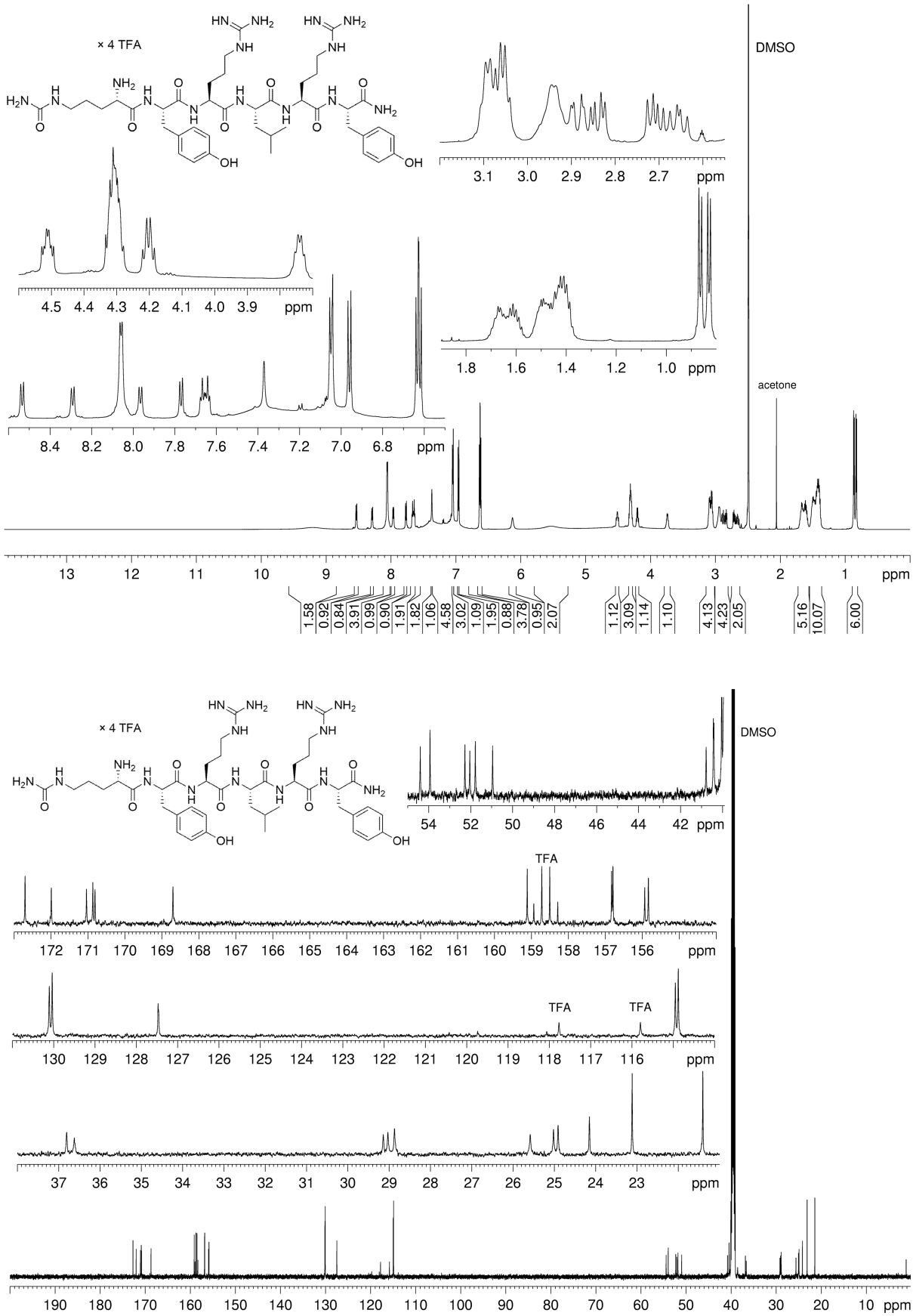

^{1}H-NMR (600 MHz, DMSO-d_6) and ^{13}C-NMR (150 MHz, DMSO-d_6) spectrum of compound **2.14**

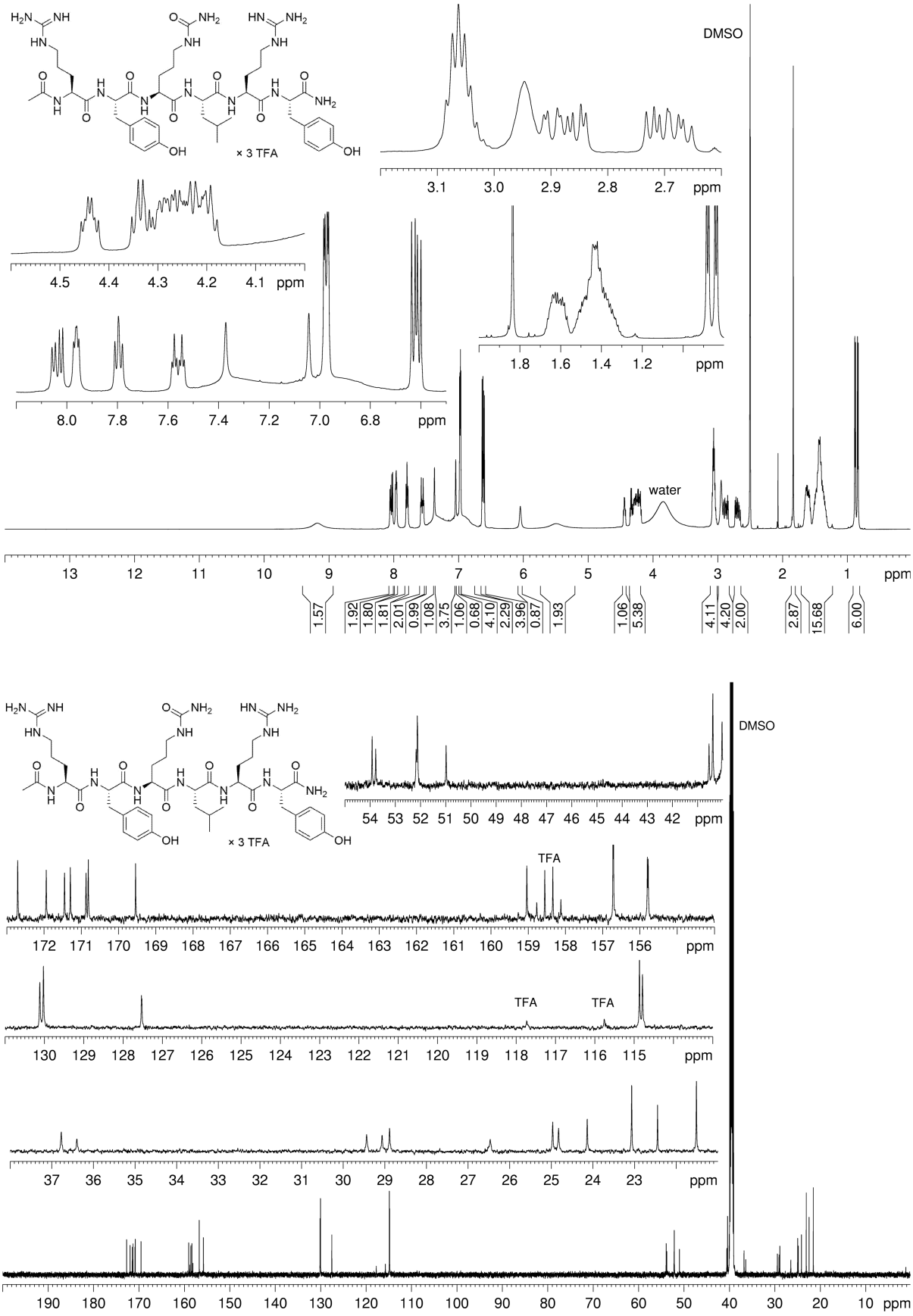

^{1}H-NMR (600 MHz, DMSO-d_6) and ^{13}C-NMR (150 MHz, DMSO-d_6) spectrum of compound **2.15**

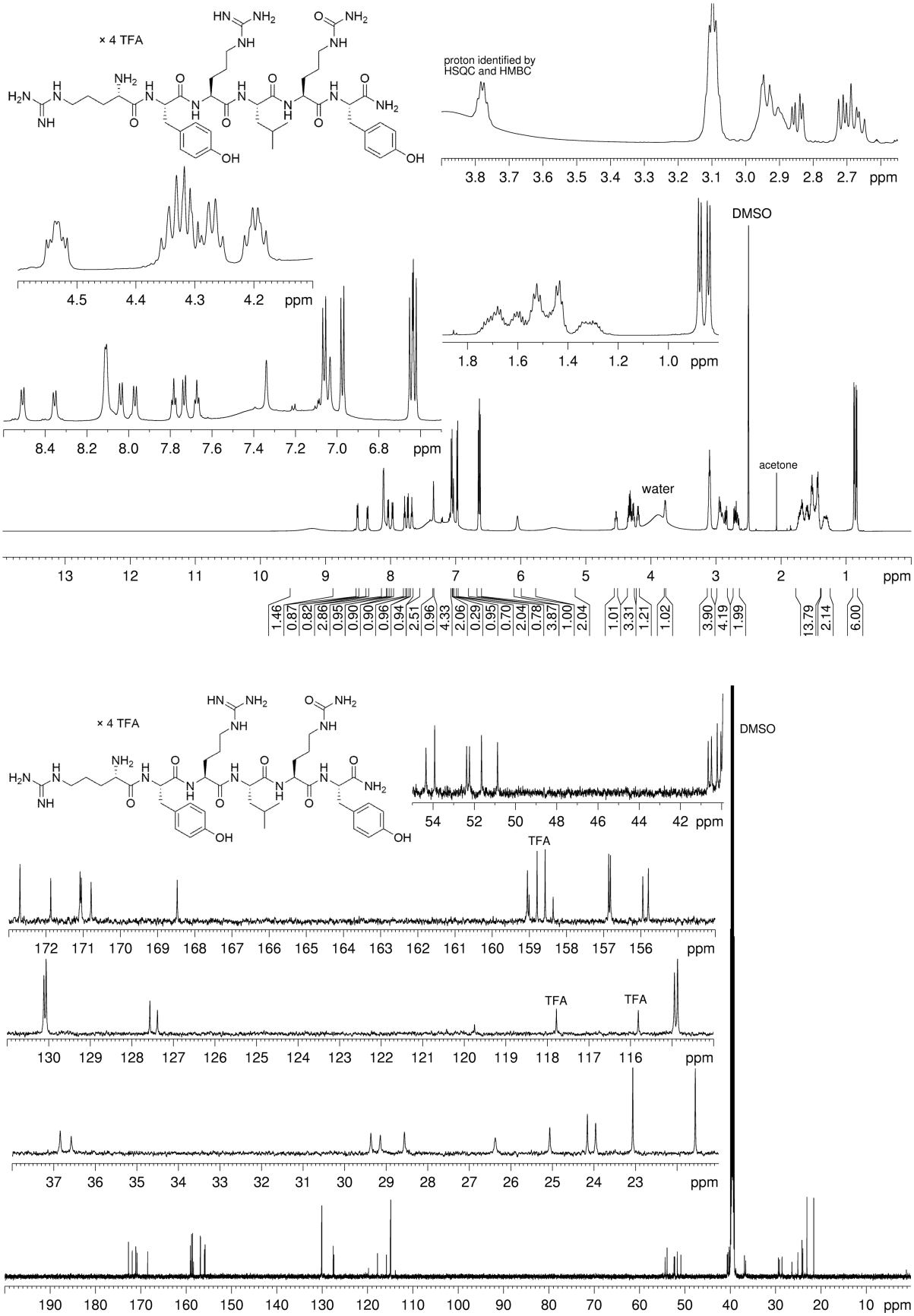

^{1}H-NMR (600 MHz, DMSO-d_6) and ^{13}C-NMR (150 MHz, DMSO-d_6) spectrum of compound **2.16**

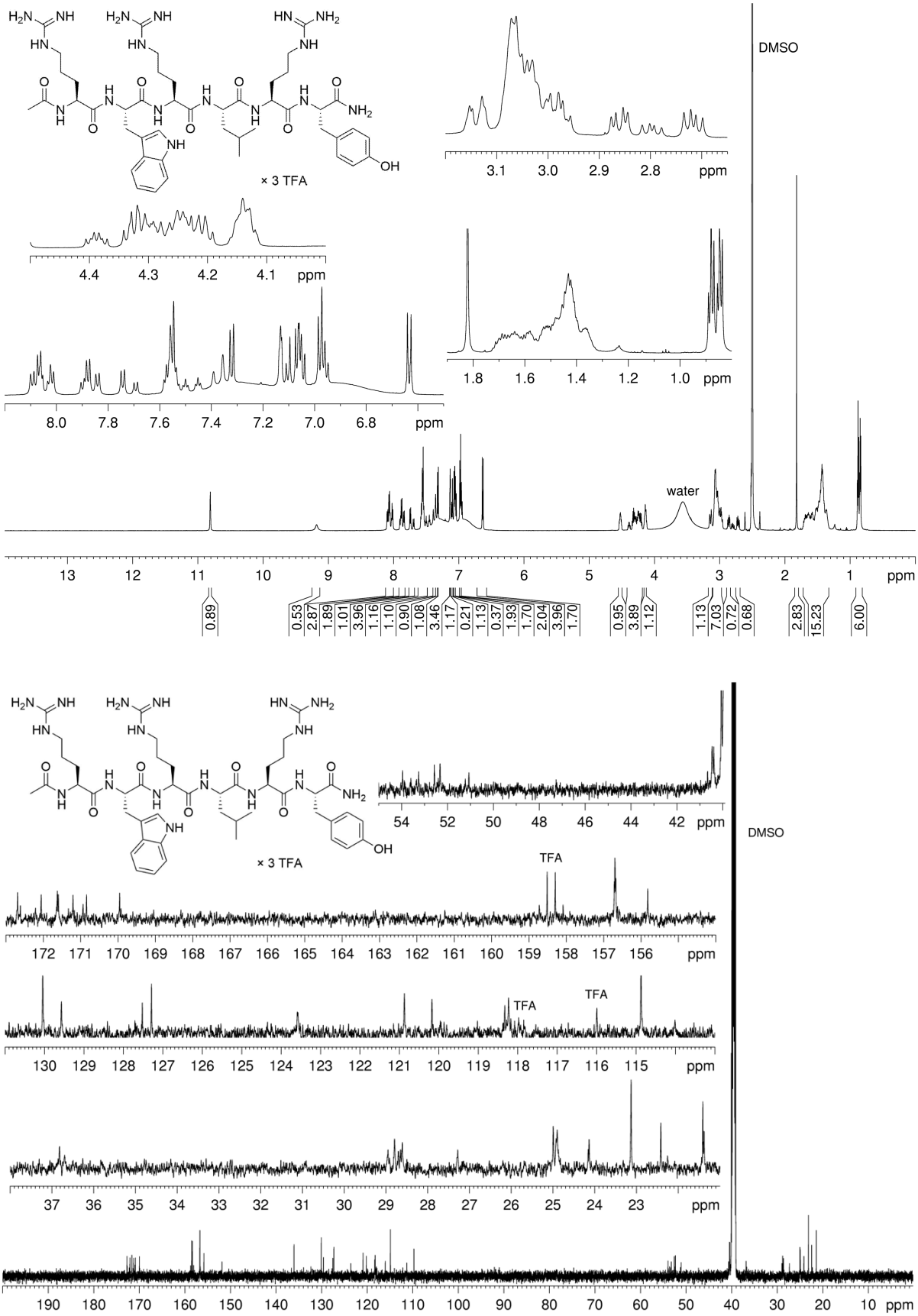

^{1}H-NMR (600 MHz, DMSO-d_6) and ^{13}C-NMR (150 MHz, DMSO-d_6) spectrum of compound **2.17**

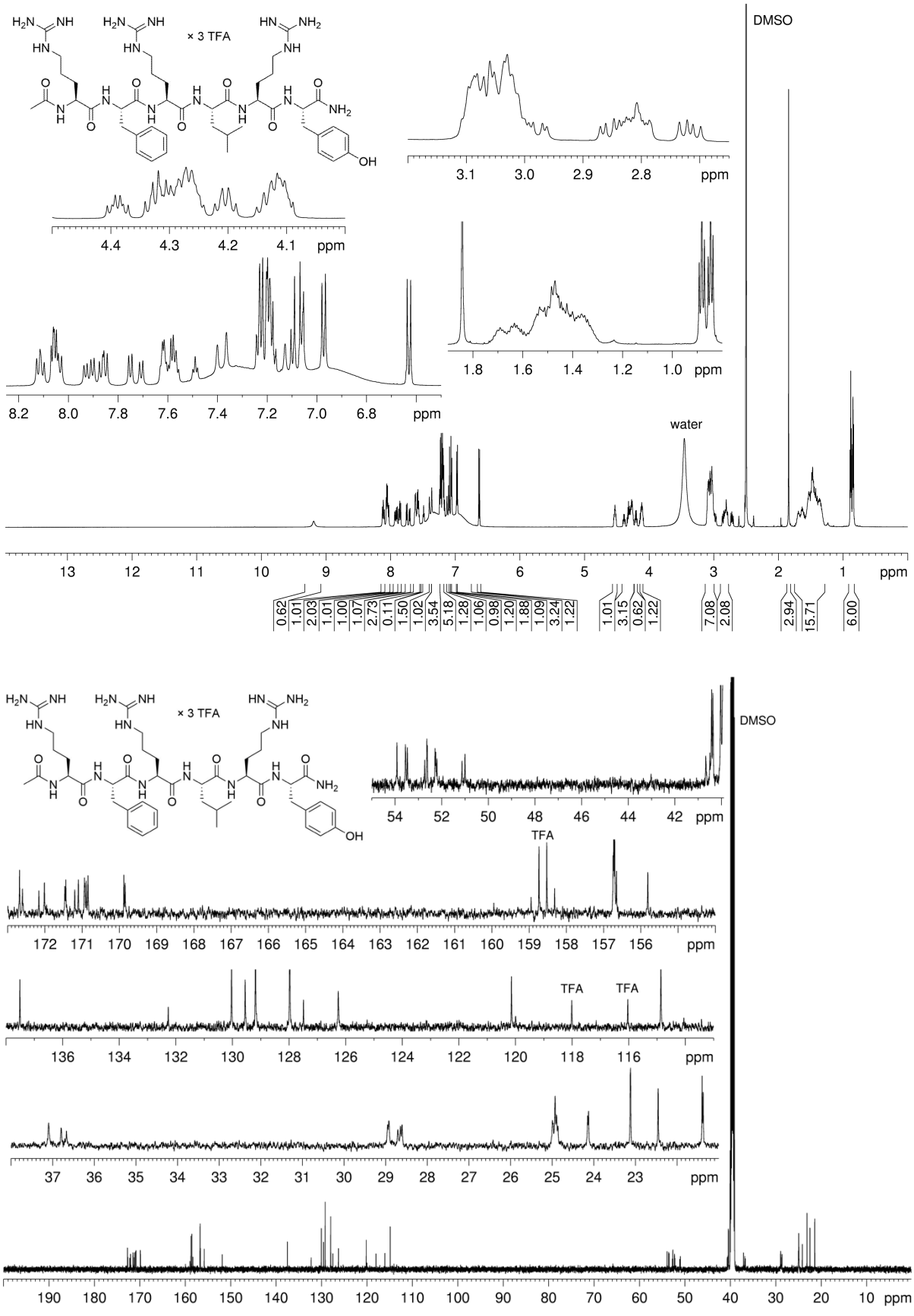

^{1}H-NMR (600 MHz, DMSO-d_6) and ^{13}C-NMR (150 MHz, DMSO-d_6) spectrum of compound **2.18**

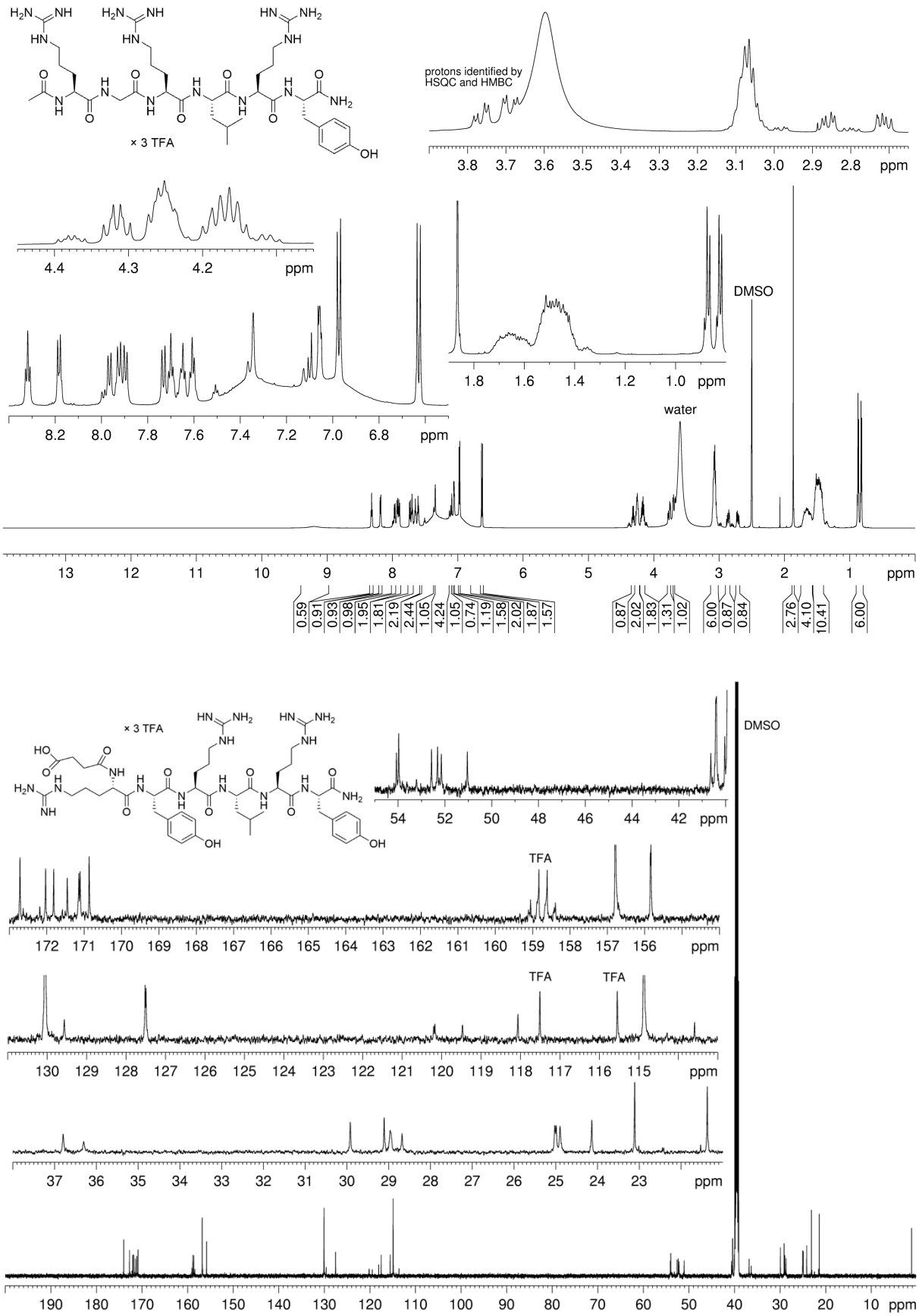

^{1}H-NMR (600 MHz, DMSO-d_6) and ^{13}C-NMR (150 MHz, DMSO-d_6) spectrum of compound **2.19**

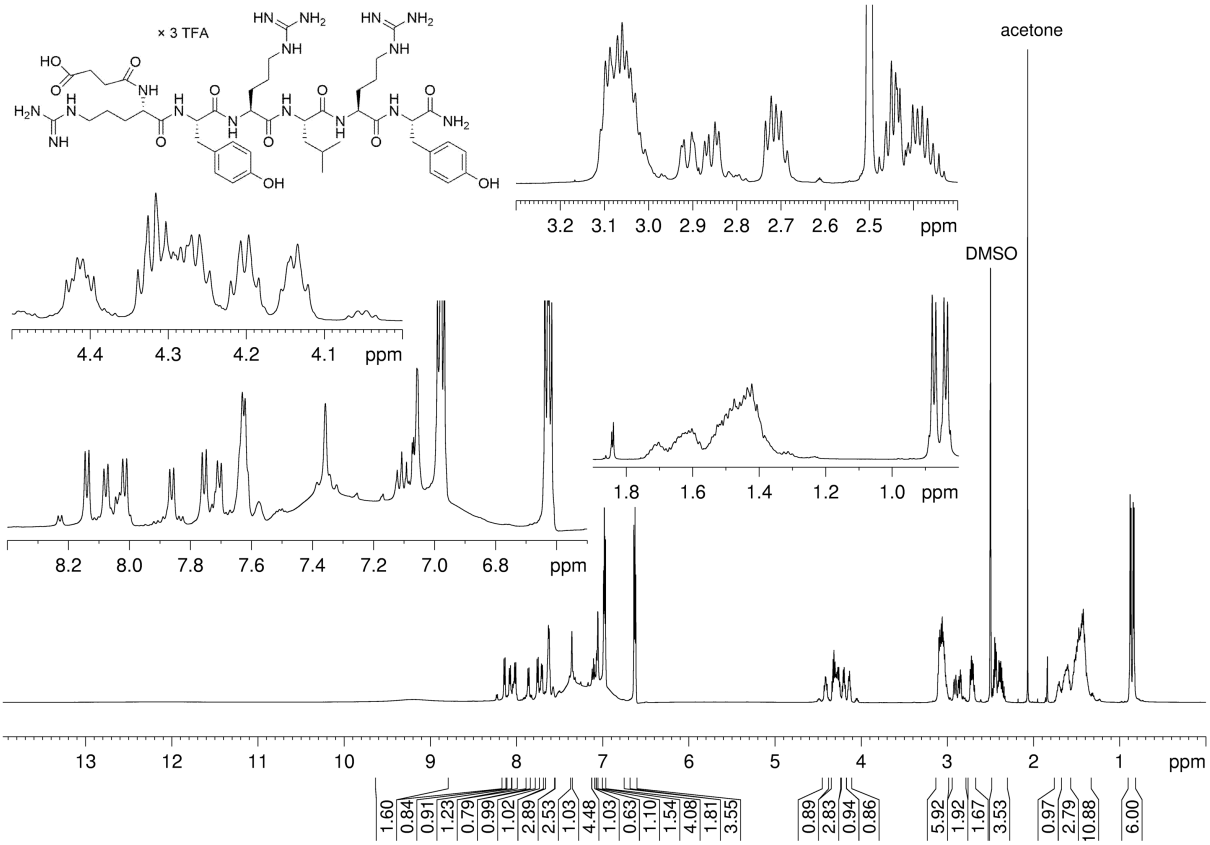

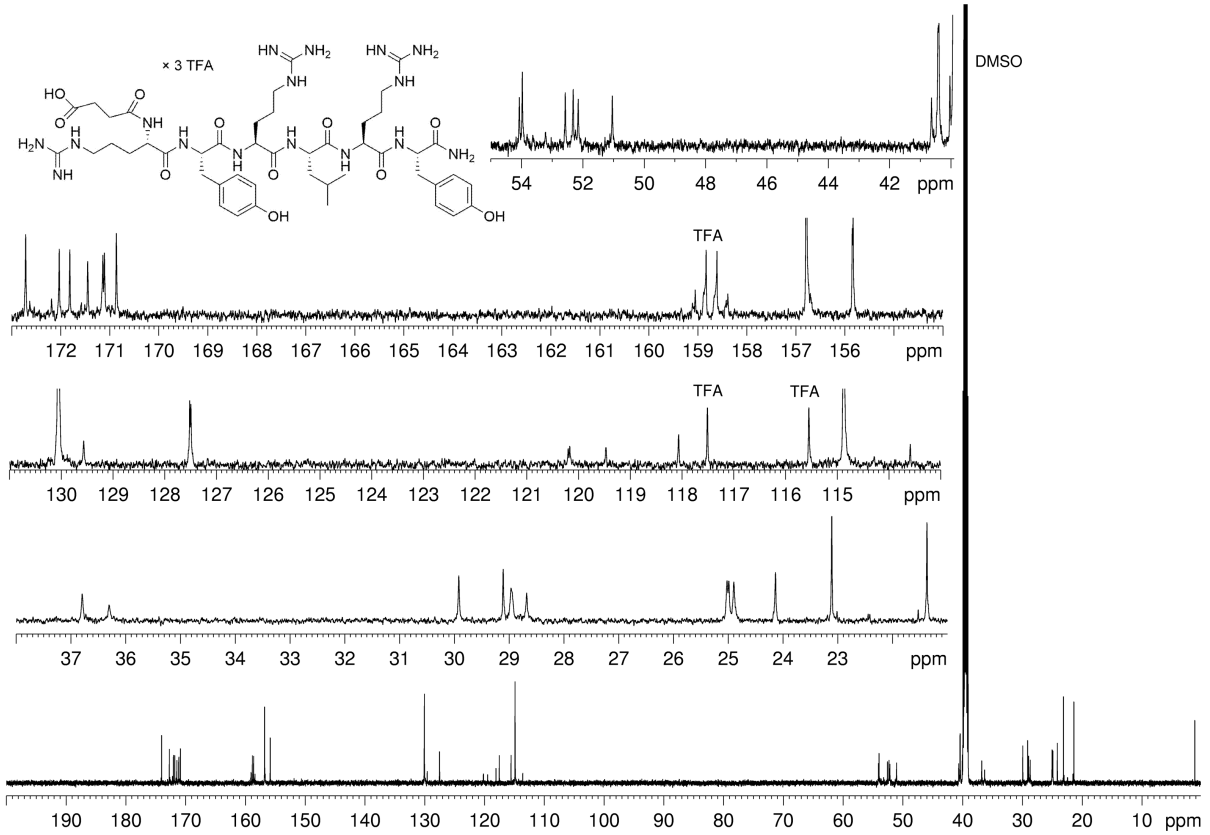

^{1}H-NMR (600 MHz, DMSO-d_6) and ^{13}C-NMR (150 MHz, DMSO-d_6) spectrum of compound **2.20**

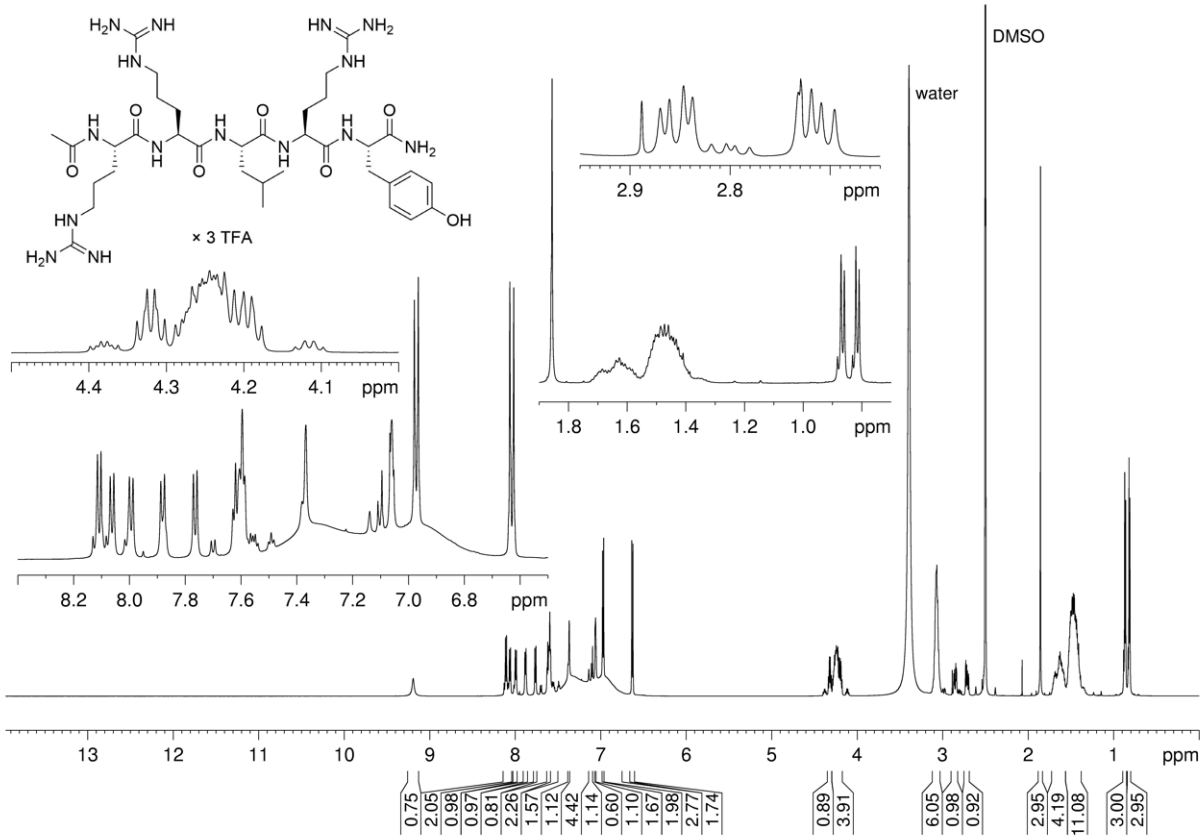

^{1}H-NMR (600 MHz, DMSO-d_6) spectrum of compound **2.21**

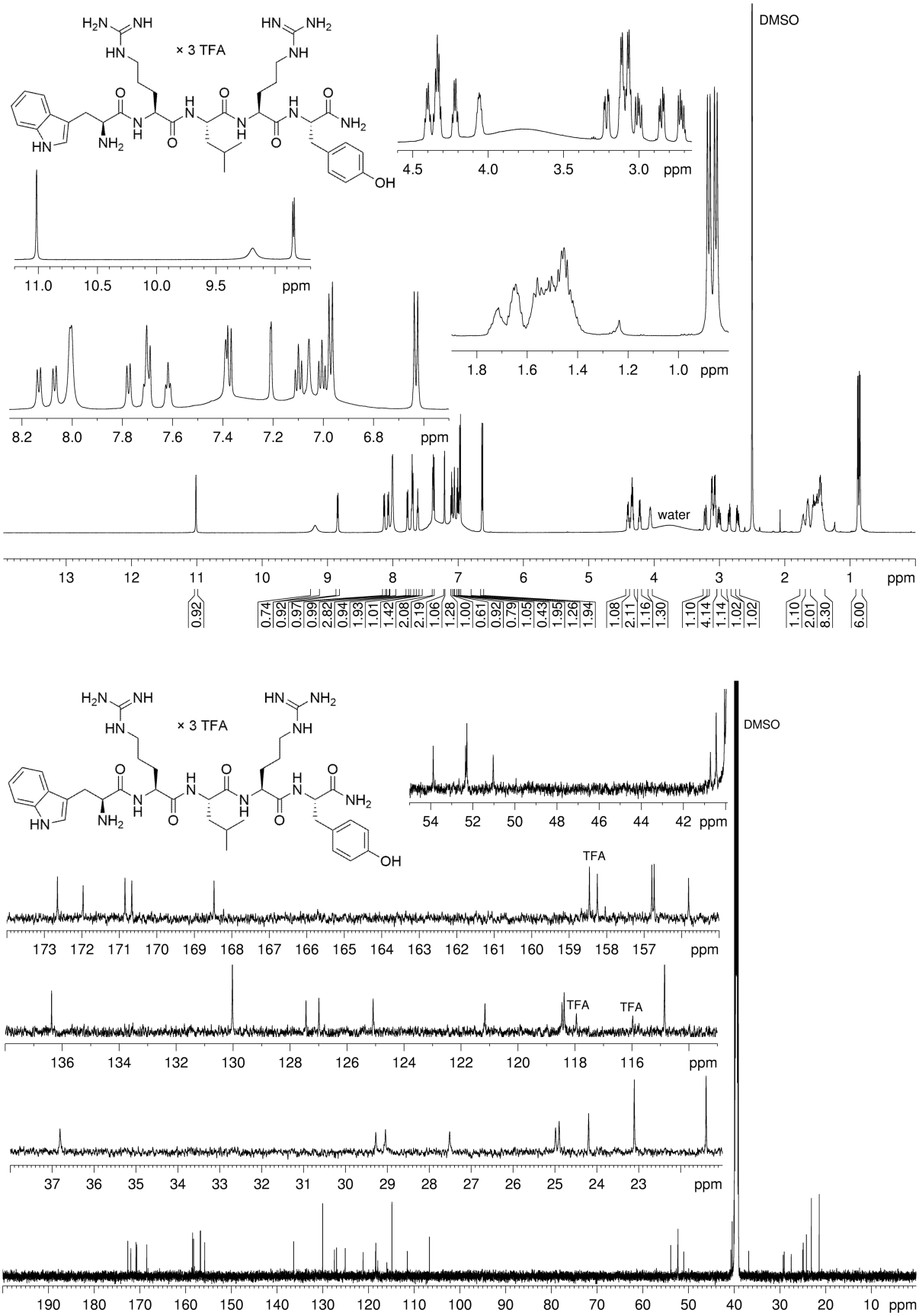

^{1}H-NMR (600 MHz, DMSO-d_6) and ^{13}C-NMR (150 MHz, DMSO-d_6) spectrum of compound **2.22**

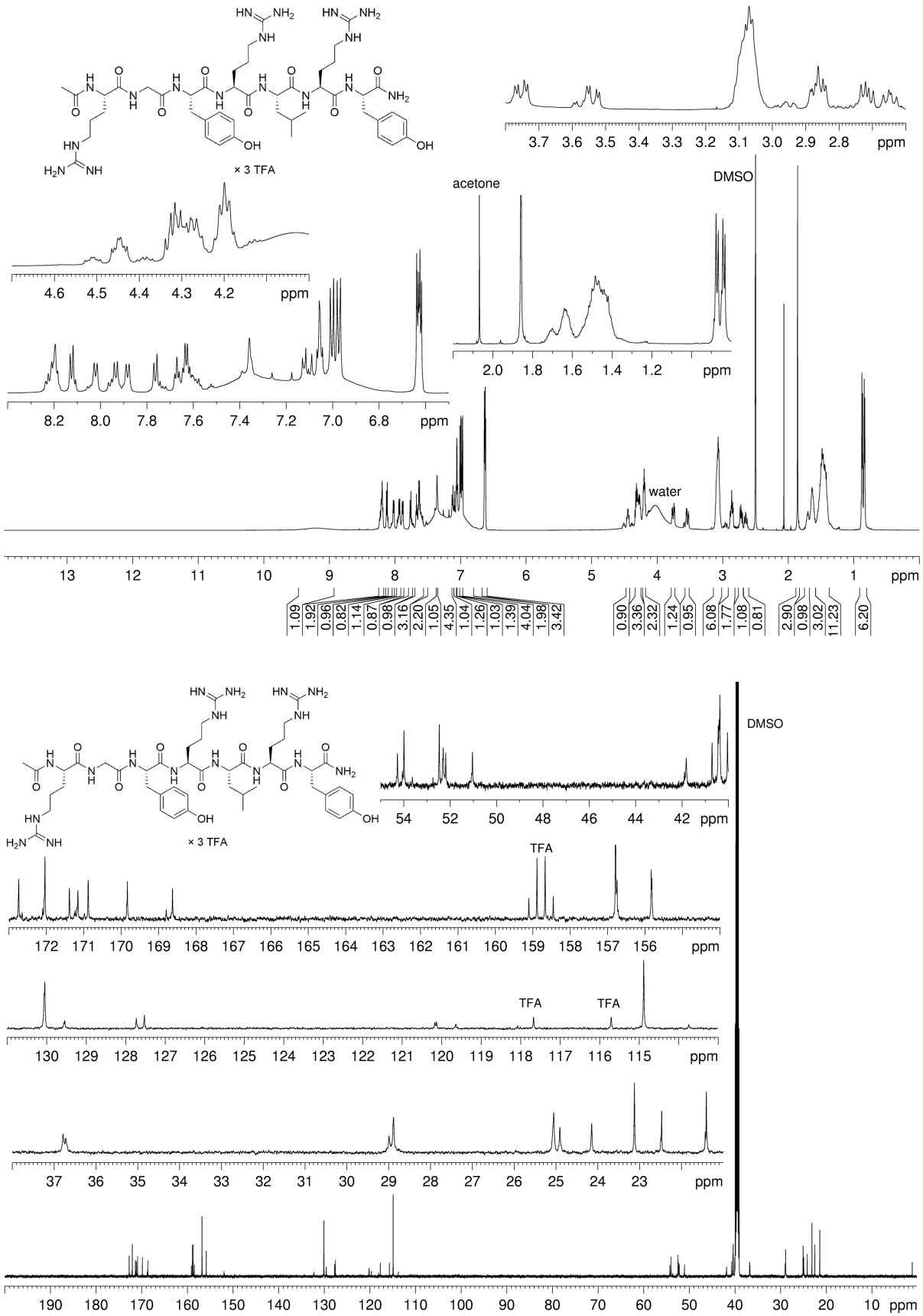

^{1}H-NMR (600 MHz, DMSO-d_6) and ^{13}C-NMR (150 MHz, DMSO-d_6) spectrum of compound **2.23**

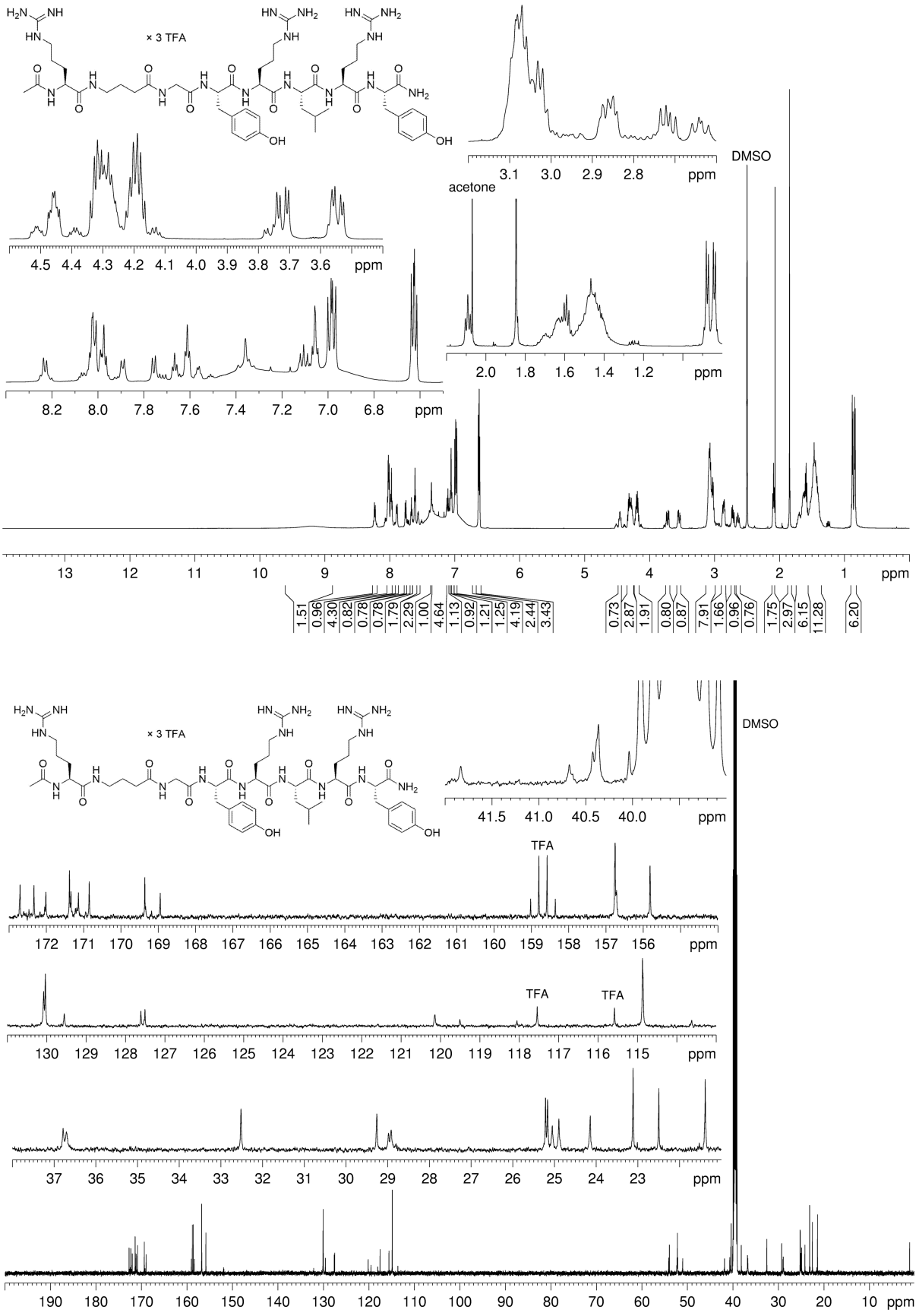

^{1}H-NMR (600 MHz, DMSO-d_6) and ^{13}C-NMR (150 MHz, DMSO-d_6) spectrum of compound **2.24**

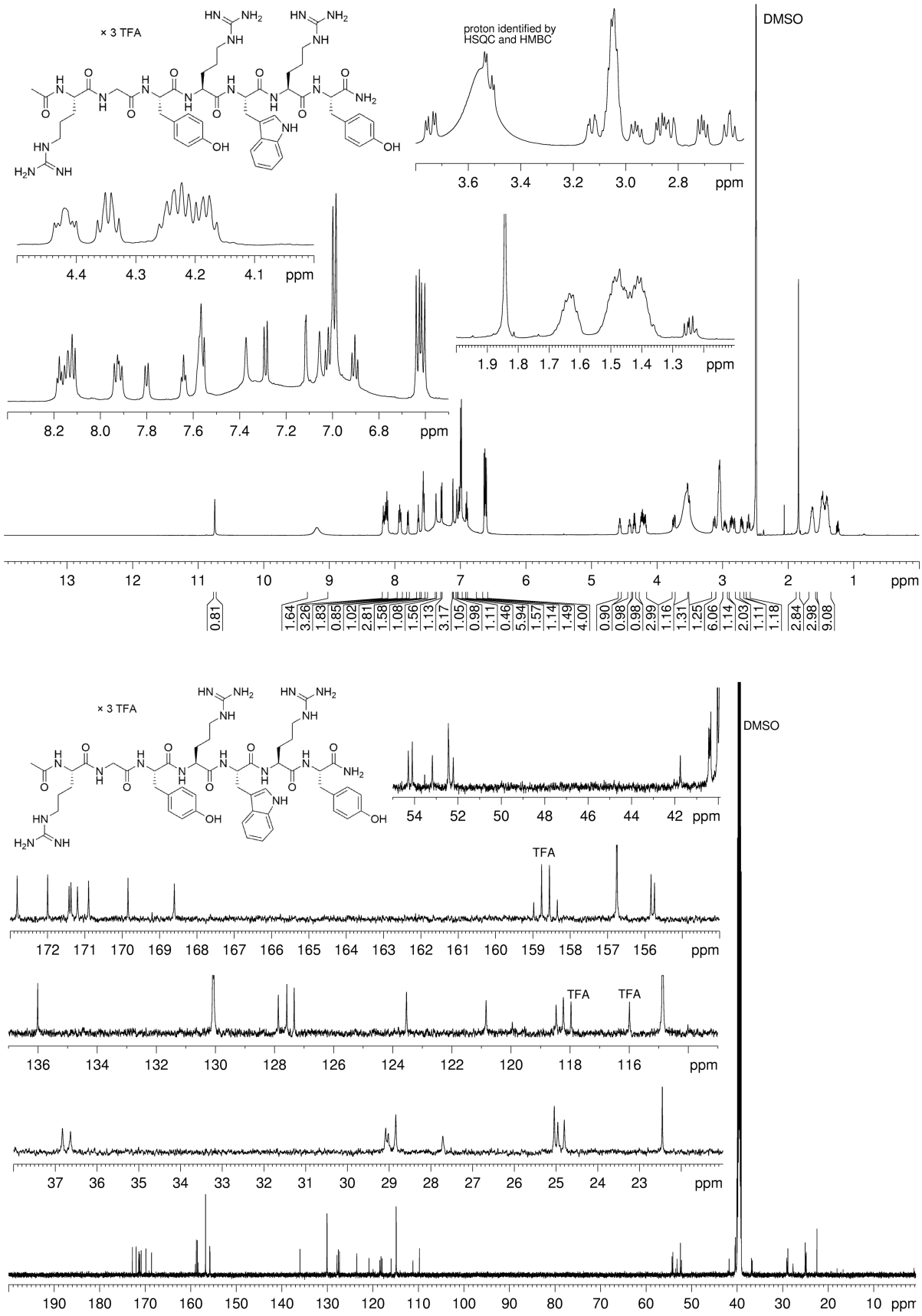

^{1}H-NMR (600 MHz, DMSO-d_6) and ^{13}C-NMR (150 MHz, DMSO-d_6) spectrum of compound **2.25**

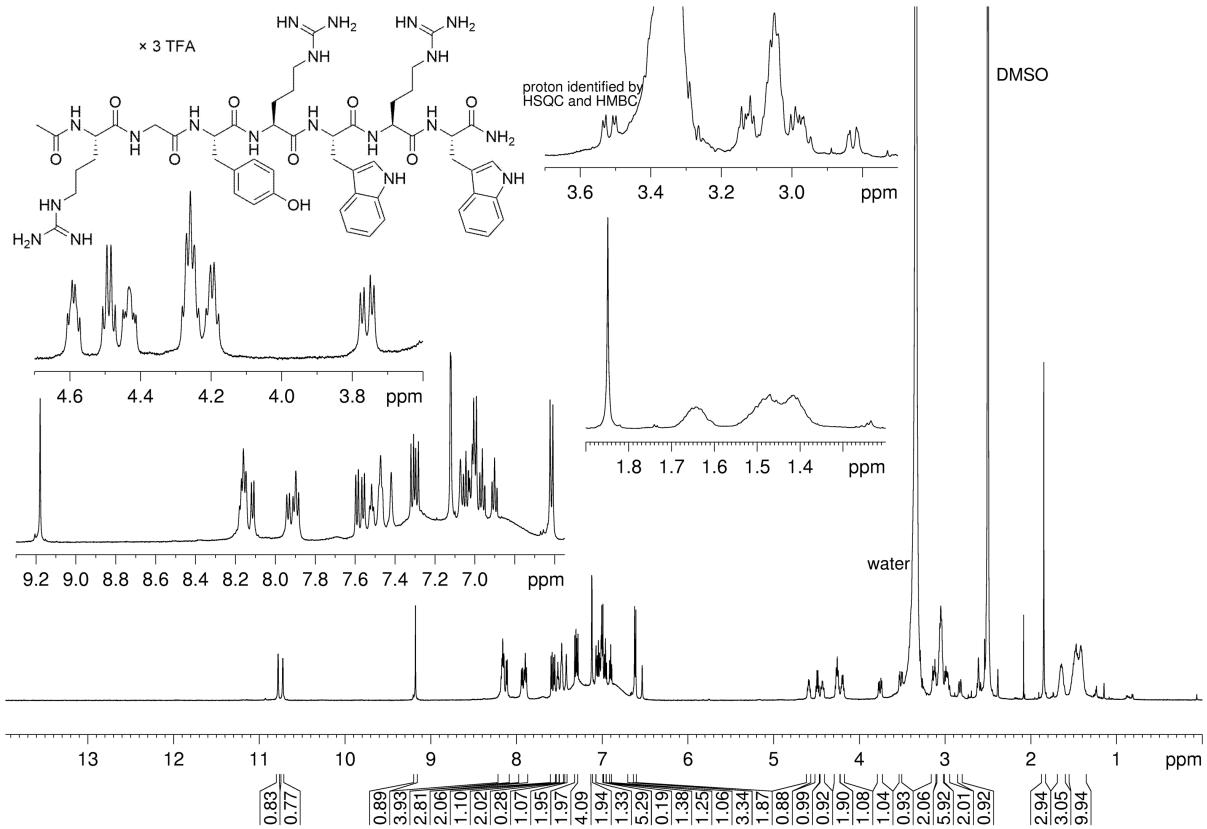

^{1}H-NMR (600 MHz, DMSO-d_6) spectrum of compound **2.26**

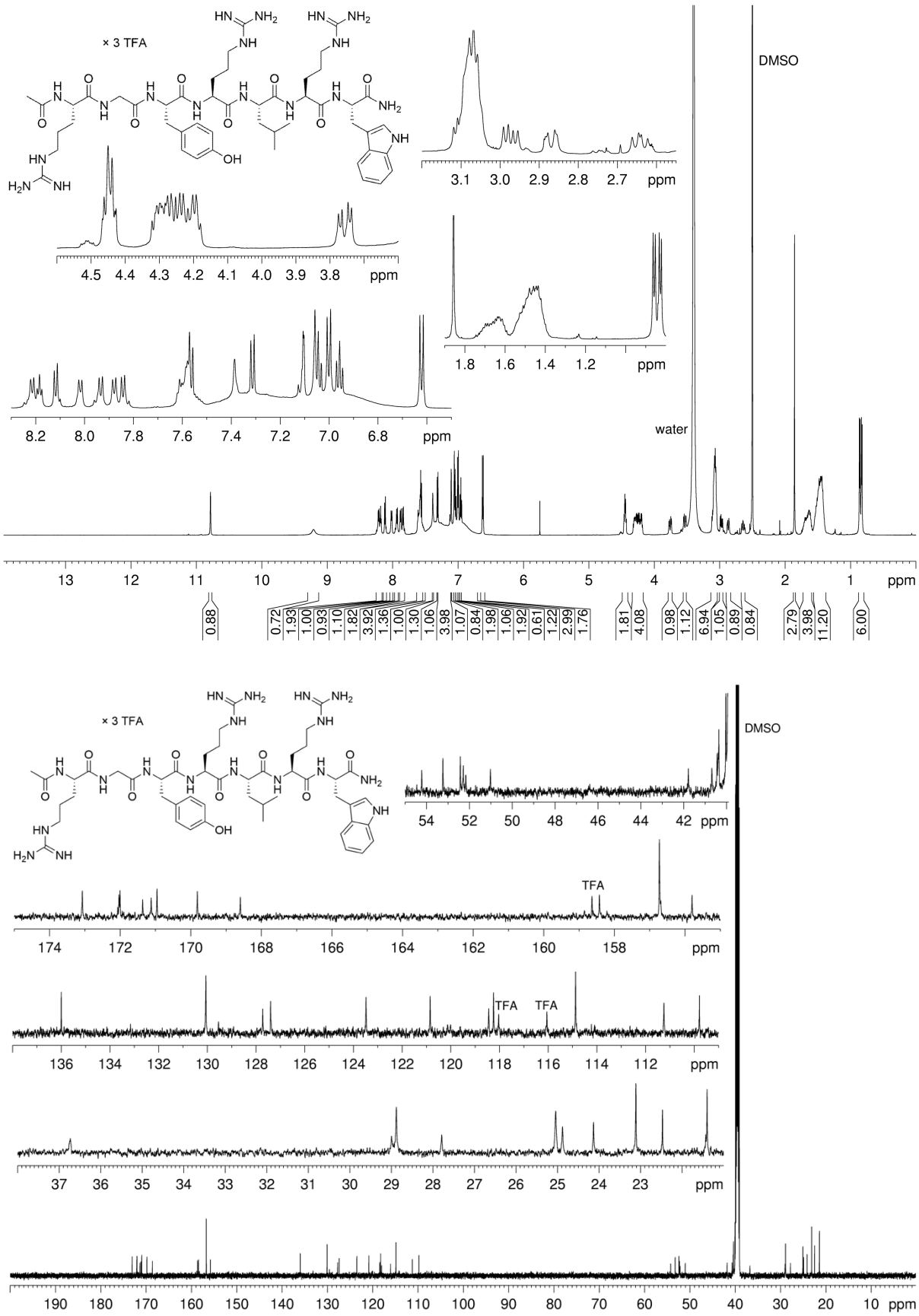

^{1}H-NMR (600 MHz, DMSO-d_6) and ^{13}C-NMR (150 MHz, DMSO-d_6) spectrum of compound **2.27**

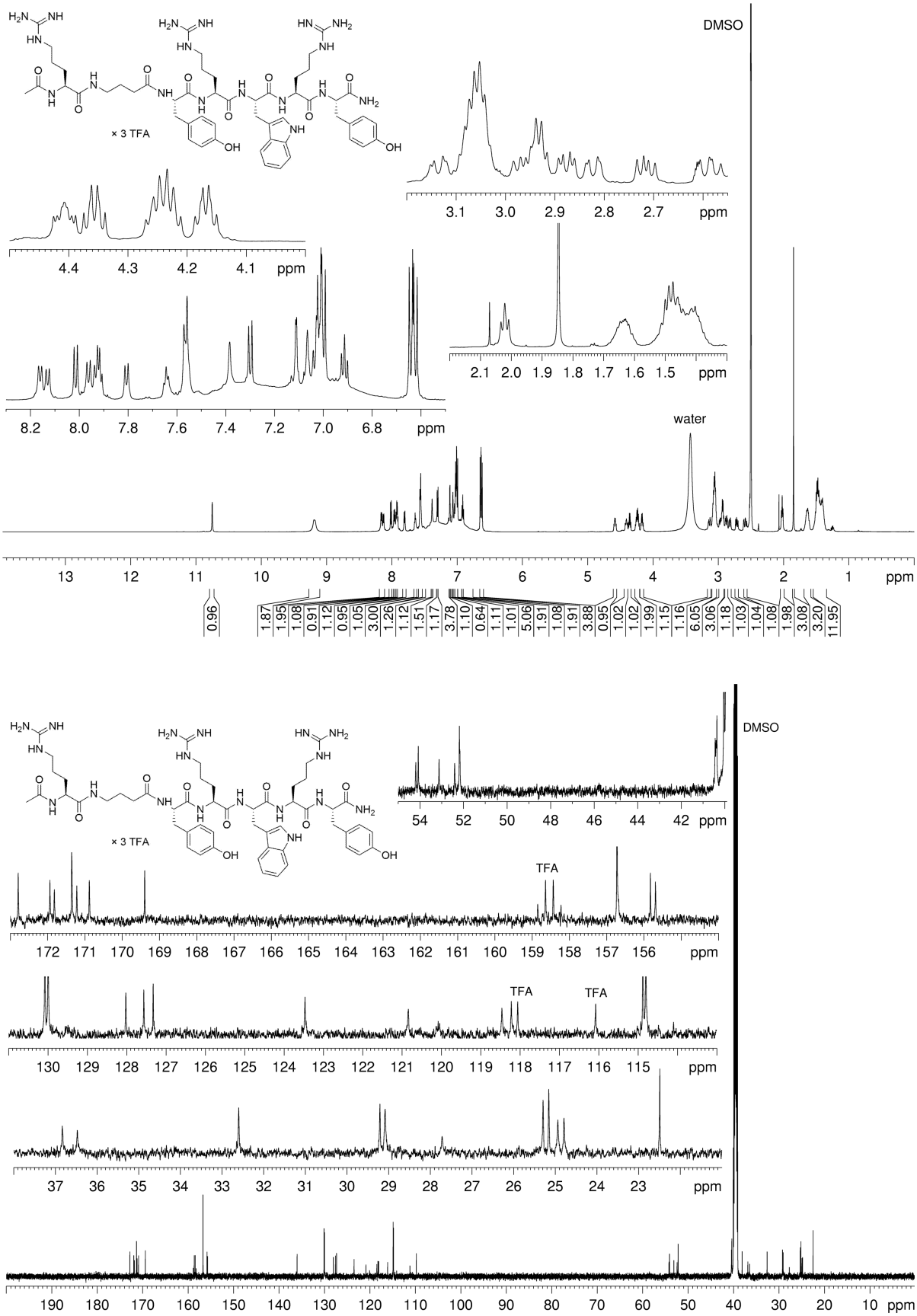

^{1}H-NMR (600 MHz, DMSO-d_6) and ^{13}C-NMR (150 MHz, DMSO-d_6) spectrum of compound **2.28**

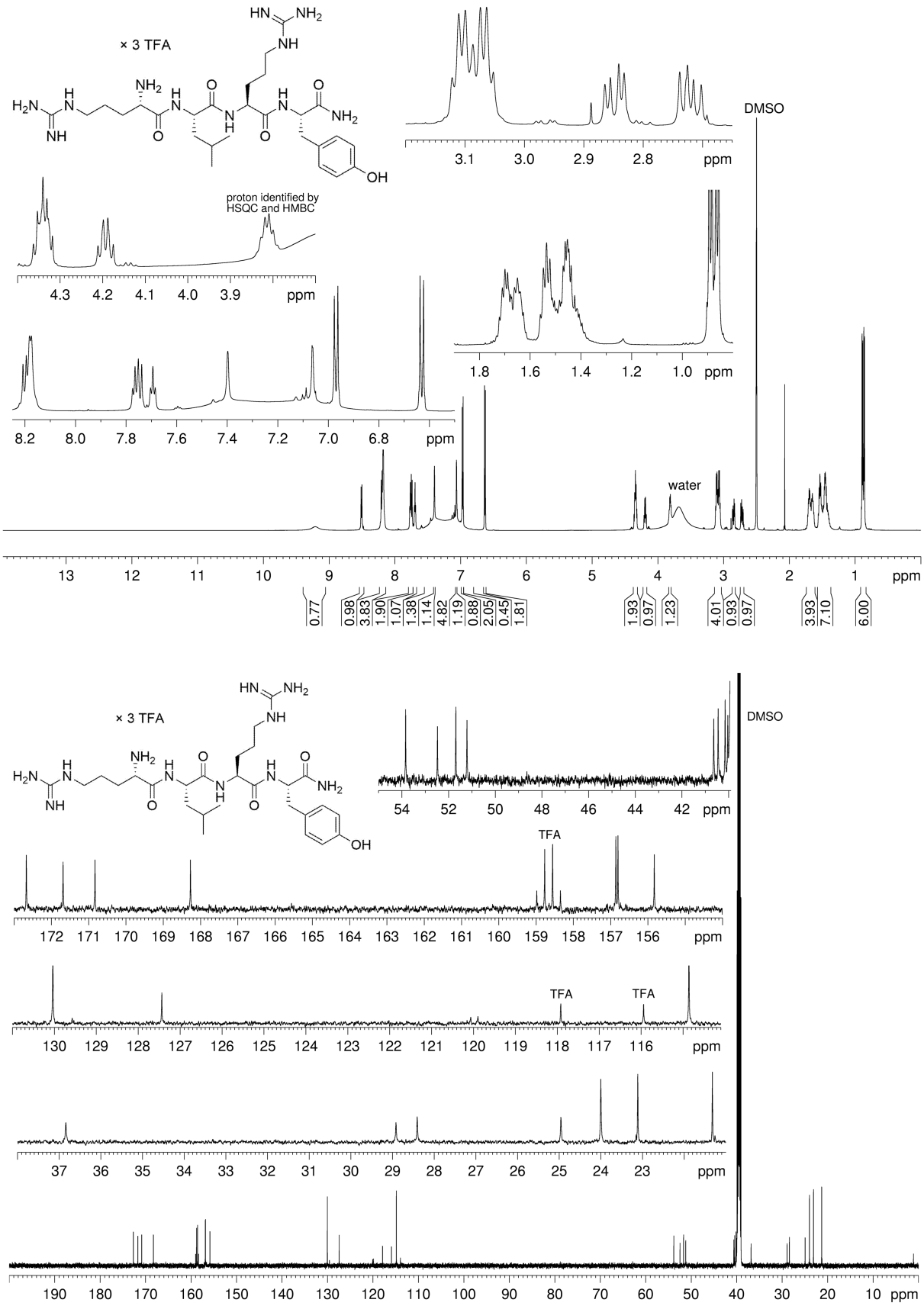

^{1}H-NMR (600 MHz, DMSO-d_6) and ^{13}C-NMR (150 MHz, DMSO-d_6) spectrum of compound **2.29**

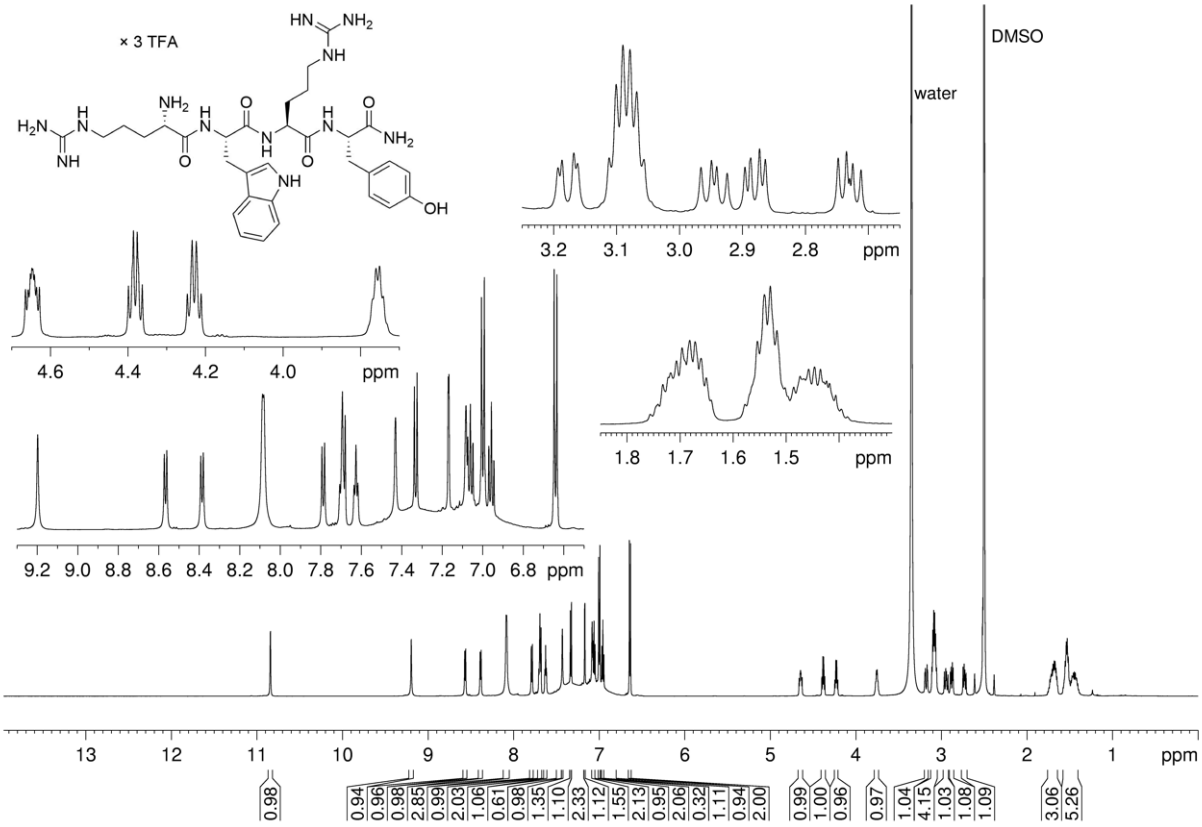

^{1}H-NMR (600 MHz, DMSO-d_6) spectrum of compound **2.30**

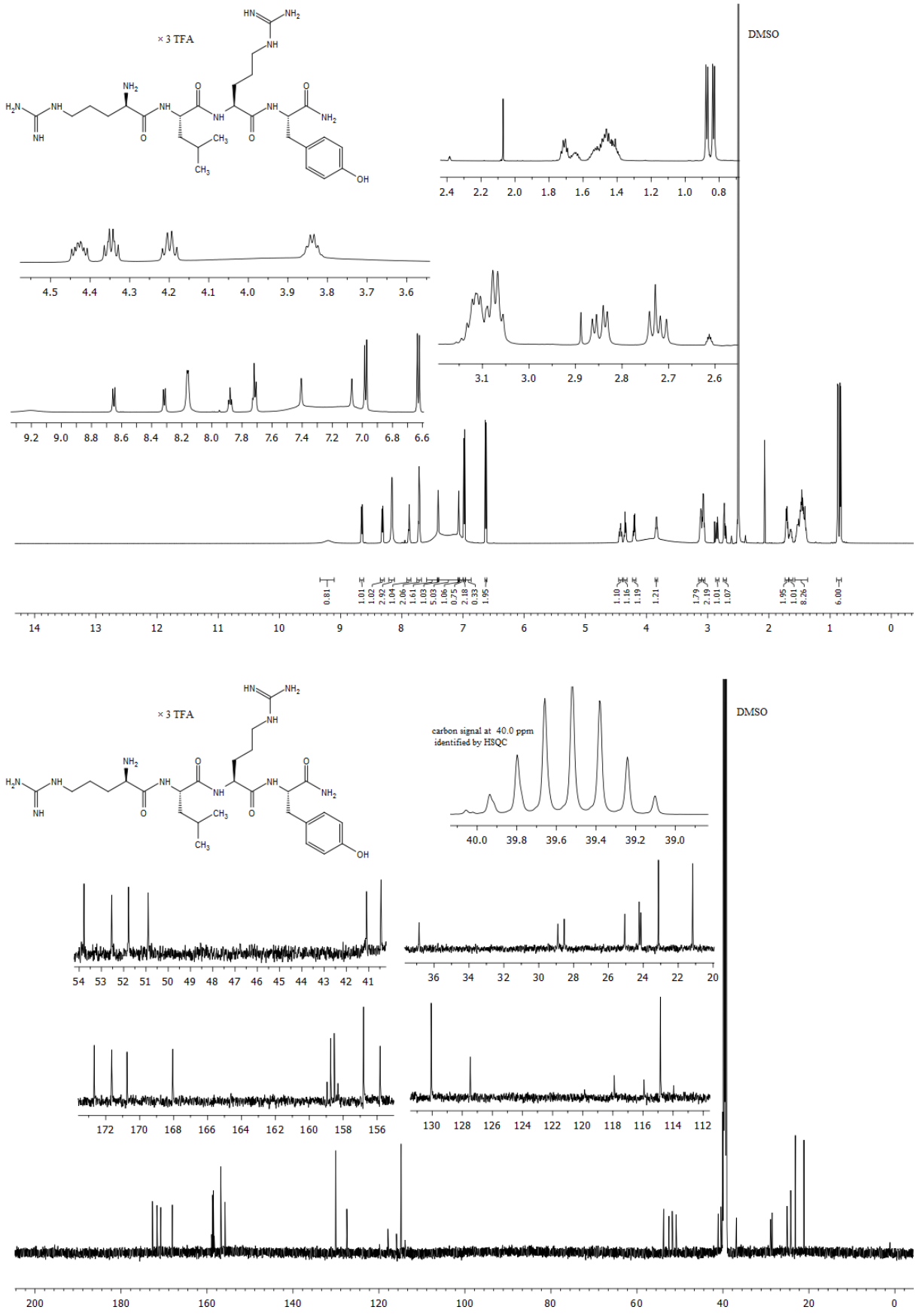

^{1}H-NMR (600 MHz, DMSO-d_6) and ^{13}C-NMR (150 MHz, DMSO-d_6) spectrum of compound **2.31**

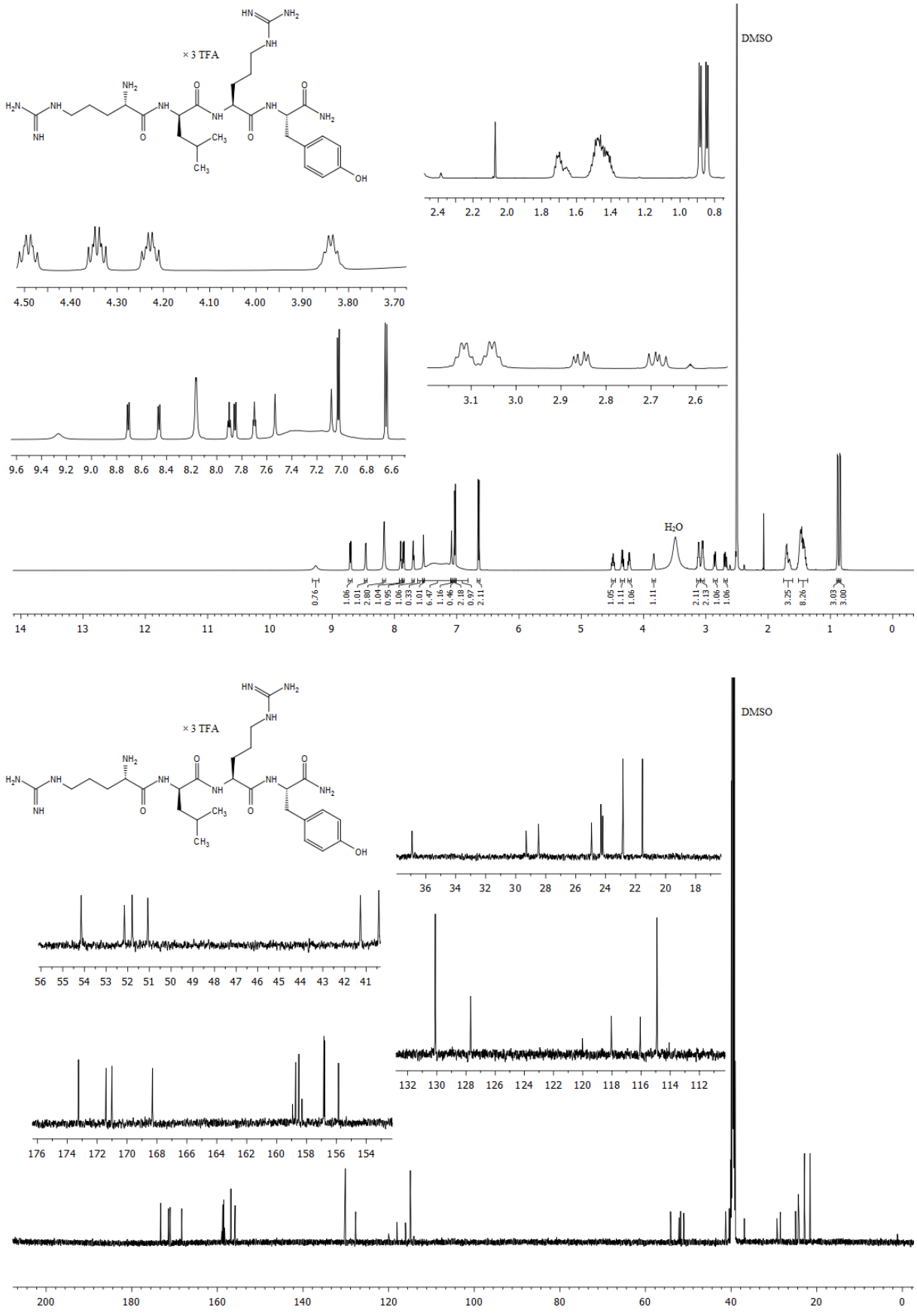

^{1}H-NMR (600 MHz, DMSO-d_6) and ^{13}C-NMR (150 MHz, DMSO-d_6) spectrum of compound **2.32**

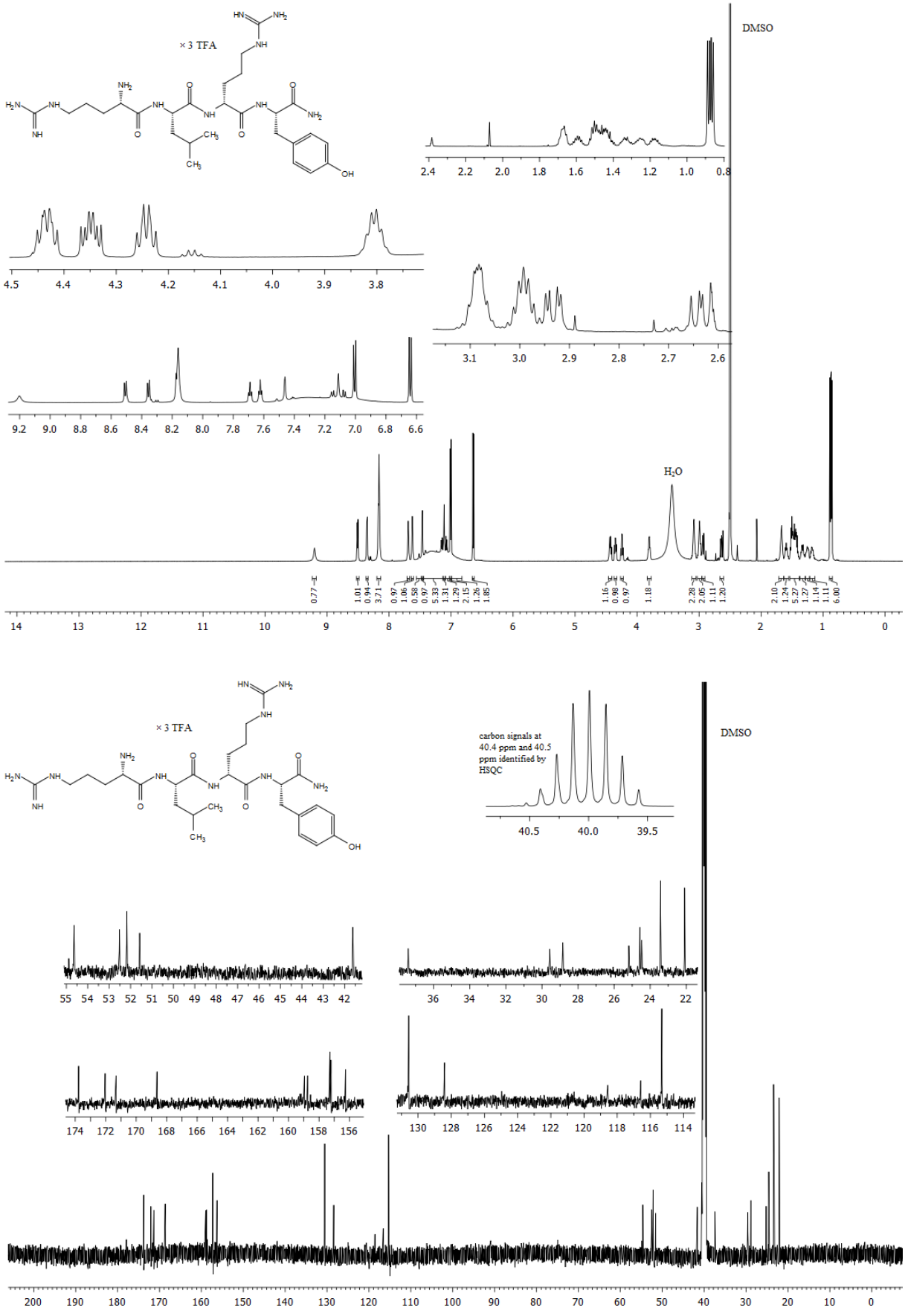

^{1}H-NMR (600 MHz, DMSO-d_6) and ^{13}C-NMR (150 MHz, DMSO-d_6) spectrum of compound **2.33**

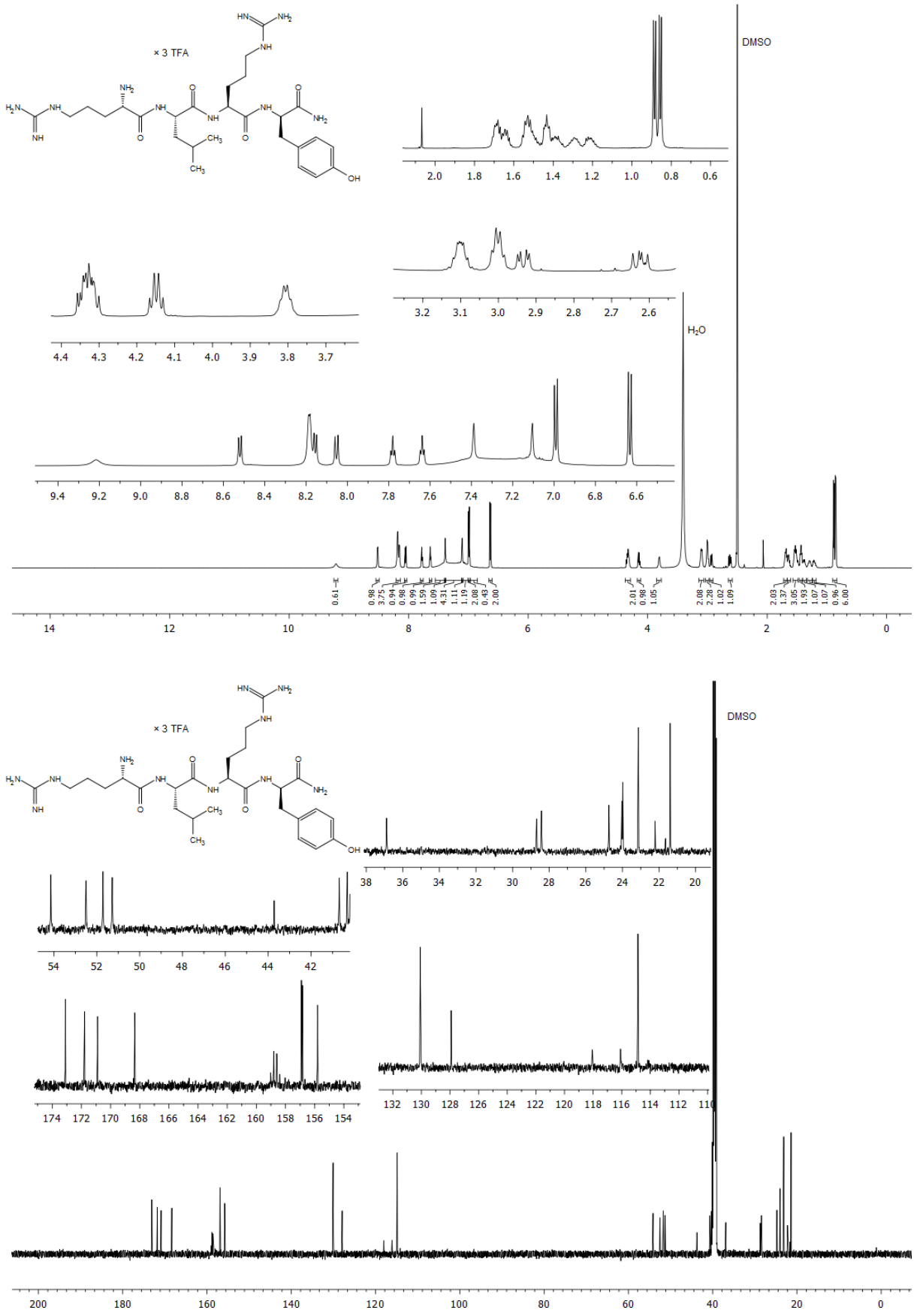

^{1}H-NMR (600 MHz, DMSO-d_6) and ^{13}C-NMR (150 MHz, DMSO-d_6) spectrum of compound **2.34**

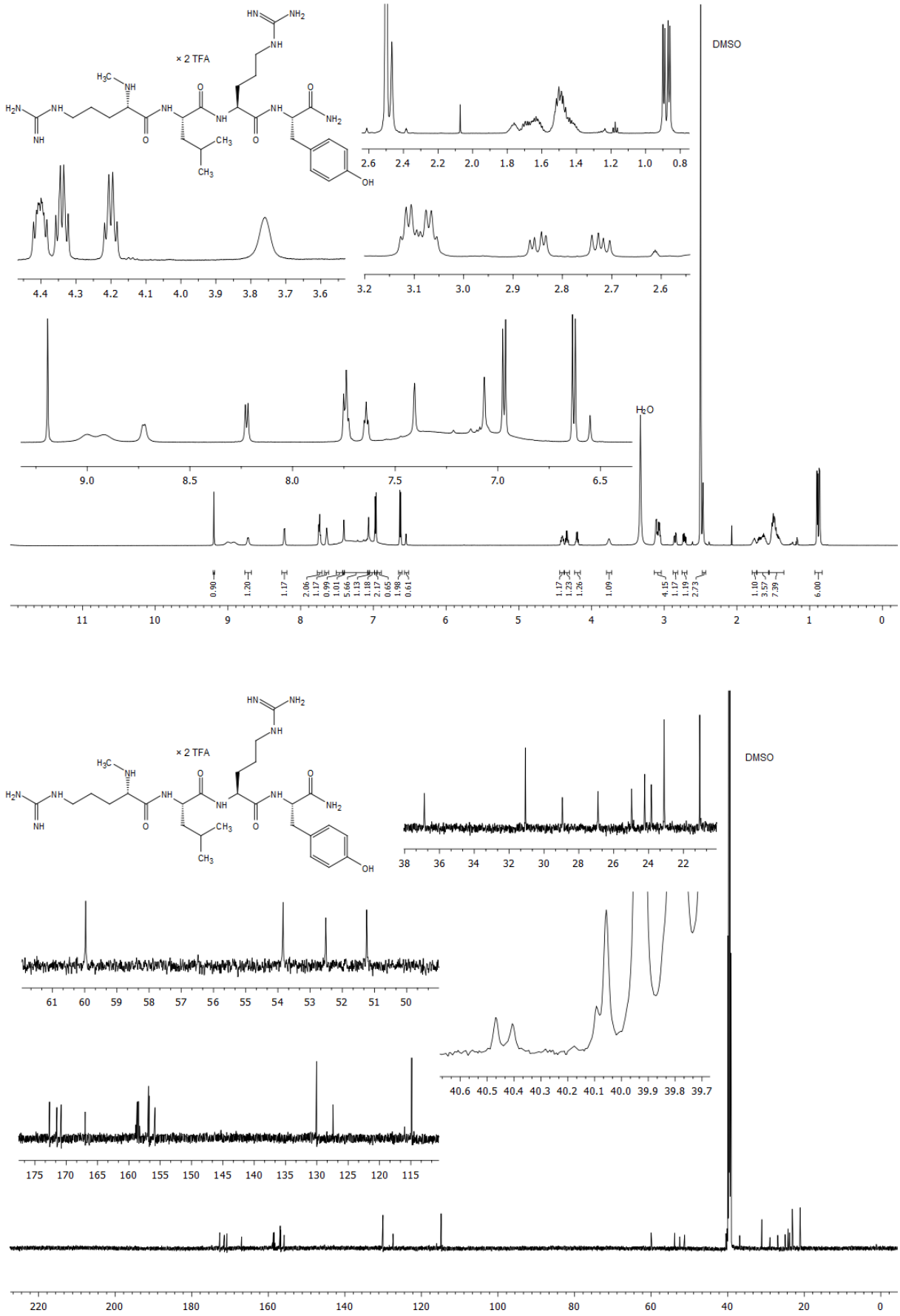

^{1}H-NMR (600 MHz, DMSO-d_6) and ^{13}C-NMR (150 MHz, DMSO-d_6) spectrum of compound **2.35**

7.2 Appendix Chapter 3

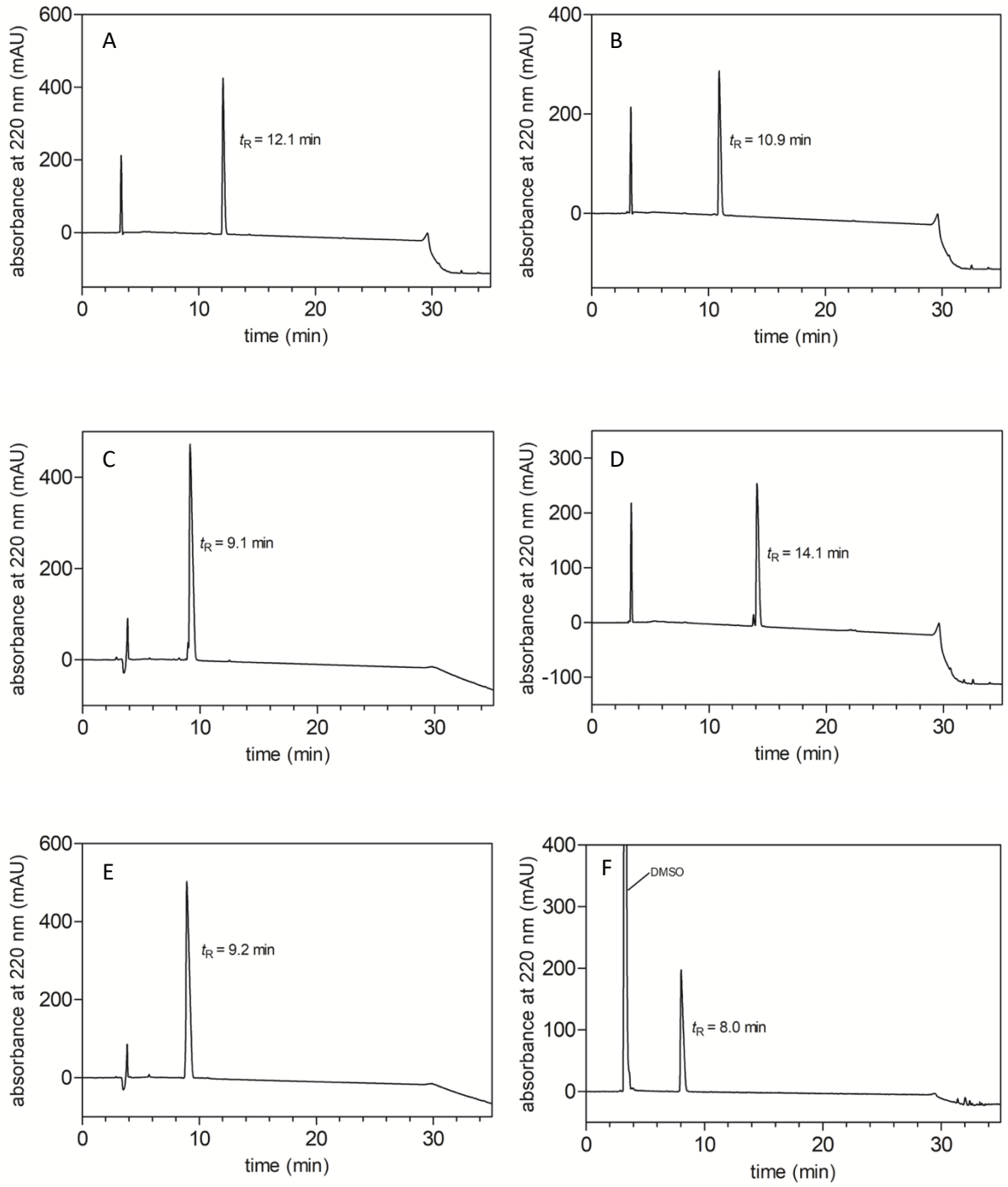

RP-HPLC analysis of compound **3.3** (A), **3.4** (B), **3.5** (C), **3.6** (D), **3.7** (E) and **3.8** (F).

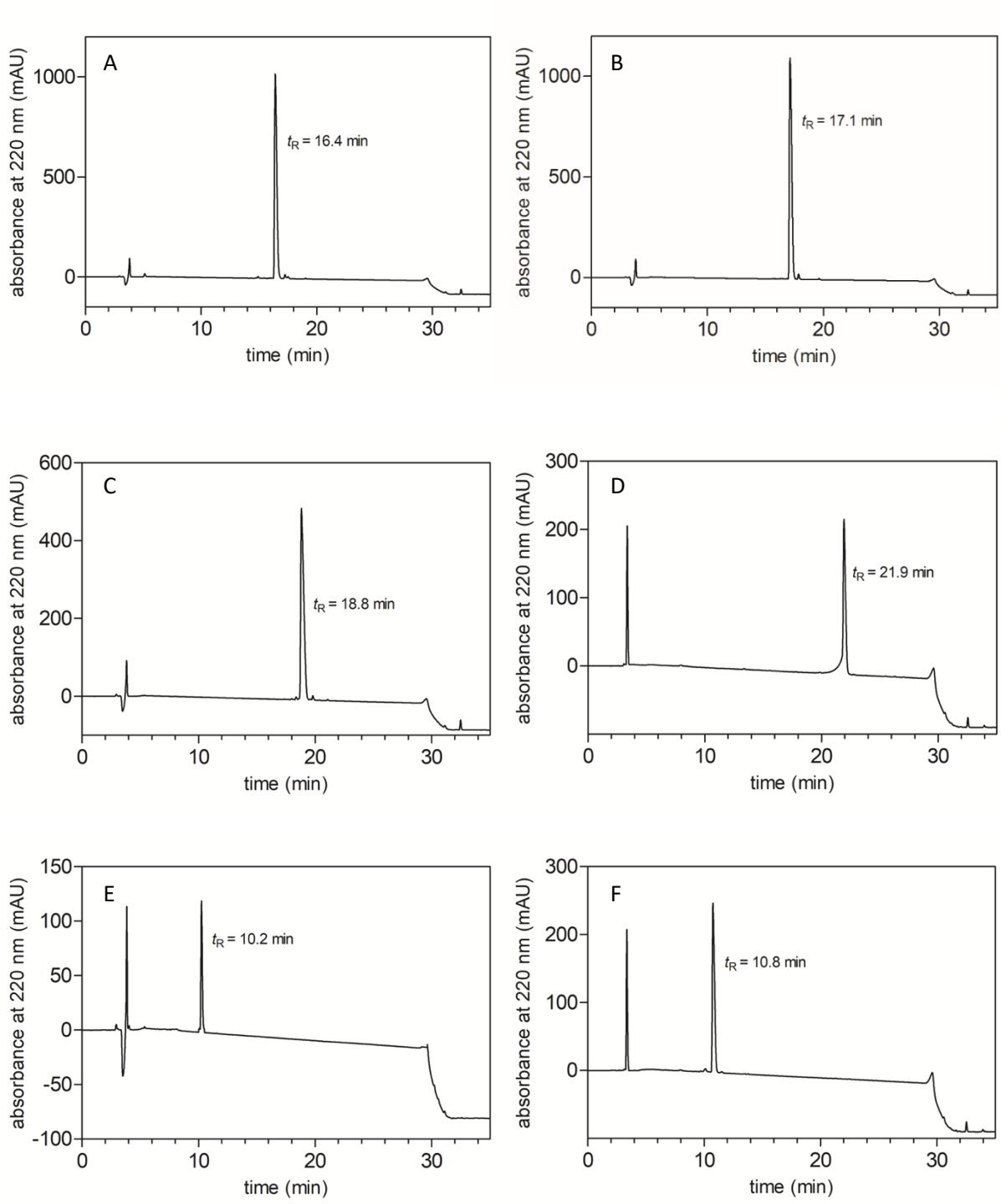

RP-HPLC analysis of compound **3.9** (A), **3.10** (B), **3.11** (C), **3.12** (D), **3.13** (E) and **3.14** (F).

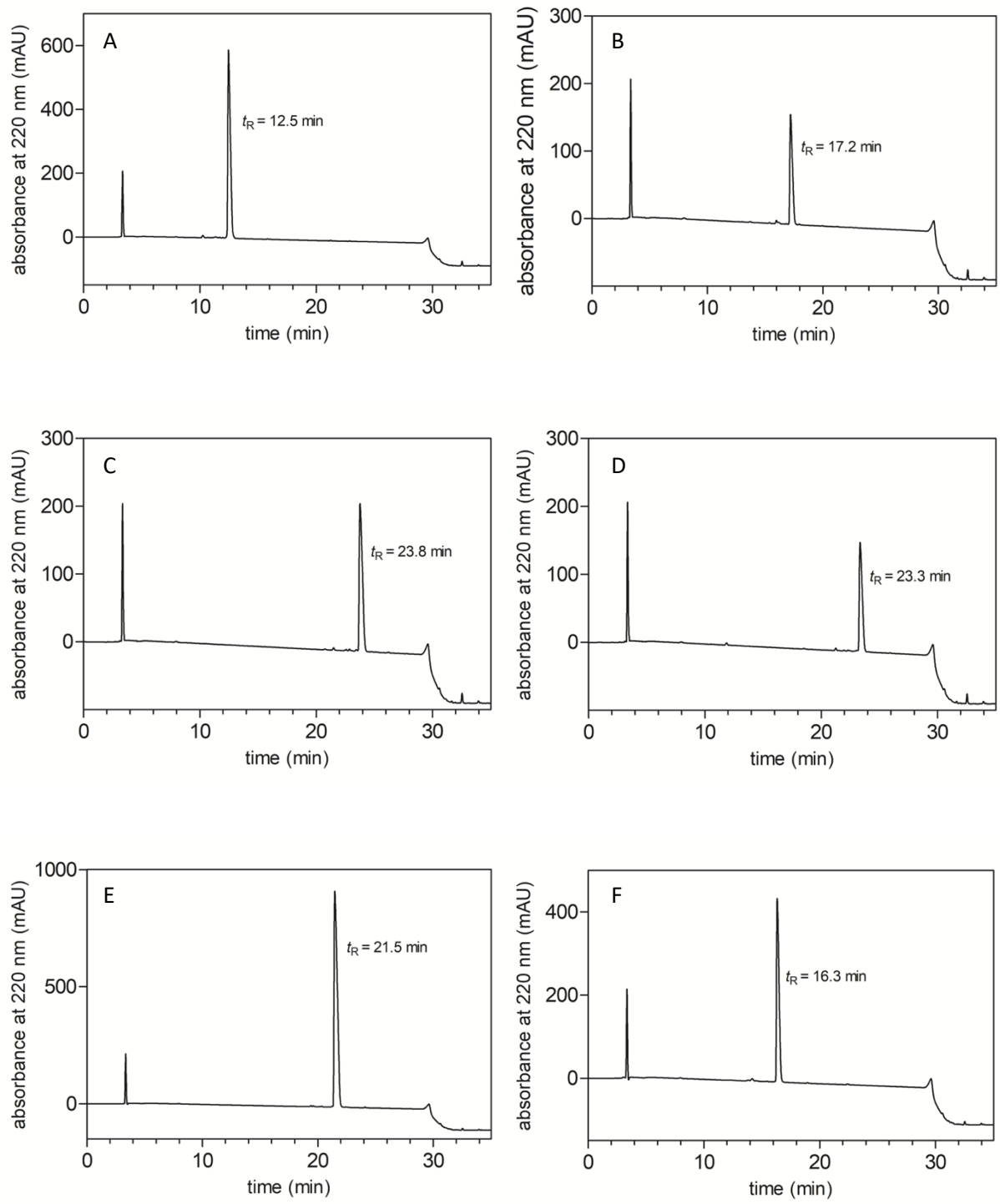

RP-HPLC analysis of compound **3.15** (A), **3.16** (B), **3.17** (C), **3.18** (D), **3.19** (E) and **3.20** (F).

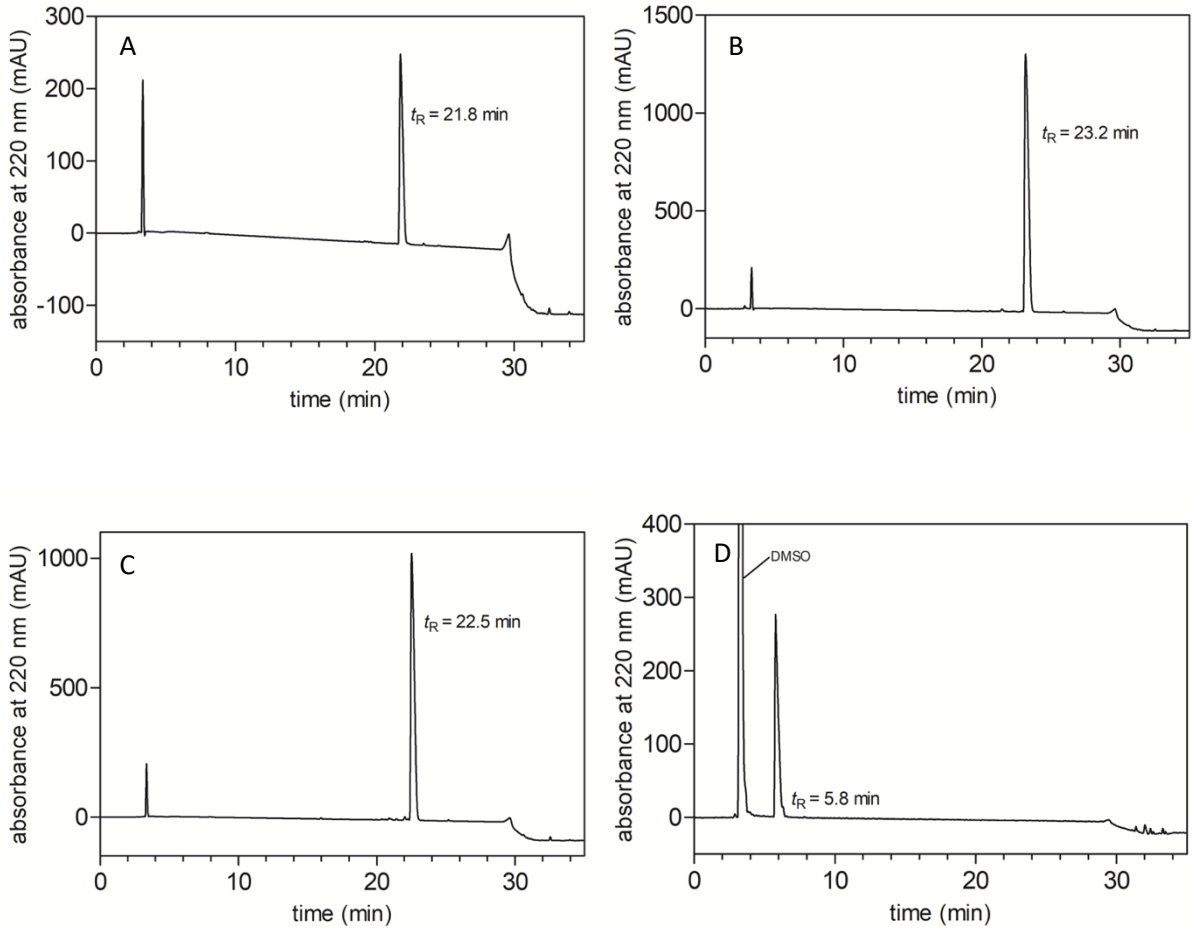

RP-HPLC analysis of compound **3.21** (A), **3.22** (B), **3.23** (C) and **3.24** (D),

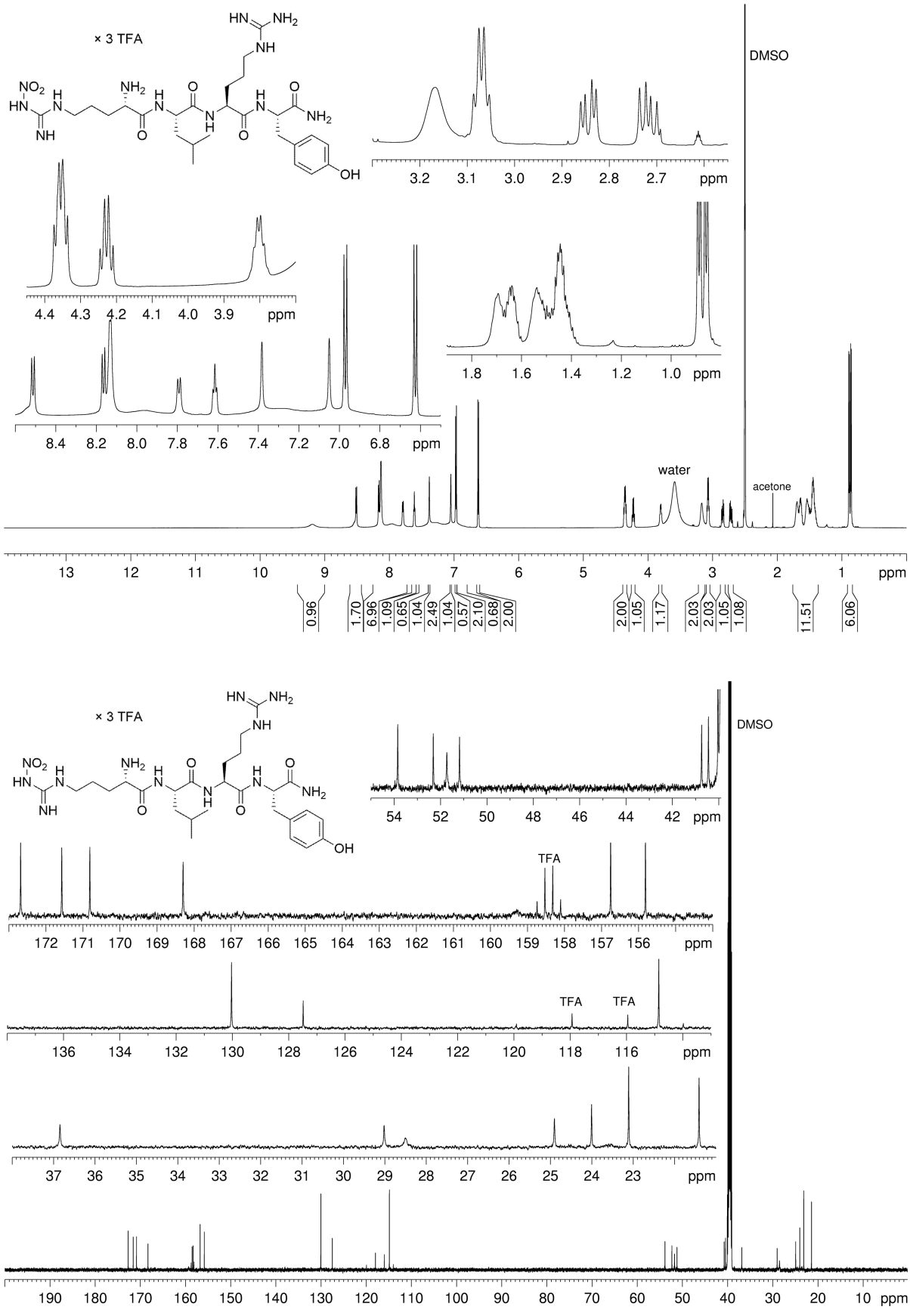

^{1}H-NMR (600 MHz, DMSO-d_6) and ^{13}C-NMR (150 MHz, DMSO-d_6) spectrum of compound **3.3**

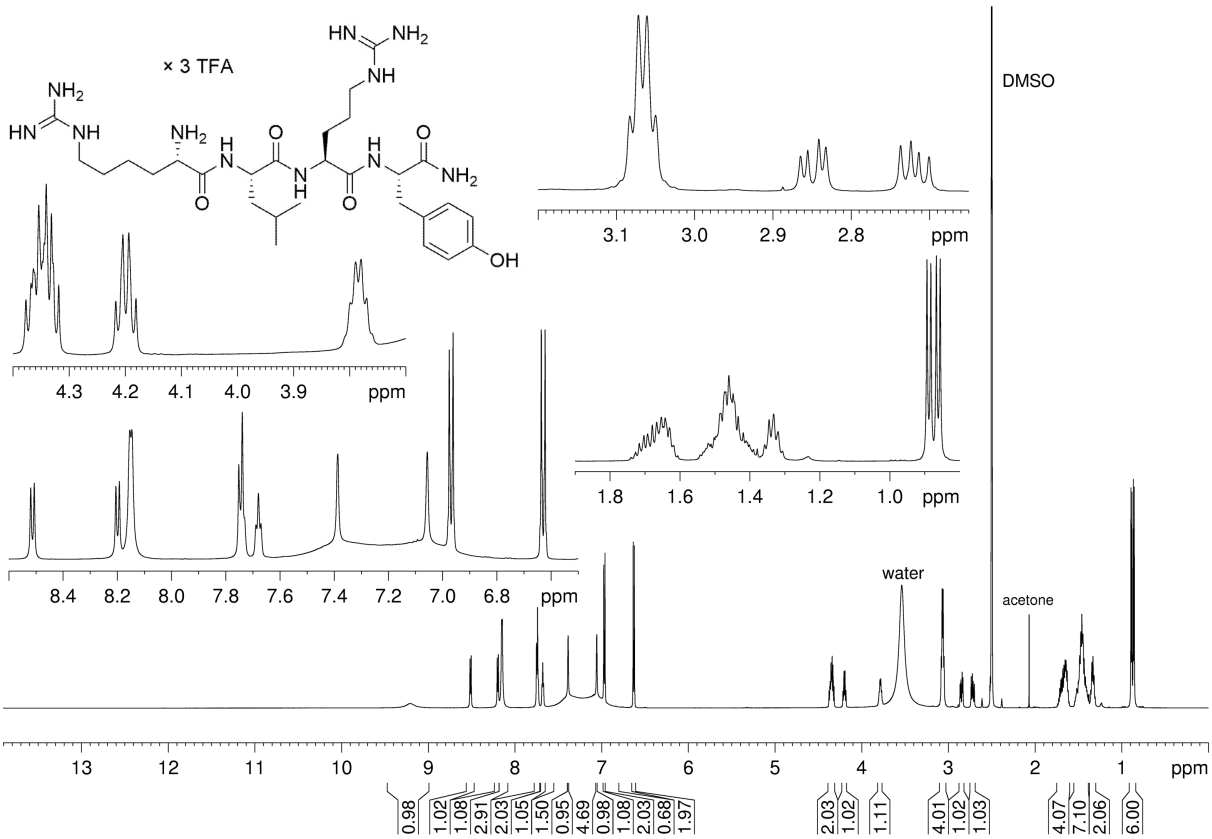

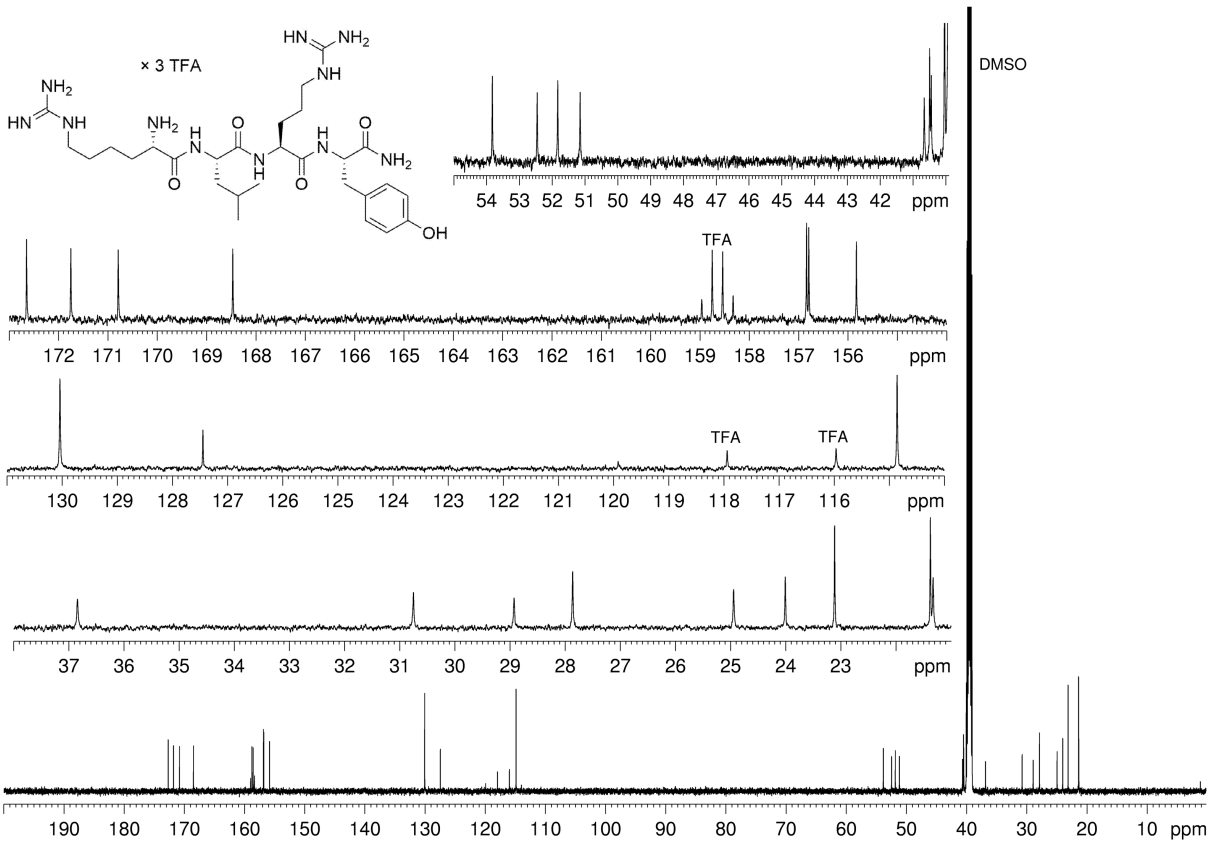

^{1}H-NMR (600 MHz, DMSO-d_6) and ^{13}C-NMR (150 MHz, DMSO-d_6) spectrum of compound **3.4**

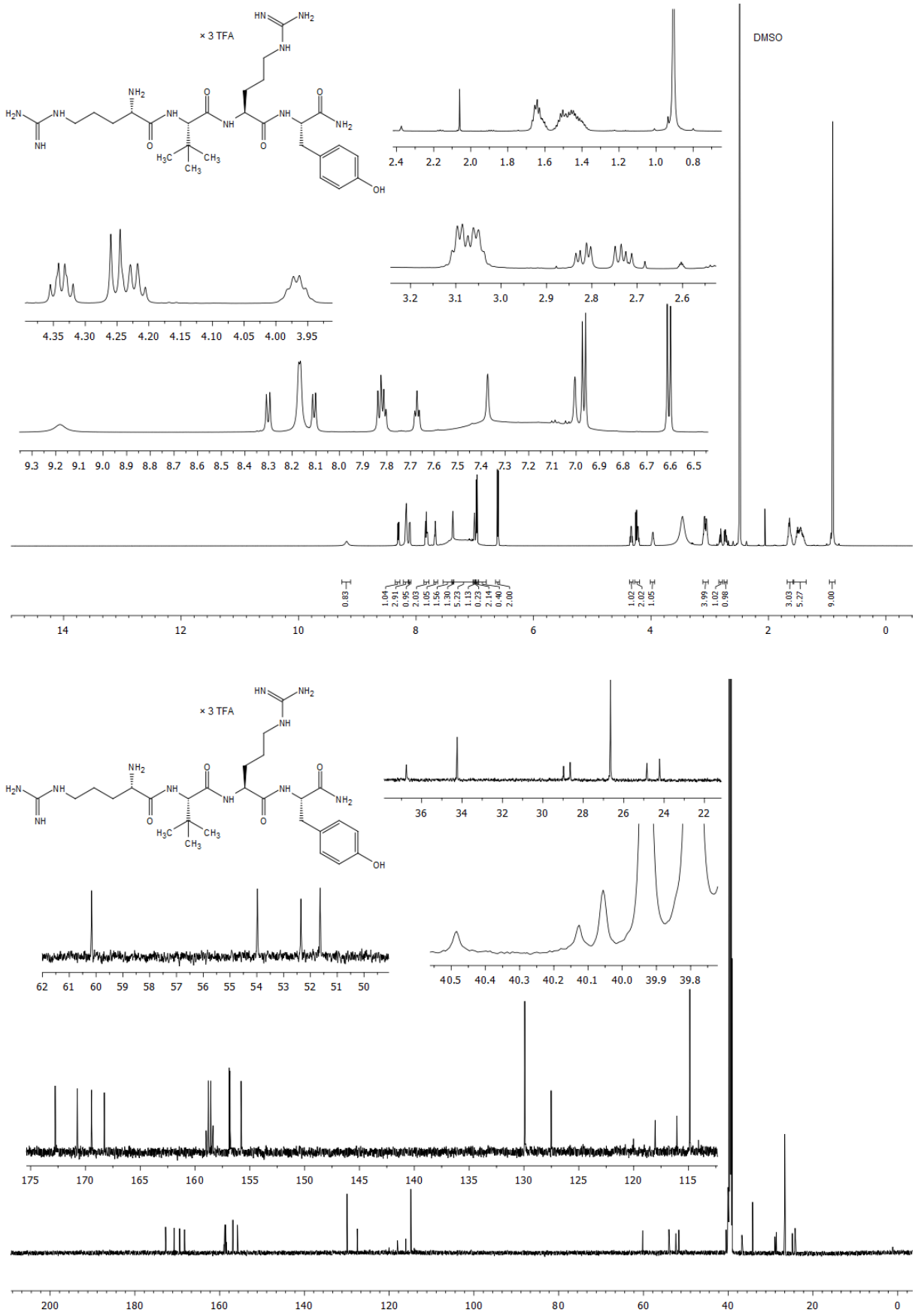

^{1}H-NMR (600 MHz, DMSO-d_6) and ^{13}C-NMR (150 MHz, DMSO-d_6) spectrum of compound **3.5**

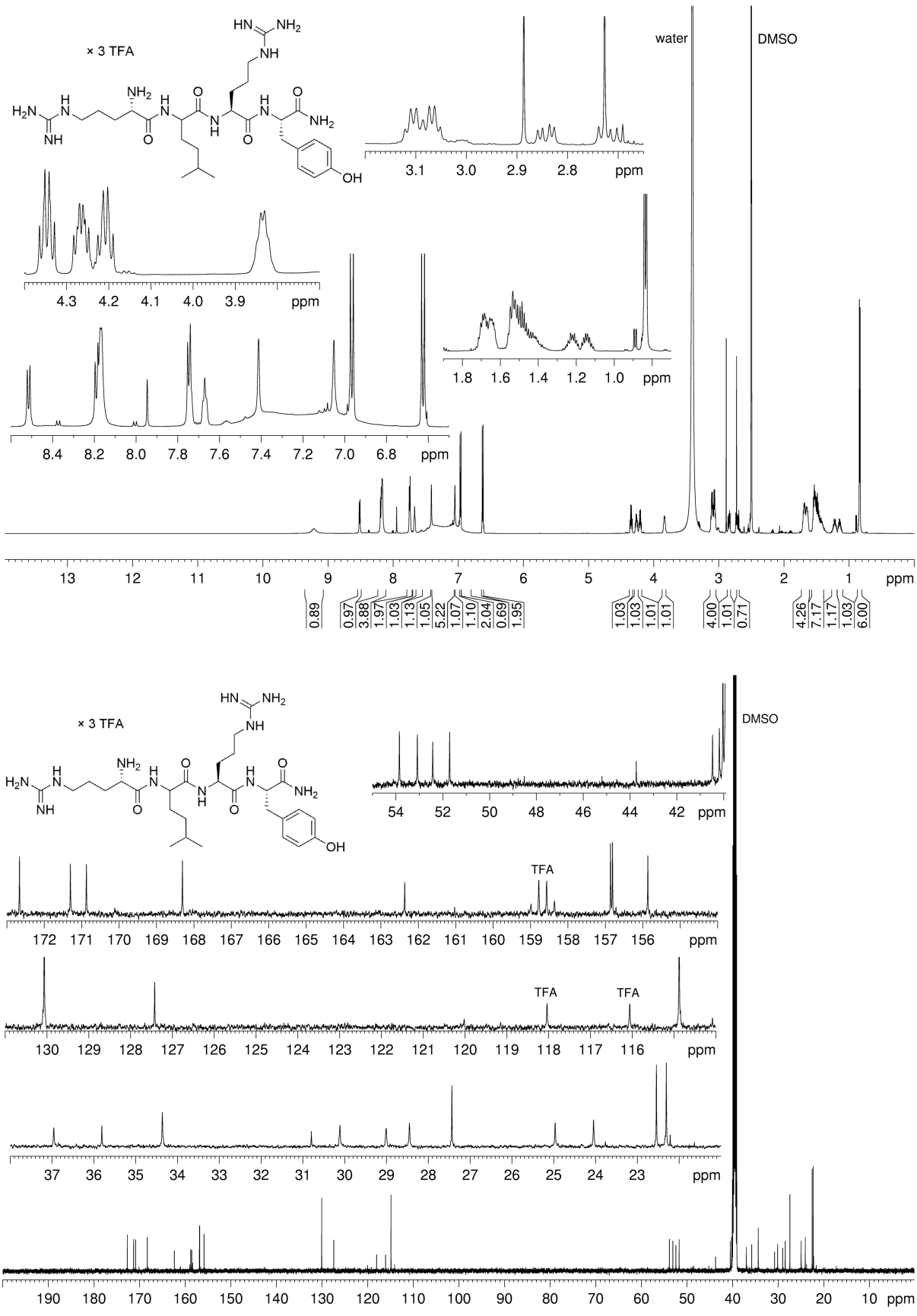

^{1}H-NMR (600 MHz, DMSO-d_6) and ^{13}C-NMR (150 MHz, DMSO-d_6) spectrum of compound **3.6**

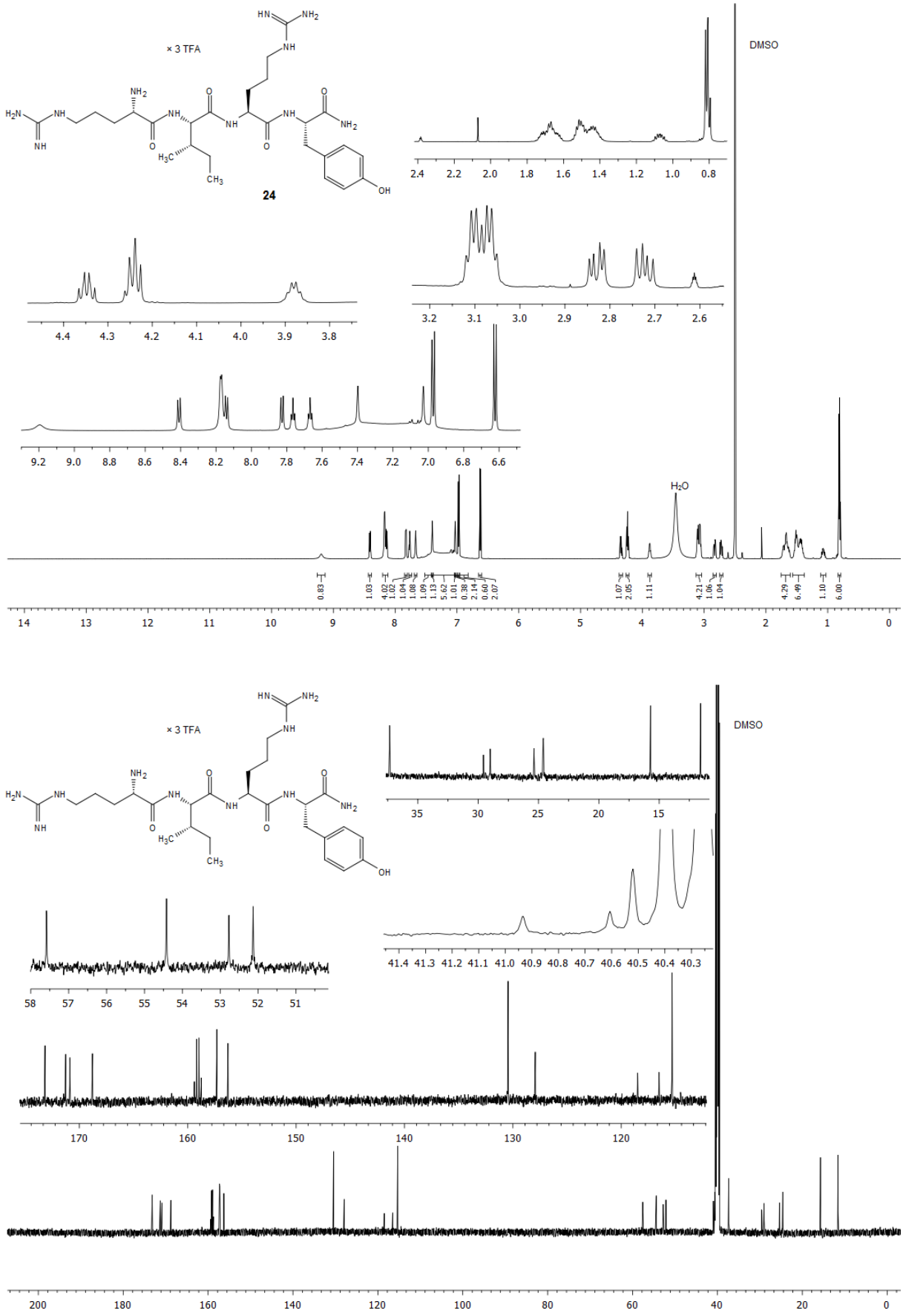

^{1}H-NMR (600 MHz, DMSO-d_6) and ^{13}C-NMR (150 MHz, DMSO-d_6) spectrum of compound **3.7**

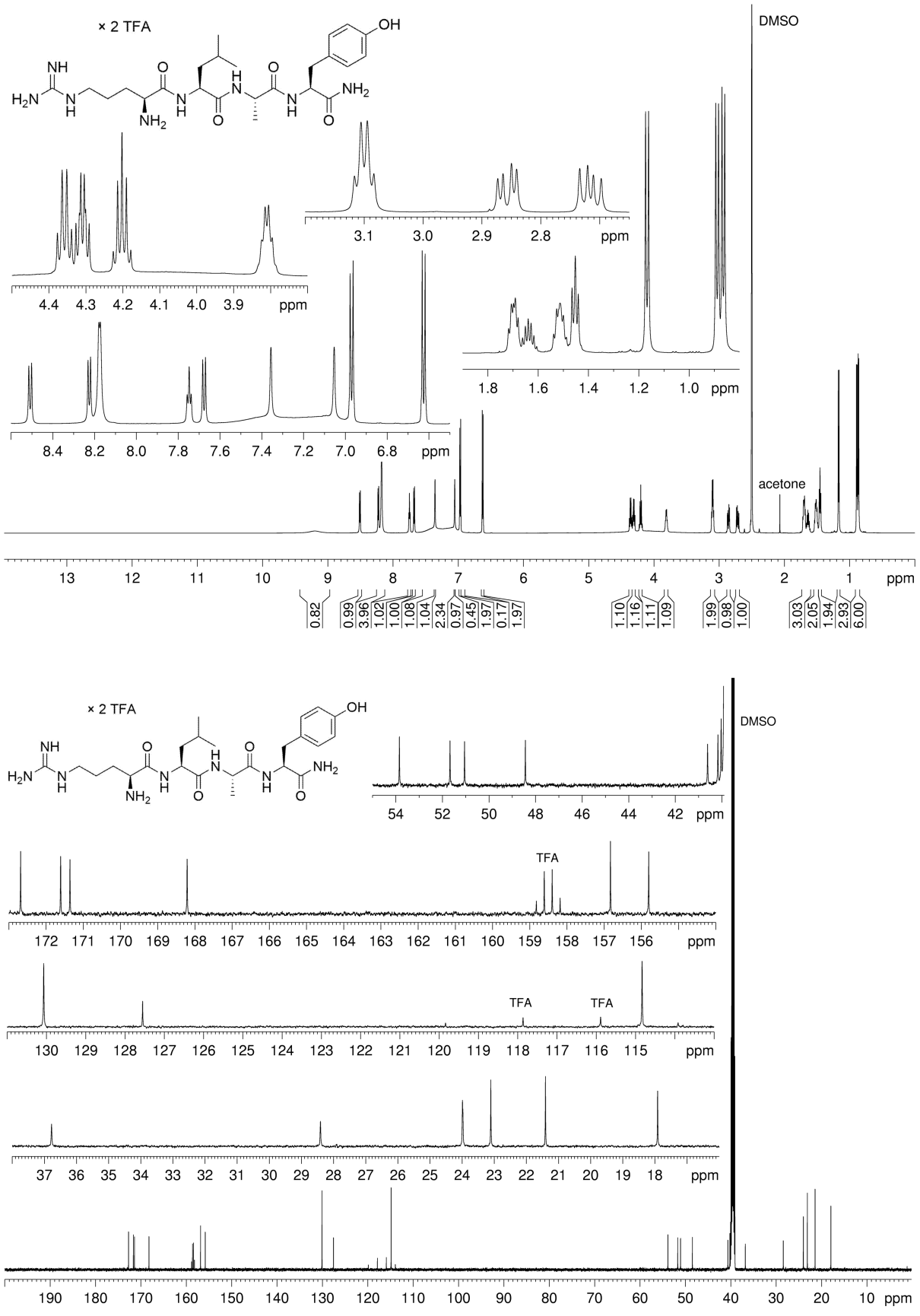

^{1}H-NMR (600 MHz, DMSO-d_6) and ^{13}C-NMR (150 MHz, DMSO-d_6) spectrum of compound **3.8**

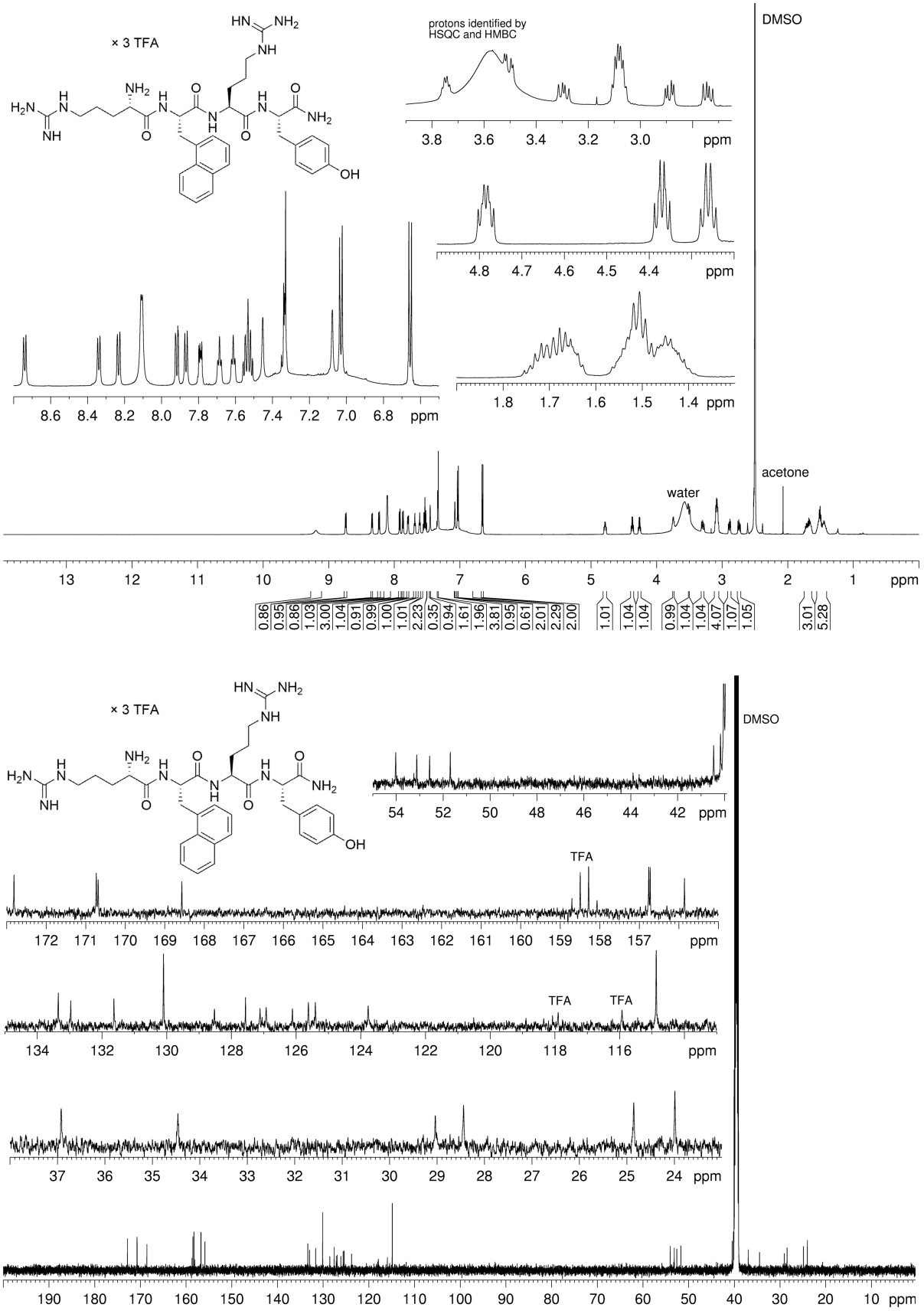

^{1}H-NMR (600 MHz, DMSO-d_6) and ^{13}C-NMR (150 MHz, DMSO-d_6) spectrum of compound **3.9**

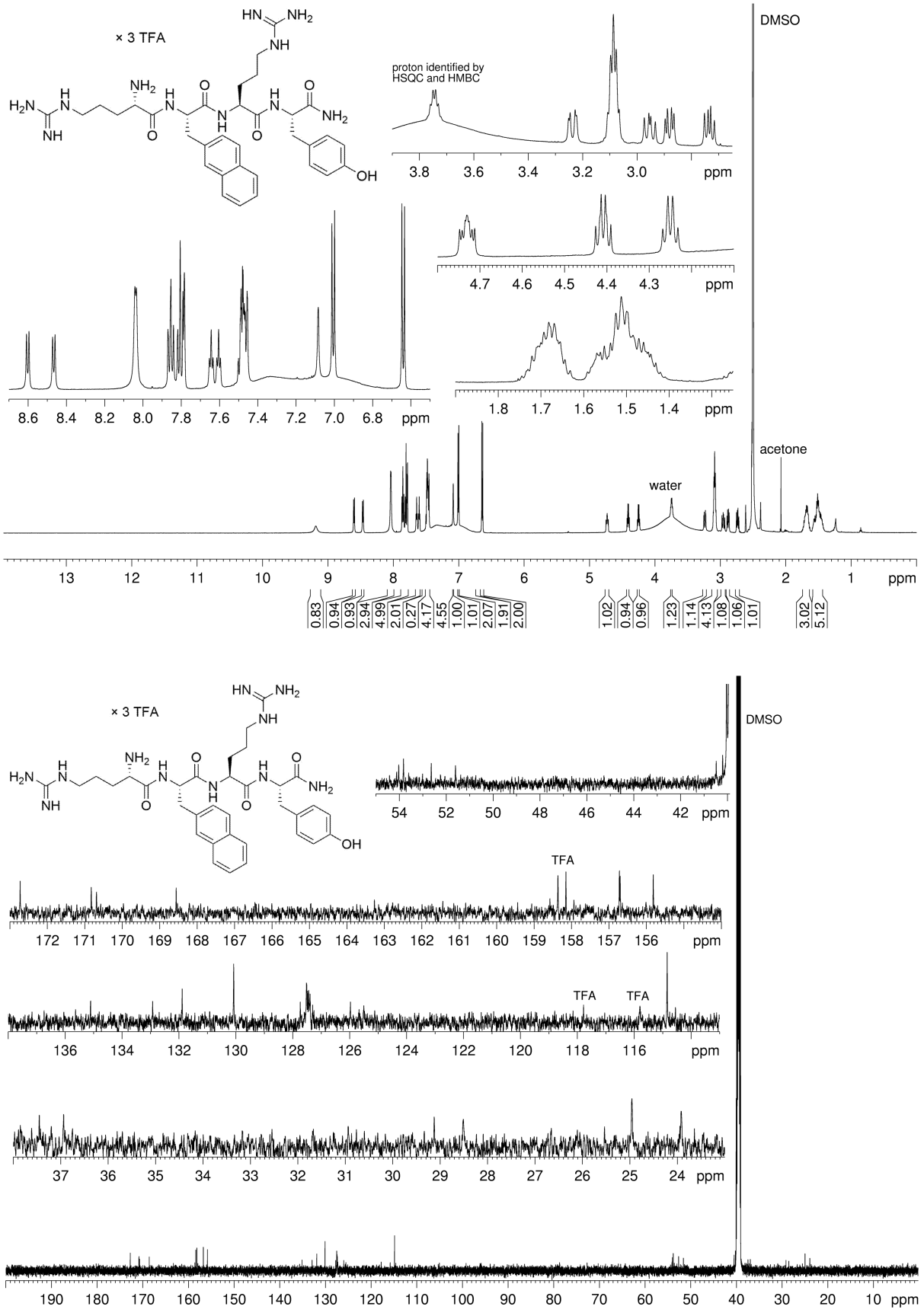

^{1}H-NMR (600 MHz, DMSO-d_6) and ^{13}C-NMR (150 MHz, DMSO-d_6) spectrum of compound **3.10**

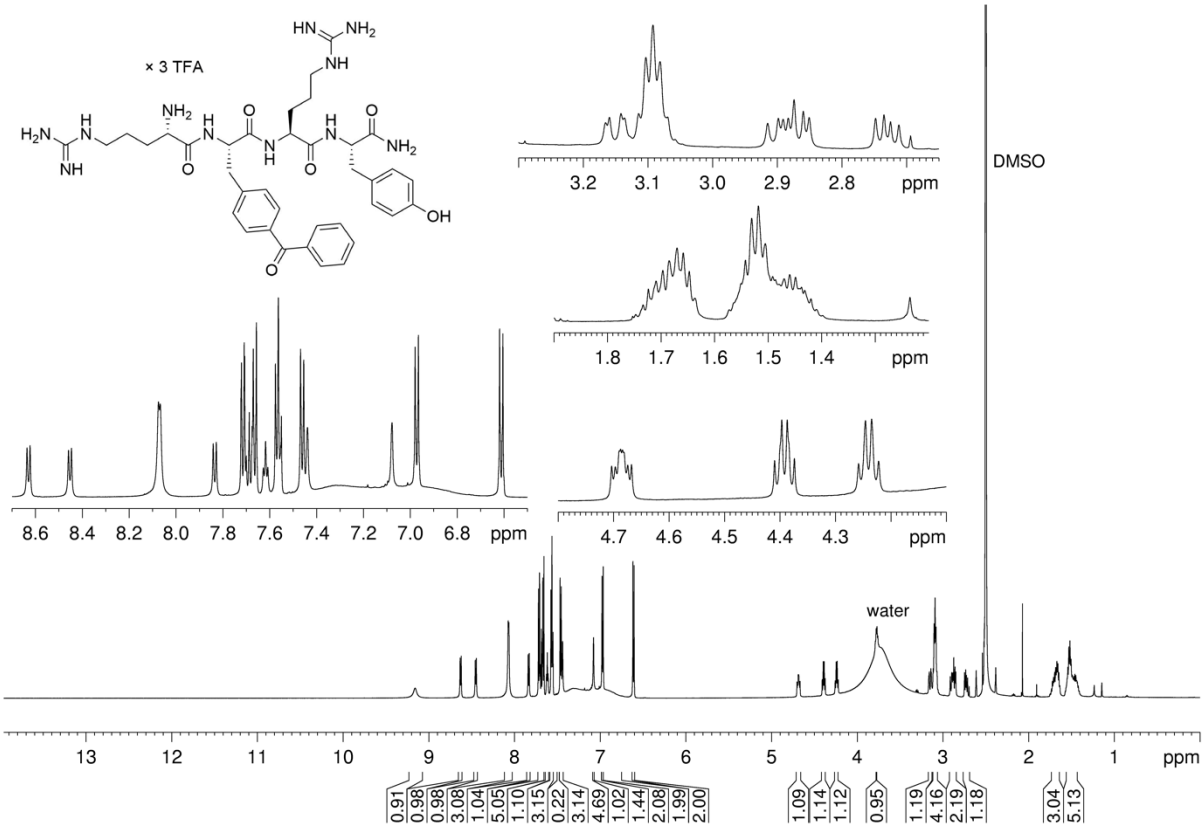

^{1}H-NMR (600 MHz, DMSO-d_6) spectrum of compound **3.11**

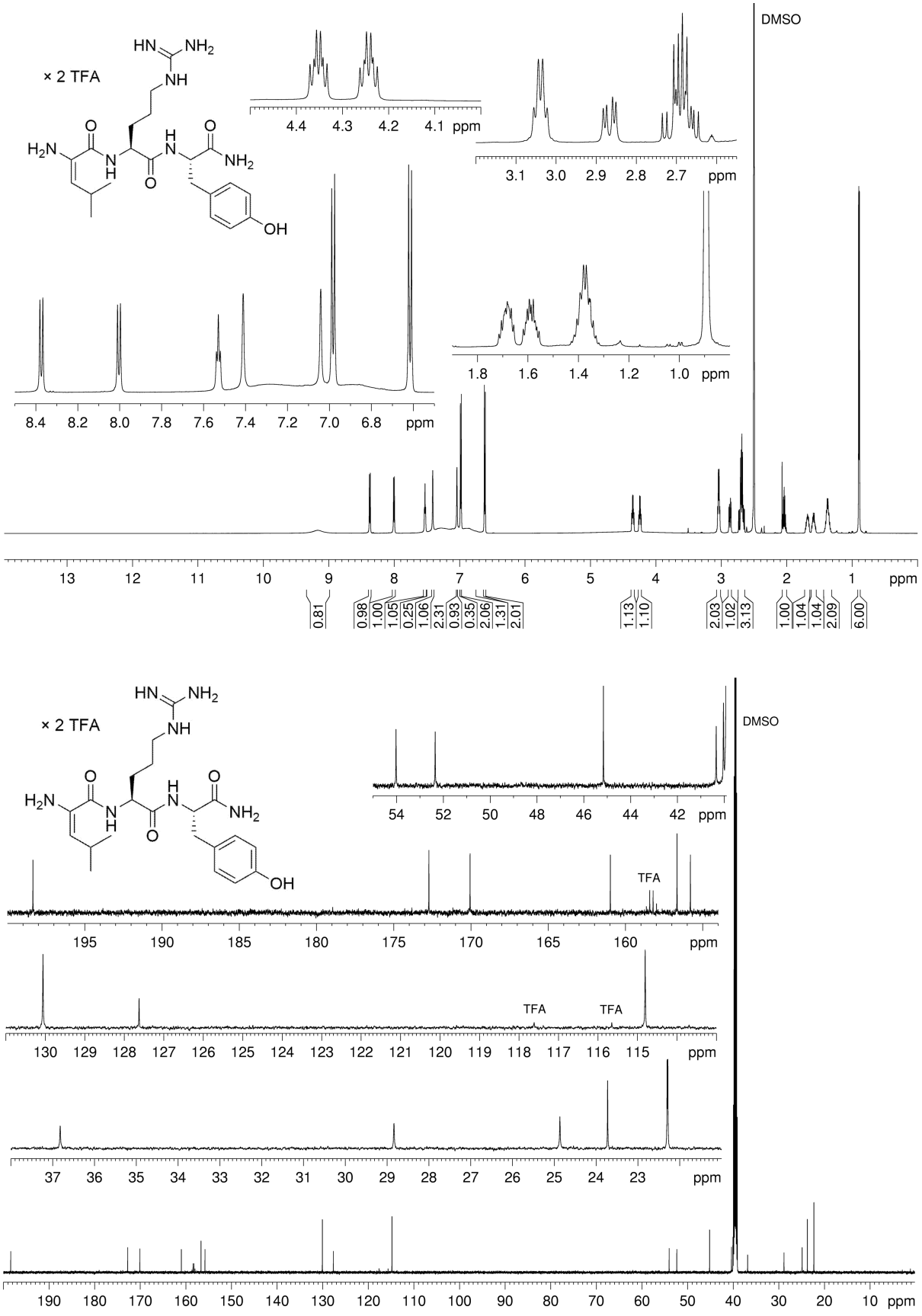

^{1}H-NMR (600 MHz, DMSO-d_6) and ^{13}C-NMR (150 MHz, DMSO-d_6) spectrum of compound **3.12**

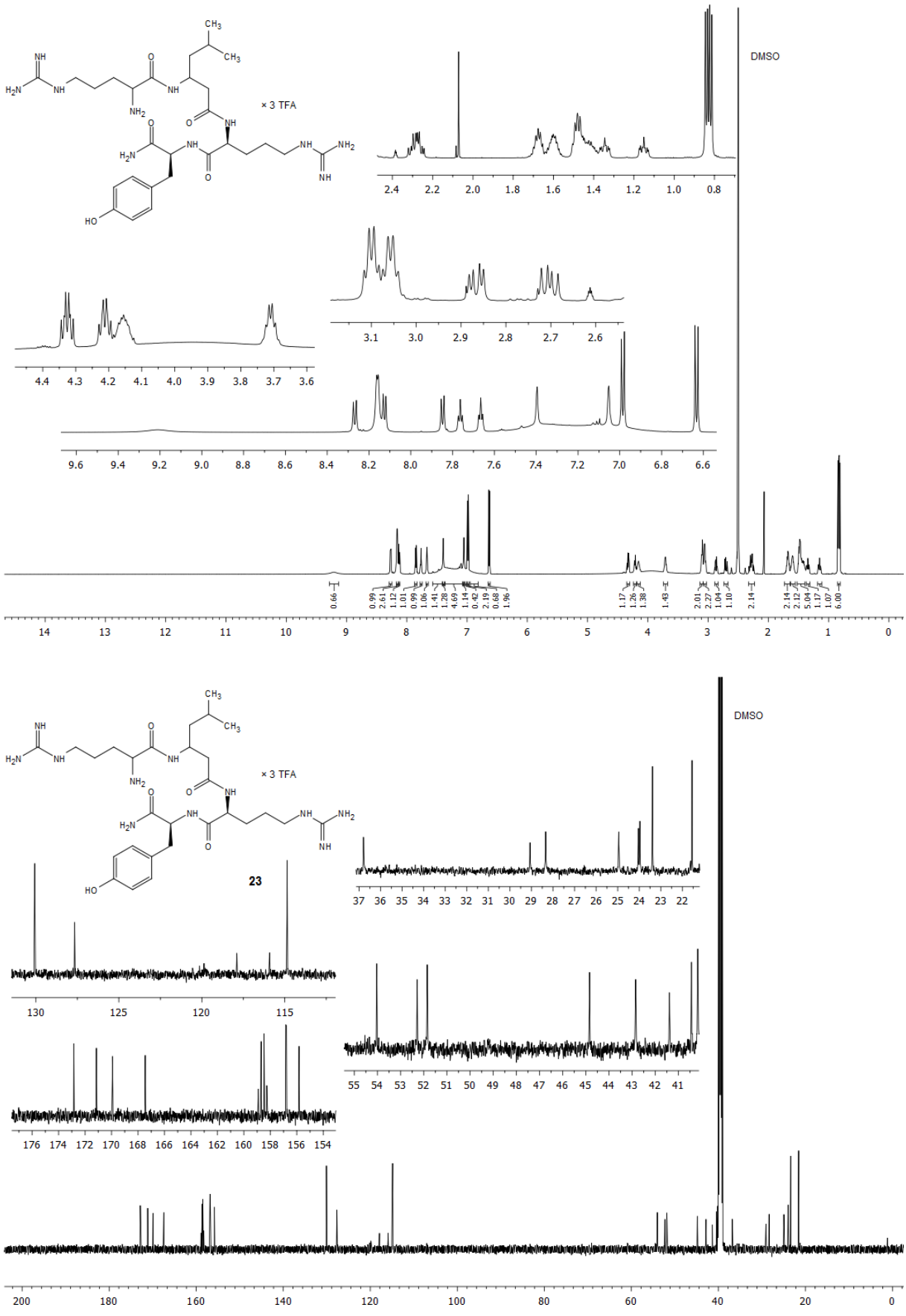

^{1}H-NMR (600 MHz, DMSO-d_6) and ^{13}C-NMR (150 MHz, DMSO-d_6) spectrum of compound **3.13**

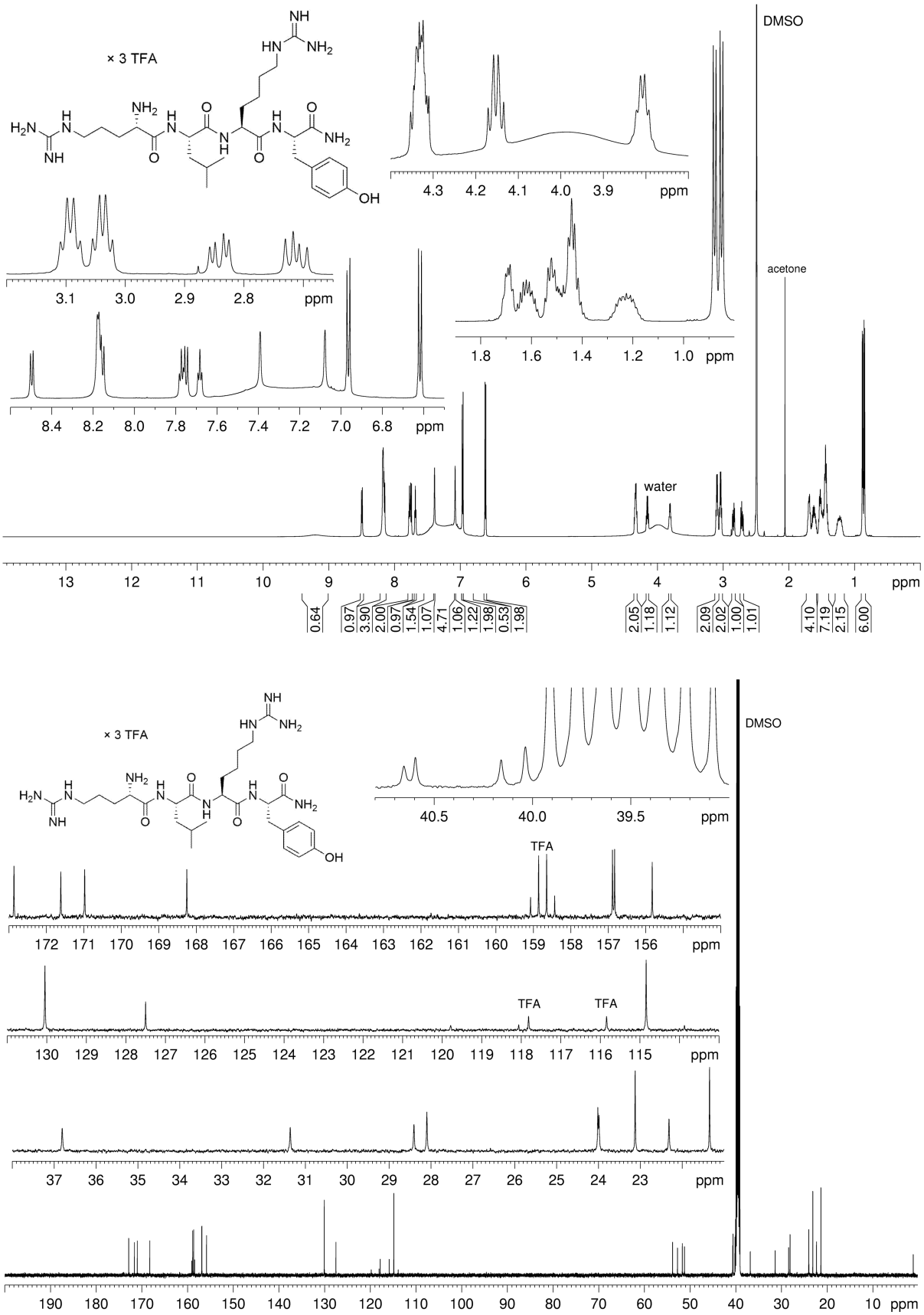

^{1}H-NMR (600 MHz, DMSO-d_6) and ^{13}C-NMR (150 MHz, DMSO-d_6) spectrum of compound **3.14**

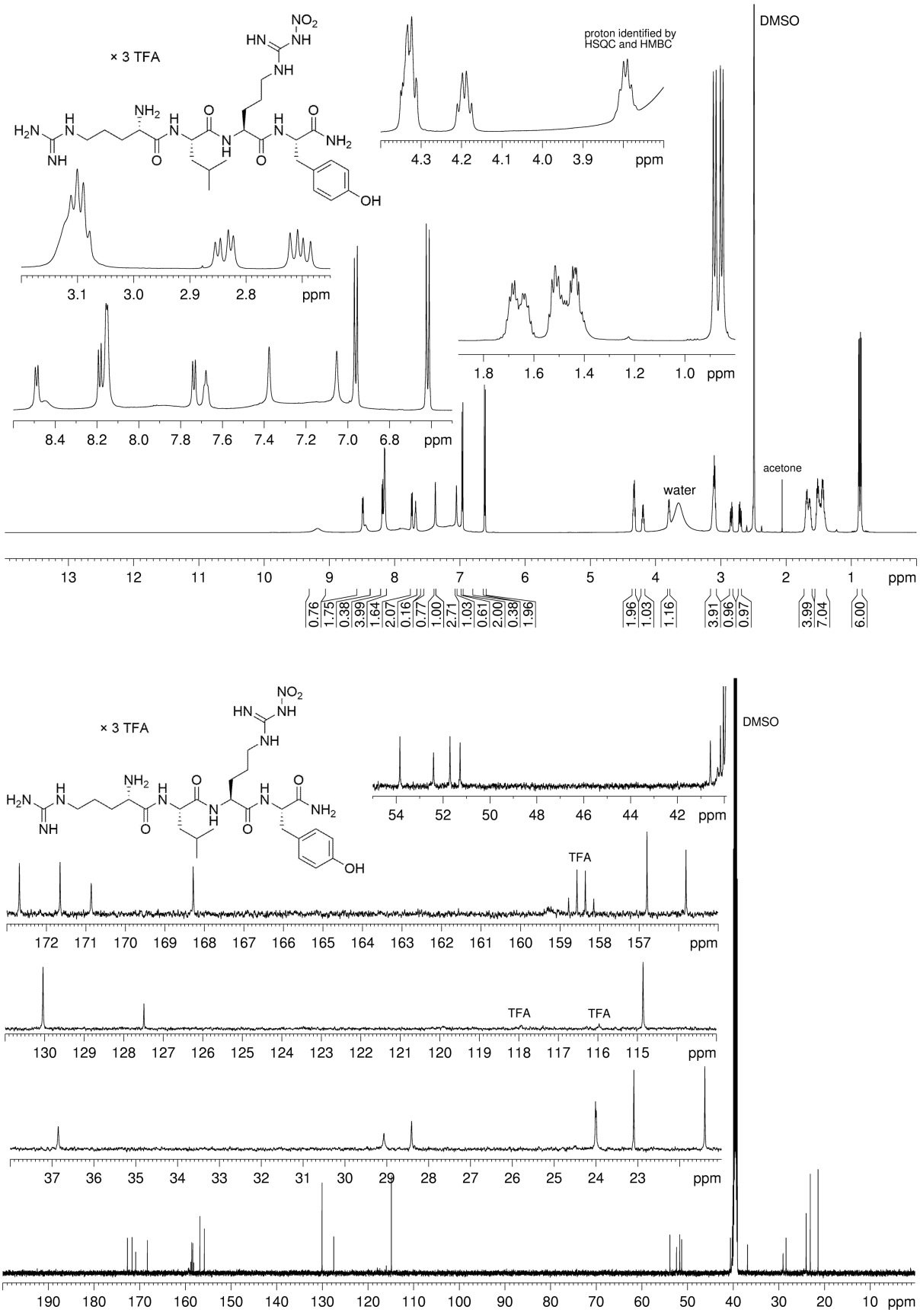

^{1}H-NMR (600 MHz, DMSO-d_6) and ^{13}C-NMR (150 MHz, DMSO-d_6) spectrum of compound **3.15**

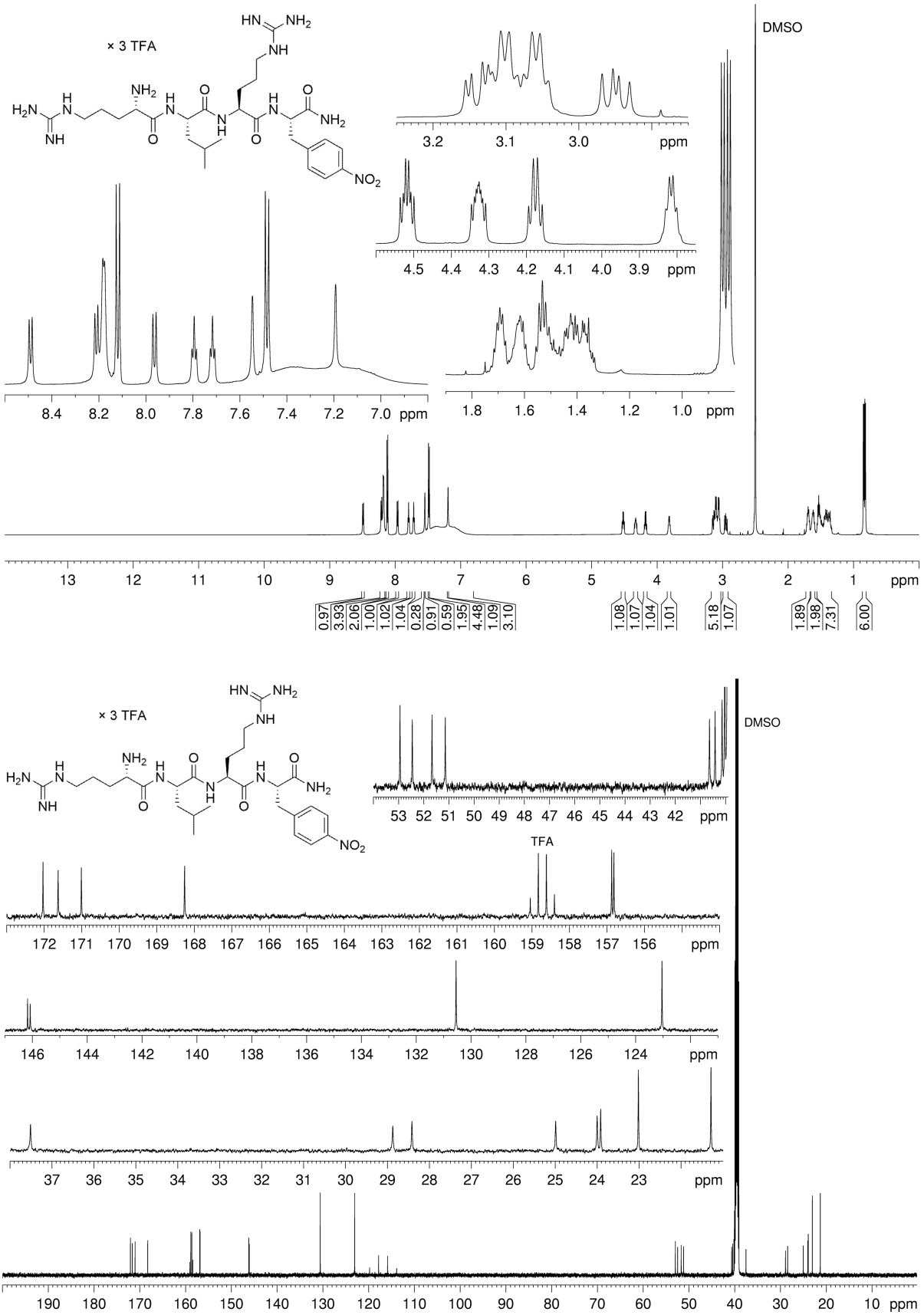

^{1}H-NMR (600 MHz, DMSO-d_6) and ^{13}C-NMR (150 MHz, DMSO-d_6) spectrum of compound **3.16**

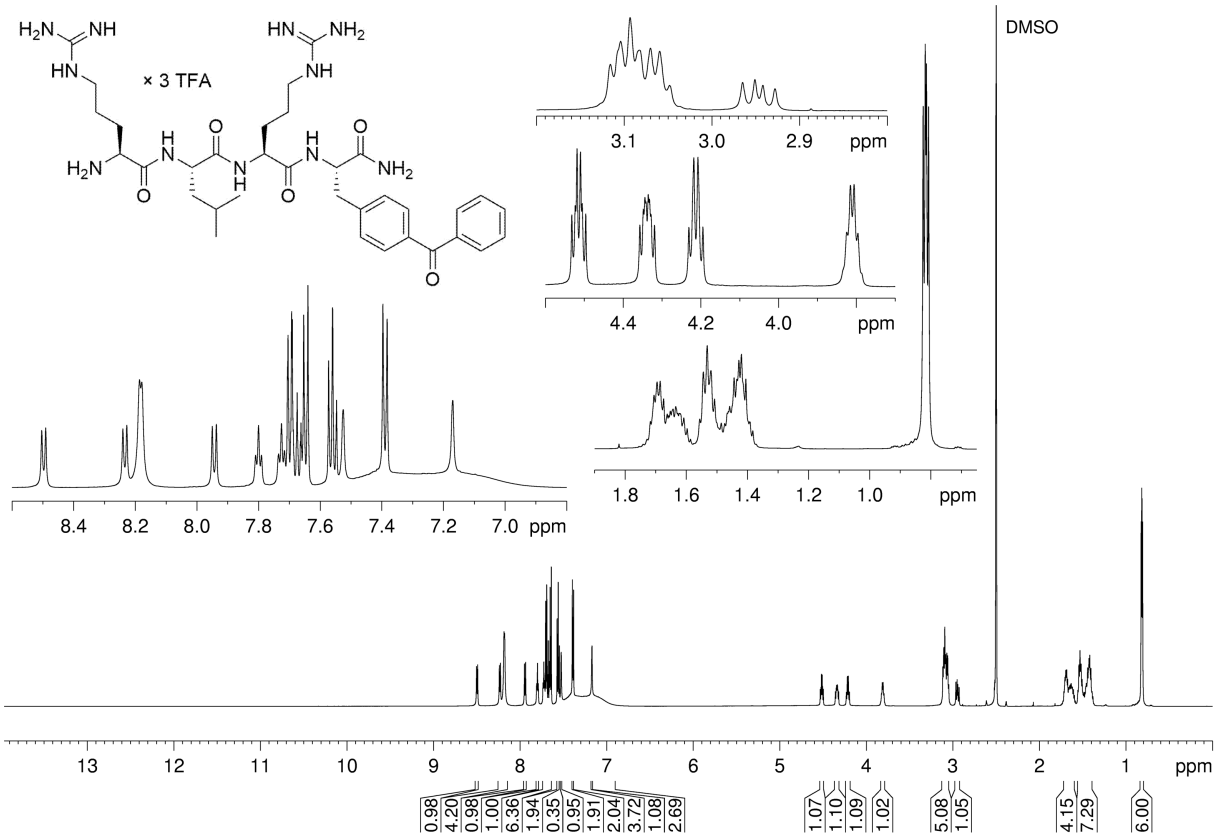

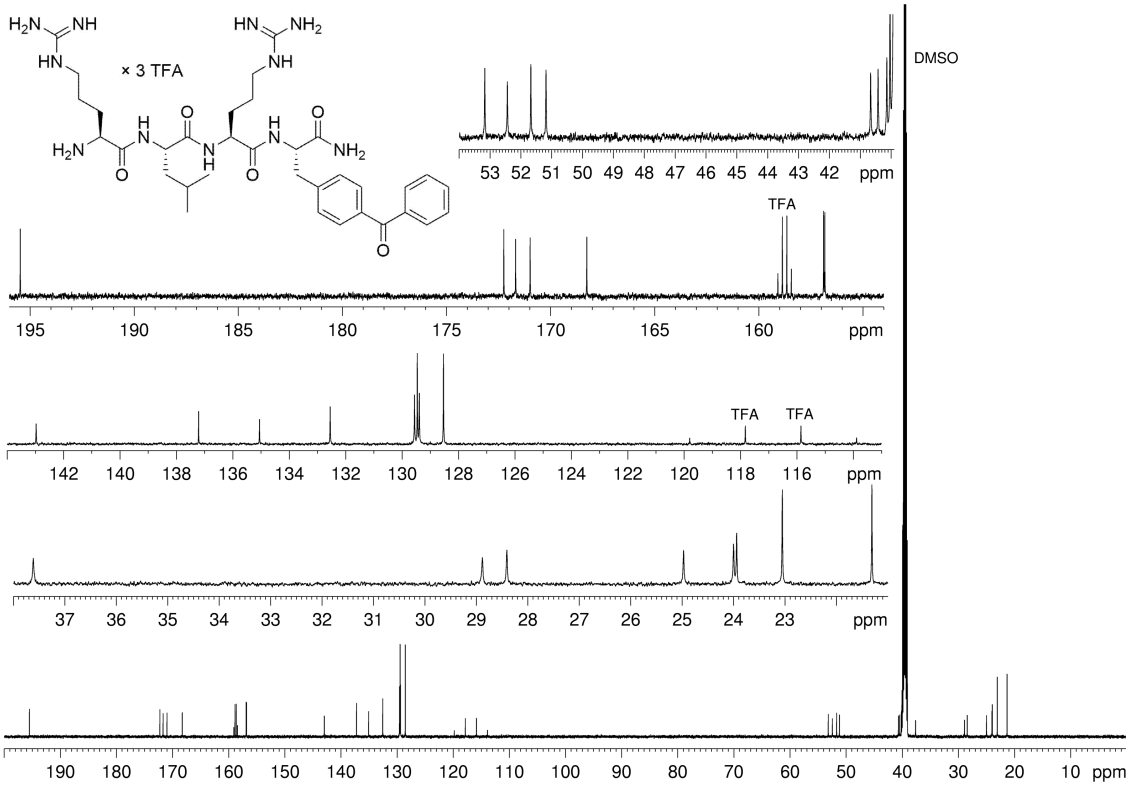

^{1}H-NMR (600 MHz, DMSO-d_6) and ^{13}C-NMR (150 MHz, DMSO-d_6) spectrum of compound **3.17**

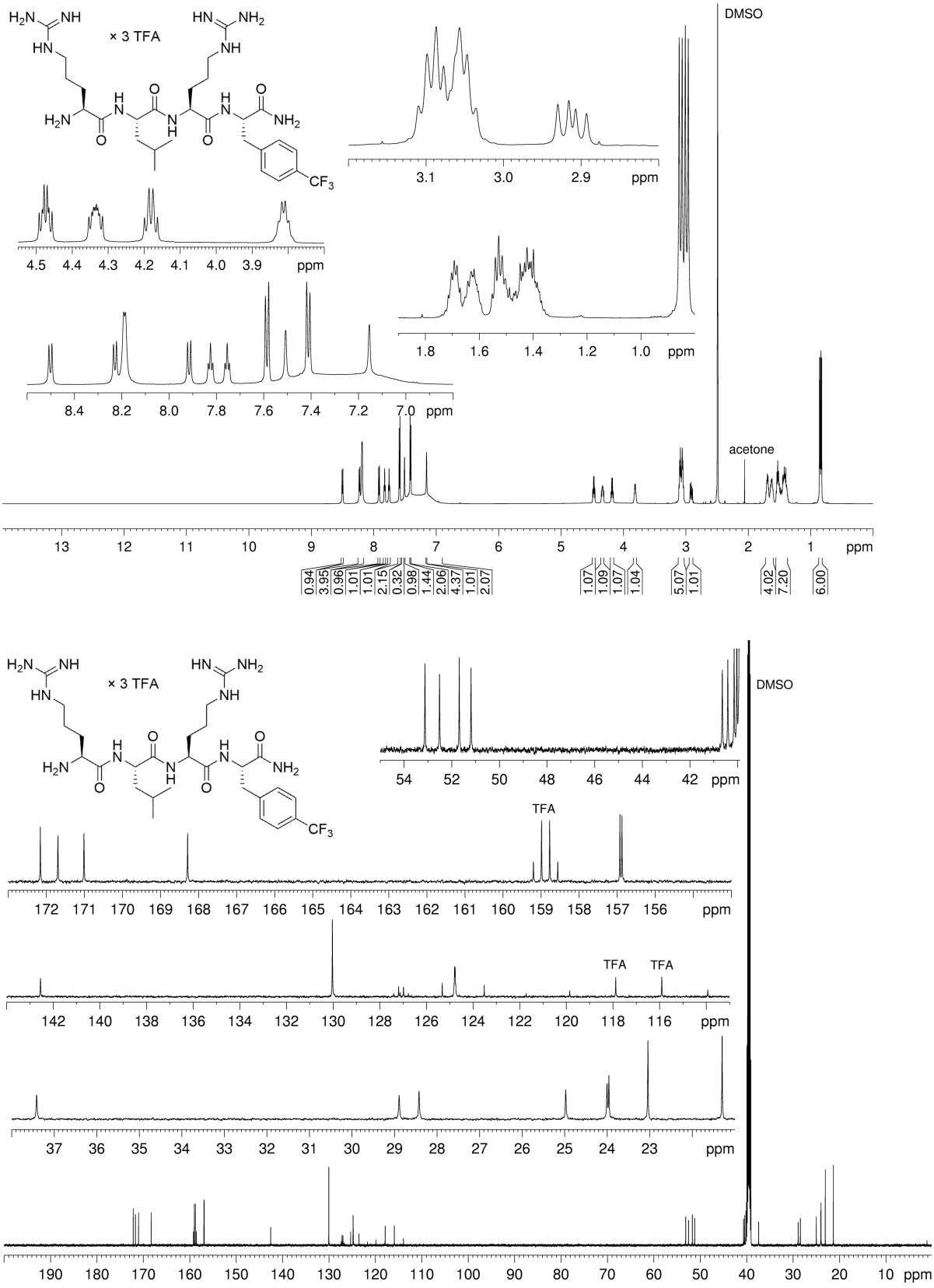

^{1}H-NMR (600 MHz, DMSO-d_6) and ^{13}C-NMR (150 MHz, DMSO-d_6) spectrum of compound **3.18**

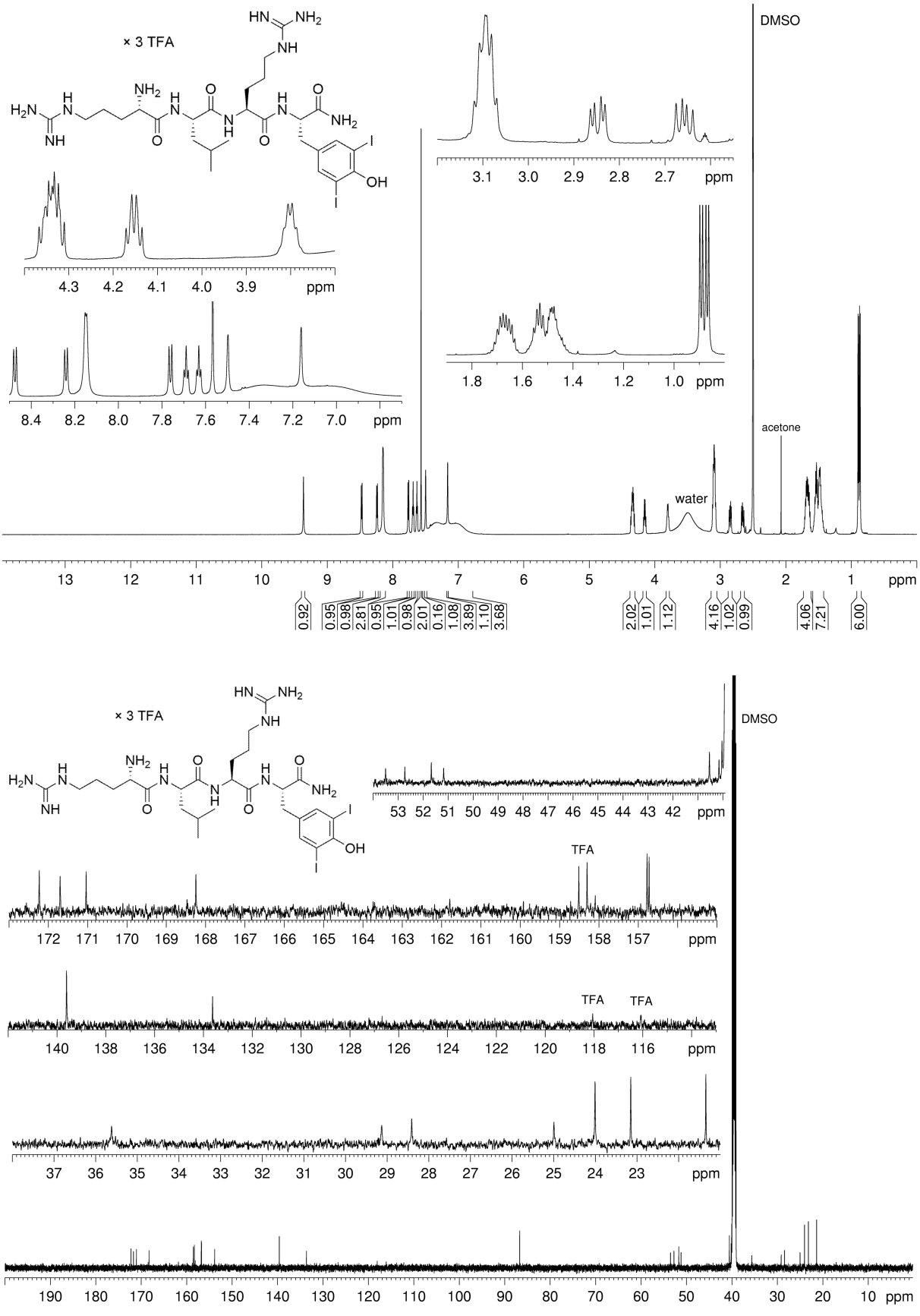

^{1}H-NMR (600 MHz, DMSO-d_6) and ^{13}C-NMR (150 MHz, DMSO-d_6) spectrum of compound **3.19**

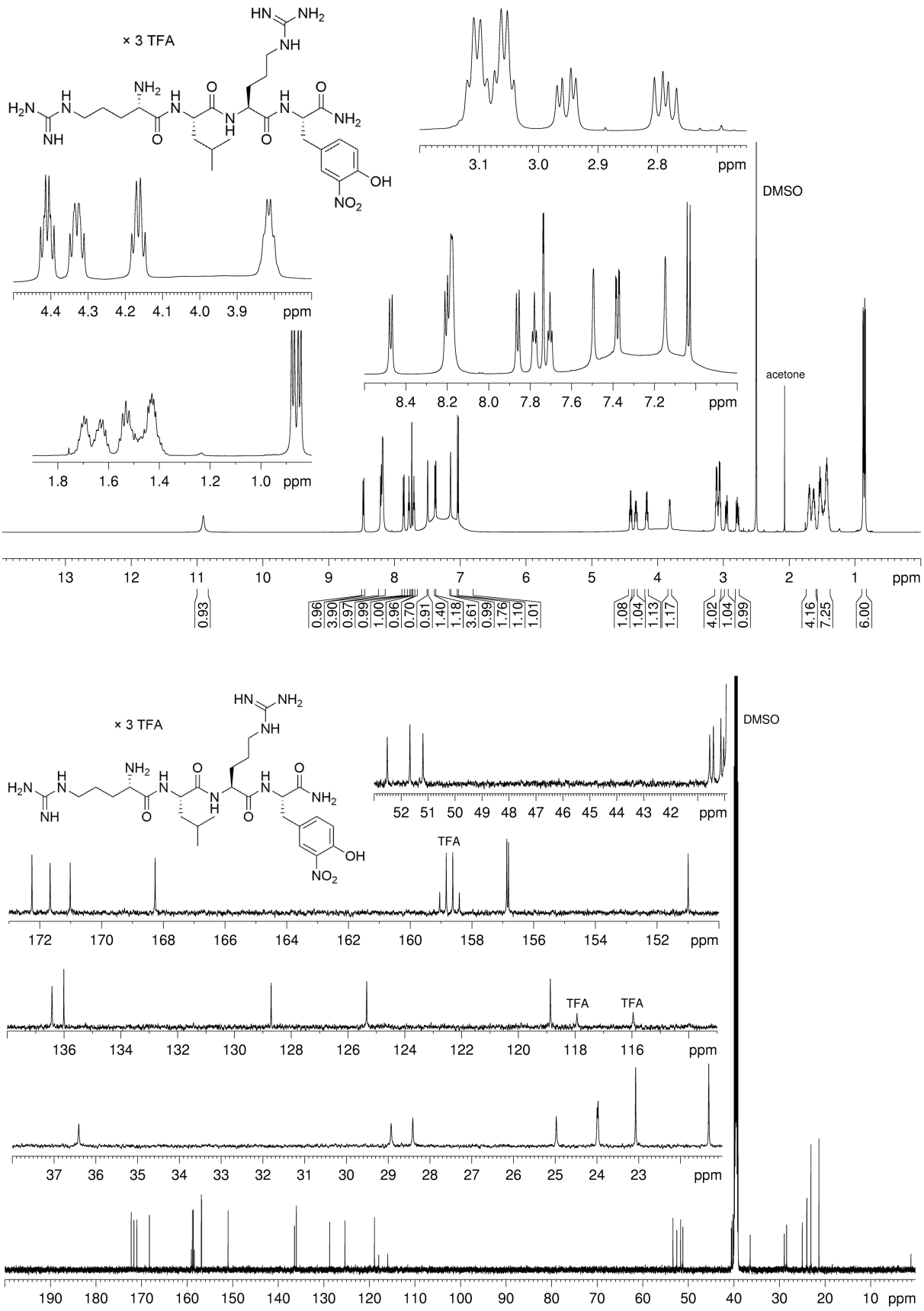

^{1}H-NMR (600 MHz, DMSO-d_6) and ^{13}C-NMR (150 MHz, DMSO-d_6) spectrum of compound **3.20**

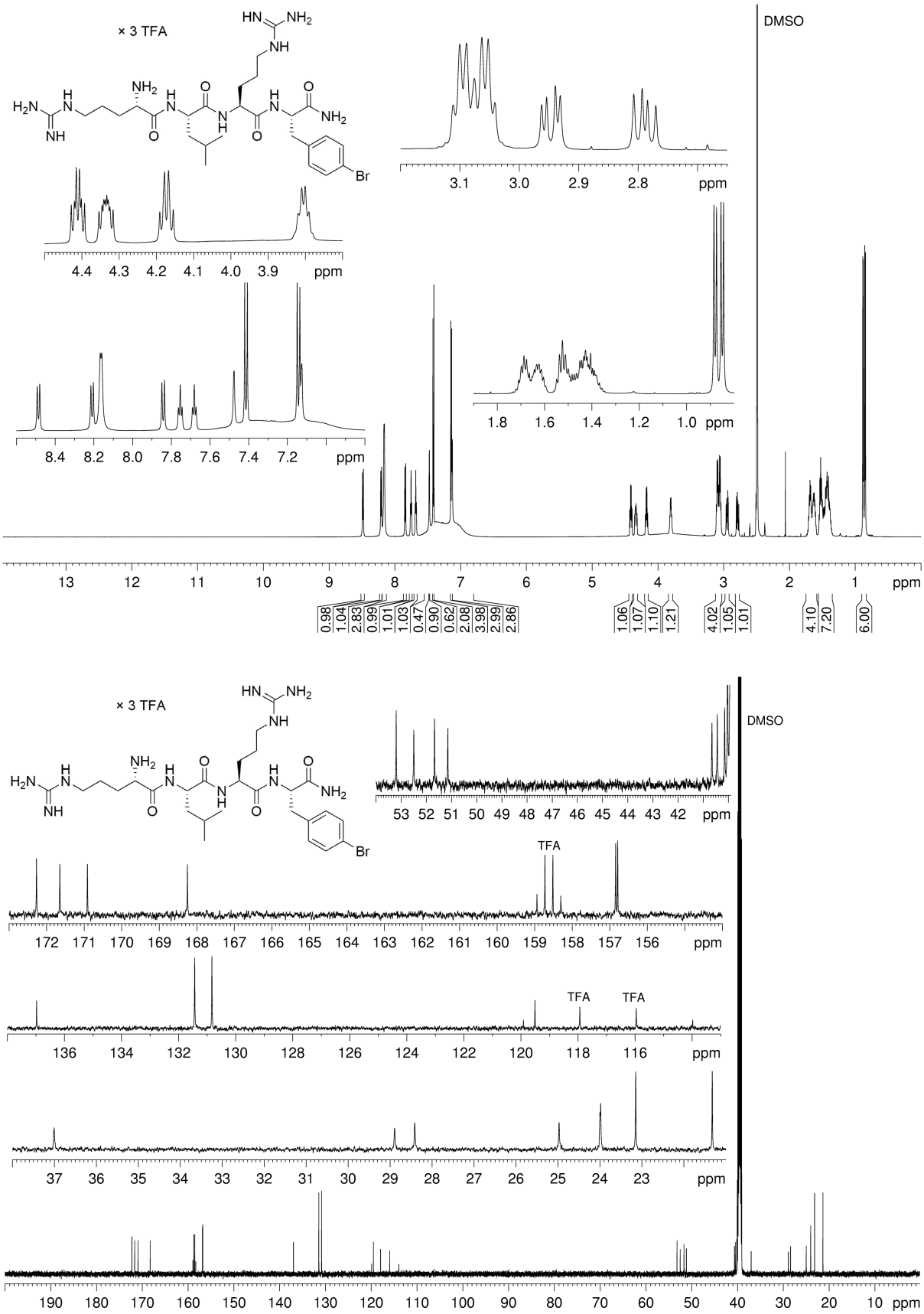

^{1}H-NMR (600 MHz, DMSO-d_6) and ^{13}C-NMR (150 MHz, DMSO-d_6) spectrum of compound **3.21**

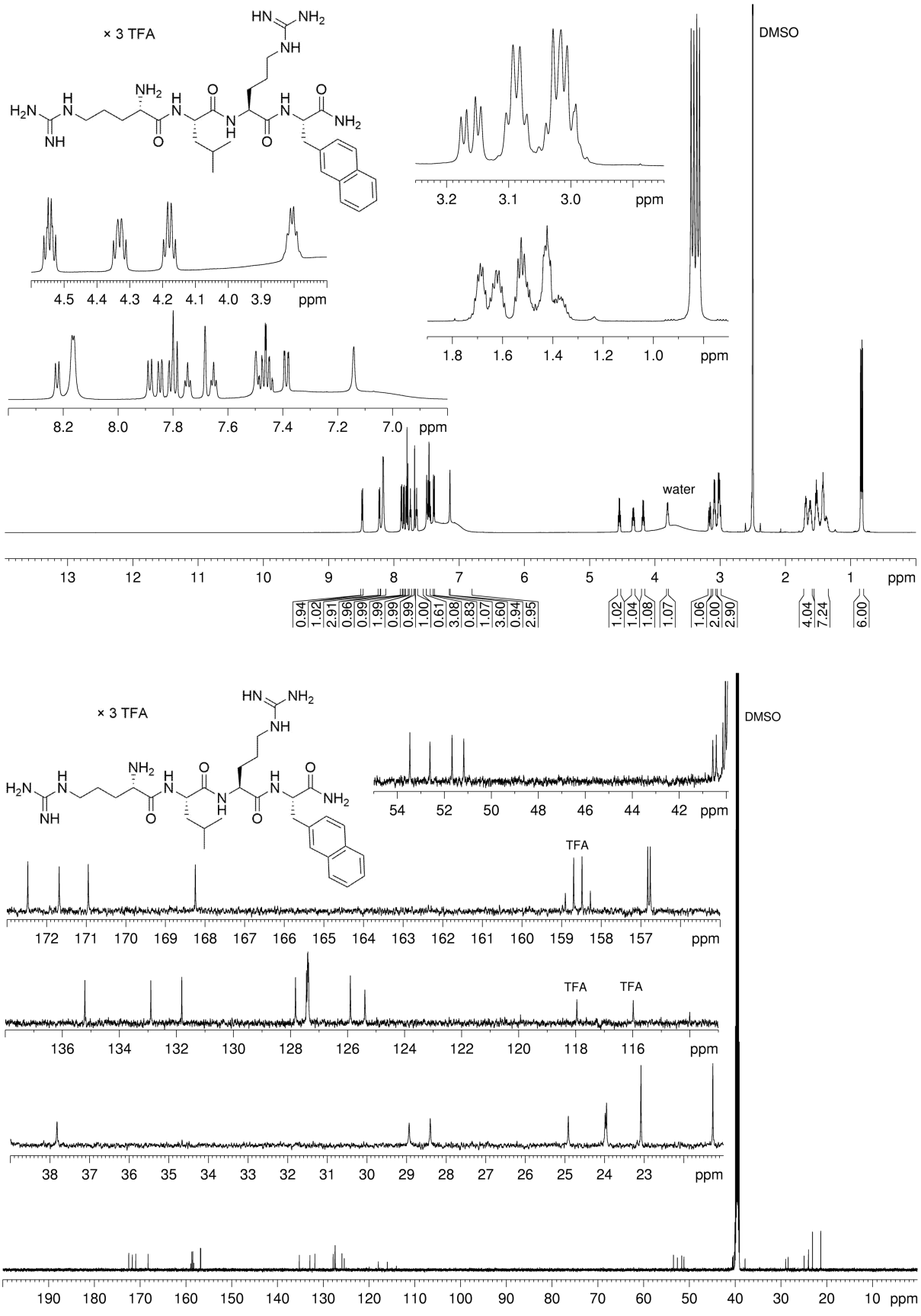

^{1}H-NMR (600 MHz, DMSO-d_6) and ^{13}C-NMR (150 MHz, DMSO-d_6) spectrum of compound **3.22**

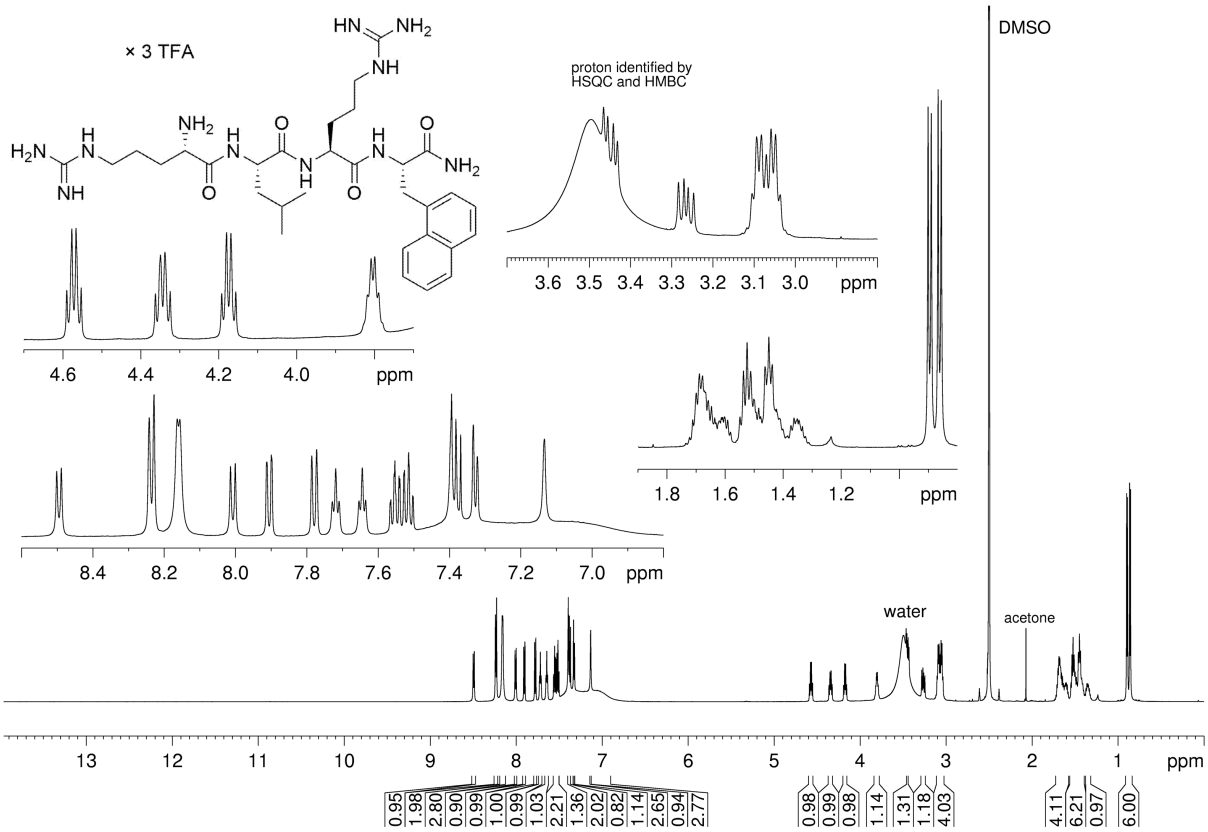

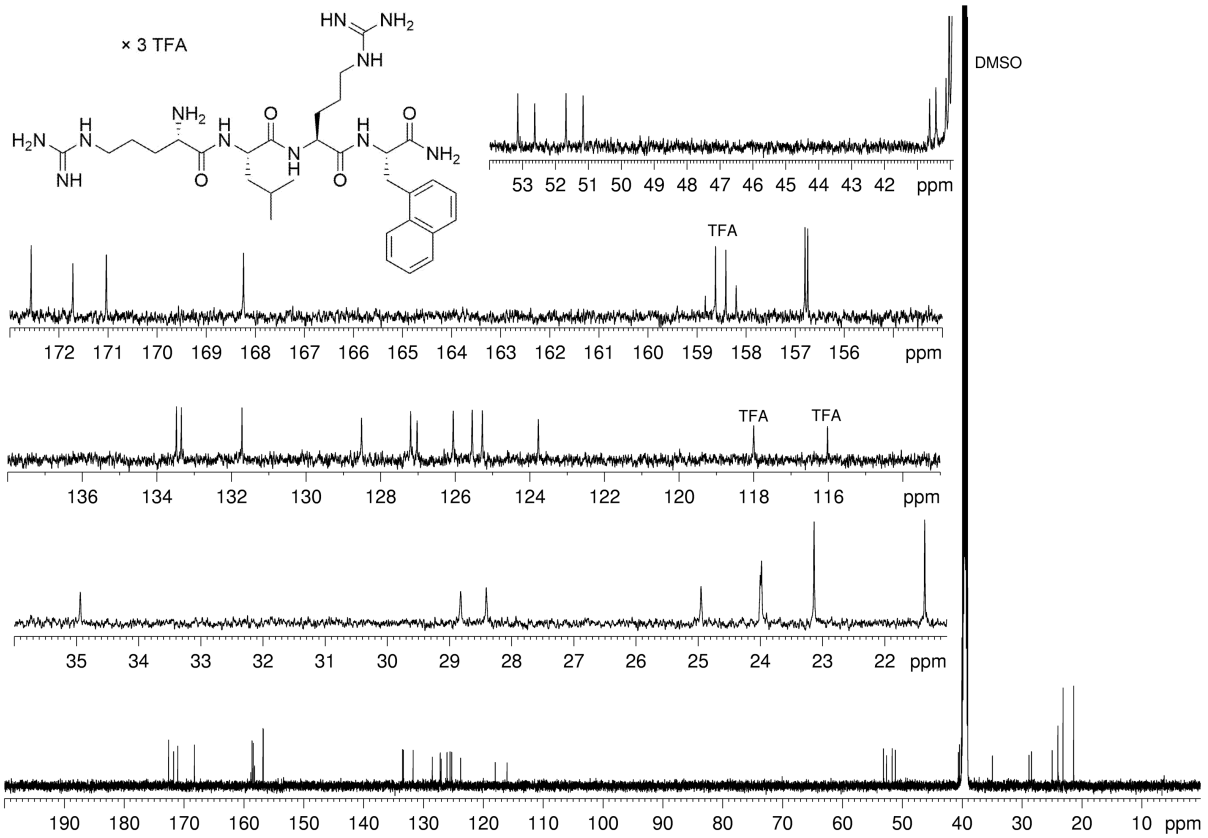

^{1}H-NMR (600 MHz, DMSO-d_6) and ^{13}C-NMR (150 MHz, DMSO-d_6) spectrum of compound **3.23**

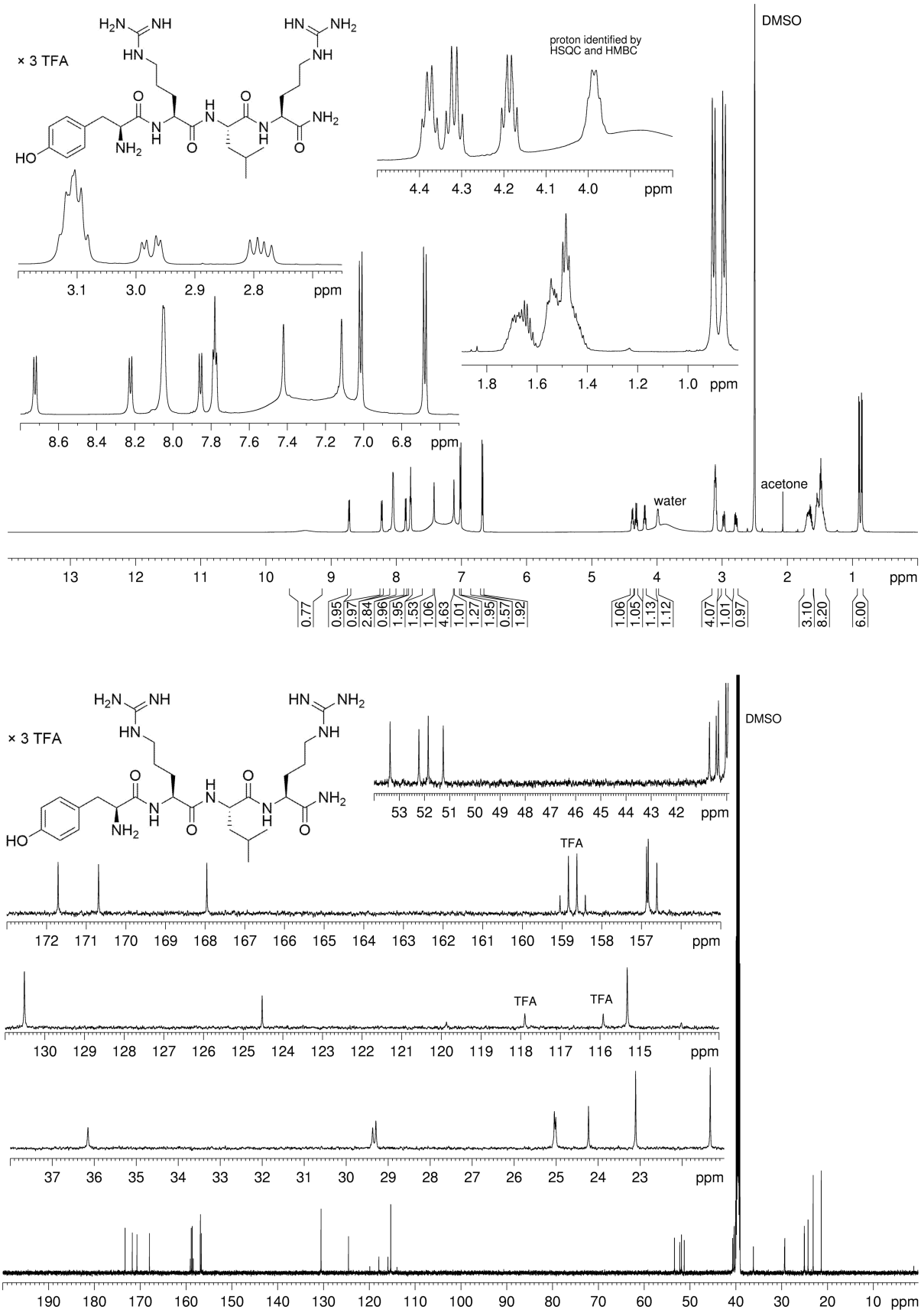

^{1}H-NMR (600 MHz, DMSO-d_6) and ^{13}C-NMR (150 MHz, DMSO-d_6) spectrum of compound **3.24**

7.3 Appendix Chapter 4

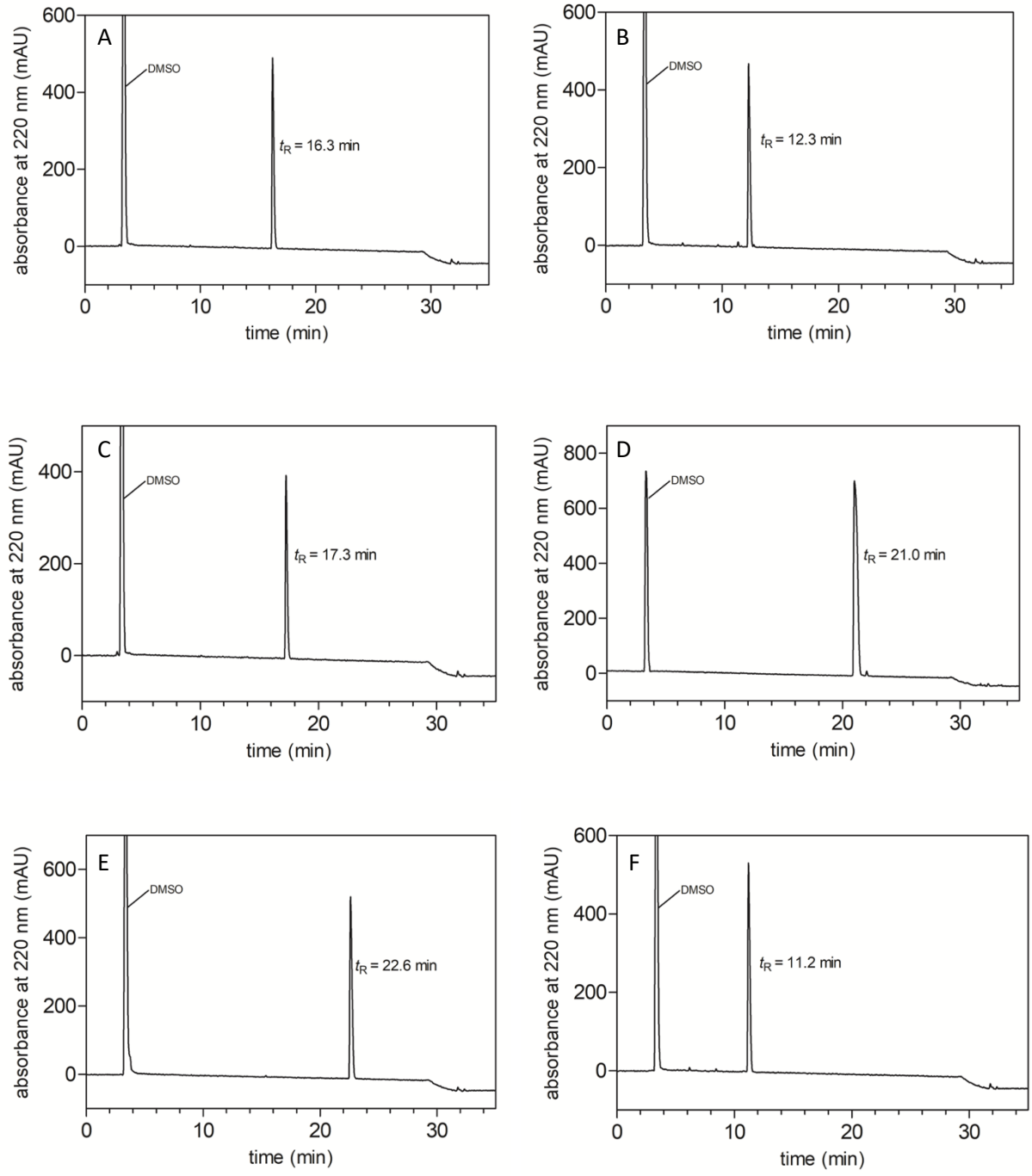

RP-HPLC analysis of compound **4.11** (A), **4.12** (B), **4.25** (C), **4.26** (D), **4.27** (E) and **4.28** (F).

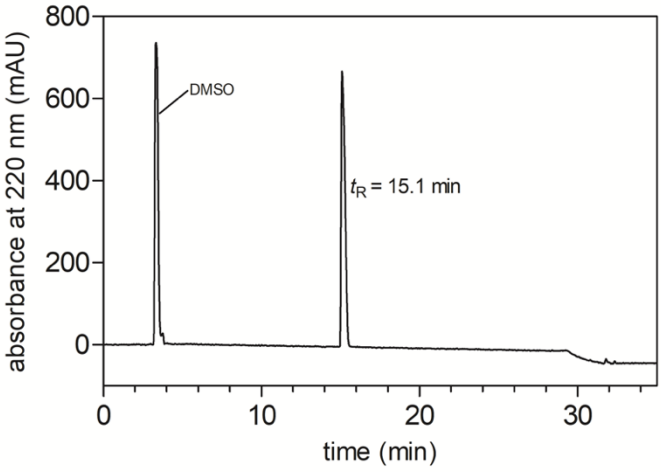

RP-HPLC analysis of compound **4.29**

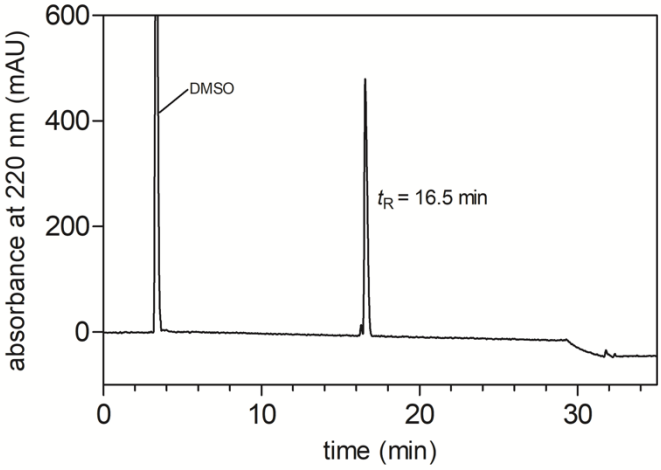

RP-HPLC analysis of compound **4.30**

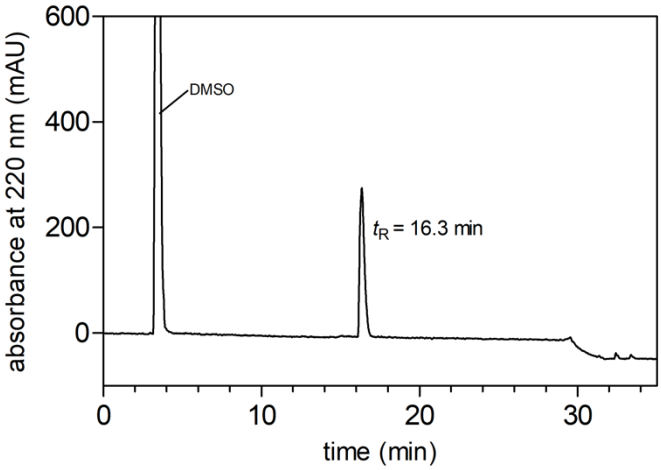

RP-HPLC analysis of compound **4.32**

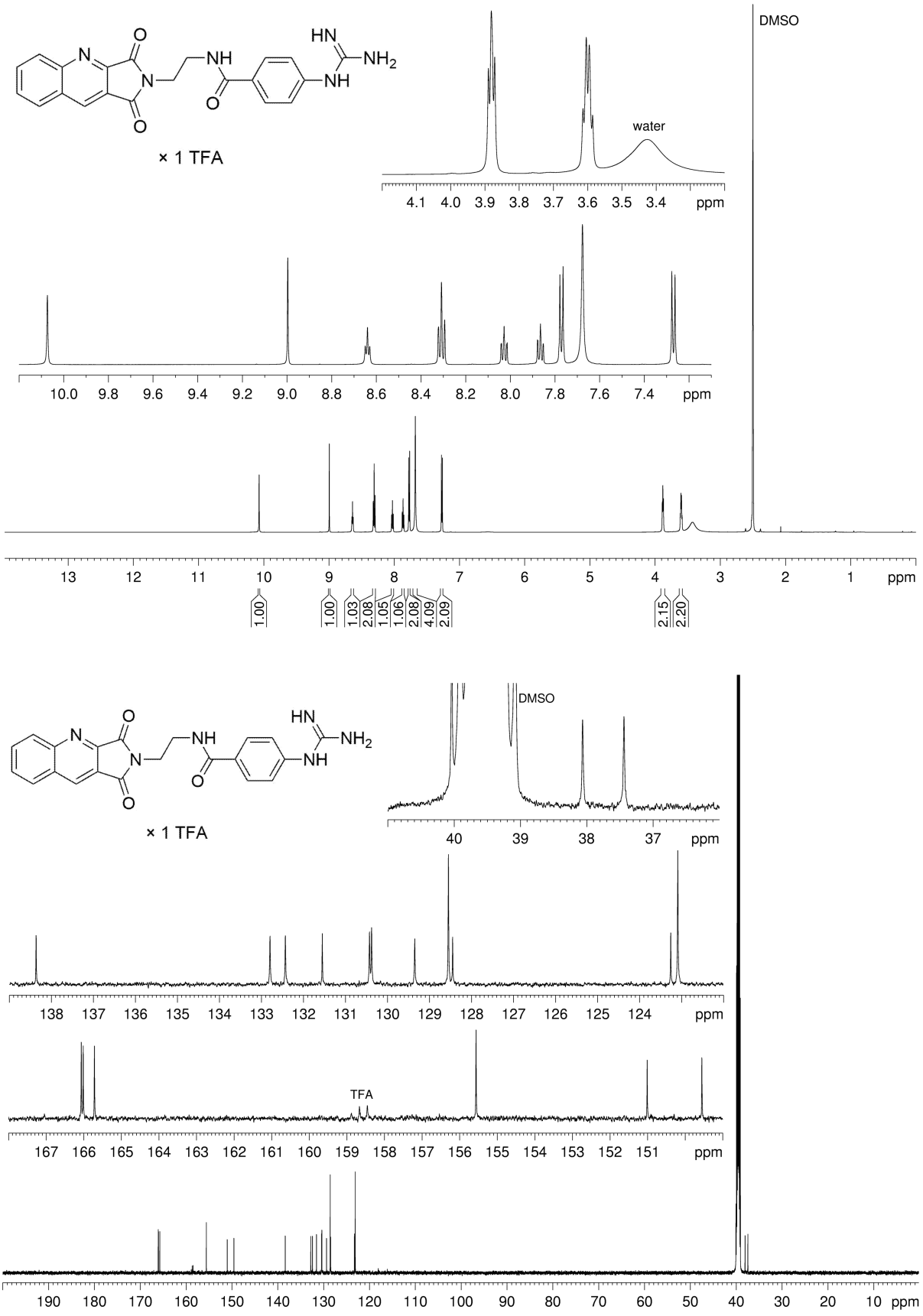

^{1}H-NMR (600 MHz, DMSO-d_6) and ^{13}C-NMR (150 MHz, DMSO-d_6) spectrum of compound **4.11**

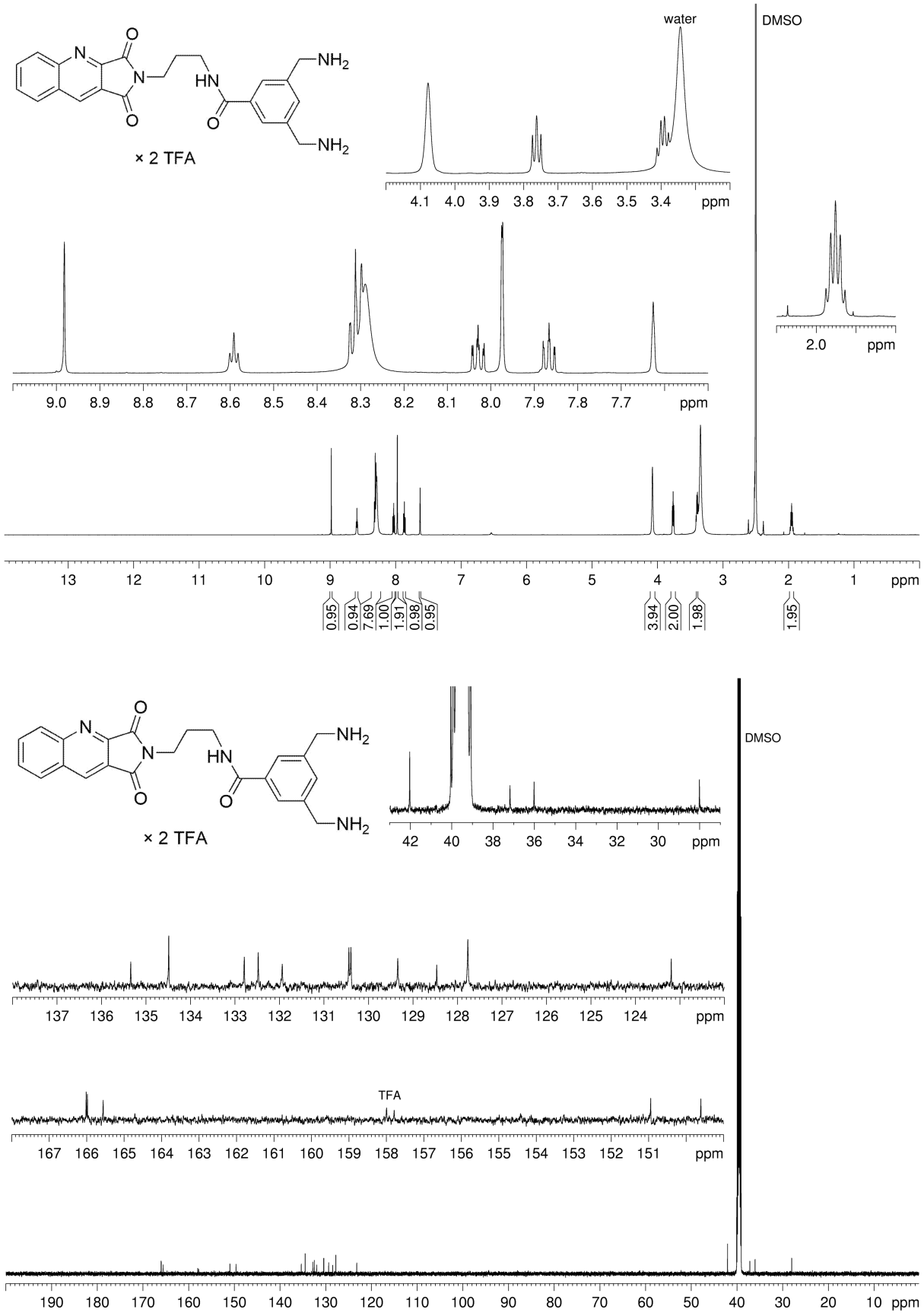

^{1}H-NMR (600 MHz, DMSO-d_6) and ^{13}C-NMR (150 MHz, DMSO-d_6) spectrum of compound **4.12**

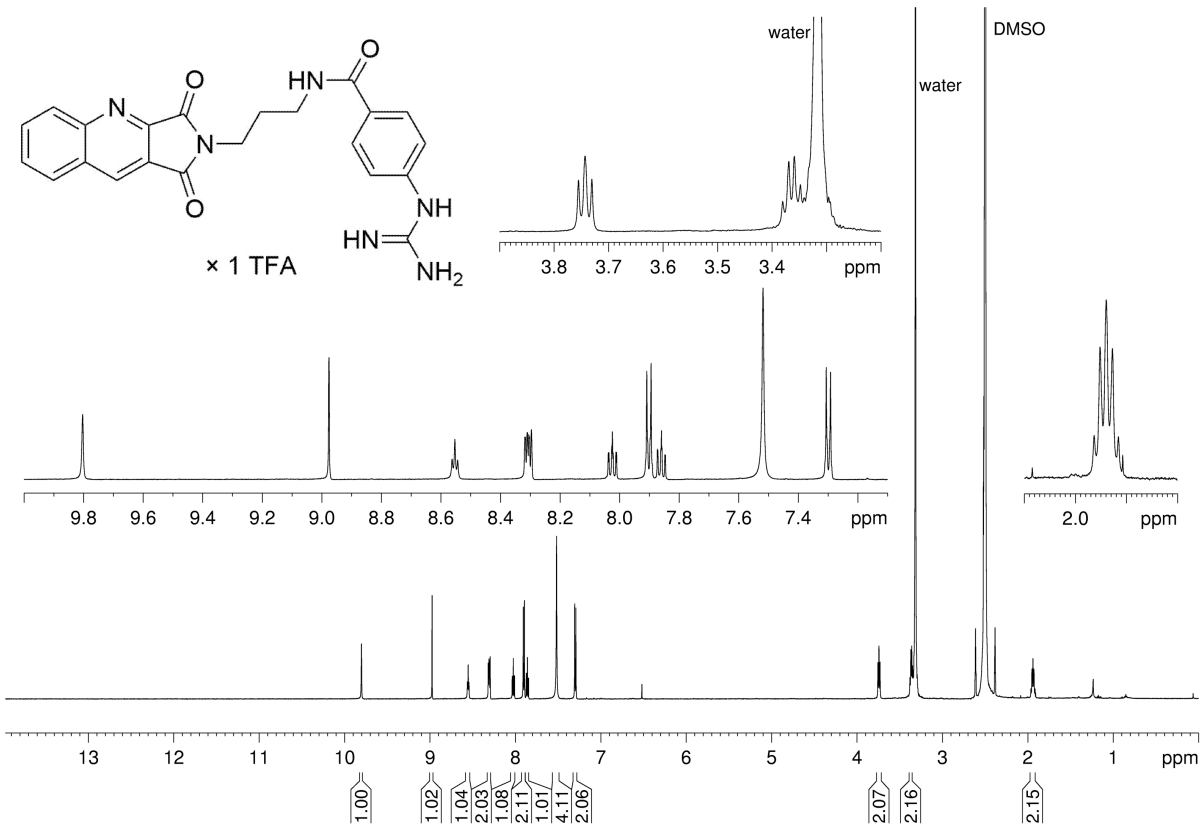

^{1}H-NMR (600 MHz, DMSO-d_6) spectrum of compound **4.25**

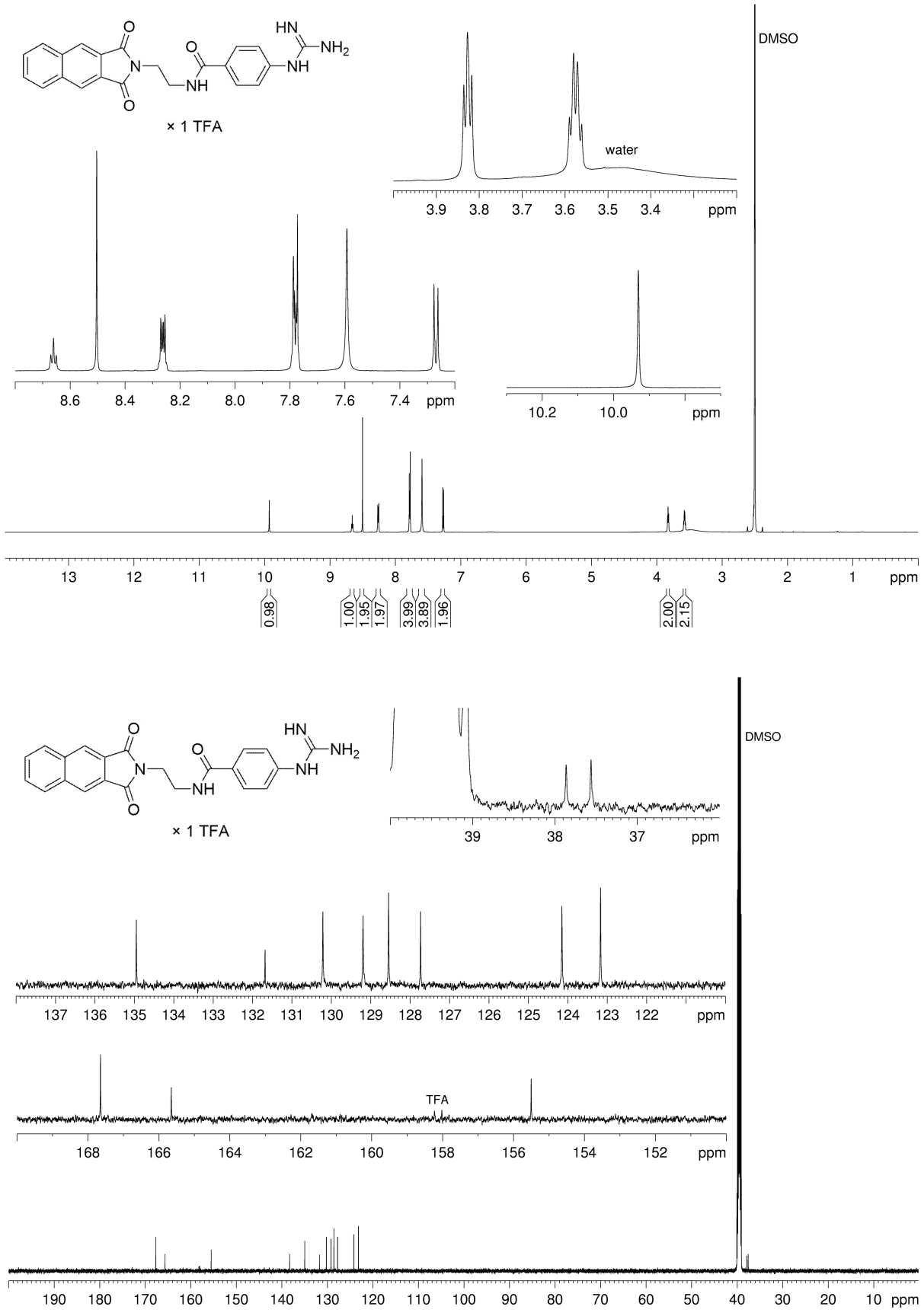

^{1}H-NMR (600 MHz, DMSO-d_6) and ^{13}C-NMR (150 MHz, DMSO-d_6) spectrum of compound **4.26**

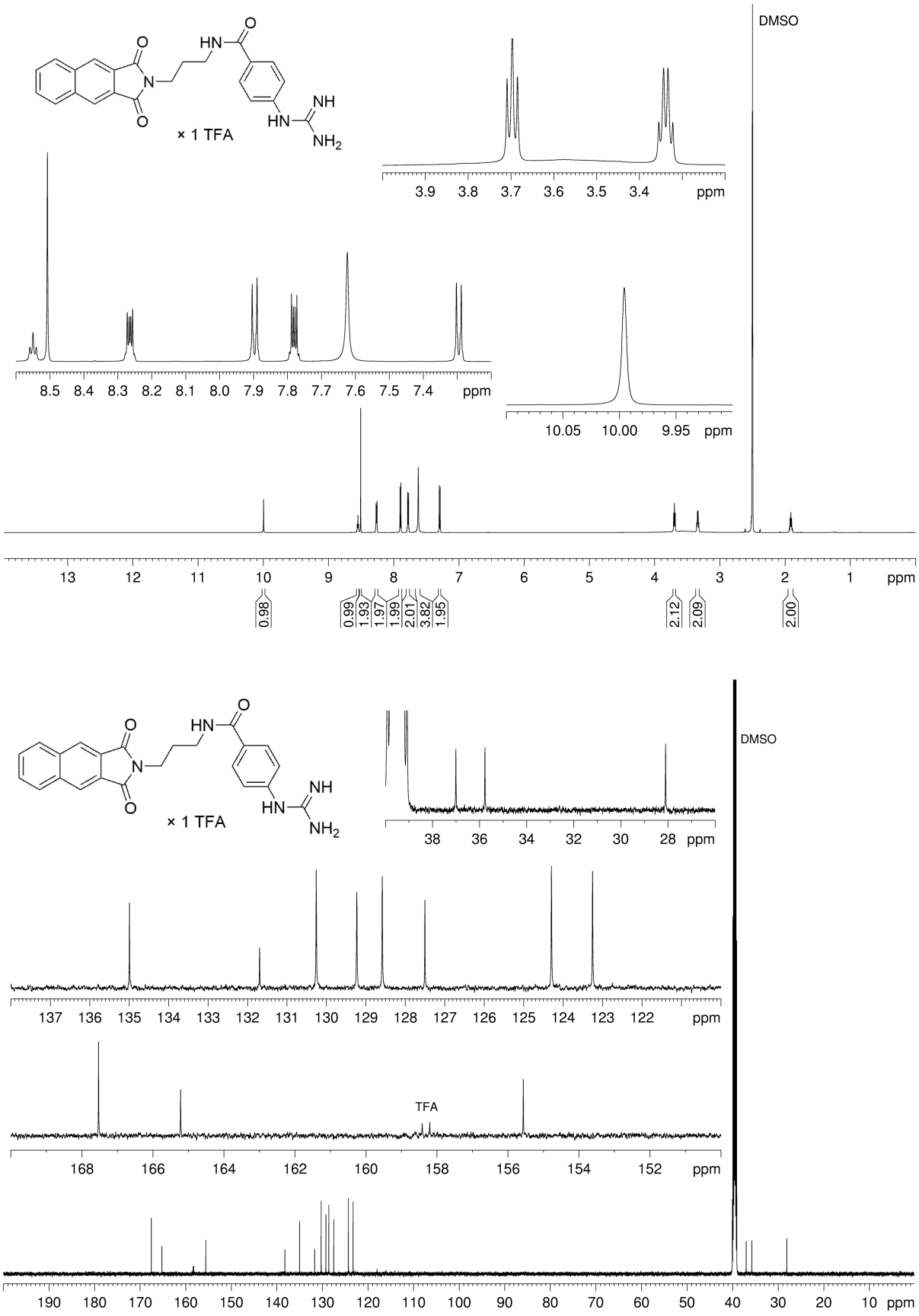

^{1}H-NMR (600 MHz, DMSO-d_6) and ^{13}C-NMR (150 MHz, DMSO-d_6) spectrum of compound **4.27**

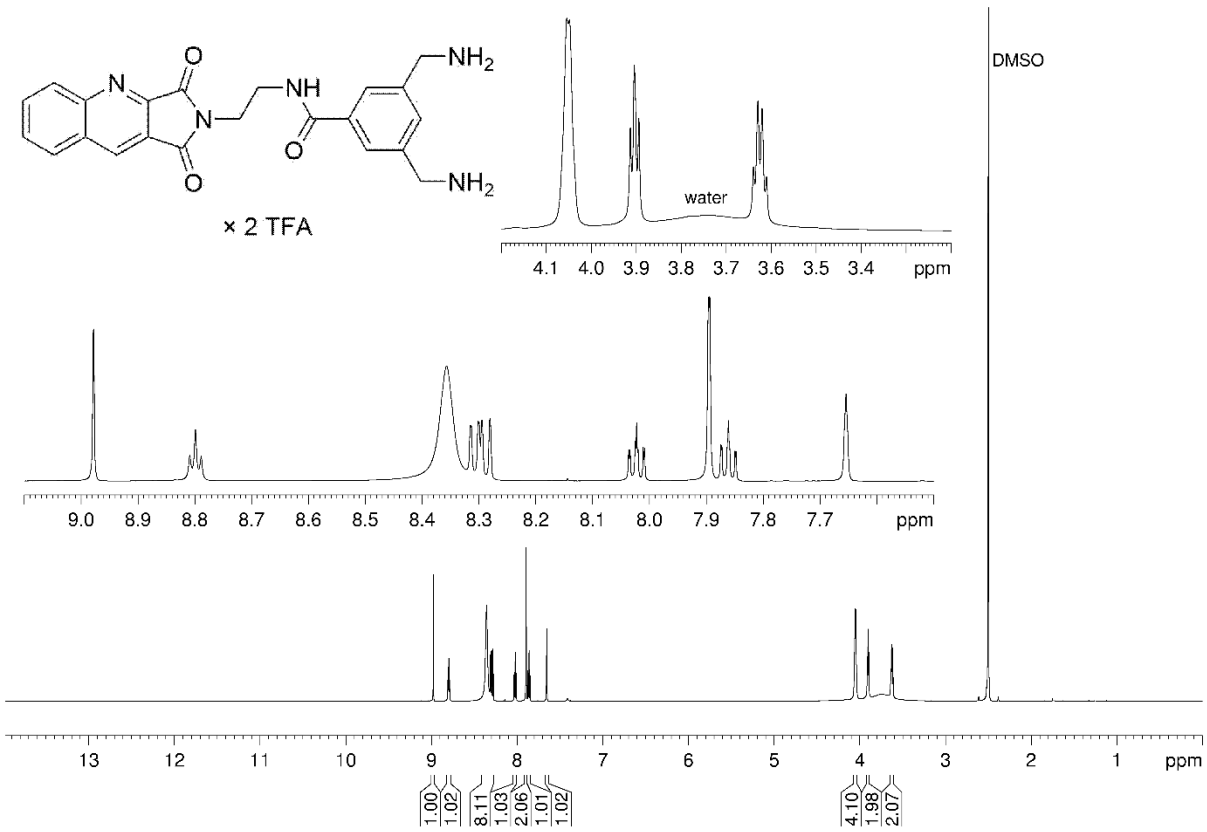
NH2
NH
NH2
× 2 TFA
water
DMSO
4.1 4.0 3.9 3.8 3.7 3.6 3.5 3.4 ppm
9.0 8.9 8.8 8.7 8.6 8.5 8.4 8.3 8.2 8.1 8.0 7.9 7.8 7.7 ppm
13 12 11 10 9 8 7 6 5 4 3 2 1 ppm
1.00 1.02 8.11 1.03 2.06 1.01 1.02 4.10 1.98 2.07

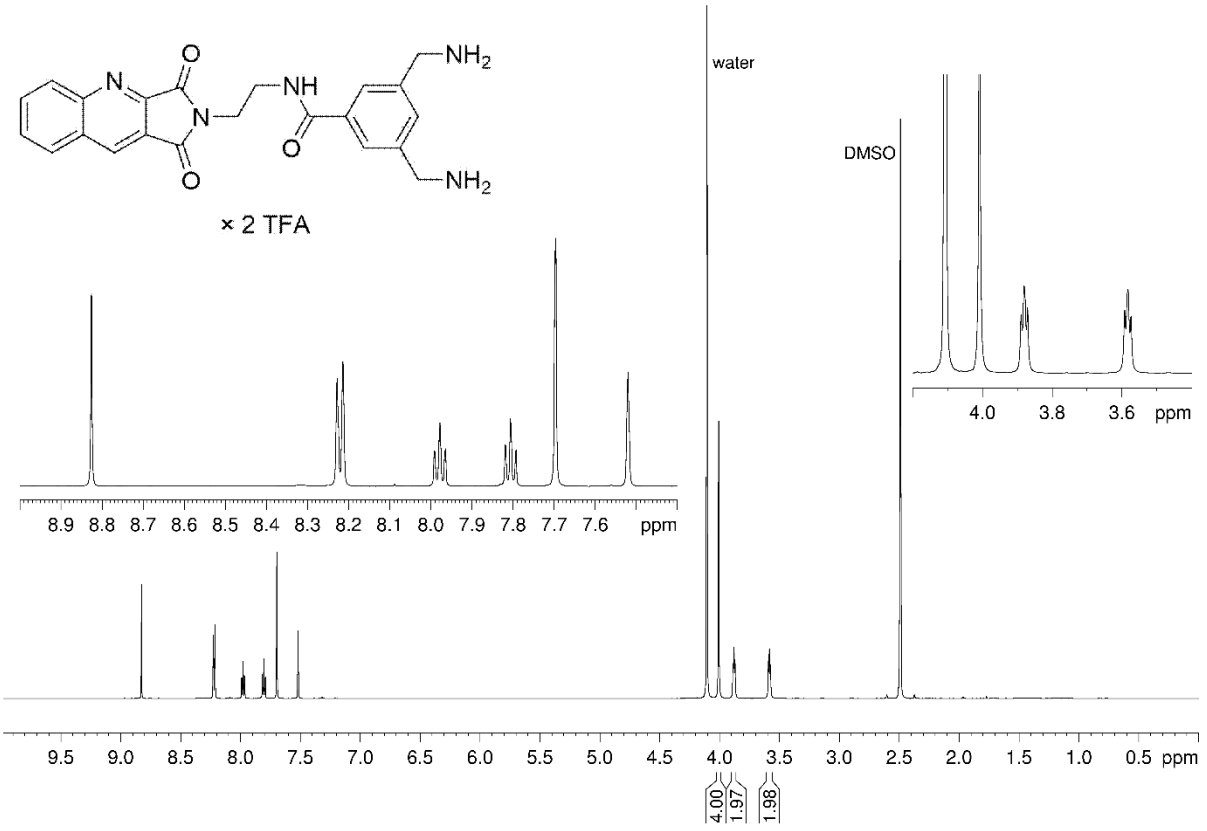
NH2
NH
NH2
× 2 TFA
water
DMSO
4.0 3.8 3.6 ppm
8.9 8.8 8.7 8.6 8.5 8.4 8.3 8.2 8.1 8.0 7.9 7.8 7.7 7.6 ppm
9.5 9.0 8.5 8.0 7.5 7.0 6.5 6.0 5.5 5.0 4.5 4.0 3.5 3.0 2.5 2.0 1.5 1.0 0.5 ppm
4.00 1.97 1.98

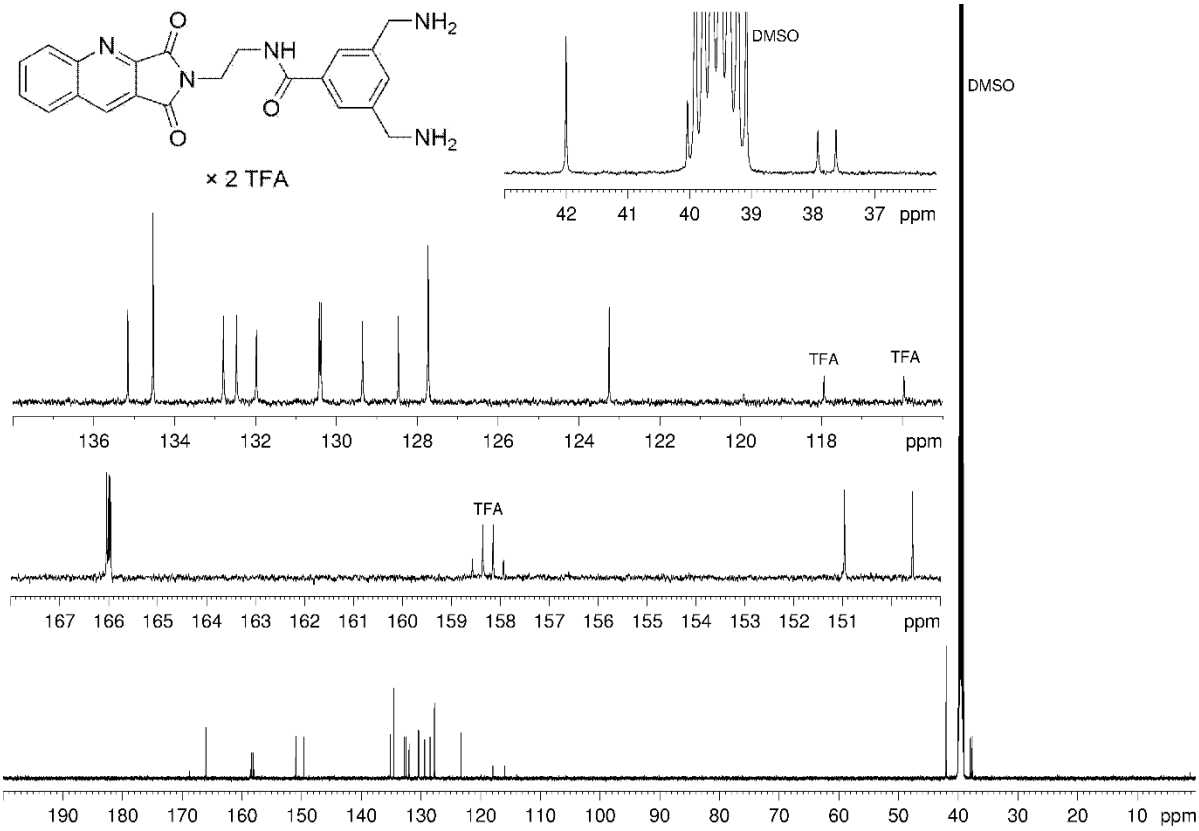

^{1}H-NMR (600 MHz, DMSO-d_6), ^{1}H-NMR (600 MHz, DMSO-d_6/D_2O 4:1 v/v) and ^{13}C-NMR (150 MHz, DMSO-d_6) spectrum of compound **4.28**

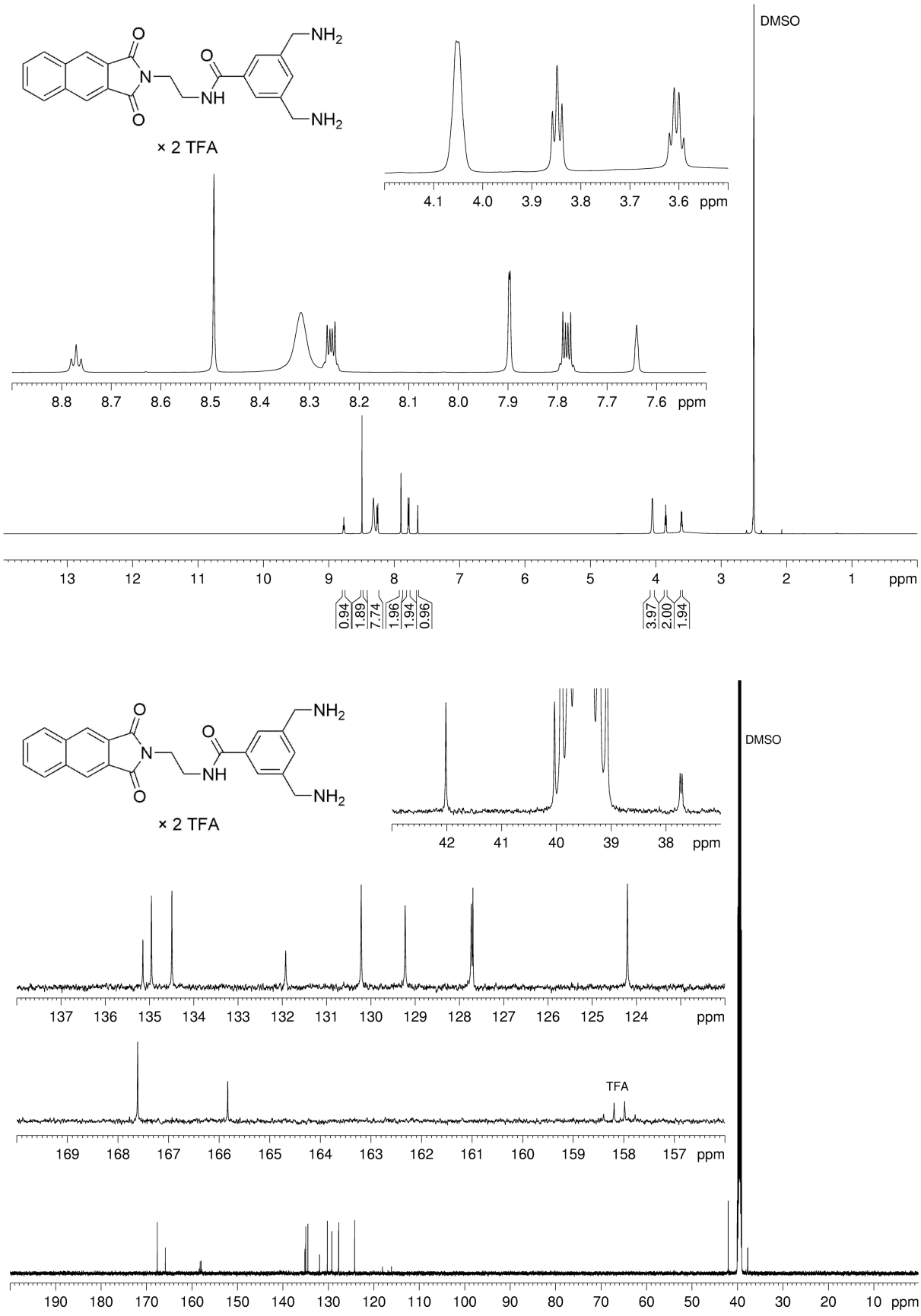

^{1}H-NMR (600 MHz, DMSO-d_6) and ^{13}C-NMR (150 MHz, DMSO-d_6) spectrum of compound **4.29**

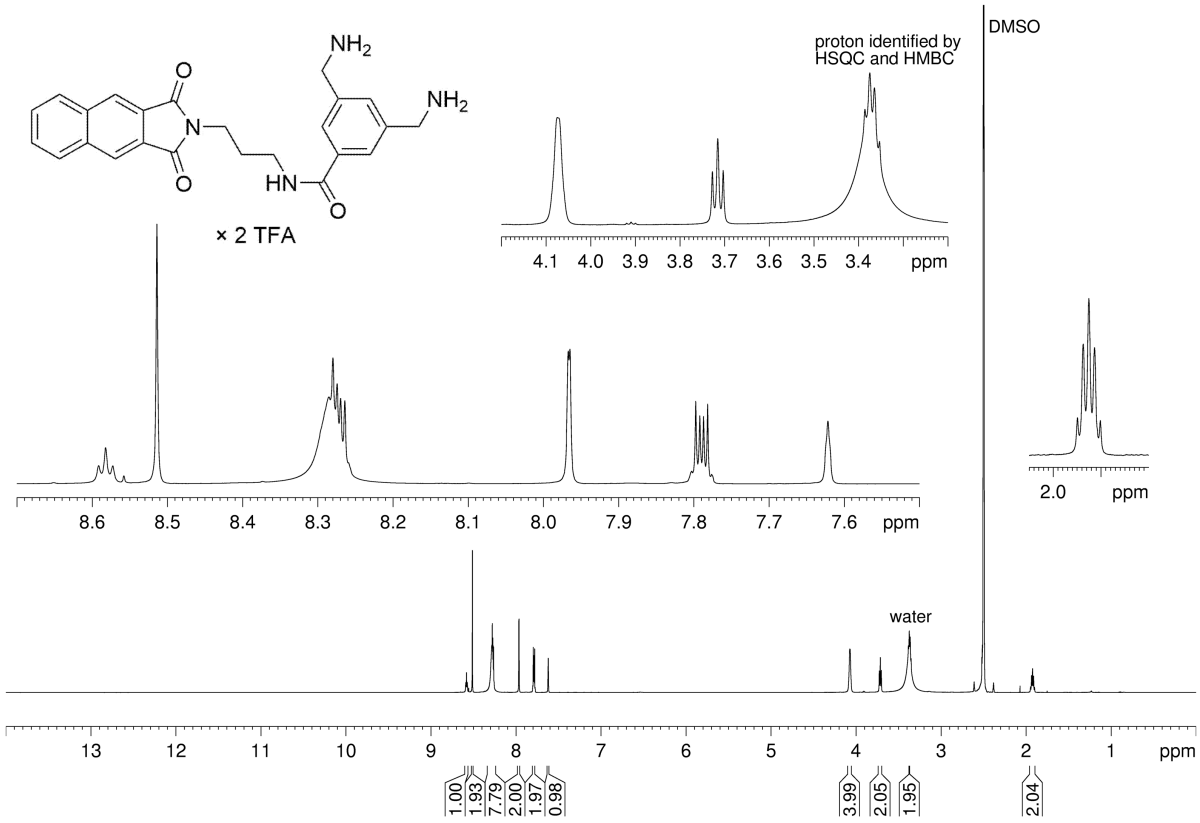
NH2
NH2
O
N
O
HN
O
× 2 TFA
proton identified by HSQC and HMBC
DMSO
water
ppm

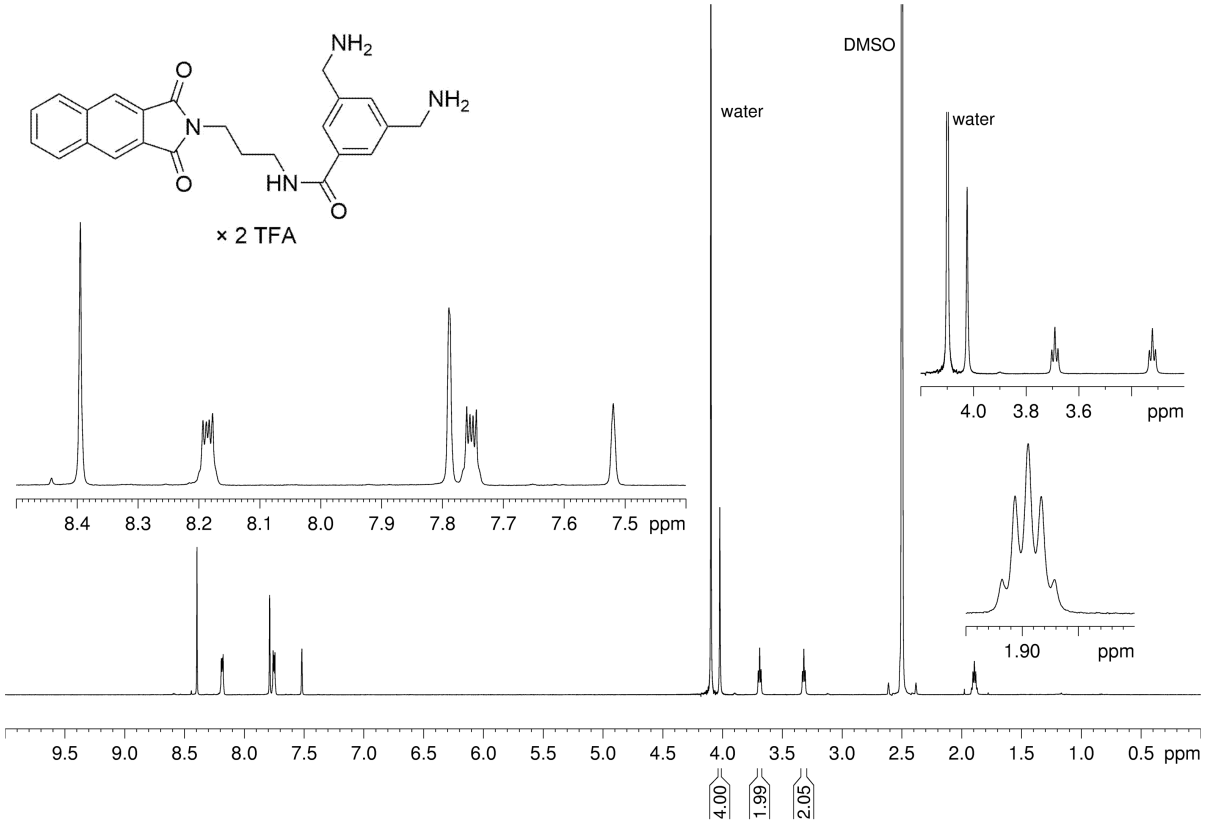
NH2
NH2
O
N
O
HN
O
× 2 TFA
water
DMSO
water
1.90
ppm

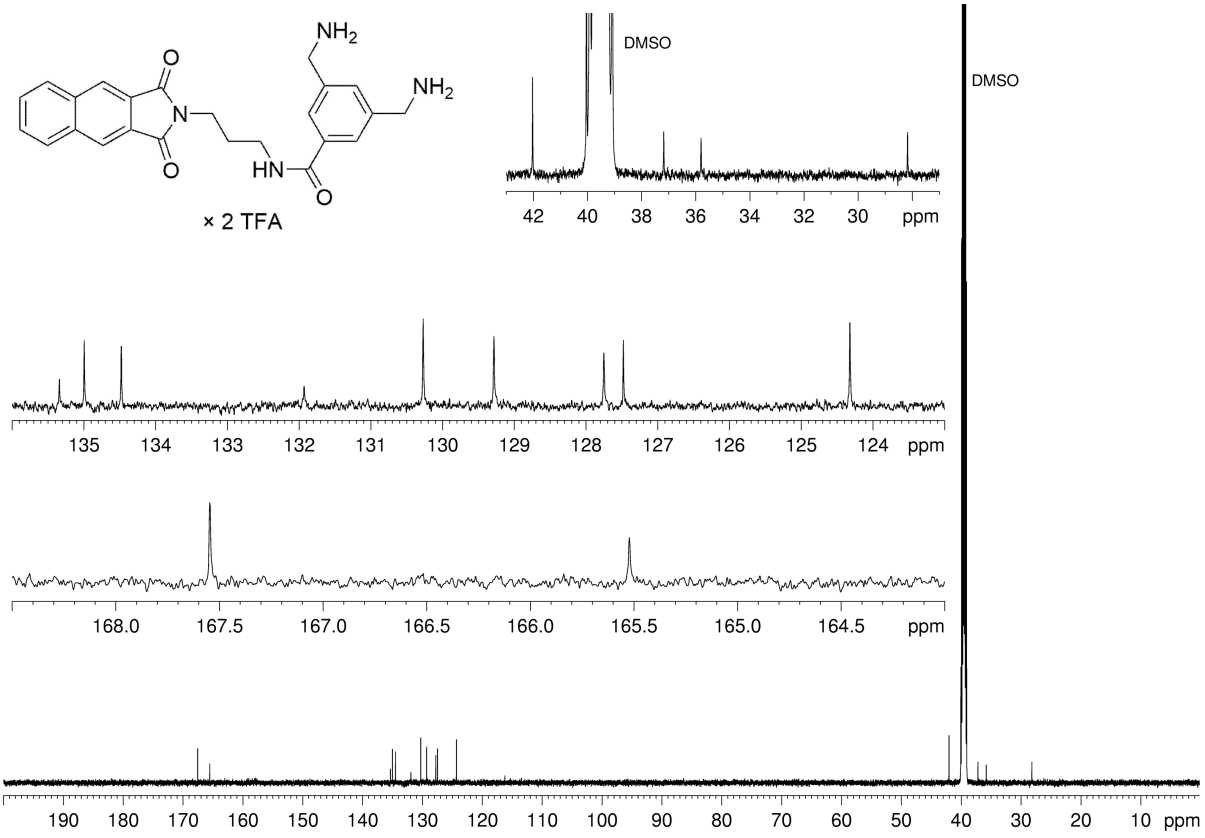

^{1}H-NMR (600 MHz, DMSO-d_6), ^{1}H-NMR (600 MHz, DMSO-d_6/D_2O 4:1 v/v) and ^{13}C-NMR (150 MHz, DMSO-d_6) spectrum of compound **4.30**

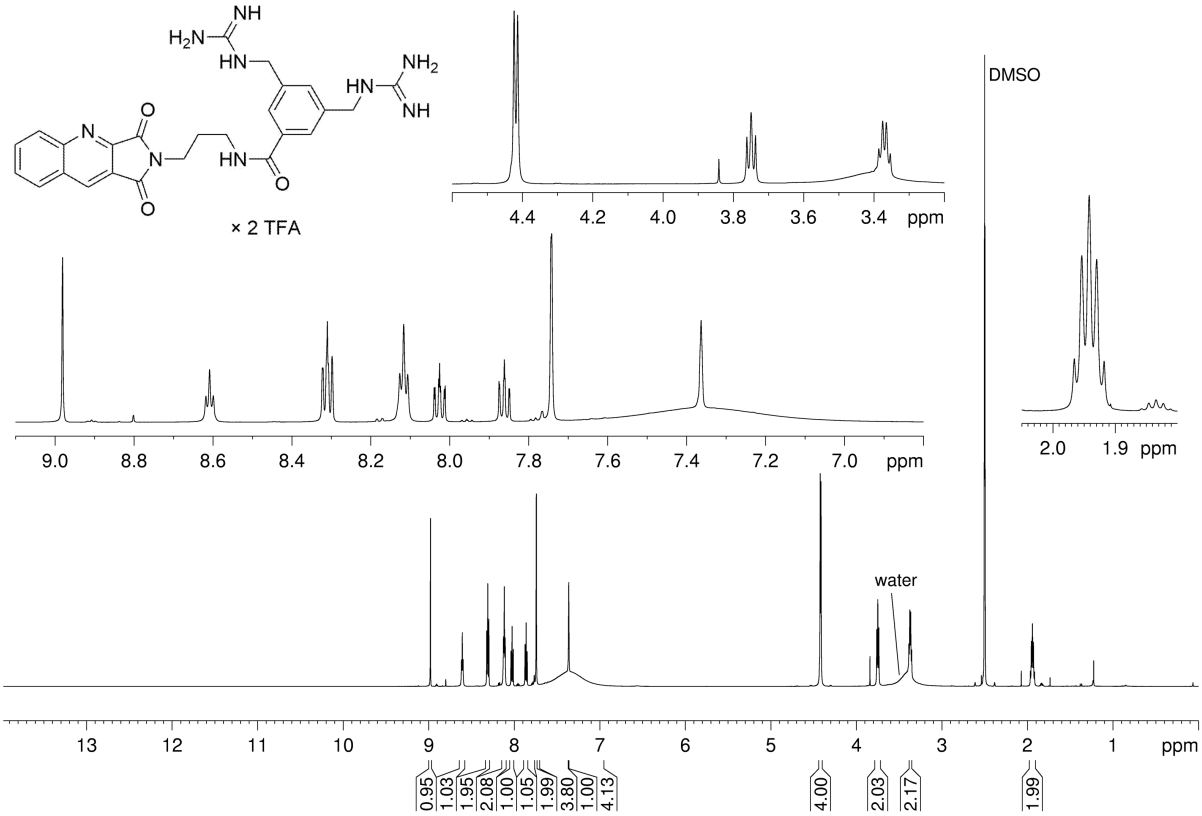
× 2 TFA
DMSO
water
ppm
0.95
1.03
1.95
2.08
1.00
1.05
1.99
3.80
1.00
4.13
4.00
2.03
2.17
1.99

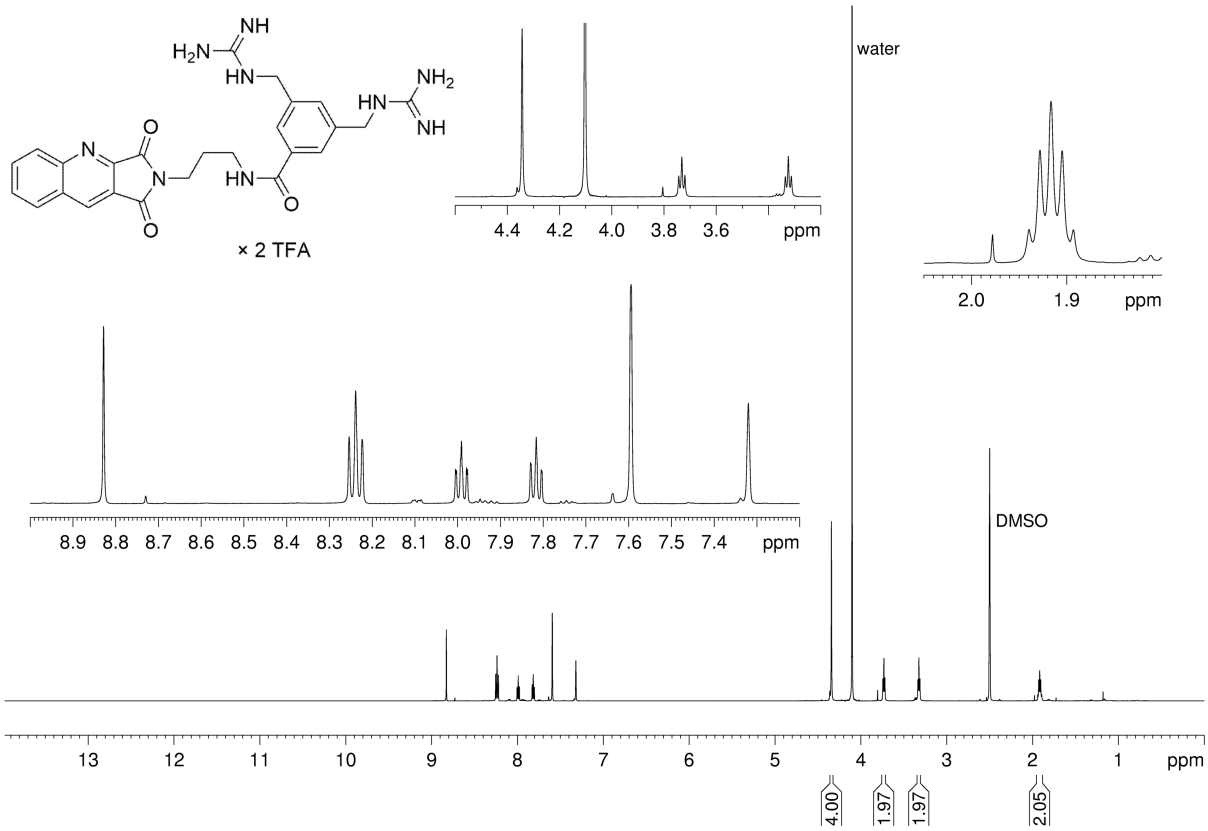
× 2 TFA
water
DMSO
ppm
4.00
1.97
1.97
2.05

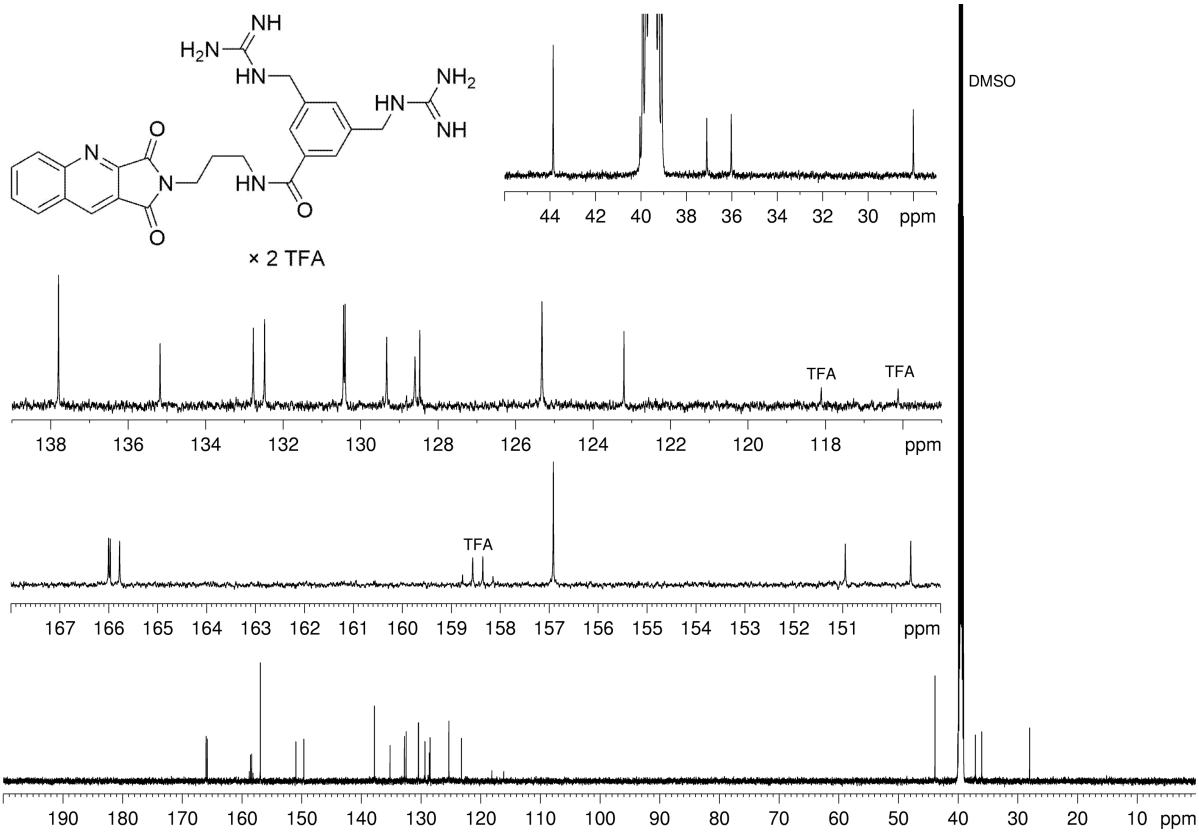

^{1}H-NMR (600 MHz, DMSO-d_6), ^{1}H-NMR (600 MHz, DMSO-d_6/D_2O 4:1 v/v) and ^{13}C-NMR (150 MHz, DMSO-d_6) spectrum of compound **4.32**

SMILES-strings of all compounds that were investigated by induced-fit docking to the hY_4R homology model:

Cyclopentene core:

N=C(N)NCCCC1=C(CCCNC(N)=N)CC(C(NC(CC2=CC=C(O)C=C2)C(N)=O)=O)C1

O=C(N)C(NC(C1CC(CCCNC(N)=N)=C1CCCNC(N)=N)=O)CC2=CC=C(O)C=C2

N=C(NCCCC1=C(CCCNC(N)=N)CC(C(NC(C(N)=O)CC2=CC=C(O)C=C2)=O)C1)N

N=C(NCCCC1=C(CCCNC(N)=N)CC(C(NC(C(N)=O)CCCN)=O)C1)N

N=C(NCCCC1=C(CCCNC(N)=N)CC(C(NC(C(N)=O)CCCCN)=O)C1)N

N=C(N)NCCCC1=C(CC(C1)C(NC(CCCCN)C(N)=O)=O)CCCNC(N)=N

N=C(N)NCCCC1=C(CCCCNC(N)=N)CC(C1)C(NC(CCCCN)C(N)=O)=O

N=C(N)NCCCCC1=C(CCCCNC(N)=N)CC(C1)C(NC(CCCCN)C(N)=O)=O

Homopiperazine core:

O=C(CC(NC(CC1=CC=C(O)C=C1)C(N)=O)=O)NC2CN(CCNC(N)=N)CCN(CCNC(N)=N)C2

O=C(CC(NC(CC1=CC=C(O)C=C1)C(N)=O)=O)NC2CN(CCCNC(N)=N)CCN(CCCNC(N)=N)C2

O=C(CC(NC(CC1=CC=C(O)C=C1)C(N)=O)=O)NC2CN(CCCCNC(N)=N)CCN(CCCCNC(N)=N)C2

O=C(CCC(NC(C(N)=O)CC1=CC=C(O)C=C1)=O)NC2CN(CCCCNC(N)=N)CCN(CCCCNC(N)=N)C2

O=C(CCC(NC(C(N)=O)CC1=CC=C(O)C=C1)=O)NC2CN(CCCNC(N)=N)CCN(CCCNC(N)=N)C2

O=C(CCCC(NC(C(N)=O)CC1=CC=C(O)C=C1)=O)NC2CN(CCCNC(N)=N)CCN(CCCNC(N)=N)C2

O=C(CCCC(NC(C(N)=O)CC1=CC=C(O)C=C1)=O)NC2CN(CCCCNC(N)=N)CCN(CCCCNC(N)=N)C2

NC(NCCCN1CCN(CCCNC(N)=N)CC(NC(CCCC(NC(CC2=CNC3=CC=CC=C23)C(N)=O)=O)=O)C1)=N

NC(NCCCN1CCN(CCCNC(N)=N)CC(NC(CCCCCNC(C2=CN=CC=C2)=O)=O)C1)=N

NC(NCCCN1CCN(CCCNC(N)=N)CC(NC(CCCCCNC(C2=CC=NC=C2)=O)=O)C1)=N

NC(NCCCN1CCN(CCCNC(N)=N)CC(NC(CCCCCNC(C2=CC=NC(C(F)(F)F)=C2)=O)=O)C1)=N

NC(NCCCN1CCN(CCCNC(N)=N)CC(NC(CCCCCNC(C2=CC=C(OC3=CC=CN=C3)N=C2)=O)=O)C1)=N

NC(NCCCN1CCN(CCCNC(N)=N)CC(NC(CCCN2C(C(C=C(C=CC=C3)C3=N4)=C4C2=O)=O)=O)C1)=N

NC(NCCCN1CCN(CCCNC(N)=N)CC(NC(CCC(NCC2=C(C=CC=C3)C3=NC=C2)=O)=O)C1)=N

NC(NCCCN1CCN(CCCNC(N)=N)CC(NC(CCCNC(C2=C(C=CC=C3)C3=CC=N2)=O)=O)C1)=N

NC(NCCCN1CCN(CCCNC(N)=N)CC(NC(CCCNC(C2=C(C=CC=N3)C3=CC=C2)=O)=O)C1)=N

NC(NCCCN1CCN(CCCNC(N)=N)CC(NC(CCCCCNC(C2=NC=CC=N2)=O)=O)C1)=N

NC(NCCCN1CCN(CCCNC(N)=N)CC(NC(CCCCCNC(C2=CN=CN=C2)=O)=O)C1)=N

NC(NCCCN1CCN(CCCCNC(N)=N)CC(C1)NC(CCCC(NC(C(N)=O)CC2=CNC3=CC=CC=C23)=O)=O)=N

NC(NCCCN1CCN(CCCCNC(N)=N)CC(C1)NC(CCCCC(NC(C(N)=O)CC2=CNC3=CC=CC=C23)=O)=O)=N

NC(NCCCN1CC(C)N(CCCCNC(N)=N)CC(C1)NC(CCCCC(NC(C(N)=O)CC2=CNC3=CC=CC=C23)=O)=O)=N

NC(NCCCN1CC(C)N(CCCNC(N)=N)CC(C1)NC(CCCCC(NC(C(N)=O)CC2=CNC3=CC=CC=C23)=O)=O)=N

NC(NCCCN1CC(C)N(CCCNC(N)=N)CC(C1)NC(CCC(NC(C(N)=O)CC2=CNC3=CC=CC=C23)=O)=O)=N

NC(NCCCN1C(C)C(C)N(CCCNC(N)=N)CC(C1)NC(CCC(NC(C(N)=O)CC2=CNC3=CC=CC=C23)=O)=O)=N

NC(NCCCN1C(C)C(C)N(CCCNC(N)=N)CC(C1)NC(CCC(NC(C(N)=O)CC2=NNC3=CC=CC=C23)=O)=O)=N

NC(NCCCN1CC(C)N(CCCNC(N)=N)CC(C1)NC(CCC(NC(C(N)=O)CC2=NNC3=CC=CC=C23)=O)=O)=N

NC(NCCCN1CCN(CCCNC(N)=N)CC(C1)NC(CCC(NC(C(N)=O)CC2=NNC3=CC=CC=C23)=O)=O)=N

NC(NCCCN1CC(C)N(CC(C1)NC(CCCNC(C2=C3C=CC=CC3=CC=N2)=O)=O)CCCNC(N)=N)=N

NC(NCCCN1C(C)C(C)N(CC(C1)NC(CCCNC(C2=C3C=CC=CC3=CC=N2)=O)=O)CCCNC(N)=N)=N

NC(NCCCN1C(C)C(C)N(CC(C1)NC(CCCNC(C2=C3C=CC=CC3=NC=N2)=O)=O)CCCNC(N)=N)=N

NC(NCCCN1C(C)CN(CC(C1)NC(CCCNC(C2=C3C=CC=CC3=NC=N2)=O)=O)CCCNC(N)=N)=N

Pyrrolidine core:

NC(NCCN1C[C@H](NC(C(N)CCCNC(N)=N)=O)[C@H](C(NC(C(N)=O)CC2=CC=C(O)C=C2)=O)C1)=N

NC(NCCCN1C[C@H](NC(C(N)CC2=CC=C(O)C=C2)=O)[C@H](C(NC(C(N)=O)CCCNC(N)=N)=O)C1)=N

NC(NCCCN1C[C@@H](C(NC(CC2=CC=C(O)C=C2)C(N)=O)=O)[C@@H](N)C1)=N

O=C(NC(C(N)=O)CC1=CC=C(O)C=C1)C2C(NC(C(N)CCCNC(N)=N)=O)CNC2

NC1CN(CCCNC(N)=N)CC1C(NCCNC(C2=CC=CN=C2)=O)=O

NC1CN(CCCNC(N)=N)CC1C(NCCNC(C2=CC=NC=C2)=O)=O

NC1CN(CCCNC(N)=N)CC1C(NCCNC(C2=CC=C(OC3=CC=CN=C3)N=C2)=O)=O

NC1CN(CCCNC(N)=N)CC1C(NCCN2C(C(C=C(C=CC=C3)C3=N4)=C4C2=O)=O)=O

NC1CN(CCCNC(N)=N)CC1C(NCC(NCC2=CC=NC3=C2C=CC=C3)=O)=O

NC1CN(CCCNC(N)=N)CC1C(NCCNC(C2=CC=CC3=C2C=CC=N3)=O)=O

NC1CN(CCCNC(N)=N)CC1C(NCCNC(C2=CN=CN=C2)=O)=O

O=C(CC(NC(CC1=CC=C(O)C=C1)C(N)=O)=O)N2C3=CC(N)=CC=C3C4=C2C=C(N)C=C4

O=C(CC(NC(CC1=CC=C(O)C=C1)C(N)=O)=O)N2C3=CC(C(N)=N)=CC=C3C4=C2C=C(C(N)=N)C=C4

NC(C1=CNC2=C(CNC(NC(CC3=CC=C(O)C=C3)C(N)=O)=O)C=C(C(N)=N)C=C21)=N

O=C(CC(NC(CC1=CC=C(O)C=C1)C(N)=O)=O)N2C3=CC(CC(N)=N)=CC=C3C4=C2C=C(CC(N)=N)C=C4

NC1CN(CCCNC(N)=N)CC1C(NCCCC(NCC2=CC=NC3=C2C=CC=C3)=O)=O

NC1CN(CCCNC(N)=N)CC1C(NCCCCNC(C2=CN=CN=C2)=O)=O

C[N](C)(C)C1=NC(OCCCN2C(C(C(C2=O)=C3)=CC4=C3C=CC=C4)=O)=CC([N](C)(C)C)=N1

C[N+](C)(C)C1=NC(OCCCCCN2C(C(C(C2=O)=N3)=CC4=C3C=CC=C4)=O)=CC([N+](C)(C)C)=N1

O=C1C2=C(N=C(C=CC=C3)C3=C2)C(N1CCCCCCNCCC4NCCNC4)=O

O=C([C@H]1[C@@H](N)CN(CCCNC(N)=N)C1)NCCN2C(C3=CC4=CC=CC=C4N=C3C2=O)=O (**4.9**)

Metabenzene core:

O=C(N)C(NC(C1=CC=C(CCCNC(N)=N)C(CCCNC(N)=N)=C1)=O)CC2=CC=C(O)C=C2

O=C(N)C(NC(C1=CC(CCCNC(N)=N)=CC(CCCNC(N)=N)=C1)=O)CC2=CC=C(O)C=C2

O=C(CC(NC(CC1=CC=C(O)C=C1)C(N)=O)=O)NCC2=CC(C(CCCNC(N)=N)=O)=CC(C(CCCNC(N)=N)=O)=C2

O=C(CC(NC(CC1=CC=C(O)C=C1)C(N)=O)=O)NCC2=CC(C(CCCCNC(N)=N)=O)=CC(C(CCCCNC(N)=N)=O)=C2

O=C(CCC(NC(CC1=CC=C(O)C=C1)C(N)=O)=O)NCC2=CC(C(NC(CCCNC(N)=N)C(N)=O)=O)=CC(C(NC(CCCNC(N)=N)C(N)=O)=O)=C2

O=C(CCCC(NC(CC(C)=C)C(N)=O)=O)NCC1=CC(C(NC(CCCNC(N)=N)C(N)=O)=O)=CC(C(NC(CCCNC(N)=N)C(N)=O)=O)=C1

O=C(NC(CCCNC(N)=N)C(N)=O)C1=CC(C(NCC(NC(C(N)=O)CC2=CC=C(O)C=C2)=O)=O)=CC(C(NC(C(N)=O)CCCNC(N)=N)=O)=C1

O=C(NCCNC(N)=N)C1=CC(C(NC(C(N)=O)CC2=CC=C(O)C=C2)=O)=CC(C(NCCCNC(N)=N)=O)=C1

O=C(NCCNC(N)=N)C1=CC(C(NC(C(N)=O)CC2=CC=C(O)C=C2)=O)=CC(C(NCCCCNC(N)=N)=O)=C1

O=C(NCCCNC(N)=N)C1=CC(C(NC(C(N)=O)CC2=CC=C(O)C=C2)=O)=CC(C(NCCCCNC(N)=N)=O)=C1

O=C(CC(NC(CC1=CC=C(O)C=C1)C(N)=O)=O)NCC2=CC(C(CCNC(N)=N)=O)=CC(C(CCCNC(N)=N)=O)=C2

O=C(CC(NC(CC1=CC=C(O)C=C1)C(N)=O)=O)NCC2=CC(C(CCNC(N)=N)=O)=CC(C(CCCCNC(N)=N)=O)=C2

O=C(CC(NC(CC1=CC=C(O)C=C1)C(N)=O)=O)NCC2=CC(C(CCCNC(N)=N)=O)=CC(C(CCCCNC(N)=N)=O)=C2

O=C(CC(NC(CC1=CC=C(O)C=C1)C(N)=O)=O)NCC2=CC(C(NCCNC(N)=N)=O)=CC(C(NCCCNC(N)=N)=O)=C2

O=C(CC(NC(CC1=CC=C(O)C=C1)C(N)=O)=O)NCC2=CC(C(NCCCCNC(N)=N)=O)=CC(C(NCCCCNC(N)=N)=O)=C2

O=C(CC(NC(CC1=CC=C(O)C=C1)C(N)=O)=O)NCC2=CC(C(NCCNC(N)=N)=O)=CC(C(NCCCCNC(N)=N)=O)=C2

O=C(CC(NC(CC1=CC=C(O)C=C1)C(N)=O)=O)NCC2=CC(C(NCCCNC(N)=N)=O)=CC(C(NCCCCNC(N)=N)=O)=C2

O=C(CC(NC(CC1=CC=C(O)C=C1)C(N)=O)=O)NCC2=CC(C(NCCCNC(N)=N)=O)=CC(C(NCCCNC(N)=N)=O)=C

O=C(NCC(NC(CC1=CC=C(O)C=C1)C(N)=O)=O)C2=CC(C(NC(C(N)=O)CCNC(N)=N)=O)=CC(C(N)=O)=C22

O=C(NCCNC(N)=N)C1=CC(C(NCCCNC(N)=N)=O)=CC(C(NCC(NC(CC2=CC=C(O)C=C2)C(N)=O)=O)=O)=C1

O=C(NCCNC(N)=N)C1=CC(C(NCCNC(N)=N)=O)=CC(C(NCC(NC(CC2=CC=C(O)C=C2)C(N)=O)=O)=O)=C1

O=C(NCCNC(N)=N)C1=CC(C(NCCCNC(N)=N)=O)=CC(C(NCC(NC(CC2=CNC3=C2C=CC=C3)C(N)=O)=O)=O)=C1

O=C(NCCNC(N)=N)C1=CC(C(NCCNC(N)=N)=O)=CC(C(NCC(NC(CC2=CNC3=C2C=CC=C3)C(N)=O)=O)=O)=C1

O=C(NCCCNC(N)=N)C1=CC(C(NCCNC(C2=CC=CN=C2)=O)=O)=CC(C(N)=O)=C1

O=C(NCCCNC(N)=N)C1=CC(C(NCCNC(C2=CC=NC=C2)=O)=O)=CC(C(N)=O)=C1

O=C(NCCCNC(N)=N)C1=CC(C(NCCNC(C2=CN=C(OC3=CC=CN=C3)C=C2)=O)=O)=CC(C(N)=O)=C1

O=C(NCCCNC(N)=N)C1=CC(C(NCCN2C(C(C=C(C=CC=C3)C3=N4)=C4C2=O)=O)=O)=CC(C(N)=O)=C1

O=C(NCCCNC(N)=N)C1=CC(C(NCC(NCC2=CC=NC3=C2C=CC=C3)=O)=O)=CC(C(N)=O)=C1

O=C(NCCCNC(N)=N)C1=CC(C(NCCNC(C2=CC=CC3=C2C=CC=N3)=O)=O)=CC(C(N)=O)=C1

O=C(NCCCNC(N)=N)C1=CC(C(NCCNC(C2=CN=CN=C2)=O)=O)=CC(C(N)=O)=C1

NC1=NC(OCC(NC(CC2=CC=C(O)C=C2)C(N)=O)=O)=CC(N)=N1

O=C(NCCCNC(N)=N)C1=CC(C(NCCNC(C2=CN=C(OC3=CC=CN=C3)C=C2)=O)=O)=CC(CNC)=C1

O=C(NCCCNC(N)=N)C1=CC(C(NCCN2C(C(C=C(C=CC=C3)C3=N4)=C4C2=O)=O)=O)=CC(CNC)=C1

O=C(NCCCNC(N)=N)C1=CC(C(NCCCC(NCC2=CC=NC3=C2C=CC=C3)=O)=O)=CC(CNC)=C1

O=C(NCCCNC(N)=N)C1=CC(C(NCCCCNC(C2=CN=CN=C2)=O)=O)=CC(CNC)=C1

O=C(CCC1=CC=C(C(CN2C(C(N=C(C=CC=C3)C3=C4)=C4C2=O)=O)=O)C=C1)N5C6=CC(C(N)=N)=CC=C6C7=C5C=C(C(N)=N)C=C7

O=C(CCC1=CC=C(C(CN2C(C(N=C(C=CC=C3)C3=C4)=C4C2=O)=O)=O)C=C1)N5C6=CC(C(N)=N)=CC=C6C7=C5C=C(C(N)=N)C=C7

O=C(OC1=CC([N+](C)(C)C)=NC([N+](C)(C)C)=N1)C2=CN=C(OC3=CC=CN=C3)C=C2

O=C(C1=CC=C(N2C(C(N=C(C=CC=C3)C3=C4)=C4C2=O)=O)C=C1)CNCCC5NCCCN5

O=C(C1=CC(O)=C(N2C(C(N=C(C=CC=C3)C3=C4)=C4C2=O)=O)C=C1)CNCCC5NCCCN5

O=C(C1=CC(O)=C(N2C(C(N=C(C=CC=C3)C3=C4)=C4C2=O)=O)C=C1)CNCCC5=NCCCN5

O=C(C1=C(O)C=C(N2C(C(N=C(C=CC=C3)C3=C4)=C4C2=O)=O)C=C1)CNCCC5=NCCCN5

O=C1C(C(C(N1CCNC(C2=CC(NC(N)=N)=CC(NC(N)=N)=C2)=O)=O)=N3)=CC4=C3C=CC=C4

O=C1C(C(C(N1CCCNC(C2=CC(NC(N)=N)=CC(NC(N)=N)=C2)=O)=O)=N3)=CC4=C3C=CC=C4

O=C1C(C(C(N1CCNC(C2=CC=C(NC(N)=N)C=C2)=O)=O)=N3)=CC4=C3C=CC=C4

O=C1C(C(C(N1CCCNC(C2=CC=C(NC(N)=N)C=C2)=O)=O)=N3)=CC4=C3C=CC=C4

O=C1C(C(C(N1CCNC(C2=CC=CC(NC(N)=N)=C2)=O)=O)=N3)=CC4=C3C=CC=C4

O=C1C(C(C(N1CCCNC(C2=CC=CC(NC(N)=N)=C2)=O)=O)=N3)=CC4=C3C=CC=C4

O=C1C(C(C(N1CCNC(C2=CC(CN)=CC(CN)=C2)=O)=O)=N3)=CC4=C3C=CC=C4

O=C1C(C(C(N1CCCNC(C2=CC(CN)=CC(CN)=C2)=O)=O)=N3)=CC4=C3C=CC=C4

O=C1C(C(C(N1CCNC(C2=CC(CNC(N)=N)=CC(CNC(N)=N)=C2)=O)=O)=N3)=CC4=C3C=CC=C4

O=C1C(C(C(N1CCCNC(C2=CC(CNC(N)=N)=CC(CNC(N)=N)=C2)=O)=O)=N3)=CC4=C3C=CC=C4

O=C(C1=CC(O)=C(N2C(C(N=C(C=CC=C3)C3=C4)=C4C2=O)=O)C=C1)CNCCC5NCCNC5

O=C(C1=CC(O)=C(N2C(C(N=C(C=CC=C3)C3=C4)=C4C2=O)=O)C=C1)CNCCC5NCCNC5

O=C1C2=C(N=C(C=CC=C3)C3=C2)C(N1CCCCCCNCCN4CCN(C)CC4)=O

O=C(C1=CC(C(NCCNC(C2=CN=C(N=C2)OC3=CC=CN=C3)=O)=O)=CC(CNC)=C1)NCCCNC(N)=N

O=C1N(C2=C(O)C=C(C(CNCCC3=NCCCN3)=O)C=C2)C(C4=CC5=CC=CC=C5N=C41)=O (**4.10**)

O=C(C1=C(N)C(C(NCCNC(C2=CN=C(N=C2)OC3=CC=CN=C3)=O)=O)=CC(CNC)=C1)NCCCNC(N)=N

O=C(C1=C(N)C(C(NCCNC(C2=CN=C(N=C2)OC3=CC=CN=C3)=O)=O)=CC(C)=C1)NCCCNC(N)=N

O=C(C1=C(N)C(C(NCCNC(C2=CN=C(N=C2)OC3=CC=CN=C3)=O)=O)=CC=C1)NCCCNC(N)=N

O=C(C1=C(N(C)C)C(C(NCCNC(C2=CN=C(N=C2)OC3=CC=CN=C3)=O)=O)=CC=C1)NCCCNC(N)=N

O=C(C1=C(N(C)C)C(C(NCCNC(C2=CN=C(N=C2)OC3=C(C)C(C)=CN=C3)=O)=O)=CC=C1)NCCCNC(N)=N

O=C1N(CCNC(C2=CC=C(NC(N)=N)C=C2)=O)C(C3=CC4=CC=CC=C4N=C31)=O (**4.11**)

O=C(NCC1=CC(C(CCCCNC(N)=N)=O)=CC(C(CCCCNC(N)=N)=O)=C1)C(C)C(NC(C(N)=O)CC2=CC=CC=C2)=O

O=C1N(CCCNC(C2=CC(CN)=CC(CN)=C2)=O)C(C3=CC4=CC=CC=C4N=C31)=O (**4.12**)

O=C(NCC1=CC(C(CCCCNC(N)=N)=O)=CC(C(CCCCNC(N)=N)=O)=N1)C(C)C(NC(C(N)=O)CC2=CC=NC=C2)=O

7.4 Appendix Chapter 5

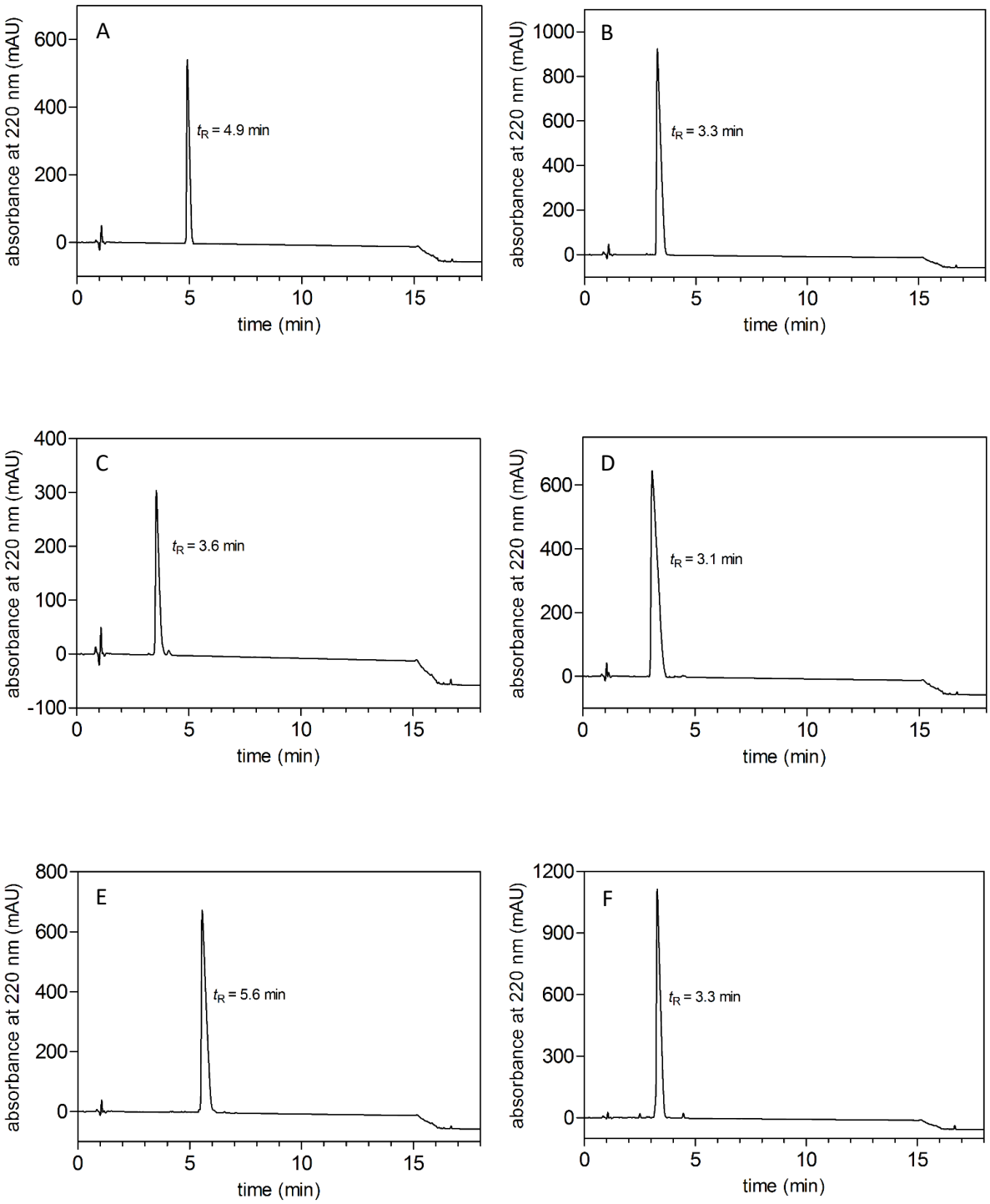

RP-HPLC analysis of compound **5.14** (A), **5.15** (B), **5.16** (C), **5.17** (D), **5.18** (E) and **5.19** (F).

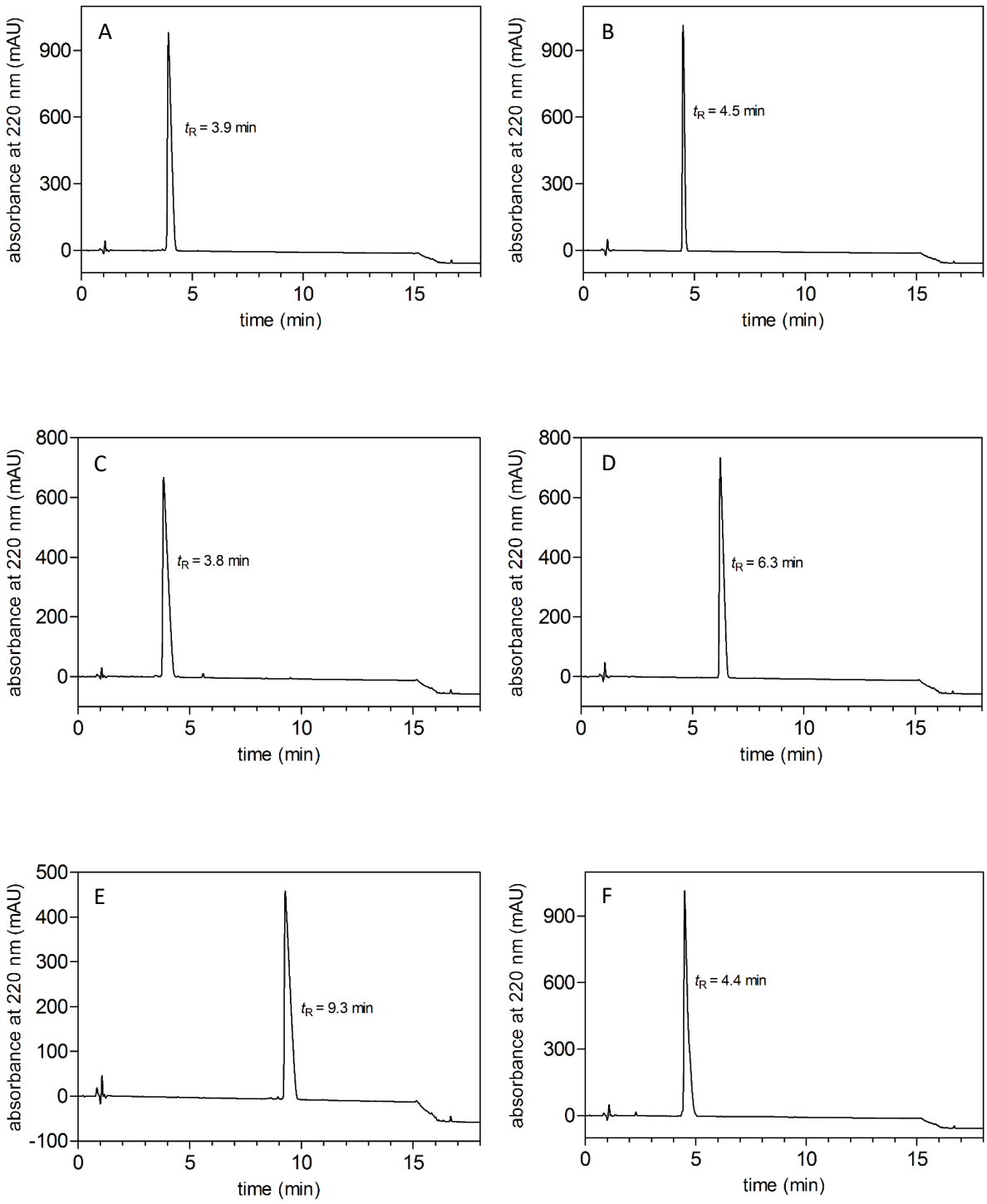

RP-HPLC analysis of compound **5.20** (A), **5.21** (B), **5.22** (C), **5.23** (D), **5.24** (E) and **5.25** (F).

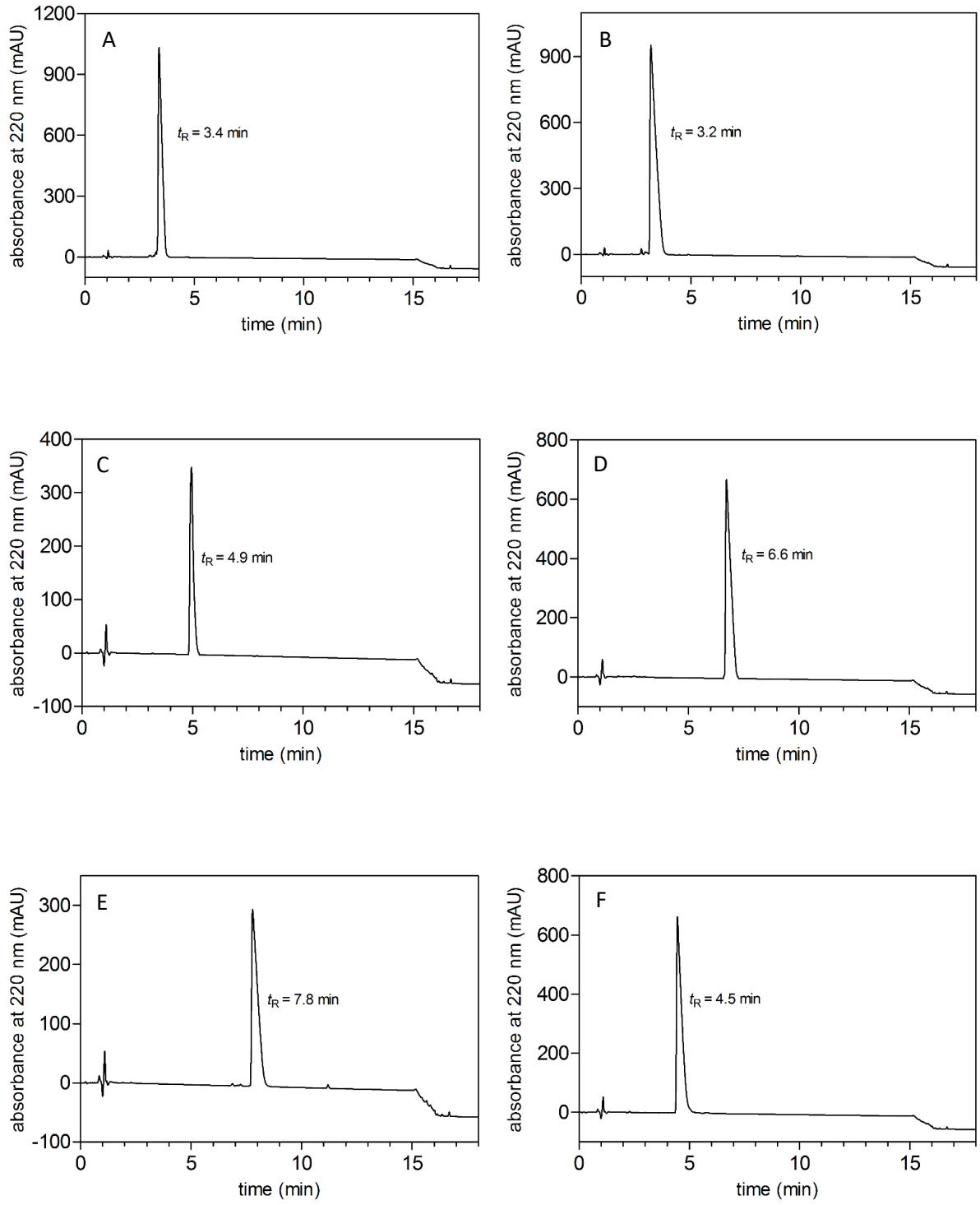

RP-HPLC analysis of compound **5.26** (A), **5.27** (B), **5.28** (C), **5.29** (D), **5.30** (E) and **5.31** (F).

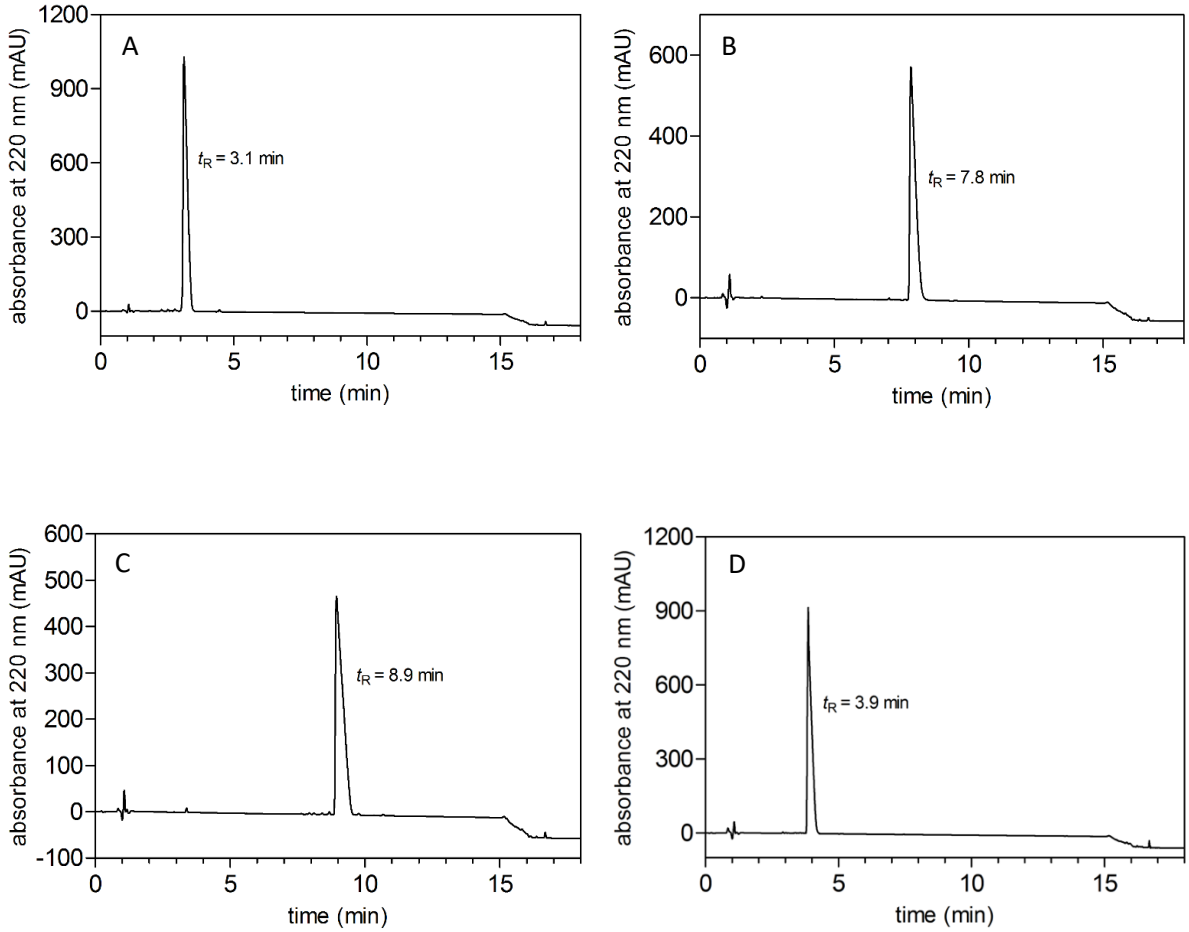

RP-HPLC analysis of compound **5.32** (A), **5.33** (B), **5.34** (C) and **5.35** (D).

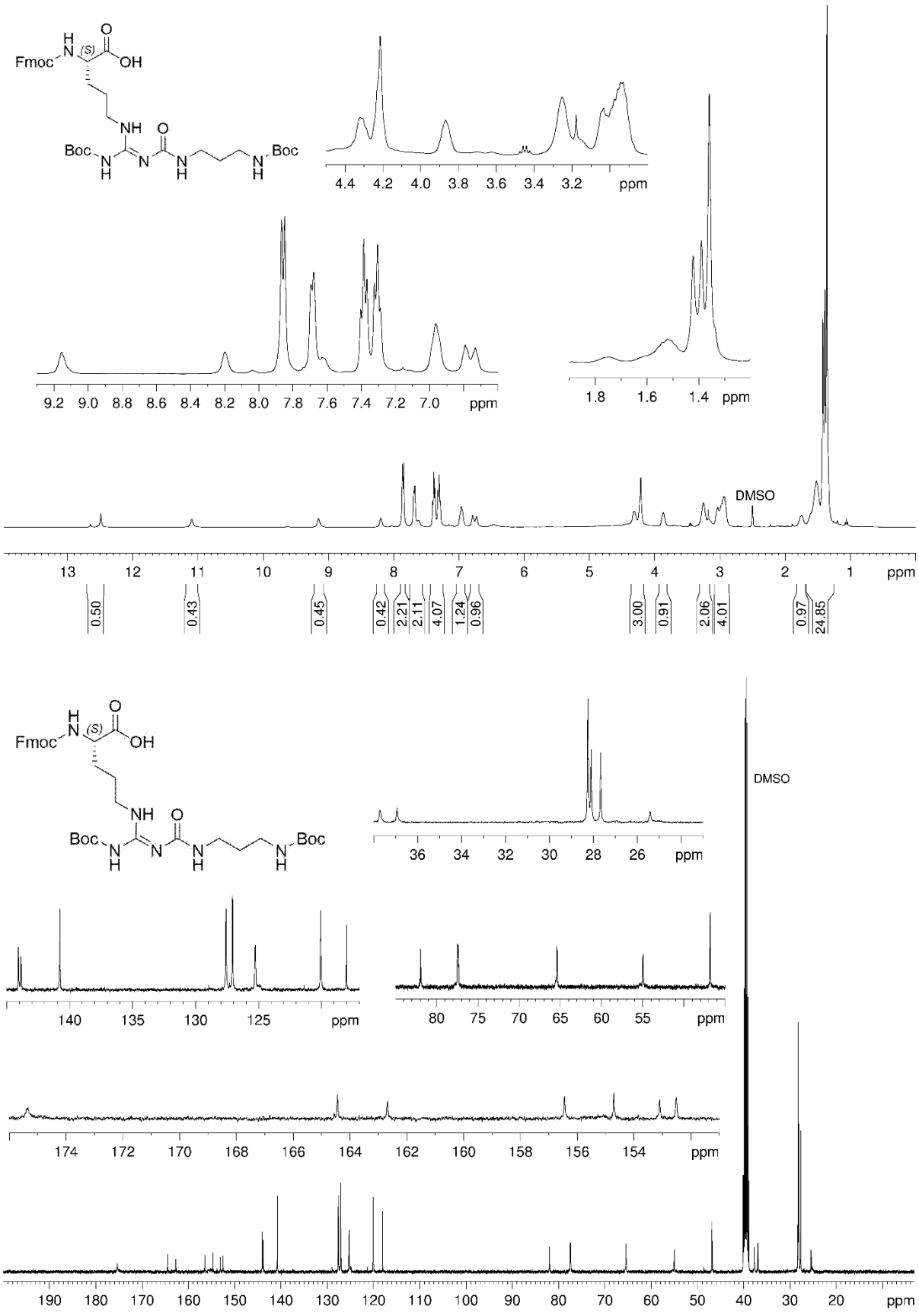

^{1}H-NMR (400 MHz, DMSO-d_6) and ^{13}C-NMR (100 MHz, DMSO-d_6) spectrum of compound **5.9**

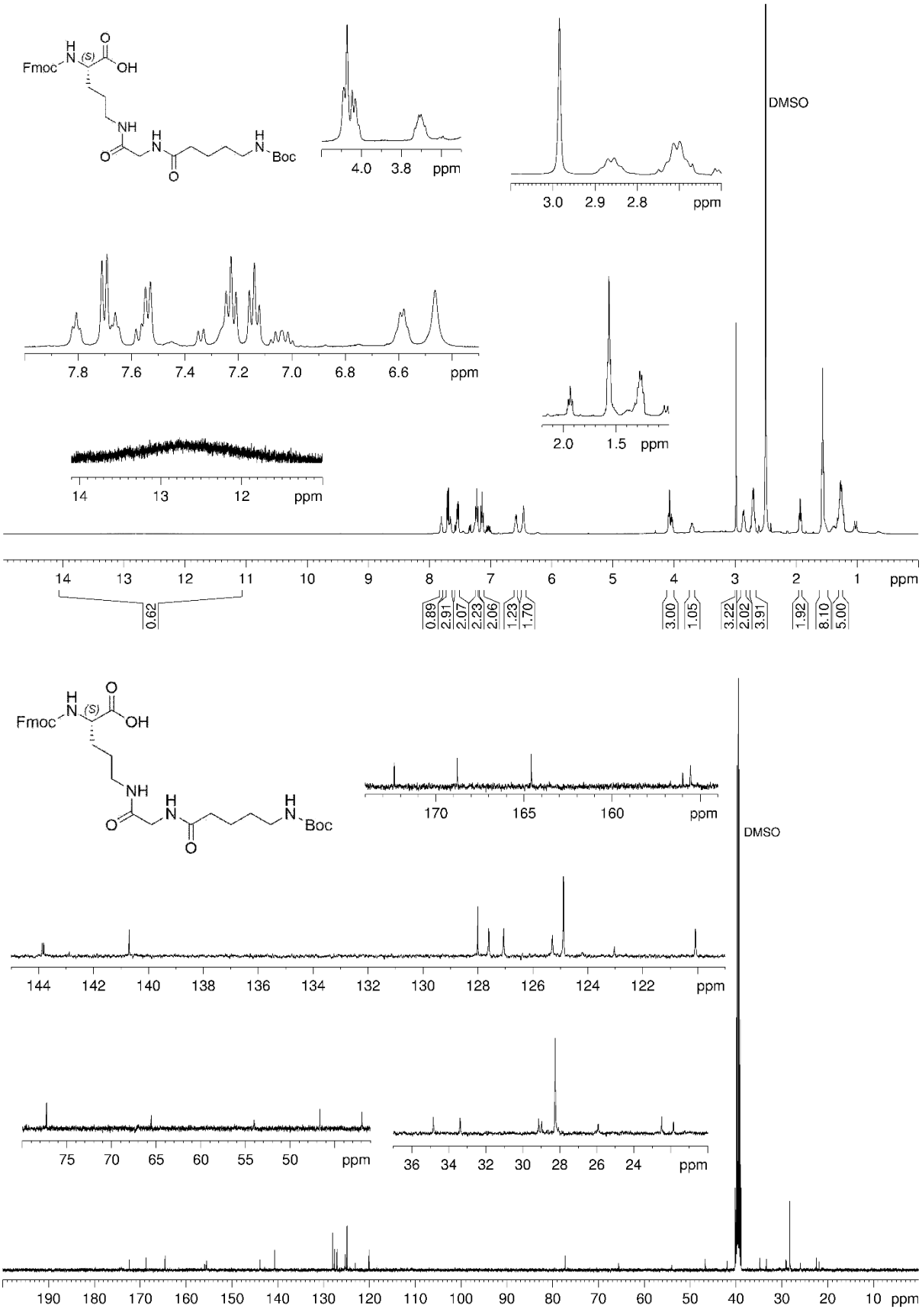

^{1}H-NMR (400 MHz, DMSO-d_6) and ^{13}C-NMR (100 MHz, DMSO-d_6) spectrum of compound **5.13**

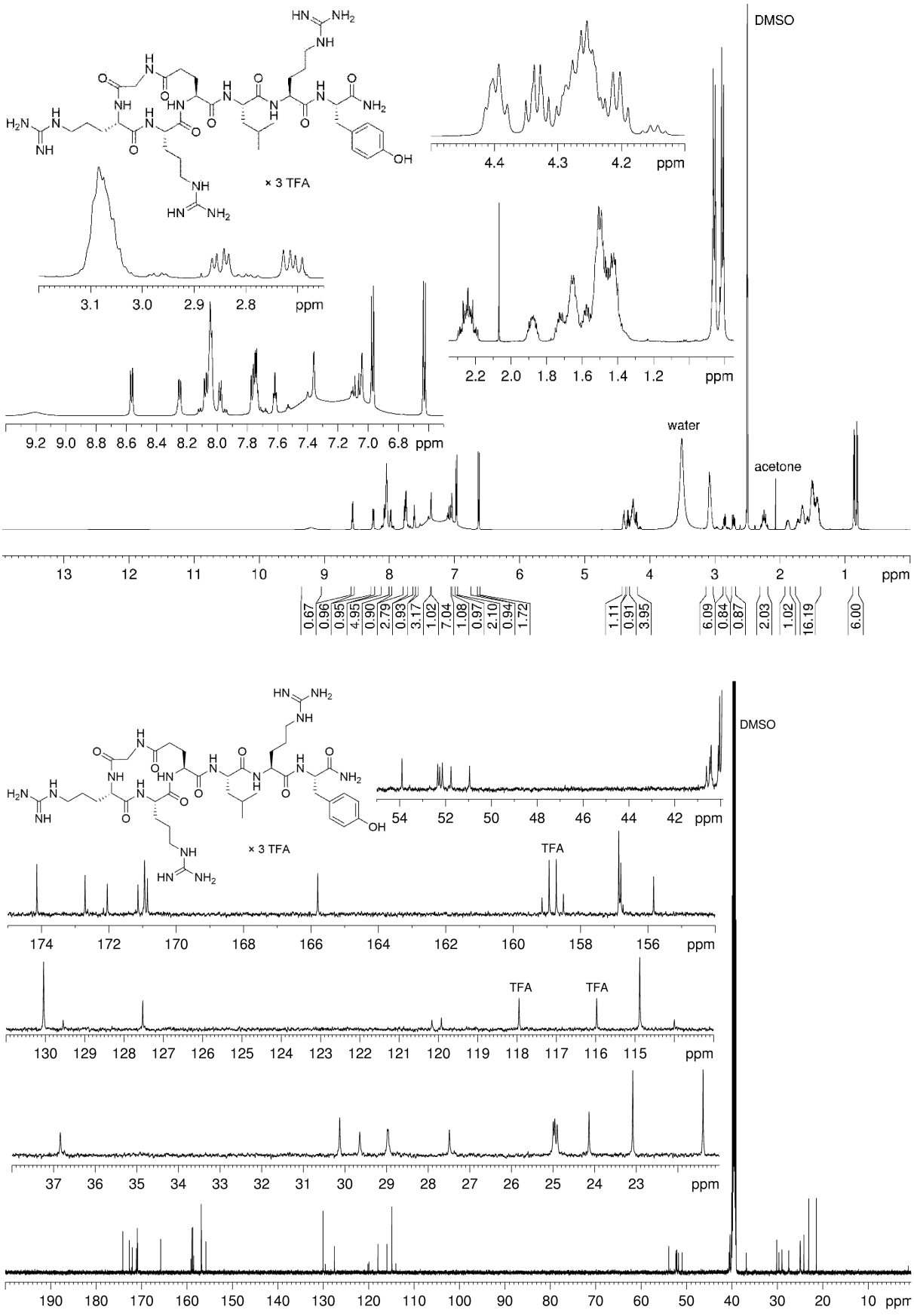

^{1}H-NMR (600 MHz, DMSO-d_6) and ^{13}C-NMR (150 MHz, DMSO-d_6) spectrum of compound **5.14**

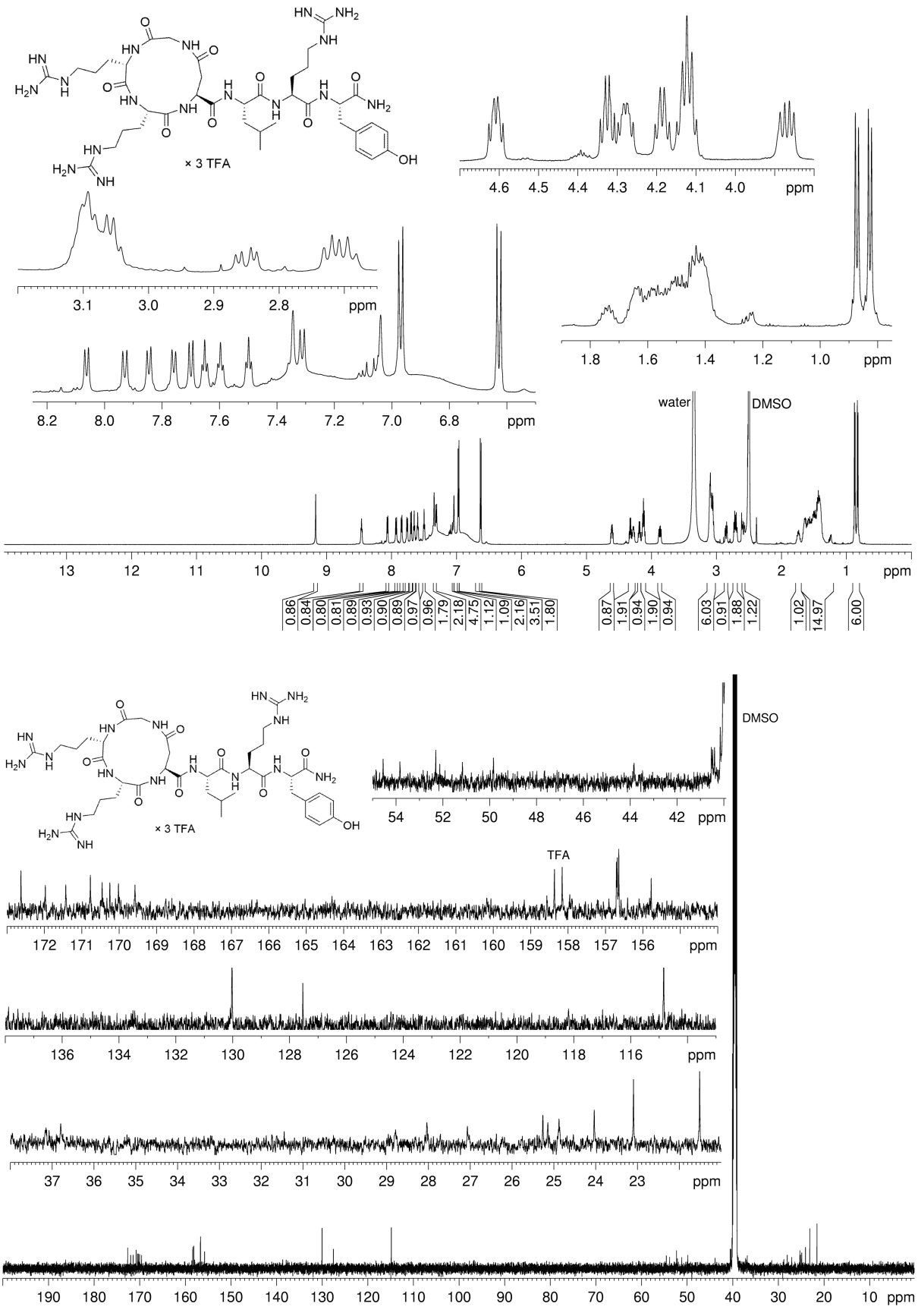

^{1}H-NMR (600 MHz, DMSO-d_6) and ^{13}C-NMR (150 MHz, DMSO-d_6) spectrum of compound **5.15**

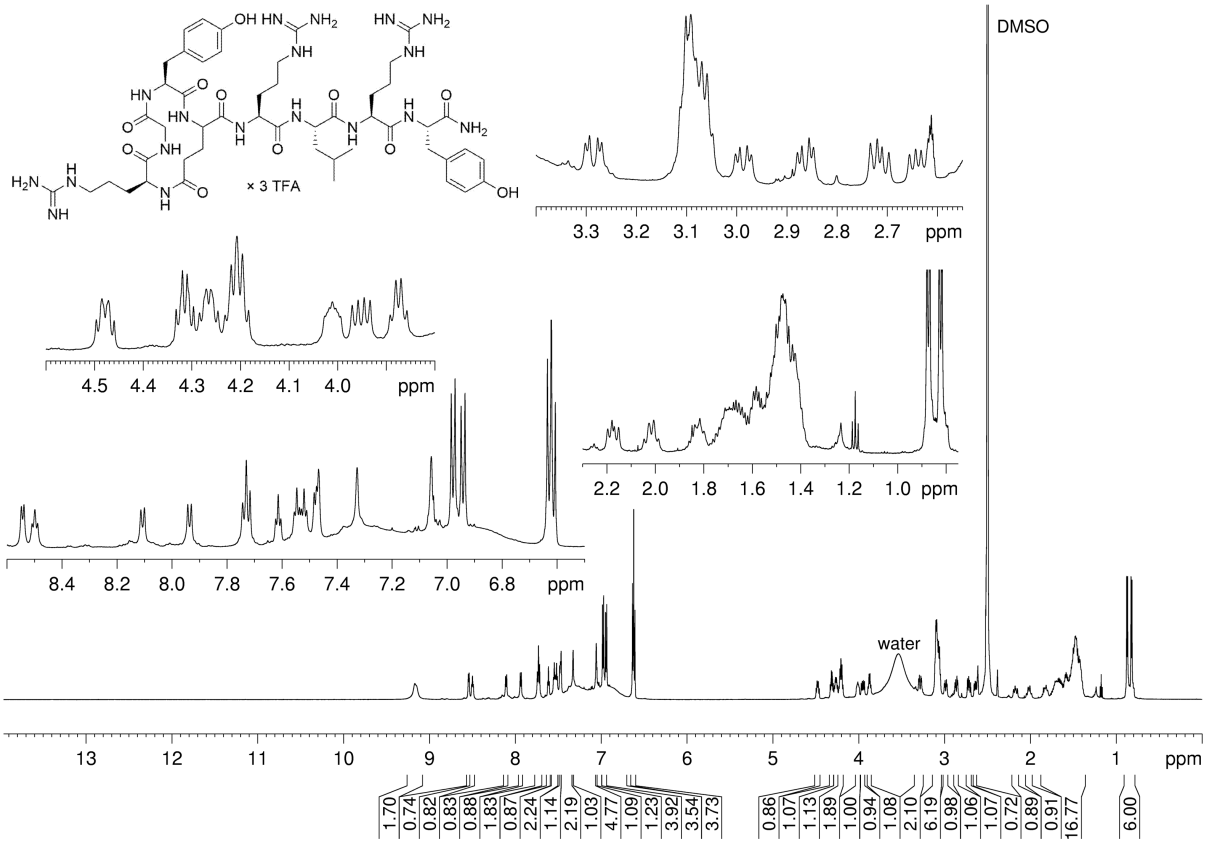

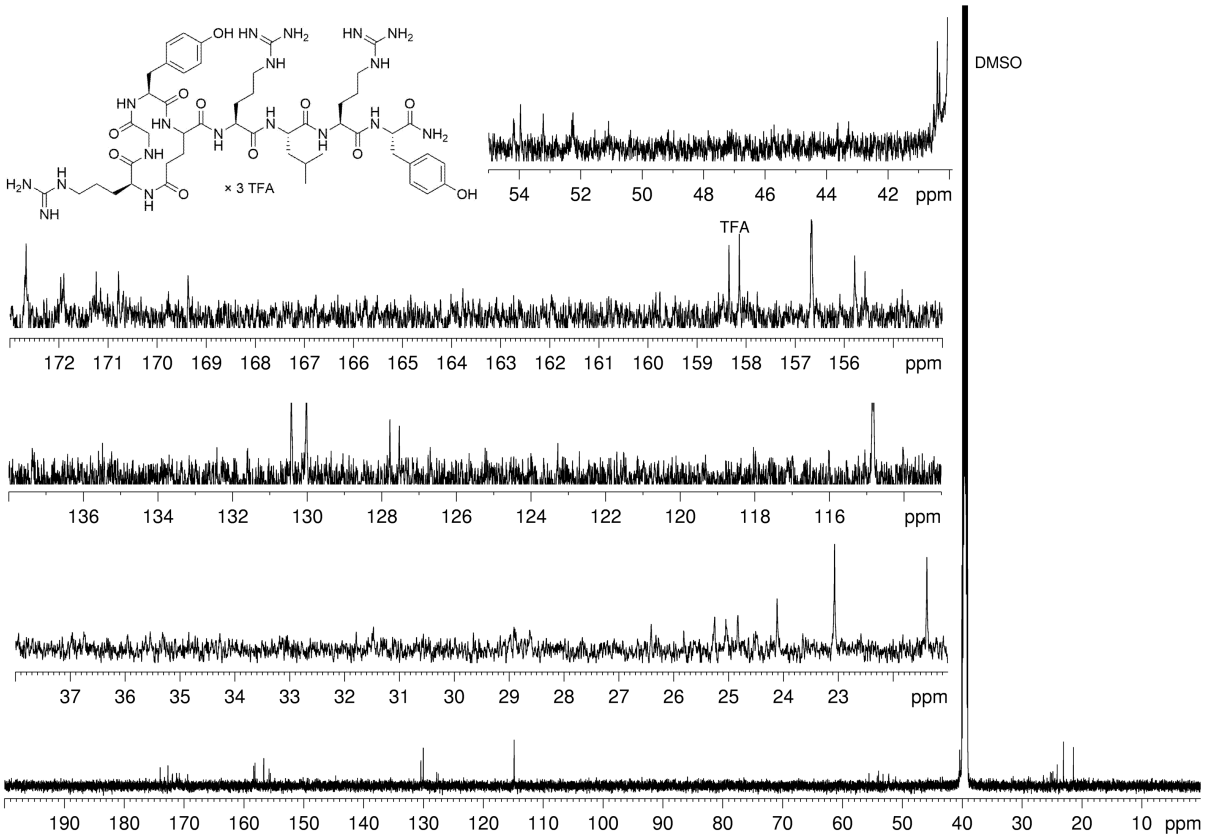

^{1}H-NMR (600 MHz, DMSO-d_6) and ^{13}C-NMR (150 MHz, DMSO-d_6) spectrum of compound **5.16**

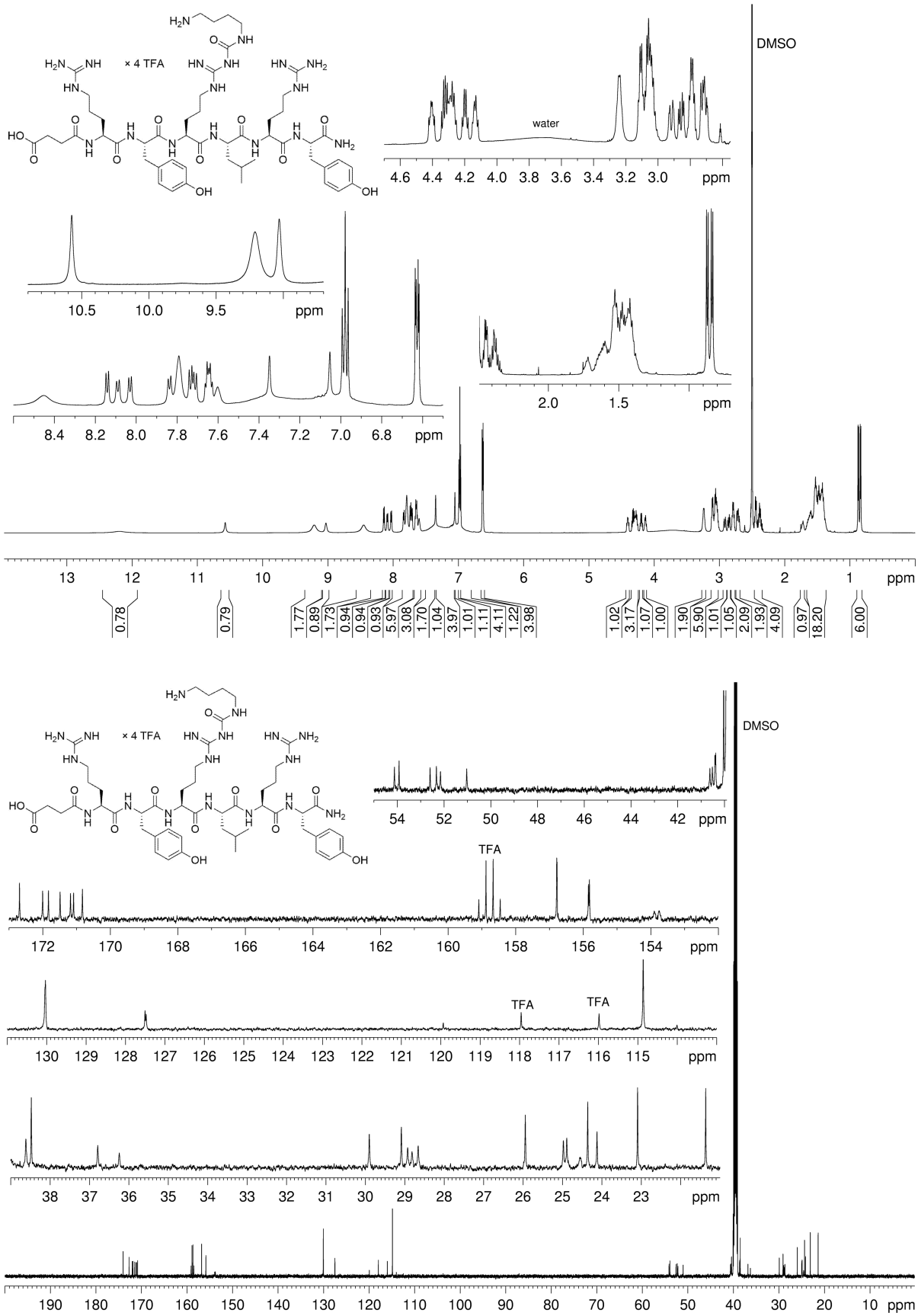

^{1}H-NMR (600 MHz, DMSO-d_6) and ^{13}C-NMR (150 MHz, DMSO-d_6) spectrum of compound **5.17**

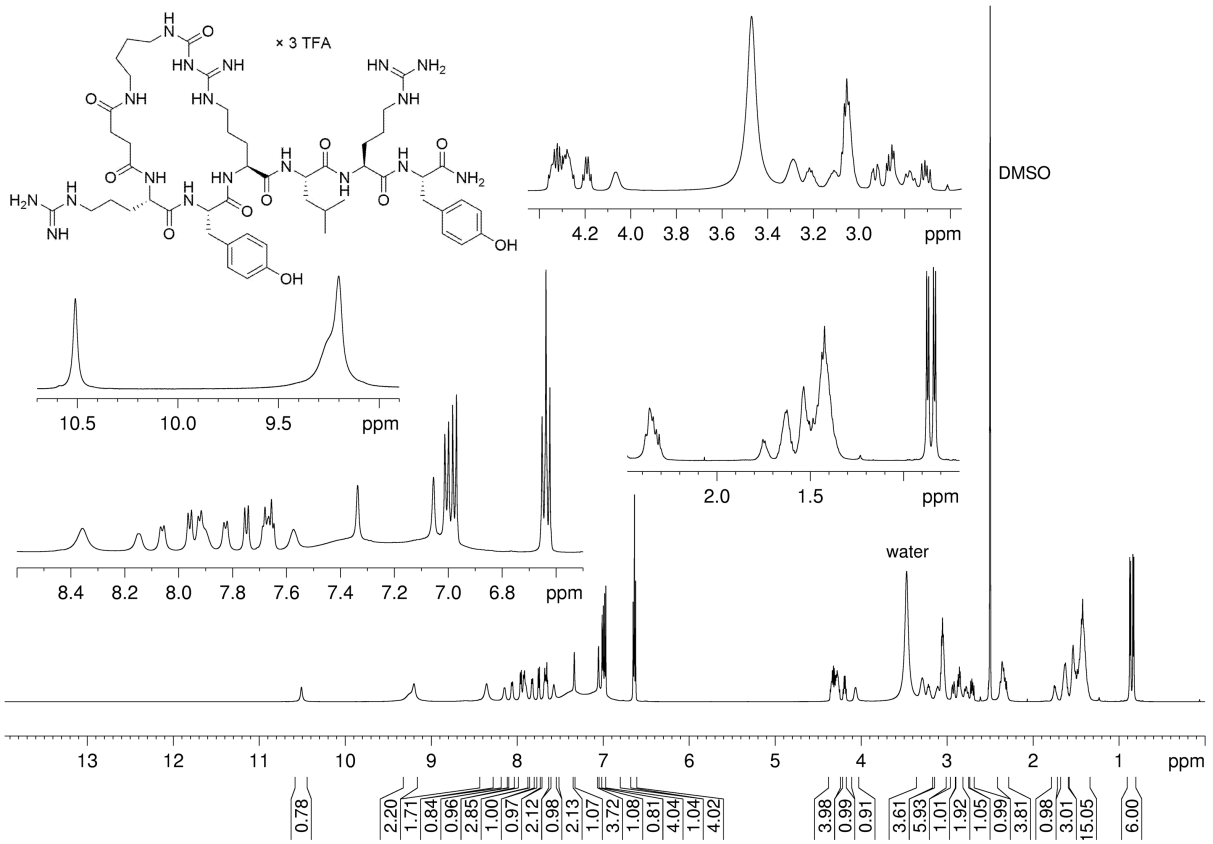
× 3 TFA
DMSO
water
ppm
0.78
2.20
1.71
0.84
0.96
2.85
1.00
0.97
2.12
0.98
2.13
1.07
3.72
1.08
0.81
4.04
1.04
4.02
3.98
0.99
0.91
3.61
5.93
1.01
1.92
1.05
0.99
3.81
0.98
3.01
15.05
6.00

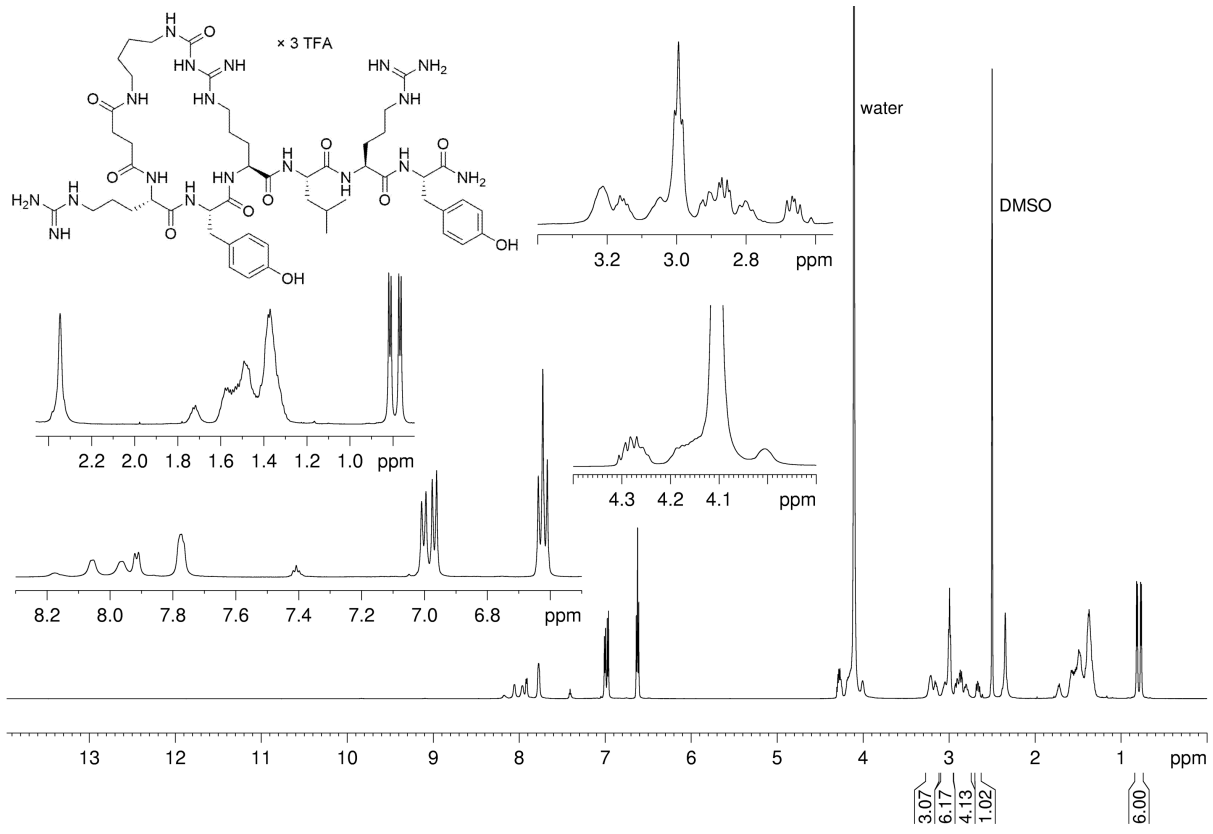
× 3 TFA
water
DMSO
ppm
3.07
6.17
4.13
1.02
6.00

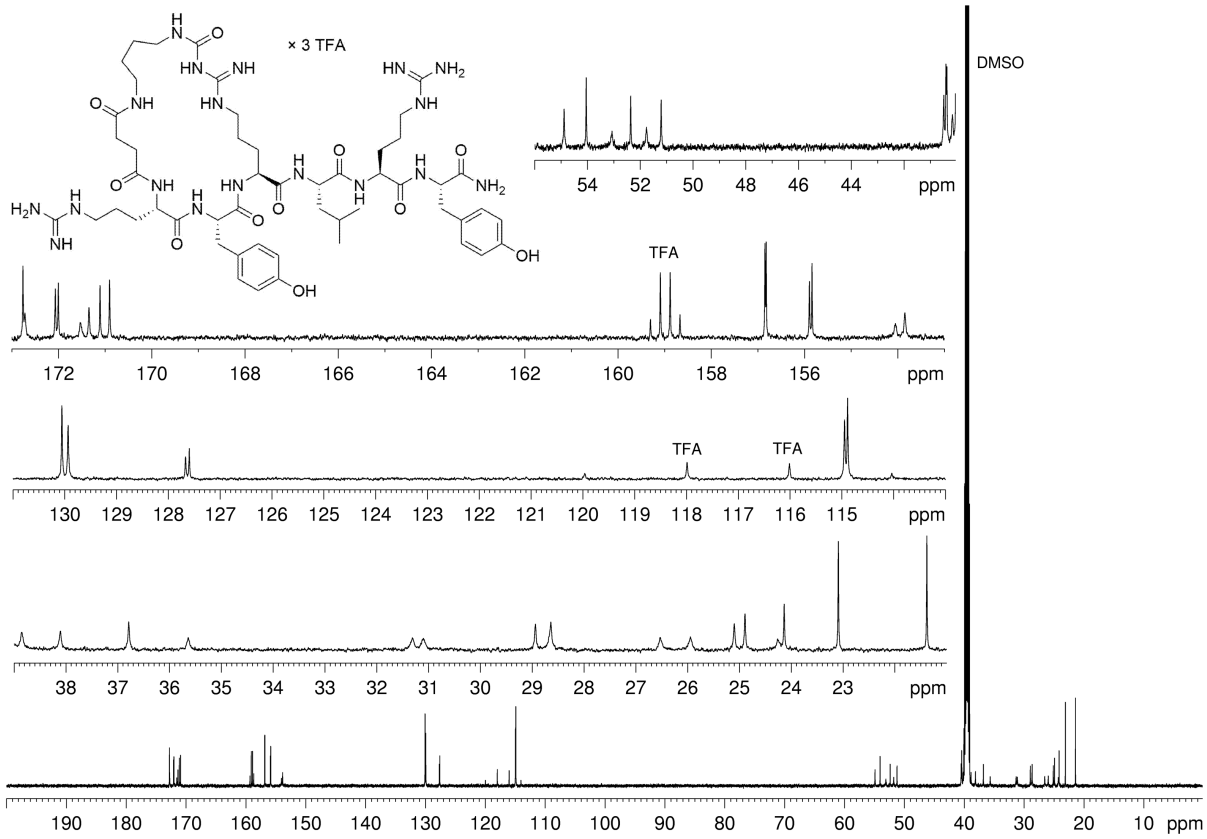

^{1}H-NMR (600 MHz, DMSO-*d*$_6$), ^{1}H-NMR (600 MHz, DMSO-*d*$_6$/D_2O 4:1 v/v) and ^{13}C-NMR (150 MHz, DMSO-*d*$_6$) spectrum of compound **5.18**

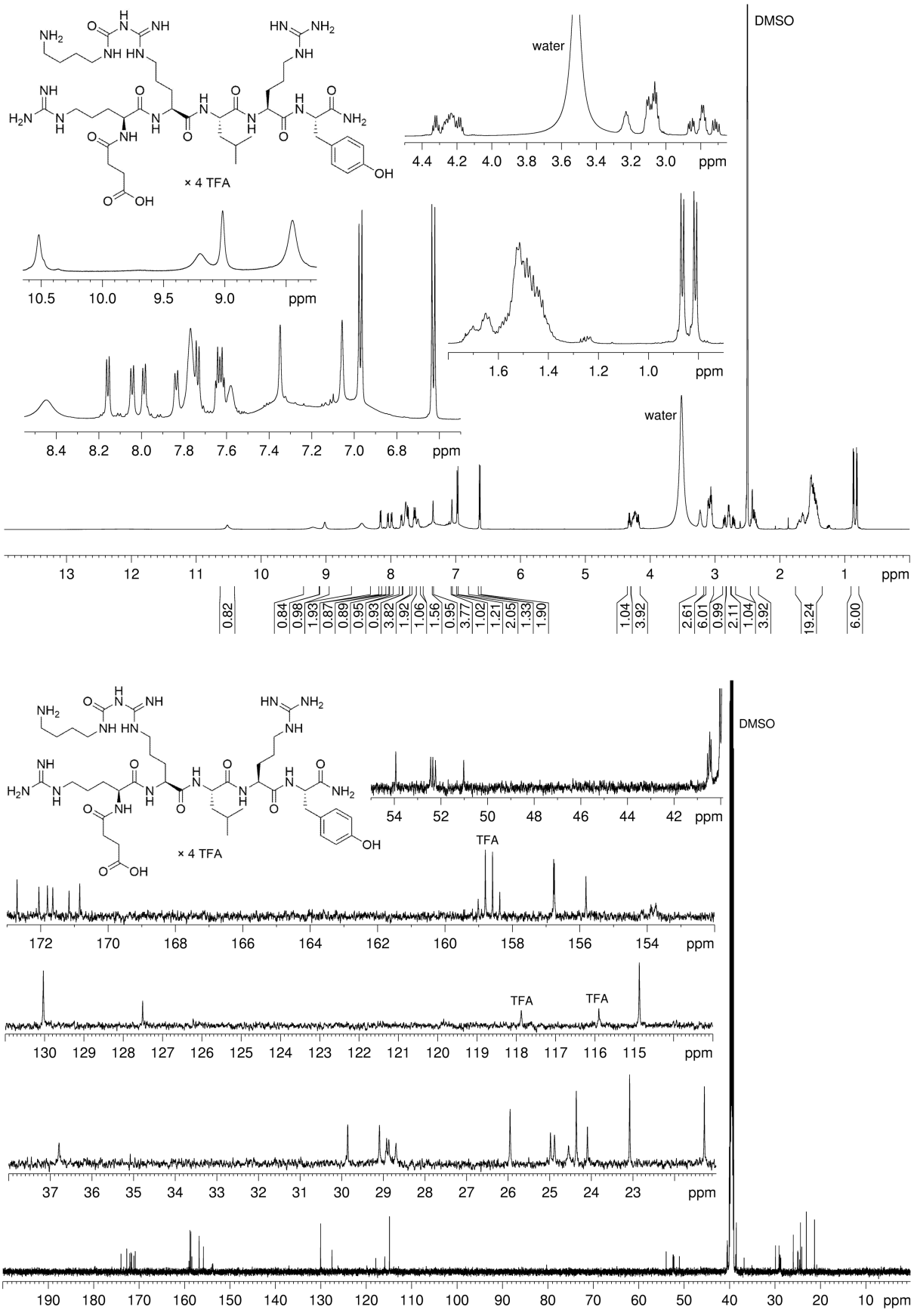

^{1}H-NMR (600 MHz, DMSO-d_6) and ^{13}C-NMR (150 MHz, DMSO-d_6) spectrum of compound **5.19**

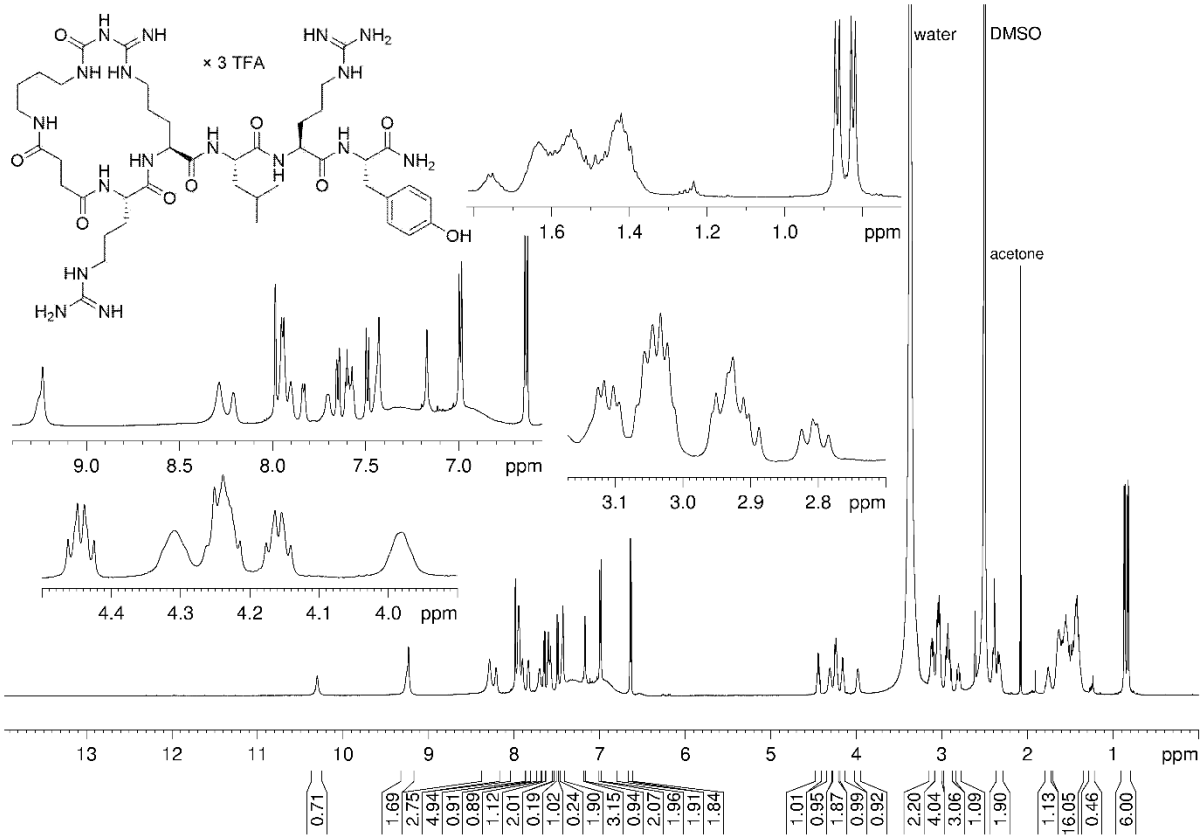

^{1}H-NMR (600 MHz, DMSO-d_6) spectrum of compound **5.20**

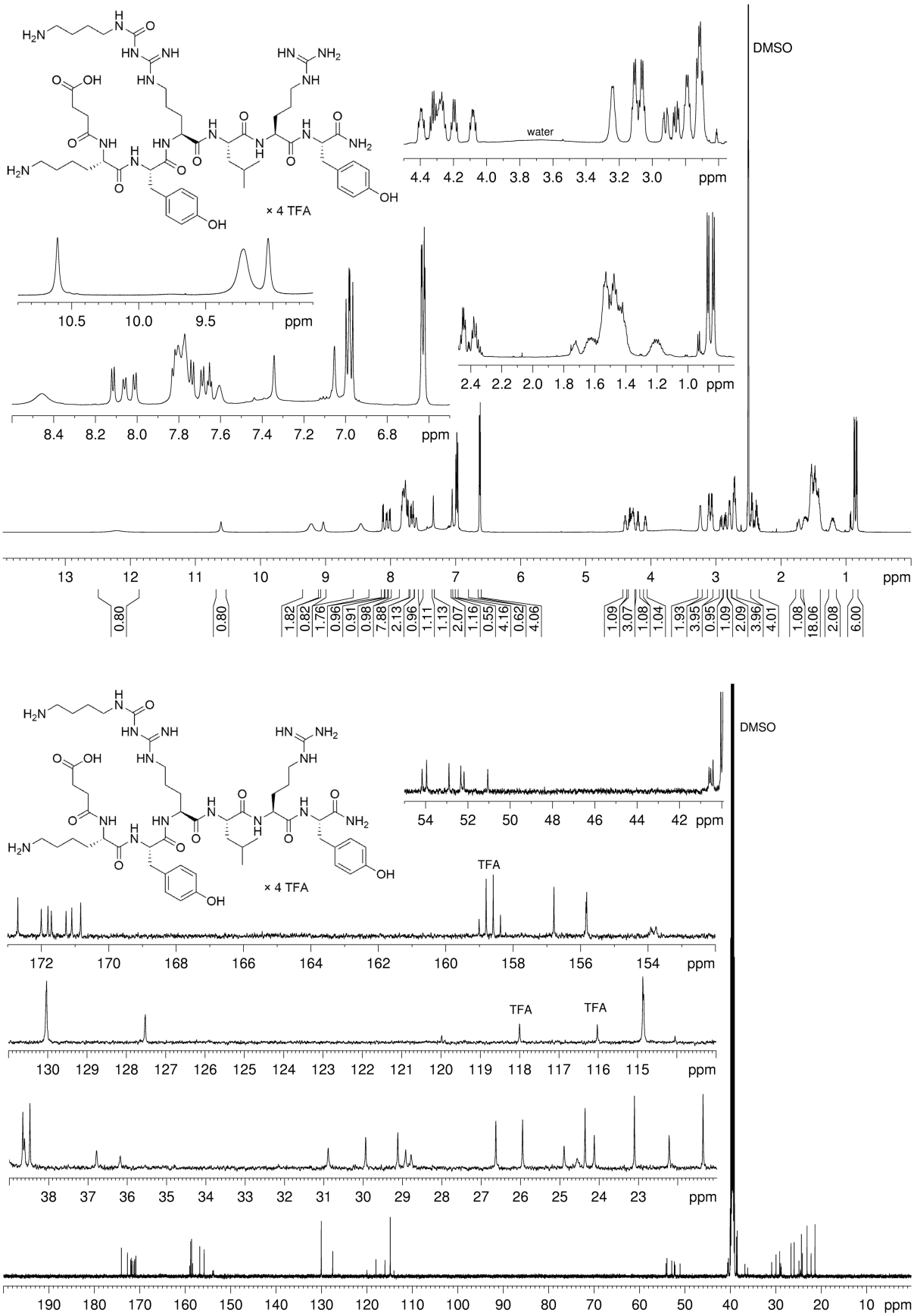

^{1}H-NMR (600 MHz, DMSO-d_6) and ^{13}C-NMR (150 MHz, DMSO-d_6) spectrum of compound **5.21**

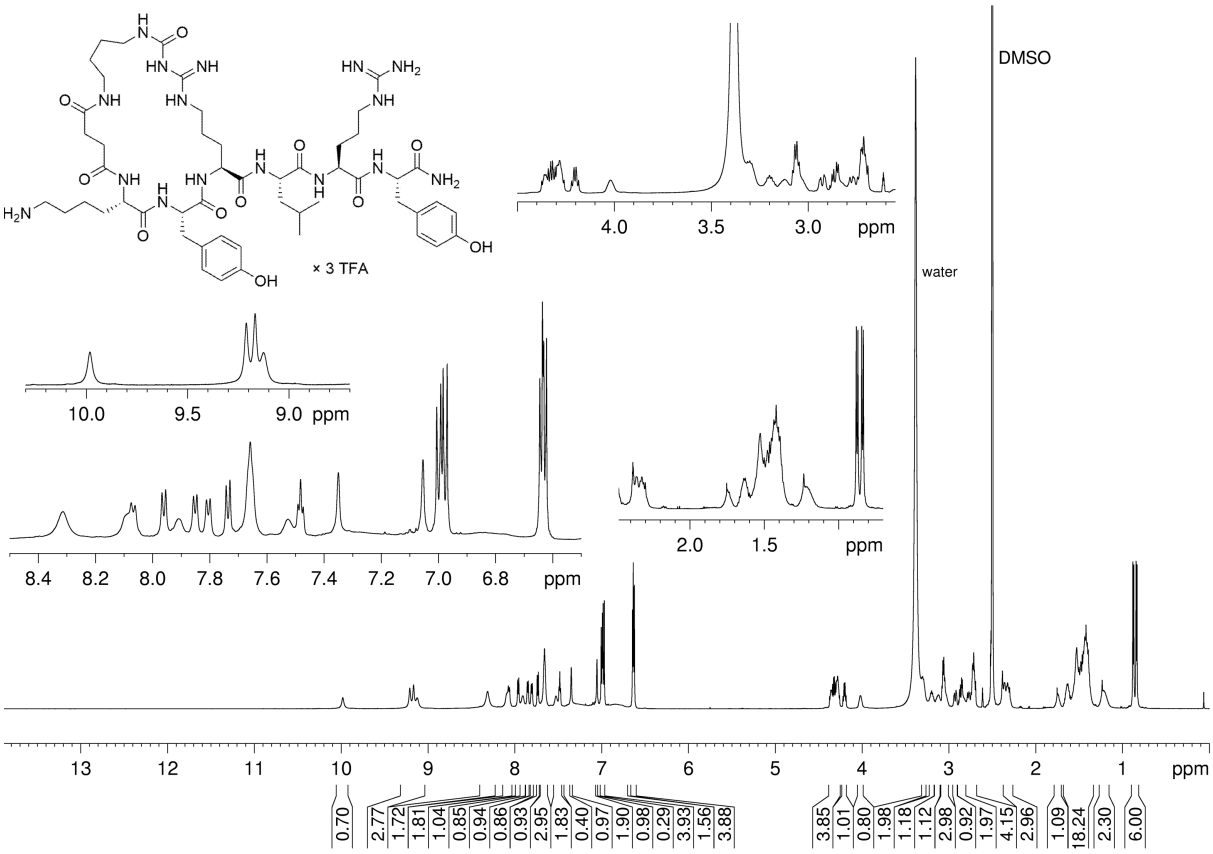
× 3 TFA
DMSO
water
4.0 3.5 3.0 ppm
10.0 9.5 9.0 ppm
8.4 8.2 8.0 7.8 7.6 7.4 7.2 7.0 6.8 ppm
2.0 1.5 ppm
13 12 11 10 9 8 7 6 5 4 3 2 1 ppm
0.70 2.77 1.72 1.81 1.04 0.85 0.94 0.86 0.93 2.95 1.83 0.40 0.97 1.90 0.98 0.29 3.93 1.56 3.88
3.85 1.01 0.80 1.98 1.18 1.12 2.98 0.92 1.97 4.15 2.96 1.09 18.24 2.30 6.00

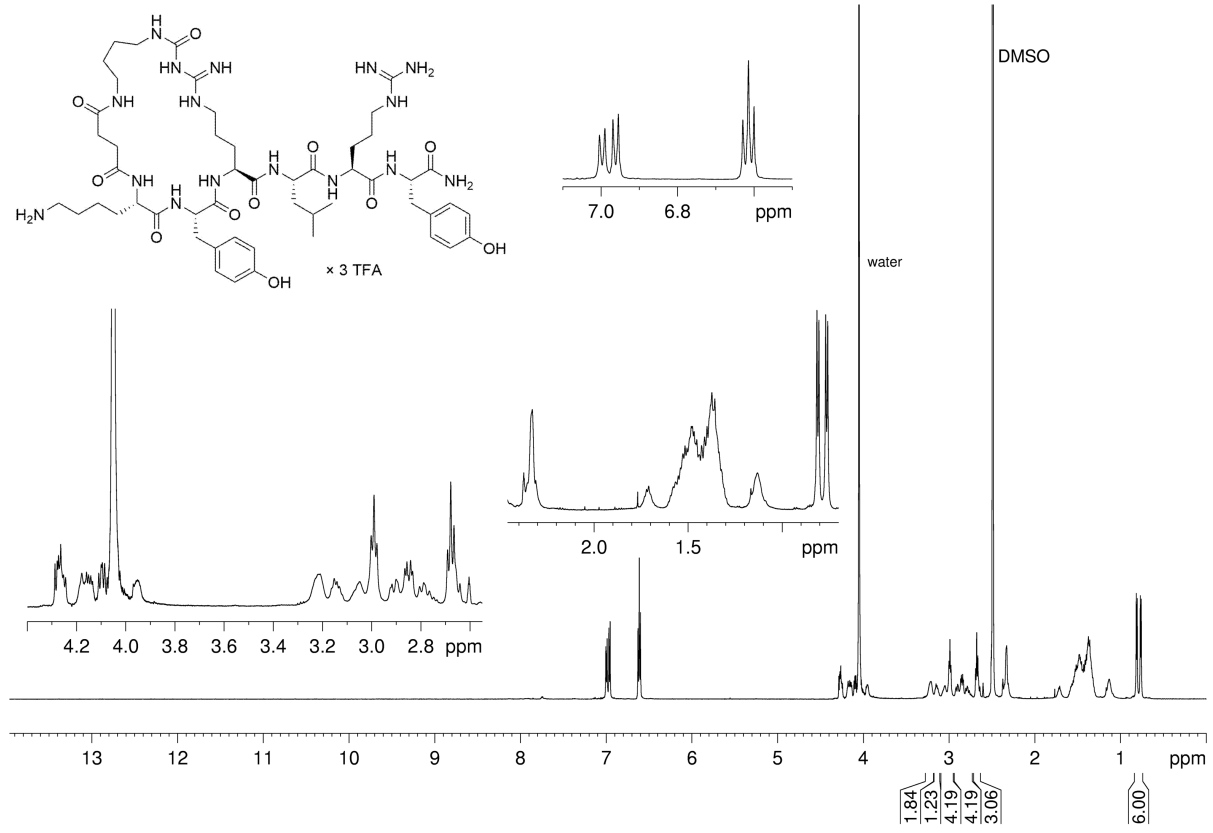
× 3 TFA
DMSO
water
7.0 6.8 ppm
4.2 4.0 3.8 3.6 3.4 3.2 3.0 2.8 ppm
2.0 1.5 ppm
13 12 11 10 9 8 7 6 5 4 3 2 1 ppm
1.84 1.23 4.19 4.19 3.06 6.00

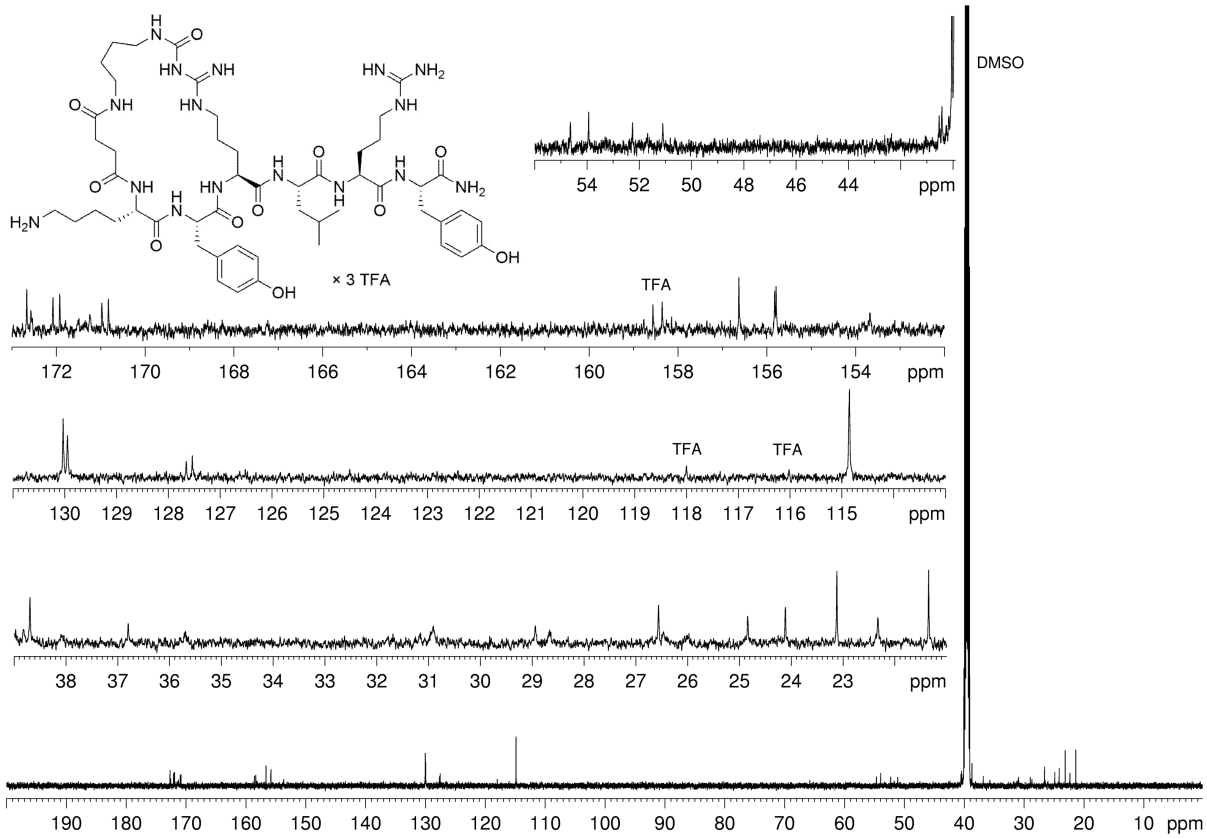

^{1}H-NMR (600 MHz, DMSO-d_6), ^{1}H-NMR (600 MHz, DMSO-d_6/D_2O 4:1 v/v) and ^{13}C-NMR (150 MHz, DMSO-d_6) spectrum of compound **5.22**

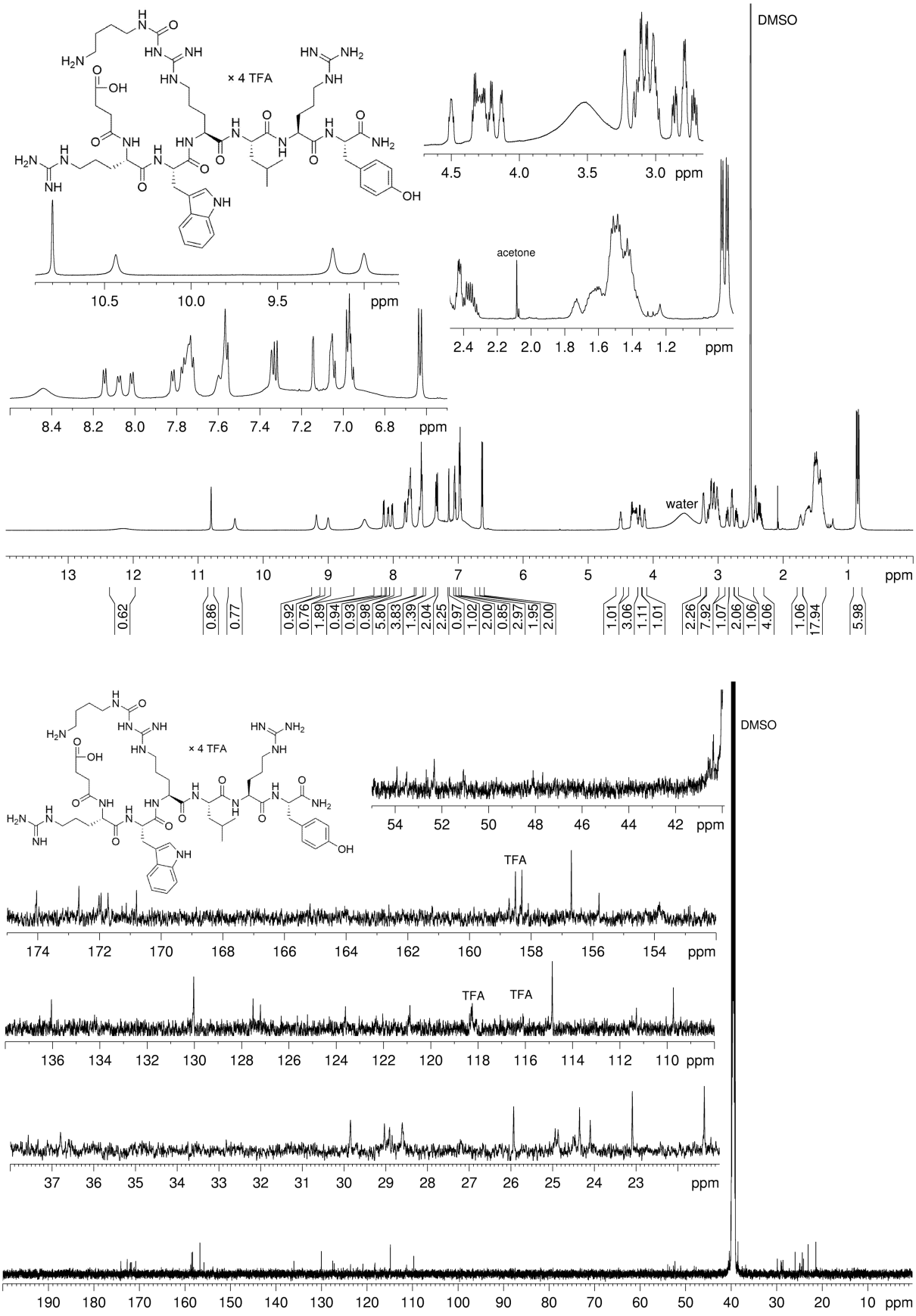

^{1}H-NMR (600 MHz, DMSO-d_6) and ^{13}C-NMR (150 MHz, DMSO-d_6) spectrum of compound **5.23**

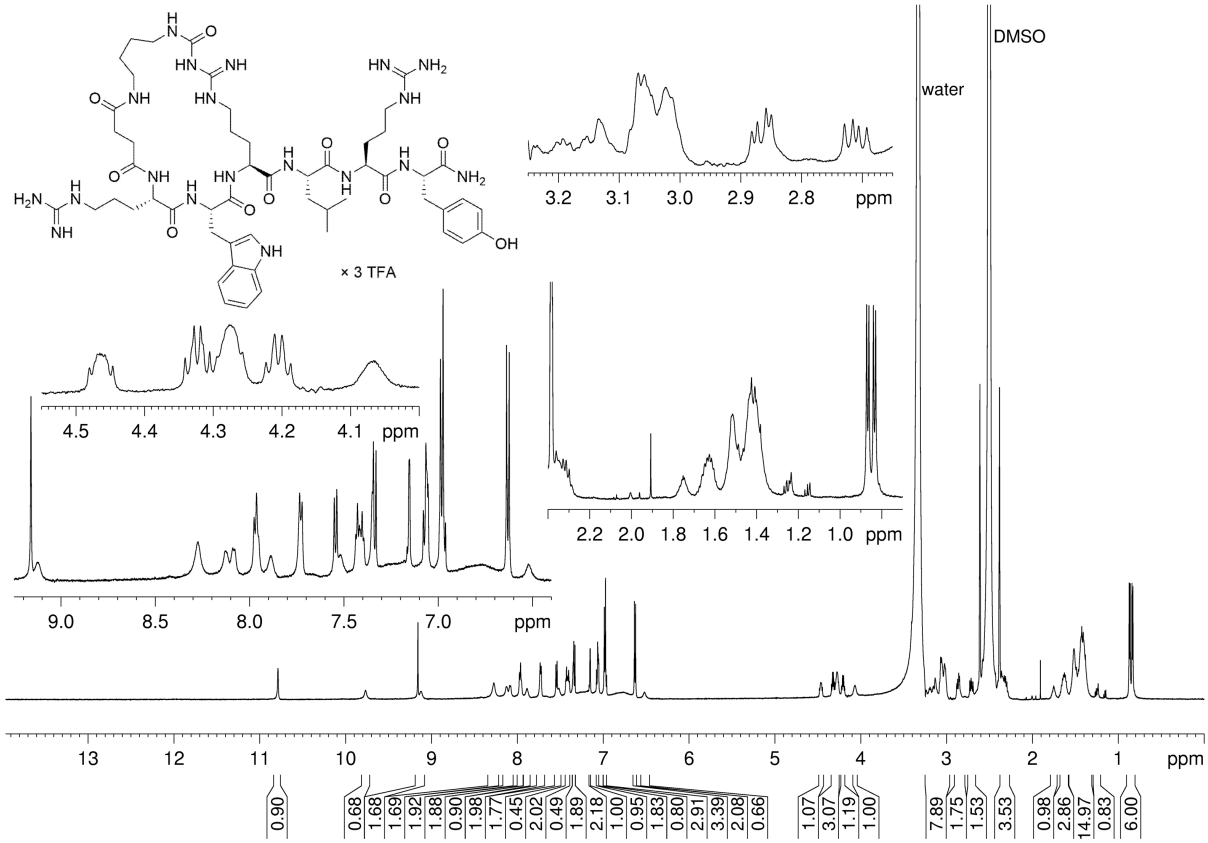

^{1}H-NMR (600 MHz, DMSO-d_6) spectrum of compound **5.24**

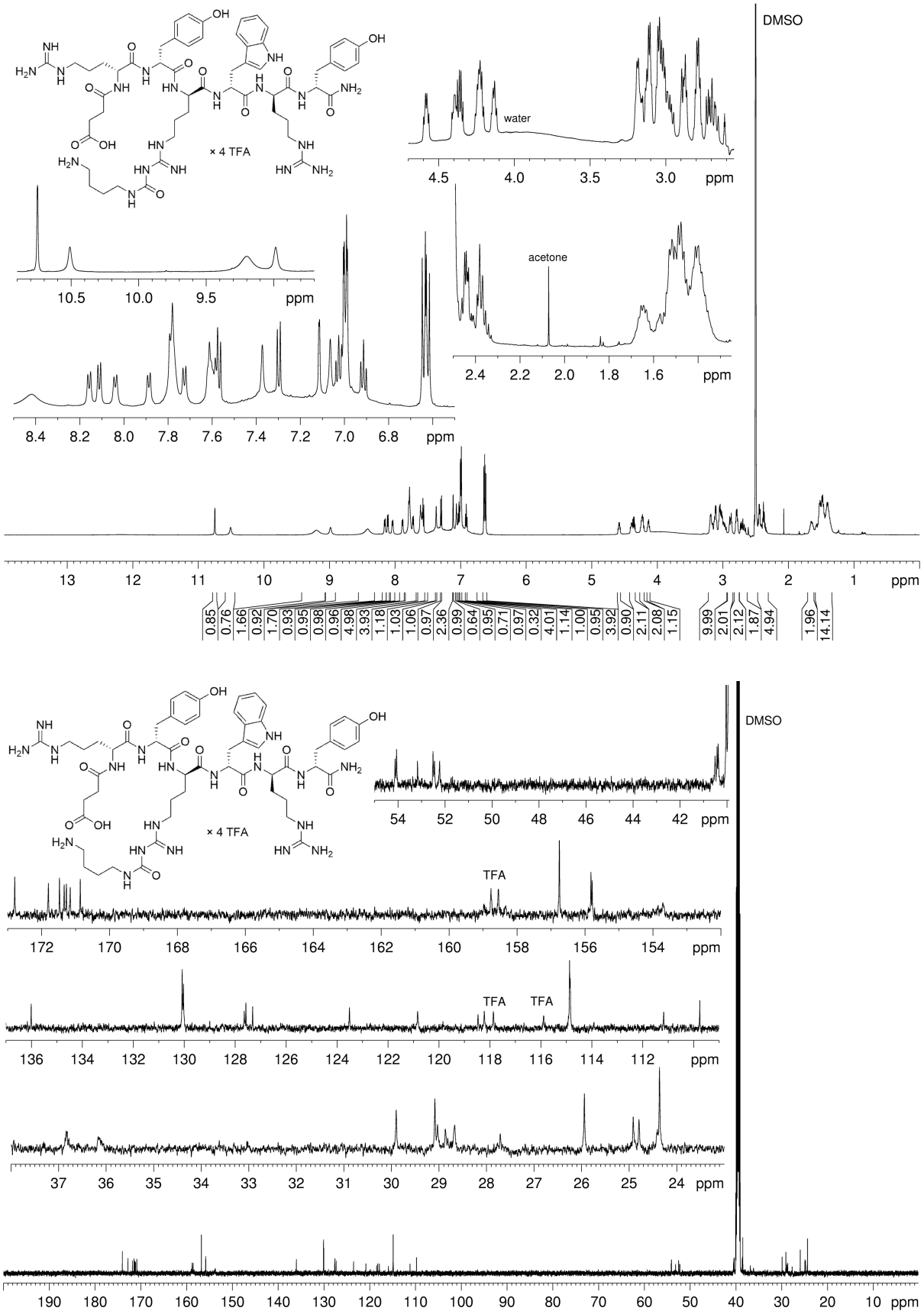

^{1}H-NMR (600 MHz, DMSO-d_6) and ^{13}C-NMR (150 MHz, DMSO-d_6) spectrum of compound **5.25**

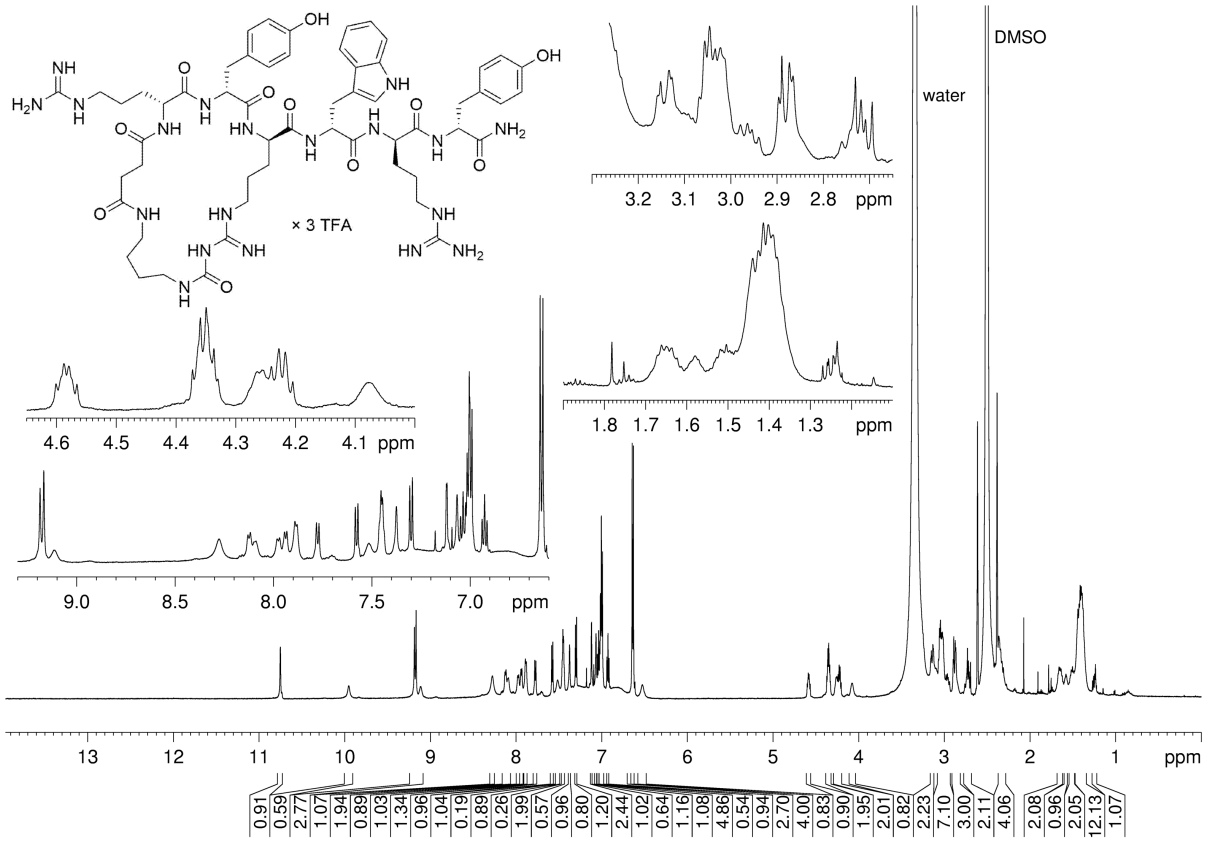

^{1}H-NMR (600 MHz, DMSO-d_6) spectrum of compound **5.26**

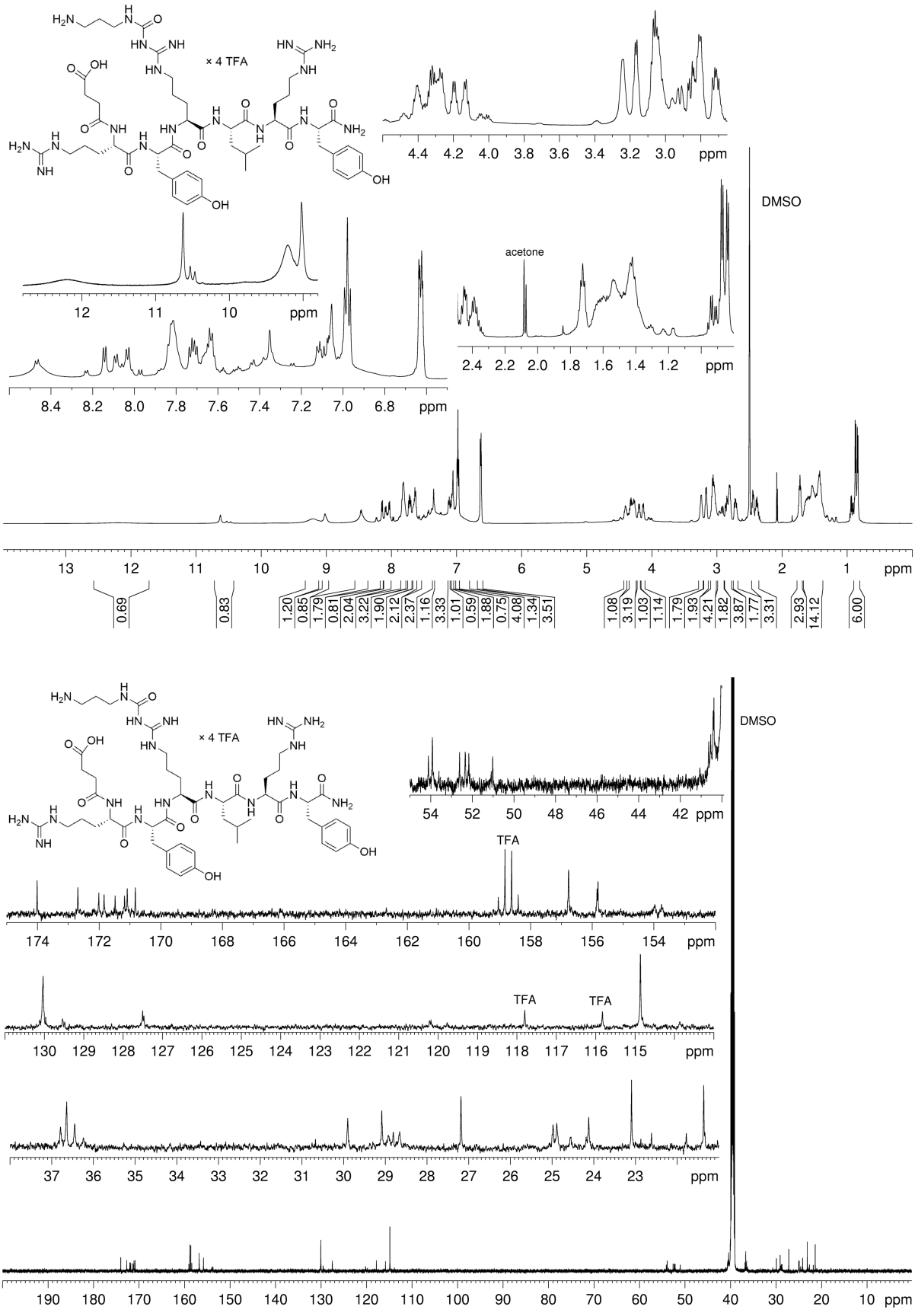

^{1}H-NMR (600 MHz, DMSO-d_6) and ^{13}C-NMR (150 MHz, DMSO-d_6) spectrum of compound **5.27**

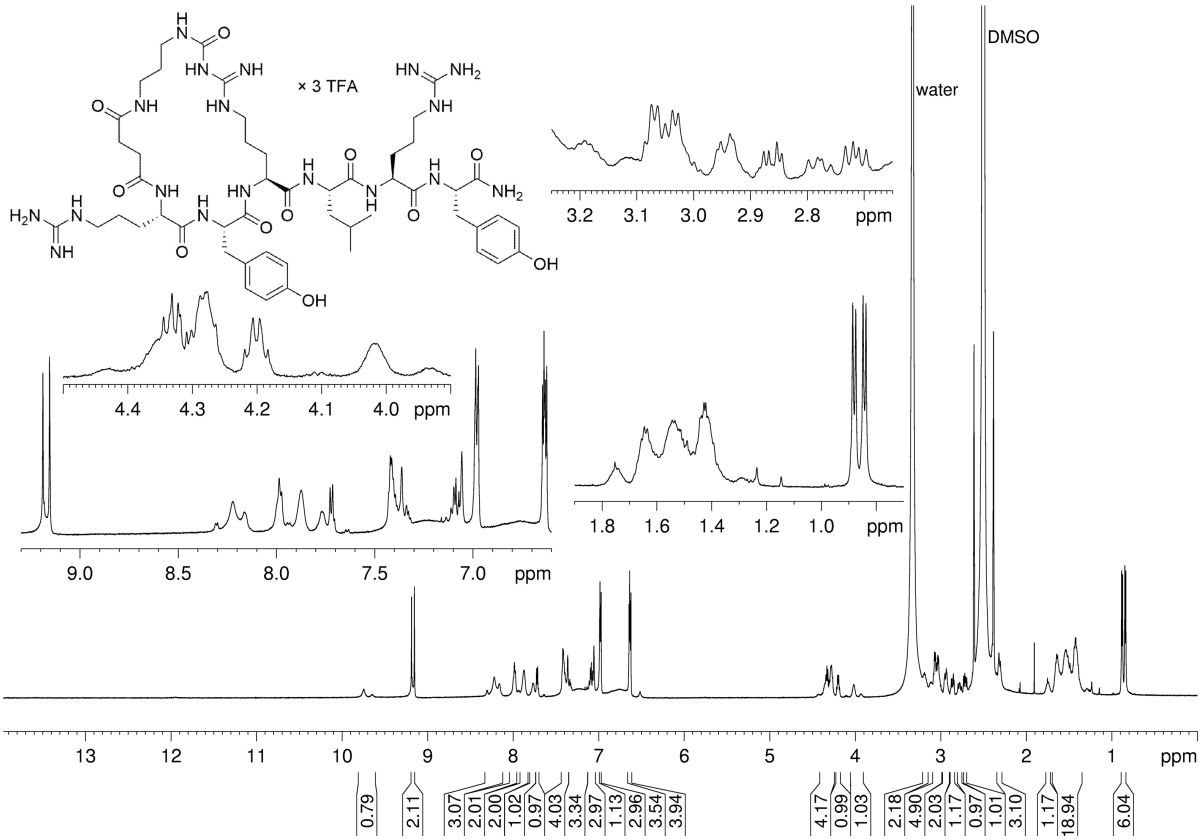

^{1}H-NMR (600 MHz, DMSO-d_6) spectrum of compound **5.28**

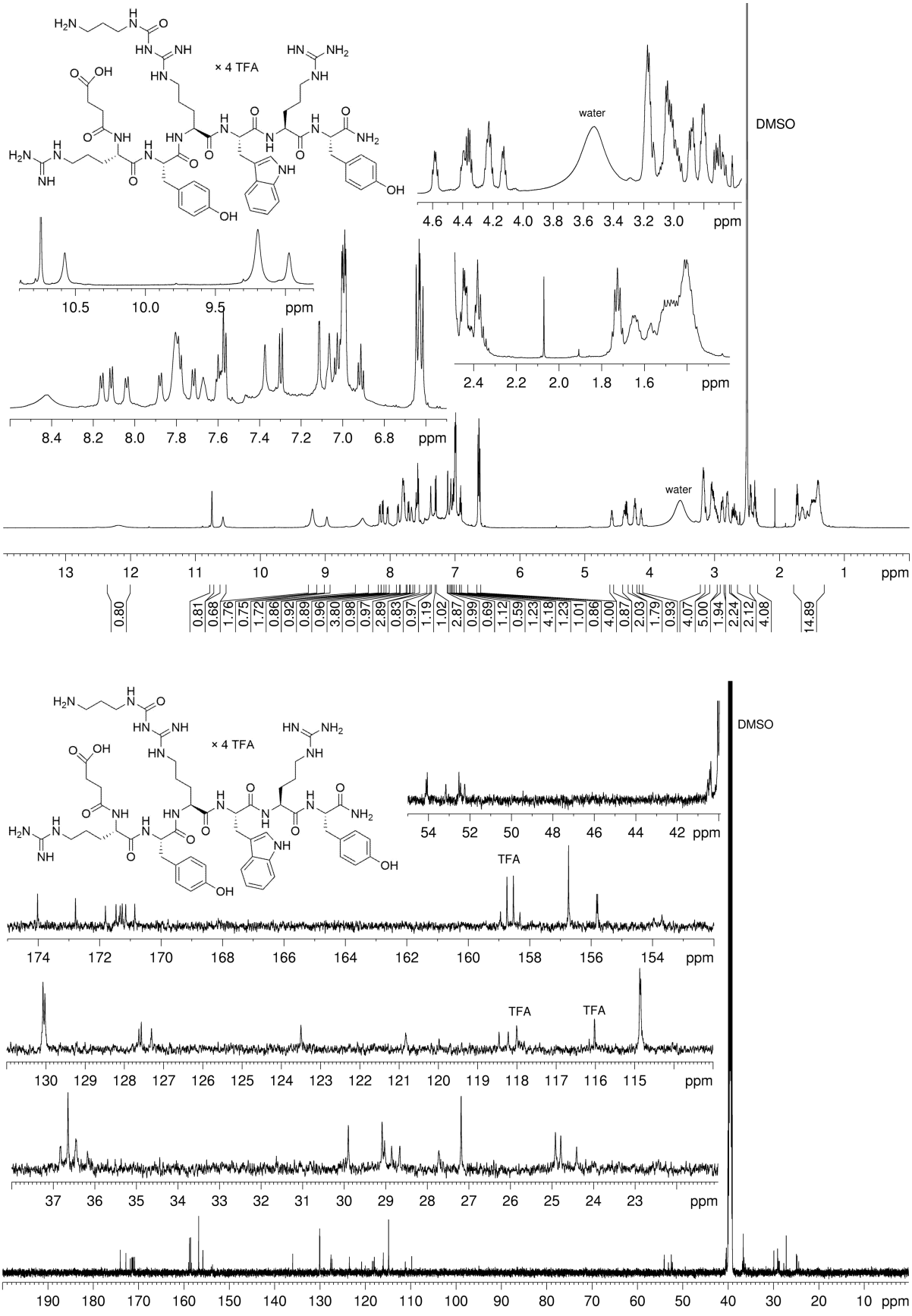

^{1}H-NMR (600 MHz, DMSO-d_6) and ^{13}C-NMR (150 MHz, DMSO-d_6) spectrum of compound **5.29**

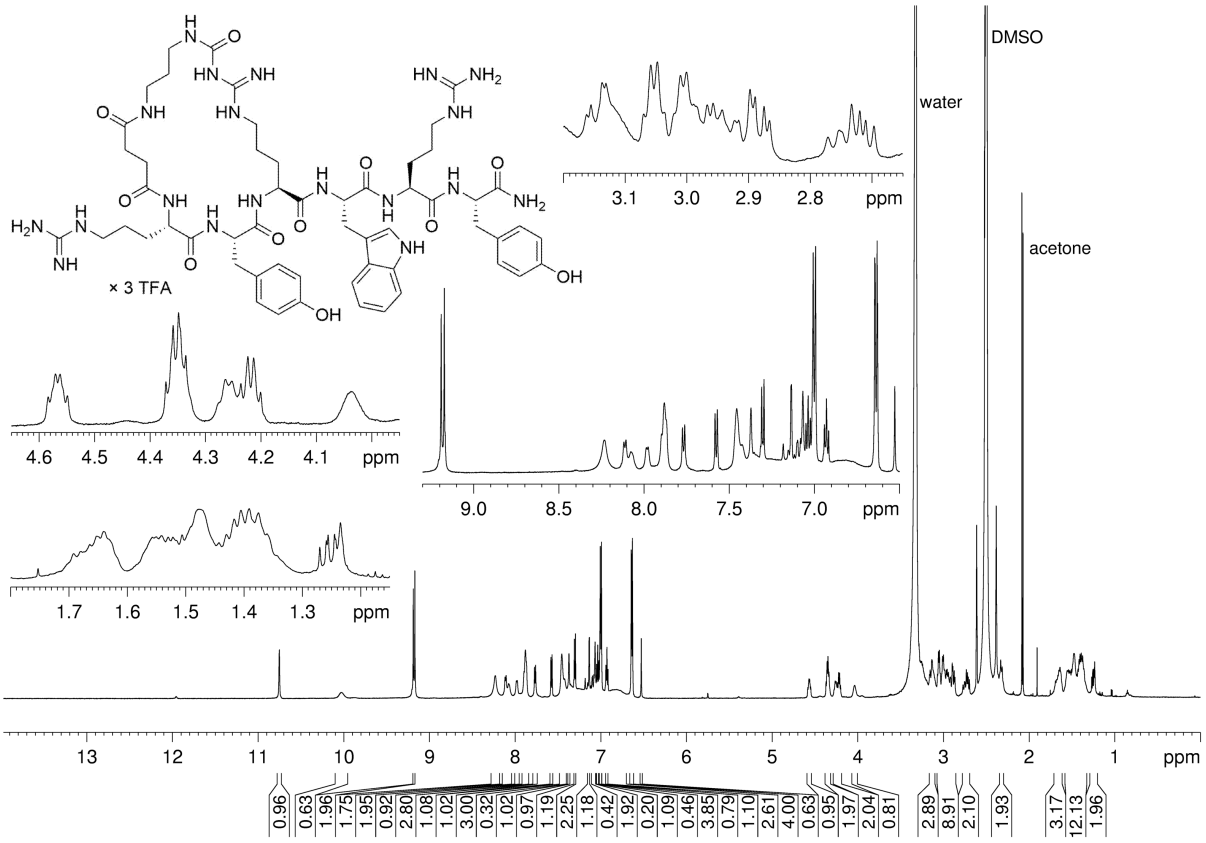

^{1}H-NMR (600 MHz, DMSO-d_6) spectrum of compound **5.30**

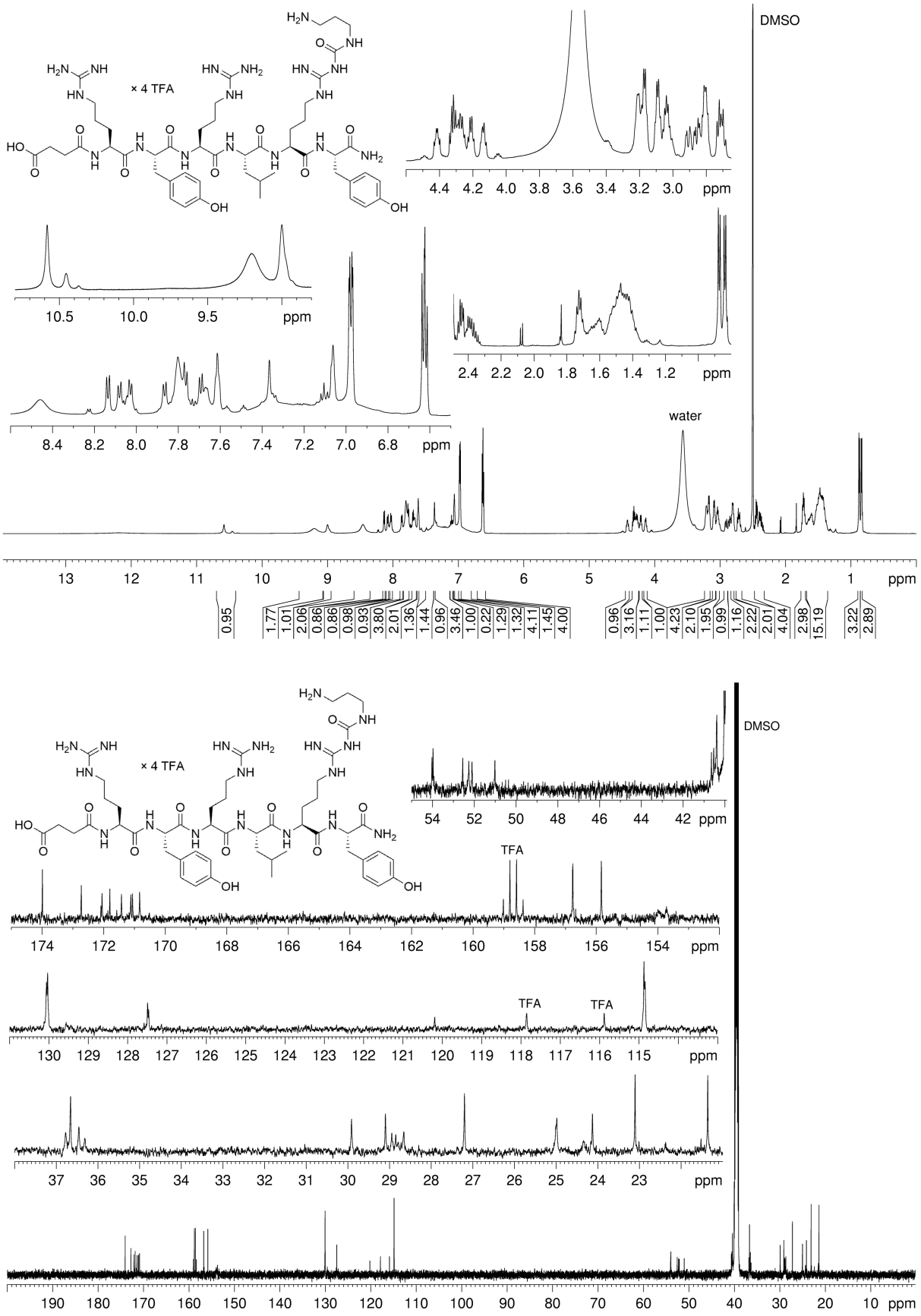

^{1}H-NMR (600 MHz, DMSO-d_6) and ^{13}C-NMR (150 MHz, DMSO-d_6) spectrum of compound **5.31**

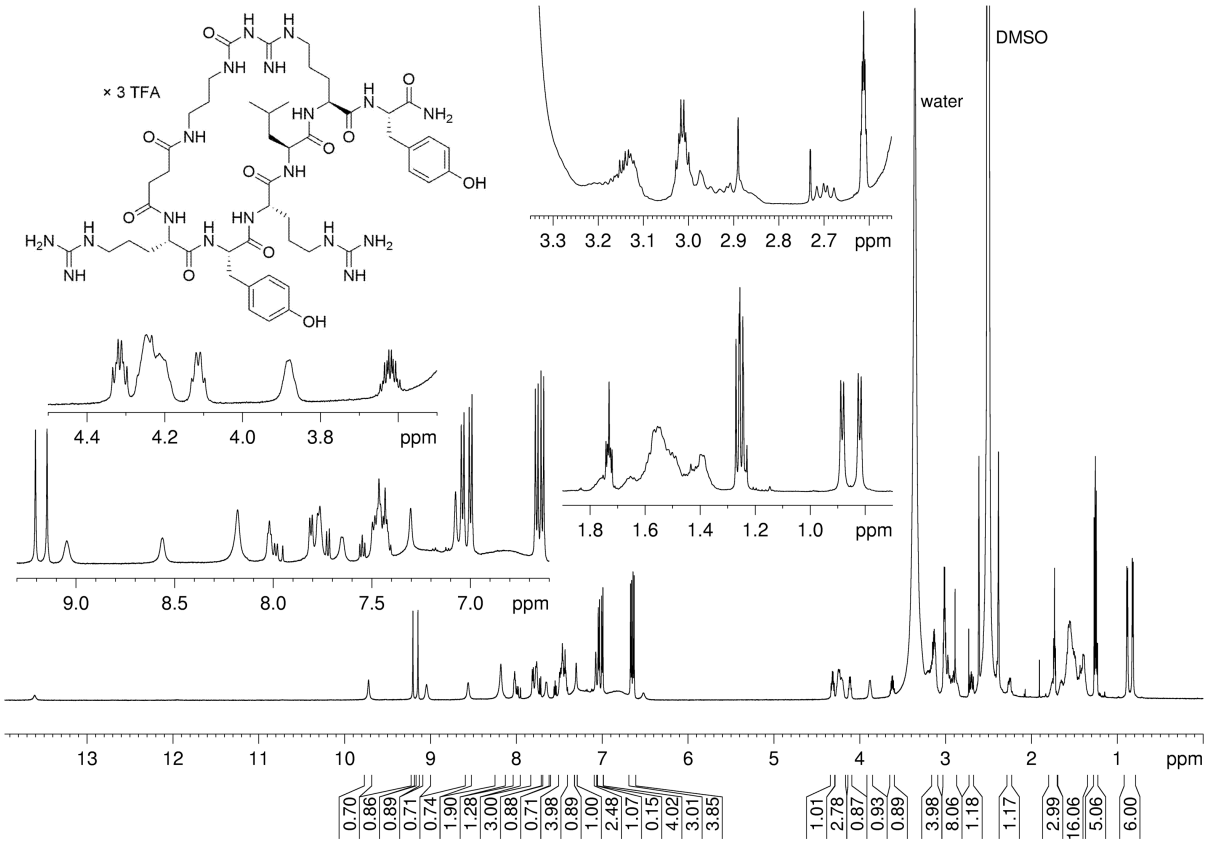

^{1}H-NMR (600 MHz, DMSO-d_6) spectrum of compound **5.32**

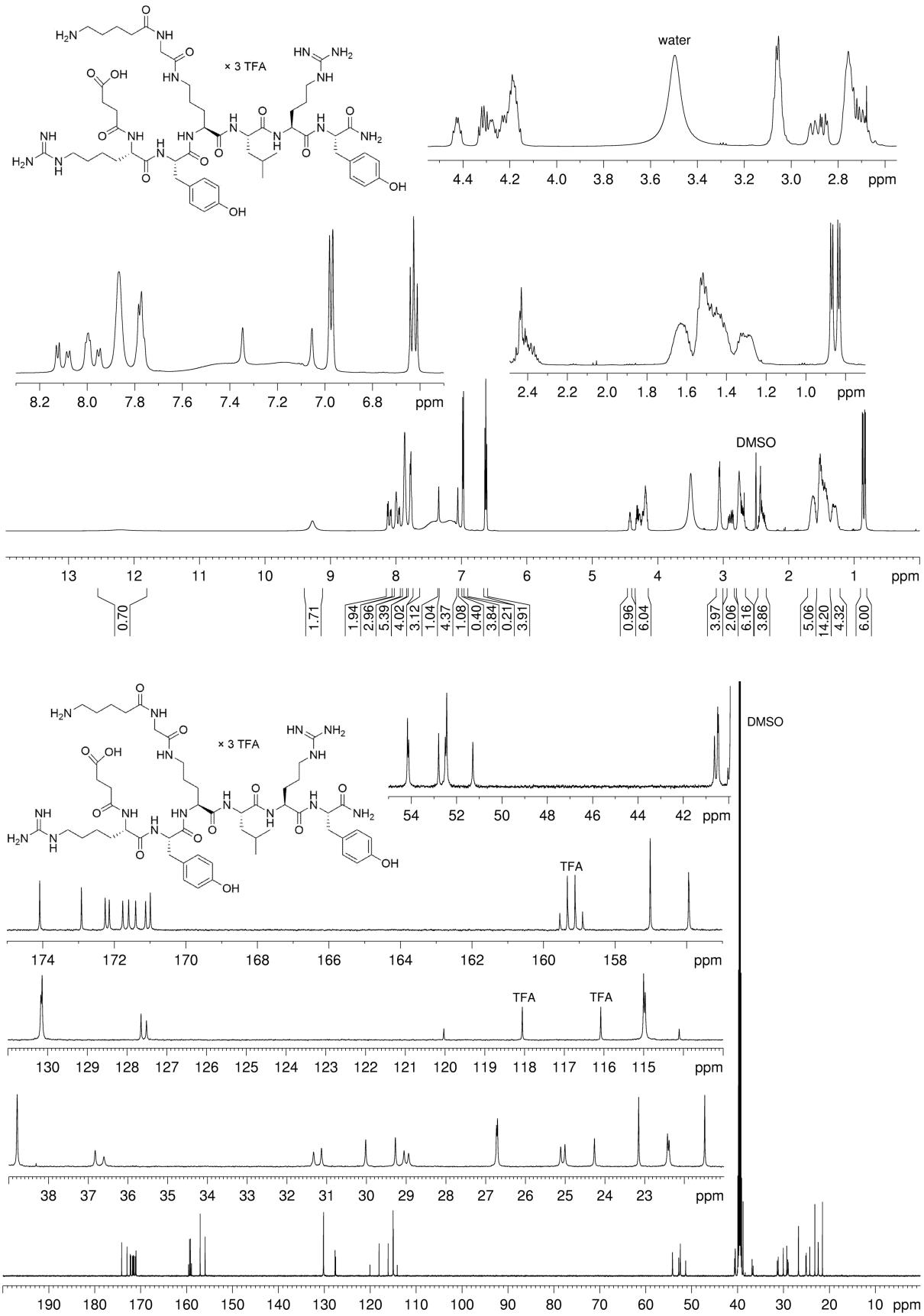

^{1}H-NMR (600 MHz, DMSO-d_6) and ^{13}C-NMR (150 MHz, DMSO-d_6) spectrum of compound **5.33**

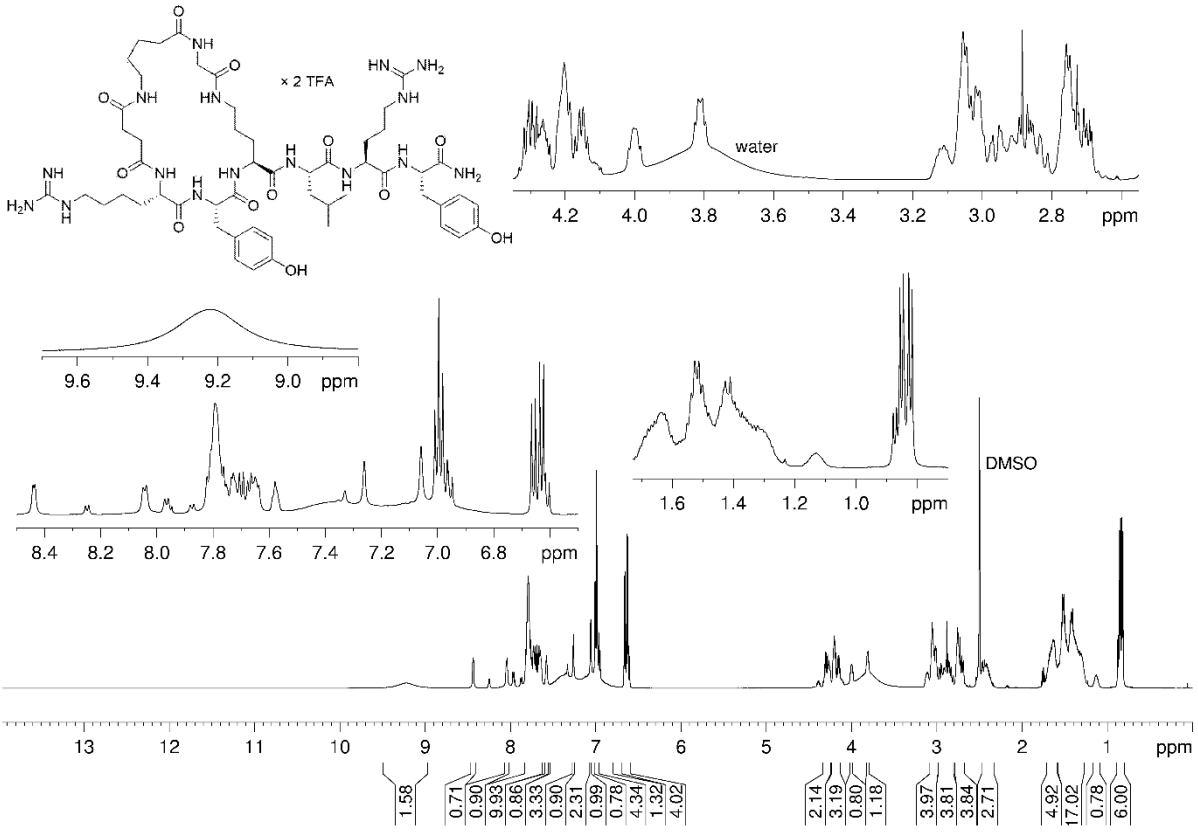
× 2 TFA
water
DMSO
ppm

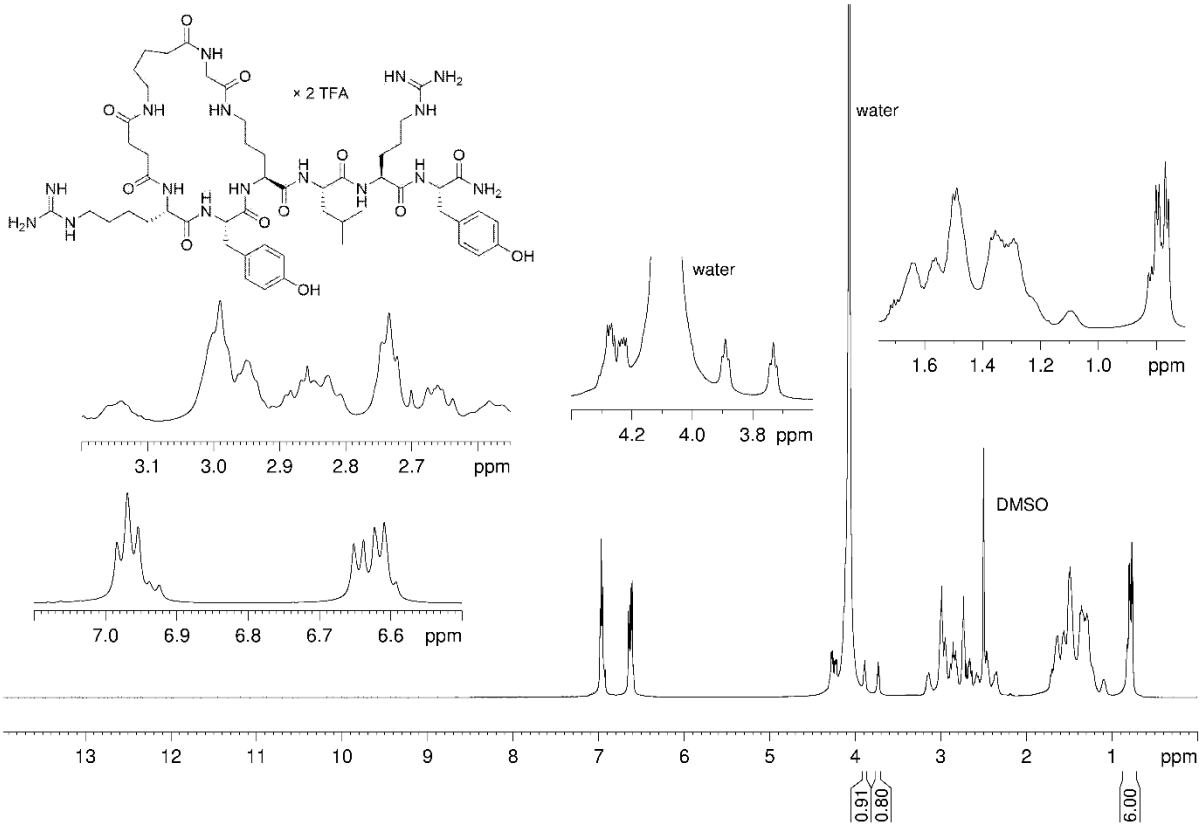
× 2 TFA
water
DMSO
ppm

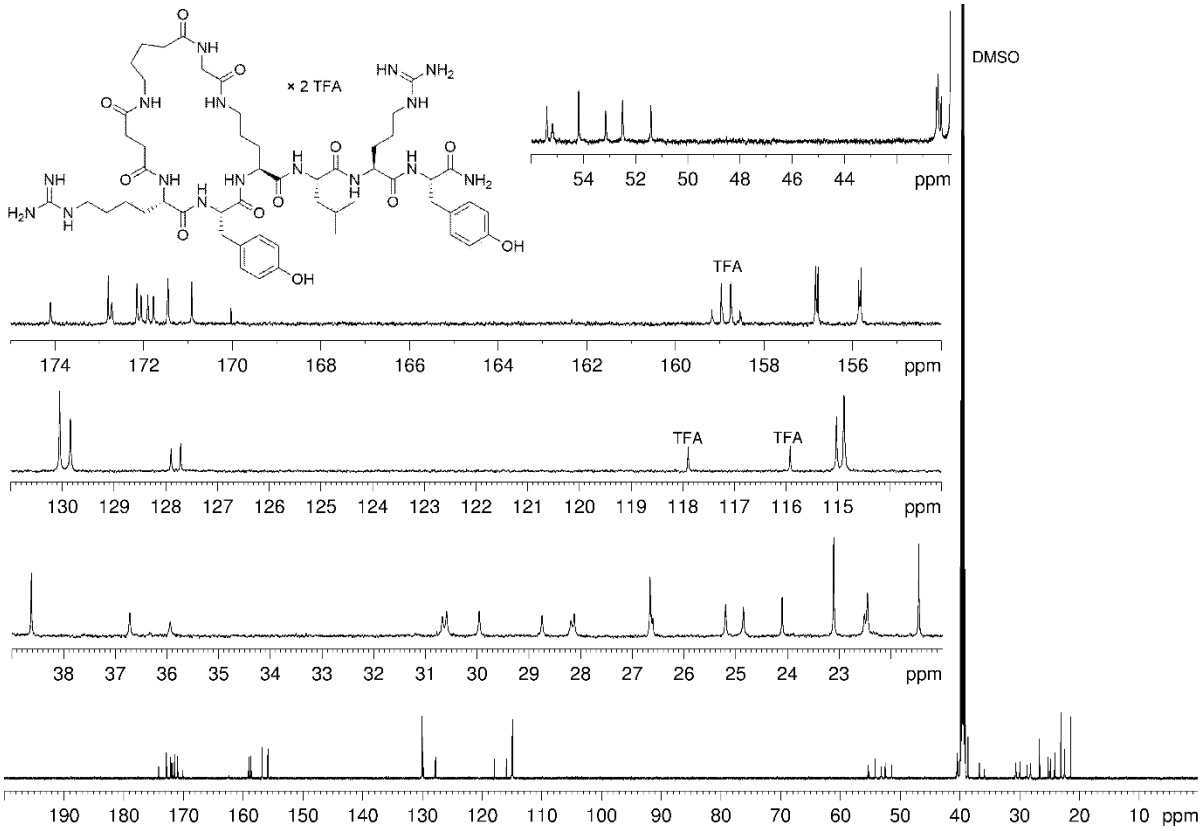

^{1}H-NMR (600 MHz, DMSO-d_6), ^{1}H-NMR (600 MHz, DMSO-d_6/D_2O 4:1 v/v) and ^{13}C-NMR (150 MHz, DMSO-d_6) spectrum of compound **5.34**

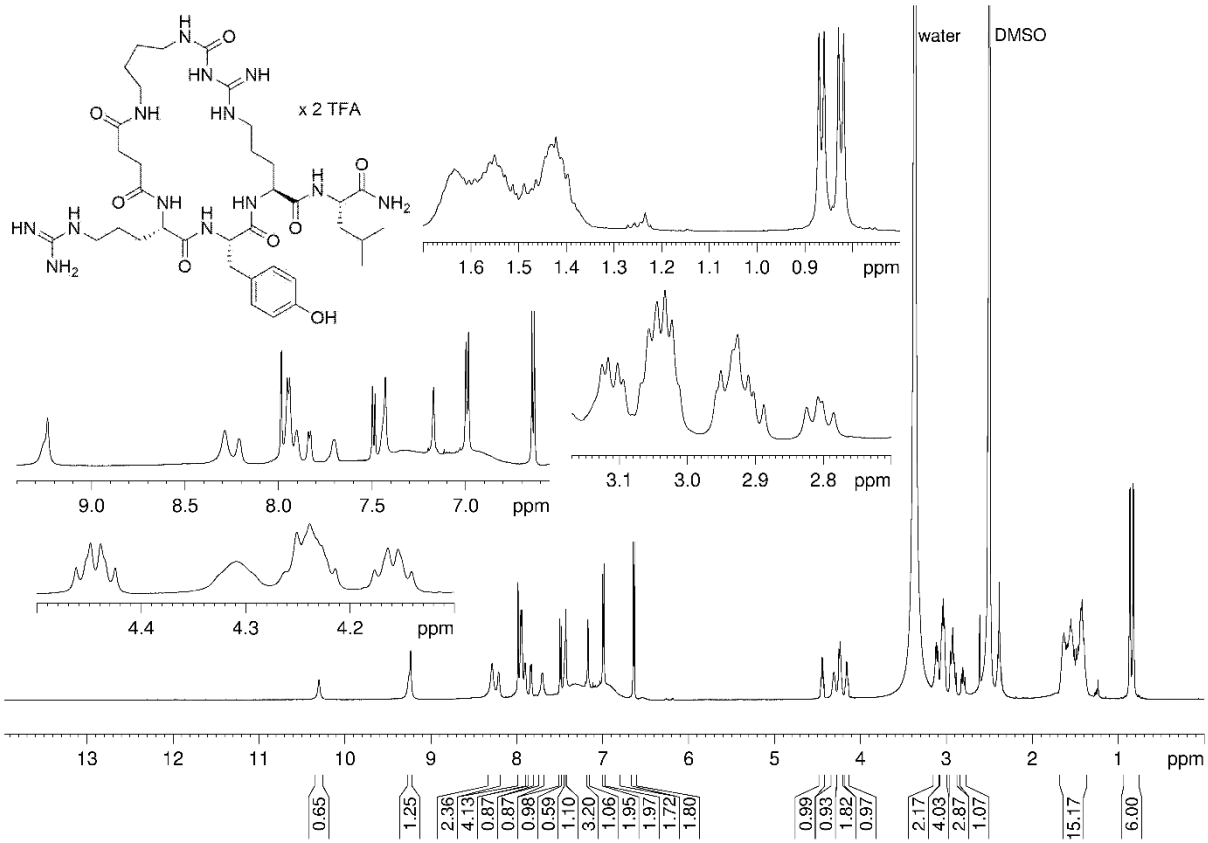

^{1}H-NMR (600 MHz, DMSO-d_6) spectrum of compound **5.35**

7.5 Abbreviations

AA	amino acids(s)
aq.	aqueous
Ac	acetyl
Boc	*tert*-butoxycarbonyl
Bq	becquerel
bs	broad singulet
BSA	bovine serum albumin
c	concentration
cAMP	cyclic adenosine monophosphate
Cbz	benzyloxycarbonyl
CHO	cells Chinese hamster ovary cells
COSY	correlated spectroscopy
d	doublet
δ	chemical shift
DCM	dichloromethane
DIPEA	*N*,*N*-diisopropyl-ethylamine
DMEM	dulbecco's modified eagle's medium
DMF	*N*,*N*-dimethylformamide
DMSO	dimethylsulfoxide
EC_{50}	agonist concentration which induces 50% of the maximum response
EtOAc	ethyl acetate
EtOH	ethanol
eq.	equivalent(s)
ESI	electrospray ionization
FACS	fluorescence activated cell sorter
FCS	fetal calf serum
Fmoc	9-fluorenylmethoxycarbonyl
GI	gastro intestinal
GPCR	G-protein coupled receptor
h	hour(s)
HBTU	2-(1*H*-benzotriazole-1-yl)-1,1,3,3-tetramethyluronium hexafluorophosphate
HEC	human endometrial carcinoma cells
HEK293	human embryonic kidney cells
HEPES	2-(4-(2-hydroxyethyl)-1-piperazinyl)-ethanesulfonic acid
HMBC	heteronuclear multiple bond correlation
HPLC	high-performance liquid chromatography

hPP	human pancreatic polypeptide
HOBt	1-hydroxybenzotriazole (monohydrate)
HR-MS	high resolution mass spectrometry
HSQC	heteronuclear single quantum coherence
IC_{50}	inhibitor concentration which suppresses 50% of an agonist induced effect or displaces 50% of a labeled ligand from the binding site
k	retention (capacity) factor
K_b	dissociation constant derived from a functional assay
K_d	dissociation constant derived from a saturation experiment
K_i	dissociation constant derived from a competition binding assay
m	multiplet
M	molar (mol/L)
MCF-7 cells	human breast adenocarcinoma cells
MeCN	acetonitrile
MeOH	methanol
mol	mole(s)
N^G	guanidine nitrogen
NMP	*N*-methyl-2-pyrrolidone
NMR	nuclear magnetic resonance
NPY	neuropeptide Y
Pbf	2,2,4,6,7-pentamethyldihydrobenzofuran-5-sulfonyl
PBS	phosphate buffered saline
PE	petroleum ether
PyBOP	benzotriazol-1-yl-oxytripyrrolidinophosphonium-hexafluorophosphat
PYY	peptide YY
RP	reversed phase
rt	room temperature
s	(1) singulet, (2) second(s)
SEM	standard error of the mean
SK-N-MC	human neuroblastoma cell line
Suc	succinyl
t	(1) time, (2) triplet
*t*Bu	*tert*-butyl
TFA	trifluoroacetic acid
THF	tetrahydrofurane
t_R	retention time
UV	ultraviolet
Y_n	NPY receptor subtypes, n = 1, 2, 4, 5

7.6 Overview of Lab Codes and Bold Compound Numerals

Lab code:	compound number:
AK1	**2.13**
AK2	**2.9**
AK3	**2.15**
AK4	**2.19**
AK5	**2.24**
AK8	**2.12**
AK10	**2.20**
AK21	**2.26**
AK22	**2.27**
AK23	**2.25**
AK24	**2.28**
AK25	**2.17**
AK26	**2.18**
AK28	**5.16**
AK29	**5.14**
AK30	**5.15**
AK31	**2.30**
AK32	**2.29**
AK34	**2.21**
AK35	**2.23**
AK36	**2.8**
AK37	**2.10**
AK38	**2.11**
AK40	**2.16**
AK41	**2.14**
AK49	**3.13**
AK50	**3.3**
AK51	**3.4**
AK52	**3.19**
AK53	**3.20**
AK54	**3.21**
AK55	**3.22**
AK56	**3.23**
AK57	**3.12**
AK58	**3.5**
AK59	**3.15**
AK60	**3.14**
AK61	**3.16**
AK62	**3.17**
AK63	**3.18**
AK65	**3.9**
AK66	**3.10**
AK67	**3.11**
AK71	**3.8**
AK76	**3.24**
AK83c	**5.35**
AK86l	**5.17**
AK86c	**5.18**
AK93l	**5.25**
AK93c	**5.26**
AK94l	**5.19**
AK94c	**5.20**
AK95l	**5.23**
AK95c	**5.24**
AK96l	**5.27**
AK96c	**5.28**
AK97l	**5.29**
AK97c	**5.30**
AK98l	**5.31**
AK98c	**5.32**
AK100	**2.22**
AK104	**4.26**
AK105	**4.27**
AK106	**4.29**
AK107	**4.30**
AK110	**4.11**
AK111	**4.25**
AK112	**4.28**
AK113	**4.32**
AK115l	**5.21**
AK115c	**5.22**
AK116l	**5.33**
AK116c	**5.34**
AK118	**4.12**

7.7 Eidesstattliche Erklärung

Ich erkläre hiermit an Eides statt, dass ich die vorliegende Arbeit ohne unzulässige Hilfe Dritter und ohne Benutzung anderer als der angegebenen Hilfsmittel angefertigt habe; die aus anderen Quellen direkt oder indirekt übernommenen Daten und Konzepte sind unter Angabe des Literaturzitats gekennzeichnet.

Regensburg, 18.11.2020 _____

Adam Konieczny